21 September 2007 | S10

Science

MARS
Reconnaissance Orbiter

AAAS

MORE NOVEL.

MORE NOVEX.®

Novex® products unite gels, stains, standards, and blotting products to tackle every protein analysis challenge.

With Novex® products, you can complete an entire western analysis in less than one workday—even for extremely large proteins. This innovative line includes the industry's first precast blue native protein gels: NativePAGE™ Novex® gels, which enable efficient analysis of native proteins, including large membrane protein complexes up to 10,000 kDa. Other standouts in the line are the iBlot™ System for 7-minute protein transfers, NativeMark™ Protein Standard, and WesternBreeze® Immunodetection Kits. Novex® products bring it all together for you. Isn't it time your protein analysis workflow was as novel as your thinking? Make it happen at www.invitrogen.com/novex.

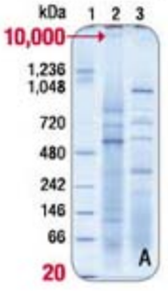

A. NativePAGE™ Novex® 3–12% Bis-Tris Gel stained with Colloidal Blue Staining Kit.*

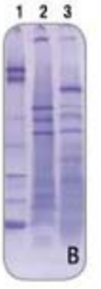

B. Effective transfer of high molecular weight proteins to PVDF using the iBlot™ System.

C. Duplicate of blot in panel B probed with antibody,** using WesternBreeze® Immunodetection Kit.

invitrogen™

*Lane 1: NativeMark™ Protein Standard, 5 µl; lane 2: bovine mitochondrial extract, 1% dodecylmaltoside, 5 µl (20 µg); lane 3: bovine mitochondrial extract, 2% digitonin, 5 µl (20 µg).
** Mouse anti–Complex I (Molecular Probes®).

2007 © Invitrogen Corporation. All rights reserved. These products may be covered by one or more Limited Use Label Licenses (see the Invitrogen catalog or our website, www.invitrogen.com).

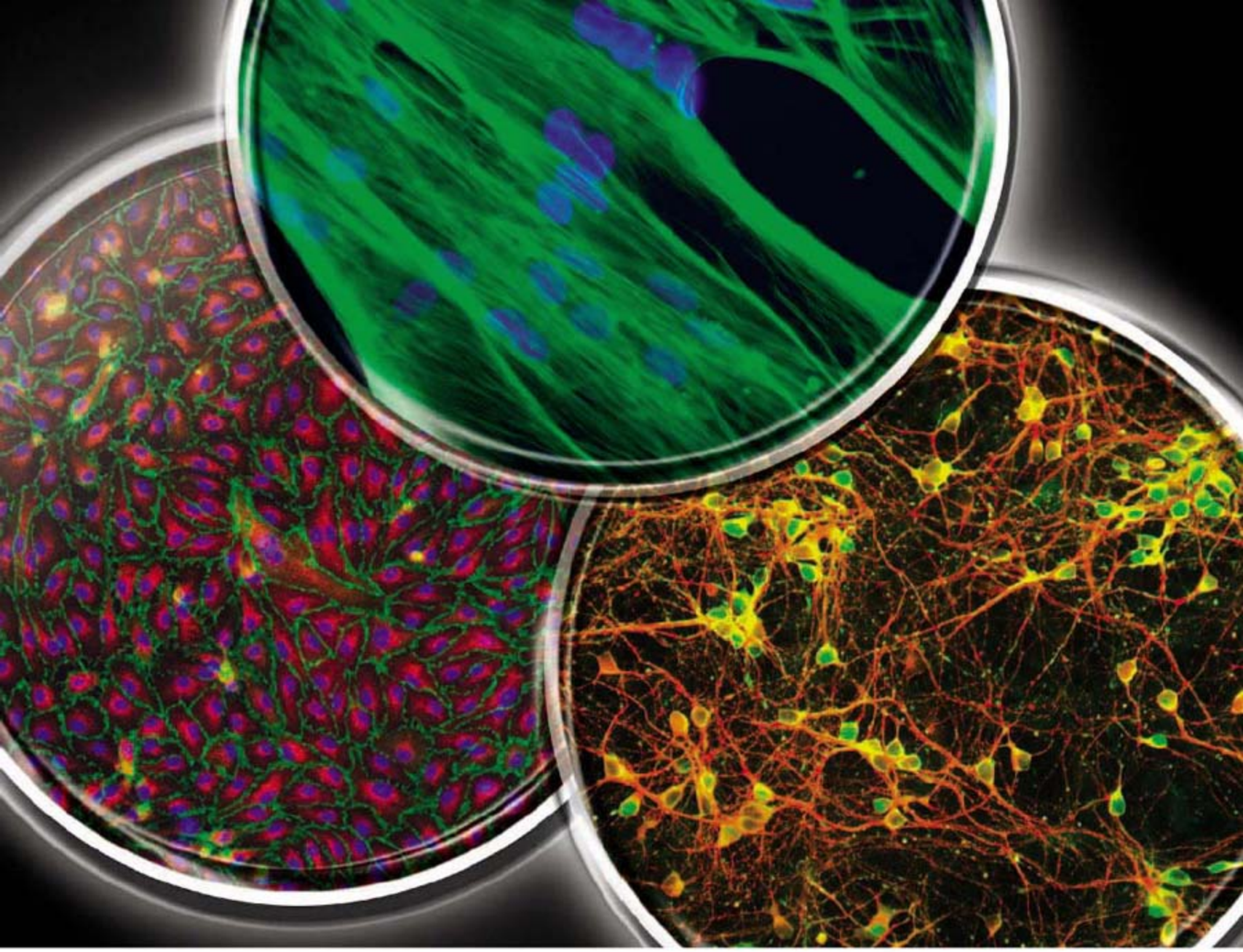

Clonetics® Primary Cells & Media

In Vivo Relevance. *In Vitro* Results.

From the leaders in primary cell culture:

- Normal and non-immortalized cells, ideal for simulating *in vivo* physiology in an *in vitro* environment
- Clonetics® cells and media, tested together under strict QC standards for risk-free cell culture
- Optimized, convenient media kits for cell growth and expansion
- Cryopreserved ampules, proliferating plates, or flasks for your specific application

Choose Clonetics® with the widest offering of ready-to-use primary cells, including epithelial, endothelial, fibroblast, keratinocyte, bone, neural, muscle and hepatocyte cells for your research applications.

Visit our website at www.lonzabioscience.com/clonetics to receive a FREE Lonza Cell Mug.

Lonza Walkersville, Inc., 8830 Biggs Ford Road, Walkersville, MD 21793

Clonetics is a registered trademark of Lonza Group or its subsidiaries. © 2007 Lonza Walkersville, Inc.

www.lonza.com

Lonza

Volume 317, Issue 5845

COVER

False-color image of gully channels in a crater in the southern highlands of Mars, taken by the High-Resolution Imaging Science Experiment (HiRISE) camera on the Mars Reconnaissance Orbiter. The gullies emanating from the rocky cliffs near the crater's rim (upper left) show meandering and braided patterns typical of water-carved channels. North is approximately up and illumination is from the left; image width is about 1 kilometer. See the special section beginning on page 1705.

Image: NASA/JPL/University of Arizona

DEPARTMENTS

1643 *Science* Online
1645 This Week in *Science*
1651 Editors' Choice
1654 Contact *Science*
1657 Random Samples
1659 Newsmakers
1773 New Products
1776 *Science* Careers

EDITORIAL

1649 A Critical Vote Down Under
by Ian Lowe

SPECIAL SECTION

Mars Reconnaissance Orbiter

INTRODUCTION

Water, Water, Not Everywhere? 1705

REPORTS

A Closer Look at Water-Related Geologic Activity on Mars 1706
A. S. McEwen et al.

Athabasca Valles, Mars: A Lava-Draped Channel System 1709
W. L. Jaeger et al.

Meter-Scale Morphology of the North Polar Region of Mars 1711
K. E. Herkenhoff et al.

Accumulation and Erosion of Mars' South Polar Layered Deposits 1715
R. Seu et al.

Density of Mars' South Polar Layered Deposits 1718
M. T. Zuber et al.

>> News story p. 1673

NEWS OF THE WEEK

Continuing Indonesian Quakes Putting Seismologists on Edge 1660

Tsunami Warning System Shows Agility—and Gaps in Indian Ocean Network 1661

Arecibo Advocates Agitate to Reverse Planned NSF Cut 1663

SCIENCESCOPE 1663

A New Body of Evidence Fleshes Out *Homo erectus* 1664

Questions Remain on Cause of Death in Arthritis Trial 1665

Climate Change: Panel Gives U.S. Program Mixed Grades 1667

Australian Scientist to Head California Stem Cell Effort 1667

NEWS FOCUS

The Geneticist's Best Friend 1668
Europe Going to the Dogs

Is Mars Looking Drier and Drier for Longer and Longer? 1673
>> Mars Reconnaissance Orbiter section p. 1705
Read My Slips: Speech Errors Show How Language Is Processed 1674

European Universities: Barroso's Brainchild 1676

CONTENTS continued >>

Science

SCIENCE EXPRESS

www.sciencexpress.org

PHYSICS

Quantum Spin Hall Insulator State in HgTe Quantum Wells
M. König et al.
A predicted, novel state of matter in which a spin-induced current flows across an insulator in the absence of a magnetic field is demonstrated in a doped thin film.
10.1126/science.1148047

PALEOCLIMATE

Mixed-Layer Deepening During Heinrich Events: A Multi-Planktonic Foraminiferal $\delta^{18}O$ Approach
H. Rashid and E. A. Boyle
Massive releases of icebergs into the North Atlantic during the last glacial period, and the associated storminess, periodically mixed the ocean to greater depths than usual.
10.1126/science.1146138

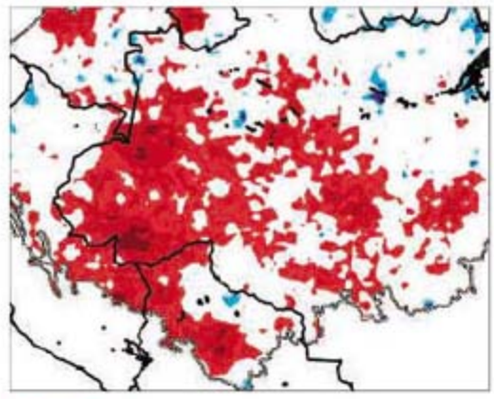

ECOLOGY

BREVIA: Amazon Forests Green-Up During 2005 Drought
S. R. Saleska, K. Didan, A. R. Huete, H. R. da Rocha
Showing unexpected resilience, tropical forests in the Amazon apparently increased photosynthesis in response to the 2005 drought, according to satellite measurements.
10.1126/science.1146663

LETTERS

Factory Flies Are Not Equal to Wild Flies 1678
J. S. Terblanche and S. L. Chown
Promoting Science and Technology from the Top
A. K. Ventura
How Old Is the Human Presence on Cyprus?
A. H. Simmons and R. D. Mandel
Ethics and Refinement in Animal Research
I. A. S. Olsson, A. K. Hansen, P. Sandøe
CORRECTIONS AND CLARIFICATIONS 1682

BOOKS *ET AL.*

Human–Machine Reconfigurations 1684
Plans and Situated Actions, 2nd ed.
L. A. Suchman, reviewed by B. Laurel and R. Tow
Müller's Lab 1685
L. Otis, reviewed by L. K. Nyhart

POLICY FORUM

The Future of Personal Genomics 1687
A. L. McGuire, M. K. Cho, S. E. McGuire, T. Caulfield

PERSPECTIVES

The Root of Platelet Production 1689
A. E. Geddis and K. Kaushansky
>> Report p. 1767
Coding and Computing Join Forces 1691
B. Chazelle
Easter Island Revisited 1692
J. Diamond
Electrons Acquire a Split Personality in Bismuth 1694
A. Huxley and A. G. Green
>> Report p. 1729
How Cells Control Zinc Homeostasis 1695
D. H. Nies
>> Report p. 1746
Home for the Precious Few 1696
S. DiNardo and R. E. Braun
>> Research Article p. 1722

TECHNICAL COMMENT ABSTRACTS

PLANETARY SCIENCE

Comment on "Organics Captured from Comet 81P/Wild 2 by the Stardust Spacecraft" 1682
M. K. Spencer and R. N. Zare
full text at www.sciencemag.org/cgi/content/full/317/5845/1680c
Response to Comment on "Organics Captured from Comet 81P/Wild 2 by the Stardust Spacecraft"
S. A. Sandford and D. E. Brownlee
full text at www.sciencemag.org/cgi/content/full/317/5845/1680d

REVIEW

PHYSICS

Circuits with Light at Nanoscales: Optical Nanocircuits Inspired by Metamaterials 1698
N. Engheta

BREVIA

PALEONTOLOGY

Feather Quill Knobs in the Dinosaur *Velociraptor* 1721
A. H. Turner, P. J. Makovicky, M. A. Norell
Regularly spaced knobs on a fossil ulna of a *Velociraptor*, a 1- to 2-meter-long theropod, are similar to knobs housing secondary feathers on modern birds.

RESEARCH ARTICLES

DEVELOPMENTAL BIOLOGY

A Vasculature-Associated Niche for Undifferentiated Spermatogonia in the Mouse Testis 1722
S. Yoshida, M. Sukeno, Y. Nabeshima
Time-lapse imaging reveals that the stem cells that generate sperm are located near blood vessels in the testis of mice, a different organization than in invertebrates. >> Perspective p. 1696

APPLIED PHYSICS

Universality Classes for Domain Wall Motion in the Ferromagnetic Semiconductor (Ga,Mn)As 1726
M. Yamanouchi et al.
Walls between magnetic domains can be moved by changing the magnetic field or the spin-polarized current, but each acts through a different exponential relationship.

CONTENTS continued >>

REPORTS

PHYSICS

Signatures of Electron Fractionalization in Ultraquantum Bismuth 1729

K. Behnia, L. Balicas, Y. Kopelevich

At very high magnetic fields, charge transport in bismuth crystals behaves like a quantum fluid, an effect previously seen only in two-dimensional materials.

>> *Perspective p. 1694*

CHEMISTRY

Free-Solution, Label-Free Molecular Interactions Studied by Back-Scattering Interferometry 1732

D. J. Bornhop et al.

Binding constants for biomolecules paired with ions or proteins can be determined using interferometry to detect changes in refractive indices upon mixing in small channels.

CHEMISTRY

Asymmetric Catalysis of the Transannular Diels-Alder Reaction 1736

E. P. Balskus and E. N. Jacobsen

A chiral catalyst facilitates carbon bond formation across a large ring, yielding several edge-sharing smaller rings and offering efficient synthesis of complex polycyclic molecules.

GEOPHYSICS

Spin Transition Zone in Earth's Lower Mantle 1740

J.-F. Lin et al.

Iron in one of the major minerals in the lower mantle, (Mg,Fe)O, undergoes a gradual transition from a high-spin state to a denser low-spin state over a large pressure range.

ANTHROPOLOGY

The Primitive Wrist of *Homo floresiensis* and Its Implications for Hominin Evolution 1743

M. W. Tocheri et al.

Homo floresiensis, the enigmatic diminutive hominin from Flores, Indonesia, retains primitive wrist bones, implying that it is not closely related to modern humans.

STRUCTURAL BIOLOGY

Structure of the Zinc Transporter YiiP 1746

M. Lu and D. Fu

The crystal structure of a bacterial membrane transporter reveals that it uses an unusual two-site, zinc-for-proton exchange mechanism.

>> *Perspective p. 1695*

BIOCHEMISTRY

Multicolor Super-Resolution Imaging with Photo-Switchable Fluorescent Probes 1749

M. Bates, B. Huang, G. T. Dempsey, X. Zhuang

A super-resolution imaging method that uses a family of multicolor fluorescent probes yields images of fixed cells with a spatial resolution of 20 to 30 nanometers.

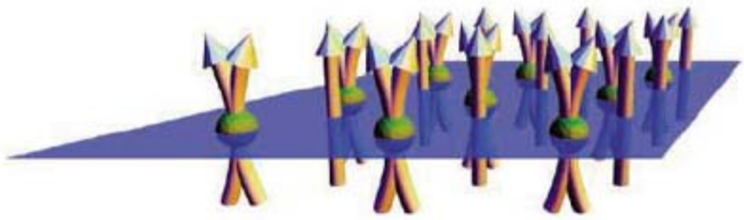

1694 & 1729

EVOLUTION

Widespread Lateral Gene Transfer from Intracellular Bacteria to Multicellular Eukaryotes 1753

J. C. Dunning Hotopp et al.

Unexpectedly, the symbiont *Wolbachia* can transfer segments of DNA consisting of individual genes or almost its entire genome to its insect or nematode hosts.

GENETICS

Draft Genome of the Filarial Nematode Parasite *Brugia malayi* 1756

E. Ghedin et al.

The genome sequence of a parasitic nematode shows that, in comparison to its free-living relative *Caenorhabditis elegans*, its genes are adapted for its parasitic life-style.

MOLECULAR BIOLOGY

UHRF1 Plays a Role in Maintaining DNA Methylation in Mammalian Cells 1760

M. Bostick et al.

Epigenetic DNA methylation patterns that persist through cell division depend on a protein that binds to hemimethylated DNA and a methyltransferase.

MOLECULAR BIOLOGY

MicroRNA Inhibition of Translation Initiation in Vitro by Targeting the Cap-Binding Complex eIF4F 1764

G. Mathonnet et al.

In vitro, microRNAs can act to repress the initial step of protein translation.

IMMUNOLOGY

Dynamic Visualization of Thrombopoiesis Within Bone Marrow 1767

T. Junt et al.

Imaging of living bone marrow confirms that platelets form when long protrusions from sessile cells extend through the blood vessel wall and are then sheared by blood flow. >> *Perspective p. 1689*

AAAS

ADVANCING SCIENCE, SERVING SOCIETY

SCIENCE (ISSN 0036-8075) is published weekly on Friday, except the last week in December, by the American Association for the Advancement of Science, 1200 New York Avenue, NW, Washington, DC 20005. Periodicals Mail postage (publication No. 484460) paid at Washington, DC, and additional mailing offices. Copyright © 2007 by the American Association for the Advancement of Science. The title SCIENCE is a registered trademark of the AAAS. Domestic individual membership and subscription (51 issues): $142 ($74 allocated to subscription). Domestic institutional subscription (51 issues): $710; Foreign postage extra: Mexico, Caribbean (surface mail) $55; other countries (air assist delivery) $85. First class, airmail, student, and emeritus rates on request. Canadian rates with GST available upon request, GST #1254 88122. Publications Mail Agreement Number 1069624. SCIENCE is printed on 30 percent post-consumer recycled paper. **Printed in the U.S.A.**

Change of address: Allow 4 weeks, giving old and new addresses and 8-digit account number. **Postmaster:** Send change of address to AAAS, P.O. Box 96178, Washington, DC 20090–6178. **Single-copy sales:** $10.00 current issue, $15.00 back issue prepaid includes surface postage; bulk rates on request. **Authorization to photocopy** material for internal or personal use under circumstances not falling within the fair use provisions of the Copyright Act is granted by AAAS to libraries and other users registered with the Copyright Clearance Center (CCC) Transactional Reporting Service, provided that $18.00 per article is paid directly to CCC, 222 Rosewood Drive, Danvers, MA 01923. The identification code for *Science* is 0036-8075. *Science* is indexed in the *Reader's Guide to Periodical Literature* and in several specialized indexes.

Printed on 30% post-consumer recycled paper.

CONTENTS continued >>

Buzz kill.

SCIENCENOW

www.sciencenow.org DAILY NEWS COVERAGE

Honey Bee Defense Leaves Hornets Breathless
Social insects suffocate their enemies by swarming them.

Brits in Space
U.K. panel endorses the concept of crewed missions to the moon and beyond.

Loneliness Is in the Genes
Research reveals how feelings of isolation can compromise the body's defenses.

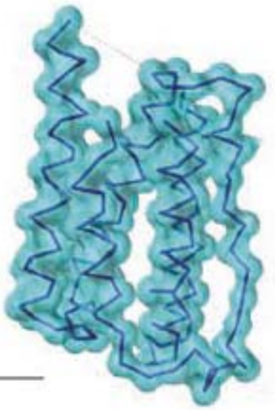

Improving interferon-α.

SCIENCE'S STKE

www.stke.org SIGNAL TRANSDUCTION KNOWLEDGE ENVIRONMENT

PERSPECTIVE: Interferon at 50—New Molecules, New Potential, New (and Old) Questions
J. A. Langer
Variant IFN-α proteins with novel activity profiles may translate into better therapeutics and provide mechanistic insights.

PERSPECTIVE: The Spark of Life—Electricity and Regeneration
J. M. W. Slack
A proton pump may play a critical role in *Xenopus* tadpole tail regeneration.

Big opportunities in nanotechnology.

SCIENCECAREERS

www.sciencecareers.org CAREER RESOURCES FOR SCIENTISTS

GLOBAL: Special Feature—Sizing Up Nano
J. Austin
"Nano" is a size, not a discipline or industry, but job prospects in nanotechnology are anything but small.

US: Starting Small
R. Service
There is plenty that budding scientists and engineers can do to improve their prospects for top-flight jobs in the nanotechnology industry.

GLOBAL: Skills Survey Highlights Varied Nanotech Needs
K. Travis
There is no single career path in nanotech, but there are some patterns and broad themes.

EUROPE: How Will Nanotech Fare in Europe?
A. Swarup
In Europe, the nanotech industry has garnered funding and policy-maker enthusiasm, but what about jobs?

SCIENCEPODCAST

Download the 21 September *Science* Podcast to hear about the history of water on Mars, unraveling the mysteries of Easter Island, new insights into dog genetics, and more.
www.sciencemag.org/about/podcast.dtl

CREDITS: (SCIENCE CAREERS) NATIONAL SCIENCE FOUNDATION; (SCIENCE NOW) EMMANOUIL FILIPPOU.

Separate individual or institutional subscriptions to these products may be required for full-text access.

EDITED BY STELLA HURTLEY AND PHIL SZUROMI

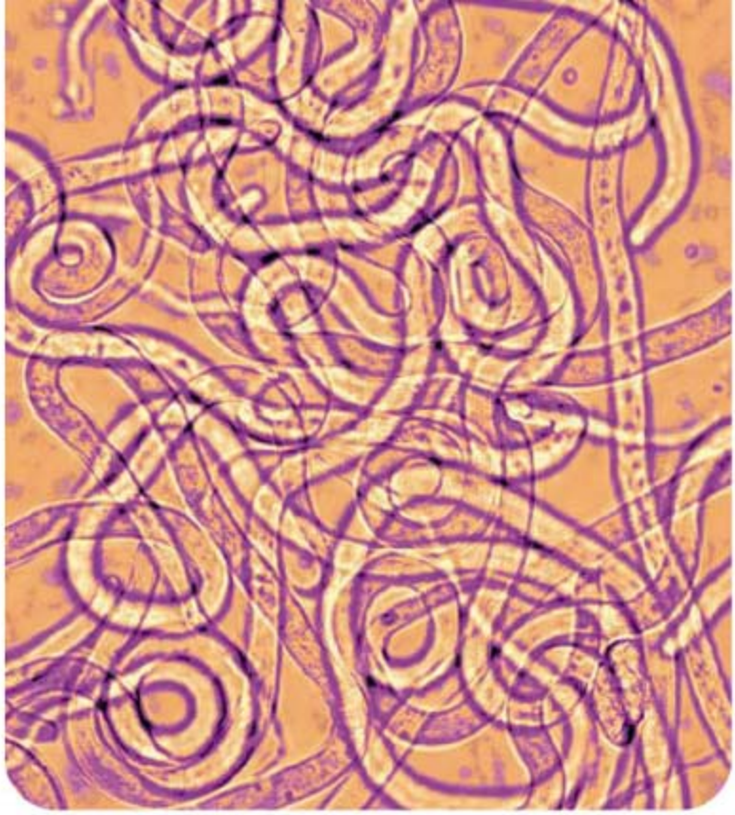

Completing a Life Cycle of Genomes

Filarial nematodes, which are important pathogens that infect large numbers of people in developing countries within the tropics, have complex life cycles involving one or more intermediate hosts. **Ghedin *et al.*** (p. 1756) now present the genome sequence of *Brugia malayi*. The free-living *Caenorhabditis elegans* nematode genome sequences allow comparisons with the sequence for the filarial worm and offer the potential to identify the genes involved in parasitism. The genomes for all of the hosts involved in this parasite's life cycle are now available—human, mosquito, *Wolbachia*, and the filarial worm itself, which opens the door to system-based studies of these relationships.

Fractional Quantum Hall Effect in 3D

In a two-dimensional (2D) electron gas, condensation can occur at particular magnetic fields to create a state that hosts remarkable liquidlike properties. Prior work has indicated this fractional quantum Hall effect arises from intrinsically many-body quantum ground states specific to 2D systems. **Behnia *et al.*** (p. 1729, published online 16 August; see the Perspective by **Huxley and Green**) report heat- and charge-transport measurements that suggest that a similar state might also be observed in bismuth crystals at very high magnetic fields, in part because this metal has such a small Fermi surface and electrons travel with very long mean-free paths. The authors found that electron correlations in bismuth are stronger than what has been commonly assumed, and that this elemental metal may host an exotic quantum Hall fluid.

From One Ring, Many

The Diels-Alder cyclization has proven widely useful in organic synthesis for introducing structural complexity in a single reaction step. Through formation of two carbon-carbon bonds, the reaction presents the opportunity to control the stereochemistry at four different centers simultaneously. **Balskus and Jacobsen** (p. 1736) show that a chiral oxazaborolidine derivative catalyzes an asymmetric Diels-Alder reaction across preformed organic macrocycles to create ring systems with high stereoselectivity in which three rings with five to eight members are linked by edge-sharing. The broad substrate scope spans a range of macrocycles bearing *E,E* dienes, and the authors applied this approach specifically to the synthesis of a sesquiterpene natural product.

Optical Nanocircuits

Increasing the clock speed of electronic circuits will begin to push the operating frequencies toward the optical regime and will require advances in addition to reducing the size of components. Challenges include the unacceptable losses in conventional microelectronics circuitry when operated at optical frequencies as well as a lack of basic circuit elements, such as resistors, capacitors, and inductors, when operating at such high frequencies. **Engheta** (p. 1698) overviews a proposed route which considers the optical response of subwavelength nanoparticles as the nanocircuit building blocks. By combining the ability to tune the optical response of metamaterials with the ability to join the building blocks together, it may be possible to create "lumped" optical circuitry akin to the circuit diagrams and structures in microelectronics.

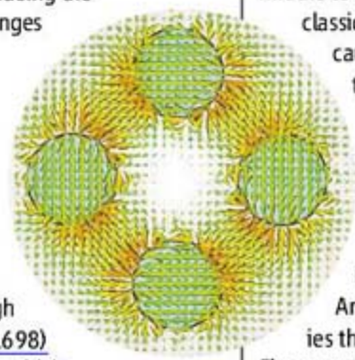

Deep Spin-Transition Region

The structure, composition, and dynamics of the Earth's lower mantle are affected by the quantum spin states of iron within minerals at high pressure and temperature. However, this behavior is not well established experimentally. **Lin *et al.*** (p. 1740) have determined the spin state of iron in ferropericlase at lower-mantle pressures and temperatures using an x-ray emission spectrometer with in situ synchrotron x-ray diffraction in the laser-heated diamond cell. A continuous change in spin properties occurs in a region spanning the middle to lower mantle (1300 to 2200 kilometers in depth). In the lowermost mantle, low-spin ferropericlase is stable. The spin transition in the middle to low mantle cannot be described by classical equations of state and may possibly cause steep velocity and density gradients there that may be detected seismically.

All in the Wrist?

The origins and affinity of the small-bodied hominins, *Homo floresiensis*, remain widely debated and enigmatic. Are these the fossils of a primitive species that somehow persisted in isolation on Flores until the Holocene, or pathologic modern humans, or something else? **Tocheri *et al.*** (p. 1743) show that the wrist bones of the original specimen are markedly primitive and completely unlike those of modern humans or of Neandertals.

Sperm Stem Cells

Little is known about the mammalian spermatogenic stem cell niche. **Yoshida *et al.*** (p. 1722; see the Perspective by **DiNardo and Braun**) used time-lapse imaging and three-dimensional reconstruction to reveal the localization of the

Continued on page 1647

CREDITS (TOP TO BOTTOM): GHEDIN ET AL.; ENGHETA

Continued from page 1645

candidate stem cells (undifferentiated spermatogonia) and found that these cells localize to the vasculature surrounding the seminiferous tubules in the mouse testis. Upon differentiation, the germ cells leave these regions to spread all through the seminiferous tubules.

Transporting Zinc

The divalent zinc cation is found in multiple guises in prokaryotic and eukaryotic cells. **Lu and Fu** (p. 1746, published online 23 August; see the Perspective by **Nies**) present the 3.8 angstrom structure of YiiP, a bacterial membrane protein that imports Zn^{2+} by exchanging it for H^+. The structure of YiiP is a Y-shaped homodimer, through which a presumptive pathway for Zn^{2+}/H^+ exchange can be discerned. YiiP is a member of the cation diffusion facilitator family of transport proteins. Another family member, ZnT-8, is expressed solely in pancreatic β cells and has recently been associated with risk for type 2 diabetes.

Technicolor Super-Resolution Imaging

The ability to visualize molecular interactions at 20- to 50-nanometer (nm) resolution requires multicolor super-resolution imaging and has remained challenging. **Bates *et al.*** (p. 1749, published online 16 August) report the implementation of multicolor stochastic optical reconstruction microscopy (STORM) using a family of photoswitchable activator-reporter pairs. Combinatorial pairing of three reporters and three activators allowed up to nine distinguishable fluorescent probes. Three-color imaging of a model DNA sample and two-color imaging of fixed cells was obtained at 20- to 30-nm resolution.

Taking a Peek at Platelet Production

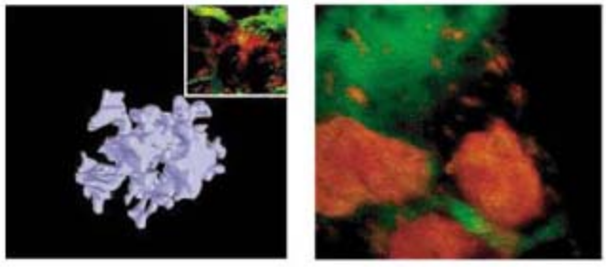

Current models of thrombopoiesis (platelet formation) have largely been derived from in vitro studies and static imaging approaches. **Junt *et al.*** (p. 1767; see the Perspective by **Geddis and Kaushansky**) use dynamic intravital imaging to reveal the behavior of active platelet-producing megakaryocytes within the bone marrow. Megakaryocytes remained in close contact with microvessels of the bone marrow, protruding long extensions into the blood stream. It appears that the shear force exerted by the bloodstream then plays an active role in the release of larger megakaryocyte protrusions that allows platelets and proplatelets to move into the peripheral circulation.

Crossing Kingdoms

Whole eukaryote genome sequencing projects routinely exclude bacterial sequences on the assumption that they represent contamination. However, **Dunning Hotopp *et al.*** (p. 1753, published online 30 August) found examples of genetic insertions from the bacterial endosymbiont *Wolbachia* into eukaryotic genomes in eleven species across six genera, three insect orders, and two different phyla. These inserts range from almost an entire *Wolbachia* genome to short 100–base pair inserts and are found as degenerate and transcribed genes. Thus, the movement of DNA between bacteria and eukaryotes may not be as rare as has been assumed.

Reconstituting MicroRNA Gene Regulation

MicroRNAs are small, ~21-nucleotide noncoding RNAs present in the genomes of almost all eukaryotes. They regulate gene expression in animals by repressing translation of target RNAs and also destabilizing them. The precise mechanism of repression has remained something of a mystery. **Mathonnet *et al.*** (p. 1764; published online 26 July) developed an in vitro messenger RNA (mRNA) translation system that recapitulates the ability of miRNAs to down-regulate gene expression. In this cell-free system, Let-7 miRNA acts to block the initial step of translation—recognition of the mRNA 5′ cap. Thus, degradation of mRNA is not critical for gene repression, at least at in the early stages of the process.

CREDIT: JUNT ET AL.

The Art of Global Discovery Chemistry

CHEMBRIDGE CORPORATION IS THE WORLD'S LARGEST GLOBAL DISCOVERY CHEMISTRY CRO AND PREMIER PROVIDER OF ADVANCED SCREENING LIBRARIES FOR SMALL MOLECULE DRUG DISCOVERY.
PLEASE VISIT WWW.CHEMBRIDGE.COM

CHEMBRIDGE™

Ian Lowe is an emeritus professor at Griffith University, Brisbane, Australia. He was previously the head of the university's School of Science.

A Critical Vote Down Under

AN ELECTION WILL BE HELD IN AUSTRALIA LATER THIS YEAR. THE CONSERVATIVE government of John Howard has been in power for 11 years—bad years for basic science. Although medical research has done well, overall public funding of science has declined from 0.77 to 0.59% of gross domestic product, placing Australia among the bottom countries of the Organization for Economic Cooperation and Development in science investment. Public policies have also caused a decline in commercial research and innovation. Whereas previous governments had encouraged private-sector R&D with a 150% tax concession, the first Howard budget cut that program, doubling the cost of research for profitable private companies. Commercial research spending fell dramatically and has only just returned to the 1996 level.

The Cooperative Research Centres program, set up nearly 20 years ago to solve Australia's failure to turn science into practical innovations, provided attractive funding for proposals bringing scientists together with various organizations, including corporations, industry groups, and public agencies dedicated to applications of basic research results. In the early funding rounds, there was a healthy balance between commercial ventures and those aimed at the public interest such as renewable energy, integrated pest management, tropical rainforests, and the coastal zone. Under the Howard government, every one of those public interest centers was eliminated, leaving the program totally oriented toward commercial outcomes.

Previous governments had specific projects to fund R&D in energy. In the 1980s, the Australian energy research council funded pioneering work that led to efficient solar cells, improved technology for solar thermal energy and wind power, the harnessing of coal seam methane, and efficiency improvements. The Howard government dismantled that effort, and as veteran science policy analyst Julian Cribb pointed out, the absence of a concerted program of R&D on energy alternatives has left Australia dangerously exposed to the volatility of world oil supply and unprepared for the carbon-constrained world of the future. Until very recently, senior government figures, including Finance Minister Nicholas Minchin and Industry Minister Ian Macfarlane, were still denying the science of climate change. Only last month, four government members of a parliamentary committee investigating carbon capture and storage wrote a dissenting note to the committee's report. The note included the full litany of climate change denial, quoting all the usual discredited suspects from Australia and the United States. Australia has joined the United States in failing to ratify the Kyoto Protocol. Energy-related greenhouse gas emissions, now more than 30% above the Kyoto baseline, are spiraling out of control in the absence of concerted policies.

The general decline in funding has intensified competition for grants. Last year, the science minister intervened after the normal peer-review process and invited a group of unqualified ideologues to vet the recommendations of the Australian Research Council. Four grants were vetoed by the group. A chapter in my recent book *Silencing Dissent*, documents several cases in which distinguished scientists have been sidelined. The main government science organization, the Commonwealth Scientific and Industrial Research Organisation (CSIRO), instructed scientists not to comment on issues with policy implications. The head of atmospheric research, Graeme Pearman, said that science pointed to the need for Australia to cut greenhouse gas emissions by at least 60%. This was seen by CSIRO managers as criticizing the government's refusal to set targets; Pearman was forced out of his job. Other scientists have since refused to comment on options for reducing emissions.

The Howard years have been gloomy for public interest research. The Labor Party, ahead in opinion polls, has promised to restore the funding and independence of science, but no specific commitments have been made. A Labor-held climate change summit in March convened scientists, policy-makers, and business leaders, and a promise was made to ratify Kyoto and set national targets (a 60% emissions reduction by 2050). That is a start. The scientific community will be watching with more interest than usual as we move into the election campaign.

– Ian Lowe

10.1126/science.1148839

CREDITS (TOP TO BOTTOM): DR. PATRICIA KELLY/GRIFFITH UNIVERSITY; MARK BAKER/REUTERS

Poison ivy (above) and poison oak (right).

IMMUNOLOGY

Managing Contact Dermititis

Mast cells are traditionally, and perhaps unfairly, associated with the unwanted face of immunity: namely allergies. Yet these cells perform a variety of vital front-line roles, from ejecting worms from the gut, to regulating T cell responses, to protecting us against the toxic effects of animal venoms. Grimbaldeston *et al.* extend this list of virtues to the attenuation of skin inflammation caused by toxins and ultraviolet (UV) radiation. Mice deficient in mast cells were found to develop a severe form of contact hypersensitivity—similar to the T cell–dependent contact dermatitis seen in humans—after exposure to the hapten dinitrofluorobenzene or to the allergenic plant compound urushiol. Replenishing the mast cell population in these animals with cells cultured from wild-type mice, but not from mice deficient in the immune regulatory cytokine IL-10, was sufficient to significantly reduce the degree of skin inflammation. The ability of mast cells to produce IL-10 depended on engagement of the immunoglobulin Fc γ receptor and corresponded with the suppression of inflammation achieved by administering antigen-specific immunoglobulin. Inflammation caused by UVB irradiation was also dampened by mast cell activities but in this case appeared generally independent of the ability to produce IL-10. These findings may open up new avenues for harnessing the anti-inflammatory power of mast cells to treat inflammatory skin disorders. — SJS

Nat. Immunol. **8**, 10.1038/ni1503 (2007).

CREDITS (TOP TO BOTTOM): (MAIN) SONKE JOHNSEN; (INSET) NPS.GOV; MEDNIKOV ET AL., *J. AM. CHEM. SOC.* **129**, 10.1021/JA073945Q (2007)

GEOCHEMISTRY

Charting Sorption Variations

The extraordinary diversity of organic matter in soil and aquatic environments has posed a considerable challenge to researchers seeking to predict the fate of specific molecular contaminants. As a starting point, the enormous array of functionalized hydrocarbons has traditionally been divided into three broad classes of material: humin, humic acids, and fulvic acids. Even within these categories, however, chemical and physical properties can vary from place to place. Niederer *et al.* have undertaken a systematic survey of the differing sorption properties of 10 distinct terrestrial and aquatic humic and fulvic acids. Using inverse gas chromatography, they measured the air/sorbent partition coefficients characteristic of these materials for ~100 small organic molecules of widely varying polarities. The coefficients varied by as much as a factor of 10, but somewhat surprisingly, the changes were manifested as constant shifts. This result implies that despite the chemical diversity of the samples, sorption is primarily a function of the abundance of available binding sites. The authors rationalize this finding by invoking the high degree of cross-linking tying up functional groups beneath the surface of the material. A series of parametrized linear free-energy relations derived from the data shows promise for predictive applications. — JSY

Environ. Sci. Technol. **41,** 10.1021/es0709932 (2007).

CHEMISTRY

Bigger with Platinum

Palladium is exceptional in its tendency to form large well-defined clusters capped with CO and phosphine ligands; clusters with up to 145 Pd atoms have been characterized. Mednikov *et al.* now report that platinum can get into the act if the synthesis starts with a smaller Pd cluster, $Pd_{10}(CO)_{12}(PPh_3)_6$ (where PPh_3 is triphenylphosphine), which reacts with added $Pt(CO)_2(PPh_3)_2$ to yield a 165-atom Pt-Pd cluster, nominally $Pd_{157}Pt_8(CO)_{72}(PPh_3)_{20}$. The crystallographic occupancy analysis was augmented by wide-angle dispersive spectroscopy to establish the Pt stoichiometry. The structure can be described as four concentric shells. At the center is a Pt atom, surrounded by a 12-atom Pd icosahedron, and the second shell is a 42-atom icosahedron with either 3 or 4 Pt atoms; the third and fourth shells are high-symmetry structures with 60 and 50 atoms, respectively. This cluster is unusual in that its outermost shell has fewer atoms than the underlying shell, and CO ligands bridge inter-shell metal atoms. — PDS

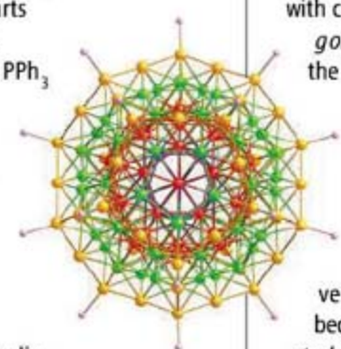

J. Am. Chem. Soc. **129**, 10.1021/ja073945q (2007).

GENETICS

Sweeping Through Toxoplasma

Though particularly notorious for its association with cats, the protozoan parasite *Toxoplasma gondii* is ubiquitous among vertebrates, to the extent that a quarter of the human population is infected. Unusually, it propagates both sexually and asexually, but tends to have a clonal population structure with three geographically distinct lineages. Unexpectedly, all lineages share a nearly monomorphic version of one chromosome, which has become fixed in natural populations. Khan *et al.* have traced the population structure of *T. gondii* by sequencing introns and find that South American strains show variation not seen in other lineages. The date of this divergence correlates with the reappearance of the Pana-

Continued on page 1653

Continued from page 1651

manian land bridge roughly 1 million years ago and the southerly migration and diversification of the Felidae. The lineages appear to have evolved in two phases, first by the generation of northern and southern haplogroups emerging by rare recombination events, and second by a global sweep spreading the monomorphic chromosome into the South American haplogroups. The selective advantage of the monomorphic chromosome has yet to be revealed, although it is probably involved in virulence and transmission. — CA

Proc. Natl. Acad. Sci. U.S.A. **104**, 14872 (2007).

GEOLOGY

Carved from the Surface

Hawaii is sometimes referred to as Earth's greatest mountain because its height above the seafloor exceeds the height of Mt. Everest above the plains of India. Recent work has identified several huge submarine slides extending off of several of the Hawaiian islands, and the large-scale topography of these islands, including underwater features, in

Kohala, Hawaii.

part reflects the feedback between growth of the islands by volcanism and this mass wasting. Lamb *et al.* argue that these slides may trigger some of the more dramatic smaller topographic features found in some of the wetter parts of the islands, specifically, amphitheaters containing a series of large waterfalls. They show that waterfalls can drill into the Hawaiian basalt at a rate sufficient to cut these amphitheaters from a cliff produced by a slump in a few hundred thousand years. An alternative model has been that erosion from groundwater seepage or springs produced these features, and that this process may have produced similar features on Mars, but the rates of spring flow and other features seem insufficient to have produced the observed features on Hawaii. — BH

Geol. Soc. Am. Bull. **119**, 805 (2007).

CHEMISTRY

Blocks on the Move

Living polymerization is a double-edged sword. On the one hand, this class of techniques—all of which feature a tight association between catalyst and growing chain that inhibits termination—affords exquisite control over the molecular structure of the polymer and the uniformity of the bulk product distribution. On the other hand, such control comes at the expense of cost and throughput efficiency, as each chain requires its own appended catalyst and monomers must be added in batches. Hustad *et al.* present an alternative approach to the preparation of diblock copolymers, in which, rather than adding consecutive batches of different monomers to a living system, they set up successive continuous reactors and limit polydispersity by using a chain shuttling agent. Rapid chain transfers between a hafnium catalyst and zinc shuttling agent allow each catalyst molecule to extend >300 chains while keeping the chain lengths roughly uniform across the sample. By feeding pure ethylene into the first reactor and adding a longer α-olefin to the second, the authors achieve a product distribution with two distinct segments (high- and very-low-density polyethylene) in each chain and a polydispersity of only 1.67. — JSY

Macromolecules **40**, 10.1021/ma0717791 (2007).

Science STKE AAAS

www.stke.org

<< Helping Plants Survive Heat

Plants rely on microorganisms in the local environment for various important processes, one of which is nitrogen fixation by symbiotic bacteria that colonize the roots of some plants. McLellan *et al.* provide evidence that fungi in the rhizosphere (the soil surrounding the plant roots) may also contribute to heat tolerance. Previously, two inhibitors of mammalian heat shock protein 90 (Hsp90) were discovered in extracts from Sonoran desert plant–associated fungi. McLellan *et al.* follow up this result by showing that monocillin I specifically binds and inhibits the chaperone activity of *Arabidopsis* Hsp90 in vitro. Exposure of *Arabidopsis* seedlings to monicillin increased the expression and abundance of the heat shock response protein AtHsp101. Pretreatment of seedlings with monicillin before what would be a lethal heat stress for untreated plants increased survival, and this protective effect required Hsp101. When *Arabidopsis* seedlings were cultured with the fungus that produces monicillin, hypocotyl elongation decreased; however, the plants tolerated heat stress much better in the presence of the fungus. — NRG

Plant Physiol. **145**, 174 (2007).

CREDIT: USGS

www.sciencemag.org

Science

1200 New York Avenue, NW
Washington, DC 20005
Editorial: 202-326-6550, FAX 202-289-7562
News: 202-326-6581, FAX 202-371-9227

Bateman House, 82-88 Hills Road
Cambridge, UK CB2 1LQ
+44 (0) 1223 326500, FAX +44 (0) 1223 326501

SUBSCRIPTION SERVICES For change of address, missing issues, new orders and renewals, and payment questions: 866-434-AAAS (2227) or 202-326-6417, FAX 202-842-1065. Mailing addresses: AAAS, P.O. Box 96178, Washington, DC 20090-6178 or AAAS Member Services, 1200 New York Avenue, NW, Washington, DC 20005

INSTITUTIONAL SITE LICENSES please call 202-326-6755 for any questions or information

REPRINTS: Author Inquiries 800-635-7181
Commercial Inquiries 803-359-4578

PERMISSIONS 202-326-7074, FAX 202-682-0816

MEMBER BENEFITS Bookstore: AAAS/BarnesandNoble.com bookstore www.aaas.org/bn; Car purchase discount: Subaru VIP Program 202-326-6417; Credit Card: MBNA 800-847-7378; Car Rentals: Hertz 800-654-2200 CDP#343457, Dollar 800-800-4000 #AA1115; AAAS Travels: Betchart Expeditions 800-252-4910; Life Insurance: Seabury & Smith 800-424-9883; Other Benefits: AAAS Member Services 202-326-6417 or www.aaasmember.org.

science_editors@aaas.org	(for general editorial queries)
science_letters@aaas.org	(for queries about letters)
science_reviews@aaas.org	(for returning manuscript reviews)
science_bookrevs@aaas.org	(for book review queries)

Published by the American Association for the Advancement of Science (AAAS), *Science* serves its readers as a forum for the presentation and discussion of important issues related to the advancement of science, including the presentation of minority or conflicting points of view, rather than by publishing only material on which a consensus has been reached. Accordingly, all articles published in *Science*—including editorials, news and comment, and book reviews—are signed and reflect the individual views of the authors and not official points of view adopted by the AAAS or the institutions with which the authors are affiliated.

AAAS was founded in 1848 and incorporated in 1874. Its mission is to advance science and innovation throughout the world for the benefit of all people. The goals of the association are to: foster communication among scientists, engineers and the public; enhance international cooperation in science and its applications; promote the responsible conduct and use of science and technology; foster education in science and technology for everyone; enhance the science and technology workforce and infrastructure; increase public understanding and appreciation of science and technology; and strengthen support for the science and technology enterprise.

INFORMATION FOR AUTHORS

See pages 120 and 121 of the 5 January 2007 issue or access www.sciencemag.org/feature/contribinfo/home.shtml

EDITOR-IN-CHIEF **Donald Kennedy**
EXECUTIVE EDITOR **Monica M. Bradford**
DEPUTY EDITORS **R. Brooks Hanson, Barbara R. Jasny, Katrina L. Kelner**
NEWS EDITOR **Colin Norman**

EDITORIAL SUPERVISORY SENIOR EDITOR Phillip D. Szuromi; **SENIOR EDITOR/PERSPECTIVES** Lisa D. Chong; **SENIOR EDITORS** Gilbert J. Chin, Pamela J. Hines, Paula A. Kiberstis (Boston), Marc S. Lavine (Toronto), Beverly A. Purnell, L. Bryan Ray, Guy Riddihough, H. Jesse Smith, Valda Vinson, David Voss; **ASSOCIATE EDITORS** Jake S. Yeston, Laura M. Zahn; **ONLINE EDITOR** Stewart Wills; **ASSOCIATE ONLINE EDITORS** Robert Frederick, Tara S. Marathe; **BOOK REVIEW EDITOR** Sherman J. Suter; **ASSOCIATE LETTERS EDITOR** Etta Kavanagh; **EDITORIAL MANAGER** Cara Tate; **SENIOR COPY EDITORS** Jeffrey E. Cook, Cynthia Howe, Harry Jach, Barbara P. Ordway, Jennifer Sills, Trista Wagoner; **COPY EDITORS** Lauren Kmec, Peter Mooreside; **EDITORIAL COORDINATORS** Carolyn Kyle, Beverly Shields; **PUBLICATIONS ASSISTANTS** Ramatoulaye Diop, Chris Filiatreau, Joi S. Granger, Jeffrey Hearn, Lisa Johnson, Scott Miller, Jerry Richardson, Brian White, Anita Wynn; **EDITORIAL ASSISTANTS** Emily Guise, Patricia M. Moore, Jennifer A. Seibert; **EXECUTIVE ASSISTANT** Sylvia S. Kihara; **ADMINISTRATIVE SUPPORT** Maryrose Madrid

NEWS SENIOR CORRESPONDENT Jean Marx; **DEPUTY NEWS EDITORS** Robert Coontz, Eliot Marshall, Jeffrey Mervis, Leslie Roberts; **CONTRIBUTING EDITORS** Elizabeth Culotta, Polly Shulman; **NEWS WRITERS** Yudhijit Bhattacharjee, Adrian Cho, Jennifer Couzin, David Grimm, Constance Holden, Jocelyn Kaiser, Richard A. Kerr, Eli Kintisch, Andrew Lawler (New England), Greg Miller, Elizabeth Pennisi, Robert F. Service (Pacific NW), Erik Stokstad; **INTERNS** Benjamin Lester, Marissa Cevallos, Veronica Raymond; **CONTRIBUTING CORRESPONDENTS** Barry A. Cipra, Jon Cohen (San Diego, CA), Daniel Ferber, Ann Gibbons, Robert Irion, Mitch Leslie, Charles C. Mann, Evelyn Strauss, Gary Taubes; **COPY EDITORS** Rachel Curran, Linda B. Felaco, Melvin Gatling; **ADMINISTRATIVE SUPPORT** Scherraine Mack, Fannie Groom; **BUREAUS** New England: 207-549-7755, San Diego, CA: 760-942-3252, FAX 760-942-4979, Pacific Northwest: 503-963-1940

PRODUCTION DIRECTOR James Landry; **SENIOR MANAGER** Wendy K. Shank; **ASSISTANT MANAGER** Rebecca Doshi; **SENIOR SPECIALISTS** Jay Covert, Chris Redwood; **SPECIALIST** Steve Forrester; **PREFLIGHT DIRECTOR** David M. Tompkins; **MANAGER** Marcus Spiegler; **SPECIALIST** Jessie Mudjitaba

ART DIRECTOR Kelly Buckheit Krause; **ASSOCIATE ART DIRECTOR** Aaron Morales; **ILLUSTRATORS** Chris Bickel, Katharine Sutliff; **SENIOR ART ASSOCIATES** Holly Bishop, Laura Creveling, Preston Huey, Nayomi Kevitiyagala; **ASSOCIATE** Jessica Newfield; **PHOTO EDITOR** Leslie Blizard

***SCIENCE* INTERNATIONAL**

EUROPE (science@science-int.co.uk) **EDITORIAL: INTERNATIONAL MANAGING EDITOR** Andrew M. Sugden; **SENIOR EDITOR/PERSPECTIVES** Julia Fahrenkamp-Uppenbrink; **SENIOR EDITORS** Caroline Ash, Stella M. Hurtley, Ian S. Osborne, Stephen J. Simpson, Peter Stern; **ASSOCIATE EDITOR** Joanne Baker; **EDITORIAL SUPPORT** Deborah Dennison, Rachel Roberts, Alice Whaley; **ADMINISTRATIVE SUPPORT** Janet Clements, Jill White; **NEWS: EUROPE NEWS EDITOR** John Travis; **DEPUTY NEWS EDITOR** Daniel Clery; **CONTRIBUTING CORRESPONDENTS** Michael Balter (Paris), John Bohannon (Vienna), Martin Enserink (Amsterdam and Paris), Gretchen Vogel (Berlin)

ASIA Japan Office: Asca Corporation, Eiko Ishioka, Fusako Tamura, 1-8-13, Hirano-cho, Chuo-ku, Osaka-shi, Osaka, 541-0046 Japan; +81 (0) 6 6202 6272, FAX +81 (0) 6 6202 6271; asca@os.gulf.or.jp; **ASIA NEWS EDITOR** Richard Stone +66 2 662 5818 (rstone@aaas.org); **CONTRIBUTING CORRESPONDENTS** Dennis Normile (Japan: +81 (0) 3 3391 0630, FAX 81 (0) 3 5936 3531; dnormile@goL.com); Hao Xin (China: + 86 (0) 10 6307 4439 or 6307 3676, FAX +86 (0) 10 6307 4358; cindyhao@gmail.com); Pallava Bagla (South Asia: +91 (0) 11 2271 2896; pbagla@vsnl.com)

AFRICA Robert Koenig (contributing correspondent, rob.koenig@gmail.com)

EXECUTIVE PUBLISHER **Alan I. Leshner**
PUBLISHER **Beth Rosner**

FULFILLMENT SYSTEMS AND OPERATIONS (membership@aaas.org) **DIRECTOR** Waylon Butler; **CUSTOMER SERVICE SUPERVISOR** Pat Butler; **SPECIALISTS** Laurie Baker, Latoya Casteel, Lavanda Crawford, Vicki Linton; **DATA ENTRY SUPERVISOR** Cynthia Johnson; **SPECIALISTS** Tomeka Diggs, Tarrika Hill, Erin Layne, Sheila Thomas; **SYSTEMS ANALYST** Tim Popoola

BUSINESS OPERATIONS AND ADMINISTRATION DIRECTOR Deborah Rivera-Wienhold; **ASSISTANT DIRECTOR, BUSINESS OPERATIONS** Randy Yi; **SENIOR FINANCIAL ANALYSTS** Michael LoBue, Jessica Tierney; **FINANCIAL ANALYSTS** Nicole Nicholson, Farida Yeasmin; **RIGHTS AND PERMISSIONS: ADMINISTRATOR** Emilie David; **ASSOCIATE** Elizabeth Sandler; **MARKETING DIRECTOR** John Meyers; **MARKETING MANAGERS** Darryl Walter, Allison Pritchard; **MARKETING ASSOCIATES** Julianne Wielga, Mary Ellen Crowley, Alison Chandler, Marcia Leach, Wendy Wise; **INTERNATIONAL MARKETING MANAGER** Wendy Sturley; **MARKETING EXECUTIVE** Jennifer Reeves; **MARKETING/MEMBER SERVICES EXECUTIVE** Linda Rusk; **JAPAN SALES** Jason Hannaford; **SITE LICENSE SALES DIRECTOR** Tom Ryan; **SALES MANAGER** Russ Edra; **SALES AND CUSTOMER SERVICE** Mehan Dossani, Iquo Edim, Kiki Forsythe, Catherine Holland, Phillip Smith; **ELECTRONIC MEDIA: MANAGER** Lizabeth Harman; **PROJECT MANAGER** Trista Snyder; **ASSISTANT MANAGER** Lisa Stanford; **SENIOR PRODUCTION SPECIALIST** Walter Jones; **PRODUCTION SPECIALISTS** Nichele Johnston, Kimberly Oster

ADVERTISING DIRECTOR WORLDWIDE AD SALES Bill Moran

PRODUCT (science_advertising@aaas.org); **CONSUMER & SPONSORSHIP SALES MANAGER** Tina Morra: 202-326-6542; **MIDWEST** Rick Bongiovanni: 330-405-7080, FAX 330-405-7081; **WEST COAST/W. CANADA** Teola Young: 650-964-2266; **EAST COAST/E. CANADA** Christopher Breslin: 443-512-0330, FAX 443-512-0331; **UK/EUROPE/ASIA** Michelle Field: +44 (0) 1223-326-524, FAX +44 (0) 1223-325-532; **JAPAN** Mashy Yoshikawa: +81 (0) 33235 5961, FAX +81 (0) 33235 5852; **SENIOR TRAFFIC ASSOCIATE** Deiandra Simms

COMMERCIAL EDITOR Sean Sanders: 202-326-6430

CLASSIFIED (advertise@sciencecareers.org); **U.S.: RECRUITMENT SALES MANAGER** Ian King: 202-326-6528, FAX 202-289-6742; **INSIDE SALES MANAGER: MIDWEST/CANADA** Daryl Anderson: 202-326-6543; **NORTHEAST** Alexis Fleming: 202-326-6578; **NORTHEAST** Allison Millar: 202-326-6572; **SOUTHEAST** Tina Burks: 202-326-6577; **WEST** Nicholas Hintibidze: 202-326-6533; **SALES COORDINATORS** Erika Foard, Rohan Edmonson, Leonard Marshall, Shirley Young; **INTERNATIONAL: SALES MANAGER** Tracy Holmes: +44 (0) 1223 326525, FAX +44 (0) 1223 326532; **SALES** Marium Hudda, Alex Palmer, Alessandra Sorgente; **SALES ASSISTANT** Louise Moore; **JAPAN** Jason Hannaford: +81 (0) 52 757 5360, FAX +81 (0) 52 757 5361; **ADVERTISING PRODUCTION OPERATIONS MANAGER** Deborah Tompkins; **SENIOR PRODUCTION SPECIALISTS** Robert Buck, Amy Hardcastle; **SENIOR TRAFFIC ASSOCIATE** Christine Hall; **PUBLICATIONS ASSISTANT** Mary Lagnaoui

AAAS BOARD OF DIRECTORS RETIRING PRESIDENT, CHAIR John P. Holdren; **PRESIDENT** David Baltimore; **PRESIDENT-ELECT** James J. McCarthy; **TREASURER** David E. Shaw; **CHIEF EXECUTIVE OFFICER** Alan I. Leshner; **BOARD** John E. Dowling, Lynn W. Enquist, Susan M. Fitzpatrick, Alice Gast, Linda P. B. Katehi, Cherry A. Murray, Thomas D. Pollard, Kathryn D. Sullivan

AAAS
ADVANCING SCIENCE, SERVING SOCIETY

SENIOR EDITORIAL BOARD

John I. Brauman, *Chair, Stanford Univ.*
Richard Losick, *Harvard Univ.*
Robert May, *Univ. of Oxford*
Marcia McNutt, *Monterey Bay Aquarium Research Inst.*
Linda Partridge, *Univ. College London*
Vera C. Rubin, *Carnegie Institution*
Christopher R. Somerville, *Carnegie Institution*
George M. Whitesides, *Harvard Univ.*

BOARD OF REVIEWING EDITORS

Joanna Aizenberg, *Harvard Univ.*
R. McNeill Alexander, *Leeds Univ.*
David Altshuler, *Broad Institute*
Arturo Alvarez-Buylla, *Univ. of California, San Francisco*
Richard Amasino, *Univ. of Wisconsin, Madison*
Meinrat O. Andreae, *Max Planck Inst., Mainz*
Kristi S. Anseth, *Univ. of Colorado*
John A. Bargh, *Yale Univ.*
Cornelia I. Bargmann, *Rockefeller Univ.*
Marisa Bartolomei, *Univ. of Penn. School of Med.*
Brenda Bass, *Univ. of Utah*
Ray H. Baughman, *Univ. of Texas, Dallas*
Stephen J. Benkovic, *Pennsylvania St. Univ.*
Michael J. Bevan, *Univ. of Washington*
Ton Bisseling, *Wageningen Univ.*
Mina Bissell, *Lawrence Berkeley National Lab*
Peer Bork, *EMBL*
Dianna Bowles, *Univ. of York*
Robert W. Boyd, *Univ. of Rochester*
Paul M. Brakefield, *Leiden Univ.*
Dennis Bray, *Univ. of Cambridge*
Stephen Buratowski, *Harvard Medical School*
Jillian M. Buriak, *Univ. of Alberta*
Joseph A. Burns, *Cornell Univ.*
William P. Butz, *Population Reference Bureau*
Peter Carmeliet, *Univ. of Leuven, VIB*
Gerbrand Ceder, *MIT*
Mildred Cho, *Stanford Univ.*
David Clapham, *Children's Hospital, Boston*
David Clary, *Oxford University*
J. M. Claverie, *CNRS, Marseille*
Jonathan D. Cohen, *Princeton Univ.*
Stephen M. Cohen, *EMBL*
Robert H. Crabtree, *Yale Univ.*
E. Fleming Crim, *Univ. of Wisconsin*
William Cumberland, *UCLA*
George Q. Daley, *Children's Hospital, Boston*
Edward DeLong, *MIT*
Emmanouil T. Dermitzakis, *Wellcome Trust Sanger Inst.*
Robert Desimone, *MIT*
Dennis Discher, *Univ. of Pennsylvania*
Scott C. Doney, *Woods Hole Oceanographic Inst.*
W. Ford Doolittle, *Dalhousie Univ.*
Jennifer A. Doudna, *Univ. of California, Berkeley*
Julian Downward, *Cancer Research UK*
Denis Duboule, *Univ. of Geneva/EPFL Lausanne*
Christopher Dye, *WHO*
Richard Ellis, *CalTech*
Gerhard Ertl, *Fritz-Haber-Institut, Berlin*
Douglas H. Erwin, *Smithsonian Institution*
Mark Estelle, *Indiana Univ.*
Barry Everitt, *Univ. of Cambridge*
Paul G. Falkowski, *Rutgers Univ.*
Ernst Fehr, *Univ. of Zurich*
Tom Fenchel, *Univ. of Copenhagen*
Alain Fischer, *INSERM*
Jeffrey S. Flier, *Harvard Medical School*
Scott E. Fraser, *CalTech*
Chris D. Frith, *Univ. College London*
John Gearhart, *Johns Hopkins Univ.*
Wulfram Gerstner, *EPFL Lausanne*
Charles Godfray, *Univ. of Oxford*
Christian Haass, *Ludwig Maximilians Univ.*
Dennis L. Hartmann, *Univ. of Washington*
Chris Hawkesworth, *Univ. of Bristol*
Martin Heimann, *Max Planck Inst., Jena*
James A. Hendler, *Rensselaer Polytechnic Inst.*
Ray Hilborn, *Univ. of Washington*
Ove Hoegh-Guldberg, *Univ. of Queensland*
Ary A. Hoffmann, *La Trobe Univ.*
Ronald R. Hoy, *Cornell Univ.*
Evelyn L. Hu, *Univ. of California, Santa Barbara*
Olli Ikkala, *Helsinki Univ. of Technology*
Meyer B. Jackson, *Univ. of Wisconsin Med. School*
Stephen Jackson, *Univ. of Cambridge*
Steven Jacobsen, *Univ. of California, Los Angeles*
Peter Jonas, *Universität Freiburg*
Daniel Kahne, *Harvard Univ.*
Bernhard Keimer, *Max Planck Inst., Stuttgart*
Elizabeth A. Kellog, *Univ. of Missouri, St. Louis*
Alan B. Krueger, *Princeton Univ.*
Lee Kump, *Penn State*
Mitchell A. Lazar, *Univ. of Pennsylvania*
Virginia Lee, *Univ. of Pennsylvania*
Anthony J. Leggett, *Univ. of Illinois, Urbana-Champaign*
Michael J. Lenardo, *NIAID, NIH*
Norman L. Letvin, *Beth Israel Deaconess Medical Center*
Olle Lindvall, *Univ. Hospital, Lund*
John Lis, *Cornell Univ.*
Richard Losick, *Harvard Univ.*
Ke Lu, *Chinese Acad. of Sciences*
Andrew P. MacKenzie, *Univ. of St. Andrews*
Raul Madariaga, *École Normale Supérieure, Paris*
Anne Magurran, *Univ. of St. Andrews*
Michael Malim, *King's College, London*
Virginia Miller, *Washington Univ.*
Yasushi Miyashita, *Univ. of Tokyo*
Richard Morris, *Univ. of Edinburgh*
Edvard Moser, *Norwegian Univ. of Science and Technology*
Naoto Nagaosa, *Univ. of Tokyo*
James Nelson, *Stanford Univ. School of Med.*
Roeland Nolte, *Univ. of Nijmegen*
Helga Nowotny, *European Research Advisory Board*
Eric N. Olson, *Univ. of Texas, SW*
Erin O'Shea, *Harvard Univ.*
Elinor Ostrom, *Indiana Univ.*
Jonathan T. Overpeck, *Univ. of Arizona*
John Pendry, *Imperial College*
Philippe Poulin, *CNRS*
Mary Power, *Univ. of California, Berkeley*
Molly Przeworski, *Univ. of Chicago*
David J. Read, *Univ. of Sheffield*
Les Real, *Emory Univ.*
Colin Renfrew, *Univ. of Cambridge*
Trevor Robbins, *Univ. of Cambridge*
Barbara A. Romanowicz, *Univ. of California, Berkeley*
Nancy Ross, *Virginia Tech*
Edward M. Rubin, *Lawrence Berkeley National Lab*
J. Roy Sambles, *Univ. of Exeter*
Jürgen Sandkühler, *Medical Univ. of Vienna*
David S. Schimel, *National Center for Atmospheric Research*
Georg Schulz, *Albert-Ludwigs-Universität*
Paul Schulze-Lefert, *Max Planck Inst., Cologne*
Terrence J. Sejnowski, *The Salk Institute*
David Sibley, *Washington Univ.*
Montgomery Slatkin, *Univ. of California, Berkeley*
George Somero, *Stanford Univ.*
Joan Steitz, *Yale Univ.*
Elsbeth Stem, *ETH Zürich*
Thomas Stocker, *Univ. of Bern*
Jerome Strauss, *Virginia Commonwealth Univ.*
Marc Tatar, *Brown Univ.*
Glenn Telling, *Univ. of Kentucky*
Marc Tessier-Lavigne, *Genentech*
Michiel van der Klis, *Astronomical Inst. of Amsterdam*
Derek van der Kooy, *Univ. of Toronto*
Bert Vogelstein, *Johns Hopkins*
Christopher A. Walsh, *Harvard Medical School*
Graham Warren, *Yale Univ. School of Med.*
Colin Watts, *Univ. of Dundee*
Julia R. Weertman, *Northwestern Univ.*
Detlef Weigel, *Max Planck Inst., Tübingen*
Jonathan Weissman, *Univ. of California, San Francisco*
Ellen D. Williams, *Univ. of Maryland*
R. Sanders Williams, *Duke University*
Ian A. Wilson, *The Scripps Res. Inst.*
Jerry Workman, *Stowers Inst. for Medical Research*
John R. Yates III, *The Scripps Res. Inst.*
Martin Zatz, *NIMH, NIH*
Huda Zoghbi, *Baylor College of Medicine*
Maria Zuber, *MIT*

BOOK REVIEW BOARD

John Aldrich, *Duke Univ.*
David Bloom, *Harvard Univ.*
Angela Creager, *Princeton Univ.*
Richard Shweder, *Univ. of Chicago*
Ed Wasserman, *DuPont*
Lewis Wolpert, *Univ. College, London*

NET WATCH

Taking Back Archaeology

Cranks continually shanghai archaeological discoveries to support nutty arguments about lost civilizations and visits from ancient astronauts. Now, two self-described angry archaeologists in Britain want to set the record straight.

Bad Archaeology debunks a range of pseudoscience, including claims that a 1513 Ottoman map (above) accurately depicts Antarctica. Touted as evidence that ancient mariners—or even aliens—surveyed the continent long ago, the map actually reflects belief in an as-yet-undiscovered southern landmass with little resemblance to Antarctica. The site also reveals the pseudoscientists' habit of plucking puzzling artifacts out of context to undermine orthodox interpretations. An example: the "batteries of Babylon," 2000-year-old Iraqi jars that some authors assert were used to generate current even though no electrical devices existed. >> www.badarchaeology.net

"Sharp" Numbers Better For Sellers

According to a new study conducted at Cornell University, the digits in the price of a house can subliminally manipulate how much you're willing to pay for it.

In housing data from Long Island and south Florida, consumer behavior researcher Manoj Thomas and colleagues found that the number of zeroes in a house's list price affected the sale price, with each zero reducing the final price by about a third of a percent. Thus, a house listed for $484,700 will sell for about $1300 more than a house listed for $485,000. "This is arguably the most important purchase we make," Thomas says. "So this is not an error of neglect, it's the way our brains work."

The researchers hypothesize that everyday experience teaches us that round (imprecise) numbers are usually larger than nonround (sharp) numbers. Buyers perceive the more precise price as being lower already—and firmer—and do not try to undercut it by as much. If the phenomenon holds up, says Priya Raghubir, a consumer behavior expert at the University of California, Berkeley, it could be useful in other settings. For example, a speed limit of 24 or 26 could cause drivers to slow down more than a speed limit of 25.

Let England Be England

For more than a decade, British shopkeepers have had to display both metric and imperial measurements in preparation for a full conversion to metric. But many traditionalists have fought the trend—such as the Metric Martyrs, inspired by a grocer who in 2001 was convicted of selling bananas by the pound.

Now, after getting extensive feedback from both industry and the public, the European Commission has backed off plans to eradicate imperial measurements by 31 December 2009. Instead, it will allow the United Kingdom to keep its pounds, feet, miles, and pints for domestic use. Exports have to be metric.

E.U. Commission Vice President Günter Verheugen said the decision "honors the culture and tradition of Great Britain," adding that he hoped this sign of E.U. flexibility would help the United States see the virtue of accepting "metric-only labeled" imports. The U.K. and the U.S. stand alone among major nations in refusing to capitulate to metrication.

Chess for Drudges?

Good chess players are really smart, right? Only up to a point, according to a study that concludes practice is more important than brains.

Merim Bilalić, a psychology doctoral student at Oxford University in the U.K., studied 57 primary and secondary school chess players, giving them chess problems and IQ tests and logging their daily chess practice.

Although years of experience and IQ correlated with chess skills, the researchers found that the highest correlation was with the number of hours a day the children spent playing or studying the game. And among the top 23 players (all boys), the correlation of chess skill with IQ disappeared. Within this high-IQ group (average 133, versus 114 for the other 34 players), it wasn't the brightest but those who practiced the most who did best, the researchers report in the September issue of *Intelligence*. The smartest ones actually practiced less.

Chess has long pitted proponents of "expertise" theory, which emphasizes the cultivation of specific skills, against those who argue that talent is important. Psychologist Neil Charness of Florida State University in Tallahassee says that the study bears out "the drudge theory of expertise. Once you're about average IQ, the most important predictor is deliberate practice." But Robert Howard of the University of New South Wales in Sydney, Australia, points out that chess prodigies "rapidly outpace the average grandmaster" despite much less practice time.

CREDITS (TOP TO BOTTOM): WIKIPEDIA; DYLAN MARTINEZ/REUTERS; GETTY IMAGES

EDITED BY YUDHIJIT BHATTACHARJEE

Celebrities

RISING. A lightweight amateur boxer with a background in computer vision and artificial-intelligence research will be South Korea's first astronaut, officials announced this month. Ko San will board a Russian Soyuz spacecraft next April to travel to the international space station.

A graduate of Seoul National University with degrees in mathematics and cognitive science, the 30-year-old Ko was working at the Samsung Advanced Institute of Technology in Yongin before he was selected for astronaut training from more than 36,000 applicants. South Korean officials hope his participation will boost public interest in South Korea's nascent space program. In addition to building a $265 million space center, the country is readying its first homegrown rocket for launch next year after having built 11 satellites launched by other countries.

Ko reportedly wants to be known as a space scientist rather than as an astronaut. During his week on the space station, he hopes to conduct 18 experiments that include how microgravity affects the fermentation of kimchi, South Korea's national dish.

AWARDS

BALZAN WINNERS. Two immunologists and a nanoscientist are among the winners of this year's Balzan Prizes, set up in 1956 in memory of Eugenio Balzan, a former editor and co-owner of Italy's *Corriere della Sera* newspaper.

Sumio Iijima of Meijo University in Nagoya, Japan, will receive the $830,000 award (half of which has to be spent on research) for his discovery of single-walled carbon nanotubes. Bruce Beutler of The Scripps Research Institute in San Diego, California, and Jules Hoffmann of the French national research agency in Strasbourg—also the current president of the French Academy of Sciences in Paris—will share the same sum for their work on innate immunity.

The winners will join awardees in international law, literature, and peace at a 23 November ceremony in Berne, Switzerland.

MEDICAL MESSIAHS. An immunologist who discovered key cells of the immune system known as dendritic cells and two cardiac surgeons who developed implantable heart valves have won this year's research awards from the Lasker Foundation.

The winner of the basic research award is Ralph Steinman, 64, of Rockefeller University in New York City, for his work with dendritic cells, which he says at first glance reminded him of "a swimmer treading water." Steinman found that dendritic cells spurred T cells to attack invading pathogens.

Alain Carpentier (right), 74, of the European Hospital Georges Pompidou in Paris and Albert Starr (left), 81, of the Providence Health System in Portland, Oregon, share the clinical research award. Starr developed a mechanical heart valve that was first successfully implanted in 1960. Carpentier took the technology a step further by using pig valves after encountering a patient with a mechanical valve who'd been paralyzed by a blood clot. The man, he remembers, had been an artist but could no longer wield a paintbrush. Carpentier was inspired "to devote my professional life" to finding valves that wouldn't pose a clotting risk. Heart valves today help save 300,000 people a year.

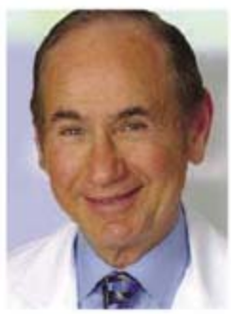

The Lasker Foundation also honored Anthony Fauci, 66, director of the National Institute of Allergy and Infectious Diseases, for building up U.S. government programs on AIDS and biodefense.

HEINZ AWARDS. A Nebraska mom whose concern for her son's well-being led her to launch a campaign against drinking-water pollution has won a share of the $250,000 environmental prize awarded by the Heinz Family Foundation. Susan Seacrest, who started the Groundwater Foundation 2 decades ago, shares the award with civil engineer Bernard Amadei, founder of Engineers Without Borders, a Colorado-based nonprofit that implements clean water, sanitation, and other engineering projects in developing communities around the world. Read about other Heinz Awards winners at www.heinzawards.net.

IN THE COURTS >>

A RULING DEFIED. A fight over water rights is the latest wrinkle in the controversial and long-delayed plan by the U.S. government to build a nuclear waste dump in the Nevada desert.

On 31 August, federal District Judge Roger L. Hunt ruled that Nevada's state engineer could deny water to teams drilling for rock samples at the site of the planned Yucca Mountain Repository, 140 km northwest of Las Vegas. The Department of Energy (DOE) is supporting the drilling to gather data for a license that it plans to file next summer to build the $58 billion facility to store waste from the country's 104 nuclear power plants, which most state officials and residents bitterly oppose.

Hunt blasted DOE for ramping up its drilling program 5 years after Congress approved the project. "The Court entertains the suspicion that either DOE wants to look busy, or it wants to keep its contractor occupied during its lengthy delays in filing for a license," he wrote.

DOE declined to comment, citing the ongoing litigation, but geoscientists familiar with the project say the drillers are most likely studying the area's seismic and volcanic history. The work continues, with DOE officials asserting that Hunt's ruling doesn't apply to the 58 boreholes due to be completed this month. Nevada has vowed to keep up the fight. "One way or another, we're going to try to get the court to assist us," says Steven Frishman, technical policy coordinator for the Nevada Agency for Nuclear Projects.

CREDITS (TOP TO BOTTOM): KOREA AEROSPACE RESEARCH INSTITUTE; PROVIDENCE HEALTH SYSTEM/OREGON

Primitive *Homo erectus* 1664

Behind the latest gene therapy death 1665

A milder shock. A suprisingly small quake generated only small tsunami waves.

SEISMOLOGY

Continuing Indonesian Quakes Putting Seismologists on Edge

How predictable are earthquakes? Most seem to barge in unannounced, but many seismologists have long seen evidence that—at least in some places—the same faults break over and over, producing similar quakes at roughly similar intervals. This regularity, they say, may offer a chance of forecasting earthquakes. The recent run of large quakes off the Indonesian island of Sumatra, which began with a megaquake and tsunami in 2004 and continued last week, is providing fodder for both sides in the debate over whether earthquakes behave consistently enough to be reliably anticipated.

Both sides now have their eyes on one section of the fault offshore of the coastal Sumatran city of Padang. If that part of the fault follows the pattern some geologists expect, a tsunami-generating magnitude-8 or larger quake could well strike there in the coming months. "It's really looking ominous to me," says geologist Kerry Sieh of the California Institute of Technology (Caltech) in Pasadena, who is watching developments while on sabbatical in nearby Singapore.

The great Asian quake and tsunami of December 2004 certainly caught researchers by surprise. But once alerted, they knew where to look for the next big one—just to the south of the December break. The earlier rupture would have transferred stress down the fault to the next 350-kilometer-long segment, which last broke in 1861. Sure enough, a magnitude-8.7 quake reruptured that segment in March 2005. If segments of the offshore Sunda fault continued chatting in this "language of stress," the researchers believed, the next quake should break all or part of the adjacent 700-kilometer segment to the south. That segment hadn't ruptured since 1833 (in the south) and 1797 (in the north).

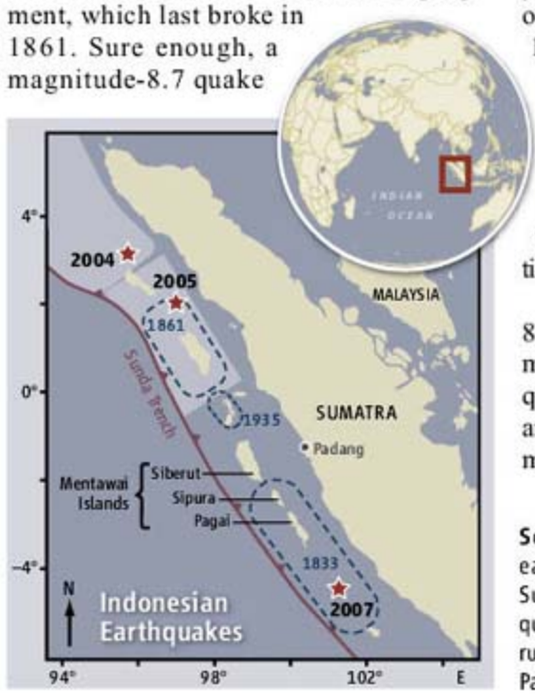

Last week's quakes off Sumatra offer some support for the idea that similar earthquakes repeat on the same fault segment at similar intervals, perhaps after feeling a nearby quake. The classic characteristic quake repeatedly struck Parkfield, California, from the 19th century into the 20th century. But as seismologists were reminded by Parkfield's misbehavior in its last appearance (*Science*, 8 October 2004, p. 206), fault behavior and communication can be frustratingly subtle, even perverse. Last week, on 12 September, a magnitude-8.4 quake did indeed strike south of the 2005 break. But it wasn't the quake called for in the stress communication script. The sequence of 2004, 2005, and now 2007 quakes skipped over the segment that last broke in 1797. Instead, much of the 1833 segment broke farther to the south.

Even if the latest quake ruptured the same part of the fault as before, that fault slipped only a couple of meters, Sieh says, not the 10 meters it slipped in 1833. That made the quake one-twentieth the size in terms of energy released. So the falling dominoes from the north for some reason passed over a fault segment that had accumulated 200 years' worth of stress. And a more distant fault did fail, but not in the characteristic quake that might have been expected.

Some seismologists see the magnitude-8.4 quake and an accompanying pair of magnitude-7 quakes as another sign that quakes mostly pop off in a range of sizes and break a largely unpredictable assortment of fault segments. "This sure looks ▶

Second-generation quakes. The 2004 great earthquake (red star and light-blue zone) on the Sunda Trench fault (red line) triggered the 2005 quake where the fault ruptured in 1861, but the next rupture came far to the south, leaving the fault off Padang as a lingering threat.

CREDITS (TOP TO BOTTOM): CRACK PALINGGI/REUTERS/LANDOV; ADAPTED FROM S. S. NALBANT *ET AL.*, *NATURE* 435, 756 (2005)

Dogging genes
1668

Insights from slips of the tongue
1674

like a large distribution of magnitudes" generated by a random process, says geophysicist Eric Geist of the U.S. Geological Survey in Menlo Park, California, who doubts that the 2005 quake could have reached this far south to trigger the next one.

Others are more open to a link to the previous rupture. "It's hard for me to imagine that after 170 years of no [larger-than-magnitude-8] earthquakes, the 2004, 2005, and 2007 earthquakes aren't somehow involved in triggering" subsequent earthquakes, says Sieh, who, with colleagues, published a forecast for a post-2005 quake. His Caltech colleague, seismologist Jean-Philippe Avouac, agrees. Stress from the 2005 rupture may have propagated farther but more slowly along the deep parts of the fault to trigger last week's quake, he says.

However this fault is working, last week's events are both good news and bad news for people in the region of Padang, says seismologist John McCloskey of the University of Ulster in Coleraine, U.K. Good news in that the magnitude-8.4 quake relieved some of the stress on the fault; the next quake could be in the low 8s rather than pushing a 9. But bad news in that last week's activity could only have increased the stress on the segment off Padang, making another rupture more likely. The threat of another huge quake has receded there, says McCloskey, "but in terms of an 8, it's still the most likely place on the planet."

–RICHARD A. KERR

Tsunami Warning System Shows Agility—And Gaps in Indian Ocean Network

Within 15 minutes after a magnitude-8.4 earthquake rocked Indonesia's Sumatra Island last week, tsunami warnings were blaring from mosque loudspeakers in local villages. By then, many residents had already fled. "We tell people that if the shaking is strong, don't wait for a warning, evacuate," says Patra Rina Dewi, executive director of the Komunitas Siaga Tsunami (Kogami), a nonprofit in Padang, Indonesia. For several hours after the quake, small tsunamis hit Sumatra's west coast, causing minor damage but no casualties.

Indonesia's warning and similar alerts across the region were the fruits of a nascent Indian Ocean Tsunami Warning and Mitigation System. Officials are pleased with the performance of the partly deployed operation, which relies on a network of sensors. But the experience also reinforced the notion that technology is just one facet of a strategy, along with boosting awareness and developing evacuation and response plans.

The need for tsunami preparedness was driven home by the 26 December 2004 magnitude-9.3 earthquake off Sumatra that triggered a monster tsunami. Many of the 230,000 deaths could have been prevented had coastal dwellers been warned of the impending waves.

In response, Indian Ocean nations, buttressed by the United Nations Educational, Scientific and Cultural Organization's Intergovernmental Oceanographic Commission and donor countries, started stitching together the Tsunami Warning System, a $130 million network of seismometers, buoys for measuring swells, sea-bottom pressure sensors, and tide gauges, as well as mechanisms for sharing data (*Science*, 9 December 2005, p. 1602). Only a handful of the deep-ocean sensors are in place, and countries are still installing seismometers and tide gauges.

Relying solely on seismic data to determine the magnitude and location of the 12 September earthquake, Indonesia's Meteorological and Geophysical Agency issued a tsunami warning to authorities near the epicenter "within 5 minutes of the earthquake," boasts Fauzi, an official in charge of tsunami warnings, who, like many Indonesians, has only a given name. Residents fled low areas on their own initiative—a good response, says Kogami's Dewi. But she would like to see accurate and timely follow-up advice based on an analysis of sensor data on whether a tsunami is actually on its way. Fauzi says that's his agency's goal.

Other countries, with the advantage of distance from the epicenter, were able to forecast the threat more accurately. The Indian Tsunami Warning System, at India's National Centre for Ocean Information Services in Hyderabad, picked up the quake on its seismometers and put authorities on the Andaman and Nicobar Islands on alert but stopped short of issuing a warning. After weighing data from tide gauges and recently placed ocean-bottom pressure sensors, the Hyderabad staff concluded that neither the islands nor the mainland faced a tsunami. Three hours after the earthquake, India issued an "all clear." The network "performed admirably," says Vinod Menon of the National Disaster Management Authority in New Delhi. But Menon admits that poor communications left people in some coastal regions in a panic. "Messaging and outreach really needs to be fine-tuned," he says.

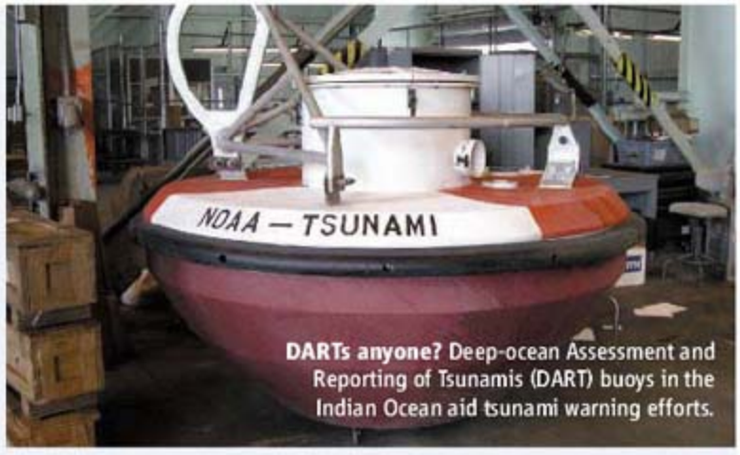

DARTs anyone? Deep-ocean Assessment and Reporting of Tsunamis (DART) buoys in the Indian Ocean aid tsunami warning efforts.

CREDIT: NOAA

Thailand's National Disaster Warning Center also concluded early on that the chance of a tsunami was small. It alerted officials to stand by but issued no public statements. Smith Dharmasaroja, chair of the National Disaster Warning Administration committee, says the center worried about losing public trust if it broadcast warnings unnecessarily. But many residents heard from the news that warnings had been issued in other countries and evacuated on their own. The center has revised its procedures and, when the next big quake strikes, will issue bulletins to keep the public informed.

Sri Lankan officials, meanwhile, played it safe and evacuated people from areas hardest hit by the 2004 tsunami. Writing in Sri Lanka's *Sunday Times* on 16 September, Dulip Jayawardene, former director of the Geological Survey Department, called on the government to "train seismologists and geophysicists in interpretation of seismic data" for more accurate tsunami forecasts.

The latest earthquake to rattle South Asia provided "the best drill ever," says Tavida Kamolvej, a disaster management expert at Thammasat University in Bangkok. Now, she says, it's time to find the gaps in the system and fill them.

–DENNIS NORMILE

With reporting by Pallava Bagla.

ASTRONOMY

Arecibo Advocates Agitate To Reverse Planned NSF Cut

Supporters of the world's largest radio telescope in Arecibo, Puerto Rico, gathered last week in the shadow of the U.S. Capitol in hopes of keeping the observatory alive. But time is running short, and the advocates face an uphill struggle to keep the 40-year-old observatory, whose receiving dish extends 305 meters across a natural sinkhole, operating into the next decade.

Last fall, the National Science Foundation (NSF) endorsed the recommendations of an independent panel to reduce the astronomy division's support for Arecibo from $8 million to $4 million to free up funds for new projects such as the Atacama Large Millimeter Array being built in Chile (*Science*, 10 November 2006, p. 904). All NSF funding for the telescope would cease after 2011 if outside donors can't be found, although the observatory's planetary radar could close as early as October 2009, says Robert Brown, director of the National Astronomy and Ionosphere Center (NAIC), based at Arecibo and operated by Cornell University.

The radar is especially important for imaging planets such as Venus and computing exact trajectories of near-Earth objects that might pose a hazard. NASA decided in 2001 to halt funding for the radar, which now costs $1 million a year to operate, in order to focus on space-based observatories.

Brown, who helped organize last week's meeting in Washington, D.C., argues that the independent panel's recommendations are outdated because their premise—that NSF's astronomy budget would remain static—now seems unlikely, given the strong political support for increased federal spending in the physical sciences. "The plan … should be rethought," he says. One New York legislator who sits on the powerful appropriations committee and is a leader of the Hispanic community is already convinced. "The Arecibo Observatory is an important scientific tool for our nation," says Representative José Serrano (D–NY). "I will be monitoring its funding situation and making sure that the correct decisions are being made." Serrano declined to say how and when he might push for more money.

That appeal to Congress doesn't sit well with NSF officials. "We commissioned a panel to determine scientific priorities," says Wayne van Citters, who heads the agency's astronomy division. "To involve Congress in one aspect of it is not a productive way to go." Van Citters fears that legislators might shift money from newer, more promising projects. "We have to recognize [there are] limited funds," says Garth Illingworth, a University of California, Santa Cruz, astronomer at Lick Observatory, who also serves as chair of the Astronomy and Astrophysics Advisory Committee that advises NSF, NASA, and the Department of Energy. "Focusing on whole new wavelength areas may be more appropriate."

One participant at the meeting, held in a building near the Capitol, complains that the NSF panel underestimated the importance of the radar. Steven Ostro, an astronomer at the Jet Propulsion Laboratory in Pasadena, California, says that Van Citters "effectively stonewalled" its advocates because its mission fell outside NSF's purview. But Van Citters says that NAIC and Cornell proposed to cut the radar to cope with the decreasing budget, without prodding from NSF.

Brown says that the Puerto Rico government, private individuals, and commercial companies have expressed some interest in supporting the telescope's operations, including the radar. And although Van Citters says he's optimistic that a white knight will appear, he warns that any plan to keep Arecibo going "has to be sustainable."

–ANDREW LAWLER

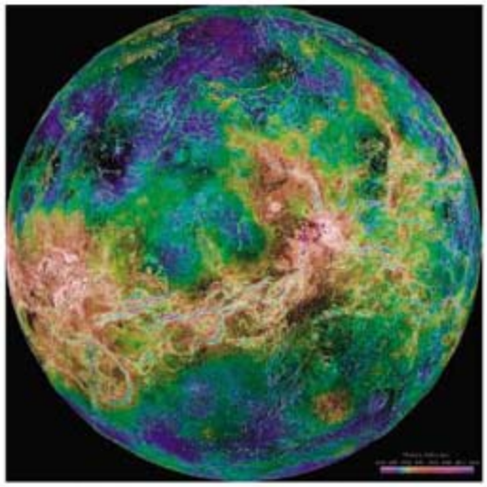

CREDIT: NASA/JPL/MIT/USGS

Venus finder. This radar image of Venus is made up of data from both NASA's Magellan spacecraft and Arecibo, which peered beneath the planet's total cloud cover.

The Young and the Innovative

Are early-career scientists more likely than their senior colleagues to suggest out-of-the-box research? That's the thinking behind a new grants program at the National Institutes of Health (NIH) that gives junior faculty members a chance to launch their biomedical research careers.

This week, the agency announced the first batch of 29 awardees for the 5-year, $1.5 million New Innovator Awards. Ideas from the 2200 applicants, who have never received an individual-investigator NIH grant and who earned their Ph.D. in the past 10 years, run the gamut from basic to therapeutic research. "Early-career types are historically the ones who come up with the most innovative ideas," says Jeremy Berg, director of the National Institute of General Medical Sciences, adding that he hopes the awards pave the way to subsequent R01 grants. NIH also announced the fourth round of Pioneer Awards to established investigators. –YUDHIJIT BHATTACHARJEE

Peru to Get Artifacts

Artifacts recovered from the famed Inca site of Machu Picchu are going home. After years of squabbling, Yale University this week agreed to return more than 350 pieces uncovered by Yale archaeologist Hiram Bingham III in the 1920s. Yale maintained it had approval to remove the artifacts, but Peru insisted that they be returned and recently threatened to go to court. Under the deal, Yale acknowledges Peru's title to the material but retains an unspecified number of artifacts. It will also co-sponsor a traveling exhibit that will raise money for a museum in the ancient Inca capital of Cuzco to open by the centennial of Machu Picchu's rediscovery by Bingham in 2011. Yale President Richard Levin says the agreement sets "a new model" for collaboration. –ANDREW LAWLER

China's Spending Boom

China is continuing to pour money into research. A new government report says that spending this year has reached $40 billion, up 22% to a record-high 1.4% of gross domestic product, with 72% of that coming from the private sector. China's R&D spending has risen by 19% a year since 1995, according to a new analysis by the Organisation for Economic Co-operation and Development (OECD). That sustained surge has moved China into sixth place globally, says the OECD report, but it adds that top-down decision-making and a limited investment in basic research have hindered the payoff from such investments. –DENNIS NORMILE

PALEOANTHROPOLOGY

A New Body of Evidence Fleshes Out *Homo erectus*

The long-legged human ancestor *Homo erectus* is known for breaking records: It has been seen as the first globetrotter, the first inventor of stone hand axes, and the first human to dramatically expand its brain and to reach the height of people today. But such views of the body of *H. erectus* rely heavily on a single partial skeleton of a strapping youth from Nariokotome, Kenya. Now the discovery of incredibly rare trunk and limb bones of early *H. erectus* shows that the species wasn't always so tall and brainy—and, according to some interpretations, suggests that it may have emerged in Asia, not Africa.

In this week's issue of *Nature*, researchers unveiled 32 postcranial bones from three adults and a teenager who lived 1.77 million years ago at Dmanisi, Georgia. The hominids resembled the Nariokotome Boy but would have stood only as high as his shoulders. "All of the individuals are small—they are not NBA players," says team leader David Lordkipanidze of the Georgian National Museum in Tbilisi. Although their feet and body proportions are modern, the Dmanisi skeletons had more primitive shoulders and arms and are considered the most primitive members of *H. erectus* yet found.

But not everyone agrees. The bones are so primitive that a few researchers aren't even sure they are members of *Homo*. "They are truly transitional forms that are neither archaic hominins nor unambiguous members of our own genus," says paleoanthropologist Bernard Wood of George Washington University in Washington, D.C.

The debate reflects how little is known about the murky period at the dawn of our genus, partly because there are so few fossils of postcranial bones. The famous partial skeleton of Lucy offers a view of *Australopithecus afarensis*, which lived 3.6 million to 3 million years ago. But the next good window into body anatomy doesn't appear until 1.55 million years ago, with the 12-year-old Nariokotome Boy from Kenya. He had a dramatically bigger brain and would have stood about 180 centimeters tall had he survived to adulthood. "We've got Lucy's body and then Nariokotome, and this gap in the middle with a lot of scrappy stuff in between," says paleoanthropologist Susan Antón of New York University. The earliest of those in-between fossils have been called *H. habilis*, which is something of a grab bag species for specimens too small or primitive to be considered *H. erectus*.

The remarkably well-preserved Dmanisi fossils, among the earliest members of *H. erectus* found anywhere, fall into that gap. The postcranial bones, some of them articulated with each other, fit nicely with four previously published small skulls. The skeletons suggest that the Dmanisi people ranged from 145 to 166 centimeters tall and weighed between 40 and 50 kilograms—bigger than an australopithecine but on the very low end of the range for modern humans. These small specimens also fit with a tiny *H. erectus* skull from Kenya published last month (*Science*, 10 August, p. 733). But another African *H. erectus* skull is both 225,000 years older and larger, so the species now encompasses a wide size range, perhaps because of sexual dimorphism between males and females or adaptations to varied habitats.

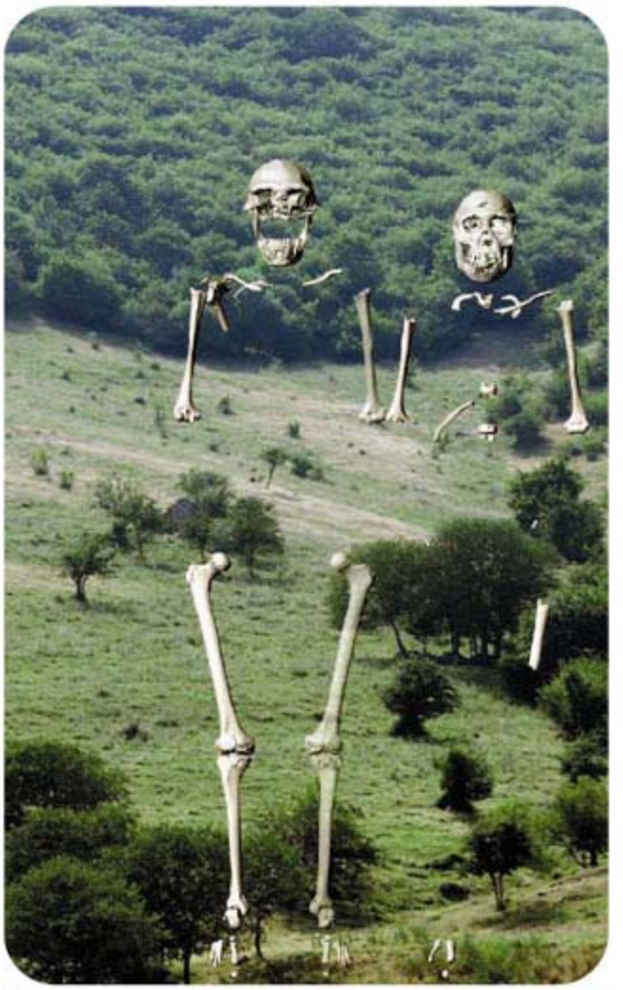

Short people. Skeletons from Dmanisi, Georgia, shown on a forested landscape are surprisingly short-statured.

CREDIT: M. PONCE DE LEÓN AND C. ZOLLIKOFER, UNIVERSITY OF ZURICH

The Dmanisi skeletal bones also have other primitive traits: The bone of the upper arm is straight rather than twisted, and the shoulder blades might have been closer to the sides rather than the back. Those traits are seen in australopithecines and also in the tiny 18,000-year-old *H. floresiensis* from Indonesia (*Science*, 19 May 2006, p. 983). Nariokotome Boy's upper arm bone is incomplete but looks relatively straight. In any case, the Dmanisi bones suggest that a dramatic reorganization of the orientation of the upper arm and shoulder, which allows overhead throwing (and piano playing), came relatively late in the evolution of humans. Yet the small-brained Dmanisi people were adept at using their archaic arms to butcher meat with stone tools, says co-author Christoph Zollikofer, a neurobiologist at the University of Zurich, Switzerland.

The fossils' small size might suggest they belong to *H. habilis* or a new species, but their more modern traits, such as long legs and modern body proportions, place them in *H. erectus* and show they were adapted for long-distance locomotion, says Zollikofer. Their feet are also quite modern, including a big toe that was not grasping, as in apes and australopithecines.

Lordkipanidze thinks the fossils were either very early *H. erectus* or "the best candidates to be the ancestors of *H. erectus*." He suggests that they arose in Asia from an early *Homo* that was part of a very early radiation out of Africa. Some of the Dmanisi fossils' descendents returned to Africa while others spread out later into Asia as full-fledged *H. erectus*. Paleoanthropologist Alan Walker of Pennsylvania State University in State College doesn't buy that scenario. He and Antón prefer a model in which the species arose in Africa and continued to evolve separately on different continents—including at Dmanisi—giving rise to variation as it adapted to different habitats. Either way, "the real story here is variation, variation, variation," says co-author Philip Rightmire of Harvard University. **–ANN GIBBONS**

GENE THERAPY

Questions Remain on Cause of Death in Arthritis Trial

An investigation into the death of a 36-year-old woman in a gene therapy trial has revealed a complex tragedy but reached no firm conclusion on whether the experiment was to blame. At a meeting this week, the National Institutes of Health's Recombinant DNA Advisory Committee (RAC) largely discounted a theory that a vector used in the trial multiplied out of control, among other hypotheses. Participants noted that the patient apparently died because she had a severely compromised immune system and succumbed to a fungal infection.

Gene therapy, which has been blamed for two deaths in the past 8 years, did not get charged with a third. Some concern had focused on the popular vector used in this experiment, adeno-associated virus (AAV). Results presented at the meeting did not challenge the consensus that it is relatively safe. However, questions remain about how well the patient was informed and how she was selected for the trial; her disease was not life-threatening. Concluded Arthur Nienhuis, president of the American Society of Gene Therapy: "We see areas in which we need to be concerned."

The patient, Jolee Mohr of Springfield, Illinois, had suffered from rheumatoid arthritis since she was 21. Through her rheumatologist, she enrolled in a phase I/II safety trial of a new treatment for arthritis sponsored by Targeted Genetics Corp. in Seattle, Washington. The study involved injecting into joints AAV that carried a gene coding for a protein that inhibits a proinflammatory cytokine called tumor necrosis factor α (TNF-α). Mohr received an initial injection in her right knee on 26 February and a second on 2 July.

After the second injection, she developed flulike symptoms. Ten days later, she was admitted to the hospital and was later transported to the University of Chicago Hospital. She died there after massive organ failure on 24 July. The Food and Drug Administration immediately put the trial on hold (*Science*, 3 August, p. 580).

The main cause of death was apparently infection with *Histoplasma capsulatum*, a common fungus, University of Chicago doctors said at the RAC meeting. Mohr's liver, lungs, and other tissues were "loaded with" the organism, which was not picked up in lab tests during her hospitalization, reported pathologist John Hart of the University of Chicago Medical Center. In addition, she had a large abdominal hematoma, or a blood clot.

Tests done after Mohr died show that she already had a mild *Histoplasma* infection on 2 July. Because she also tested positive for herpes simplex virus, some experts have suggested that herpes proteins, along with wild AAV, could have helped the AAV vector to replicate and weaken her immune system. But although the AAV vector did escape from the injected joint to other tissues, the levels were extremely low, making it unlikely the virus was replicating, RAC found.

Medical mystery. It's not clear whether gene therapy contributed to the death of 36-year-old Jolee Mohr, shown with her family.

CREDIT: AP PHOTO/COURTESY OF THE MOHR FAMILY

A more likely culprit is an immune-suppressing drug she was taking. This drug, called Humira, is a TNF-α blocker like the gene therapy product and has been associated with *Histoplasma* infections. One possibility is that the combination pushed Mohr over the edge. The RAC members hope an experimental assay can tease apart levels of gene product and drug in Mohr's blood.

More definitive results should be available by the next RAC meeting in December, said chair Howard Federoff of Georgetown University in Washington, D.C. Meanwhile, however, Federoff and others say other questions remain unanswered—such as whether Mohr realized that patients weren't expected to benefit from this study. **–JOCELYN KAISER**

Taking ADHD to Heart

U.S. academic researchers are teaming up with health insurers to learn whether drugs used to treat hyperactivity also cause heart problems. They will be looking at the health records of 500,000 children and adults who have taken any of a half-dozen drugs for attention deficit hyperactivity disorder (ADHD) in search of higher rates of sudden cardiac death, heart attacks, and stroke. The $4 million study may also provide clues about "how risk changes with age, gender," and other variables, says Michigan State University's Marsha Rappley, chair of the pediatric advisory committee at the Food and Drug Administration. FDA is co-funding the study with the federal Agency for Healthcare Research and Quality.

–JENNIFER COUZIN

Space for Rent ...

With no money for new biomedical research aboard the international space station, NASA is hoping that a sister agency will open its pocketbook. A new agreement between NASA and the National Institutes of Health is intended to open doors for NIH-funded scientists proposing projects to take advantage of the station's microgravity environment. "The funding will come if we have competitive, highly meritorious grants," says cell biologist Danny Riley, president-elect of the American Society for Gravitational and Space Biology. The station is scheduled to open for business in 2011.

–BENJAMIN LESTER

... And Google Air?

Two Gulfstream jets took off recently from NASA Ames Research Center at Moffett Field in California to observe a meteor shower high above the haze of San Francisco Bay. The front-row seats for astronomers came courtesy of a deal between NASA and a private company run by Larry Page and Sergey Brin, founders of the Internet giant Google.

Last month, NASA granted the planes access to Moffett Field, located near Google's base in Silicon Valley and typically off-limits to private aircraft, in exchange for their use on research missions. The two Gulfstreams and a Boeing 767 will be housed for $1.3 million to $2.3 million a year, says Steven Zornetzer, Ames associate director for institutions and research, and outfitted with a suite of atmospheric sensors that will be activated whenever the planes are in the air. Outside researchers, who are welcome to submit proposals, may be attracted to the king-sized beds on the Boeing jet, whose commercial version carries 180 passengers. **–ANDREW LAWLER**

CLIMATE CHANGE

Panel Gives U.S. Program Mixed Grades

An expert panel says the Bush Administration deserves "a pat on the back" for advancing the science of climate change. But the scientists assembled by the National Academies' National Research Council (NRC) have serious concerns about the management, funding, and emphasis of the $1.7-billion-a-year Climate Change Science Program (CCSP).

President George H. W. Bush created the U.S. Global Change Research Program in 1990 to bring under one umbrella the government's efforts to understand climate change. In 2002, his son reshuffled the climate deck to create CCSP. Last week, the NRC panel took the first outside look at that program and concluded, says chair V. Ramanathan, an atmospheric scientist at the Scripps Institution of Oceanography in San Diego, California, that its efforts to understand how and why climate has changed and to make predictions are "proceeding well."

At the same time, the 15-member panel identified serious shortcomings. The country's ability to monitor climate is being eroded, it says, by a projected one-third reduction in the number of operating instruments by 2010. "The loss of existing and planned satellite sensors is perhaps the single greatest threat to the future success of the CCSP," the report concludes.

Wants more. NRC committee chair V. Ramanathan sees progress and shortcomings in U.S. effort.

The report also criticizes the program's management structure. "Interagency working group members often have little budgetary authority to implement the research directions that they define," the panel wrote, because the program only controls the $1.4 million needed to manage its nine-person office. Ramanathan says CCSP often can make progress only when its interests happen to coincide with those of the 13 participating agencies.

Ramanathan says he's troubled by the program's limited success in "assessing [climate change] impacts on human well-being and adaptation capacities." Those assessments would require reliable forecasts of climate change at the regional if not the local level, Ramanathan notes, a capability the world's climate modelers are still struggling with. But gauging impacts on humans and figuring out how humans might adapt to climate change will take far more than the $20 million per year now spent within the program on social science studies, the committee said. It will also take better communication between the program and business interests, other agencies, and the general public. For starters, 21 synthesis and assessment reports were due from CCSP by now, but only two have been delivered.

John Marburger, the president's science adviser, called the review "thoughtful" and said the Administration would "take their recommendations very seriously." The same NRC committee is already working on a second report, due out early next year, on how to improve the program. **–RICHARD A. KERR**

REGENERATIVE MEDICINE

Australian Scientist to Head California Stem Cell Effort

California has landed one of the biggest fish in the Pacific to head its stem cell venture. Late last Friday, the board of the California Institute for Regenerative Medicine (CIRM) approved the appointment of Alan Trounson, one of Australia's premier researchers, as the institute's president.

Trounson, director of stem cell research at Monash University in Melbourne, Australia, thus joins the international roster of big-name researchers who have been lured by California's $3 billion stem cell program, launched in 2004. "Things are booming in California right now," says former CIRM president Zach Hall, who says Trounson's varied experience makes him "almost uniquely qualified for the job."

Trounson says things happened fast. "I was passing through California 6 weeks ago" when CIRM's board chair Robert Klein, whom he had met in Melbourne last spring, encountered him at a dinner and asked if he was interested in the job. "I thought he must have been joking," says Trounson.

Trounson, 61, began his career working on sheep and cattle reproduction but quickly made a name for himself in human in vitro fertilization. He was neck and neck with James Thomson of the University of Wisconsin, Madison, in the race to cultivate the first human embryonic stem cell lines in 1998. He is also well-versed in managerial and entrepreneurial issues as founder of a number of Australian biotech companies and co-founder of the Singapore-based ES Cell International.

Big fish. Alan Trounson expects to start by year's end.

Those who know Trounson say his personal skills should make for smooth relations with Klein, who has more than once ruffled colleagues with his propensity to take unilateral actions. "Alan is charming, … a lovely human being," says stem cell researcher Evan Snyder of the Burnham Institute in San Diego, California. Johns Hopkins University researcher John Gearhart says he has "political savvy" on top of a "very broad base of knowledge." Trounson himself likes to talk about "partnerships"—in this case with Klein, whom he calls a "visionary financier."

Trounson is one of several stem cell scientists Australia has lost to the United States, including Martin Pera, now at the University of Southern California in Los Angeles, and Paul Simmons, now at the University of Texas, Houston. Trounson has made it clear he regards the CIRM presidency as the capstone of his career. "I thought would another two or three *Science* papers make a difference, or would taking this job really make a difference? It's a no-brainer to come here and do this." **–CONSTANCE HOLDEN**

CREDITS (TOP TO BOTTOM): SCRIPPS INSTITUTION OF OCEANOGRAPHY, UCSD; MONASH UNIVERSITY

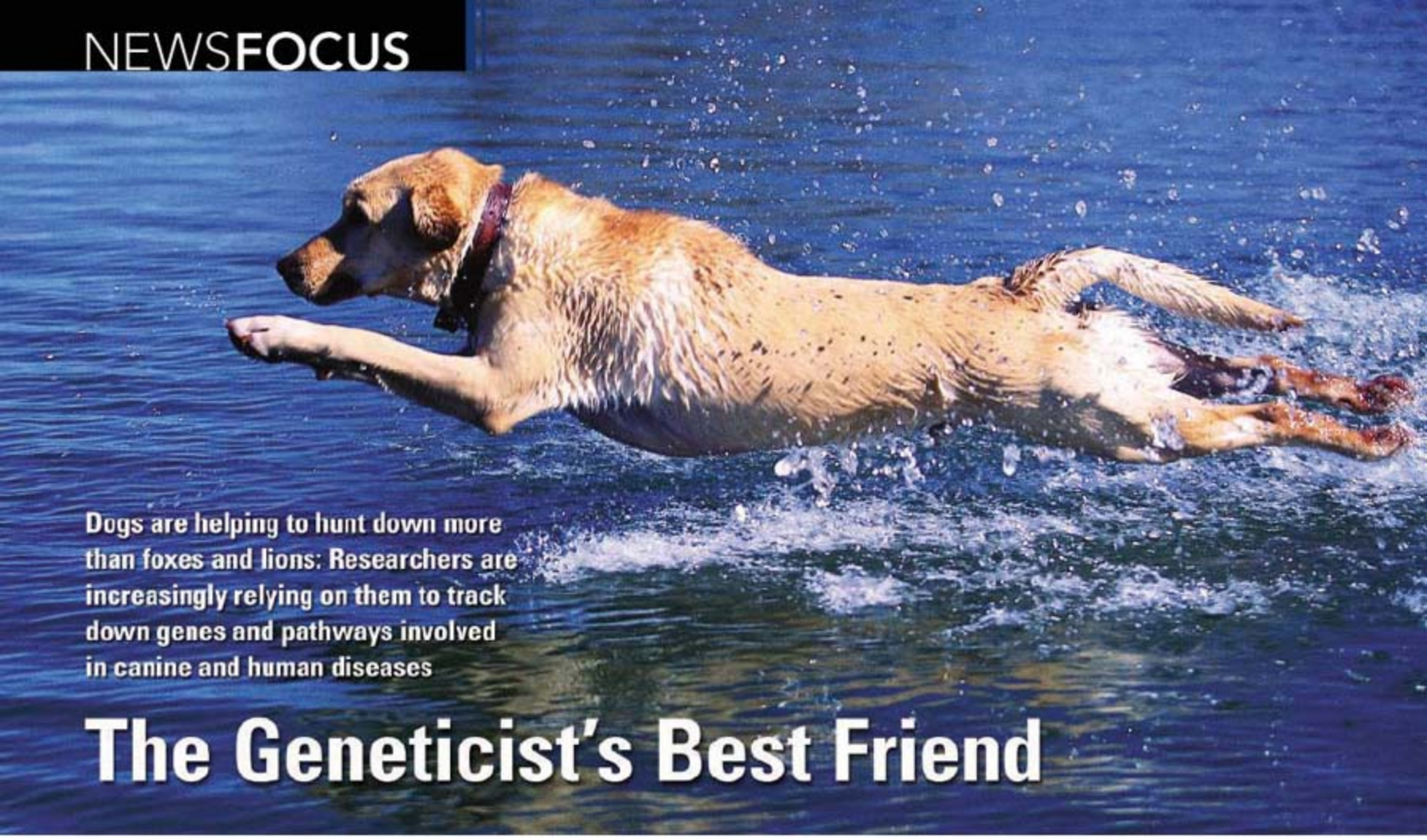

Dogs are helping to hunt down more than foxes and lions: Researchers are increasingly relying on them to track down genes and pathways involved in canine and human diseases

The Geneticist's Best Friend

TALK ABOUT BLIND FAITH. TWENTY YEARS ago, Gustavo Aguirre and his colleague Gregory Acland were struggling to understand a common cause of inherited blindness in dogs. They had bred affected and unaffected individuals and traced the inheritance patterns in the offspring, but "there was no hope of finding the gene," recalls Aguirre, a veterinarian at the University of Pennsylvania's School of Veterinary Medicine in Philadelphia. At the time, researchers hadn't even assigned numbers to the canine chromosomes, let alone begun to map the locations of genes. Nonetheless, "I decided that in the future, someone somewhere would come up with [a way] to come up with the gene," he says. So they banked blood from their dogs and waited.

Their patience paid off. A decade later, their freezers provided the raw material for a linkage map of the dog genome and, eventually, the discovery of the long-sought gene for progressive rod-cone degeneration. With that map as a starting point, researchers have built a community that has proven the value of dog genetics not just for veterinarians and dog breeders but also for human geneticists.

Dogs are a geneticist's dream. Pure breeds, as the name implies, are often highly inbred for specific traits. They have large families and well-documented genealogies, all of which greatly simplifies the task of tracking down mutations that cause disease or genes that underlie traits such as size, coat color, or even behavior. And the link to humans can be direct: The top 10 diseases in dogs include cancer, epilepsy, allergy, and heart disease—disorders that affect many millions of people. Also, because dogs live in the same environment as people, they share some of the same environmental risk factors. As a result, more and more researchers, including a consortium about to be announced in Europe (see p. 1670), are turning to the dog for clues to human genetics. "All of a sudden, people from a wide range of disciplines can see the value, power, and practicality of genetic studies in dogs to shed light on issues of concern to them," says Acland, a geneticist now at Cornell University.

Dogged pursuit. Elaine Ostrander helped jumpstart canine genomics.

Pooch politics

It wasn't always that way. In fact, it took years of work by a small but dedicated band of researchers for the dog's scientific value to be appreciated. Jasper Rine got the ball rolling almost 20 years ago. A yeast geneticist at the University of California, Berkeley, he recognized that dogs were bred for specific behaviors and that those behaviors probably had a very strong, and perhaps easily identifiable, genetic basis. Rine crossed Border collies with Newfoundlands to see if he could pinpoint the genes underlying the former's predilection for herding and the latter's love of swimming. But he lacked a key tool: a map of genetic markers—known stretches of DNA prone to variation—that he could track from parents to offspring to determine which were passed along with the best swimmers and which were associated with herding. The markers associated with a particular behavior should lie near genes that contribute to that behavior. To develop such a tool, Rine conceived the idea of a dog genome project.

For Elaine Ostrander, the timing was fortuitous. She had just come to Berkeley in 1990 as a postdoc to study plant genetics, and to tide her over until her new fellowship kicked in, she took a temporary job with Rine. Her assignment: to begin building the dog map. She never made it to the plant lab. When she left in 1993 for the Fred Hutchinson Cancer Research Center in Seattle, Washington,

CREDITS (TOP TO BOTTOM): CHASE SWIFT/CORBIS; THERESA NAUJACK

Dog DNA deciphered. Researchers have sequenced this boxer's genome.

she was a complete convert, as comfortable soliciting blood samples from breeders at dog shows as she was poring over gels. Her puppy, a Border collie named Tess, became her lab's mascot, providing Ostrander and her students with welcome distractions and, once, posing for the cover photo on *Mammalian Genome*. Ostrander's home became a meeting place for colleagues interested in promoting dog genetics. "She drove this whole canine genome initiative," says Matthew Breen, a cytogeneticist at North Carolina State University's College of Veterinary Medicine in Raleigh.

Eventually, Rine closed down his dog-behavior studies for lack of funding and to avoid being hassled by animal-rights activists. Ostrander persisted on the map, but progress was slow until 1996, when she, Acland, and Aguirre joined forces. "We figured out we needed to check our egos at the door and pool our efforts," Ostrander recalls. Because Aguirre and Acland had samples from a large number of dogs with known genealogies spanning several generations, Ostrander and colleagues were able to determine the relative order of scores of markers by following which ones were inherited together in these dog families. A year after they began working together, they produced the first map showing the positions of 150 of these markers on the dog genome. With this tool, they quickly narrowed down the location of the gene for progressive rod-cone degeneration to a region of chromosome 9, although it would take several more years to get to the gene itself.

Very quickly, that map was superseded by a much more comprehensive one, a joint effort by Breen, Ostrander, and Francis Galibert, a human geneticist at the University of Rennes, France. Galibert, who became convinced of the value of dogs for gene hunting after hearing Ostrander give a talk at a Cold Spring Harbor Laboratory meeting, had located markers along the genome in a so-called radiation hybrid map. Ostrander and Breen added their markers to it to create a detailed atlas for tracking genes. With it, researchers "could pull DNA samples from their pedigrees out of their freezers and begin to do genome scans," Ostrander says.

Ostrander and Aguirre had long suspected that dog studies could lead to the discovery of genes important to humans. "But at the time, we were fighting the perception that dogs couldn't tell you anything," recalls Aguirre. That changed in 1998, when Emmanuel Mignot of Stanford University in Palo Alto, California, and his colleagues tracked down a gene that causes narcolepsy in dogs. After a decade of work, they found causative mutations in the *Hcrtr2* gene in narcoleptic dachshunds, Labrador retrievers, and Doberman pinschers, a discovery that clued researchers in to a new molecular pathway involved in sleep. With these results, "it was crystal clear that by studying dog genetics, we were going to learn things we couldn't learn in mice," says Ostrander.

That realization helped Ostrander achieve her ultimate goal: a complete genome sequence of the dog. She and her colleagues had their appetites whetted when J. Craig Venter, then president of Celera Genomics in Rockville, Maryland, turned his sequencing machines on his pet poodle, churning out a very rough sketch of its genome in 2001. An analysis was published 2 years later (*Science*, 26 September 2003, p. 1898). About the same time, the National Human Genome Research Institute (NHGRI) at the National Institutes of Health in Bethesda, Maryland, began supporting the deciphering of other vertebrate genomes, and Ostrander and her collaborators wasted no time writing up a white paper arguing that the dog be given high priority. She convinced the Broad Institute of the Massachusetts Institute of Technology and Harvard University in Cambridge, Massachusetts—a leader in high-throughput genome sequencing and analysis—to sign on. In 2002, the dog beat out the cat and the cow for a spot in the sequencing pipeline.

Ostrander put out a call to dog breeders for a highly inbred candidate. (The more inbred the individual, the more similar the animal's two sets of chromosomes and the easier it would be to piece the genome together.) After studying hundreds of samples of dog DNA submitted by owners, Ostrander and her colleagues chose a boxer named Tasha as the first canine to have its genome deciphered.

As part of that sequencing effort, researchers at the Broad Institute compared Tasha's genome with the rough draft of the poodle genome and DNA sequences from nine other dog breeds and five wild canids and came up with 2.5 million single-nucleotide polymorphisms (SNPs): points on the genome where a change in a single nucleotide frequently occurs. The analysis, published in the 8 December 2005 issue of *Nature*, "is a masterpiece," says geneticist Greg Barsh of Stanford University. Broad's Kerstin Lindblad-Toh, who led the dog genome sequencing project, has since worked with Affymetrix in Santa Clara, California, to develop a SNP chip, a microarray that allows researchers to screen samples rapidly for these variations across the genome. Dog genetics studies were primed for takeoff. These tools, says Aguirre, "put us into the 21st century."

CREDITS (TOP TO BOTTOM): GREGORY M. ACLAND; COURTESY OF NIH

Community outreach. NHGRI's Heidi Parker gets DNA from a dog-show competitor.

The power of inbreeding

The dog's power in tracking genes comes largely from inbreeding. "Each [breed] is a mini Iceland or Finland," explains Ostrander,

now at NHGRI. Many breeds stem from a few individuals whose progeny were interbred, not because of geographic isolation but to select for specific features and behaviors. As a result, members of a given breed have extremely long stretches of identical DNA in common—millions of bases long compared to the typical tens of thousands of bases in humans. In humans, "there's a lot of background cackling, but when you look at the dog genome, the message is loud and clear, without a lot of background noise," Breen explains. That means researchers can track down recessive genes involved in disease using many fewer animals. They also need an order of magnitude fewer SNPs than are needed for human studies.

The inbreeding in dogs is especially valuable in studies of genetic risks in complex diseases. In people, different mutations, even different genes, may be at fault in the same disease. Dozens of genes contribute to the risk of common cancers, for example, with no single one jumping out as key. But because each dog breed is an isolated, inbred population that typically dates back just a few hundred years, not a lot of time has passed for the dogs in any one breed to develop multiple mutations for the same disorder, or for several mutations to have been introduced from outbreeding. "In dogs of one breed, you will have exactly the same mutation in the same gene," geneticist Mark Neff of the University of California, Davis, explains. Breeds derived from a common ancestral breed might share a mutation, but distantly related breeds will not, offering the potential of revealing other genes, perhaps in the same pathway involved in a disease.

Born to point. Even as puppies, German shorthaired pointers live up to their names.

To help sort out how different breeds are related to each other, Ostrander, Heidi Parker in her lab, and their colleagues have looked for genetic variants that are shared across breeds: The more shared variants, the more closely the breeds are related. They initially studied 85 breeds, and the results helped them home in on a gene for short stature (*Science*, 6 April, p. 112). They have now expanded the work—called the PhyDo Project—to 130 of the 155 breeds recognized by the American Kennel Club. In work in press at *Genome Research*, they report that breeds cluster into five genetically defined groups, with some subdivisions within each group.

As these researchers will report, they have used these relationships to track down a gene causing collie eye anomaly, which is the canine equivalent of a human birth defect in which part of the eye does not form properly. In 2003, they had narrowed the gene's location down to a 1.7-million-base stretch of dog chromosome 37. Then they went further: "By comparing different herding breeds with the same disease, we whittled down [the possibilities] to four genes," Ostrander explains.

A close look revealed the likely culprit: a gene called *NHEJ1* missing 7800 bases. They found the same mutation in two more distantly related breeds, Nova Scotia duck tolling retrievers and longhaired whippets, which likely had farm collies in their family trees. But unrelated soft-coated wheaten terriers, which also get this disease, don't have the mutation. "We think we will be able to play that trick [of looking for mutations in closely related breeds] again and again," says Nathan Sutter, who recently left Ostrander's lab for Cornell University.

PhyDo is also helping Ostrander's group make sense of bladder cancers. Five breeds tend to develop this cancer. The most susceptible, with a 30-fold increase in risk, is the Scottish terrier. Three other at-risk breeds are terriers, which likely share the same

Europe Going to the Dogs

While U.S. researchers were beginning to piece together the first genetic maps for dogs in the 1990s, University of Copenhagen pig researcher Merete Fredholm was wringing her hands in frustration at the lack of funds to support a European consortium with the same goal. But now, she and collaborators from more than 20 institutions are poised to make a champion showing in this field, thanks to a pending European Union award for about $16 million.

Named after the legendary wolf who nourished the founders of Rome, the LUPA consortium plans to get DNA samples and health histories from 8000 dogs and hunt down genes for 18 diseases, including four cancers, four inflammatory disorders, and three heart diseases. "We have decided to focus on certain areas and to standardize the clinical characterization of these diseases," explains Leif Andersson, a geneticist at Uppsala University in Sweden. In this way, they use the DNA from animals across different countries, as well as across different breeds, to find genes. Once they have found the gene, they plan to see what role it plays in humans, says LUPA coordinator Michel Georges of the University of Liege in Belgium.

Georges is a recent convert, having never studied dogs before. But joining him are key players in canine genomics. Kerstin Lindblad-Toh, who headed the dog sequencing project at the Broad Institute of Massachusetts Institute of Technology and Harvard University in Cambridge, Massachusetts, is now spending three-quarters of her time at Uppsala University. "Her recognition, competence, and working capacity will change [European dog genomics]," says collaborator Åke Hedhammar, a long-term dog researcher at the Swedish University of Agricultural Sciences in Uppsala, who has used kennel club records and records from companies that provide health insurance for pets to sort out which individual dogs and breeds are best suited for particular gene searches.

Best of Show. Olle Kämpe, Göran Andersson, Kerstin Lindblad-Toh, Åke Hedhammar, and Leif Andersson (left to right) have teamed up to tackle human diseases through dog studies.

The European effort promises to push the field to warp speed. "We're going to learn a lot more about a lot of diseases," says Elaine Ostrander, a geneticist at the National Human Genome Research Institute in Bethesda, Maryland. Until recently, much of the high-profile work on dog genetics came from Ostrander and her collaborators, but already Europe is churning out a slew of key papers. With LUPA, "there will be a lot of competition," says Fredholm. **–E.P.**

CREDITS (TOP TO BOTTOM): DALE C. SPARTAS/CORBIS; ERIK BONGCAM

mutation. But PhyDo data verify that the fifth susceptible breed, the beagle, is not at all related, so its bladder tumor risk probably stems from a different genetic abnormality.

Dog fanciers

Ostrander's group is working with Carlos Bustamante of Cornell University to make SNP profiles of individual breeds available in a public database called "CANMAP." It should provide researchers and breeders with powerful tools to track down the traits in which they are most interested. Already, researchers are intrigued by the possibilities.

The data set includes wolves, the common ancestor of all dogs, which should give evolutionary biologists a "wonderful perspective on the evolution of the dog," says collaborator Robert Wayne, an evolutionary biologist at the University of California, Los Angeles. Since the 1980s, he's wanted to find the genes underlying the evolution of dogs and dog breeds. Back then, "it was clear we didn't have the technology to address the basic questions," he recalls. Now, says Sutter, by comparing SNP profiles of dogs and wolves, "we will know what changes occurred in the dog during domestication."

Stanford's Barsh has a different quarry in his sights. Over the past 15 years, he has worked on the genetics of coat color in mice, but recently he's focused on dogs and is well on his way to understanding the genetic basis of the stripes in the brindle coat of Great Danes. Like Barsh, Danielle Karyadi in Ostrander's lab is also a recent convert to dog genetics. She has spent much of her career chasing down genes that make people more susceptible to prostate cancer. Now, she has turned her attention to squamous cell carcinoma, a cancer found only in solid black dogs, such as poodles. "It will be really exciting when we can identify genes in dog cancers" and use them to understand human cancers, says Karyadi.

Lindblad-Toh has also been won over to the hounds. She specialized in human genetics when she came to Cambridge but by chance got roped into running the mouse genome sequencing project and eventually all mammalian sequencing projects at the Broad Institute. Working with European collaborators, Lindblad-Toh's group has two papers in press demonstrating the power of genomewide association studies in dogs to pin down genes. In one, they used fewer than two dozen boxers to track down the gene for white coat color. The gene is the same one that is mutated in humans with Waardenburg syndrome, an inherited disease characterized by hearing loss and skin and pigmentation abnormalities, and in several mouse pigmentation disorders. A second study on Rhodesian ridgebacks has led the group to a mutation possibly involved in neural tube defects; that study required fewer than two dozen animals as well. "It shows how little material you need," says Åke Hedhammar, a geneticist at the Swedish University of Agricultural Sciences in Uppsala.

He and Lindblad-Toh expect to make progress understanding more complex diseases as well. For example, boxers, bull terriers, and West Highland white terriers are prone to atopic dermatitis, a skin disease that in both dogs and humans has environmental and genetic components. Genetic studies are under way in these breeds to find the genes that influence this risk.

Common ills. Dogs and humans suffer from many of the same diseases, such as atopic dermatitis (*left*).

A window on behavior

The rapid progress in dog genetics is prompting some researchers to get back to studies that motivated a canine genome project in the first place: tracking down genes associated with behavioral traits. Neff has teamed up with Illumina Inc. in San Diego, California, to use a microarray to look for SNPs associated with "pointing." About 40 breeds point—freezing and lifting a paw in the direction of a rabbit or other quarry. "I finally feel we have a chance to understand the behavior," says Neff, who worked with Rine in the 1990s.

Even with the best genetic resources, however, the work is still challenging. "The problem is identifying the phenotype and separating what is learned versus what they are born with," says Parker. Adds Barsh: "We know whether [a dog] is yellow or black, but sometimes it's not so easy to tell how good a dog is at herding versus retrieving." In Ostrander's lab, Tyrone Spady—who used to study visual behavior in fish—depends on DNA from dogs that live in different places, with different upbringings and lifestyles. So Spady asks owners to fill out questionnaires: how frequently does the dog chase other animals, what quarry gets it running, and so on. By pooling surveys from many people, he corrects for bias in the owners' responses and uses the data in genomewide association studies.

At the Norwegian School of Veterinary Science in Oslo, Frode Lingaas is taking a similar tack in looking into "cocker rage." In this syndrome, generally amiable pets turn on their owners, exhibiting frighteningly aggressive behavior. He and his European colleagues assess the dogs' personalities through interviews with the owners and questionnaires. Several hundred samples will come from English cocker spaniels, but a few will come from English springer spaniels, which are also prone to this mental disorder. These dogs should get the researchers close to the gene, and a comparison with golden retrievers, which can also be four-legged Jeckylls and Hydes, should get them within striking distance. Because rage is often a symptom in schizophrenia, bipolar disease, obsessive-compulsive disorder, and other mental problems, finding this gene could help researchers understand why it develops in patients with mental illness.

Swedish researchers have a leg up on Spady and Lingaas. In Sweden, breeders often evaluate their young dogs using a standardized personality test. By looking at aggression, boldness, shyness, and sociability, they are able to better assess which ones should be trained as working dogs and for what jobs. So they have a large data set to work with and are moving forward with those studies, says Hedhammar. And in Russia, a long-term breeding program in foxes has yielded docile, doglike animals whose genes might yield insights into what makes dogs so affectionate and loyal.

Although Ostrander is curious about the genetic basis of why dogs get sick, grow tall, or excel at hunting, the intimacy she and others share with their canine pets is not something she cares to be intellectual about. Just the thought of the death of her lab's mascot a year ago still brings tears to her eyes. "There's some genetics buried in that," she says, "but I am going to leave that to someone else."

–ELIZABETH PENNISI

CREDITS (TOP TO BOTTOM): KERSTIN BERGVALL; LESTER V. BERGMAN/CORBIS

PLANETARY SCIENCE

Is Mars Looking Drier and Drier For Longer and Longer?

The more closely planetary scientists scrutinize the Red Planet, the less wet and weathered its surface appears to be, even in the solar system's earliest days

In recent years, "water, water everywhere" might have been the motto for Mars exploration. Shallow, salty seas ruled on early Mars, and water has been gushing down gullies in the geologically recent past, some even in the past few years. But the tide is now receding, at least a ways.

As highlighted in the 21 September issue of *Science* and elsewhere, more leisurely consideration of observations from rovers and orbiters and the unprecedented detail afforded by Mars Reconnaissance Orbiter (MRO)—the latest arrival at Mars—are bringing into question many earlier geologic interpretations involving surface water. Mars has been "a desolate place for a long time," concludes geochemist Scott McLennan of Stony Brook University in New York state.

The drier touch is the result of terabytes of data coming down from MRO's High Resolution Imaging Science Experiment (HiRISE), which can image features such as boulders as small as a half-meter in size. With that powerful new resolution, HiRISE principal investigator Alfred McEwen of the University of Arizona, Tucson, and his team went gully hunting.

On page 1706, they report imaging the bright-looking deposits that appeared in two gullies between passes by the Mars Orbiter Camera (MOC) onboard the now-defunct Mars Global Surveyor. From the way the bright material appeared to have flowed, the MOC team concluded that it had been charged with a fluid, presumably water. HiRISE has now discovered four other distinctively bright gullies, but "we've seen nothing to confirm" the presence of water, says McEwen. "We could change our minds, but for now, there's nothing here that isn't explained just as well by a dry flow" of loose debris down Mars's steepest slopes.

New gullies aren't the only young, watery features that the HiRISE team is calling into question. In a paper in press at *Geophysical Research Letters*, Frank Chuang of the Planetary Science Institute in Tucson, Arizona, McEwen, and colleagues report seeing a slight hollowing out of dark streaks running down martian slopes. A few researchers thought water might have caused such streaks (*Science*, 30 March, p. 1788), but the relief detected through late-day shadowing suggests dry dust avalanches instead, the group says.

Further back in geologic time, the HiRISE team is questioning some of its own aqueous interpretations. Most researchers believed that water, gushing from a great crack in the ground, sliced through lava flows to form Athabasca Valles (*Science*, 30 November 2001, p. 1820). McEwen still thinks that the original valleys were probably cut by water, but now with HiRISE's greater resolution, the valleys and the sediments deposited there—possibly containing traces of subsurface life—appear to be buried beneath several meters of lava, as Windy L. Jaeger of the U.S. Geological Survey in Flagstaff, Arizona, and HiRISE colleagues report on page 1709.

The observation might help explain why so many Mars landers put down on putative lakebeds and outflow channels have found nothing but lava, says McEwen. It would also flatly contradict the contention that expanses of flat plains—where waters from Athabasca Valles supposedly drained millions of years ago—are still a "frozen sea" of ice (*Science*, 4 March 2005, p. 1390).

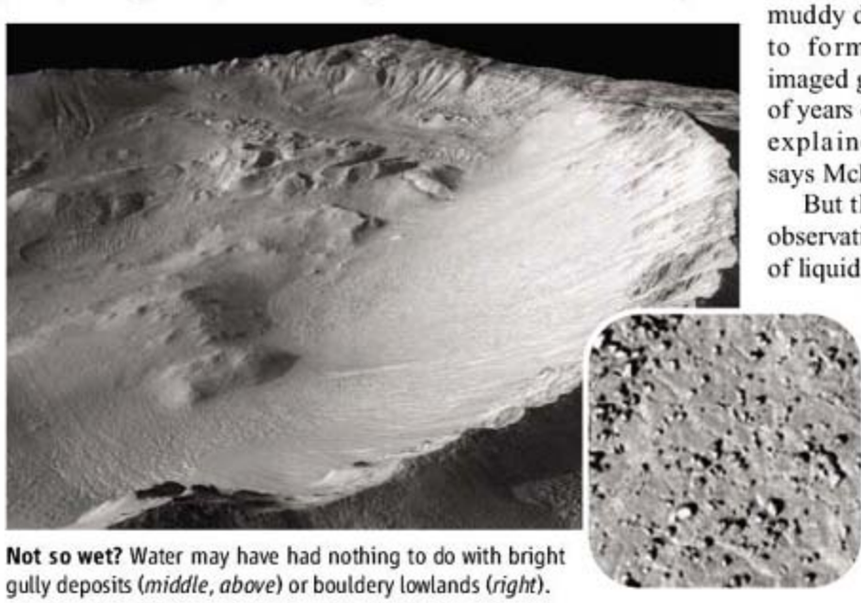

Not so wet? Water may have had nothing to do with bright gully deposits (*middle, above*) or bouldery lowlands (*right*).

CREDITS (TOP TO BOTTOM): NASA/JPL/UNIVERSITY OF ARIZONA; A. S. MCEWEN ET AL./SCIENCE

Finally, new HiRISE data from the northern lowlands of Mars cast doubt on one hypothesis that there was an ancient ocean there. Lingering shorelines have been reported around the broad, flat basin. But HiRISE images reveal ubiquitous boulders up to 2 meters in size strewn across the northern lowlands where a deep, long-lived ocean should have left nothing as large as a grain of sand. Either an ocean sediment layer is far thinner than proposed, say McEwen and colleagues, or there was never any ocean.

Not that Mars has dried out entirely. Sixty-kilometer Mojave crater looks for all the world as though drenching rains had gouged its slopes and dumped the debris in great conical fans (*Science*, 9 April 2004, p. 196). With a closer look through HiRISE, McEwen and his team think they see a deeper source for the water. Rather than water falling from the sky, they think an impactor may have hit a water-rich crust, creating muddy debris that flowed down to form fans. And HiRISE imaged gullies possibly millions of years old that are "most easily explained as flowing water," says McEwen.

But the tendency of HiRISE observations to diminish the role of liquid surface water may reinforce recent trends. Ice and snow have obviously moved around the planet when Mars periodically tilted on its axis, but observations from the Opportunity and Spirit rovers reveal excruciatingly slow rates of erosion (*Science*, 8 April 2005, p. 192). Running water could not have been much of a player in the past 3 billion years or more, researchers are concluding. And the rust-colored martian visage long attributed to moist weathering seems to be only a thin patina on fresh rock untouched by the eons (*Science*, 22 August 2003, p. 1037). A slight dampness may have sufficed.

Even the early days of Mars—often called "warm and wet"—are looking drier. The apparent remains of "shallow, salty seas" where Opportunity roved have shrunk to ephemeral puddles in a hyperarid desert (*Science*, 5 January, p. 37). When planetary scientists gather next month to narrow their landing site options for the next Mars rover, their search for signs of martian water will need be well focused indeed.

–RICHARD A. KERR

Say what? Panbanisha ponders lexigrams.

LINGUISTICS

Read My Slips: Speech Errors Show How Language Is Processed

Researchers are analyzing spoonerisms and other slips of the tongue to help understand how humans—and even apes—can comprehend and use language

Kanzi, a 27-year-old bonobo, knows the difference between a blackberry and a hot dog. But sometimes, when researchers asked him to touch the abstract visual symbol, called a lexigram, that means blackberry, he touched the lexigram for hot dog, blueberries, or cherries instead.

Kanzi's errors weren't random mistakes, nor an indication of apes' language limitations, says Heidi Lyn, a comparative cognitive scientist at the University of St. Andrews in Fife, U.K. Rather, they show the complex way in which his mind had organized the lexigrams. For example, if Kanzi made a mistake when asked for "blackberry," he was more likely than chance to choose a lexigram for another fruit, much as you or I might say "red" instead of "black," says Lyn, whose paper on Kanzi's mistakes was published online in *Animal Cognition* in April and will appear in print later this year or early next.

Analyzing errors for insight into the covert mental processes of animals is a new direction for a technique that language scientists have used for 40 years to study language processing in humans. For all its power, human language remains something of a scientific mystery. Researchers are still struggling to understand exactly how humans hear, comprehend, and produce words and sentences. Slips of the tongue, or linguistic mistakes made inadvertently by speakers who do know the correct form, offer potent clues about language processing in the brain. Speech error research is currently on the upswing with new methods and theories and increased attention to groups such as children and users of sign language—and, now, animals. "We have a long way to go before we understand how to put the multiple pieces of language systems together in the seamless way that we experience it," says psycholinguist Merrill Garrett of the University of Arizona, Tucson, who has studied slips of the tongue since the 1970s. "Error profiles that arise during spontaneous conversation are going to be an important part of the agenda."

Barn doors and darn bores

Early in the 20th century, collecting speech errors was chiefly a hobby, especially for people who found Freud's emotional explanations lacking. (Psychoanalysis had no way to account for the diverse, often mundane slips of the tongue that people make.) In the 1960s, Noam Chomsky sparked a wave of grammatical theorizing that transformed speech errors into theoretical gold. Linguist Victoria Fromkin, among others, argued in the late 1960s that speech errors showed that abstract mental units of sounds and words were also concrete symbols in speakers' minds.

Using speech errors as scientific data posed some problems: Waiting for speakers to make an error required an inordinate amount of time, and some questioned the reliability of what listeners heard. But the field got a boost in the 1970s when researchers created ways to elicit many (but not all) types of speech errors in the lab. One method involved giving people word pairs like "duck bill," "dart board," and "dust bin," then asking them to say "barn door." About 10% of the time, subjects said "darn bore." By eliciting speech errors, researchers can control for higher frequency sounds (in English, "s" is more frequent than "k") and words ("latrine" is more frequent than "tureen"). Words used more frequently are less likely to be involved in speech errors. For example, more errors occur with content words ("cat," "hat") than grammatical words ("the," "in"), because grammatical words are used more frequently. The effect of frequency also implies that what one usually talks about affects how one slips.

Lyn was the first to apply the study of errors to bonobos. Kanzi and a female bonobo, Panbanisha, who now live at the Great Ape Trust in Des Moines, Iowa, can comprehend instructions and descriptions in spoken English, and they can respond by using 384 lexigrams, which they touch on a keyboard. From 1990 to 2001, researchers tested the bonobos thousands of times, showing them a photo or lexigram or saying an English word. The bonobos then had to select the matching lexigram. The apes chose correctly 12,157 times and made 1497 incorrect choices, although no one thought to consider the errors as data until now.

Handy. German signers can catch more of their mistakes than speakers can.

Lyn found that Kanzi and Panbanisha have arranged hundreds of lexigrams in their minds in a complex, hierarchical manner based mainly on their meaning. She coded the relations between all 1497

CREDITS (TOP TO BOTTOM): GREAT APE TRUST; EVA WALESCHKOWSKI

sample-error pairs along seven dimensions, including whether the lexigrams looked alike, had English words that sounded alike, or referred to objects in the same category. She found that the errors were not random but patterned. If the lexigram stood for "blackberry," the error was more likely than chance to sound like blackberry, be edible, be a fruit, or be physically similar. Errors were also more likely to be associated with more than one category. For example, "cherries" are both edibles and fruits, and the word sounds like the correct one, "blackberries." All this indicated to Lyn that mental representations of the lexigrams must be stored not as simple one-to-one associations but in more complex arrangements. This suggests that, given the chance, bonobos and other apes can acquire systems of meaning that are closer than anyone has thought to what humans do, and that some aspects of language acquisition are not unique to humans. "We begin to see that the biological or species variable is far less important than we thought," says Susan Savage-Rumbaugh of the Great Ape Trust.

Kid talk. Children make slips in stages, as they acquire language.

CREDIT: HOLGER WINKLER/A.B./ZEFA/CORBIS

Out of the mouths of babes

Lyn's analysis is not the first to study errors in creatures that haven't mastered all the complexities of human speech: For about 20 years, researchers have also used speech errors to study language acquisition in children. Kids do say the darnedest things, but by definition, the true errors are the ones they make with linguistic levels and units they know, explains linguist Jeri Jaeger of the University at Buffalo in New York state, who in 2005 published a book that capped 20 years of collecting kids' slips, many of them from her three children. It was the first study of the same children's speech errors over a long period, allowing her to match their errors with their stages of language development. Jaeger's collection is "unique," says linguist Annette Hohenberger of Middle East Technical University in Ankara, Turkey, and shows how slips change over time.

Distinguishing true slips took a linguist's ear and a mother's patience. Jaeger's youngest daughter's exclamation that "She already showed me tomorrow!" wasn't a true slip, because she didn't yet know the meaning of "yesterday." On the other hand, at 16 months, her eldest daughter said "one two three, one two three, one tuwee"—a fusion of "two" and "three," which was a true slip because she knew the two words were distinct and had regularly pronounced them correctly. This anchors Jaeger's point that children only make slips with what they know.

Analysis of such speech errors can provide a novel perspective on how children acquire language. Linguists have debated, for instance, whether children need syntactic knowledge to speak in two-word clumps. Jaeger says no. Her data show that when children begin to combine words, at about age 2, they don't blend phrases or confuse intonations. Such slips require a mature knowledge of syntax. Not until children speak in sentences of three or more words do syntactic errors, such as "sit down this immediately!" (a blend of "sit down this minute" and "sit down immediately") appear.

It's long been known that children make more speech errors than adults, but it wasn't known how or if aging affected error rates. In 2006, Janet Vousden and Elizabeth Maylor at the University of Warwick in the U.K. published the first study tracking speech errors across the life span and reported no significant increase in total errors between young and older adults. However, compared to children, adults made proportionately more errors in which a sound segment was anticipated (frive frantic fat frogs) rather than perseverated (five frantic fat fogs).

That fits with a widely used model of speech errors developed in the 1980s by cognitive scientist Gary Dell of the University of Illinois, Urbana-Champaign. Most linguists think that words and sounds are stored in a kind of network in the brain, connected by variables such as how they sound, their parts of speech, and their meaning. Dell proposed that when sounds or words stored in such a network are selected, this also strengthens or "activates" neighboring words or sounds, which may be misread as the right ones. In his model, people forced to speak quickly make more errors not because they have more opportunities to do so but because the stimulation of neighboring units has less opportunity to fade. Dell also proposes that practice tends to activate present and future units more than past ones. As a result, the more practice a speaker has, the higher the proportion of anticipatory errors, although overall errors decrease. "Whatever makes you more error-prone makes your errors more perseveratory," explains Dell. Caroline Palmer, a psychologist at McGill University in Montreal, Canada, has found the same effect (among others) in piano performances.

Language need not be spoken, and linguists have long been interested in whether speech and sign are processed the same way. German linguists Hohenberger and Daniela Happ and Helen Leuninger at the University of Frankfurt used a newer method for eliciting slips from German speakers and signers of Deutsche Gebärdensprache (DGS, or German Sign Language), in the first slip study of signers in a language other than American Sign Language. In a series of papers, the most recent published in 2007, they asked speakers and signers to narrate a series of pictures under various stress conditions, such as putting pictures out of order.

They found that all types of slips found in spoken German are also present in DGS, although in different frequencies. The slips also occur with the same basic units. This indicates that signs and words are both stored in the brain as clusters of primary elements that can be flexibly recombined, and it underscores that humans possess a single language faculty regardless of how they deploy it, says Hohenberger.

But there are some differences. For instance, both signers and speakers catch and repair utterances that include mistakes. But signing is relatively slower, so signers catch more errors involving exchanges of individual signing elements, such as hand shapes or location of the sign.

Because of this, Hohenberger speculates that slips of the hand may next contribute to an emerging question in slip-of-the-tongue research. Based on ultrasound studies of speakers' tongues as they make sound exchanges (better known as spoonerisms, such as "jeef berky" instead of "beef jerky"), phonetician Marianne Pouplier of the University of Munich, Germany, has suggested

in several recent papers that speakers don't substitute one whole sound segment for another as was previously thought. Rather, they attempt to pronounce the two sounds at the same time. This way of thinking about speech errors—as a collision of motor commands rather than as substitutions of mental symbols—might be more reliably investigated in slips of the hand, Hohenberger says, because researchers can capture the slower hand movements more clearly than tongue movements.

Although error studies offer intriguing data, their implications are not always clear. Take the bonobo findings. The apes confused fewer target-error pairs that were either both nouns or both verbs, implying that they don't take note of parts of speech. "This result argues against the claims made elsewhere that Kanzi has spontaneously developed an elementary grammar," says primatologist Robert Seyfarth of the University of Pennsylvania.

But Lyn says the error results don't directly address the question of grammar and don't contradict earlier findings in which bonobos appeared to prefer certain semantic sequences. Instead, she says, "the results support the idea that [apes'] representation of semantic information is much more complex than has been shown to date."

Still, the study of bonobo errors does rebut two frequent criticisms of ape language research: that the apes have simply been trained to respond, and that researchers may inadvertently shape the bonobos' responses. Errors can't be trained, nor can patterns of errors be deliberately produced. And if researchers were subtly guiding the apes by eye gaze or body posture, Kanzi and Panbanisha might have made far more errors based on simple proximity in the keyboard.

Lyn plans to continue analyzing the error data for other insights into the bonobos' conceptual world. "For me, the error analysis was not to just study one aspect of their symbolic representation," Lyn says, "but to get a glimpse of how it all hangs together." Such a big question hasn't been answered for human language, either, but speech errors will likely be central to the search. Says the University of Arizona's Garrett: "We have most certainly not reached the limits of that kind of research." **–MICHAEL ERARD**

Michael Erard is the author of *Um…: Slips, Stumbles, and Verbal Blunders, and What They Mean*.

EUROPEAN UNIVERSITIES

Barroso's Brainchild

Thanks to the influence of José Manuel Barroso, Europe may soon have its new European Institute of Technology. But few scientists are celebrating

"Just think what Europe could be. … Think of its untapped potential to create prosperity and offer opportunity and justice for all its citizens." Thus began a February 2005 memorandum from José Manuel Barroso, president of the European Commission—the European Union's (E.U.'s) executive branch—aimed at salvaging the Lisbon strategy. This ambitious plan to create economic growth and jobs in Europe was faltering and, Barroso wrote, "immediate action" and "a new start" were needed.

Next week, the European Parliament (EP) is slated to vote on one of the remedies Barroso presented in his memo: the European Institute of Technology (EIT). As *Science* went to press, one major issue—where to find the €300-plus million now budgeted for the project—remained unresolved, and the commission and the Parliament were in frenetic discussions. A commission spokesperson said that a solution was "imminent."

Yet few in the European research community are elated. A supposed engine for Europe's economy, EIT was envisioned as bringing together the smartest minds around top-notch research that will lead to new industries. Its name echoes that of the Massachusetts Institute of Technology (MIT) in Cambridge to show that the commission is aiming high. A series of reports, however, has argued that the plan will do very little for innovation in Europe.

The League of European Research Universities, for instance, concluded in a study last year that the EIT plan was "misconceived and doomed to failure," and Euroscience, a Europe-wide movement of scientists and policy experts, called it "a politically motivated idea, starting from a wrong premise." EIT, says former U.K. science adviser Robert May, "is based on a misunderstanding" about innovation: namely, that it can be bought with government money.

And 2 years of political wrangling have watered down the EIT proposal to the point that critics say it will only add a layer of bureaucracy to the E.U.'s funding system. Indeed, the real MIT could be forgiven for not recognizing itself in its European competitor. EIT won't have a campus; it will be a virtual institute made up of scientists based at universities, research labs, and companies across the continent. It also won't award diplomas, as was originally proposed. And although more money is supposed to flow from various sources, the amount promised so far until 2013 boils down to about €50 million a year, less than 3% of MIT's annual budget and about 13% of what Barroso had proposed.

Homeless institute

EIT is meant to address what is sometimes called the European paradox. Although Europe's scientific output, measured in papers, is bigger than that of the United States—and arguably of the same quality—Europe seems far less able to turn knowledge into thriving industries. The Lisbon strategy, launched in 2000, aimed to reverse the trend and make Europe the world's most competitive and dynamic "knowledge-based economy"—that is, based on high-tech. But a 2004 report by Wim Kok, former prime minister of the Netherlands, concluded that Lisbon was stalled—hence Barroso's call for action.

Despite widespread skepticism, the plan had political legs—apparently because it had been presented by Barroso himself, European policy watchers say. "He put his entire weight behind it," says Helga Nowotny, vice-chair of the European Research Council (ERC) and another critic of the idea. "Governments just couldn't just say no."

The EIT plan has changed considerably, however. Initially, the commission entertained the idea of a brick-and-mortar, degree-granting institute somewhere in Europe. Poland and other new E.U. members began lobbying for the prize, offering significant financial incentives. After a wide consultation made clear that countries were unlikely to agree on a site—and that universities didn't like a new competitor—EIT went virtual. In the commission's formal proposal in October 2006, EIT became a small governing board plus six or more Knowledge and Innovation Communities (KICs), independent networks that would each focus on a different field and

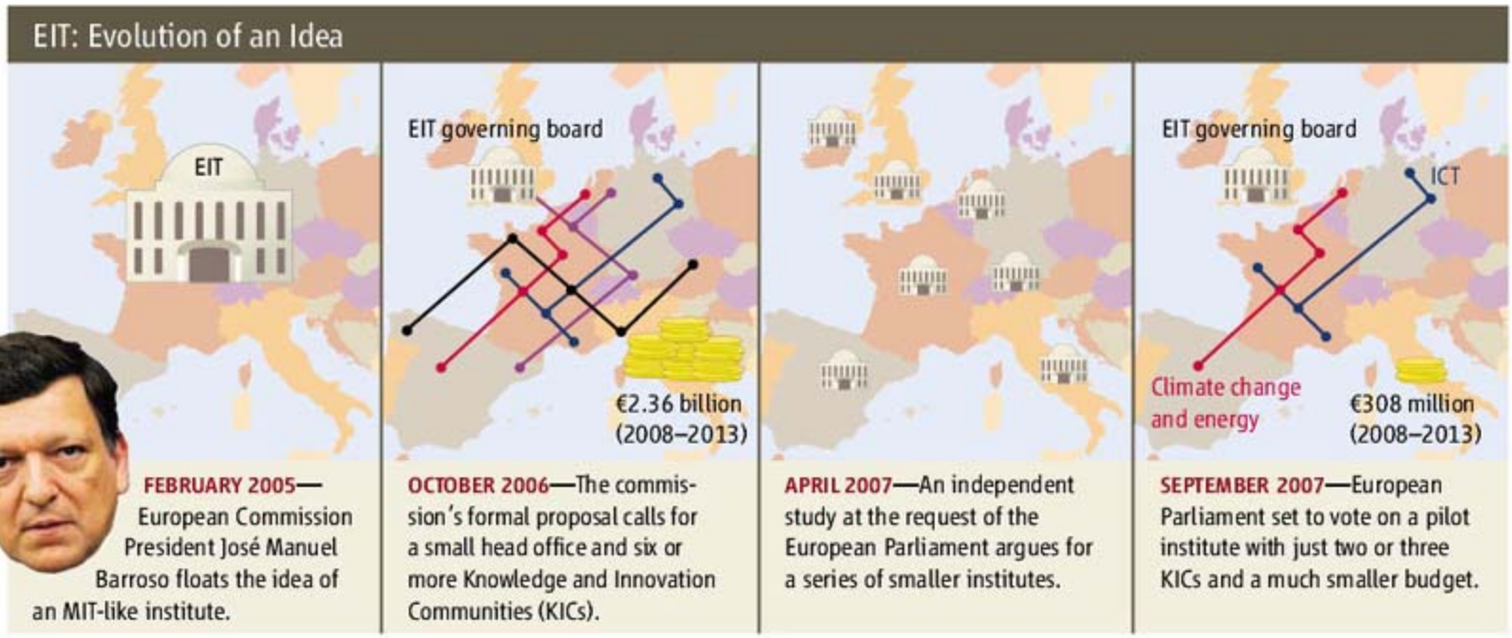

employ scientists at existing institutes and companies around the E.U. Its budget, however, would still have been a healthy €2.36 billion for the period 2008–2013.

Laws and new initiatives such as this begin with the E.U. Commission, but they need to be approved by the Council of the E.U.—in which ministers of member states meet—and by the Parliament. Insiders say that in the council, several countries, including the United Kingdom and Germany, were very skeptical about the EIT plan. Several Parliament committees were divided as well. But intense diplomacy by the German government, which chaired the E.U. during the first 6 months of this year, led to a compromise in June. A key Parliament committee endorsed EIT in July.

Negotiations chipped down its scope, however, leaving a pilot phase of 4 years and a gradual start with just two or three KICs. (Climate change, energy, and information technology were suggested as their themes.) They also took away EIT's right to give out diplomas, replacing it with an EIT label on existing university degrees. To top it off, "Innovation" was added to EIT's name—although the acronym was left intact.

The money issue remains unresolved. Even if the commission does find the €308 million, it's a long way away from what Barroso wanted, and it's not clear what other sources will be tapped. The KICs can seek aid from Europe's Framework Programme 7 (FP7), the E.U.'s main source of research funding. But Parliament members want guarantees that the centers won't get preferential treatment. "We don't want them to cannibalize" other programs, says Reino Paasilinna of Parliament's Industry, Research and Energy committee.

Barroso's plan for EIT has always anticipated a significant financial contribution from industry—the intended beneficiary of the institute's output—but that support has not yet materialized. The problem is that industry cannot commit to an institute that doesn't exist, says Horst Soboll, chair of the now-defunct European Research Advisory Board and a former director of technology at DaimlerChrysler. That might change once the KICs take shape and concrete business opportunities come up, he says.

To EIT critics, the final compromise isn't an institute but a funding mechanism, and one that looks remarkably like existing ones. Most of the FP7 money also goes to topic-specific Networks of Excellence; other E.U. funding streams favor large collaborative efforts as well. As to innovation, such scattered organizations are unlikely to generate strong ties with industry, says Peter Tindemans, an independent consultant who studied the commission's plan together with Luc Soete of the United Nations University in Maastricht at the request of EP. "There's not a shadow of a chance that this will have any major impact," says Tindemans.

But a senior official at the commission's directorate-general for education—who, in accordance with commission rules, declined to be named—says that analysis is wrong. Already, there has been an "unending procession" of companies telling the commission that EIT is a "wonderful idea" and that they would like to participate, says the official. Still, Nowotny predicts KICs will have trouble hiring excellent staff, because researchers with thriving careers are unlikely to jump to an organization whose future is so uncertain.

Solving a paradox

Is there a better alternative? There's no consensus among the innovation experts, although there are some other proposals. In their study, Tindemans and Soete launched the idea of a Cluster EIT, a series of smaller institutes with 300 to 500 researchers, each focusing on a specific field and big enough to attract company interest. But Parliament has done nothing with the idea.

Frank Gannon, former director of the European Molecular Biology Organization in Heidelberg, Germany, believes the answer is even simpler. His solution is to bet more on ERC, the funding agency launched in February that picks investigator-initiated projects based on merit without any political or geographical considerations (*Science*, 2 March, p. 1205). "If we had more high-quality research, I think the European paradox would just disappear," says Gannon, who is trying the same recipe in his new job at the helm of the Science Foundation Ireland.

May, meanwhile, believes the problem isn't in the science funding at all—it's Europe's "culture of coziness and adversity to risk" that makes people shy to invest in new technologies. To him, changing tax and bankruptcy laws to reward entrepreneurship might be a better solution.

For now, the research community has largely resigned itself to the idea of EIT. Whether the slimmed-down version of the grand idea proposed in 2005 can help make Europe a "beacon of economic, social, and environmental progress to the rest of the world," as Barroso hoped—well, they're not holding their breath.

–MARTIN ENSERINK

CREDIT: CHRISTOPHE KARABA/EPA/CORBIS

Between humans and computers 1684

How Easter Island lost its forests 1692

LETTERS

edited by Etta Kavanagh

Factory Flies Are Not Equal to Wild Flies

IN HIS NEWS FOCUS ARTICLE "WELCOME TO ETHIOPIA'S FLY FACTORY" (20 July, p. 310), Martin Enserink highlights the controversy generated by the use of the sterile insect technique (SIT) and its application for controlling and eradicating tsetse (*Glossina* spp.) in Africa. Although it is clear that SIT has a history of successes and failures, and has both champions and critics, much of the focus, especially in this discussion, is on costs and benefits from the social and political perspectives and the problems posed by a multitude of tsetse species. We agree that such a focus is useful and necessary, but it is not sufficient.

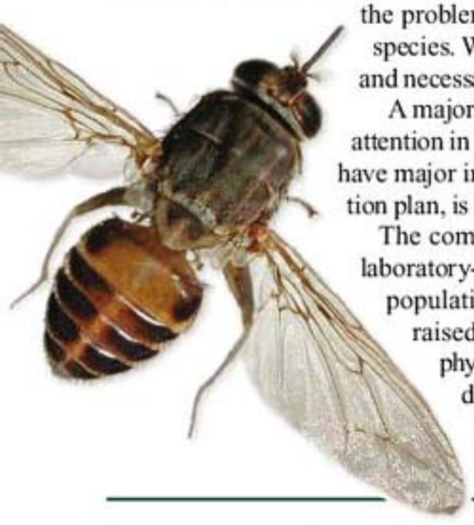

A major avenue of concern receiving scant attention in Enserink's article, and one that will have major implications for Ethiopia's eradication plan, is laboratory adaptation of the flies. The compatibility and competitiveness of laboratory-reared tsetse for release into wild populations are concerns that have been raised previously in behavioral (*1*) and physiological work (*2*, *3*). Substantial differences are typically found between natural populations and colony-reared flies, ranging from physiological tolerance of lethal temperatures to mating compatibility. Moreover, feeding behavior in tsetse appears to be a learned response obtained during early adult development (*4*), suggesting that laboratory-reared flies raised on artificial membranes may not feed on wild animals. Thus, they would not survive for more than a few days in the wild. Similarly, caged rearing conditions are known to be deleterious to flight and locomotor performance because flight muscle development is restricted, which in turn may limit mating success in the wild (*5*). Other work on insects has shown that laboratory adaptation substantially alters animal performance (*6*).

Thus, the SIT program for eradicating tsetse hinges on a crucial and neglected question: the performance capabilities in the wild of flies reared in the laboratory. If colony flies are substantially outperformed by their wild counterparts, which seems likely on present evidence, the SIT program might fail for reasons that have little to do with financial investment, commitment, or species numbers.

JOHN S. TERBLANCHE AND STEVEN L. CHOWN

Centre for Invasion Biology, Department of Botany and Zoology, Stellenbosch University, Stellenbosch 7602, South Africa. E-mail: jst@sun.ac.za

References

1. J. Brady, A. J. Crump, *Physiol. Entomol.* **3**, 177 (1978).
2. J. S. Terblanche *et al.*, *Am. J. Trop. Med. Hyg.* **74**, 786 (2006).
3. P. Taylor, *Physiol. Entomol.* **2**, 317 (1977).
4. J. Bouyer *et al.*, *Biol. Lett.* **3**, 113 (2007).
5. E. Bursell, *Proc. R. Entomol. Soc. London* **36A**, 69 (1961).
6. A. A. Hoffmann *et al.*, *Evolution* **55**, 1621 (2001).

Promoting Science and Technology from the Top

GOVERNMENTS IN DEVELOPING COUNTRIES are the primary source of resources and guidance for science and technology (S&T). Despite an apparent recognition of the importance of S&T for socioeconomic growth and poverty reduction (as shown by a modicum of investment), the full benefits of S&T have not been achieved. Chief among the reasons for this are (i) lack of political vision and will, (ii) low business confidence in S&T and innovation, (iii) imprecise decision-making and archaic management, (iv) suboptimal investments, (v) national inertia and illiteracy, (vi) puerile dependency, (vii) a lack of imagination, and (viii) corruption.

S&T are tools that motivate, propel, and dictate change, which often demands incisive administrative management and cultural shifts of varying degrees. S&T may threaten ministries jostling for power. Furthermore, bureaucracy is steeped in the orthodoxy of seniority and political favoritism and tends to be uncritically rigid and suspicious of fresh intellectual talent. Changes in management structures and methods, decision-making, implementation, and reviews of effectiveness and coordination are often stoutly resisted.

Consequently, national S&T management bodies and coordinating systems that are installed to implement policies and execute plans often prove ineffectual. Strong political leadership at the top of the S&T structure is needed. Prime ministers or presidents should take charge.

The decision to have prime ministers or presidents lead the knowledge transfiguration of a country will circumvent unnecessary layers of government, while quelling political rivalries. Additionally, the private sector needs assurance and accessible incentives from government to support research and development (R&D) and thereby create new businesses, jobs, and skills. The top levels of government must make the necessary budgetary decisions to support local R&D, which has, until now, been left to the whims and fancies of foreign technical assistance and investment. It is very difficult for ministers of finance and other cabinet officers to allocate funds to seemingly intangible S&T development when there is pressure on the budget to satisfy immediate and pressing needs like education, health care, and roads. Science and technology courses

CREDIT: SAN-HO CORREWYN/INSTITUTE OF TROPICAL MEDICINE

specifically designed to educate top political leaders regarding the long-term benefits are therefore necessary.

The ultimate challenge is to convince busy prime ministers and presidents to take charge of these efforts. This is where national S&T advisors are vital. **ARNOLDO K. VENTURA**

Special Science and Technology Advisor to the Prime Minister of Jamaica, Office of the Prime Minister, Kingston 6, Jamaica.

How Old Is the Human Presence on Cyprus?

ALBERT AMMERMAN'S CONTRIBUTIONS TO archaeology are substantial, but his comments about Cyprus may mislead the reader ("Exploring the prehistory of Europe, in a few bold leaps," J. Bohannon, News Focus, 13 July, p. 188). Current studies on this Mediterranean island have indeed indicated a human presence much earlier than previously believed. As the article notes, research by Peltenburg and others has pushed back the island's Neolithic presence to ~8200 calibrated B.C.E.

Ammerman suggests that his sites are approximately 12,000 years old and are the remains of seafaring pre-Neolithic hunters and gatherers. Whether or not aeolianite dunes would have made suitable camps, we commend Ammerman for examining ephemeral sites that all too often have been ignored. However, he believes that these are "the oldest evidence of seafaring in the Mediterranean," a claim presently based only on artifactual data, and as Peltenburg points out, "independent evidence" is needed to confirm their antiquity.

An early human presence on Cyprus has been well established at Akrotiri Aetokremnos for nearly two decades (*1*). It is thus no surprise that there may be other sites dating to this time period, and many of us hope that Ammerman's sites are as old as he claims. But until this can be confirmed by defensible dating of materials in good context, these sites should not enter the literature as examples of a pre-Neolithic presence on Cyprus. **ALAN H. SIMMONS[1] AND ROLFE D. MANDEL[2]**

[1]Anthropology and Ethnic Studies, University of Nevada, Las Vegas, 4505 Maryland Parkway, Las Vegas, NV 89154, USA. [2]Kansas Geological Survey, University of Kansas, Lawrence, KS 66047, USA.

Reference

1. A. Simmons, *Faunal Extinction in an Island Society* (Klewer/Plenum, New York, 1999).

Nominations for the Penn Vet World Leadership in Animal Health Award are being accepted now through December 12, 2007.

The World Leadership in Animal Health Award has been created as a prestigious international tribute to veterinarians whose research and/or other contributions have profoundly influenced the course of animal and/or human health. The annual award, a medal and cash prize of US $100,000, is intended to heighten public awareness of veterinary medicine's essential contributions to the health and well-being of all types of animals, the environment, and society as a whole.

The World Leadership in Animal Health Award will be presented to a veterinarian who has dramatically changed the practice and image of the profession and substantially influenced the lives and careers of others. Nominations are being accepted now through December 12, 2007 at www.vet.upenn.edu/worldaward/nominationguidelines.pdf

The awards program has been established by a generous gift from the Vernon and Shirley Hill Foundation.

World's Largest Mouse ES Cell Library
CLICK ON IT

TIGM
TEXAS INSTITUTE FOR GENOMIC MEDICINE
713-677-7429 | 888-377-TIGM

THE
TACONIC
ADVANTAGE

ADME-Tox

Another Taconic breakthrough:
The first and only portfolio
of commercially available, fully
licensed transgenic ADME-Tox
mouse models.

Includes:
Mrp2
Oct1/2
Bcrp
Mdr1a
Mdr1a/b
Mdr1a/b-Bcrp

Coming soon:
PXR
and
HRN™

Available exclusively from Taconic.

Call today to put the Taconic
Advantage to work for you.

Taconic
Smart Solutions To Improve Human Health

1.866.382.6549
www.taconic.com/adme_sci

Ethics and Refinement in Animal Research

SCIENTISTS AND JOURNALS COULD AND should do more to secure the ethical standards of animal use in biomedical research. Scientists often justify animal use by referring to the scientific value and biomedical importance (*1*). However, except from a purely anthropocentric perspective, ethical concerns about compromised animal welfare cannot be eased by human benefits alone (*2*). It is equally important that the benefits are achieved with a minimum of negative effects to the animals involved. Thus, scientists must apply "refinement," the third R of the so-called 3 Rs (*3*). But scientists sometimes seem to do less than they should, and journals fail in their duty to enforce high ethical standards.

We studied the use of animals as models for Huntington's disease. In this model, refinement should focus on limiting the negative impact of declining sensorimotor function as the neurodegenerative disease progresses: Housing adaptations facilitating food and water intake and humane endpoints (using earlier, less severe clinical signs as endpoint parameters rather than awaiting spontaneous death) are two possible approaches (*4*). We asked to what extent animal welfare problems and refinements addressing them were reported in publications of the most common rodent models by analyzing 90 research reports published in international peer-reviewed journals during 2003–04. These include quinolinic acid (*5*, *6*) and 3-nitropropionic acid (*6*, *7*) administration to rats and mice and R6/1, R6/2, and N171-82Q transgenic mice (*8*–*10*). Our results show that the majority of experiments (53) were in the two most severe categories, in which animals have sensorimotor deficits interfering with their capacity to eat and drink normally from the cage top. Very few papers reporting such severe experiments included information on refinement measures: Out of 14 survival studies of transgenic animals with a progressive neurodegenerative phenotype, only 6 referred to humane endpoints and only 2 to housing adaptations. Among the majority of studies referring to compliance with official regulations and/or efforts to reduce animal suffering, we also found experiments using far from best practices, such as administration of rising neurotoxin doses until high animal mortalities were reached.

Journals should ensure that referees seriously consider whether submitted studies were indeed carried out with the smallest achievable negative impact on the animals. Although important results might be found in a paper not complying with current refinement standards, a journal like *Science* should still reject such a paper, thereby sending an important signal to the research community, similar to what is common practice for studies involving human research subjects. Furthermore, journals should give authors space to describe refinement and welfare precautions. We demonstrate that such descriptions are rare, which means that other researchers cannot benefit from refinement ideas (*11*), in turn implying a real danger that animals will have to suffer unnecessarily, and that animal welfare will be improved later than necessary.

I. ANNA S. OLSSON,[1,2] AXEL K. HANSEN,[3] PETER SANDØE[2]

[1]Laboratory Animal Science, IBMC–Instituto de Biologia Molecular e Celular, Universidade do Porto, Rua do Campo Alegre 823, 4150-180 Porto, Portugal. [2]Danish Centre for Bioethics and Risk Assessment, Faculty of Life Sciences, University of Copenhagen, Rolighedsvej 25, 1958 Frederiksberg C, Denmark. [3]Division of Laboratory Animal Science and Welfare, Faculty of Life Sciences, University of Copenhagen, Dyrlaegevej 88, 1870 Frederiksberg C, Denmark.

References and Notes

1. E. Frankel Paul, J. Paul, Eds., *Why Animal Experimentation Matters: The Use of Animals in Medical Research* (Transaction Publishers, New Brunswick, NJ, 2000).
2. I. A. S. Olsson, P. Robinson, K. Pritchett, P. Sandøe, in *Handbook of Laboratory Animal Science*, G. Van Hoosier, J. Hau, Eds. (CRC Press, Boca Raton, FL, ed. 2, 2002), pp. 13–30.
3. W. M. S. Russell, R. L. Burch, *The Principles of Humane Experimental Technique* 1959/1992 (http://altweb.jhsph.edu/publications/humane_exp/het-toc.htm).
4. D. B. Morton, J. Hau, in *Handbook of Laboratory Animal Science*, G. Van Hoosier, J. Hau, Eds. (CRC Press, Boca Raton, FL, ed. 2, 2002), pp. 457–486.
5. M. F. Beal *et al.*, *Nature* **321**, 168 (1986).
6. E. Brouillet, F. Condé, M. F. Beal, P. Hantraye, *Prog. Neurobiol. (Oxf.)* **59**, 427 (1999).
7. E. Brouillet *et al.*, *J. Neurochem.* **60**, 356 (1993).
8. L. Mangiarini *et al.*, *Cell* **87**, 493 (1996).
9. E. Hockly, B. Woodman, A. Mahal, C. M. Lewis, G. Bates, *Bn Res. Bull.* **61**, 469 (2003).
10. G. Schilling *et al.*, *Hum. Mol. Genet.* **8**, 397 (1999).
11. H. Würbel, *Nature* **445**, 357 (2007).
12. We thank colleagues in the COST Action B24 Laboratory Animal Science and Welfare; researchers N. Dantuna, C. Maynard, C. Kosinski, E. Diguet, D. Emerich, and H. H. Phuc Nguyen, who provided information on clinical signs in different models; and P. Robinson, who commented on a previous version of the Letter. Preparation of this Letter was part of the interdisciplinary project Comparative Genomics of Man and Pig, funded by the Danish Agency for Science, Technology and Innovation.

Letters to the Editor

Letters (~300 words) discuss material published in *Science* in the previous 3 months or issues of general interest. They can be submitted through the Web (www.submit2science.org) or by regular mail (1200 New York Ave., NW, Washington, DC 20005, USA). Letters are not acknowledged upon receipt, nor are authors generally consulted before publication. Whether published in full or in part, letters are subject to editing for clarity and space.

CORRECTIONS AND CLARIFICATIONS

Editors' Choice: "Timing is everything" (31 August, p. 1147). The phrase "…HPV clearance rates—measured as cell-mediated immunity to the virus—were comparable…" should have read "…HPV clearance rates—a measure of cell-mediated immunity to the virus—were comparable…"

Newsmakers: "Indelible" (10 August, p. 731). George Cotzias's name was misspelled in the story.

Policy Forum: "Critical assumptions in the Stern Review on climate change" by W. Nordhaus (13 July, p. 201). On page 202, part of reference 7 was incorrect; the complete reference is K. J. Arrow *et al.*, *Climate Change 1995—Economic and Social Dimensions of Climate Change*, J. Bruce, H. Lee, E. Haites, Eds. (Cambridge Univ. Press, Cambridge, 1996), pp. 125–144.

Policy Forum: "Taking science out of the box—foresight recast" by D. A. King and S. M. Thomas (22 June, p. 1701). The URL in reference 6 is incorrect. It should be www.discoverysoftware.co.uk/FloodRanger.htm.

Perspectives: "Nuclear actin as choreographer of cell morphology and transcription" by J. I. Wu and G. R. Crabtree (22 June, p. 1710). The surname of the second author, while correctly spelled in print and in the online article display, was initially spelled incorrectly in the electronic metadata associated with the online article, which led to an incorrect spelling in the electronic table of contents and in online search results, as well as in some indexing services not affiliated with *Science*. The metadata have been corrected; the proper spelling of the second author's surname is Crabtree.

Reports: "Structure of the multidrug transporter EmrD from *Escherichia coli*" by Y. Yin *et al.* (5 May 2006, p. 741). On page 744, following the sentence "In addition, certain single-site mutations in the cytoplasmic halves…," only reference 17 should be cited. In Fig. 2C, residue EmrD T128 should be EmrD T119 (and the "+" over the corresponding MdfA A137 shifted to MdfA A128 in fig. S1). Finally, the asterisk denoting residue MdfA A324 in fig. S1 was misformatted and should lay over MdfA Y323. The corrected figure has been added to the Supporting Online Material for the Report (see www.sciencemag.org/cgi/data/312/5774/741/DC1/1). The implementation of these corrections does not change the proposed mechanism, as the shifted residues still fall within the boundaries of the proposed selectivity filter.

TECHNICAL COMMENT ABSTRACTS

Comment on "Organics Captured from Comet 81P/Wild 2 by the Stardust Spacecraft"

Maegan K. Spencer and Richard N. Zare

Sandford *et al.* (Reports, 15 December 2006, p. 1720) reported on organic compounds captured from Comet 81P/Wild 2 by the Stardust spacecraft. We emphasize the difficulty in assigning the origin of compounds detected diffusely along particle impact tracks and show that rapid heating of aerogel that has never been exposed to cometary particle capture can generate complex aromatic molecules from low-mass carbon impurities present in the aerogel.

Full text at www.sciencemag.org/cgi/content/full/317/5845/1680c

Response to Comment on "Organics Captured from Comet 81P/Wild 2 by the Stardust Spacecraft"

Scott A. Sandford and Donald E. Brownlee

Caution must be taken in interpreting measurements of organics in Stardust samples. In particular, as noted in Sandford et al. and reinforced in the comment by Spencer and Zare, one component of Stardust organics, the low-mass polycyclic aromatic hydrocarbons seen diffusely along track surfaces, should be treated cautiously because they may be due to impact conversion of aerogel carbon.

Full text at www.sciencemag.org/cgi/content/full/317/5845/1680d

Applied Biosystems Real-Time PCR Licensing Programs

Applied Biosystems is proud of its historical role in developing basic PCR. As the exclusive licensor of real-time PCR and certain PCR improvement patents, Applied Biosystems continues to provide access to these newer technologies in a variety of ways.

End user customers can obtain research rights by purchasing reagents (e.g., DNA polymerase or master mix) bearing label license rights from Applied Biosystems and other licensed suppliers. Specific commercial service rights may also be granted with application kits available from some of these companies.

For companies that wish to obtain rights to manufacture and sell enzymes, application kits (in multiple fields) and/or probes conveying such label license rights, Applied Biosystems has established three worldwide licensing programs:

1 Enzyme Supplier License 2 Application Kit Manufacturing License 3 Probe Manufacturing License

Service and in-process testing laboratories that home-brew kits can access the process rights they need through Applied Biosystems' Commercial Services License and Internal Quality Assurance/Control License. Available fields include contract research, forensics and human identity testing, animal identity and breeding, environmental, agricultural, food, and GMO testing, and internal quality control testing.

For information on any or all of these programs, please contact: Director of Licensing, Applied Biosystems, 850 Lincoln Centre Drive, Foster City, CA 94404, USA | PHONE 650.554.7959 | EMAIL director_licensing@appliedbiosystems.com | FAX 650.638.6071

Applied Biosystems

COMPUTERS

A Classic Reconfigured

Brenda Laurel and Rob Tow

Human–Machine Reconfigurations
Plans and Situated Actions. 2nd ed.
by Lucy A. Suchman
Cambridge University Press, Cambridge, 2007. 326 pp. $80. ISBN 9780521858915. Paper, $29.99. ISBN 9780521675888.

In *Human–Machine Reconfigurations*, Lucy Suchman updates her seminal 1987 book *Plans and Situated Actions* (*1*). Like the earlier work, the revision takes on the issues implicit in the construction of artificial intelligence (AI). Although the book is described as being about interface design, Suchman (who spent 20 years as a researcher at Xerox's Palo Alto Research Center before moving to Lancaster University's Centre for Science Studies) remains at heart an anthropologist. She prefaces this book with a lengthy response to the arguments leveled at the earlier work by the anthropology community. It is only after the nine chapters reprising the 1987 text that Suchman's ideas pick up steam and the writing becomes accessible—or engaging—to designers interested in human-computer interaction. If they can stick with the scholarly tone long enough to get to the author's new thinking, members of that audience will find the ideas in the book potentially useful.

Up through the conclusion of the first edition, Suchman's writing, clearly aimed at the anthropology and social science communities, suffers from the coded terminology and dense sentence construction of the hidebound academic. The opening chapter, Readings and Responses, demonstrates the impact that her work has had in those domains but will discourage the "outsider" designer or engineer from proceeding further into an unfamiliar jungle of discourse. Fortunately, when she starts to reveal new methods, observations, and ideas in the later chapters, Suchman begins to speak as a person unafraid of using first-person pronouns. At last, one thinks, the arguments will not be Lilliputian, but rather large, furry ideas that anyone can hear stomping into the room.

Indeed, the large ideas are there, but they are rare big game very well camouflaged. They range from philosophical and political observations to purely (but importantly) operational ones. For example, Suchman's analysis of how and why corporate marketing types go to such lengths to prevent designers and engineers from directly engaging in human-centered research is both in-your-face and operationally relevant. The construction of "agents" as servants and the tendency of AI to model a service economy is another furry idea—and she persuasively urges that it's high time we considered it in all its implications. But surrounded by the jargon of anthropological discourse, such ideas are not as accessible as they should be to folks who can really do something about them—designers and engineers of human-computer systems.

Suchman gains credibility and shows courage as she moves beyond the traditional field ethnography methodology where the "scientist" (observer) is the measuring instrument. Suchman's use of video, for example, both removes the "interference" of the observer and allows a permanent and exteriorized record to be analyzed and shared. Like the best of contemporary practitioners in design research, she acknowledges that dyads often make for more generative interviews than conversations with single individuals. However, we wish that she had included more active practitioners among her quoted sources and that she had asked those whom she did interview, like Rodney Brooks, more about what they thought they were doing and why. Brooks—an extremely well-read practitioner—demonstrated his sensitivity to the issues involved in the Cog project in many ways, such as the inclusion of a female Christian theologian in his team.

The postmodern feminist critique can often drift into a tone of superiority over those boys who don't know what they're doing. Applied liberally, it paints all with the same brush. But there is a meaningful difference between Rodney Brooks's thoughtful work and some of the snake oil that has been extruded by other self-identified AI researchers. Most of the sources with whom Suchman aligns herself have not actually done engineering or system design. Perhaps coming the closest is Andrew Pickering, who holds doctorates in both physics and science studies and who spent time in residence in at least one research lab, which informed his concept of "mangles of practice" (*2*). But, for example, as much as Katherine Hayles's critical work is to be admired (and as much as it informs this book), it is fundamentally not the same as investigating the ideas and methods of makers themselves. A critique of makers based on the philosophies of nonmakers constitutes a stacked deck.

In her power (and in her voice), Suchman has the opportunity to let go of critique of the past and to instigate a new dialogue regarding the future. By positioning her thinking as living somewhere beyond Donna Haraway's cyborg (*3*), Suchman has gone at least half the distance. She seems to acknowledge that the cyborg was essentially a very serious feminist prank intended to draw our attention to a problematic dualism and an equally problematic re-visioning. She demonstrates that how we view human-computer symbosis depends on how and where we "cut" the relations between humans and machines. Because they and we increasingly act in complex collectives, the locus of agency refuses to adhere to either of the terms of the old dichotomy or even to the monstrous construction of the cyborg; instead it floats.

An obvious step in this new discourse is to look more deeply into biology—a step the book suggests but does not take. Just as much of the human body consists of (nested) "entities" with perception-representation-

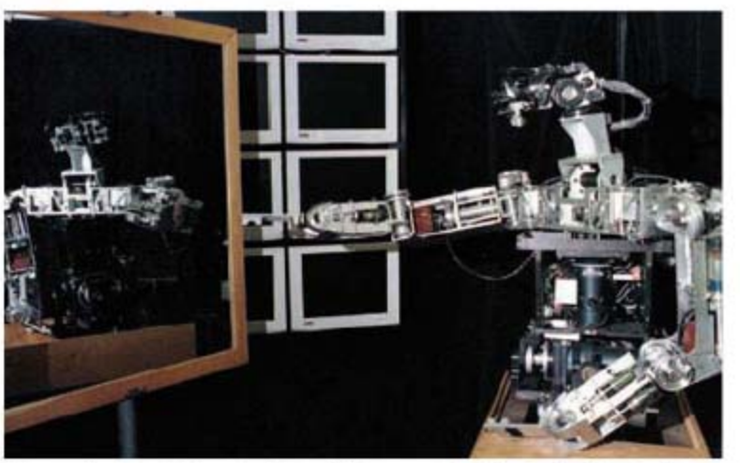

Situated robot. Seeing Rod Brooks's humanoid robot in the lab, Suchman noted "the extended network of human labors and affiliated technologies that afford Cog its agency."

CREDIT: DONNA COVENEY/MIT

Brenda Laurel is at the Graduate Program in Design, California College of the Arts, 1111 Eighth Street, San Francisco, CA 94107–2247, USA. E-mail: blaurel@tauzero.com. Rob Tow is at Tau Zero, 14004 Madrone Place, Los Gatos, CA 95033, USA. E-mail: robtow@tauzero.com

action loops (and thus that possess agency), "entities" that transcend the simple hybrid of human plus machine are intimated by Suchman's work. At work here, taking a lesson from the biological insights of Lynn Margulis, we find something like symbiogenesis: the combination of symbiotic organisms into a single, new organism in which the original partners drop the genetic codes for capabilities that they no longer need for survival. As Margulis challenges traditional evolutionary biology, and as symbiogenesis challenges the Darwinian notion of descent with modification, so Suchman positions herself to challenge both the old human-tech dichotomy and the rhetorical device of the cyborg. She gives us a beginning place for a new discourse, and we hope she runs with it.

References

1. L. Suchman, *Plans and Situated Actions: The Problem of Human-Machine Communication* (Cambridge Univ. Press, Cambridge, 1987).
2. A. Pickering, *The Mangle of Practice: Time, Agency, and Science* (Univ. of Chicago Press, Chicago, 1995).
3. D. Haraway, *Simians, Cyborgs, and Women: The Reinvention of Nature* (Routledge, New York, 1991).

10.1126/science.1142472

HISTORY OF SCIENCE

Inventing Johannes Müller

Lynn K. Nyhart

What makes a great scientist? His students. Although they do not (usually) make his scientific discoveries or theories for him, it is often students and followers who take their experiences of their mentor's personality and ideas to create the image of the great scientist revered by later generations. In this close study of Johannes Müller, the greatest "great physiologist" of 19th-century Germany, as viewed by seven of his students, the literary scholar, historian, and MacArthur award recipient Laura Otis (Emory University) shows how Müller the person became reconstructed as Müller the historical character. Her compelling analysis asks us to think hard about our access to the past and about how our understanding of long-distant events is shaped by the rhetorical work of past scientists in their everyday working lives.

Müller is an enigma. From 1833, when he assumed the professorship of anatomy and physiology at the University of Berlin, until his death (possibly by suicide) in 1858 at 56, he was Germany's leading physiologist. The author of the leading 19th-century textbook of human physiology, Müller pursued all aspects of physiology—chemical, sensory, anatomical, comparative, developmental, pathological—in a broad program to understand how life worked. He traced physiological functions through experiment, comparison across the span of the animal kingdom, and examination of healthy and diseased structures, and he was committed to rigorous investigation in all these areas. Yet he also believed in a "life force" that held all of living nature together, a view that ran against the increasingly materialistic currents of his scientific times. Letters from his adult years are sparse, and the most vivid portrayals of him come from students. But can we trust them? How can we come to know Müller?

Müller's Lab
by Laura Otis
Oxford University Press, Oxford, 2007.
336 pp. $55, £32.99.
ISBN 9780195306972.

To answer this question, Otis examines the historical constructions and reconstructions of Müller created by Theodor Schwann (of cell theory fame), the microscopists Jakob Henle and Robert Remak, the experimental physiologists Hermann von Helmholtz and Emil du Bois-Reymond (Müller's successor in Berlin), the cellular pathologist Rudolf Virchow, and the evolutionary zoologist Ernst Haeckel. These men, all of whom became distinguished scientists themselves, encountered Müller at different points in his career, for different spans of time, and interpreted him through their varying perspectives and scientific interests. They invented not one Müller but several, each according to his needs.

Through their lenses, Otis reconstructs not only Müller but also Berlin science from the 1830s to the 1890s, painting an almost Brueghelian crowdscape of scientific activity. We see aspiring scientists hunched over their microscopes in the rare windows of their crowded rooming houses for lack of lab space; we see Müller, rector of the University of Berlin in 1848, defending his institution's integrity—and his museum—against student revolutionaries, even as the radical Virchow rushed off to man the barricades and du Bois-Reymond slunk under his covers, avoiding participation altogether by being sick. We see Remak, the orthodox Jew, unable to gain a professorship or even share a convivial meal with his colleagues because of his religion, taking up a side business as an electrotherapist—an undertaking that kept him afloat financially but damaged his scientific reputation. One vivid scene after another brings 19th-century German biology to life.

Above all, though, Otis shows us these men as writers, scientists who knew the power of their words. As she demonstrates, virtually every piece of writing by these ambitious men—not just memos to bureaucratic purse-string holders, but letters, reminiscences, and historical introductions in scientific writings—had a persuasive purpose. Haeckel wrote his parents to demonstrate his diligence as a medical student and simultaneously to express his aversion to a profession as a physician. When du Bois-Reymond wrote the first major biography of Müller, Otis shrewdly argues, he needed to show that Müller had begun a revolution in physiology that only he himself would be able to complete, and then only if he had the institute, equipment, and funding that the Prussian cultural ministry could provide. This profoundly shaped his portrayal of Müller, as did the different agendas of each of the actors whose Müllers Otis delineates. The Müller that emerges from each man is part of a history his students constructed that would lead to their own goals, as they created narratives of the past intended to push history forward in the directions they wanted to take it.

In doing so, however, his students made Müller less than he was. As Otis argues, he is not best understood as the overlapping sum of their descriptions, for his students consistently underestimated him and underrecognized his support of their different projects. Even where they clearly led away from his own commitment to a life force uniting all of life, he advocated their work as fruitful science, supporting them both intellectually and institutionally far more than they acknowledged. Otis's Müller is more than the sum of the recollections and reconstructions of his students.

As powerful as scientists are in constructing biography and history in the course of their careers, and as dependent as historians are on the records scientists leave for their own reconstructions and analyses, Otis shows what historical and literary perspectives can add to scientists' own accounts. Her rhetorical analysis calls attention to the power of scientists' writings in all their forms, while her historical reconstructions make sense of the scientific and personal agendas underlying these scientists' rhetoric. Thus, while we may never know the "real" Müller, we come away with a deeper and richer understanding of the many Müllers his successors created—and of the making of great scientists more generally.

10.1126/science.1146670

The reviewer is at the Department of the History of Science, University of Wisconsin, Madison, 7143 Social Science, 1180 Observatory Drive, Madison, WI 53706–1363, USA. E-mail: lknyhart@wisc.edu

MEDICINE

The Future of Personal Genomics

Routine generation of whole-genome sequences will pose many health system challenges.

Amy L. McGuire,[1] Mildred K. Cho,[2] Sean E. McGuire,[3] Timothy Caulfield[4]

On 31 May 2007, James Watson was handed a miniature hard drive containing his personal genome sequence, which was subsequently uploaded onto publicly accessible databases. Craig Venter's personal genome was published a few months later (*1*). These projects represent research milestones. They also present an opportunity to examine the ethical, social, and clinical implications of personal genomics.

Excitement over these projects has been tremendous. Many are willing to pay a hefty price to be next. Scientists predict that within 5 years DNA sequencing technologies will be affordable enough that personal genomics will be integrated into routine clinical care (*2*). Companies are responding by offering their services for ancestry tracing, forensics, nutritional advice, reproductive assistance, and even social networking. It will not be long before companies are able to offer a "Facebook-like service centered around our genomes" (*3*). The medical community needs to consider the ways in which routine generation of this information will affect our health system and how this information might be used outside the medical context.

Despite limited treatment options for many genetic conditions, genetic testing has revolutionized the clinical management of patients for many disorders. Building on this history, companies and genetic testing laboratories have begun to develop technologies for genetic testing on a broader scale. For example, Baylor College of Medicine offers microarray analyses to evaluate a fetus for over 65 disorders or for genomic errors associated with autism or mental retardation (*4*).

We currently face an inflection point in clinical medicine as we move from specific diagnostic tests for particular disorders to much broader assays for variants whose effects we do not yet fully understand. In addition, the effects of any single gene on common diseases are generally small, and their interactions with environmental factors remain largely unknown. For example, despite enthusiasm about recent genomewide association studies that report an association between coronary heart disease and a common variant on chromosome 9, the actual risk of heart disease was only increased from 1% to 1.6% in homozygotes (*5*, *6*).

These studies are invaluable for understanding disease pathogenesis, but the present utility of this information for making treatment decisions is limited. Just because an association between genetic variation and disease is statistically significant does not mean that it is clinically meaningful (*7*). Moreover, simply knowing genetic risks and disease predispositions may not lead to better health decisions (*8*). For some, it might lead to fatalism and reduced compliance with healthy choices. As a result, many clinicians are "not at all enthusiastic about rushing out to test people in the clinic" for these genes (*7*). Although the scientific value of genomic research has been enormous, these emerging technologies have only had marginal impact on health care to date, at least at the population level (*9*).

Some fear that personal genomes may become the genetic version of whole-body magnetic resonance imaging scans, which might lead to a population of "worried well" seeking follow-up investigations that could burden already-strained health-care systems. Physicians knowledgeable in genetics are the best guard against this concern. However, physicians are ill-prepared for current genetic testing information (*10*). The deluge of risk information from widespread use of whole-genome sequencing would greatly magnify this dilemma (*11*). Research and training for health-care providers is necessary for personal genomic information to affect patient care.

Only clinically meaningful genomic test results should be integrated into medical decision-making. Clinical practice guidelines should be developed, considering how best to use and present genomic information, and whether and how to withhold information that patients do not want to know. Failure to anticipate what may become standard of care could result in these issues being decided through malpractice litigation.

As personal genomics advances, questions about social justice and the cost of whole-genome sequencing will loom large, especially in countries (including the United States) where there is limited access to basic health-care services for many. Should private health insurance companies and public health systems pay for DNA sequencing, genetic analysis, counseling, and follow-up clinical care? (*12*). Will physicians be reimbursed for the additional time spent educating patients about the significance of genetic risk information? Payers will likely decline coverage for genomic testing and counseling until it can be associated with improved patient outcomes and quality of care (*13*).

The potential clinical application of genomic information is great, as exemplified by the recent U.S. Food and Drug Administration approval of a label change for warfarin to include information on how genetic variations may affect drug response (*14*). However, successful integration of personal genomics into routine clinical care will require clear standards, multidisciplinary collaboration, and careful consideration of the ethical, social, and clinical implications.

[1]Center for Medical Ethics and Health Policy, Baylor College of Medicine, Houston, TX 77030, USA. [2]Stanford Center for Biomedical Ethics, Stanford University, Palo Alto, CA, USA. [3]Division of Radiation Oncology, University of Texas MD Anderson Cancer Center, Houston, TX, USA. [4]Health Law Institute, University of Alberta, Edmonton, AB, Canada.

*Author for correspondence. E-mail: amcguire@bcm.edu

CREDIT: C. BICKEL/SCIENCE

References and Notes

1. S Levy *et al.*, *PLoS Biology* **5**, 0001-0032 (2007); www.plosbiology.org.
2. N. Wade, *New York Times*, 1 June 2007, p. A19; www.nytimes.com/2007/06/01/science/01gene.html?ex=1183521600&en=3ff34724cb1d6a0c&ei=5070.
3. H.-H. Lei, "Personal genome company 23andMe receives Google investment" (22 May 2007), www.eyeondna.com/2007/05/22/personal-genome-company-23andme-receives-google-investment/.
4. Chromosomal Microarray Analysis, Baylor College of Medicine, www.bcm.edu/cma/professional.htm.
5. R. McPherson *et al.*, *Science* **316**, 1488 (2007).
6. A. Helgadottir, *et al.*, *Science* **316**, 1491 (2007).
7. J. Couzin, J. Kaiser, *Science* **316**, 820 (2007).
8. C. Carlsten, W. Burke, *JAMA* **296**, 2480 (2006).
9. M. T. Scheuner, J. I. Rotter, *Genet. Med.* **8**, 141 (2006).
10. A. E. Guttmacher, M. E. Porteous, J. D. McInerney, *Nat. Rev. Genet.* **8**, 151 (2007).
11. S. D. Grosse, M. J. Khoury, *Genet. Med.* **8**, 448 (2006).
12. A. Silversides, *Can. Med. Assoc. J.* **176**, 315 (2007).
13. Department of Health and Human Services (DHHS), *Coverage and Reimbursement of Genetic Tests and Services: Report of the Secretary's Advisory Committee on Genetics, Health, and Society* (February 2006); www4.od.nih.gov/oba/SACGHS/reports/CR_report.pdf.
14. Center for Drug Evaluation and Research, U.S. Food and Drug Administration, DHHS, *"New labeling information for warfarin (marketed as Coumadin)"* (16 August 2007); www.fda.gov/cder/drug/infopage/warfarin/default.htm.
15. We thank R. A. Gibbs for valuable contributions. Supported by the Greenwall Foundation, Baylor College of Medicine, Genome Alberta, and The Ethical, Legal, and Social Implications (ELSI) Research Program, National Human Genome Research Institute (NHGRI-ELSI), NIH, grants R01HG004333 and P50HG003389.

10.1126/science.1147475

IMMUNOLOGY

The Root of Platelet Production

Megakaryocytes are caught in the act of shedding platelets into blood vessels, settling a debate on how this process occurs.

Amy E. Geddis and Kenneth Kaushansky

Blood platelets are the first line of defense against uncontrolled hemorrhage, yet they also play a pathological role in atherosclerosis, acute coronary syndromes, and cancer. The production of an individual platelet begins when a hematopoietic stem cell begins to differentiate, and is complete when a fragment of a bone marrow megakaryocyte is released into the vasculature and begins to circulate. Details of the final step in this process are reported by Junt *et al.* (*1*) on page 1767 in this issue. Through live imaging with multiphoton intravital microscopy, they show that platelets arise from long "proplatelet" processes that extend from the surface of mature megakaryocytes, through sinusoidal endothelial cells, and into blood vessels (see the figure).

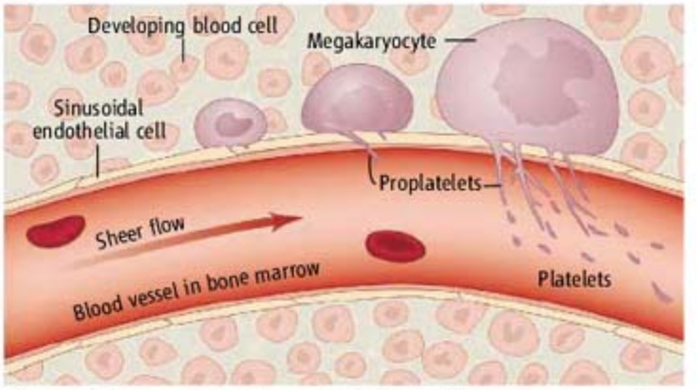

Flow and fragmentation. Junt *et al.* observed how mature megakaryocytes in mouse bone marrow routinely extend protrusions (proplatelets) into blood vessels. Sheer stress from blood flow fragments these protrusions, generating platelets.

Blood flow must be fluid to traffic vital gases, nutrients, and waste products to and from tissues, yet upon vascular injury, this flow must be locally arrested and the vessel repaired so that exsanguination does not occur. Platelets are discoid, anucleate cells, ~2 μm in diameter. Under steady-state conditions, they are nonreactive with the vascular wall, but upon injury they change shape, adhere to the injured site, and aggregate to form a plug in the vessel that stops bleeding. In forging this plug, platelets form the scaffold and secrete the cytokines that initiate vascular repair. Hence, a continuous supply of platelets is an indispensable component of life, and thrombocytopenia (deficiency of blood platelets) can cause bleeding symptoms ranging from simple bruising to intracranial or gastrointestinal hemorrhage and death.

To maintain the normal circulating level of blood platelets of 150,000 to 350,000 per mm^3, ~1×10^{11} new platelets are produced daily in the adult human. However, platelet production (thrombopoiesis) can increase 20-fold or more under conditions of increased demand. Platelets are produced by bone marrow megakaryocytes, very large, polyploid cells that develop from hematopoietic stem cells under the influence of the cytokine thrombopoietin. Despite progress in understanding the mechanisms regulating megakaryocyte growth and differentiation, the process by which they produce platelets has been more difficult to decipher.

Our understanding of thrombopoiesis was greatly advanced with the development of methods to culture bone marrow cells committed to megakaryocyte lineage (*2*, *3*), the recognition of transcription factors that influence megakaryocytic differentiation (*4*, *5*), and the cloning and characterization of thrombopoietin (*6*, *7*). These contributions provided important insights into the steps by which hematopoietic stem cells commit to the megakaryocyte lineage, how committed progenitors differentiate into megakaryocytes, and the signals that emanate from the thrombopoietin receptor that drive and amplify these events. However, these studies did not directly address the process of platelet formation, the final step in thrombopoiesis.

For decades, two major models of platelet formation—cytoplasmic fragmentation and proplatelet process elaboration—competed for attention. Electron microscopic images of mature megakaryocyte cytoplasm have revealed abundant cell membranes that divide the cytoplasm into "platelet territories," a term suggesting a function in walling off prospective platelets that are released by cytoplasmic fragmentation (*8*). By contrast, microscopic evaluation of bone marrow and in vitro assays have suggested that platelets arise from the elaboration of long, microtubule-based "proplatelet" processes that extend from the surface of mature megakaryocytes (*9*, *10*). In support of the latter model, platelets formed from proplatelet processes in vitro are functional (*11*). Moreover, an alternative function has been suggested for the demarcation membranes—that of providing a reservoir of membrane for growth of the proplatelet processes (*12*).

Much of our current understanding of the cell biology of proplatelet formation has been derived from videomicroscopy of cultured megakaryocytes. A series of striking video-micrographs of thrombopoietin-stimulated cultures of murine fetal liver cells illustrated the birth of proplatelets from the surface of megakaryocytes (*13*). Subsequent studies have revealed the cytoskeletal components that contribute to their elongation and terminal platelet formation. Purified extracellular matrix components, such as vitronectin (*14*) and fibrinogen (*15*), have been added to cultured megakaryocytes to re-create the bone marrow environment and better understand the physiological stimuli for proplatelet formation. Nevertheless, it remained possible that what investigators were studying was an in vitro artifact. The report of Junt *et al.* definitively puts that concern to rest.

Using intravital fluorescence microscopy to examine the opened cranial marrow cavity of mice, the authors caught living megakaryocytes (expressing a fluorescent protein) in the act of protruding proplatelet processes into the vascular lumen, and witnessed the hydrodynamic force of flowing blood shear these processes off, releasing large proplatelet masses. They also observed that occasionally, proplatelets occlude the vascular lumen, leading to their further fragmentation. Their findings confirm the decades-old observation that the platelet count in the pulmonary veins (leading out of the lung) is higher than in the pulmonary arteries (leading into the lung), because single proplatelet processes undergo further hydrodynamic processing in the lung into two or more platelets.

As with all biological insights, answering one question raises new ones. Though elegant, the study by Junt *et al.* does not provide mechanistic insights. What determines when a megakaryocyte is ready to begin proplatelet

The authors are in the Departments of Pediatrics and Medicine, University of California, San Diego, CA 92103–8811, USA. E-mail: kkaushansky@ucsd.edu

CREDIT: P. HUEY/SCIENCE

process extension, and how is the megakaryocyte submembrane cytoskeleton disrupted to allow proplatelet protrusion? Does iron deficiency or inflammation change platelet size and number by affecting proplatelet formation? And because proplatelets issue only from large polyploid megakaryocytes, what are the mechanisms that uncouple megakaryocyte DNA replication and cell division, leading to polyploidy? The elegant intravital look at platelet formation provided by Junt and colleagues has only increased our appetite to more fully understand thrombopoiesis, and in so doing, potentially intervene in the process for therapeutic benefit of patients who lack an adequate homeostatic defense.

References

1. T. Junt *et al.*, *Science* **317**, 1767 (2007).
2. D. Metcalf *et al.*, *Proc. Natl. Acad. Sci. U.S.A.* **72**, 1744 (1975).
3. W. Vainchenker *et al.*, *Blood* **54**, 940 1979.
4. D. I. Martin *et al.*, *Nature* **344**, 444 (1990).
5. P. H. Romeo *et al.*, *Nature* **344**, 447 (1990).
6. F. J. de Sauvage *et al.*, *Nature* **369**, 533 (1994).
7. K. Kaushansky *et al.*, Nature **369**, 568 (1994).
8. D. Zucker-Franklin, S. Petursson, *J Cell Biol.* **99**, 390 (1984).
9. R. P. Becker, P. P. De Bruyn, *Am. J. Anat.* **145**, 183 (1976).
10. M. Tavassoli, M. Aoki, *Blood Cells* **15**, 3 (1989).
11. E. S. Choi *et al.*, *Blood* **85**, 402 (1995).
12. H. Schulze *et al.*, *Blood* **107**, 3868 (2006).
13. J. E. Italiano Jr., P. Lecine, R. A. Shivdasani, J. H. Hartwig, *J. Cell Biol.* **147**, 1299 (1999).
14. R. M. Leven, F. Tablin, *Exp. Hematol.* **20**, 1316 (1992).
15. M. K. Larson, S. P. Watson, *Blood* **108**, 1509 (2006).

10.1126/science.1148946

COMPUTER SCIENCE

Coding and Computing Join Forces

Researchers who develop theories of computation are using their insights to create improved error correction codes.

Bernard Chazelle

Unlike vinyl recordings of yore, today's CDs and DVDs are impervious to the feral assaults of even the most determined toddler. For this triumph of civilization over savagery, we owe thanks to coding theory, one of the crown jewels of the digital era. Since Claude Shannon's pioneering work in the mid-20th century, error-correcting codes are found in all manner of communication devices—so much so, in fact, that by the 1990s coding theorists began to wonder if their brightest days had not passed. However, recent developments highlight a remarkable confluence of coding and computing, which may herald the shape of things to come.

Imagine Bob communicating with Alice the 21st-century way, text messaging. Complying with her request, Bob texted Alice his age: 48. But one digit was garbled, and 28 is what she got. It might have been wise of Bob to add at least one redundant symbol so she could spot the corruption of any single digit, sparing him much grief. For example, Bob could take the sum of the digits modulo 10 [i.e., the remainder of $(4 + 8) = 12$ divided by 10, which equals 2]. Adding the "2" gives the new message "482" and Alice could detect the error by doing the same calculation. In fact, by tagging on more symbols to his message, Bob could have enabled his friend to recover it in the presence of one or more garbled digits.

If Alice is to have any chance of restoring Bob's message if corrupted by e errors, Bob would need to inject at least $2e$ redundant symbols. Courtesy of so-called Reed-Solomon codes, this is sufficient. On the downside, it requires complex computations. Yet the added complication has not stopped these codes from becoming the world's most popular.

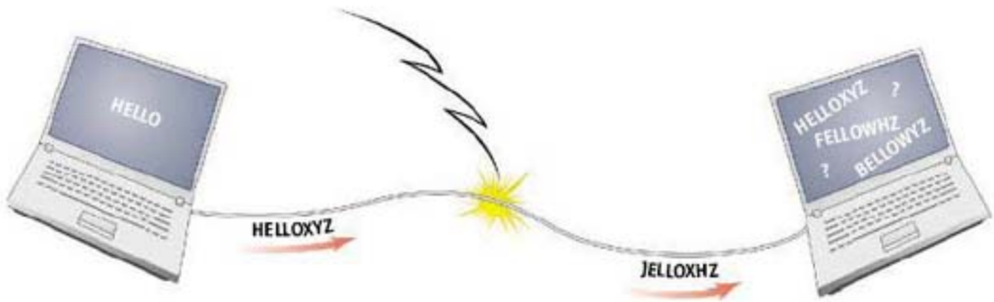

Safe transit. An example of list decoding. Additional information ("xyz") is appended to a message ("hello") sent through a noisy channel, enabling the receiver to check the message's accuracy. The garbled message is compared against a list of all possible encoded messages bearing close similarity to the one received ("jelloxhz").

If the message Alice receives differs from the one Bob sent in more than e places, the decoding may not be unique. Back at the dawn of coding theory, Elias observed (*1*) that such ambiguity is unlikely and saw in this an opportunity. Why not let Alice set a parameter $E > e$ of her choice and reconstruct a list of all the messages Bob might have written that could have produced the received message in the presence of up to E errors? If the transmission noise stays within this bound, obviously Alice's list will include his message and it will just be a matter of picking it out from the crowd. To do that, she might choose the message whose encoding matches the received message most closely; or her preference might go to the message she deems most likely to be Bob's.

The success of "list decoding," as Elias's suggestion is called, hinges on the shortness of the list (as a function of E) and the ease of collecting it. In two breakthrough papers, Sudan (*2*) and Guruswami and Sudan (*3*) showed how to list-decode Reed-Solomon codes efficiently. And here the word "efficiently" is everything, for decoding is trivial when time is not an issue. Sudan and Guruswami's key insight was to trade single-variable polynomials, the natural habitat of Reed-Solomon, for the two-variable kind. This then led to a series of improvements by Parvaresh and Vardy (*4*) and Guruswami and Rudra (*5*).

What were Sudan and Guruswami, two theoretical computer scientists, doing on the stomping grounds of coding theorists? List decoding can function as a tool for changing one computational problem into another. Suppose that I compose a message that enumerates the solutions of a given problem for all possible inputs of a certain length. With list decoding, my message can be recovered from its encoded version even if 99% of its information has been destroyed. Until the work of these researchers (*2*–*5*), a message more than 50% garbled could not be recovered.

Thinking now of the encoded message as another problem's "solution sheet," we conclude that even an algorithm so bad that it solves the new "problem" erroneously 99% of the time can be used to recover the message correctly, and hence solve the original problem, all of the time. Conversely, a problem known to be hard on just a few inputs can be transformed into one that is hard on nearly all of them. Strange as

The author is in the Department of Computer Science, Princeton University, Princeton, NJ 08540, USA. E-mail: chazelle@cs.princeton.edu

CREDIT: P. HUEY/SCIENCE

it may seem, cryptographers crave such problems because hard problems can be used to create difficult-to-break encryption.

In some cases, Alice may need to recover, say, the 217th bit of the message Bob intended without having to read all of the message she received. For this we turn to "locally decodable" codes and, specifically, to a remarkable recent result of Yekhanin (*6*): Bob's message can be encoded so that, should a small enough fraction of its symbols die in transit, Alice would still be able, with high probability, to recover the original bit anywhere in the message she chooses. The surprise: She can do it by picking at random a mere three bits of the received message and combining them the right way.

The randomness of the three single-bit lookups makes locally decodable codes ideally suited for private information retrieval. The concept was introduced by Chor *et al.* (*7*) to allow users of a database to make queries without divulging what they are. Yekhanin's scheme would keep the anonymity of a query by breaking it down into three subqueries and passing on each one to a separate copy of the database. Individually, each subquery would look random and therefore unrelated to the parent query.

Computing theorists have been borrowing from coding theory for decades. Recently they have begun to return the favor. This symbiotic relationship, it is safe to predict, is far from having run its course. The quest for a practical solution to private information retrieval is still wide open. How to turn the beautiful mathematics of local decoding into working privacy tools is one of the main challenges ahead.

References

1. P. Elias, *List Decoding for Noisy Channels*, Research Laboratory of Electronics Technical Report 335 (Massachusetts Institute of Technology, Cambridge, MA, 1957).
2. M. Sudan, *J. Complexity* **13**, 180 (1997).
3. V. Guruswami, M. Sudan, *IEEE Trans. Inform. Theory* **45**, 1757 (1999).
4. F. Parvaresh, A. Vardy, in *Proceedings of the 46th Annual IEEE Symposium on Foundations of Computer Science* (IEEE Computer Society, Los Alamitos, CA, 2005), pp. 285–294.
5. V. Guruswami, A. Rudra, in *Proceedings of the 38th Annual ACM Symposium on Theory of Computing* (Association of Computing Machinery, New York, 2006), pp. 1–10.
6. S. Yekhanin, in *Proceedings of the 39th Annual ACM Symposium on Theory of Computing* (Association of Computing Machinery, New York, 2007), pp. 266–274.
7. B. Chor, O. Goldreich, E. Kushilevitz, M. Sudan, *J. Assoc. Comp. Machinery* **45**, 965 (1998).

10.1126/science.1148064

ARCHAEOLOGY

Easter Island Revisited

New information about Easter Island is helping to identify the cause of the massive deforestation that occurred prior to European arrival, but unanswered questions remain.

Jared Diamond

Easter Island is famous for many reasons: its remoteness, its total deforestation, its hundreds of giant stone statues, their destruction by the carvers' own descendants, the violent transformation of its Polynesian society, and as a metaphor for our world today (*1*). New information about these themes has recently been flooding in from on-going projects.

When first seen by Europeans in the 1700s, Easter was almost unique among tropical Pacific islands in lacking trees over 3 m tall. But pollen in swamp cores revealed the former existence of a giant palm similar to the world's largest living palm, the Chilean wine palm (see the first figure). By identifying 78,000 bits of burned wood from raidocarbon-dated ovens and middens, Orliac and Orliac (*2*) recognized more than 20 other tree and woody plant species exterminated during human settlement. The palm was mostly gone by A.D. 1450, and the other large trees by A.D. 1650, after which the islanders had to burn grasses and sedges instead of wood for fuel.

The end of the forest brought other huge losses for islanders. The palm had yielded food (more than 400 liters of sap per tree per year, plus nuts and palm hearts) and material for baskets, sails, thatching, and mats (*3*). Other vanished tree species had yielded edible fruits, fiber for rope, bark cloth, and wood for canoes, levers, and carvings (*2*).

Deforestation also forced changes in horticultural practices (*3–6*). Easter's early farmers planted crops between the palms, which provided fertilizer, shade, and protection for the soil. In that first phase, erosion was negligible, and horticulture was sustainable (*3*). Around A.D. 1280, the islanders began felling the palms, removing the trunks (presumably for timber), and burning the debris, as shown by a radiocarbon-dated charcoal layer, burned roots and palm nuts, and burned palm stumps chopped off near the ground, but no large pieces of trunk wood at these sites (*3*). The loss of the palm canopy exposed soil to heating, drying, wind, and rain. The resulting sheet erosion proceeded uphill at 3 m/year, removing fertile topsoil and burying down-slope settlements and gardens (*3*). Palm burning and sheet erosion have been studied especially at Poike but also appear elsewhere until A.D. 1520.

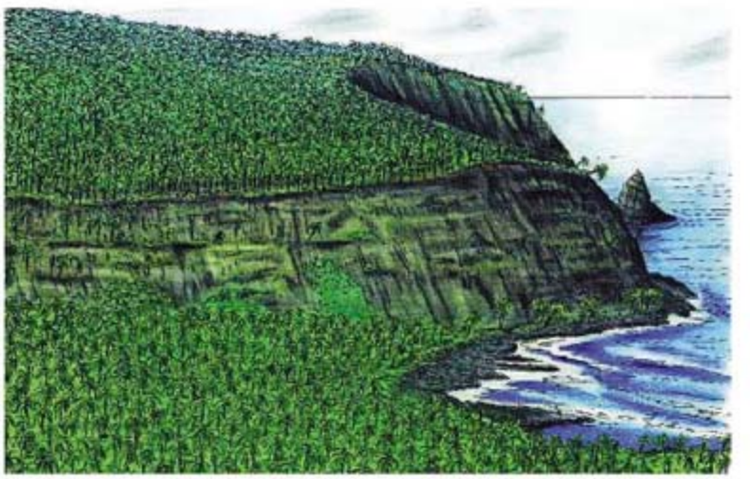

Before human arrival. In this artist's view, the Poike Peninsula is covered with a forest dominated by a giant palm tree, now extinct.

Faced with lower crop yields as a result of deforestation, the islanders responded around A.D. 1400 by occupying the formerly little-used uplands, and by introducing the remarkable labor-intensive gardening method of "stone mulching" on a vast scale (*3–6*). That meant covering half of the island with more than a billion stones averaging 2 kg in weight (*6*). In experiments, stone mulching decreases soil water evaporation, protects against wind and rain erosion, and reduces daily temperature fluctuations (*7*). Pulverized stones may also raise soil fertility by slowly releasing nutrients (*8*). That function would have been valuable, because nutrient levels (especially phosphorus) often limit tropical

The author is in the Geography Department, University of California at Los Angeles, Los Angeles, CA 90095–1524, USA. E-mail: jdiamond@geog.ucla.edu

CREDIT: ANDREAS MIETH/UNIVERSITY OF KIEL, REPRINTED FROM (*22*) WITH PERMISSION FROM THE WISSENSCHAFTLICHE BUCHGESELLSCHAFT, DARMSTADT, GERMANY.

plant growth. Phosphorus levels in most Easter soils are low today, and the islanders' extermination of former seabird colonies eliminated phosphorus input in guano (*9*).

Van Tilburg and Arévalo have inventoried the more than 900 statues on Easter Island (*10*). They have also mapped the interior of Rano Raraku crater, from whose stone most statues were carved. The carving areas define 19 distinct quarries, grouped into a western and an eastern set of quarries. The crater's western half produced statues resembling those on platforms (ahu) in the island's western part, whose clans had higher social status, and where ahu occur earlier. The crater's less accessible eastern half produced bigger statues resembling those on the late eastern Ahu Tongariki, with 15 huge statues of up to 90 tons. This contrast suggests that easterners challenged westerners for status and supremacy by erecting larger statues (see the second figure) (*11*).

See podcast online at www.sciencemag.org/multimedia/podcast/#20070921

Vargas *et al.* (*12*) recognized archaeological style changes toward the 1600s as wood became scarce. There was a proliferation of more than 1000 stone buildings 2 m in height, described in oral tradition as chicken houses; Vargas *et al.* indeed found chicken bones, feathers, eggshells, and guano in many of them. Human houses became smaller and were built with less wood. Earth ovens became stone-lined for efficiency when firewood was scarce. Oral traditions describe caves as refuges during the late period of chronic fighting; that tradition was confirmed by features indicating prolonged occupation of a defensible site. The caves were closed by massive stone walls, accessible through a narrow entrance, and provided with food and utensils.

Thus, major changes unfolded on Easter Island before European arrival. Those changes included deforestation; the loss of palm sap as a food and water source; switching from wood to grasses and sedges as fuel; establishing stone mulching; ceasing to carve statues, because deforestation meant no more big logs and fiber rope for transport; abandoning upland plantations, probably used to feed workers transporting statues; and (as described in oral traditions) increases in warfare, statue destruction by rival clans, and use of refuge caves. However, alternative views have been proposed.

One view is a version of Rousseau's noble savage myth: the claim that bad things began happening on Easter only after European arrival (*13*–*15*). Undoubtedly, Europeans on Easter, as elsewhere in the Pacific, did serious harm through slave raids, worsened erosion, and introduced diseases, grazing animals, and plants. But this view ignores or dismisses the abundant evidence, summarized above, for pre-European impacts.

Another view recognizes pre-European deforestation but blames it on hypothesized droughts (*2*). However, there is no direct information about climate change on Easter between A.D. 1000 and 1700. Easter's forests had already survived tens of thousands of years of climate fluctuations (*1*), and it seems unlikely that a drought in the 1600s (if there was one) destroyed the forests just coincidently soon after human arrival.

According to a third view, deforestation was caused by introduced rats, as suggested by rat gnaw marks on many nuts of the extinct palm (*15*). This hypothesis does not account for all those palm stumps cut off at the ground and burned, nor for the larger number of palm nuts burned rather than gnawed, nor for the disappearance of the long-lived palm trees themselves (with an estimated life span of up to 2000 years) (*16*). If rats were responsible, they were unusual ones, equipped with fire and hatchets. Thousands of other Pacific islands overrun by introduced rats were not deforested, and many other tree species that survived on other rat-infested islands disappeared on Easter (*16*).

No mean feat. Van Tilburg and Ralston (*11*) enlisted modern islanders to drag a 9-ton statue over a distance of 10 km, using methods described in oral traditions. The task required 70 adults pulling in unison, supported and fed by their families numbering about 400 people. By extrapolation, Ahu Tongariki's big statues required a population of thousands in the eastern chiefdoms alone.

Instead, Easter's deforestation can be understood in terms of its environmental fragility. Throughout the Pacific, islanders brought rats and felled and burned trees. The resulting pre-European deforestation ranged from negligible on some islands to complete on Easter. Among 81 islands analyzed, this variation in deforestation parallels measured variation in nine environmental parameters that determine tree growth rates: The more slowly trees grow back, the more extensive was deforestation (*17*). All parameters were stacked against Easter: It is relatively cold, dry, low, small, and isolated, with negligible nutrient inputs from atmospheric dust and volcanic ash, relatively old leached soils, and no uplifted-reef terrain. Thus, Easter became deforested not because its inhabitants were uniquely improvident, nor because its European visitors were uniquely evil, but because Easter Islanders had the misfortune to inhabit one of the Pacific's most fragile environments.

Much remains to understand about Easter. Here are my six favorite unsolved questions.

First, was Easter's mysterious rongorongo writing invented after or before the arrival of Europeans? If the latter were true, Easter would have been by far the world's smallest society to invent writing independently. Orliac's recent ^{14}C-dating of one surviving rongorongo object is a tantalizing first step toward an answer (*18*).

Second, did Easter Islanders live in isolation from other humans from the time of colonization until European arrival, or did further Polynesian settlers arrive? For instance, was the sweet potato brought by the first settlers, or only later (*19*)?

Third, when, within the period from A.D. 800 to 1200, did the first settlers arrive (*12*, *16*, *20*)? This question is unlikely to be solved by finding and dating the first settlement site itself, which would be like seeking a needle in a haystack. Instead, the answer will come from dating widespread impacts left by the first settlers, such as burned charcoal (*16*) and annual sediment layers (*21*) in swamp cores, appearance of rat bones, and declines in numbers of bones of native birds killed by settlers (*9*).

Fourth, along what time course did Easter's human population rise and fall, and what was the peak population? Vargas *et al.* have reported an initial analysis based on hundreds of dated archaeological sites (*12*).

Fifth, was each of Rano Raraku's 19 quarries owned by a different one of the dozen or more territorial clans described in Easter oral traditions (*10*)?

Finally, stone itself cannot be radiocarbon-

CREDIT: EASTER ISLAND STATUE PROJECT

dated. By what other method can we date the statues and ahu, recognize stylistic changes with time, and specify (independently of the oral tradition suggesting around A.D. 1680) when the last statue was carved?

References

1. J. Flenley, P. Bahn, *The Enigmas of Easter Island* (Oxford Univ. Press, Oxford, 2003).
2. C. Orliac, M. Orliac, *Nouv. Archéol.* **102**, 29 (2006).
3. A. Mieth, H. Bork, in *Soils and Societies*, J. McNeill, V. Winiwarter, Eds. (White Horse Press, Isle of Harris, UK, 2006), pp. 273–321.
4. J. Wozniak, *Rapa Nui J.* 13, 95 (1999).
5. C. Stevenson, T. Jackson, A. Mieth, H. Bork, T. Ladefoged, *Antiquity* **80**, 919 (2006).
6. H. Bork, A. Mieth, B. Tschochner, *Rapa Nui J.* **18**, 10 (2004).
7. C. White, D. Dreesen, S. Loftin, *N. Mex. J. Sci.* **38**, 251 (1998).
8. T. Ladefoged, C. Stevenson, P. Vitousek, O. Chadwick, *Rapa Nui J.* **19**, 100 (2005).
9. D. Steadman, P. Vargas, C. Cristino, *Asian Perspect.* **33**, 79 (1994).
10. J. Van Tilburg, C. Arévalo in *Abstracts of VII International Conference on Easter Island and the Pacific*, Visby, Sweden, 20 to 25 August 2007, p. 14.
11. J. Van Tilburg, T. Ralston, in *Onward and Upward*, K. Johnson, Ed. (Stansbury Publications, Chico, CA, 2005), pp. 279–306.
12. P. Vargas, C. Cristino, R. Izaurieta, *1000 Años en Rapa Nui: Arqueología del Asentamiento* (Univ. of Chile, Santiago, 2006).
13. P. Rainbird, *World Archaeol.* **33**, 436 (2002).
14. B. Peiser, *Energy Environ.* **16**, 513 (2005).
15. T. Hunt, *Am. Sci.* **94**, 412 (2006).
16. J. Flenley, P. Bahn, *Rapa Nui J.* **21**, 12 (2007).
17. B. Rolett, J. Diamond, *Nature* **431**, 443 (2004).
18. C. Orliac, *Archaeol. Oceania* **40**, 115 (2005).
19. P. Wallin, C. Stevenson, T. Ladefoged, in *The Sweet Potato in Oceania: A Reappraisal*, C. Ballard *et al.*, Eds. (Oceania Monograph, Sydney, 2005).
20. T. Hunt, C. Lipo, *Science* **311**, 1603 (2006).
21. H. Fukusawa, M. Kato, K. Gotanda, Y. Yasuda, *Monsoon* **6**, 32 (2005).
22. H.-R. Bork, *Landschaften der Erde* (Wissenschaftliche Buchgesellschaft, Darmstadt, Germany, 2006).

10.1126/science.1138442

PHYSICS

Electrons Acquire a Split Personality in Bismuth

Unusual collective quantum states seen only in two-dimensional layers of electrons may have now been observed in a three-dimensional metal.

Andrew Huxley and Andrew G. Green

When many identical particles such as electrons interact with each other, new and unusual quantum states can emerge. Given that a single cubic centimeter of condensed matter may contain as many as 10^{23} electrons, however, one cannot hope to identify from theory all the states that may form. Guidance from experiment is crucial. For example, fractional quantum Hall states, which occur when electrons interact and regroup to create new "quantum particles" with noninteger electrical charge, were identified only after the experimental observation of strange features in the electrical conductance of a two-dimensional (2D) sample. On page 1729 of this issue, Behnia *et al.* report measurements revealing signatures similar to those associated with fractional quantum Hall states, but in 3D crystals of bismuth (*1*). Because 2D confinement of the electrons is fundamental to the accepted understanding of fractional quantum Hall states, this presents a new challenge: to understand how the observed behavior can occur in a 3D host.

Magnetic fields are the key. An applied magnetic field causes electrons to move in quantum orbits that are organized in levels somewhat similar to the energy levels in an atom. In this case, the number of orbits in each level is proportional to the strength of the magnetic field, and in 2D materials the levels have distinct energies. Physical properties such as electrical conductance show oscillations as the magnetic field increases, reflecting successive changes in the number of levels needed to accommodate the electrons. Impurities can provide a reservoir of electrons, preserving the complete filling of a level over a range of fields. This changes the oscillations into steps, and such steps are seen in the so-called integer quantum Hall effect. Above a certain field, the quantum limit is reached where the lowest-energy level can accommodate all of the electrons. Gathering all the electrons together in this way provides perfect conditions for the formation of new collective states.

Fractional states. In this schematic picture of a fractional quantum Hall state, the electrons (represented by spheres) are confined to move on a 2D surface traversed by flux tubes (represented by arrows). A pair of flux tubes is associated with each electron to form a composite object. A third flux tube per electron remains unbound. This causes the composite objects to move in quantum orbits, completely filling one orbit level.

Tsui *et al.* (*2*) observed plateaus in the Hall resistance corresponding to fractional electron filling of the lowest-energy orbits, evidence that new states form when the field is increased above the quantum limit in 2D electron gases. In other words, these states behave as though they are composed of particles possessing fractions of the charge of an electron. Laughlin (*3*) subsequently proposed a wave function that could account for the plateaus.

One way to visualize Laughlin's wave function is to consider the magnetic field to be composed of flux tubes with each electron attached to a specific number of flux tubes to form a composite object (see the figure). The objects behave as fermions or bosons (the two categories into which all quantum particles must fall), depending upon whether they are made with even or odd numbers of flux tubes (*4*). In the standard fractional quantum Hall state, an even number of flux tubes are bound to each electron so that the composite objects behave like fermions. The composite fermions orbit around remaining unattached flux tubes, giving rise to plateaus of the Hall resistance as with the integer quantum Hall effect. The plateaus occur for fractional fillings of the lowest electron orbit type because the unbound flux tubes correspond to only a fraction of the total magnetic flux.

In 3D materials, such as bismuth, each orbit spans a range of electron energies owing to the motion of the electrons along the third direction. This means that the quantum Hall effect does not occur, but as the magnetic field is increased, physical properties still undergo small oscillations known as quantum oscilla-

A. Huxley is with the Scottish Universities Physics Alliance, University of Edinburgh, Edinburgh EH9 3JZ, UK. A. G. Green is with the Scottish Universities Physics Alliance, University of St. Andrews, St. Andrews KY16 9SS, UK. E-mail: ahuxley@ph.ed.ac.uk

tions. Above the quantum limit, all the electrons are in the lowest-orbit level but still have a range of kinetic energies owing to their motion along the field direction. The experiments of Behnia *et al.* explore what happens in this case.

They report measurements of the transverse voltage induced across a single crystal of bismuth by a longitudinal temperature gradient as the magnetic field is varied. Such voltages, known as the Nernst signal, have been used as sensitive probes of the motion of electrons in superconductors (*5*). The origin of the Nernst signal in bismuth, which is not a superconductor even in zero magnetic field, is different and at low magnetic field is ascribed to normal electrons. Behnia *et al.* now show that the Nernst signal has well-defined peaks at high fields (well above the quantum limit) indicating the presence of fractional charge behavior in a bulk metal.

Although the detailed behavior of the Hall coefficient at low fields around and below the quantum limit is not yet understood in bismuth, Behnia *et al.* also observe signatures at high field reminiscent of the fractional quantum Hall effect in 2D electron gases. However, the lack of clear plateaus of the Hall resistance makes it very difficult to assign filling factors to these features. Behnia *et al.* tentatively assign a level filling of ½ to the first such feature, based on the magnetic field at which it occurs. Because this filling factor is atypical for 2D electron gases in the archetype fractional quantum Hall system gallium arsenide, understanding why it might be stabilized in bismuth will be one of many challenges for theoreticians.

The main theoretical challenge, however, is to understand the role of dimensionality. A way to construct a 3D quantum Hall state is to start with 2D sheets of electrons stacked along the third dimension. The electron behavior becomes 3D through quantum tunneling of electrons between the layers. Experimental systems of this behave like normal metals in the direction perpendicular to the layers and exhibit fractional quantum Hall states within the plane, as predicted theoretically. The data reported by Behnia *et al.* for bismuth also display these two types of behavior. However, in bismuth the natural starting point is a 3D metal, and a theoretical understanding of how similar states may form from this starting point does not exist.

As well as presenting challenges to theory, the work is also a catalyst for future experimental studies. For example, in the 2D fractional quantum Hall state, many more fractional states appear as purity is increased. It will be interesting to see whether similar phenomena occur in bismuth.

References

1. K. Behnia *et al.*, *Science* **317**, 1729 (2007).
2. D. C. Tsui *et al.*, *Phys. Rev. Lett.* **48**, 1559 (1982).
3. R. B. Laughlin, *Phys. Rev. Lett.* **50**, 1395 (1983).
4. J. K. Jain, *Composite Fermions* (Cambridge Univ. Press, Cambridge, 2007).
5. Y. Wang *et al.*, *Science* **299**, 86 (2003).

10.1126/science.1148554

BIOCHEMISTRY

How Cells Control Zinc Homeostasis

The structure of a transport protein for divalent metal cations sheds light on how metal concentrations in the cell are regulated.

Dietrich H. Nies

Divalent metal cations are essential for all living cells. For example, Mg^{2+} stabilizes the phosphates in adenosine triphosphate (ATP), and Zn^{2+} is required for transcription, immune functions, and neurotransmission. On page 1746 of this issue, Lu and Fu report the structure of a zinc transport protein that elucidates how the zinc concentration of the cell is controlled (*1*).

Tight control of the cellular concentration of divalent metals (a process referred to as metal homeostasis) prevents the formation of metal complexes or the occurrence of redox reactions that are toxic to the cell. Sequestration of transition metals to metal-binding and storage compounds prevents unwanted chemical reactions. However, the key to metal homeostasis is transport. This metal homeostasis can be envisioned as the equilibrium between metal uptake and efflux. Understanding metal homeostasis thus requires knowledge of the structure and function of the transport proteins involved.

The author is in the Institute for Microbiology, Martin-Luther-University Halle-Wittenberg, 06099 Halle/Saale, Germany. E-mail: d.nies@mikrobiologie.uni-halle.de

Lu and Fu now reveal the structure of YiiP, a transport protein for transition metal cations, from *Escherichia coli*. Toyoshima reported the structure of the Ca^{2+}-transporting P-type adenosine triphosphatase (ATPase) (*2*); many members of the P-type ATPase protein family transport zinc. Thus, we now have structures for the two known zinc exporter families. Common motifs in these two exporter families and that of uptake systems for divalent metal cations (*3*, *4*) indicate that flux control of transport proteins through the metal concentration may be an important contribution to metal homeostasis. Moreover, the structures demonstrate how such a process may be accomplished.

The YiiP protein belongs to the cation diffusion facilitator (CDF) protein family. CDF proteins (*5*) occur in bacteria, archaea, and eukaryotes (*6*). Their substrates are Zn^{2+}, Cd^{2+}, Co^{2+}, Ni^{2+}, Mn^{2+}, and Fe^{2+}; the ZnT (zinc transport) proteins from humans mainly transport Zn^{2+}. In addition to efflux, CDF proteins may also be involved in cation uptake when the metal concentration in the cytoplasm is too low (*7*, *8*).

YiiP (*1*) is a dimeric protein, in which the transmembrane domains of the two subunits are clearly separated but the carboxyl-terminal cytoplasmic domains are closely associated (see the figure, right). Fu and Lu identify four bound Zn^{2+} ions per subunit, two in or next to the transmembrane domain and two in the cytoplasmic domain. Three of these ions seem to be required to form and stabilize the YiiP dimer, the active form of the protein. In the Mg^{2+} uptake systems CorA and MgtE (see the figure, left), the magnesium-binding sites are in the cytoplasmic domains, which suggests that Mg^{2+} uptake is controlled by cytoplasmic Mg^{2+} concentrations (*3*, *4*); the divalent metal cation is only taken up when needed. Similarly, the YiiP structure indicates that superfluous Zn^{2+} in the cytoplasm may lead to or stabilize the formation of the active dimer, which exports Zn^{2+} until homeostasis is attained.

Control of zinc efflux via activity (rather than gene expression) might be required for two reasons. First, flux control enables much quicker and finer control of the cytoplasmic zinc concentration than can be achieved by gene expression, which happens in addition to flux control for many known Zn^{2+} efflux sys-

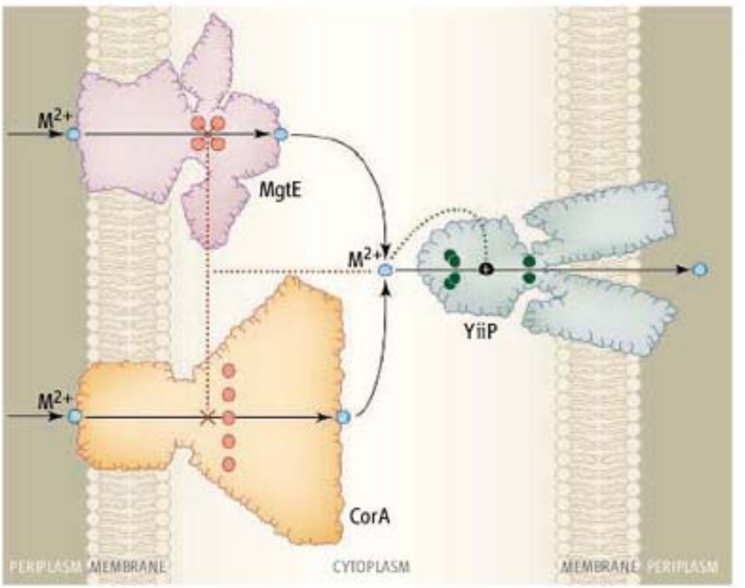

Controlling cellular metal homeostasis. The backbone of cellular metal homeostasis is a flow equilibrium of uptake and efflux reactions. Activity of either transport process seems to be controlled by cytoplasmic concentrations of divalent metal cations (M^{2+}). Solid lines, transport, dashed lines, regulation of transport activity; red, inhibition; green, activation. Uptake (**left**) can be understood from the structures of the Mg^{2+} uptake systems MgtE (*4*) and CorA (*3*), which also transport other divalent metal cations. Binding of Mg^{2+} to sites in cytoplasmic domains of either protein (red circles) closes the gate and prevents cation uptake at sufficient cytoplasmic concentrations (red dashed line with crosses). Similarly, the Zn^{2+} efflux gate (**right**) may be opened through binding of Zn^{2+} to sites Z2, Z3, and Z4 (green circles) in the cytoplasmic domain of YiiP (*1*). Thus, superfluous cytoplasmic Zn^{2+} concentrations may stimulate efflux (green dashed line ending with "+").

tems (*9*). Second, Zn^{2+} is taken up into most cells by highly specific Zn^{2+} uptake systems that are expressed under conditions of zinc starvation. However, other uptake systems (such as Mg^{2+} uptake systems) also transport Zn^{2+} nonspecifically. Because these nonspecific systems are regulated by their specific substrate, but not by Zn^{2+}, this may lead to superfluous zinc concentration in the cytoplasm, necessitating activated Zn^{2+} efflux.

These nonspecific uptake systems import a range of divalent metal cations until the concentration of the main substrate, such as Mg^{2+}, reaches the desired cytoplasmic concentration. Following that, the various efflux systems (for example, CDF proteins and P-type ATPases for Zn^{2+}) select and remove with high specificity all those cations that reach dangerous concentrations. Thus, the controlled flow of metal cations though a cellular compartment regulates not only the ambient concentration of one metal cation but also the composition of the complete set.

The YiiP structure far increases our understanding of CDF proteins and of zinc homeostasis, but many questions remain open. YiiP transports Zn^{2+} in vitro (*10*), but in vivo (*11*), its main substrate is Fe^{2+}. Thus, YiiP is the first model not only for a transition metal transporter but also for a bacterial Fe^{2+} efflux system. However, it is currently not known which metal cation binds to which site in vivo and what consequences these binding events have on stabilization of the structure, regulation, or transport.

Answers may come from an unexpected direction. The cytoplasmic domain of YiiP forms a metallochaperone-like structure (*1*), and interactions between metallochaperones and transport proteins are essential for cellular copper homeostasis mechanisms (*12*). No cytoplasmic zinc chaperone is known. Nevertheless, knowledge of the interaction between transport and binding processes may be the key to unraveling the mechanisms by which the cell controls zinc concentrations.

References and Notes

1. M. Lu, D. Fu, *Science* **317**, 1746 (2007).
2. C. Toyoshima, N. Nomura, T. Tsuda, *Nature* **432**, 361 (2007).
3. V. Lunin *et al.*, *Nature* **440**, 833 (2006).
4. M. Hattori, Y. Tanaka, S. Fukai, R. Ishitani, O. Nureki, *Nature*, 10.1038/nature06093 (2007).
5. I. T. Paulsen, M. H. Saier Jr., *J. Membr. Biol.* **156**, 99 (1997).
6. D. H. Nies, *FEMS Microbiol. Rev.* **27**, 313 (2003).
7. R. A. Valentine *et al.*, *J. Biol. Chem.* **282**, 14389 (2007).
8. T. Bloss, S. Clemens, D. H. Nies, *Planta* **214**, 783 (2002).
9. C. E. Outten, T. V. O'Halloran, *Science* **292**, 2488 (2001).
10. Y. N. Wei, D. Fu, *J. Biol. Chem.* **280**, 33716 (2005).
11. G. Grass *et al.*, *Arch. Microbiol.* **183**, 9 (2005).
12. L. Banci *et al.*, *Nat. Chem. Biol.* **2**, 367 (2006).
13. Work on CDF proteins was supported by Deutsche Forschungsgemeinschaft, grants Ni262/4 and Ni262/8. I thank G. Sawers for helpful discussions.

10.1126/science.1149048

DEVELOPMENTAL BIOLOGY

Home for the Precious Few

Live imaging reveals that branching of blood vessels in the mammalian testes may define the location of niches for germline stem cells.

Steve DiNardo and Robert E. Braun

Cells in multicellular organisms rarely escape the influence of other cell types. This is especially true for stem cells, which reside in tissue-specific niches, or homes. Niche cells regulate fundamental stem cell properties, including long-term survival, proliferation, and the balance between cell divisions that are self-renewing or differentiative. Simply identifying a niche can stimulate hypotheses about these properties. For instance, the identification of neural stem cells in a vascular niche (*1*) suggested correctly that co-culture of these stem cells with vascular endothelial cells could affect their potency (*2*). Similarly, in fruit fly gonads, identifying the germline stem cell niche led to the elucidation of locally acting self-renewal signals, and revealed how oriented cell divisions contribute to stem cell fate (*3*–*6*). On page 1722 in this issue, Yoshida *et al.* (*7*) take an exciting step toward identifying stem cell niches in the mammalian testis.

It was initially surmised that testis stem cells must exist because men make sperm for decades. Then, in rodent models, it was observed that spermatogenesis would naturally be reestablished after a severe toxic insult. Spermatogonial stem cells were eventually identified when a preparation of cells from a donor mouse testis was shown to repopulate spermatogenesis when transplanted into the testis of a sterile recipient animal (*8*). As with any tissue maintained by stem cells, only a small fraction of testis cells are spermatogonial stem cells. But where is home for these precious, few cells?

In mice, putative spermatogonial stem cells were initially identified histologically, as type A single (A_s), undifferentiated cells. A_s cells gen-

S. DiNardo is in the Department of Cell and Developmental Biology, University of Pennsylvania, Philadelphia, PA 19104–6058, USA. R. E. Braun is in the Department of Genome Sciences, University of Washington, Seattle, WA 98195–7730, USA. E-mail: sdinardo@mail.med.upenn.edu, braun@washington.edu

CREDIT: ADAPTED BY P. HUEY/SCIENCE

erate a transit-amplifying pool of interconnected daughter cells, A_{pr} (paired) and A_{al} (aligned), which mature into more differentiated germ cells. Recent studies have determined that genes expressed in the A_s, A_{pr}, and A_{al} cells act autonomously to regulate spermatogonial stem cell self-renewal (*9*, *10*). Despite this progress, the specific identity of bona fide spermatogonial stem cells is still in question. Are some or all A_s cells—or even some of the transit-amplifying cells—spermatogonial stem cells? Yoshida and colleagues (*11*) recently combined a creative labeling method with a transplantation/repopulation assay to follow spermatogonial stem cells in normal mouse testes and in testes (depleted of resident spermatogonial stem cells) that were recipients of transplanted cells. Remarkably, these two analyses gave different results, suggesting that the stem cell population is not homogeneous. Instead, their data suggest that the A_s, A_{pr}, and A_{al} cells exhibit differing degrees of stem cell potential, with the highest potential perhaps in the A_s cells. Spermatogonial stem cell potential is revealed by the degree of niche occupancy. In normal testes, niches are generally occupied by stem cells with the highest potential for self-renewal. But in recipient testes depleted of resident spermatogonial stem cells, transplanted cells can fill unoccupied niches, even if the cells have a low potential for self-renewal.

Unlike in fruit flies and worms, however, the mammalian seminiferous tubules—sites in the testis where spermatozoa mature—do not offer an obvious anatomical niche. Although spermatogonial stem cells are in direct contact with constituents of the tubules—Sertoli cells (that nourish developing spermatogonia) and the basal lamina that surrounds each tubule—no functional subcompartment has been identified among the vast area delimited by these components. Glial cell line–derived neurotrophic factor (GDNF), secreted by Sertoli cells, affects spermatogonial stem cell behavior (*12*), but whether this factor is made by all or only a subset of Sertoli cells is uncertain. Additionally, a receptor subunit for this factor is selectively enriched on undifferentiated gonial cells (*13*), which is not consistent with a simple model in which GDNF determines spermatogonial stem cell fate.

So, where is home for resident spermatogonial stem cells? Yoshida *et al.* use heroic three-dimensional reconstructions and live imaging (up to 4 days) of the mouse testis to draw inferences about the niche. Of necessity, the authors followed undifferentiated spermatogonia, and not "pure" stem cells, but they analyze the data exhaustively and interpret it with great care. They conclude that these primitive cells are not randomly positioned around or along a seminiferous tubule, but rather are enriched at defined positions, usually where the interstitial area just outside the tubule is filled with various cell types and, curiously, branching blood vessels (see the figure). Although an association with the interstitium had been suggested for spermatogonial stem cells, the external vasculature had not been implicated (*14*). In addition, although spermatogonial migration had been previously proposed, it had never been visualized live. Now, Yoshida *et al.* see that once small chains of A_{al} cells are produced, they migrate along the inside surface of the basal lamina. Later, these cell groups divide to form larger chains of differentiating spermatogonia. The extent of this process had not been appreciated until now.

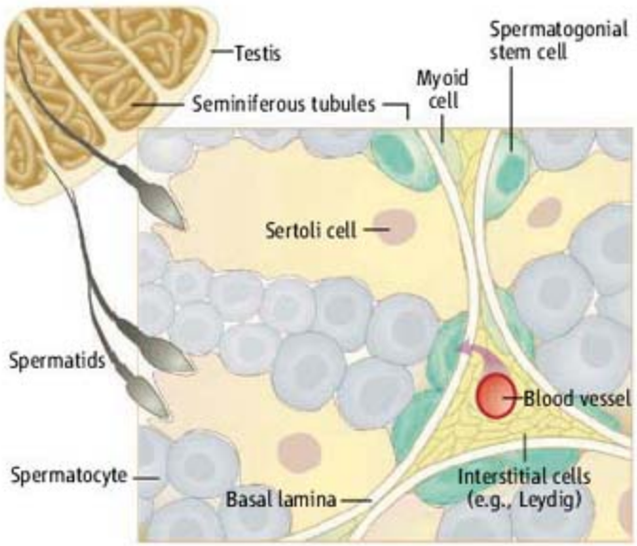

At home, in small narrow places. Spermatogonial stem cells localize to interstitial regions between seminiferous tubules in the mouse testis. This implies that interstitial cells and branching blood vessels secrete factors (arrow) that influence stem cell fate.

The position of spermatogonial stem cells near the interstitium implies the existence of secreted factors that must act over a distance to influence the niche. Factors emanating from interstitial cells must traverse a cellular and biochemical barrier (the myoid cell layer surrounding seminiferous tubules, and the basal lamina upon which myoid cells are situated; see the figure) before they can gain access to the niche compartment. Interstitial factors—perhaps testosterone from Leydig cells in the interstitium or unknown factors from the blood vessels—could act directly on the spermatogonial stem cells. Alternatively, a relay might be engaged, whereby signals act on myoid or Sertoli cells, which in turn act on the spermatogonial stem cells.

Regardless of the mechanism, the limited number of active niches suggests strongly that all Sertoli cells cannot be equal. Perhaps, as the present work suggests, only Sertoli cells near interstitia that harbor a branched vasculature can support spermatogonial stem cells. To investigate this possibility, the authors grafted a tubule segment, labeled with green fluorescent protein, from a donor testis into an unmarked host testis. They found that undifferentiated cells were enriched near the realigned host vasculature. Despite the intriguing association of other progenitor cells with vasculature (*1*), it remains unclear whether vascular branches in the mouse testis generate the niches (where spermatogonial stem cells are found), or whether stem cells, under hypoxic stress, cause nearby vessels to branch.

Spermatogonial stem cells make only spermatozoa. However, cells cultured from mouse testes have been coaxed toward multipotency and even pluripotency (*15*, *16*). These cultures were enriched (and not "pure") in spermatogonial stem cells, so precisely which cells were manipulated is questionable. The location of the niche might suggest new candidate signals that influence stem cell behavior, leading to the eventual purification and efficient expansion of spermatogonial stem cells in culture. That, in turn, might lead to the coaxing of human spermatogonial stem cells toward pluripotency, yielding a ready source of cells untainted by ethical concerns associated with deriving embryonic stem cells.

References

1. T. D. Palmer, A. R. Willhoite, F. H. Gage, *J. Comp. Neurol.* **425**, 479 (2000).
2. Q. Shen *et al.*, *Science* **304**, 1338 (2004).
3. T. Xie, A.C. Spradling, *Cell* **94**, 251 (1998).
4. N. Tulina, E. Matunis, *Science* **294**, 2546 (2001).
5. A. A. Kiger *et al.*, *Science* **294**, 2542 (2001).
6. Y. M. Yamashita, D. L. Jones, M. T. Fuller, *Science* **301**, 1547 (2003).
7. S. Yoshida, M. Sukeno, Y.-I. Nabeshima, *Science* **317**, 1722 (2007).
8. R. L. Brinster, J. W. Zimmermann, *Proc. Natl. Acad. Sci. U.S.A.* **91**, 11298 (1994).
9. F. W. Buaas *et al.*, *Nat. Genet.* **36**, 647 (2004).
10. J. A. Costoya *et al.*, *Nat. Genet.* **36**, 653 (2004).
11. T. Nakagawa, Y. Nabeshima, S. Yoshida, *Dev. Cell* **12**, 195 (2007).
12. X. Meng *et al.*, *Science* **287**, 1489 (2000).
13. S. Yoshida *et al.*, *Dev. Biol.* **269** 447 (2004).
14. H. Chiarini-Garcia, A. M. Raymer, L. D. Russell, *Reproduction* **126**, 669 (2003).
15. M. Kanatsu-Shinohara *et al.*, *Cell* **119**, 1001 (2004).
16. K. Guan *et al.*, *Nature* **440**, 1199 (2006).

10.1126/science.1149533

CREDIT: ADAPTED BY P. HUEY/SCIENCE

Circuits with Light at Nanoscales: Optical Nanocircuits Inspired by Metamaterials

Nader Engheta

A form of optical circuitry is overviewed in which a tapestry of subwavelength nanometer-scale metamaterial structures and nanoparticles may provide a mechanism for tailoring, patterning, and manipulating local optical electric fields and electric displacement vectors in a subwavelength domain, leading to the possibility of optical information processing at the nanometer scale. By exploiting the optical properties of metamaterials, these nanoparticles may play the role of "lumped" nanocircuit elements such as nanoinductors, nanocapacitors, and nanoresistors, analogous to microelectronics. I show that this concept of metamaterial-inspired nanoelectronics ("metactronics") can bring the tools and mathematical machinery of the circuit theory into optics, may link the fields of optics, electronics, plasmonics, and metamaterials, and may provide road maps to future innovations in nanoscale optical devices, components, and more intricate nanoscale metamaterials.

In microelectronics, the notion of a circuit is a powerful concept in which a flow of a certain quantity (e.g., electric current as the "flow" of charges) is related to a potential of another quantity (e.g., electric potential) through the functions of "lumped" elements (e.g., resistor, inductor, capacitor, diode). This "lumpedness" of circuit elements is an important assumption in modeling, allowing simplification and, effectively, modularization of the function of each element. From a systems point of view, in effect what is happening inside the element becomes less relevant to the connectivity and functionality of this modularized element to the rest of the system. This notion has been extensively and successfully used in the radio frequency (RF) and microwave domains and has been proven to be a powerful tool in the design, innovation, and discovery of new functionalities in circuits in those frequency domains. Extending the operating frequency to higher frequency regimes—for example, terahertz, infrared (IR), and visible wavelengths—may in general lead to miniaturization of devices, higher storage capacities, and larger data transfer rates. Therefore, a natural question may be asked: Can this concept of lumped circuit elements, and the mathematical machinery and tools of circuit theory, be extended and applied to the optical domain? Initially, one may imagine that merely scaling down the sizes of elements from the microwave to optical wavelengths may achieve this goal. However, several obstacles must be overcome before such optical lumped elements can be conceived. The first challenge is the size of such an optical module. Just as circuits in the lower frequency domains (e.g., in RF and microwave domains) indeed involve elements that are much smaller than the wavelength of operation, fabrication techniques can be used to construct nanoparticles with subwavelength dimensions at optical wavelengths. Therefore, the obstacle of size reduction may be overcome. The second, more limiting, hurdle is the response of metals at IR and optical frequencies, which cannot be simply scaled from RF to optics. Metals such as gold, silver, aluminum, and copper are highly conductive materials at RF and microwaves and consequently are commonly used in many circuits in these regimes. However, at optical frequencies, some noble metals behave differently in that they do not exhibit conductivity in the usual sense but instead exhibit plasmonic resonance (i.e., coupling of optical signals with collective oscillation of conduction electrons at these metal surfaces) as a result of the negative real part of their permittivities. Therefore, clearly, at optical wavelengths the conduction current may not be the main current flowing in such lumped optical elements. Instead, the other well-known current term, which arises from the Maxwell equations, that is, the electric displacement current density $\frac{\partial \mathbf{D}}{\partial t}$, can be used as the "flowing optical current." Therefore, just scaling down the element size may not provide answers to the above questions.

Lumped Optical Nanoelements

With these issues in mind, my group took an entirely different approach to address the above questions (*1*). Imagine a deeply subwavelength-size nanoparticle made of a nonmagnetic material with permittivity ε illuminated with a monochromatic optical signal with angular frequency ω (Fig. 1A) (*2*). After solving the Maxwell equations for the optical electric and magnetic vector fields inside and near this small particle, one can specify and evaluate the optical electric

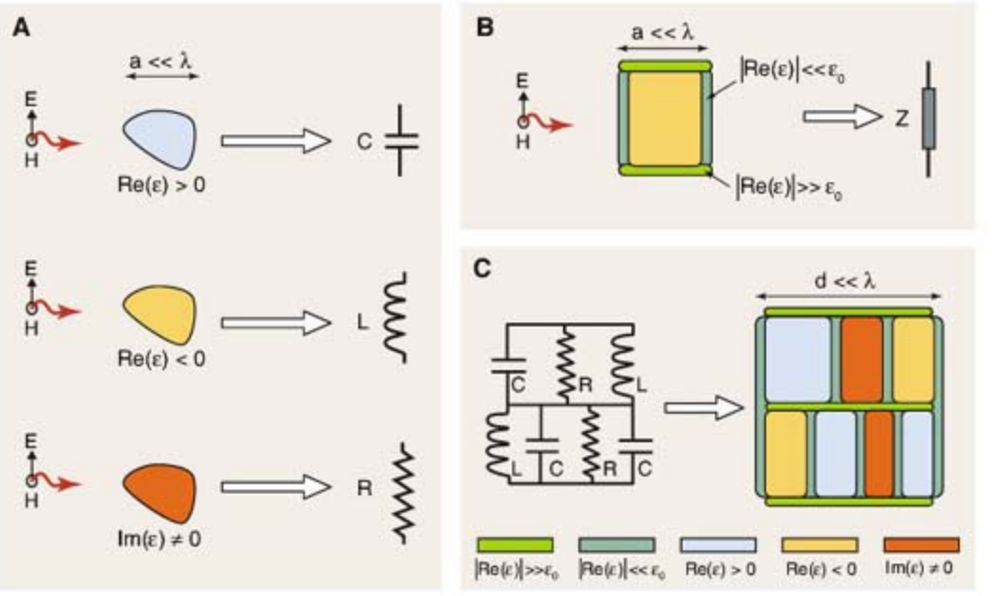

Fig. 1. Subwavelength nanoparticles as lumped nanocircuit elements at optical frequencies, and the collections of such nanoparticles. **(A)** A nanoparticle, with subwavelength size, when illuminated by a monochromatic optical signal, can effectively play the role of a lumped optical circuit element, depending on the permittivity of its material (*2*). **(B)** An optical nanomodule, formed by a material nanoparticle with subwavelength size, covered on its sides by layers of material with a very low real part of relative permittivity and on its two ends by layers of material with a very high real part of relative permittivity. This may perform as an insulated, lumped optical nanoelement with two connecting terminals. **(C)** Illustration of the concept of mn-circuits, several lumped optical nanomodules of (B), arranged next to each other, with a subwavelength dimension. When this mn-circuit is excited by an optical signal, the optical electric fields and displacement currents in these elements are tailored and patterned such that this collection of particles may behave approximately as the circuit shown on the left in a specific frequency band.

University of Pennsylvania, Department of Electrical and Systems Engineering, Philadelphia, PA 19104, USA. E-mail: engheta@ee.upenn.edu

displacement current flowing into and out of this particle, and because the particle is small compared with the wavelength one can also define an averaged optical electric potential across this particle (*1*, *2*). The ratio of these two quantities, optical potential to displacement current, can then be assigned as the optical "lumped impedance" of this nanoparticle. Such an impedance is clearly dependent on the shape and size of the particle, the materials forming the particle, the optical frequency, and possibly its orientation with respect to the impressed optical electric field. It turns out that the choice of material can determine the type of lumped impedance the nanoparticle may represent (*1*): If the material is a conventional dielectric (e.g., SiO2 or Si) with $\mathrm{Re}(\varepsilon) > 0$ at optical frequencies, the nanoparticle will act as a capacitive impedance (i.e., nanocapacitor); if, however, the particle is made of material with $\mathrm{Re}(\varepsilon) < 0$ at optical wavelengths (e.g., noble metals such as Ag and Au), the particle may behave as a negatively capacitive impedance, which implies that it will behave as an inductive impedance (i.e., nanoinductor) (*3*); and when the material exhibits some material loss, that is, when its $\mathrm{Im}(\varepsilon) \neq 0$ (which is almost always the case), a "nanoresistor" element should be included in the nanocircuit representation of the nanoparticle. This behavior is consistent with the dispersion properties of dielectric functions of optical materials discussed in (*4*). Other nonlinear lumped elements, such as an optical lumped nanorectifier-nanodiode, may also be envisioned when nonlinear optical materials are mixed with plasmonic nanoparticles. Before moving forward toward such optical nanocircuits, we need to expand on the analogy with conventional RF circuits. In standard RF circuits, the individual lumped elements are insulated from each other by nonconducting insulating materials (e.g., dielectric or air) and are connected to other elements only at their terminals using conducting wires. In short, one does not usually have to be concerned about the leakage of conduction current from the middle of the lumped elements. In the optical domain, however, the optical electric displacement current in the nanoparticles considered here can in general leak into and out of different parts of the nanoparticle surface. This current leakage, which can lead to coupling among various tightly packed nanoelements, can be accounted for as dependent sources in the circuit paradigm (*1*). To strengthen the analogy between the two paradigms of the conventional RF circuits and the optical nanocircuits envisioned here, we have proposed the use of additional thin layers of materials with proper values of permittivity around the nanoparicles (*5*). For these layers to act as "insulators" for the optical displacement current, that is, to allow negligibly small displacement current and to stop the leakage, the real part of their relative permittivities needs to be very small. Such "epsilon-near-zero" (ENZ) materials, if designed properly, should prevent leakage of the optical electric displacement current, because inside such materials the displacement vector $\boldsymbol{D}$ should be negligibly small for a finite electric field. On the other hand, if one wants layers of materials that allow an easy flow of displacement current without introducing a noticeable optical electric field, materials with high relative real part of permittivity should be considered, because in such high-permittivity media a very small electric field can produce a high amount of displacement current. Such "epsilon-very-large" (EVL) materials can play the role of nanoscale "conduit" for the optical displacement current, analogous to the role that metallic wires play for the conduction current in the RF domains. Now let us consider a subwavelength nanoparticle that has a thin layer of an ENZ material around its sides and thin layers of EVL materials on its two ends (Fig. 1B). Such a composite nanoparticle can allow the flow of the optical displacement current in and out of its two EVL terminals and yet confine this current within it without any leakage from its ENZ side (*5*). Depending on the permittivity of the main material in the particle, this composite nanostructure can indeed act approximately as a modularized lumped nanoelement at optical frequencies. Thus, the addition of the ENZ and EVL materials for shielding and connecting the nanoparticle, although not always necessary, can provide us with

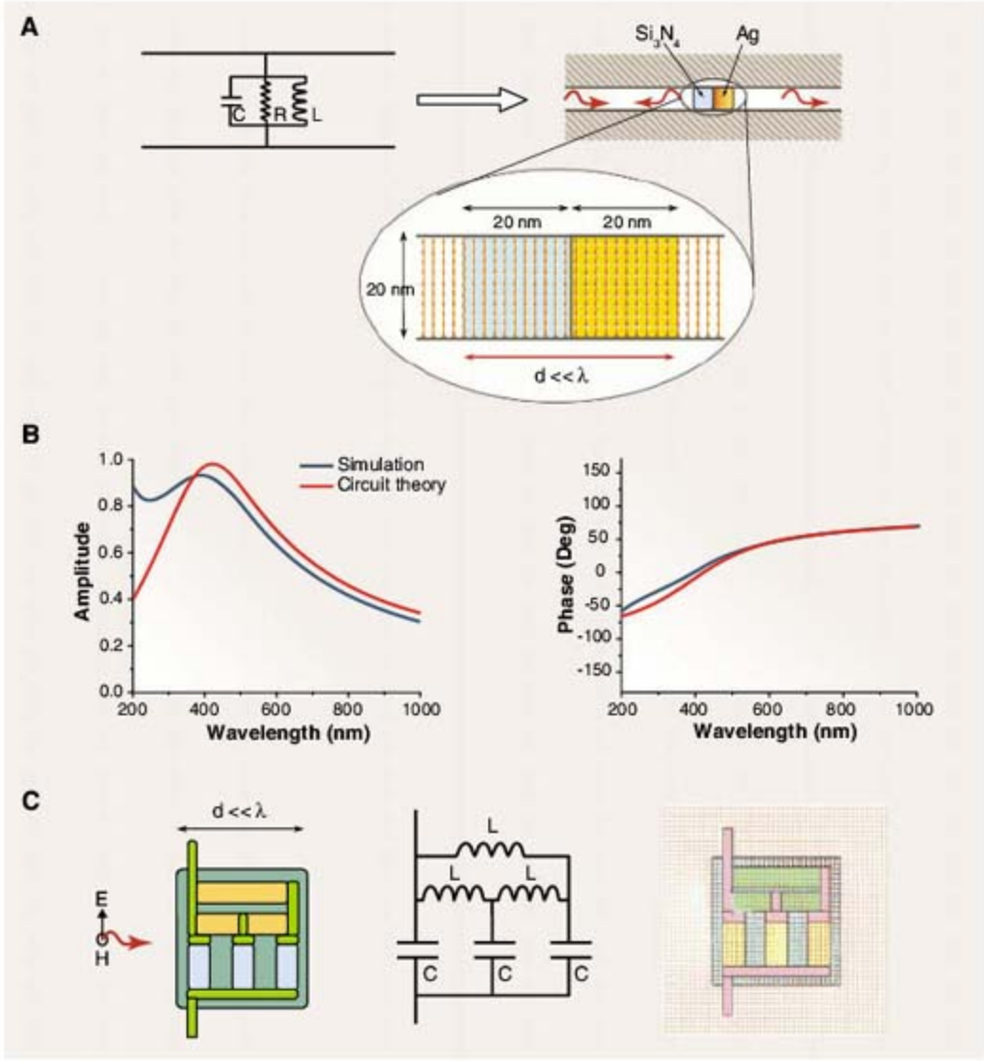

Fig. 2. Designed functionality: an example of filtering properties of optical mn-circuits. **(A)** RF circuit on the left shows a standard band-pass RLC filter; the mn-circuit on the right shows the cross section of a 2D optical counterpart of such nanofilters, formed by juxtaposing two nanorods, one made of Si_3N_4 with permittivity of $\sim 4.33\varepsilon_0$ and the other made of Ag with a Drude model dispersion consistent with the silver permittivity data from the literature. The inset shows the zoomed-in 2D full-wave numerical simulation of optical electric field vectors, when a 421-nm-wavelength optical signal guided in this waveguide impinges on these two nanorods. **(B)** Amplitude and phase of the transfer function of the 2D nanofilter shown in (A). In each plot, the two curves are shown, one representing the full-wave 2D simulation of the nanorod collection (black) and the other the result of the lumped circuit theory (red). The good agreement between the two curves supports the notion that the two nanorods indeed effectively act as lumped elements. **(C)** A cross section of a more complex 2D mn-circuit formed by six nanoelements (three nanoinductors and three nanocapacitors) is sketched in the left (color codes as in Fig. 1C), representing the circuit shown in the middle panel. A snapshot of optical electric field distribution in this cross section, when the mn-circuit is excited by a plane wave from the left, is obtained using the full-wave 2D numerical simulation and is shown on the right.

a closer analogy between the RF and the optical circuit concepts and can also lead to lumped impedance values that would effectively be independent of the orientation of this nanomodule with respect to the impressed optical electric field (*5*). Before discussing how various arrangements of such nanoparticles positioned next to one another can give us functional optical nanocircuits, I need to mention the role of metamaterials in this paradigm.

Metamaterials

Metamaterials are engineered composite media, formed by packing and embedding various subwavelength inclusions and inhomogeneities, which can exhibit unconventional response functions not observed in their individual constituents or in natural media, such as negative, low, or near-zero permittivities or permeabilities. When both permittivity and permeability are negative at a given frequency, the result is a negative refractive index (*6*). Metamaterials, particularly those with negative refraction, have attracted a great deal of interest in recent years (*7*–*26*). After the first experimental verification of a metamaterial with negative refraction at microwave frequencies (*13*), inspired by the work of Pendry on split-ring resonators (*14*), experimental and theoretical development of this area started in the microwave regime and has been steadily moving into the higher frequency regime, with recent experimental breakthroughs in the THz, infrared, and visible ranges (*15*–*20*). It is important to emphasize that the concept of metamaterials is not limited to the negative-index phenomenon. Indeed, other artificially engineered materials with unusual parameter values, such as ENZ materials (*21*, *22*), EVL materials (*5*, *23*), and single-negative (SNG) media, may offer exciting potential applications as well. For instance, using ENZ materials, we have theoretically shown the possibility of squeezing light through very narrow channels and tight bends (*21*), as well as its role in transparency and cloaking (*22*, *25*). Broadly speaking, metamaterials provide a platform for dispersion engineering and management, namely, the possibility of developing materials with desired temporal and spatial dispersions, which would provide powerful tools in manipulating and tailoring electromagnetic waves. For instance, it is well known that by stacking pairs of thin layers of plasmonic material (e.g., Ag) and conventional dielectric, one can form an anisotropic metamaterial whose permittivity tensor elements can achieve near zero or very high values (*27*–*29*). This suggests an example for our ENZ and EVL materials around the nanoelements.

A Tapestry of Nanostructures: "Metananocircuits"

For our optical nanocircuit elements, metamaterials, including plasmonic media, play important roles in the development of this concept. Using the notion of optical nanomodules described above, let us now imagine that one can position next to each other a set of these lumped nanoelements, each of deeply subwavelength size and composed of specific materials (*2*). This tapestry of composite nanoparticles as optical nanomodules indeed forms a new paradigm as an optical nanocircuit with subwavelength dimensions (Fig. 1C). Such a "metananocircuit" (mn-circuit), when excited by an optical signal, manifests a pattern of local optical electric and displacement vector fields that is analogous to the pattern of voltage and current distributions in a conventional RF circuit (Fig. 1C). This circuit can be excited by an optical signal through various means, such as optical nanoantennas or optical plasmonic waveguides feeding this circuit, or direct optical illuminations. The arrangement of nanomodules can be used to tailor the local optical electric and displacement vector fields in a desired manner in a subwavelength domain, analogous to the way, on an RF test bench in an electronic circuit laboratory, one connects different conventional circuit elements by using conducting wires on a circuit board. I argue that this patterning of local optical field can, under proper conditions, provide us with functionalities for information processing (e.g., low-pass, high-pass, or band-pass filtering), as a regular circuit does in the RF domain. Let us take the case of a filter with a two-dimensional (2D) geometry as an example (Fig. 2A). In the RF domain, a simple conventional band-pass (or band-stop) filter can be designed using a parallel (or series) combination of an inductor (L), a capacitor (C), and a resistor (R). If we want to have an analogous filter function in our optical mn-circuit, we will need to use two nanomodules—one nanoparticle (or nanorod in this 2D case) made of a material with negative permittivity (e.g., plasmonic materials such as noble metals) acting as a nanoinductor accompanied by a nanoresistor due to the material loss, and the other nanoparticle formed by a dielectric material acting as a nanocapacitor. With proper design, juxtaposing these two nanomodules, either in parallel or in series, may provide us with an optical mn-circuit with, respectively, the band-pass or the band-stop filtering functionality at a certain range of optical wavelengths. For the parallel case with 2D geometry (Fig. 2A), this assertion has been shown numerically using full-wave simulations of Maxwell equations, when a Drude dispersion model is assumed for the plasmonic material (e.g., Ag) forming the nanoinductor module (including material loss representing a nanoresistor) and a simple dielectric permittivity is assumed for the nanocapacitor module. This 2D nanofilter is placed within a thin parallel-plate waveguide with impenetrable walls at the top

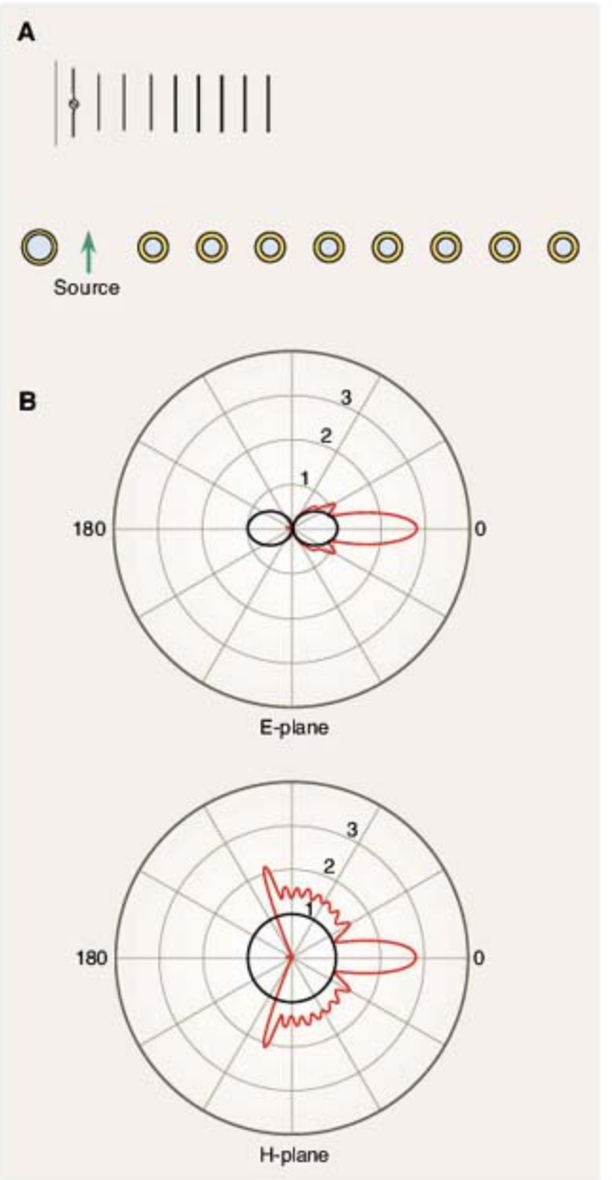

Fig. 3. Metananocircuit as a tool in the design of optical Yagi-Uda nanoantennas (*30*). **(A)** A sketch of conventional Yagi-Uda RF antenna is shown above. The collection of nanoshell particles (with two different ratios of radii) around an optical point dipole source (e.g., a molecule) can form Yagi-Uda–type optical nanoarrays. **(B)** The theoretically evaluated radiation patterns of the optical Yagi-Uda–like nanoarrays in (A) at 620 nm (red), compared with that of a dipole alone (black). In (*30*), we used the core of SiO2 and the shell of Ag in our analysis, with outer radius of $0.2\lambda_o$ and ratios of radii of 0.851 and 0.834 for the left and right nanoshells, respectively. The distance between the left nanoshell and the source is $0.25\lambda_o$, while that on the right (and between the right particles) is $0.65\lambda_o$. [From (*30*)].

and bottom [thus supporting a transverse electromagnetic (TEM) mode], acting as a two-port network. The transfer function of this filter, that is, the ratio of the optical potential at the output port to that of the incoming potential, shows a band-pass behavior, which confirms our approach to this nanofilter design at optical wavelengths (Fig. 2B). (The dispersion of the waveguide alone is excluded.) More complex nanocircuits can be envisioned when more than two nanomodules can be arranged, providing higher order transfer function for such circuits. The left panel of Fig. 2C presents the cross section of another 2D example with six optical nanoelements in a specific layout, providing the functionality essentially analogous to that of the circuit shown in the middle panel of Fig. 2C. In the right panel, we see that the full-wave 2D simulation of a snapshot of the optical electric vector field in the cross section of this 2D mn-circuit reveals field patterns that are analogous to voltage distributions in the circuit. Various material dispersions used in such mn-circuits can provide an even richer variety of transfer functions beyond the conventional RF counterparts. The performance and quality factors of such optical nanocircuit elements depend on the relative values of real and imaginary parts of permittivities of materials in the range of operating wavelengths and, therefore, depending on specific scenarios and applications, it may be preferable to use optical materials with proper ranges of ratios of imaginary to real parts of permittivity.

Although the concept of mn-circuits is based on the arrangement of metamaterial and plasmonic nanostructures, the converse may also be considered, namely, these optical mn-circuits can be envisioned as lumped inclusions to be used for synthesizing metamaterials with prescribed, and even more intricate, dispersion properties. As in the case of microwave metamaterials in which distributions of resonant elements [for instance, either split-ring (L-C) resonators in the 3D realizations (*13*) or lumped RF circuit elements (e.g., lumped inductors and capacitors) in the planar transmission line metamaterials (*10*, *11*)] are considered, here optical mn-circuits can be the building blocks as inclusions for more diverse classes of engineered materials in the future, providing a road map for tailoring novel optical metamaterials with various dispersion features.

Designing Optical Nanodevices and Components

To illustrate how such mn-circuits may contribute to the understanding and innovation of other nano-optical devices and components, we have studied and analyzed several problems in which these concepts can provide guides to solutions. One such problem is how some of the well-known antenna designs in the RF and microwave domains, for example, the Yagi-Uda antennas, can be brought into the nanoscale optical domain (*30*). In the Yagi-Uda antenna, the main element is known to be a resonant dipole, accompanied by several parasitic (i.e., passive) wire elements in order to narrow the antenna radiation patterns and point the main beam in a given direction (Fig. 3). To transplant this concept from the microwave into the optical domain, in (*30*) we considered two-material nanostructures [e.g., nanoshell particle with dielectric core and plasmonic shell (*31*)] resembling resistor-inductor-capacitor (RLC) resonant circuit at optical frequencies. It is known that at a particular ratio of core-to-shell radii, this particle is at resonance (*31*, *32*). Figure 3A shows this idea where several nanoshell particles, with a core of SiO2 and a shell of Ag and a certain ratio of radii, are placed at the right side of an optical point-dipole source (e.g., a quantum dot or a fluorescent molecule), and a single similar nanoshell particle but with a different ratio of radii is situated at the left side of this source (*30*). The radiation pattern of this nanoantenna, as obtained from our theoretical analysis (*30*), may indeed, under proper conditions, show a right-pointed main beam that is narrower than that of a single dipole, as expected and anticipated from such an antenna array (Fig. 3B). Therefore, the presence of these nanoparticles in the vicinity of the optical source, for example, a molecule, can indeed affect its emission properties. Because this design is sensitive to the operating wavelength, one can envision a set of several optical Yagi-Uda nanoantennas coupled to the same molecule, but each designed for a different specific wavelength and placed at a different orientation around a molecule. In such a scenario, each nanoantenna array, which is optimized for a specific wavelength, has its main beam pointed in a different direction. This set-up will analyze the spectral information of the molecular emission and transform the spectral contents into specific angular variations of emitted signals.

Another topic that has received inspiration from this concept of mn-circuits is the theory we

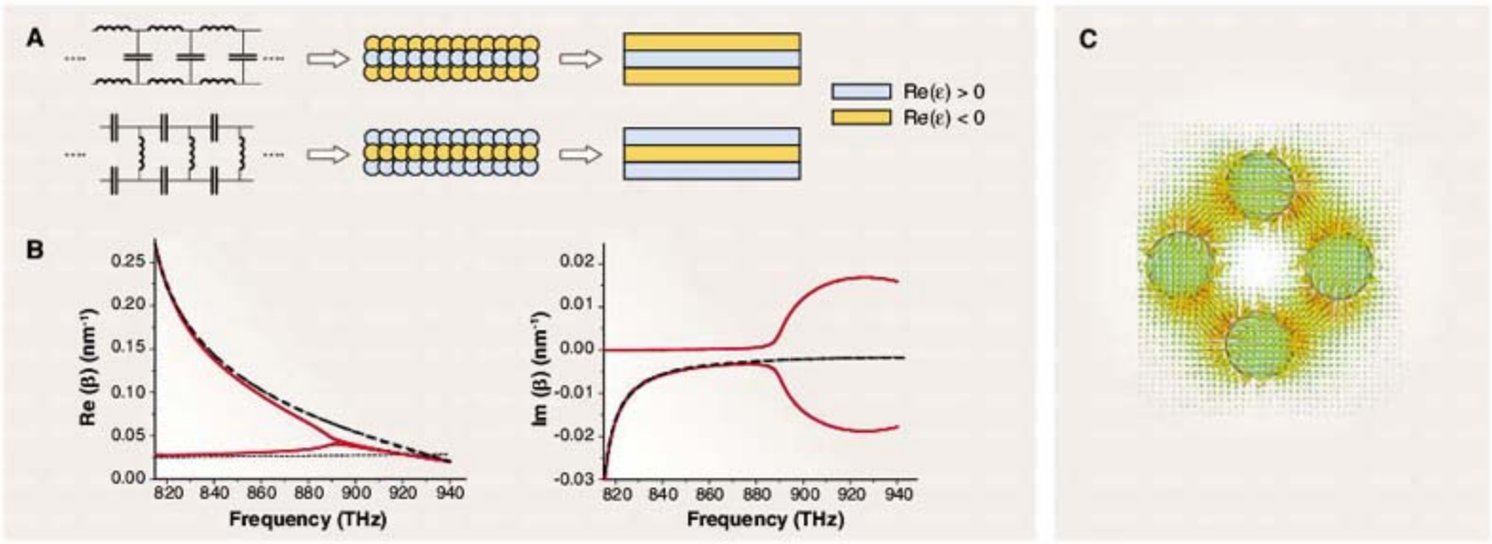

Fig. 4. Optical nanotranmission line based on the mn-circuits. **(A)** The concept of transmission lines in RF and microwave (left) can be brought into the optical domain using the notion of lumped nanocircuit elements (middle and right). By replacing the lumped inductor and capacitor with plasmonic [Re(ε) < 0] and dielectric [Re(ε) > 0] nanoparticles, respectively, the structures shown in the middle panel can be obtained. In the limit, when these nanoparticles merge into each other, the guided-wave structures sketched on the right are the result. These structures thus indeed function as optical nanotransmission (*37*). **(B)** The dispersion diagram of the waveguide shown in (A), when the SiO2 and Ag are considered for the dielectric and plasmonic materials. Solid lines are for the even mode in Ag-SiO2-Ag waveguide; dashed lines are for the odd mode in SiO2-Ag-SiO2 waveguide; the dotted line shows the light line for SiO2. For Ag, a Drude dispersion is assumed in our analysis. These results show that such optical nanotransmission lines can exhibit backward-wave and forward-wave propagation, as their RF and microwave counterparts do. [Adapted from (*37*). Copyright 2006, Optical Society of America] **(C)** Simulated electric field distribution for a nanoring composed of four plasmonic nanospheres at 655 THz. [Adapted from (*41*). Copyright 2006, Optical Society of America]

developed for the far-field subdiffraction optical microscopy (FSOM), or supermicroscopy (*29*). In this technique, an optical imaging system in the far field can in principle capture the image of two points that are placed less than half a wavelength from each other. An ordinary microscope cannot resolve two such points because of the Abbe-Rayleigh limit. However, in the theory of FSOM, we have shown that by using properly designed metamaterial crystals in the close vicinity of the object, one can magnify these objects in the near field such that their images in the output plane of the metamaterial crystal structure can be farther apart than half a wavelength, and then a regular optical microscope can detect these magnified images. Thus, the overall imaging system can in principle have a resolution better than the conventional Abbe-Rayleigh limit, although it is still a far-field system with a near-field magnification. The key section of such FSOM is the metamaterial layered structure in which stacks of pairs of thin plasmonic and dielectric layers create a medium with hyperbolic dispersion. The permittivity tensor of such a structure is similar to that of anisotropic plasma, which has been investigated by many groups. An interesting feature in wave propagation in such a medium is the cone of resonance (*33*). Balmain's group (*33*) has studied this phenomenon by analyzing two-dimensional arrays of lumped inductors and capacitors in the microwave frequencies. We investigated what would happen if we replaced their RF lumped inductors and capacitors with our optical lumped nanoinductors and nanocapacitors using negative permittivity and dielectric nanoparticles, respectively. In the limit when these nanoparticles are packed closer and closer, one would obtain the metamaterial-layered structure with hyperbolic dispersion required for supermicroscopy. It is important to note that Narimanov's group, independently and at the same time but using a quite different approach, studied such metamaterial structures for supermicroscopy, which they name "hyperlens" (*34*). Zhang's group (*35*) and Smolyaninov's group (*36*) have experimentally verified and validated this concept.

One more topic that got inspiration from the notion of mn-circuits is the possibility of the design of 1D, 2D, and 3D optical nanotransmission lines with negative refraction (*26*, *37*, *38*). In the RF and microwave domains, it has been shown by several groups (*10*, *11*) that dual transmission lines, formed by series lumped inductors and shunt lumped capacitors, support wave propagation with negative refraction. When one replaces these lumped elements with their optical counterparts (Fig. 1A), optical nanotranmission lines can be envisioned in which a subset of the allowed modes of propagation may exhibit negative refraction. Figure 4 sketches this concept. This approach provides an interesting way to obtain negative refraction at optical frequencies. Atwater's group has recently demonstrated experimentally the negative refraction in 2D metal-insulator-metal geometry (*39*). The circuit concept has also facilitated the understanding and calculation of resonant metamaterials at optical frequencies in (*40*). Moreover, the concept of mn-circuits has helped to suggest the arrangements of rings of metallic nanoparticles, as circular loops of LC elements in optics, that is, the optical version of slit-ring resonators, which can generate magnetic dipole moments at optical frequencies (Fig. 4C) (*41*). Such rings of nanoparticles can be the basic inclusions for photonic metamaterials with magnetic response and negative refraction (*41*).

Concluding Remarks

Although mn-circuits may offer exciting possibilities and may suggest new ways of tackling nano-optical data processing, they also bring new challenges and questions. As the few examples described above suggest, this notion may lead to a different method in exploring some of the future potentials in nano-optics. This concept may link together the fields of circuit designs and nano-optics, along with metamaterials and plasmonics, linking the macroworld to the nanoworld in optics and electronics, and leading to metactronics as another paradigm for nanoelectronics/nanophotonics. It can open doors to the exporting and transplanting of various ideas from RF and microwave into the IR and visible frequency domains, and it may lead to innovation in nanodevices and components—with the capability of optical detection, optical processing and storage, and data exchange on the nanoscale—and to potential applications and breakthroughs in various scientific fields.

References and Notes

1. N. Engheta, A. Salandrino, A. Alù, *Phys. Rev. Lett.* **95**, 095504 (2005).
2. Although the nanoparticles are assumed to be deeply subwavelength, they are not too small to necessitate taking into account the quantum effects in these phenomena. Therefore, we are still operating in the domain of classical electrodynamics, and permittivity functions are considered.
3. Depending on the frequency dispersion of the dielectric function, such an effective nanoinductor may itself be frequency dependent as $L_{eff} \propto \frac{1}{-\omega^2 a \mathrm{Re}(\varepsilon(\omega))}$, where a is length scale related to the size of particle. If we consider a Drude model for $\varepsilon = \varepsilon_o\left(1 - \frac{\omega_p^2}{\omega^2}\right)$ and if we operate at frequency ω sufficiently lower than ω_p, then L_{eff} will be approximately constant. If we are close to, but still lower than, ω_p, this nanoparticle can be regarded as a parallel combination of a capacitor and an inductor, with inductive impedance still dominating the effect. I thank S. Tretyakov of Helsinki University of Technology for his comments on this latter issue and the related fruitful discussion.
4. V. M. Shalaev, *Phys. Rep.* **272**, 61 (1996).
5. M. Silveirinha, A. Alù, J. Li, N. Engheta, www.arxiv.org/abs/cond-mat/0703600.
6. V. G. Veselago, *Sov. Phys. Usp.* **10**, 509 (1968).
7. D. R. Smith, J. B. Pendry, M. C. K. Wiltshire, *Science* **305**, 788 (2004).
8. J. B. Pendry, D. R. Smith, *Sci. Am.* **295**, 60 (2006).
9. V. M. Shalaev, *Nature Photonics* **1**, 41 (2007).
10. C. Caloz, T. Itoh, *Electromagnetic Metamaterials: Transmission Line Theory and Microwave Applications* (Wiley-IEEE Press, Hoboken, NJ, 2006).
11. G. V. Eleftheriades, K. G. Balmain, Eds., *Negative-Refraction Metamaterials* (Wiley-IEEE Press, Hoboken, NJ, 2005).
12. N. Engheta, R. W. Ziolkowski, Eds., *Metamaterials: Physics and Engineering Explorations* (Wiley-IEEE Press, Hoboken, NJ, 2006).
13. R. Shelby, D. R. Smith, S. Schultz, *Science* **292**, 77 (2001).
14. J. B. Pendry, A. J. Holden, D. J. Robbins, W. J. Stewart, *IEEE Trans. Microw. Theory Tech.* **47**, 2075 (1999).
15. T. J. Yen *et al.*, *Science* **303**, 1494 (2004).
16. V. M. Shalaev *et al.*, *Opt. Lett.* **30**, 3356 (2005).
17. S. Zhang *et al.*, *Phys. Rev. Lett.* **95**, 137404 (2005).
18. S. Zhang *et al.*, *J. Opt. Soc. Am. B* **23**, 434 (2006).
19. G. Dolling, C. Enkrich, M. Wegener, C. Soukoulis, S. Linden, *Opt. Lett.* **31**, 1800 (2006).
20. G. Dolling, M. Wegener, C. Soukoulis, S. Linden, *Opt. Lett.* **32**, 53 (2007).
21. M. Silveirinha, N. Engheta, *Phys. Rev. Lett.* **97**, 157403 (2006).
22. A. Alù, N. Engheta, *Phys. Rev. E Stat. Nonlin. Soft Matter Phys.* **72**, 016623 (2005).
23. J. T. Shen, P. B. Catrysse, S. Fan, *Phys. Rev. Lett.* **94**, 197401 (2005).
24. J. Li, N. Engheta, *Phys. Rev. B* **74**, 115125 (2006).
25. M. Silveirinha, A. Alù, N. Engheta, *Phys. Rev. E Stat. Nonlin. Soft Matter Phys.* **75**, 036603 (2007).
26. A. Alù, N. Engheta, *Phys. Rev. B* **74**, 205436 (2006).
27. S. Anantha Ramakrishna, J. B. Pendry, M. C. K. Wiltshire, W. J. Stewart, *J. Mod. Opt.* **50**, 1419 (2003).
28. D. Schurig, D. R. Smith, *N. J. Phys.* **7**, 162 (2005).
29. A. Salandrino, N. Engheta, *Phys. Rev. B* **74**, 075103 (2006).
30. J. Li, A. Salandrino, N. Engheta, www.arxiv.org/abs/cond-mat/0703086
31. E. Prodan, C. Radloff, N. J. Halas, P. Nordlander, *Science* **302**, 419 (2003).
32. A. Alù, N. Engheta, *J. Appl. Phys.* **97**, 094310 (2005).
33. K. G. Balmain, A. A. E. Luttgen, P. C. Kremer, *IEEE Antennas Wireless Propag. Lett.* **1**, 146 (2002).
34. Z. Jacob, L. V. Alekseyev, E. Narimanov, *Opt. Express* **14**, 8247 (2006).
35. Z. Liu, H. Lee, Y. Xiong, C. Sun, X. Zhang, *Science* **315**, 1686 (2007).
36. I. I. Smolyaninov, Y. J. Hung, C. C. Davis, *Science* **315**, 1699 (2007).
37. A. Alù, N. Engheta, *J. Opt. Soc. Am. B* **23**, 571 (2006).
38. A. Alù, N. Engheta, *Phys. Rev. B* **75**, 024304 (2007).
39. H. J. Lezec, J. A. Dionne, H. A. Atwater, *Science* **316**, 430 (2007).
40. T. P. Meyrath, T. Zentgraf, H. Giessen, *Phys. Rev. B* **75**, 205102 (2007).
41. A. Alu, A. Salandrino, N. Engheta, *Opt. Express* **14**, 1557 (2006).

42. I thank all the members of my research group, particularly A. Alù and J. Li, for their assistance in preparing parts of Fig. 2, A to C; Fig. 3, A and B; and Fig. 4, B and C, for many fruitful discussions, and for their contributions to various aspects of the metamaterial and plasmonic research in my group. I acknowledge the research support from the U.S. Air Force Office of Scientific Research (AFOSR), grant number FA9550-05-1-0442.

10.1126/science.1133268

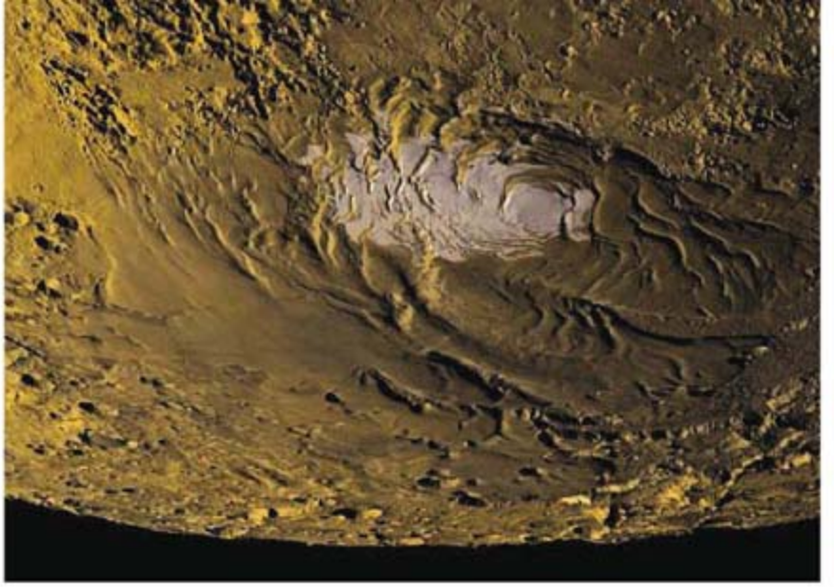

CREDIT: ZUBER ET AL.

INTRODUCTION

Water, Water, Not Everywhere?

THE STORY OF WATER ON MARS HAS A CHECKERED PAST. HISTORICALLY thought to be criss-crossed by alien canals, the arrival of the first spacecraft showed that the red planet is bone dry. A flotilla of satellites has since traveled to Mars. Water ice has been seen dusting the ground, in hydrous minerals, in glaciers draped on volcano walls, and, the vast majority, locked up in the polar caps. Such a frosting gives a clue that water was once abundant on Mars and the planet's early climate was wet. Since then, water has been lost from the surface and atmosphere. It is possible that some may have survived underground, occasionally seeping to the surface, and so signs of flowing water have been sought extensively. Such places would be top destinations for future landers to search for signs of extant or past life.

The primary mission of the latest spacecraft to reach the red planet, the Mars Reconnaissance Orbiter (MRO), is to study its hydrologic history. It is opening up new vistas with its exceptionally keen eyesight. Regional landforms were mapped before, but MRO can now spot boulders less than a few meters in size, allowing Martian global geology to be surveyed on a human scale over vast areas. Among several other instruments, it also contains a radar sounder for exploring subsurface ice deposits and is accurately measuring Mars' gravity. This special issue presents scientific results from MRO detailed images of the ice-capped poles and regions thought to have been shaped by liquid water, both recently and in the past.

The papers in this issue show that evidence for liquid water is rare and difficult to discern (see also the News story by Kerr, p. 1673). Images of supposed ancient ocean floors and riverbeds show no obvious signs that liquid water was ever present. Reexamination of some some landforms implies that they have been formed by flowing lava, not water. The only locations where features seem to indicate the presence of liquid water today or in the recent past are on the rims of craters and some gullies, suggesting that heat from impacts may have been the trigger for trickles rather than a revealed water table. Radar and gravity data show that the cap on Mars' south pole now holds the largest reservoir of relatively pure water ice on the planet, and layers there and in the north polar cap reveal seasonal oscillations in climate.

These papers thus provide a tour around the martian world of water in the first 100 days or so of the main MRO mission. More will be revealed as it continues to probe the surface, including Mars' mineralogy, and focuses several instruments on its atmosphere, dust, and clouds. But there is a lot to drink already.

– JOANNE BAKER

Mars Reconnaissance Orbiter

CONTENTS

Reports

1706 A Closer Look at Water-Related Geologic Activity on Mars
A. S. McEwen et al.

1709 Athabasca Valles, Mars: A Lava-Draped Channel System
W. L. Jaeger et al.

1711 Meter-Scale Morphology of the North Polar Region of Mars
K. E. Herkenhoff et al.

1715 Accumulation and Erosion of Mars' South Polar Layered Deposits
R. Seu et al.

1718 Density of Mars' South Polar Layered Deposits
M. T. Zuber et al.

See also related News story page 1673

Science

REPORT

A Closer Look at Water-Related Geologic Activity on Mars

A. S. McEwen,[1]* C. J. Hansen,[2] W. A. Delamere,[3] E. M. Eliason,[1] K. E. Herkenhoff,[4] L. Keszthelyi,[4] V. C. Gulick,[5] R. L. Kirk,[4] M. T. Mellon,[6] J. A. Grant,[7] N. Thomas,[8] C. M. Weitz,[9] S. W. Squyres,[10] N. T. Bridges,[2] S. L. Murchie,[11] F. Seelos,[11] K. Seelos,[11] C. H. Okubo,[1] M. P. Milazzo,[1] L. L. Tornabene,[1] W. L. Jaeger,[4] S. Byrne,[1] P. S. Russell,[8] J. L. Griffes,[7] S. Martínez-Alonso,[6] A. Davatzes,[5] F. C. Chuang,[9] B. J. Thomson,[2] K. E. Fishbaugh,[12] C. M. Dundas,[1] K. J. Kolb,[1] M. E. Banks,[1] J. J. Wray[10]

Water has supposedly marked the surface of Mars and produced characteristic landforms. To understand the history of water on Mars, we take a close look at key locations with the High-Resolution Imaging Science Experiment on board the Mars Reconnaissance Orbiter, reaching fine spatial scales of 25 to 32 centimeters per pixel. Boulders ranging up to ~2 meters in diameter are ubiquitous in the middle to high latitudes, which include deposits previously interpreted as fine-grained ocean sediments or dusty snow. Bright gully deposits identify six locations with very recent activity, but these lie on steep (20° to 35°) slopes where dry mass wasting could occur. Thus, we cannot confirm the reality of ancient oceans or water in active gullies but do see evidence of fluvial modification of geologically recent mid-latitude gullies and equatorial impact craters.

A major goal of the Mars Reconnaissance Orbiter (MRO) mission is to better understand the history of water (*1*). The High-Resolution Imaging Science Experiment (HiRISE) is imaging the martian surface at scales of 25 to 32 cm per pixel, with a center color swath that distinguishes major surface materials (dust, sand, rock, or frost) and stereo imaging for topographic studies (*2*, *3*). We highlight three new results concerning the history of water on Mars: (i) the nature of middle- to high-latitude surface deposits and relevance to putative oceans and climate change, (ii) processes forming and modifying the geologically recent gullies, and (iii) evidence for water in the ejecta of recent equatorial impact craters.

The origin of the Vastitas Borealis Formation (VBF), covering the lowest portions of the extensive northern plains, has been the subject of much debate, including (among other hypotheses) that it is the fine-grained residue of an ancient ocean (*4*) or that it represents frozen deposits of sediment-laded water from giant outflow channels (*5*). The more than 200 HiRISE images of this unit show that rocks ranging in size from the limits of resolution (~0.5 m) to ~2 m in diameter are ubiquitous (Fig. 1), except where buried by eolian or airfall materials. Boulders are concentrated around circular structures of probable impact origin, but they are present over most of the VBF at uniform densities. In addition, we have seen no light-toned layered deposits within the VBF; such deposits elsewhere are thought to be of aqueous sedimentary origin (*6*). The boulder distribution and absence of light-toned layered deposits are difficult to reconcile with the hypothesis that the VBF primarily consists of a thick (~100-m) deposit of fine-grained materials deposited from suspended sediments in an ocean (*4*). Either the VBF had a different origin or the combination of impacts and periglacial processes has raised boulders from depth and thoroughly mixed them with overlying materials; viscously relaxed topography (*7*) and ubiquitous polygonal-patterned ground (*8*) may be consistent with such processes.

One hypothesis for the origin of recent mid-latitude gullies is that they formed from the melting of snow deposited during a period of higher orbital obliquity, with remnants of the snow pack still present as "pasted-on" material (*9*). HiRISE has imaged this material at several locations, and the surfaces that it appears on include many boulders (fig. S2). We interpret these materials as rock glaciers: rocky deposits rich in ice, similar to interpretations of debris aprons elsewhere on Mars (*7*). The rockiness is inconsistent with a primary origin as dusty snowfall, unless subsequent processes have modified the deposits, but those deposits are nearly free of impact structures and are likely much younger than the VBF, making such modification unlikely. Note that a thin mantle over many mid-latitude regions (*10*) does still appear fine-grained at HiRISE resolution.

Mid-latitude gullies (*11*) are of great interest because they may indicate that liquid water can reach the surface, even today (*6*, *12*). Key questions are whether liquid water is required to form some of them (and, if so, what is the source of that water) and whether the gully-forming processes are ongoing—even in the present-day climate—rather than being the result of past climates and different insolation geometries. HiRISE images confirm that many gully morphologies on Mars, including braided channels and terraces (Fig. 2), are similar to water-carved features on Earth. Boulders 0.5 to 3 m in diameter are more concentrated in the channels than in surrounding terrains, which is consistent with processes that remove the finer particles. Erosional channels occur on slopes of less than 20° (e.g., Fig. 2, B and C), which is inconsistent with dry granular flows. We are not aware of common terrestrial processes besides running water that could explain all of these observations. HiRISE images also reveal a range of relative ages for the gullies [see the supporting online material (SOM)].

Evidence for ongoing gully activity has come from observations at two locations of new, bright deposits corresponding to depositional fans (*12*) (Fig. 3 and fig. S2). Not all bright deposits at gully termini consist of recent gully-emplaced sediment, as some appear to consist of rippled eolian deposits or patterned ground, modifying relatively old gully deposits (fig. S3).

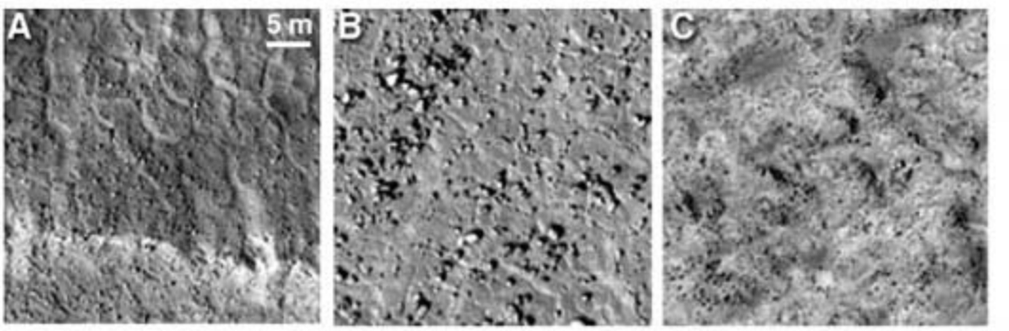

Fig. 1. Boulders over northern lowland terrains. **(A)** PSP_001964_2275 (*26*) at 47.0° N, 101.8° E. **(B)** TRA_000846_2475 at 67.0° N, 0.0° E. **(C)** PSP_001810_2175 at 37.2° N, 348.0° E. For all figures, North is at the top and time of day is near 3 p.m., and images have been reprojected to a scale of 25 cm per pixel.

[1]Lunar and Planetary Laboratory, University of Arizona, Tucson, AZ 85721, USA. [2]Jet Propulsion Laboratory, Pasadena, CA 91109, USA. [3]Delamere Support Systems, Boulder, CO 80304, USA. [4]U.S. Geological Survey, Flagstaff, AZ 86001, USA. [5]NASA Ames Research Center/SETI Institute, Moffett Field, CA 94035, USA. [6]University of Colorado, Boulder, CO 80309, USA. [7]Smithsonian Center for Earth and Planetary Studies, Washington, DC 20650, USA. [8]University of Bern, Bern, Switzerland. [9]Planetary Science Institute, Tucson, AZ 85719, USA. [10]Cornell University, Ithaca, NY 14853, USA. [11]Applied Physics Laboratory, Laurel, MD 20723, USA. [12]International Space Science Institute, Bern, Switzerland.

*To whom correspondence should be addressed. E-mail: mcewen@lpl.arizona.edu

In the Centauri–Hellas Montes region, the entire equator-facing slope of a crater is covered by narrow gully channels (Fig. 3). There is no evidence for eolian, periglacial, or other modifications of many of these channels. The lower portions of some channels do contain ripples of probable eolian origin, and boulder tracks are superimposed over some channels, so there is a range of relative ages. The bright material, deposited between 1999 and 2004 (*12*), emanates from some apparently unmodified gully channels. From stereo imaging (fig. S4), we confirm that, in some places, this bright deposit diverts around topographic obstructions like a fluid and, at the distal end, overtops low hummocks like a landslide. The shape of the deposit has not changed over the 15 months since last imaged by the Mars Orbiter Camera, which suggests that it is not bright because of frost or ice (*13*). Near-infrared spectra (*14*) do not reveal hydrated minerals in the bright deposit, as might be expected from sublimation of salty groundwater (fig. S5). There are bright materials within gullies over much of the slope, so the new deposit may have come from the redeposition of preexisting bright material (Fig. 3 and fig. S2B). Also, dust-sized materials are generally brighter than sand and rocks on Mars. Thus, the relative brightness of this material does not directly indicate a role for water.

We have imaged gully deposits with bright termini at four locations that appear to be very recent, in addition to the two locations reported previously (figs. S6 and S7). These deposits are again associated with fine channels and show no subsequent modification. All six of the deposits are near the base of relatively long, steep slopes (see the SOM, including table S1); five are on the slopes of well-preserved impact craters. There is no favored slope aspect: The bright deposits are on east-, west-, equator-, and pole-facing slopes. All are in the middle latitudes 31° to 47° N and S, but there has been no systematic monitoring of steep slopes in the equatorial regions of Mars, so a latitudinal dependence to active slope movements is unknown. The average slopes are greater than 20°, close to the stability limits of dry, unconsolidated materials, and the elevation drops by at least 500 m (table S1). Long, steep slopes are favorable to both groundwater breakouts and gravity-driven movements. In summary, although the involvement of liquid water cannot be ruled out, there is no confirmation from MRO analyses to date that water reached the surface in the past decade.

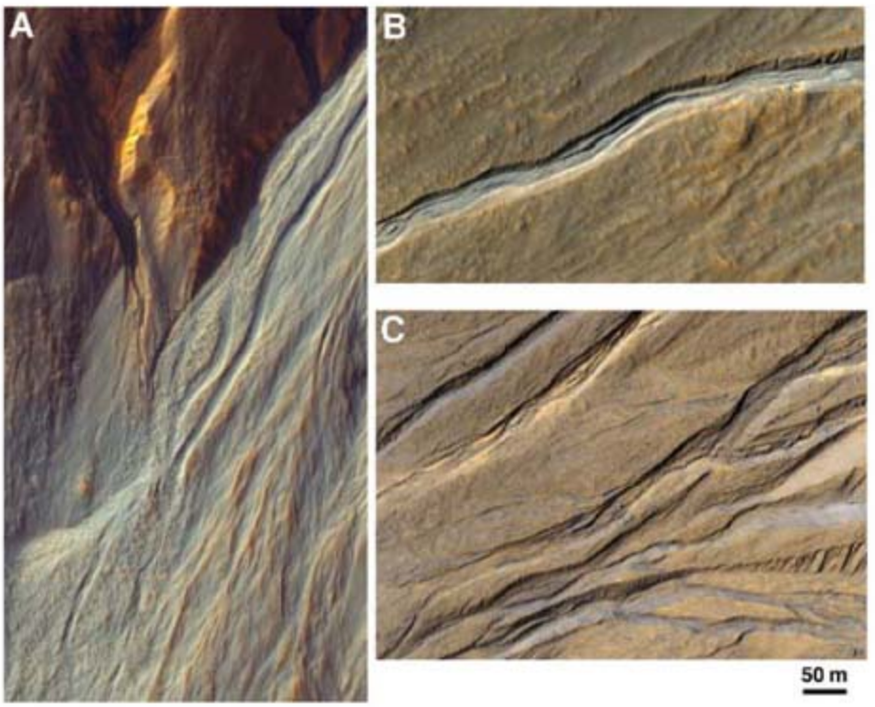

Fig. 2. Color images of gully channels. **(A)** Portion of PSP_002172_1410 at 38.9° S, 195.9° E. **(B)** and **(C)** are portions of PSP_002932_1445 at 35.1° S, 324.7° E in Hale Crater. Color (here and in other figures) is constructed from red and blue-green bandpasses and exaggerated as compared with natural color. Downslope direction is toward the bottom of (A) and the lower left of (B) and (C).

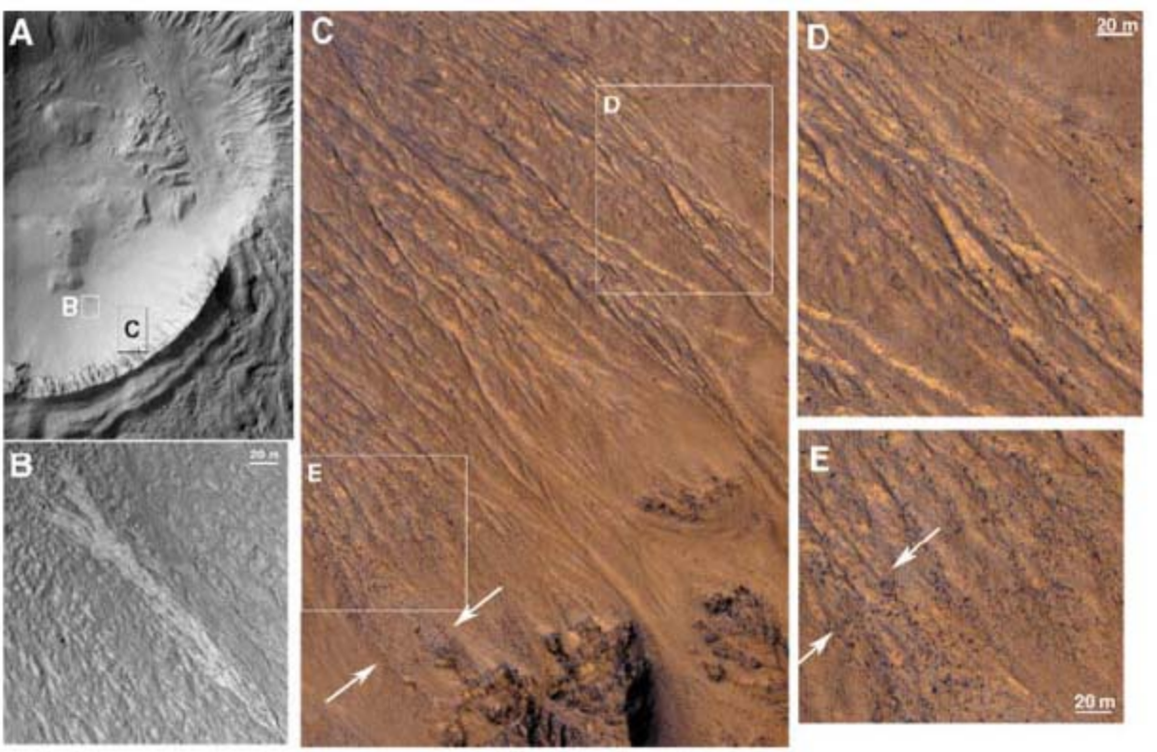

Fig. 3. Crater in Centauri–Hellas Montes region at 38.4° S, 96.8° E. **(A)** Browse image PSP_001714_1415. **(B)** Full-resolution portion of image indicated in (A), showing the bright deposit. **(C)** Color for portion of image indicated in (A). **(D)** Enlargement of channels [indicated in (C)], showing eroded bright deposits and boulders concentrated in the channels. **(E)** Enlargement of the apparent source region [indicated in (C)] above the new bright deposit. The shallow depression and uppermost channels leading to the new deposit lie between the arrow tips in (C) and (E). North is 7 degrees to the right of the top.

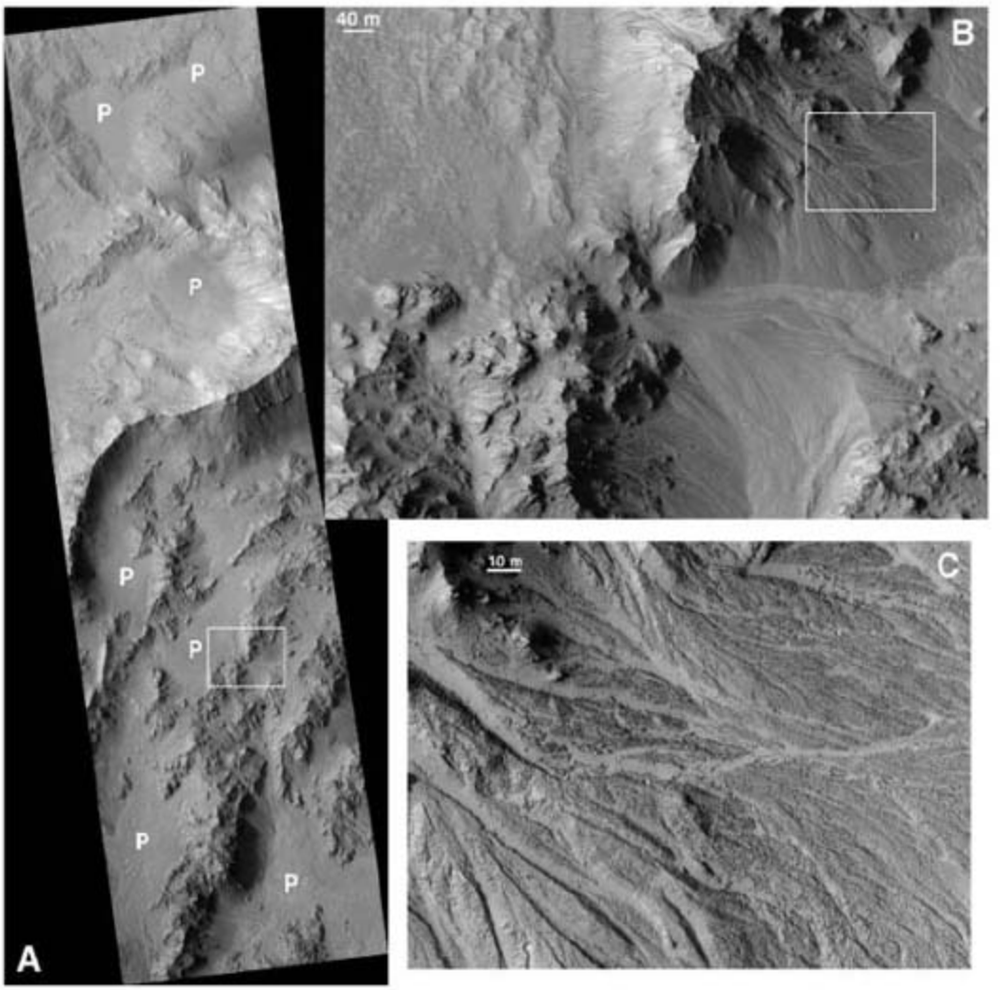

Fig. 4. Northwestern rim of Mojave Crater at 7.6° N, 327° E (PSP_001481_1875). **(A)** Full browse image at greatly reduced resolution. Several locations of ponded and pitted material are labeled with "P"; boxed area shows the location of enlargement indicated in (B). **(B)** An example of where a large fan emanates from the ponded and pitted material to the northwest; boxed area shows enlargement to the full-resolution sample indicated in (C). **(C)** Braided and distributary channels and boulders up to ~1 m in diameter.

The lobate morphology of some martian impact crater ejecta has long been considered evidence for fluidization by water (*15*) or other mechanisms (*16*), but conclusive evidence for the presence of water in the ejecta has been elusive (*17*). Meanwhile, another debate has arisen about the possibility of impact-induced "rainfall" producing the erosion of Noachian (>3.7 billion-year-old) terrains (*18*). HiRISE observations of relatively large but geologically recent and well-preserved impact craters are providing insights relative to both debates.

Mojave Crater (60 km in diameter) contains channels and fan-shaped deposits (*11*) with a marked resemblance to alluvial fans in desert regions on Earth (*19*). The branching channels of third or fourth order include first-order channels at topographic peaks and ridges (Fig. 4B), which are difficult to explain by seepage of a groundwater table, leading to the hypothesis of impact-generated precipitation (*20*). The channels and fans are present on much of the terrace and rim regions but not on all topographic features (e.g., the central uplift or ponded and pitted materials), which may prove difficult to reconcile with the precipitation theory. A geologically recent origin of the crater is indicated by the small number of impact craters superimposed on both the fans and undissected portions of the crater (*21*). Mojave appears to be one of the most recent craters on Mars that is larger than 50 km in diameter, which form on average about every 20 million years (*22*). HiRISE stereo observations show ponded materials at various levels inside and outside of the crater (Fig. 4A), which sometimes have a fractured surface similar to ponded materials in lunar craters (*23*). However, unlike lunar examples, the martian "ponds" are often covered by coalesced pits, which lack raised rims and appear to be coeval. We interpret this pitted, ponded unit to be a mix of melt and fragmented rock similar to that found in terrestrial impact craters in volatile-rich targets (*24*), with pitting due to collapse from the loss of volatiles. There is a close association between the ponded material, which does not show evidence for erosion by overland flow, and the channels and fans that extend downhill of the ponded deposits (*25*) (Fig. 4B), suggesting that water was released from the ponded deposits.

The fluvial geomorphology of Mojave Crater was thought to be an isolated occurrence (*19*, *20*), but we have found channels, alluvial-like fans, debris flows, and the presence of ponded and pitted material in other geologically recent craters, including Hale (125 to 150 km in diameter), Tooting (28 km in diameter; fig. S8), Zunil (10 km in diameter), and more than ten others (*25*). The ponded material appears to be far more voluminous than ponded materials in lunar craters of comparable size, in spite of lower primary impact velocities on Mars (i.e., less melt production if the target materials were identical). The key difference may be that the martian upper crust is rich in ice, water, and hydrated minerals, which can form muddy debris and lower the melting point of silicate minerals. The evidence for impact-induced precipitation at Mojave or elsewhere remains inconclusive, but the HiRISE observations demonstrate that landscapes with a fluvially modified appearance may be produced by syndepositional effects during impact cratering. The much larger and more numerous craters produced in the Late Noachian could explain some of the pervasive erosion of Noachian-aged terrains, thus weakening the argument that ancient Mars must have had a warmer, wetter climate on a sustained basis.

HiRISE observations are sharpening our view of when and where water has modified the martian surface. These observations inform models for past and present geologic and climatic processes and can focus future exploration to those locations with the greatest promise for discovering evidence for life.

References and Notes

1. R. Zurek, S. Smrekar, *J. Geophys. Res.* **112**, E05S01 (2007).
2. A. S. McEwen *et al.*, *J. Geophys. Res.* **112**, E05S02 (2007).
3. C. H. Okubo, A. S. McEwen, *Science* **315**, 983 (2007).
4. M. A. Kreslavsky, J. W. Head, *J. Geophys. Res.* **107**, 5121 (2002).
5. M. H. Carr, J. W. Head, *J. Geophys. Res.* **108**, 5042 (2003).
6. M. C. Malin, K. S. Edgett, *J. Geophys. Res.* **106**, 23429 (2001).
7. S. W. Squyres, S. M. Clifford, R. O. Kuzmin, J. R. Zimbelman, F. M. Costard, in *Mars*, H. H. Kieffer *et al.*, Eds. (Univ. of Arizona Press, Tucson, AZ, 1992), pp. 523–554.
8. M. T. Mellon, *J. Geophys. Res.* **102**, 25617 (1997).
9. P. R. Christensen, *Nature* **422**, 45 (2003).
10. J. F. Mustard, C. D. Cooper, M. K. Rifkin, *Nature* **412**, 411 (2001).
11. Martian gullies have been defined as landforms on relatively steep slopes that may include an alcove, channel, and depositional fan (*6*) and that may form by a variety of processes, such as dry mass wasting, wet debris flows, or running water. The gullies are typically much younger than the landforms that they eroded. The channels and fans seen in large young impact craters are similar in morphology to the gullies but are larger, occur

over shallower slopes, and appear to be the same age as the craters.
12. M. C. Malin, K. S. Edgett, L. V. Posiolova, S. M. McColley, E. Z. Noe Dobrea, *Science* **314**, 1573 (2006).
13. K. E. Williams, O. B. Toon, J. Heldmann, *Geophys. Res. Lett.* **34**, L09204 (2007).
14. S. L. Murchie *et al.*, *J. Geophys. Res.* **112**, E05S03 (2007).
15. M. H. Carr, G. G. Schaber, *J. Geophys. Res.* **82**, 4039 (1977).
16. O. S. Barnouin-Jha, P. H. Schultz, *J. Geophys. Res.* **101**, 21099 (1996).
17. R. M. E. Williams, K. S. Edgett, paper presented at the American Geophysical Union Fall Meeting, abstr. P33B-03, San Francisco, CA, 13 to 17 December 2004.
18. T. L. Segura, O. B. Toon, A. Colaprete, K. Zahnle, *Science* **298**, 1977 (2002).
19. R. M. E. Williams, J. R. Zimbelman, A. K. Johnston, *Geophys. Res. Lett.* **33**, L10201 (2006).
20. R. M. E. Williams, K. S. Edgett, M. C. Malin, *Lunar Planet. Sci.* **XXXV**, abstr. 1415 (Lunar and Planetary Institute, Houston, TX, CD-ROM, 2004).
21. There are four craters that are larger than 100 m in diameter in MRO context image 808_1874, which covers 2.1×10^3 km^2 of the interior and continuous ejecta of Mojave Crater.
22. B. A. Ivanov, *Space Sci. Rev.* **96**, 87 (2001).
23. D. J. Heather, S. K. Dunkin, *Icarus* **163**, 307 (2003).
24. G. R. Osinski, *Meteorit. Planet. Sci.* **41**, 1571 (2006).
25. L. L. Tornabene *et al.*, *Lunar Planet. Sci.* **XXXVIII**, abstr. 1338 (Lunar and Planetary Institute, Houston, TX, CD-ROM, 2004).
26. HiRISE images are identified by the format "mission phase_orbit number_orbital position." Thus, PSP_001468_1535 was acquired in the Primary Science Phase, orbit 1468, and 153.5 degrees from the night-side equator or 26.5°S latitude (MRO travels north over the day side in its orbit).
27. We thank the science, operations, and engineering teams of the HiRISE and MRO projects, whose diligent efforts enabled the results presented here, and also thank the reviewers and editor. For more information about HiRISE and image access, see (http://hirise.lpl.arizona.edu).

Supporting Online Material

www.sciencemag.org/cgi/content/full/317/5845/1706/DC1
SOM Text
Figs. S1 to S8
Table S1
References

18 April 2007; accepted 10 August 2007
10.1126/science.1143987

REPORT

Athabasca Valles, Mars: A Lava-Draped Channel System

W. L. Jaeger,[1]* L. P. Keszthelyi,[1] A. S. McEwen,[2] C. M. Dundas,[2] P. S. Russell[3]

Athabasca Valles is a young outflow channel system on Mars that may have been carved by catastrophic water floods. However, images acquired by the High-Resolution Imaging Science Experiment camera onboard the Mars Reconnaissance Orbiter spacecraft reveal that Athabasca Valles is now entirely draped by a thin layer of solidified lava—the remnant of a once-swollen river of molten rock. The lava erupted from a fissure, inundated the channels, and drained downstream in geologically recent times. Purported ice features in Athabasca Valles and its distal basin, Cerberus Palus, are actually composed of this lava. Similar volcanic processes may have operated in other ostensibly fluvial channels, which could explain in part why the landers sent to investigate sites of ancient flooding on Mars have predominantly found lava at the surface instead.

Athabasca Valles is the youngest outflow channel system on Mars (*1*–*3*). It originates at a fissure (part of the Cerberus Fossae), extends southwest for about 300 km, and debouches into a basin named Cerberus Palus (Fig. 1). In most respects, Athabasca Valles resembles the catastrophic flood-carved landscape of the Channeled Scabland in Washington State, with branching channels, streamlined "islands," and dunes interpreted to have formed subaqueously (*2*). However, its floor is remarkably uneroded at the subkilometer scale. These seemingly incongruous attributes have spawned multiple hypotheses, which depict the channel floor as either (i) a flood- or glacial-erosion surface with an uneven sediment cover (*2*, *4*), (ii) the icy or desiccated dregs of sediment-laden floodwaters that froze (*5*, *6*), or (iii) a lava flow that coursed through the channel system and solidified (*7*–*9*). Color and stereo images with high spatial resolution (27 to 117 cm/pixel) acquired by the High-Resolution Imaging Science Experiment (HiRISE) camera onboard the Mars Reconnaissance Orbiter (MRO) spacecraft provide observations that are key to resolving this debate.

HiRISE images sample Athabasca Valles from its source to its terminus, showing a solidified flow within the channels at all locations. On the north (upslope) side of the source region, the flow manifests as numerous thin, arcuate, and overlapping fronts that are concentric to the fissure-vent (Fig. 2). The fronts become progressively younger and smaller (i.e., they step up) with proximity to the fissure. They record the final surges in a waning eruption of low-viscosity fluid from the Cerberus Fossae (fig. S1).

Downstream in the channels, the flow exhibits two distinct textures: polygonal and ridged (*5*, *8*–*10*). The difference between these is surficial; the flowtop crumpled where it is ridged but remained intact where it is polygonal. Furthermore, where the flowtop rifted under tensile stress, discrete rafted plates are preserved. In several channel segments, medial ridged terrain is flanked by polygonal terrain, and the contacts between the two textures are brittle shear zones that accommodated higher flow velocities toward the center of the channel (fig. S2). These shear zones indicate that the surface of the flow was solidifying while its fluid interior continued moving downhill through Athabasca Valles.

The flow receded from its maximum stand before completely solidifying. North of the source region, it appears to have embayed a tectonic ridge while at peak discharge and then draped its flank as the eruption waned (fig. S3). However, a deposit of wind-swept, bright material obscures the stratigraphic relationship. Within Athabasca Valles, polygonal and ridged flow textures reach high onto streamlined "islands" and blanket features previously interpreted to be fluvial bedforms, including the putative subaqueous dunes (fig. S4). At its height, the flow filled and locally overbanked the channel system. Subsequently, its level dropped as fluid drained downstream into the contiguous distal basin of Cerberus Palus, where it ponded and solidified. Current channel topography suggests that, in Athabasca Valles, the flow level receded >50 m from its high stand.

The pivotal question is whether the flow is composed primarily of sediment, ice, or lava, and its answer can be educed from the thousands of ring-mound landforms (RMLs) that occur exclusively on the flow surface. RMLs are a continuum of landforms intermediate to rings and mounds (fig. S5). Various hypotheses for their origin have been advanced, each invoking a specific flow composition. If the RMLs are pingos (ice-cored mounds) in various stages of collapse, the flow is a mixture of sediment and extant ice (*5*, *11*, *12*); if the RMLs are cryophreatic cones formed by the explosive release of flow-entrained volatiles, the flow is sediment that was initially volatile-rich but is now degassed (*13*); and if the RMLs are hydrovolcanic (rootless) cones formed when groundwater heated by the overlying flow vented in steam explosions, the flow is lava (*8*, *9*). HiRISE data allow these divergent hypotheses to be tested.

Topographic information derived from HiRISE stereo image pairs shows that many RMLs are ringed by moats. The moats exhibit a frozen-in evolutionary sequence. Incipient moats have

[1]Astrogeology Team, U.S. Geological Survey, Flagstaff, AZ 86001, USA. [2]Lunar and Planetary Laboratory, University of Arizona, Tucson, AZ 85721, USA. [3]Physikalisches Institut, Universität Bern, CH-3012, Bern, Switzerland.

*To whom correspondence should be addressed. E-mail: wjaeger@usgs.gov

ring fractures at their perimeters, more-evolved moats have tilted slabs that override their surroundings, and end-stage moats show foundering plates (Fig. 3). Thus, the moats formed in response to loading of a thin, brittle crust underlain by deformable material. The crustal thickness at the time of loading can be directly measured where foundering plates are tilted edge-on, and it is on the order of a few meters.

Relict wakes bounded by levees trail downstream from many RMLs. Some of the wakes are severed where the flowtop rafted apart (Fig. 4A). This establishes that the wakes formed on the solidified surface of an active flow. However, they are not gouges left where the flowtop crumpled against anchored obstacles. Instead, they formed as gas vented from fixed sources at depth, ripping continuous openings through the moving flowtop. In some places, the wakes grade into chains of overlapping RMLs (Fig. 4B). These formed through successive explosions in a process loosely analogous to the construction of the Hawaiian Island chain, where Earth's crust moved over a fixed magma source, producing a string of volcanoes. Thus, the volatile that caused the explosions was housed beneath, not within, the flow. The RMLs are, therefore, hydrovolcanic cones, and the flow is lava. This conclusion is supported by the spatial distribution of RMLs, which preferentially occur where steam venting should be locally enhanced (fig. S6).

Previous work rejected the hydrovolcanic model on the basis that RMLs modified impact craters (*12*); however, HiRISE images show that the reverse is true. Impact craters are consistently superimposed on RMLs, indicating that the latter are older (fig. S7). Furthermore, the ejecta from these craters is strewn with boulders, suggesting that the target material is rocky. This is consistent with lava but not with ice, which would sublimate at a rate of 10^1 to 10^3 m per million years (*14*, *15*).

Several other data sets support the conclusion that the flow is lava. Although radar mapping from Earth-based radio telescopes cannot resolve Athabasca Valles proper, it shows Cerberus Palus to be exceedingly rough at the decimeter scale (*16*–*18*). The backscatter and depolarization values are consistent with blocky lava surfaces (*18*). Similarly, the Gamma-Ray Spectrometer (GRS) onboard the Mars Odyssey spacecraft showed Cerberus Palus to be among the driest regions on Mars, with a water-equivalent hydrogen abundance (~2 to 5 mass percent) suggestive of minor amounts of hydrated minerals, and no appreciable water ice, in the upper ~1 m (*19*). Both the Thermal Emission Spectrometer (TES) and the Thermal Emission Imaging System (THEMIS) found that, although the region is overlain by sufficient dust to obscure substrate mineralogy (*20*, *21*), the thermal inertia of Athabasca Valles (typically 300 to 400 J/m^{2}Ks$^{1/2}$) is still above average for Mars (*22*–*24*). These thermal inertia values do not have a unique interpretation but are comparable to the Gusev Crater and Viking 1 landing sites, both of which had an abundance of basaltic boulders (*23*). Collectively, these data point to a dust-coated, hydrogen-poor, rocky surface, which is consistent with lava.

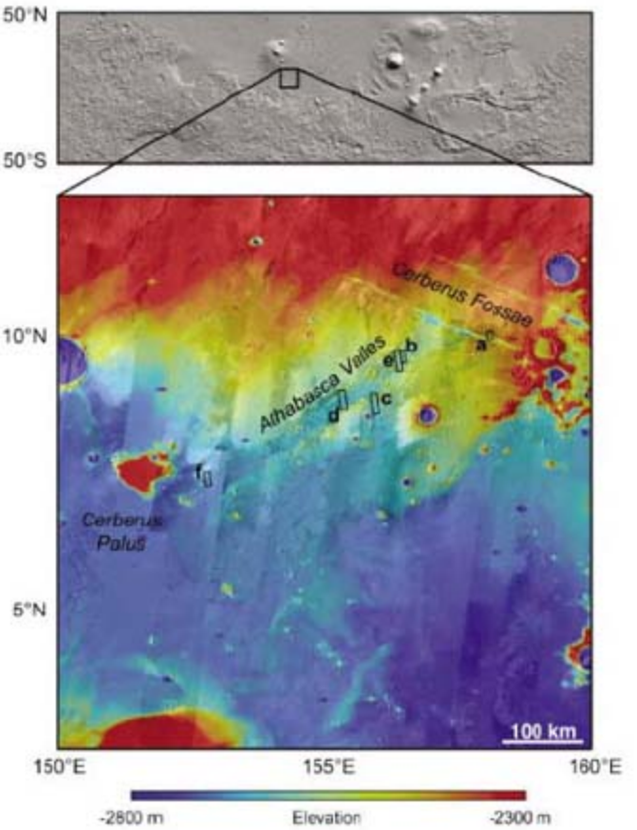

Fig. 1. (Top) Mars Orbiter Laser Altimeter (MOLA) shaded relief map of Mars covering 0° to 360°E. **(Bottom)** THEMIS infrared mosaic draped by colorized MOLA elevation data over Athabasca Valles. Key features are labeled. Black boxes locate the following HiRISE images: (a) PSP_001408_1900 (*25*), (b) stereo pair PSP_001606_1900 and PSP_002226_1900, (c) stereo pair PSP_001540_1890 and PSP_002371_1890, (d) stereo pair PSP_002938_1890 and PSP_003083_1890, (e) stereo pair PSP_002661_1895 and PSP_003294_1895, and (f) stereo pair PSP_002174_1875 and PSP_002292_1875.

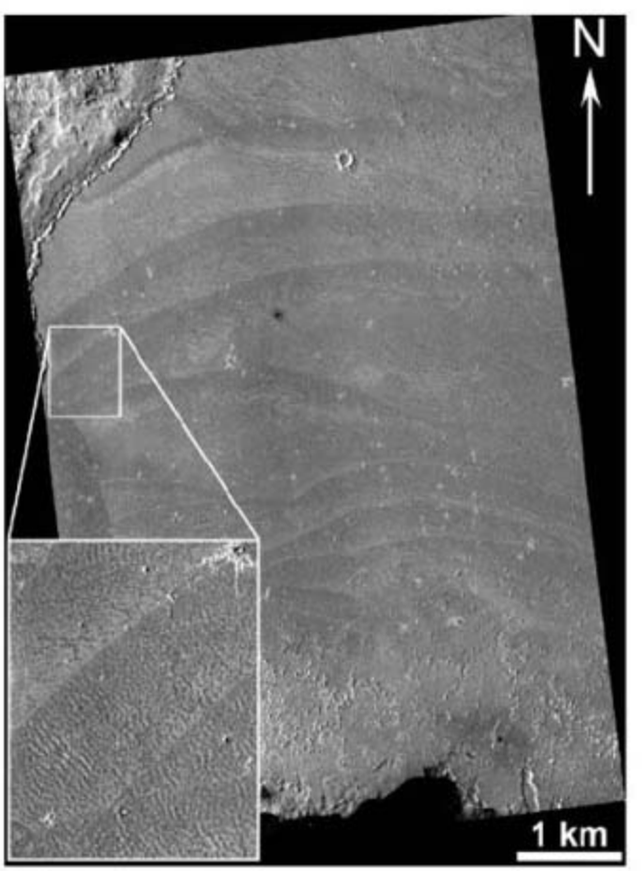

Fig. 2. HiRISE image PSP_001408_1900 shows plains north of a fissure vent at the head of an Athabasca Valles tributary. Thin, concentric flow fronts cover the plain. Shadow measurements indicate that the fronts are <1 m tall. The inset shows rough, and consequently dark, bands at their terminal edges. Illumination is from the left, and north is up in this and all subsequent HiRISE images.

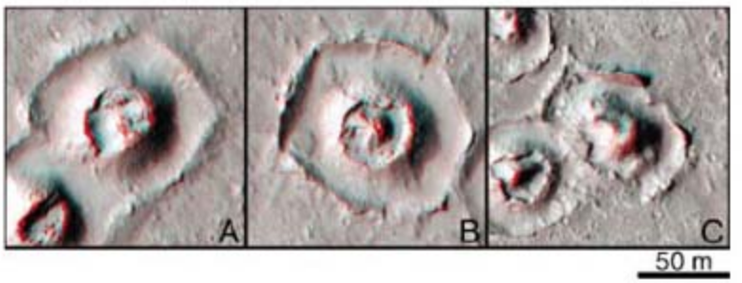

Fig. 3. Anaglyphs from subsections of HiRISE stereo image pairs PSP_001606_1900 and PSP_002226_1900 (**A** and **B**) and PSP_001540_1890 and PSP_002371_1890 (**C**). The thin flowtop cracked, shifted, and foundered under the weight of RMLs, producing a continuum of moat morphologies from (A) ring fractures, to (B) tilted plates that jut over the surrounding flow surface, to (C) foundering plates exposed edge-on.

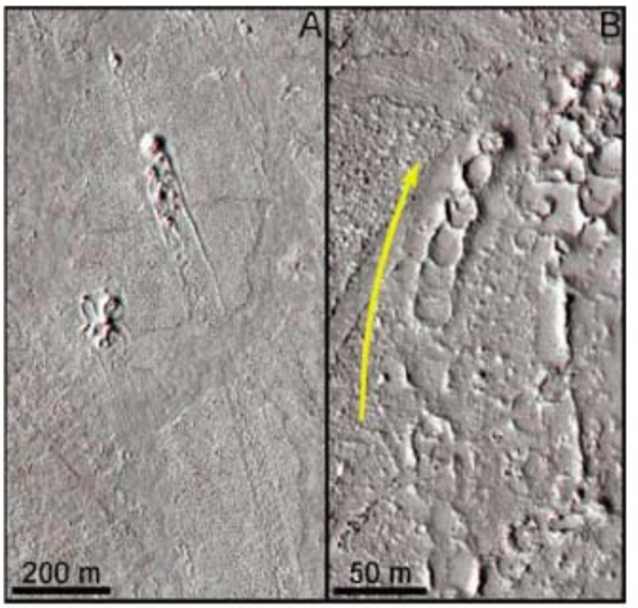

Fig. 4. (**A**) Anaglyph of a subsection of HiRISE stereo image pair PSP_001540_1890 and PSP_002371_1890 showing RMLs with wakes severed along rafted plate boundaries. Compressional ridges cover the plates, and polygonal terrain occupies the interstitial space. (**B**) Anaglyph of a subsection of HiRISE stereo image pair PSP_002938_1890 and PSP_003083_1890 showing a chain of overlapping RMLs. Cross-cutting relationships indicate that the RMLs within the chain become younger in the upstream direction (yellow arrow).

HiRISE data show that Athabasca Valles is draped by lava and riddled with hydrovolcanic cones. The purported frozen sea in Cerberus Palus (*6*) is instead a ponded distal section of this lava flow. HiRISE has imaged similar lava flows within other channels (e.g., Marte Vallis and Kasei Valles), which suggests that Athabasca Valles may be unique only in that it is exceptionally well preserved. Although it remains likely that the outflow channels were carved by aqueous floods (rather than lava), surface exposures of flood sediments may be rare on Mars. This could partially explain why every Mars lander sent to investigate fluvial or lacustrine landforms has found a surface dominated by lava.

References and Notes

1. K. L. Tanaka, D. H. Scott, *Lunar Planet. Sci.* **XVII**, 865 (abstr.) (1986).
2. D. M. Burr, J. A. Grier, A. S. McEwen, L. P. Keszthelyi, *Icarus* **159**, 53 (2002).
3. A. S. McEwen *et al.*, *Icarus* **176**, 351 (2005).
4. E. Gaidos, G. Marion, *J. Geophys. Res.* **108**, 5055 (2003).
5. J. W. Rice Jr., T. J. Parker, A. J. Russel, O. Knudsen, *Lunar Planet. Sci.* [CD-ROM] **XXXIII**, abstr. 2026 (2002).
6. J. B. Murray *et al.*, *Nature* **434**, 352 (2005).
7. J. B. Plescia, *Icarus* **88**, 465 (1990).
8. P. D. Lanagan, thesis, University of Arizona, Tucson (2004).
9. L. Keszthelyi *et al.*, *Geochem. Geophys. Geosyst.* **5**, 2004GC000758 (2004).
10. M. C. Malin, K. S. Edgett, *J. Geophys. Res.* **106**, 23,429 (2001).
11. D. M. Burr, R. J. Soare, J.-M. W. B. Tseung, *Icarus* **178**, 56 (2005).
12. D. P. Page, J. B. Murray, *Icarus* **183**, 46 (2006).
13. N. Hoffman, K. Tanaka, *Lunar Planet. Sci.* [CD-ROM] **XXXIII**, abstr. 1505 (2002).
14. M. H. Carr, *Icarus* **87**, 210 (1990).
15. M. H. Carr, *Water on Mars* (Oxford Univ. Press, New York, 1996).
16. D. O. Muhleman, B. J. Butler, A. W. Grossman, M. A. Martin, *Science* **253**, 1508 (1991).
17. K. E. Edgett, B. J. Butler, J. R. Zimbelman, V. E. Hamilton, *J. Geophys. Res.* **102**, 21,545 (1997).
18. J. K. Harmon, R. E. Arvidson, E. A. Guinness, B. A. Campbell, M. A. Slade, *J. Geophys. Res.* **104**, 14,065 (1999).
19. W. C. Feldman *et al.*, *J. Geophys. Res.* **109**, E07S06 (2004).
20. J. L. Bandfield, V. E. Hamilton, P. R. Christensen, *Science* **287**, 1626 (2000).
21. P. R. Christensen *et al.*, *J. Geophys. Res.* **106**, 23,873 (2001).
22. N. E. Putzig, M. T. Mellon, K. A. Kretke, R. E. Arvidson, *Icarus* **173**, 325 (2005).
23. M. P. Golombek *et al.*, *J. Geophys. Res.* **108**, 2002JE002035 (2003).
24. M. P. Milazzo, thesis, University of Arizona, Tucson (2005).
25. HiRISE images are identified by the format "mission phase_orbit number_orbital position." For example, PSP_001408_1900 was acquired in the Primary Science Phase, orbit 1408, and 190.0° from the night-side equator or 10°N latitude (MRO travels north over the day side in its orbit).
26. We thank both the HiRISE Team and the MRO Project for their excellent support. This work was funded by NASA through the MRO Project and the Planetary Geology and Geophysics Program.

Supporting Online Material

www.sciencemag.org/cgi/content/full/317/5845/1709/DC1
Figs. S1 to S7
Table S1
References and Notes

2 April 2007; accepted 1 August 2007
10.1126/science.1143315

REPORT

Meter-Scale Morphology of the North Polar Region of Mars

K. E. Herkenhoff,[1]* S. Byrne,[2] P. S. Russell,[3] K. E. Fishbaugh,[4]† A. S. McEwen[2]

Mars' north pole is covered by a dome of layered ice deposits. Detailed (~30 centimeters per pixel) images of this region were obtained with the High-Resolution Imaging Science Experiment on board the Mars Reconnaissance Orbiter (MRO). Planum Boreum basal unit scarps reveal cross-bedding and show evidence for recent mass wasting, flow, and debris accumulation. The north polar layers themselves are as thin as 10 centimeters but appear to be covered by a dusty veneer in places, which may obscure thinner layers. Repetition of particular layer types implies that quasi-periodic climate changes influenced the stratigraphic sequence in the polar layered deposits, informing models for recent climate variations on Mars.

Planum Boreum (the martian north polar topographic dome) has been stratigraphically divided into the irregularly layered "basal unit" (*1*–*3*), the classical polar layered deposits (PLD) (*4*), and the residual cap, which covers most of the planum and maintains a high albedo throughout the northern summer because of its relatively clean water ice composition (*4*, *5*). All of these deposits overlie older materials with a complex history (*6*). Recent climate

variations, mainly caused by changing orbital parameters, are widely believed to control the deposition of ice and dust in the PLD, creating a record of global climate history within the layers. Therefore, images that resolve PLD layer thickness and their stratigraphic variations can be used to address key questions regarding their origin and evolution, and in turn these observations can be related to theories for recent climate change on Mars (*7*). The basal unit is thought to be the source of dark sand-sized material in the circumpolar dune fields (*1*–*3*). Dark material in this unit is interbedded with brighter layers that were previously thought to be composed mostly of dust (*3*). High-Resolution Imaging Science Experiment (HiRISE) images of these strata provide new information regarding the relations between them and their geologic history.

HiRISE (*8*) uses time delay integration, which yields signal-to-noise ratios far in excess of previous high-resolution cameras. HiRISE has collected 85 images of the north polar deposits, with more images covering outlying polar material and dune fields. Most of these images were acquired between the beginning of MRO's primary science phase at solar longitude L_s = 133° (*9*) and the onset of polar cloud formation at about L_s = 150°. All the data discussed here were acquired during northern summer.

Previous observations of the patchy distribution of dark layers in the basal unit were interpreted as evidence for large-scale cross-bedding (*3*). HiRISE images show potential cross-bedding at smaller scales (Fig. 1), implying that this material was saltating before deposition and burial by overlying layers. We therefore infer that the dark material in the basal unit is composed of solid sand grains that are currently being eroded and remobilized into dunes.

HiRISE data show that the interbedded bright layers have substantial thickness and material strength and are not just thin accumulations of dust. Polygonal fracturing has broken these layers into meter-scale blocks. On the basis of the morphologic similarity between these polygonally fractured layers and the overlying ice-rich (*10*) PLD layers, we interpret the bright basal unit layers to be volatile-rich. In several locations, perhaps assisted by undercutting caused by removal of the interbedded sand-rich material, these blocks have detached from the bright layers and now lie at the bases of the scarps (Fig. 2). This style of mass wasting was not previously recognized in the polar regions. The debris at scarp bases is less common than expected from the abundance of blocks near layer edges, indicating that when these blocks detach, they are quickly eroded. This relatively rapid ablation of fallen blocks is probably due to disruption of any thin preexisting lag and increase of exposed surface area by the mass-wasting process. The persistence of recesses from which blocks have been dislodged suggests that mass wasting contributes more strongly to scarp retreat than in situ ablation of fractured layers.

Debris fans or aprons, intermediate in brightness between the darker material and brighter layers of the basal unit, are present on some basal unit erosional scarps. Large (100- to 200-m wide) fans accumulate at the break in slope below relatively steep sections of basal unit outcrop, and smaller examples occur up to the contact of the basal unit with the overlying PLD. The overall form and surface morphology of the fans are consistent with construction through a series of individual discrete, dry, granular avalanches and/or debris flows with low liquid water content (Fig. 3). Their brightness, polygonal surface texture, incorporation of bright blocks, and strong

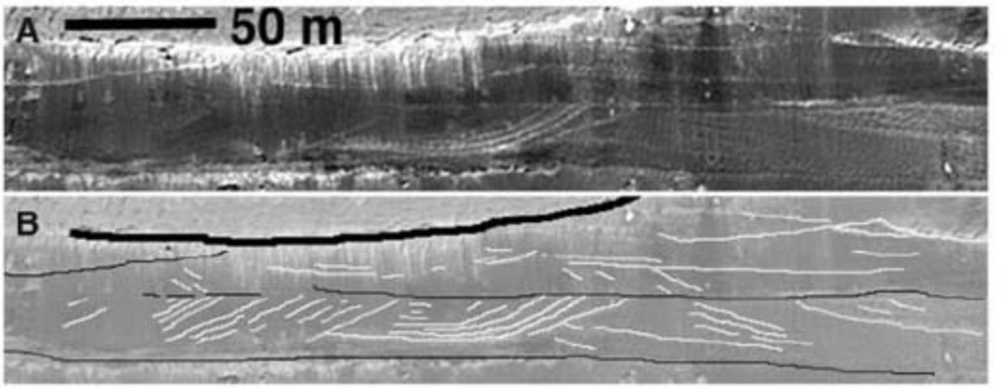

Fig. 1. Section of HiRISE image TRA_000863_2640, at 83.80°N, 235.50°E, illumination from bottom-right, slope dips toward bottom. **(A)** Section of polar scarp containing uppermost section of basal unit (dark material) and contact with PLD (brightest material). Dark basal unit layers contain structures interpreted as cross-bedding. **(B)** Annotation of beds showing truncations.

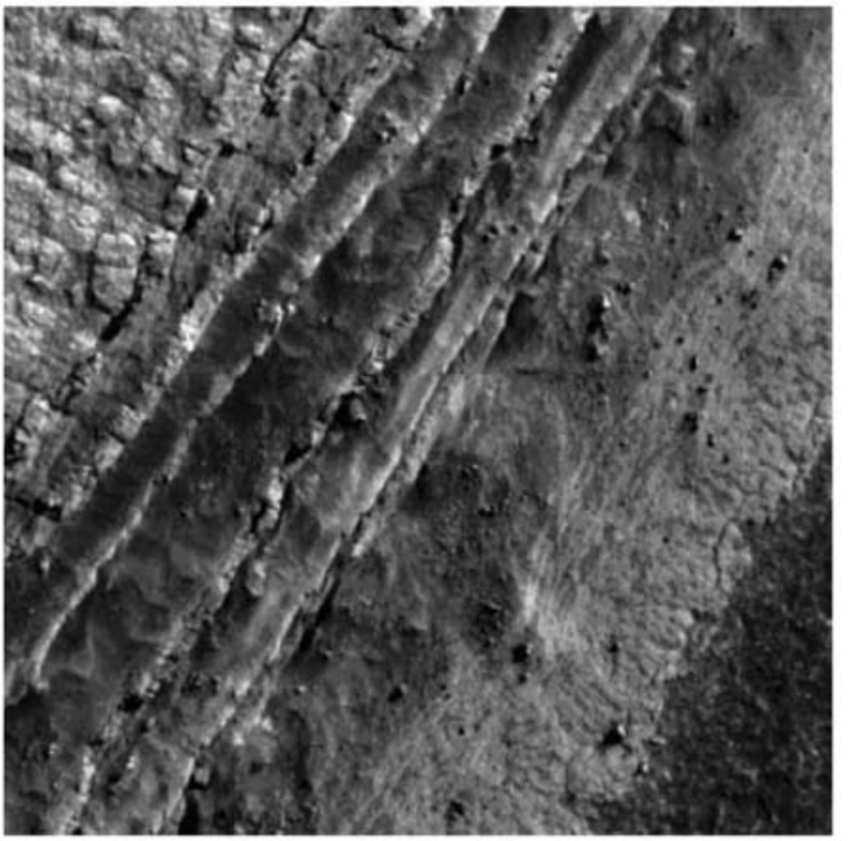

Fig. 2. Debris shed from polygonally fractured layers in basal unit. Section of HiRISE image TRA_000845_2645, at 84.635°N, 3.375°E; scene is 100 m across. Illumination from upper right, slope dips toward lower right.

[1]Astrogeology Team, United States Geological Survey (USGS), Flagstaff, AZ 86001, USA. [2]Lunar and Planetary Laboratory, University of Arizona, Tucson, AZ 85721, USA. [3]Physikalisches Institut, Universität Bern, CH-3012 Bern, Switzerland. [4]International Space Science Institute, CH-3012 Bern, Switzerland.

*To whom correspondence should be addressed. E-mail: kherkenhoff@usgs.gov

†Present address: Center for Earth and Planetary Studies, National Air and Space Museum, Washington, DC 20013, USA.

water ice absorption bands in Compact Reconnaissance Imaging Spectrometer spectra (*11*) indicate that the fans contain ice. The primary source of fan material appears to be debris wasted from the ice-rich, highly fractured lower PLD.

Some of the most distinct sets of basal unit features indicative of flow are rilles associated with fans, especially at distal margins (Fig. 3). Individual and paired rille flank deposits are probably levees formed in the flow stage, during which deposition is largely occurring at low-energy lateral margins (whereas the high-energy central flow leaves little material behind). A morphological gradation of rilles to positive-relief digitate lobes represents the transition to a lower energy stage, during which relatively steep, lobate flow fronts are preserved as the flow comes to rest [e.g., (*12*)]. We see no evidence requiring the presence of liquid water and therefore favor dry granular flows to explain the observed fans and related rille features, but wet debris flows cannot be ruled out.

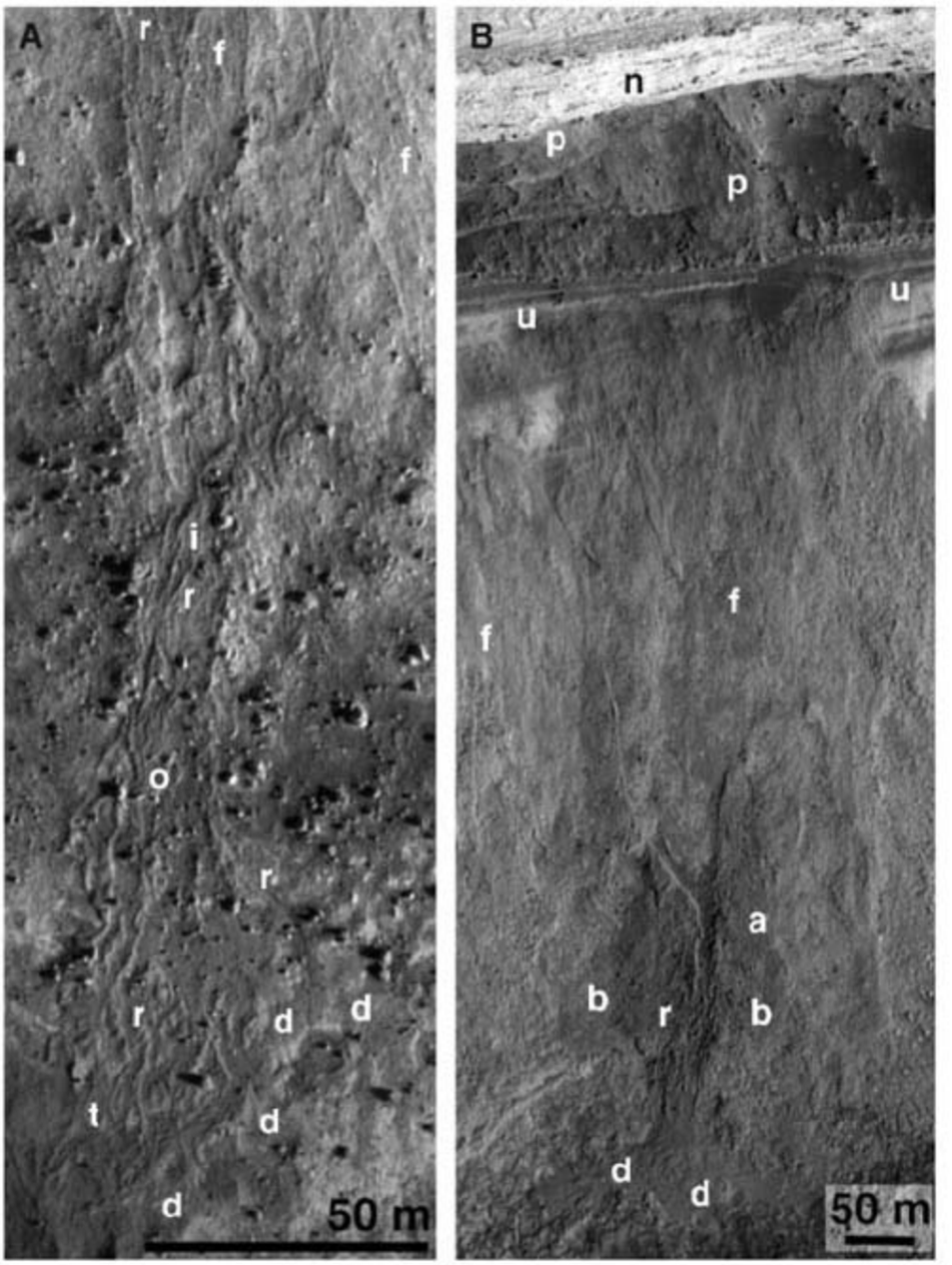

Fig. 3. Portions of image PSP_001412_2650, at 84.75°N, 3.85°E, illumination from right, slope dips toward bottom. **(A)** Rilles defined by segments of parallel ridges with little to no medial incision (r), resulting from flow of dry to low-water-content debris. Fan surface appears striated (f). Course-altering influences on flow may include obstacles (o), topography (t), or irregularities in deposition of flow fronts (i). Rilles may transition into relatively high-standing, branching, narrow, digitate lobes with abrupt fronts at mouths (d). **(B)** Similar features (r), seen in context at foot of fan (f) emplaced on basal unit layers (u) with patchy material (p) reaching up to base of lower PLD (n). Full path from mass-wasting origin to distal accumulations of large blocks (b) and digitate terminal lobes (d). Late-stage rilles may have cut through initial larger avalanche deposit (a).

The minimal apparent modification and lack of superposed aeolian bedforms suggest that these distal rille and digitate deposits represent the most recent and/or largest of the type of mass wasting-initiated flow events that contribute to the growth of the large fans. Current activity, such as fracture-aided mass wasting, raises the potential that changes in fan or scarp appearance, including the appearance of blocks or avalanche deposits, could be observed over the course of the MRO mission.

The high-relief exposures of PLD at the head of Chasma Boreale and along the margin of Olympia Planum exhibit two distinct sections on the basis of presence or absence of polygonal fractures. The lower section appears similar to the polygonally fractured bright layers in the basal unit, whereas the upper section shows no evidence of this polygonal fracturing (Fig. 4A). Dark, sandy material has not been observed in the upper section and rarely occurs in the lower section of the PLD. The lower PLD is typically exposed on steeper slopes, indicating a different resistance to erosion and/or more effective mass wasting there, perhaps enhanced by erosion of the basal unit and consequent undercutting. Although we cannot exclude the possibility that the fractures in the lower PLD are not representative of its bulk properties and were formed during erosion of the scarps, Shallow Radar (SHARAD) results (*13*) indicate that these sections differ in dielectric properties throughout the PLD. We therefore interpret the polygonal fracturing of the lower PLD to be a result of inherent material properties or historical processes that are not common to the upper PLD.

The lower-relief troughs within the northernmost PLD typically only expose layers in the upper section. Here, layers within Mars Global Surveyor (MGS) Mars Orbiter Camera (MOC) images range in apparent thickness down to the image scale [~1.5 m/pixel at best (*14*, *15*)]. However, HiRISE observations show that apparent layer thickness ranges down to the pixel scale (30 cm) only where foreshortened on relatively steep slopes. Therefore, on more typical trough slopes, HiRISE has resolved the thinnest layers visible from orbit. For example, image PSP_001738_2670 (*16*) shows layers with ~1-m apparent width on a slope (derived from MGS Mars Orbiter Laser Altimeter gridded topographic data) that implies a true thickness of ~10 cm. Any thinner layers that may exist appear to be obscured in many places by surficial deposits of frost and/or ice (white in Fig. 4, B and C) and dust (red in Fig. 4B and gray in Fig. 4C).

HiRISE images of the PLD indicate that the apparent brightness of the layers is likely controlled by topography, texture, and surficial frost distribution (Fig. 4B) and is therefore not directly related to the internal composition of the layers. This implies that apparent layer bright-

ness profiles cannot be directly compared with calculations of obliquity- or precession-driven changing insolation in an attempt to date layers (*15*, *17*, *18*).

Stratigraphic analyses using Viking and MOC images have shown that some layers can be correlated within one trough (*14*, *19*), across several troughs (*20*, *21*), and even across wide areas of the PLD (*15*, *22*). One easily traceable layer is the "marker bed" (*14*), so called because of its distinctive, knobby morphology (*23*). At full HiRISE resolution (Fig. 4C), this layer appears to have undergone localized slumping, perhaps of an overlying dust lag, and has linear grooves (possibly created by eolian erosion) and tiny knobs and pits dotting its surface near the top of the layer. The marker bed protrudes, in most places, from the surrounding layers, indicating that it is relatively resistant to erosion. By using these defining characteristics, we have identified six such layers within one HiRISE image, four of which are also traceable to another HiRISE image in a nearby trough. The presence of these newly discovered "marker

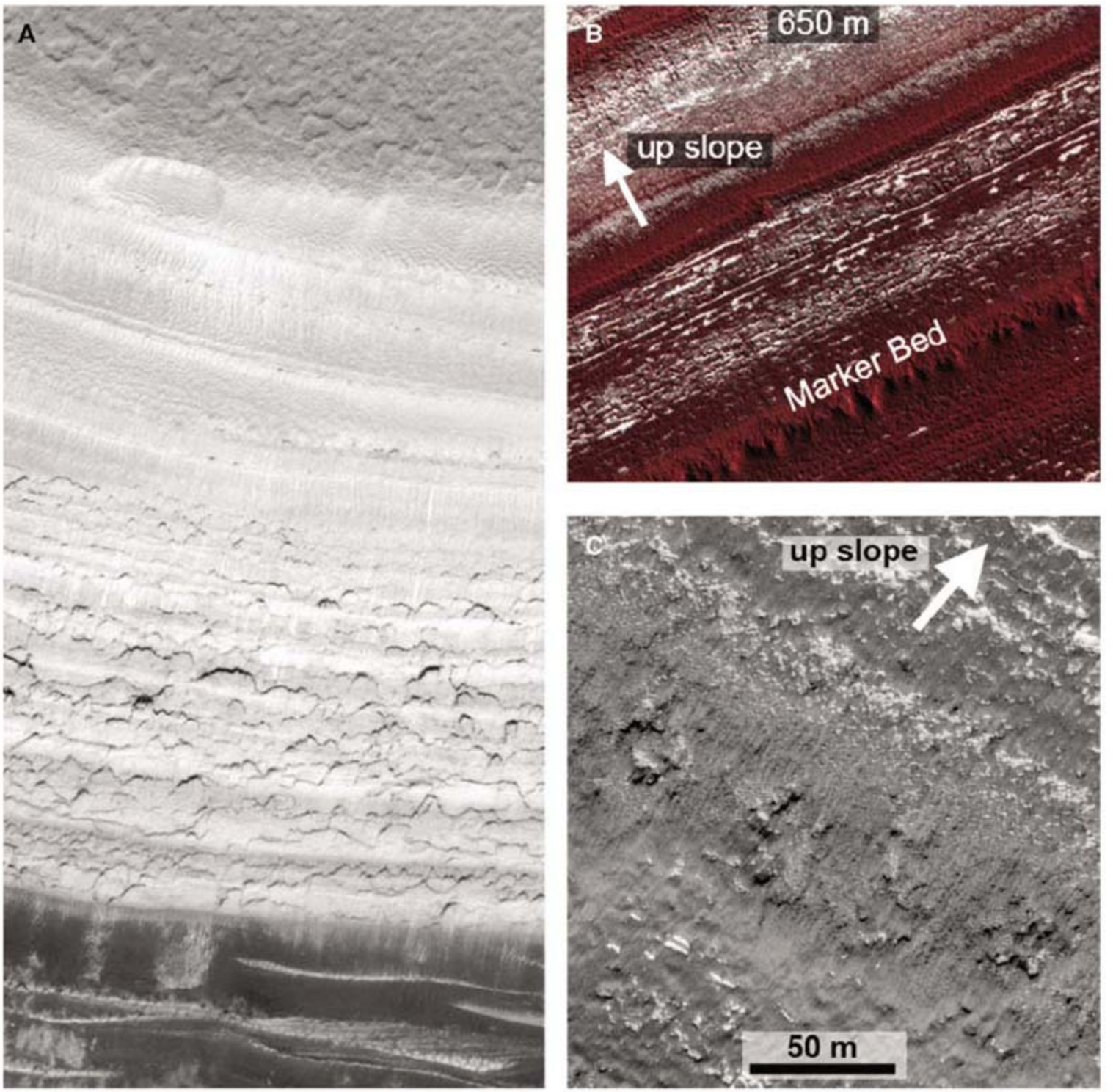

Fig. 4. North polar layered deposits. (**A**) Transition in layering over polar scarp, section of HiRISE image PSP_001550_2640, at 83.83°N, 235.30°E. Slope dips toward bottom, illumination from bottom, scene is 540 m across. (**B**) Portion of false-color HiRISE image (PSP_001738_2670, centered at 87.1°N, 92.6°E) of layers in upper portion of PLD. Illumination from upper right. (**C**) Portion of HiRISE image PSP_001488_2665 (centered at 86.51°N, 80.0°E), showing original "marker bed" (diagonally across center). Illumination from lower right.

beds" is suggestive of a repeating climate signal within the upper PLD.

These observations are consistent with the following general history of the north polar region. (i) Dark sand saltates into the north polar region during periods (possibly high obliquity) when thick accumulations of ice do not form at the north pole. (ii) Alternating with sand migration, ice accumulates and inhibits saltation of underlying dark sand (possibly during lower obliquity). (iii) Several such depositional cycles produce alternating brighter (ice and dust) and darker (sandy) layers in the basal unit. (iv) Icy layers, similar in morphology to those in the basal unit, are deposited with little or no dark sand to form the lower (polygonally cracked) PLD. This transition from the previous depositional cycles may indicate that the sand supply was exhausted or no longer transportable onto these growing deposits. (v) The upper PLD accumulates, and varying conditions during its accumulation lead to the development of the layered sequences that have been correlated in multiple exposures (*6*, *22*). (vi) Most recently, the thin north polar residual cap forms on top of the PLD and evolves to its present state by condensation and sublimation of water ice. Mass wasting of the PLD at steep scarps produces icy debris fans.

References and Notes

1. S. Byrne, B. Murray, *J. Geophys. Res.* **107**, 10.1029/2001JE001615 (2002).
2. K. Edgett, R. M. E. Williams, M. C. Malin, B. A. Cantor, P. C. Thomas, *Geomorphology* **52**, 289 (2003).
3. K. Fishbaugh, J. Head, *Icarus* **174**, 444 (2005).
4. P. Thomas, S. Squyres, K. Herkenhoff, A. Howard, B. Murray, in *Mars* (Univ. Arizona Press, Tucson, 1992).
5. Y. Langevin F. Poulet, J.-P. Bibring, B. Gondet, *Science* **307**, 1584 (2005); published online 17 February 2005 (10.1126/science.1109091).
6. K. Tanaka, *Nature* **437**, 991 (2005).
7. S. Clifford *et al.*, *Icarus* **174**, 291 (2005).
8. A. McEwen *et al.*, *J. Geophys. Res.* **112**, 10.1029/2005JE002605 (2007).
9. L_s is the solar longitude of Mars, used to define season with 0 defined as the northern vernal equinox.
10. R. J. Phillips et al., *Lunar Planet. Sci. Conf.* **XXXVIII**, abstr. 1925 (2007).
11. S. Murchie *et al.*, *Lunar Planet. Sci. Conf.* **XXXVIII**, abstr. 1472 (2007).
12. A. Johnson, *Physical Processes in Geology* (Freeman, New York, 1970).
13. R. Seu *et al.*, *Science* **317**, 1715 (2007).
14. M. Malin, K. Edgett, *J. Geophys. Res.* **106**, 23439 (2001).
15. S. Milkovich, J. Head, *J. Geophys. Res.* **110**, 10.1029/2004JE002349 (2005).
16. HiRISE images are identified by the format "mission phase_orbit number_orbital position." For example, PSP_001738_2670 was acquired in the Primary Science Phase, orbit 1738, and 267° from the night-side equator or 87°N latitude (MRO travels north over the day side in its orbit).
17. J. Cutts, B. Lewis, *Icarus* **50**, 216 (1982).
18. J. Laskar, B. Levrard, F. Mustard, *Nature* **419**, 375 (2002).
19. L. Fenton, K. Herkenhoff, *Icarus* **147**, 433 (2000).
20. A. Howard, J. Cutts, K. Blasius, *Icarus* **50**, 161 (1982).
21. E. Kolb, K. Tanaka, *Icarus* **154**, 22 (2001).
22. K. Fishbaugh, C. Hvidberg, *J. Geophys. Res.* **111**, 10.1029/2005JE002571 (2006).
23. S. M. Milkovich, J. W. Head III, *Mars* **2**, 21 (2006).

24. We thank the HiRISE science team and operations staff at the University of Arizona for continuing support in acquiring spectacular images of the martian polar regions and the USGS HiRISE team for development of software and procedures for processing the images. Two anonymous reviews and comments by J. Skinner and K. Tanaka helped to improve the manuscript and are much appreciated.

6 April 2007; accepted 28 August 2007
10.1126/science.1143544

REPORT

Accumulation and Erosion of Mars' South Polar Layered Deposits

Roberto Seu,[1]* Roger J. Phillips,[2] Giovanni Alberti,[3] Daniela Biccari,[1] Francesco Bonaventura,[4] Marco Bortone,[3] Diego Calabrese,[5] Bruce A. Campbell,[6] Marco Cartacci,[1] Lynn M. Carter,[6] Claudio Catallo,[5] Anna Croce,[5] Renato Croci,[5] Marco Cutigni,[1] Antonio Di Placido,[4] Salvatore Dinardo,[3] Costanzo Federico,[7] Enrico Flamini,[8] Franco Fois,[5] Alessandro Frigeri,[7] Oreste Fuga,[1] Emanuele Giacomoni,[1] Yonggyu Gim,[9] Mauro Guelfi,[5] John W. Holt,[10] Wlodek Kofman,[11] Carlton J. Leuschen,[12] Lucia Marinangeli,[13] Paolo Marras,[4] Arturo Masdea,[1] Stefania Mattei,[3] Riccardo Mecozzi,[5] Sarah M. Milkovich,[9] Antonio Morlupi,[4] Jérémie Mouginot,[11] Roberto Orosei,[14] Claudio Papa,[3] Tobia Paternò,[4] Paolo Persi del Marmo,[1] Elena Pettinelli,[15] Giulia Pica,[3] Giovanni Picardi,[1] Jeffrey J. Plaut,[9] Marco Provenziani,[1] Nathaniel E. Putzig,[2] Federica Russo,[1] Ali Safaeinili,[9] Giuseppe Salzillo,[3] Maria Rosaria Santovito,[3] Suzanne E. Smrekar,[9] Barbara Tattarletti,[4] Danilo Vicari[4]

Mars' polar regions are covered with ice-rich layered deposits that potentially contain a record of climate variations. The sounding radar SHARAD on the Mars Reconnaissance Orbiter mapped detailed subsurface stratigraphy in the Promethei Lingula region of the south polar plateau, Planum Australe. Radar reflections interpreted as layers are correlated across adjacent orbits and are continuous for up to 150 kilometers along spacecraft orbital tracks. The reflectors are often separated into discrete reflector sequences, and strong echoes are seen as deep as 1 kilometer. In some cases, the sequences are dipping with respect to each other, suggesting an interdepositional period of erosion. In Australe Sulci, layers are exhumed, indicating recent erosion.

A marked similarity between Mars and Earth is the presence of thick polar ice caps, which potentially provide a wealth of data about recent climate and atmospheric history (*1*, *2*). The martian polar plateaus are as much as 3.5 km thick (*3*) and composed of layers overlain by a residual (i.e., perennial) ice cap that, according to recent analyses, is no more than a few tens of meters thick (*4*–*6*). The polar residual ice in the south is predominantly CO_2 ice containing trace amounts of dust and water ice (*5*). Compared to the north, the residual ice covers only a small portion of the south polar layered deposits (SPLD), which are offset from the pole by ~2° and are asymmetrically distributed between latitudes 70°S and 80°S (*3*). Most plateau surfaces are buried under an optically thick layer of sand or of seasonal frost accumulations (*7*). The layers are composed of water ice mixed with dust, with layer thicknesses and ice/dust ratios possibly controlled by orbital cycles (*8*). They apparently formed by deposition of ice condensates or precipitates and atmospheric dust (*9*, *10*). The polar plateaus are considered to be very young. On the basis of crater counts, the surface age of Planum Australe is estimated to be on the order of tens of millions of years (*11*, *12*).

Planum Australe was probed previously with the Mars Advanced Radar for Subsurface and Ionospheric Sounding (MARSIS) onboard the European Space Agency's Mars Express (*6*, *13*). The MARSIS radar signals penetrated to depths estimated to be greater than 3.7 km (*6*). Subsurface echoes are frequently very strong, indicating minimal attenuation of the signal through

[1]Dipartimento INFOCOM, Università di Roma "La Sapienza," I-00184 Rome, Italy. [2]Washington University, St. Louis, MO 63130, USA. [3]Consorzio di Ricerca Sistemi di Telesensori Avanzati, I-80125 Naples, Italy. [4]Info Solution Spa, I-00131 Rome, Italy. [5]Thales Alenia Space Italia, I-00131 Rome, Italy. [6]Smithsonian Institution, Washington, DC 20013–7012, USA. [7]Università di Perugia, I-06123 Perugia, Italy. [8]Agenzia Spaziale Italiana, I-00198 Rome, Italy. [9]Jet Propulsion Laboratory, California Institute of Technology, Pasadena, CA 91109, USA. [10]University of Texas at Austin, Austin, TX 78758, USA. [11]CNRS and Université Joseph Fourier, 38041 Grenoble Cedex 9, France. [12]University of Kansas, Lawrence, KS 66045–7612, USA. [13]International Research School of Planetary Sciences, I-65127 Pescara, Italy. [14]Istituto Nazionale di Astrofisica, I-00133 Rome, Italy. [15]Università Roma Tre, I-00146 Rome, Italy.

*To whom correspondence should be addressed. E-mail: roberto.seu@uniroma1.it

the SPLD. Although plausible solutions to models of layer composition based on the dielectric losses are unconstrained (*14*), the SPLD may be composed of nearly pure water ice (*6*). With a vertical resolution of 150 m in free space, however, MARSIS is not suited to study the structure of the deposits, because individual layers are a few meters thick (*15*).

SHARAD (Shallow Radar) is a synthetic-aperture, orbital sounding radar on the Mars Reconnaissance Orbiter (MRO) (*16*). SHARAD was designed to complement MARSIS by trading penetration depth for improved vertical resolution (*17*, *18*) and is better suited for mapping 10-m-scale stratigraphy in the polar plateaus. Data are collected preferentially on the night side of Mars, where the Sun-excited ionosphere has a low electron density and plasma frequency, and radar echoes are thus nearly unaffected by distortions caused by propagation through a frequency-dispersive medium. SHARAD operates at a center frequency of 20 MHz, with a 10-MHz bandwidth that provides a free-space range resolution of ~15 m after pulse compression. Resolution in the across-track direction ranges from 3 to 6 km, and in the along-track direction after synthetic-aperture processing is 0.3 to 1 km. The transmitted signal is a 10-W, 85-μs chirped (linearly frequency-modulated) pulse emitted from a 10-m-long dipole antenna. After downlink to Earth, coherent azimuth sums on ~1500 pulses taken at a pulse repetition frequency of 700 Hz result in a signal-to-noise ratio of 30 to 40 dB for a relatively smooth surface (*17*, *18*). Waves that are transmitted into the subsurface reflect from dielectric discontinuities and return to the instrument at greater time delay than the nadir surface echo. The primary obstacle to the identification of subsurface echoes is interference from off-nadir surface echoes (known as "surface clutter") that arrives at the radar receiver with the same time delay as that of subsurface echoes. The data described here were acquired in January and February 2007, on orbits 2202, 2413, 2624, and 2835. The ground tracks of the radar are located within Planum Australe's Promethei Lingula region (Fig. 1). Here we report on the SPLD stratigraphy as mapped by SHARAD in Promethei Lingula and interpret this information in terms of the depositional and erosional history.

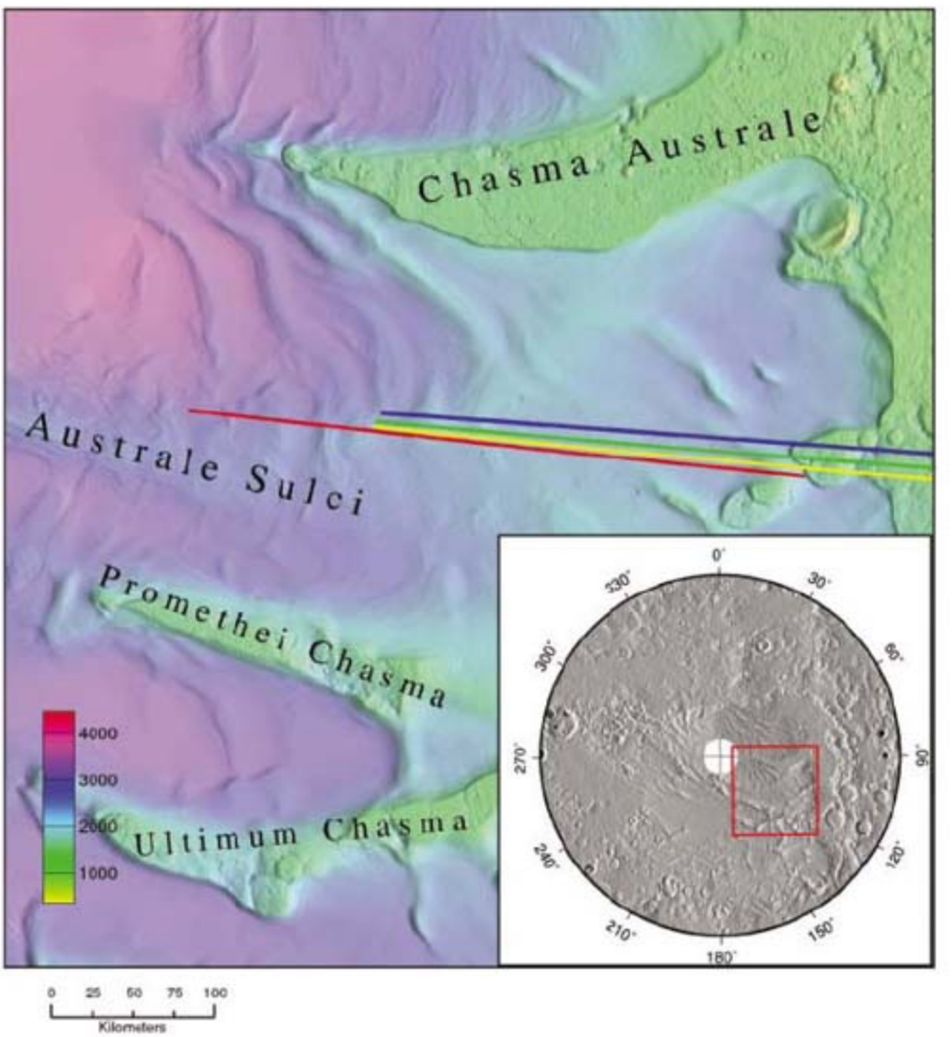

Fig. 1. Topography of the Promethei Lingula region. Promethei Lingula is the extension of the Planum Australe plateau delimited by Chasma Australe to the top, Ultimum Chasma to the bottom, and Promethei Planum to the right. The ground tracks of the MRO spacecraft during SHARAD data acquisitions are shown in red for orbit 2202, in yellow for orbit 2413, in green for orbit 2624, and in blue for orbit 2835. The inset shows the location in the south polar area of Mars.

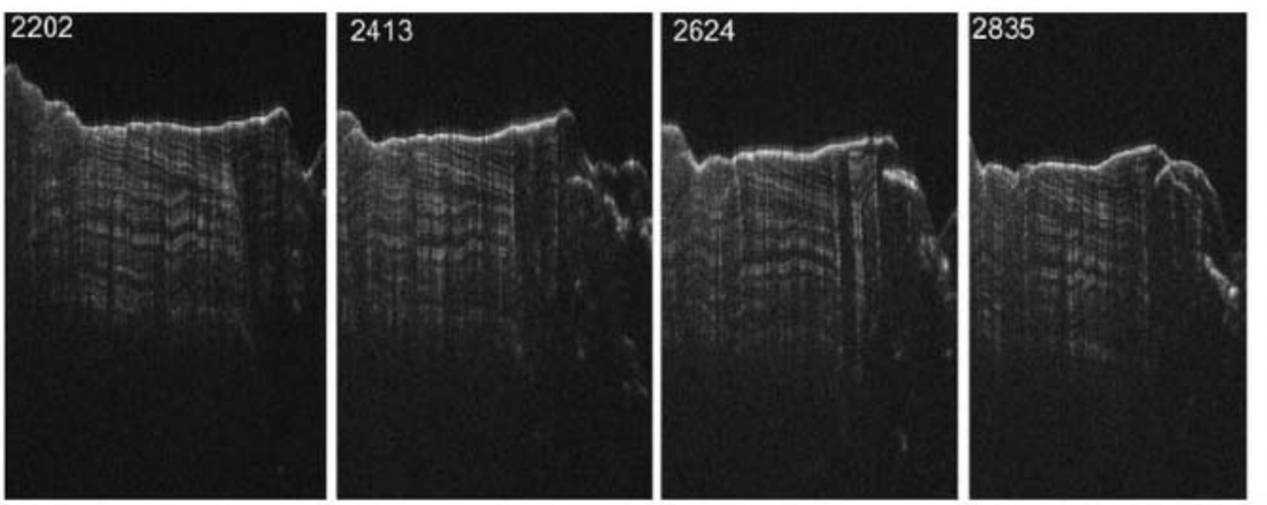

Fig. 2. Radargrams for orbits 2202, 2413, 2624, and 2835. A radargram is a two-dimensional cross section of the surface and subsurface in which brightness corresponds to echo power. The vertical axis is the two-way pulse travel time, and the horizontal axis is the distance of the spacecraft along its ground track. Similar subsurface layering structure is seen in these four closely spaced, parallel tracks.

Roughly half of Promethei Lingula is dissected by canyon systems. These include deep canyons radial to the Promethei Lingula distal margin (chasmata) and smaller, curvilinear canyons perpendicular to the chasmata commonly referred to as "spiral troughs" (Fig. 1). The origin of the chasmata has been attributed to dissection by katabatic wind (*12*, *19*, *20*) or to basal melting (*21*), whereas development of curvilinear canyons has been attributed to aeolian erosion (*20*, *22*) or to ductile deformation (*23*) of the SPLD.

SHARAD data were acquired during four closely spaced (<5 km), nearly parallel orbit segments (Fig. 1). These data (Fig. 2) are all characterized by a multilayered internal structure with dozens of internal reflections. Many of these reflections are traceable over distances of up to 150 km over the smooth area extending from the outer edge to the central part of the Planum Australe plateau (from right to left in Fig. 2). There are several bands (packets) containing many thin reflectors running parallel or subparallel to the surface, separated by thicker dark bands. To determine if they arise from subsurface interfaces or come from surface topographic features at the same time delay, we ran a high-fidelity model of the expected contribution of off-nadir topographic clutter using Mars Orbiter Laser Altimeter (MOLA) data (*7*, *24*, *25*). Results show no visible surface topographic feature that explains the observed bands; hence, we conclude that they are subsurface reflectors. This banded structure is similar, and certainly related, to the layering visible in optical images, and radar reflections are likely caused by intralayer compositional variations in dust content or density. Sets of reflectors can be correlated among the four radargrams, giving us confidence that the same layered structure extends laterally (across track) for several kilometers. Reflections are seen down to depths of about 1 km, consistent with the very low attenuation through the SPLD observed by MARSIS. However, such reflections are at a shallower depth than the deepest reflection in the MARSIS radargrams over the same area, which are found at 1.3 km and correspond to the local plateau height relative to the surrounding plains (*6*). We deem that the lack of any deeper reflectors is more likely due to attenuation or scattering of the SHARAD radar signal than to the character of the plateau basal interface.

The distinct subsurface layered structure noted above is not present along the entire length of the four SHARAD ground tracks. In some areas, these dielectric interfaces pinch out or disappear entirely. Possible reasons for these changes in the echo behavior include (i) tilting of the layers, which can move the specular reflection from a smooth interface out of the Doppler bandwidth of the processed data; (ii) increased surface roughness that decreases the effective amount of radar signal transmitted into the subsurface; or (iii) changes in the geologic structure or physical state of the materials that diminishes their dielectric contrast.

From analysis of the radargrams, it is possible to identify four main boundaries (colored lines in Fig. 3) that separate different dielectric sequences. The first sequence, limited at the base by the yellow boundary and located in time between 1.7 and 5.3 μs of depth below the surface, is dipping toward the right. Several of the upper layers in this sequence terminate at the surface, which is nearly horizontal in this segment. Below this reflector a second one (in white) is detectable at a time depth of about 4.3 to 5.6 μs. Beneath such an interface a second well-defined sequence of layers is clearly visible up to a time depth of about 5.6 to 7.1 μs where the third main reflector (in orange) closes the series. Finally, below it another multilayered structure, limited by a reflector (in light blue) located at a depth of about 11.0 to 12.9 μs, is also visible.

To convert echo time delays to depths requires assumptions about the material that the radar pulse is passing through. As mentioned above, the SPLD may consist mostly of water ice (*6*). We thus convert time to depth by assuming a real part of the relative permittivity of 3.5, corresponding to that of water ice with a few percent of dust. The four reflectors shown in Fig. 3 are located, from top to bottom, at depths of about 130 to 420 m, 340 to 450 m, 450 to 570 m, and 890 to 1030 m. Because the depths scale by the inverse of the square root of the dielectric constant, small variations in material (i.e., dust content) will not have a profound effect on calculated depths.

Above the first reflector in Fig. 3, the layers are continuous and generally of even thickness laterally. Below the second reflector the same observation applies. Between the two, the layer sequence goes from thick (about 240 m) to nearly zero. The layers become difficult to follow within this wedge-shaped region. We propose two possible interpretations for this morphology: (i) The pinching out of the layers in the wedge-shaped region is an erosional feature (an unconformity); or (ii) the shape of this region is a primary feature of the deposition, i.e., the thickness of some layers varies laterally. The first interpretation is consistent with conclusions from a study of exposed layers in Promethei and Ultimum Chasmata (Fig. 1) (*19*). However, because there is no clear image of truncation of the bedding along a dipping boundary in the wedge-shaped region, we are unable to rule out interpretation (ii).

We interpret the dipping layers that are truncated at the surface within Australe Sulci as due to erosion of the plateau surface rather than due to lateral variations in SPLD accumulation rate, because this last process would be unable to produce the observed constant thickness of the layers. This interpretation is consistent with the observation of erosional surface features in Australe Sulci, whose shape and direction may be controlled by the wind, most likely by off-pole katabatic winds (*12*). The local stratigraphic evolution can thus be interpreted as consisting of at least four stages: (i) essentially uniform deposition of a lower package; (ii) erosion at an angle, or laterally variable deposition; (iii) renewed deposition on the angled surface; and (iv) truncation of

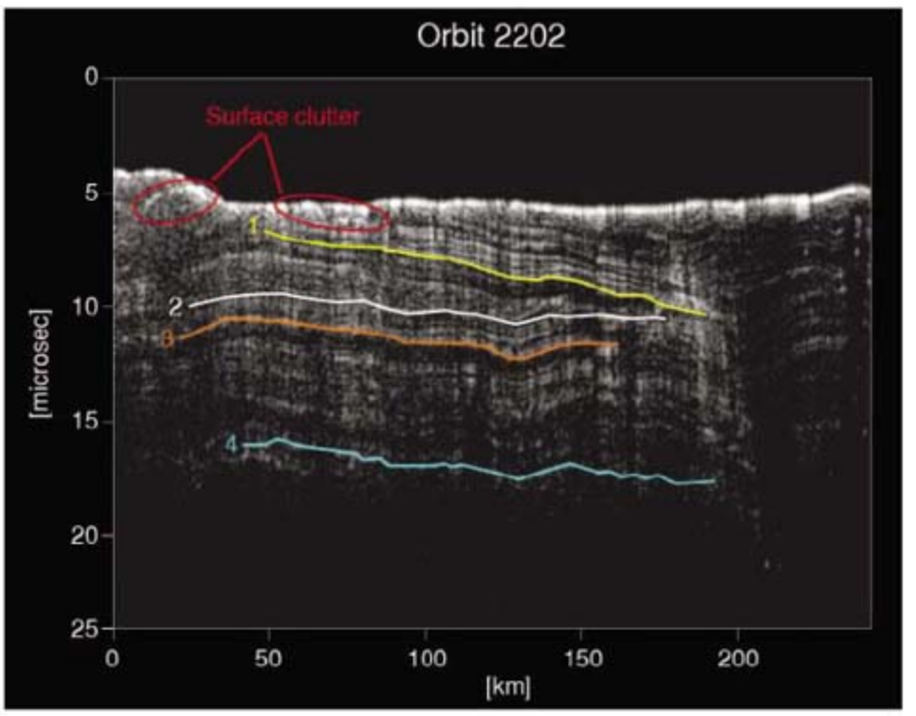

Fig. 3. Enlarged view of data for orbit 2202. Four main reflectors, which separate different dielectric sequences, are marked with lines of yellow, white, orange, and light blue. Red ellipses highlight echo features identified as surface clutter through radar surface echo simulation (see text).

the angled package to the present horizontal surface as result of erosion.

Despite the age uncertainties of the polar deposits, the strength of CO_2 ice is insufficient to support the long-term topography of the polar caps (*26*). SHARAD data are consistent with a mechanically strong plateau material, as we see no evidence, such as folding or faulting, for flow in the bulk of the plateau's layered structure. However, flow resulting in broad-scale changes in layer thickness or flow at the very base of the deposits cannot be ruled out by these observations. The continuity of layers, spanning distances of up to 150 km, is evidence that the depositional processes that formed Planum Australe were regional in scale, as already inferred from layer correlation studies of exposures in Australe Mensa (*27*) and Promethei Lingula (*19*). Spectral and albedo observations of the surface indicate that the plateau surface is covered by an optically thick layer of dust or rocky material (*7*), but we do not see evidence in our data that can be interpreted in terms of an ice-free surface layer, perhaps because of its small thickness compared to SHARAD vertical resolution.

References and Notes

1. J. R. Petit *et al.*, *Nature* **399**, 429 (1999).
2. K. L. Tanaka, E. J. Kolb, *Icarus* **154**, 3 (2001).
3. D. E. Smith *et al.*, *Science* **284**, 1495 (1999).
4. S. Byrne, A. P. Ingersoll, *Science* **299**, 1051 (2003).
5. J.-P. Bibring *et al.*, *Nature* **428**, 627 (2004).
6. J. J. Plaut *et al.*, *Science* **316**, 92 (2007).
7. S. Douté *et al.*, *Planet. Space Sci.* **55**, 113 (2007).
8. O. B. Toon, J. B. Pollack, W. Ward, J. A. Burns, K. Bilski, *Icarus* **44**, 552 (1980).
9. P. Thomas, S. Squyres, K. Herkenhoff, A. Howard, B. C. Murray, in *Mars*, H. H. Kieffer, B. M. Jakosky, C. W. Snyder, M. S. Matthews, Eds. (Univ. of Arizona Press, Tucson, 1992), pp. 767–795.
10. M. T. Mellon, *Icarus* **124**, 268 (1996).
11. K. E. Herkenhoff, J. J. Plaut, *Icarus* **144**, 243 (2000).
12. M. R. Koutnik, S. Byrne, B. C. Murray, A. D. Toigo, Z. A. Crawford, *Icarus* **174**, 490 (2005).
13. G. Picardi *et al.*, *Science* **310**, 1925 (2005).
14. D. C. Nunes, R. J. Phillips, *J. Geophys. Res.* **111**, E06521 (2006).
15. M. C. Malin, K. S. Edgett, *J. Geophys. Res.* **106**, 23429 (2001).
16. J. E. Graf *et al.*, *Acta Astronaut.* **57**, 566 (2005).
17. R. Seu *et al.*, *J. Geophys. Res.* **112**, E05S05 (2007).
18. R. Seu *et al.*, *Planet. Space Sci.* **52**, 157 (2004).
19. E. J. Kolb, K. L. Tanaka, *Mars* **2**, 1 (2006).
20. A. D. Howard, *Icarus* **144**, 267 (2000).
21. S. M. Clifford, *J. Geophys. Res.* **92**, 9135 (1987).
22. A. D. Howard, *Icarus* **34**, 581 (1978).
23. D. A. Fisher, *Icarus* **105**, 501 (1993).
24. J.-F. Nouvel, A. Herique, W. Kofman, A. Safaeinili, *Radio Sci.* **39**, RS1013 (2004).
25. MOLA topographic data at 1/128 degree per pixel grid spacing were used to simulate echoes from the cross-track region for each SHARAD subsurface sounding observation. Along-track sources were suppressed because SHARAD data processing achieves this by aperture synthesis.
26. J. F. Nye, W. B. Durham, P. M. Schenk, J. M. Moore, *Icarus* **144**, 449 (2000).
27. S. Byrne, A. B. Ivanov, *J. Geophys. Res.* **109**, E11001 (2004).

28. The Shallow Subsurface Radar (SHARAD) was provided by the Italian Space Agency, and its operations are led by the INFOCOM Department, University of Rome "La Sapienza." Thales Alenia Space Italia is the prime contractor for SHARAD and is in charge of in-flight instrument commissioning and of the SHARAD Operations Center. The Mars Reconnaissance Orbiter mission is managed by the Jet Propulsion Laboratory, California Institute of Technology, for the NASA Science Mission Directorate, Washington, DC. Lockheed Martin Space Systems, Denver, is the prime contractor for the orbiter.

23 April 2007; accepted 16 August 2007
10.1126/science.1144120

REPORT

Density of Mars' South Polar Layered Deposits

Maria T. Zuber,[1]* Roger J. Phillips,[2] Jeffrey C. Andrews-Hanna,[1] Sami W. Asmar,[3] Alexander S. Konopliv,[3] Frank G. Lemoine,[4] Jeffrey J. Plaut,[3] David E. Smith,[4] Suzanne E. Smrekar[3]

Both poles of Mars are hidden beneath caps of layered ice. We calculated the density of the south polar layered deposits by combining the gravity field obtained from initial results of radio tracking of the Mars Reconnaissance Orbiter with existing surface topography from the Mars Orbiter Laser Altimeter on the Mars Global Surveyor spacecraft and basal topography from the Mars Advanced Radar for Subsurface and Ionospheric Sounding on the Mars Express spacecraft. The results indicate a best-fit density of 1220 kilograms per cubic meter, which is consistent with water ice that has ~15% admixed dust. The results demonstrate that the deposits are probably composed of relatively clean water ice and also refine the martian surface-water inventory.

The martian south polar layered deposits (SPLD) (Fig. 1) contain the south polar residual ice cap and smooth, low-albedo surroundings that collectively rise ~3 km above the surrounding cratered highlands terrain (*1*). The residual polar-cap component is believed to be composed of water ice with an unknown admixed dust component that is overlain by a thin (1- to 10-m) predominantly CO_2 cover (*2–4*). The CO_2 veneer contains "swiss cheese–like" shallow depressions (*5*) that reveal the underlying water ice at their bases. The more spatially extensive part of the SPLD (Fig. 1) has a low albedo and a dustlike spectral signature, which raises the question of whether the dominant component of the SPLD as a whole is volatile (H_2O and/or CO_2) or dust. This question is relevant to establishing an accurate inventory of surface volatiles on Mars.

In this study, we used initial high-resolution gravity observations from X-band (8.4 GHz) Doppler tracking of the Mars Reconnaissance Orbiter (MRO) (*6*) together with the volume obtained by combining surface topography from the Mars Orbiter Laser Altimeter (MOLA) (*7*) and basal topography from the Mars Advanced Radar for Subsurface and Ionospheric Sounding (MARSIS) (*8*) to calculate the density of the SPLD and constrain their composition. The MRO's orbital periapsis altitude of ~255 km above the south pole of Mars provides considerably higher spatial resolution measurements (140-km block size) than did previous Mars missions (*9*) and permits the gravitational attraction of the SPLD and underlying crust to be resolved sufficiently for regional modeling for the first time (Fig. 2).

We found the best-fit density by calculating the predicted gravity field from the observed structures of the SPLD and of the crust and mantle. The key unknowns were the densities of the crust, mantle, and SPLD and the topography along the crust/mantle interface (the Moho). The densities of the martian crust and mantle were taken to be 2900 and 3500 kg m^{-3}, respectively (*10*). Because it is not possible to solve simultaneously for both the SPLD density and the Moho topography, we represented the Moho beneath the SPLD by assuming that the topography before loading by the SPLD is in a state of partial isostatic compensation. The best-fit degree of compensation outside the SPLD of 91% was applied to the crustal topography beneath the SPLD to estimate the depth to the Moho. The lack of observed flexure in MARSIS profiles (*8*) suggests support by a thick lithosphere (*11*). We calculated the deflection of the Moho by the

[1]Department of Earth, Atmospheric and Planetary Sciences, Massachusetts Institute of Technology, 77 Massachusetts Avenue, Cambridge, MA 02139–4307, USA. [2]Department of Earth and Planetary Sciences, Washington University, St. Louis, MO 63130, USA. [3]Jet Propulsion Laboratory, California Institute of Technology, 4800 Oak Grove Drive, Pasadena, CA 91009–8099, USA. [4]Solar System Exploration Division, NASA Goddard Space Flight Center, Greenbelt, MD 20771, USA.

*To whom correspondence should be addressed. E-mail: zuber@mit.edu

SPLD as in (*12*), using a fast Fourier transform approach (see supporting online material).

The contributions to the gravity from the topography along the Moho, crustal surface, and SPLD surface were calculated, accounting for the finite amplitude of the topography (*13*). The SPLD density was iterated to find the best fit between the modeled and observed gravity (*14*). For the preferred case of zero flexure beneath the deposits, we found a mean density of 1220 kg m^{-3}, with a 95% confidence interval (CI) of 740 to 1780 kg m^{-3} and a root mean square misfit over the SPLD of 22.9 mgal (1 gal = 10^{-2} m s^{-2}) (Fig. 2). For a flexural depression of up to 100 m beneath the SPLD [the approximate uncertainty of the MARSIS observations (*8*)], the best-fit density increased to 1290 kg m^{-3}. Reducing the crustal density to 2700 kg m^{-3} reduces the SPLD density marginally to 1200 kg m^{-3}. The result is only weakly sensitive to the assumed degree of compensation, and thus the recovered density is not highly sensitive to the key unknowns.

As an independent check, we also performed an inversion for the SPLD density. We calculated model-gravity anomalies associated with the crust and mantle, assuming crustal and Moho topography and densities as noted above. The residual gravity compared to the observed gravity was assumed to be due solely to the mass of the SPLD, which is a simplification because some of the variation is probably due to crustal sources. For this simple model, results yielded a model average density of 1290 kg m^{-3}, consistent with the forward model results.

The density of 1220 kg m^{-3}, taking into account surface spectral measurements (*3*, *4*), is most simply explained by water ice with a silicate dust content of 15%. Though the 95% CI formally allows for the possibility of pure water ice, dust is observed at the surface (Fig. 1) of the SPLD, and in the subsurface, layering that probably reflects alternating ice and dust possibly emplaced during different climatic time periods is indicated by MRO sounding-radar profiles (*15*). Our result can be compared with a dust content of 0 to 10% inferred from the dielectric loss tangent of the SPLD measured by MARSIS (*8*). It also supports an earlier inference based on laboratory measurements of rheological properties (*16*) that the SPLD are mostly water ice rather than denser (1589 kg m^{-3}) CO_2 ice.

Despite the dustlike albedo and spectral signature over most of its surface, the martian SPLD are probably composed of relatively clean water ice. These deposits represent the largest known surface reservoir of water on Mars today and the largest in the inner solar system outside of Earth.

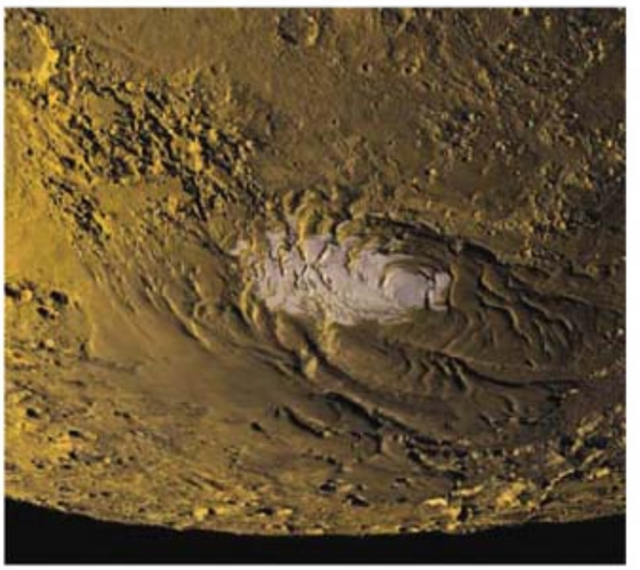

Fig. 1. MOLA shaded relief mosaic combined with color from Mars Global Surveyor imaging of Mars' south polar region showing the residual ice cap (in white) within the smooth SPLD that overlie the cratered southern highlands. [Photo credit: NASA/MOLA Science Team]

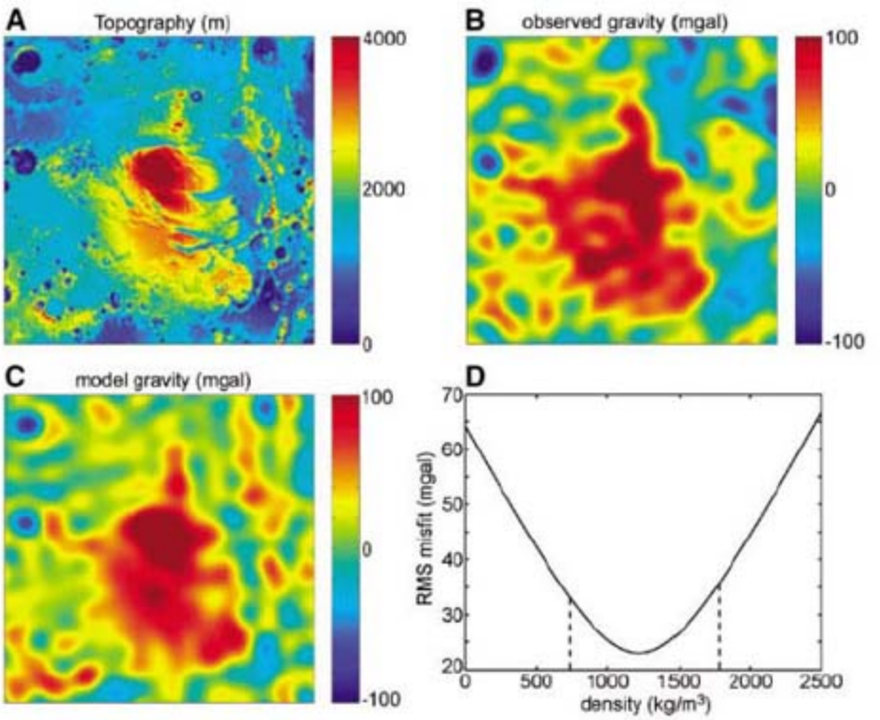

Fig. 2. (**A**) Topography (*7*), (**B**) observed gravity, and (**C**) modeled gravity for the SPLD with the best-fit density of 1220 kg m^{-3}. Map windows are 40° by 40° in stereographic projection. (**D**) 95% CIs are indicated by dashed lines. RMS, root mean square.

References and Notes

1. D. E. Smith *et al.*, *Science* **284**, 1495 (1999).
2. S. Byrne, A. P. Ingersoll, *Science* **299**, 1051 (2003).
3. T. N. Titus, H. H. Kieffer, P. R. Christensen, *Science* **299**, 1048 (2003); published online 5 December 2002 (10.1126/science.1080497).
4. J.-P. Bibring *et al.*, *Nature* **428**, 627 (2004).
5. M. C. Malin, M. A. Caplinger, S. D. Davis, *Science* **294**, 2146 (2001).
6. M. T. Zuber *et al.*, *J. Geophys. Res.* **112**, E05S07 (2007).
7. D. E. Smith *et al.*, *J. Geophys. Res.* **106**, 23689 (2001).
8. J. J. Plaut *et al.*, *Science* **316**, 92 (2007).
9. R. W. Zurek, S. E. Smrekar, *J. Geophys. Res.* **112**, E05S01 (2007).
10. G. A. Neumann *et al.*, *J. Geophys. Res.* **109**, E08002 (2004).
11. R. J. Phillips *et al.*, in *Seventh International Conference on Mars* 9 to 13 July 2007 (Lunar and Planetary Institute, Pasadena, CA, 2007).
12. C. L. Johnson *et al.*, *Icarus* **144**, 313 (2000).
13. R. L. Parker, *Geophys. J. R. Astron. Soc.* **31**, 447 (1972).
14. The observed gravity was filtered to subtract spherical harmonic degrees 2 and 3 to remove the effects of the Tharsis rise, and a cosine filter was applied to degrees 85 to 90 to reduce noise, whereas the modeled gravity was low-pass filtered to match the resolution of the observed field.
15. R. Seu *et al.*, *Science* **317**, 1715 (2007).
16. W. B. Durham, S. H. Kirby, L. A. Stern, *Geophys. Res. Lett.* **26**, 3493 (1999).

17. The MRO Radio Science investigation is supported by the NASA Mars Program.

Supporting Online Material

www.sciencemag.org/cgi/content/full/317/5845/1718/DC1
Materials and Methods
Fig. S1
References

25 June 2007; accepted 9 August 2007
10.1126/science.1146995

Feather Quill Knobs in the Dinosaur *Velociraptor*

Alan H. Turner,[1]* Peter J. Makovicky,[2] Mark A. Norell[1]

Some nonavian theropod dinosaurs were at least partially covered in feathers or filamentous protofeathers (*1*). However, a complete understanding of feather distribution among theropod dinosaurs is limited because feathers are typically preserved only in lagerstätten like that of Solnhofen, Germany or Liaoning, China. Such deposits possess clear taphonomic biases toward small-bodied animals, limiting our knowledge regarding feather presence in larger members of feathered clades.

We present direct evidence of feathers in *Velociraptor mongoliensis* based on the presence of quill knobs on the posterior forearm. In many living birds, raised knobs along the caudal margin of the ulna reveal where the quills of the secondary feathers are anchored to the bone by follicular ligaments. Quill knobs are variably present in extant bird species and are present in only a few basal taxa such as *Ichthyornis* (*2*), so their absence does not necessarily indicate a lack of feathers. Their presence, however, is a direct indicator of feathers of modern aspect (e.g., feathers composed of a rachis and vanes formed by barbs).

The specimen IGM (Geological Institute of Mongolia) 100/981 was collected at the Gilvent Wash locality near Ukhaa Tolgod (Campanian Djadokhta Formation). The specimen is estimated to have been 1.5 m long and to have weighed roughly 15 kg. It possesses several characteristics found in *V. mongoliensis*, a common dromaeosaurid in the Djadokhta Formation. IGM 100/981 preserves six low papillae on the middle third of the caudal margin of the ulna (Fig. 1). These are regularly spaced about 4 mm apart. Topographically, these papillae correspond to the quill knobs in living birds. Given their spacing in IGM 100/981, we estimated that there is space for eight additional secondary feathers. This suggests that 14 secondaries were present in *Velociraptor*, which compares well with the 12 or more secondaries in *Archaeopteryx* (*3*). About 18 secondaries are suggested for the dromaeosaurid *Microraptor* (*4*), whereas its close relative *Rahonavis* appears to have possessed just 10 (*5*).

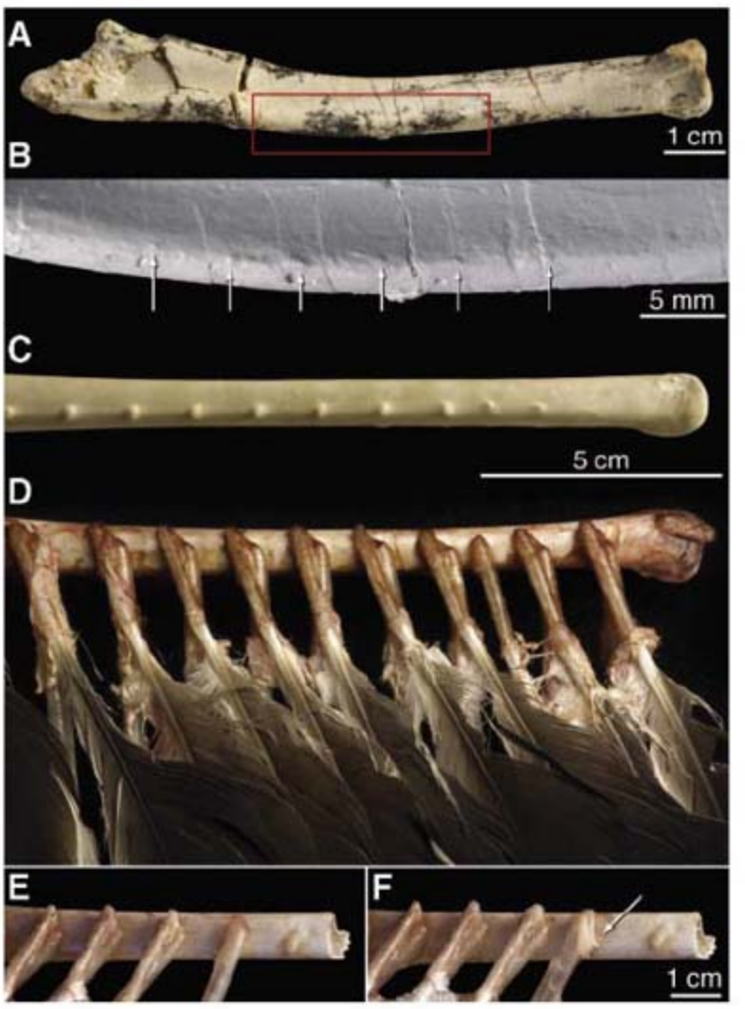

Fig. 1. (**A**) Dorsal view of right ulna of *Velociraptor* IGM 100/981. (**B**) Detail of red box in (A), with arrows showing six evenly spaced feather quill knobs. In (B), a cast of IGM 100/981 was used. (**C**) Dorsal view of right ulna of a turkey vulture (*Cathartes*). (**D**) Same view of *Cathartes* as in (C) but with soft tissue dissected to reveal placement of the secondary feathers and greater secondary coverts relative to the quill knobs. (**E**) Detail of *Cathartes*, with one quill completely removed to reveal quill knob. (**F**) Same view as in (E) but with quill reflected to the left to show placement of quill, knob, and follicular ligament. Follicular ligament indicated with arrow.

Such variation is expected because extant birds display variable counts even within species (*3*).

Known coelurosaurs with wing feathers of modern aspect are small basal members of their respective clades. Some have been considered possibly volant (*4*, *5*), and it has been suggested that the large-bodied, derived members of the feathered theropod clades may not have retained feathers or only retained feathers while juveniles (*6*). This *Velociraptor* specimen indicates this is not the case for at least one lineage of dromaeosaurids. An examination of the living families of birds shows a significant correlation between the absence of ulnar papillae and the loss and/or reduction in volancy, even though some strong flyers lack papillae (*7*). This raises the possibility that ulnar papillar reduction or absence in large-bodied derived dromaeosaurids reflects loss of aerodynamic capabilities from the clade's ancestral members. Quill knobs in *Velociraptor* could reflect retention of feathers from smaller possibly volant ancestors, but such feathers may have had other functions. Although thermoregulatory effects of secondaries on the ulna would be negligible, such feathers could have been used for display (*1*), in shielding nests for thermal control (*8*), or for creating negative lift during incline running (*9*). Whether this feature represents retention of an ancestral function or the cooption for other purposes, the presence of quilled feathers on the posterior of the arms in a medium-sized derived, clearly nonvolant dromaeosaur can now be established.

References and Notes

1. M. A. Norell, X. Xu, *Annu. Rev. Earth Planet. Sci.* **33**, 277 (2005).
2. J. A. Clarke, *Bull. Am. Mus. Nat. Hist.* **286**, 1 (2004).
3. A. Elzanowski, in *Mesozoic Birds, Above the Heads of Dinosaurs*, L. M. Chiappe, L. M. Witmer, Eds. (Univ. California Press, Berkeley, CA, 2002), pp. 129–159.
4. X. Xu *et al.*, *Nature* **421**, 335 (2003).
5. C. A. Forster, S. D. Sampson, L. M. Chiappe, D. W. Krause, *Science* **279**, 1915 (1998).
6. X. Xu *et al.*, *Nature* **431**, 680 (2004).
7. Materials and methods are available on *Science* Online.
8. T. P. Hopp, M. J. Oren, in *Feathered Dinosaurs*, P. J. Currie, E. B. Koppelhus, M. A. Shugar, J. L. Wright, Eds. (Indiana Univ. Press, Bloomington, IL, 2004), pp. 234–250.
9. K. P. Dial, *Science* **299**, 402 (2003).
10. We thank S. Nesbitt for comments, L. Barber and A. Balcarcel for preparation and casting, M. Ellison for photography, P. Sweet, P. Capainolo, and the 1998 Gobi field crew. This study was supported by NSF Division of Earth Sciences (M.A.N. and P.J.M.) and a NSF Doctoral Dissertation Improvement grant (A.H.T.).

Supporting Online Material

www.sciencemag.org/cgi/content/full/317/5845/1721/DC1
Materials and Methods
Fig. S1
References

14 May 2007; accepted 30 July 2007
10.1126/science.1145076

[1]Division of Paleontology, American Museum of Natural History, Central Park West at 79th Street, New York, NY 10024–5192, USA. [2]Department of Geology, The Field Museum, 1400 South Lake Shore Drive, Chicago, IL 60605–2496, USA.

*To whom correspondence should be addressed. E-mail: turner@amnh.org

A Vasculature-Associated Niche for Undifferentiated Spermatogonia in the Mouse Testis

Shosei Yoshida,* Mamiko Sukeno, Yo-ichi Nabeshima

Mammalian spermatogenesis produces numerous sperm for a long period based on a highly potent stem cell system, which relies on a special microenvironment, or niche, that has not yet been identified. In this study, using time-lapse imaging of green fluorescent protein–labeled undifferentiated spermatogonia (A_{undiff}) and three-dimensional reconstitution, we revealed a biased localization of A_{undiff} to the vascular network and accompanying Leydig and other interstitial cells, in intact testes. Differentiating spermatogonia left these niche regions and dispersed throughout the basal compartment of the seminiferous epithelium. Moreover, rearrangement of A_{undiff} accompanied the vasculature alteration. We propose that the mammalian germline niche is established as a consequence of vasculature pattern formation. This is different from what is observed in *Drosophila* or *Caenorhabditis elegans*, which display developmentally specified niche structures within polarized gonads.

Tissue homeostasis is ensured by the normal functioning of stem cells, which are characterized by their ability to self-renew, as well as to differentiate into specialized cell types. Stem cells are tightly linked to their niche or microenvironment, which regulates their behaviors (*1*, *2*). The *Drosophila* and *Caenorhabditis elegans* germ lines represent model systems that have provided insights into the stem cell niche. In these organisms, the gonads are polarized: One end opens out of the body wall, and the opposite end harbors a specialized somatic compartment that supports the stem cells. The somatic components of the stem cell niche are developmentally specified, and their elimination causes irreversible stem cell dysfunction (*1*, *3*).

Functional and genetic evidence suggests that the niche is also critical to mammalian spermatogenic stem cells (*4*–*7*); however, the structural basis of this niche is largely unknown. The mammalian testis lacks overall polarity: Seminiferous tubules form loops with both their ends connected to the rete testes, the outlet for sperm from the testis. Stem cells are scattered throughout the loops. The interstitium between the convoluted seminiferous tubules contains the vasculature network and Leydig cells, macrophages, as well as other cells that surround the blood vessels (*8*, *9*) (Fig. 1, A and B, see also fig. S1, A and A′). The basal compartment within the seminiferous tubules (the space between the basement membrane and the Sertoli cell tight junctions) supports all the stages of spermatogonia before meiosis, including the stem cells. However, no specialized niche substructure has been identified (*4*) (Fig. 1B).

Unequivocal identification of the spermatogenic stem cells in the mouse testis has also not been achieved. However, a subset of primitive spermatogonia (<1% of total testicular cells) termed "undifferentiated spermatogonia" or "A_{undiff}" includes stem cells that constitute an as-yet-unidentified subpopulation (*10*, *11*). The A_{undiff} population persists throughout the seminiferous epithelial cycle, which takes 8.6 days to complete and is divided into stages I to XII

Department of Pathology and Tumor Biology, Graduate School of Medicine, Kyoto University, Kyoto, Japan.

*To whom correspondence should be addressed. E-mail: shosei@lmls.med.kyoto-u.ac.jp

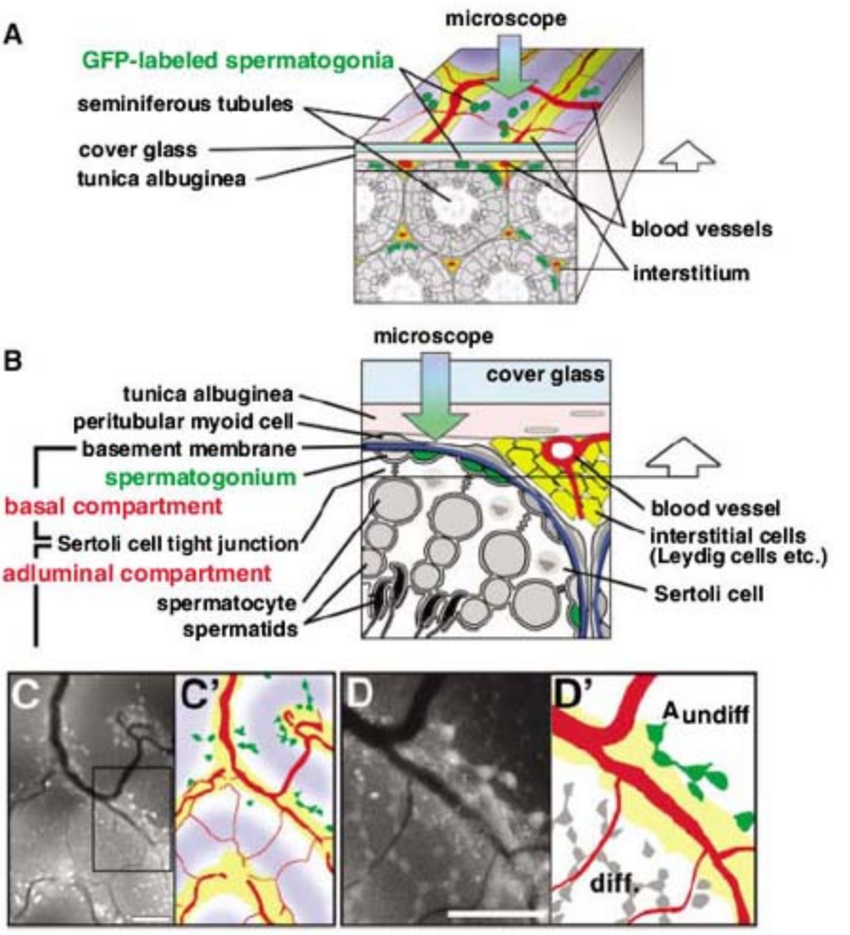

Fig. 1. Anatomy of the testis and observation of the GFP-labeled spermatogonia. (**A** and **B**) Anatomy of the testis and the observation strategy. See text for details. To observe the GFP-labeled A_{undiff}, a part of a testis of Ngn3/EGFP transgenic mouse (*20*) was flattened with a cover glass. The GFP-labeled spermatogonia in the outermost tubules were observed under a fluorescence microscope through the tunica albuginea, peritubular myoid cells, and basement membrane. Only the superficial region that covered the basal compartment could be seen (indicated by the upward-pointing arrows). (**C** and **D**) (C) A representative tiled image and (**C′**) a trace of the labeled spermatogonia (green), blood vessels (red), and interstitium (yellow); seminiferous tubule continuity is indicated in blue. (D) and (**D′**) are magnified images of a part of (C) marked by a rectangle. Labeled A_{undiff} can be observed, whereas the meshwork of cells weakly positive for GFP in (D) [indicated in gray in (D′)] constitutes the differentiating spermatogonia (diff.). Scale bars, 100 μm.

(*9*, *12*). The A_{undiff} population periodically gives rise to the A_1 differentiating spermatogonia at a specific stage (VII to VIII) of the cycle (*9*, *13*, *14*). A_1 spermatogonia subsequently go through six synchronous mitoses [generating A_2, A_3, A_4, intermediate (In), and B spermatogonia, and preleptotene spermatocytes], which are tightly linked to the seminiferous epithelial cycle progression, before undergoing meiosis. In contrast, A_{undiff} divide asynchronously under a weaker restriction of the cycle (*9*, *14*, *15*). The reconstituting colony-forming activity after transplantation is enriched in the A_{undiff} population (*16*, *17*).

The A_{undiff} population contains A_{single} (A_s, isolated cells), A_{paired} (A_{pr}, pairs of interconnected cells), and $A_{aligned}$ (A_{al}, chains of 4, 8, 16, or occasionally 32 cells) spermatogonia (*9*, *13*). Visualization of the chains requires whole-mount preparations of the seminiferous tubules, a procedure that disturbs the testicular organization and eliminates the vasculature and cells of the interstitial compartment. In paraffin sections, A_{undiff} show primitive nuclear morphology lacking prominent heterochromatin condensation; however, distinguishing A_{undiff} from differentiating A spermatogonia (A_1 to A_4) is difficult (*13*). Chiarini-Garcia *et al*. morphologically identified A_{undiff} in plastic-embedded thin sections and reported their preference for an area facing the interstitium in the mouse and rat testes (*18*, *19*).

In this study, we analyzed the localization and behaviors of A_{undiff} in undisturbed testes. For that purpose, A_{undiff} were labeled with green fluorescent protein (GFP) under the control of the *Ngn3* (*neurogenin3*) regulatory sequence (*20*, *21*). Ngn3-positive spermatogonia constitute a major, although not the entire, fraction of A_{undiff} and give rise to all of the spermatogenic cells in the mature testis (*11*, *20*, *22*).

Seminiferous epithelial stage–related distribution of the labeled spermatogonia. Our strategy for observing the GFP-labeled spermatogonia located just beneath the tunica albuginea, the outer capsule of the testis, is shown (Fig. 1, A and B) and described (*21*). By this method, the labeled A_{undiff} (green in Fig. 1, C and D) were detected because of their strong GFP signal, while the background autofluorescence allowed us to recognize the position of seminiferous tubules (blue), blood vessels (red), and interstitial cells (yellow). The differentiating progeny of A_{undiff} that remained in the basal compartment (A_1 to B spermatogonia) were also observed within the same two-dimensional image before cells moved to the adluminal compartment and entered meiosis, as long as they retained the residual GFP fluorescence (gray in Fig. 1D).

The GFP-labeled spermatogonia showed variable distribution patterns relative to the local seminiferous epithelial stages that we determined (fig. S1 and Fig. 2). At stages IV to VI, they exhibited a strong preference for the region adjacent to the blood vessels and the interstitium (Fig. 2, B to E). The preference became weaker at stages VII to VIII, when the A_{undiff} to A_1 transition occurs, and was mostly lost in stage IX, when A_1 give rise to A_2 after the first synchronous division. This is compatible with previous observations on plastic-embedded sections (*18*, *19*). A_{undiff} showed a strong correlation with intertubular vessels (arterioles and venuoles) that usually accompany interstitial cells, but not with capillaries or vessels without surrounding interstitial cells. Weakly stained differentiating spermatogonia were detectable usually up to A_3 or A_4 (stages I or II to III), or occasionally up to B at stage VI.

Biased localization of A_{undiff} and their migration during the transition to differentiating spermatogonia. To more comprehensively visualize the locations and movements of spermatogonia during the A_{undiff} to A_1 transition, we performed time-lapse imaging. A representative compilation of images of a continuous tubule segment are shown (Fig. 3), with a portion of them highlighted (Fig. 3B and movie S1). At the beginning of the imaging (around stage VII), labeled spermatogonia clustered at a position adjacent to the vessels and interstitium (star). During ~30 to 70 hours, two chains of interconnected eight GFP-positive A_{undiff} (A_{al-8}, indicated by orange and yellow asterisks in Fig. 3B) migrated out of this region and, thereafter, divided into 16-cell chains with a similar timing (at 76 hours and 73 hours). On the basis of the stage-specific distribution pattern of the GFP-labeled cells (Fig. 2), we determined that these divisions were the A_1 to A_2 division, i.e., the first synchronous division of the differentiating spermatogonia that occurs at stage IX. Similar behaviors were consistently observed of other spermatogonia undergoing the A_{undiff} to A_1 transition, which led us to conclude that this transition event coincides with migration away from their original position near the intertubular vessels. The migrating spermatogonia divided infrequently [usually >40 hours (Fig. 3B and movie S1), sometimes >70 hours], compatible with previous studies using fixed testes (*13*, *14*). The spermatogonia continued to migrate beyond the A_1 to A_2 division until they were evenly distributed throughout the basal compartment—this occurred around the A_2 to A_3 division in stage XI.

Gray ovals in Fig. 3A′ indicate the positions from which the labeled A_{undiff} migrated out and transited into A_1. Representative examples with higher magnifications are also shown (Fig. 3, C to F). Within the zone facing the interstitium and

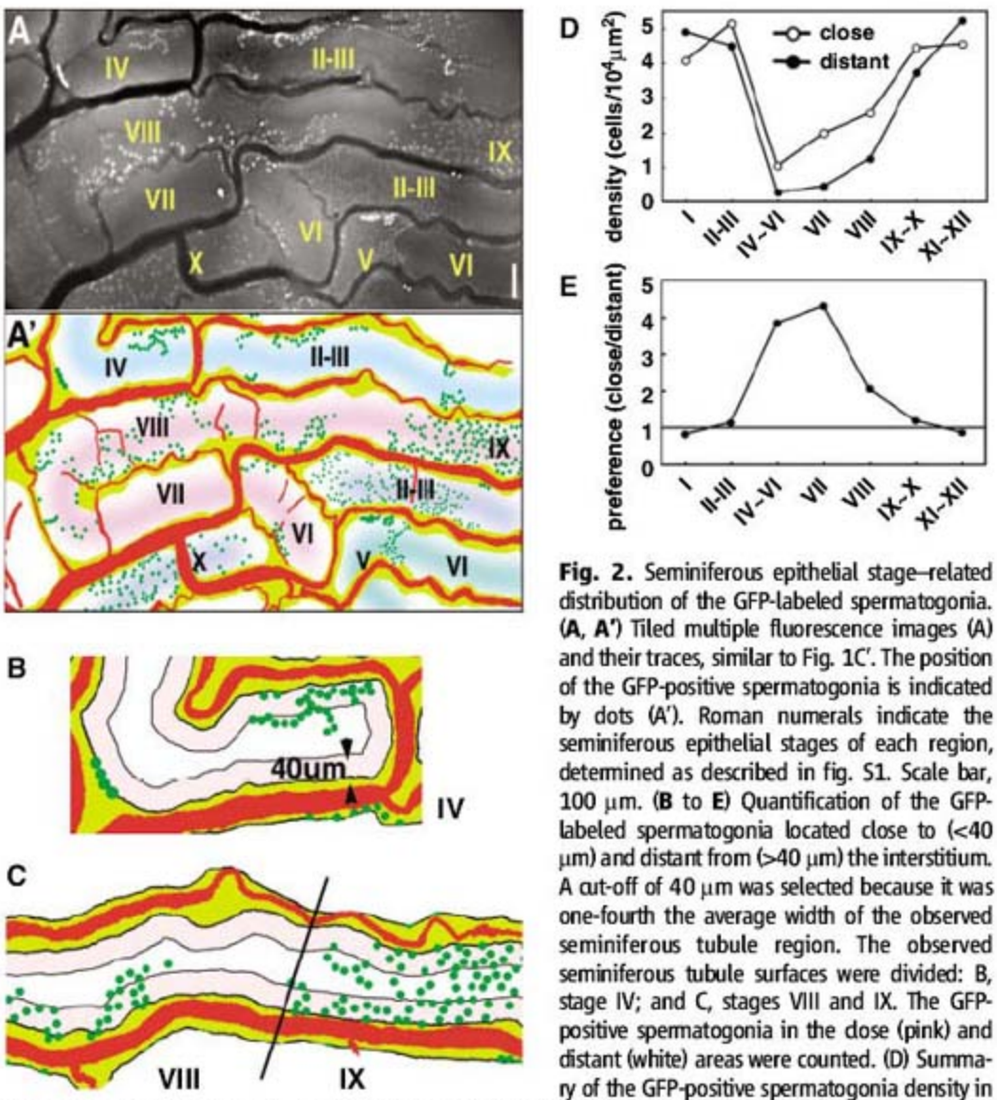

Fig. 2. Seminiferous epithelial stage–related distribution of the GFP-labeled spermatogonia. (**A**, **A′**) Tiled multiple fluorescence images (A) and their traces, similar to Fig. 1C′. The position of the GFP-positive spermatogonia is indicated by dots (A′). Roman numerals indicate the seminiferous epithelial stages of each region, determined as described in fig. S1. Scale bar, 100 μm. (**B** to **E**) Quantification of the GFP-labeled spermatogonia located close to (<40 μm) and distant from (>40 μm) the interstitium. A cut-off of 40 μm was selected because it was one-fourth the average width of the observed seminiferous tubule region. The observed seminiferous tubule surfaces were divided: B, stage IV; and C, stages VIII and IX. The GFP-positive spermatogonia in the close (pink) and distant (white) areas were counted. (D) Summary of the GFP-positive spermatogonia density in each area, classified by the seminiferous epithelial stages. (E) Their preference for the close area [(density in close area)/(density in distant area), which was expected to be 1 in the case of random distribution]. Results from 1155 GFP-positive spermatogonia in 77 seminiferous tubule segments are summarized.

blood vessels, the labeled spermatogonia exhibited a further preference for the branch points of the blood vessels, as indicated by blue circles in Fig. 3A′. Characteristically, labeled A_{undiff} spermatogonia were often found in the inner or outer corner of turning tubules, which were also associated with vascular branching (Fig. 3, E and F). It is noteworthy that such branch points always coincided with abundant interstitium. In some instances, A_{undiff} in neighboring seminiferous tubules were localized on the opposite side of the branching vessels (Fig. 3, C and D). The majority of such branch points accompanied the A_{undiff} clusters, although, in some cases, the migration of the A_{undiff} spermatogonia away from the surface of the exposed seminiferous tubule hid them from view.

Vasculature-related localization of A_{undiff} in inner seminiferous tubules. The above findings were from the superficial area of the seminiferous tubules that contacts with tunica albuginea, and the GFP-labeling was dependent on the *Ngn3*-regulatory sequence and might not represent the entire A_{undiff} population (*11*, *20*). Therefore, to obtain more universal information, we reconstructed three-dimensional images from paraffin-embedded serial sections after cell-type determination by examining nuclear morphology after hematoxylin staining (*9*) (Fig. 4). Because of the uncertainty in distinguishing A_{undiff} from A_1 to A_4 differentiating spermatogonia, we restricted our analysis to stages IV to VIII, stages that contain A_{undiff} and nascent A_1 spermatogonia, but lack more differentiated type-A spermatogonia.

Three-dimensional reconstruction allowed us to follow the convoluted seminiferous tubules and the surrounding vasculature network (Fig. 4, D to G): The yellow stripes and the blue areas represent the regions facing the interstitium and the neighboring tubules, respectively. The A_{undiff} (green) showed a clear correlation with the yellow stripes running beneath the blood vessels, with an additional preference for the blood vessel branch

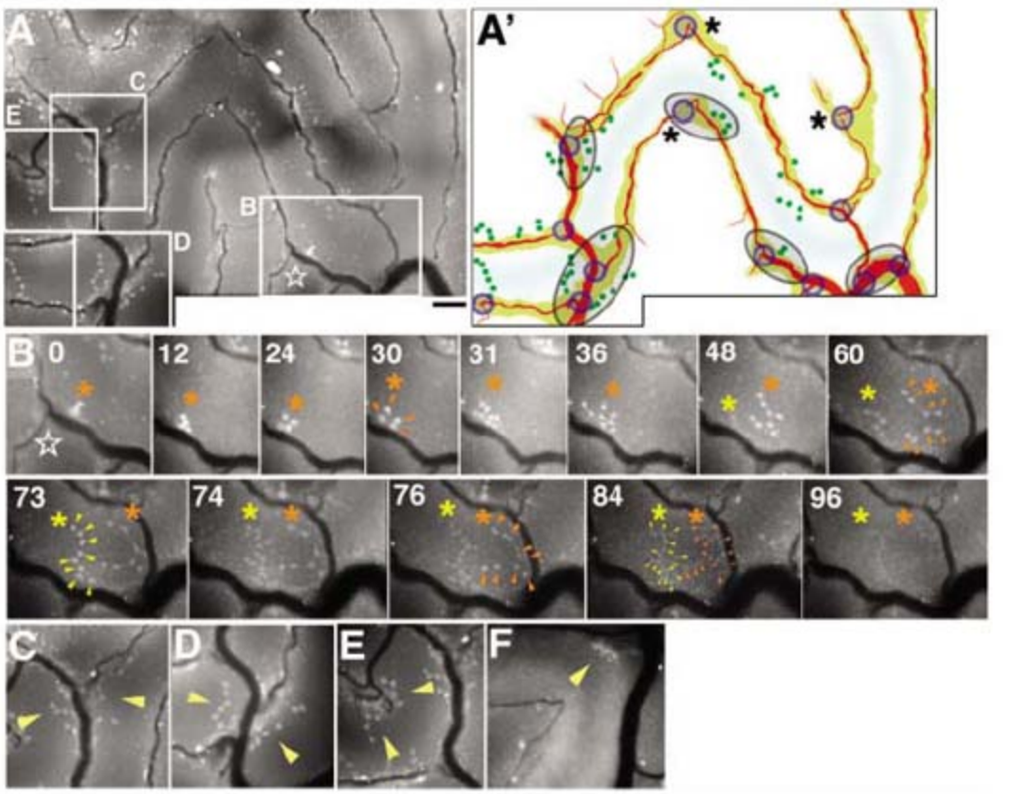

Fig. 3. Time-lapse observation of the GFP-labeled spermatogonia during the transition from undifferentiated to differentiating spermatogonia. (**A**, and **A′**) Composition of multiple fluorescence images at the beginning of the imaging (A) that includes a continuous seminiferous tubule segment represented in (A′) (as in Fig. 2A′). Rectangles in (A) indicate the positions of the images in the rest of the figure. Gray ovals in (A′) indicate the sites from which GFP-positive A_{undiff} migrated during their transition to differentiating spermatogonia. The smaller blue circles indicate the blood vessels branch points, some of which (indicated by asterisks) have branches running inward into the testis (perpendicular to the image plane). Scale bar, 100 μm. (**B**) Selected frames of the record of the area shown in (A) (also see movie S1). Numbers indicate the approximate elapsed time in hours. Orange and yellow asterisks indicate two syncytial clones that divided during the imaging. Individual cells in these clones are indicated by arrowheads in some frames; some cells of the orange clone are behind a blood vessel in frame 84 hours. Mitoses were observed at 30 hours and 76 hours in the orange clone (4 to 8 and 8 to 16 cells, respectively), and at 73 hours in the yellow clone (8 to 16 cells). Star, a blood vessel branch point, corresponds to the star in (A). (**C** to **F**) Typical examples of the regions wherein A_{undiff} are located before they transit to differentiating spermatogonia. Arrowheads indicate clustered GFP-positive A_{undiff}. (C) to (E) Magnified images of the areas presented in (A); (F) a different observation.

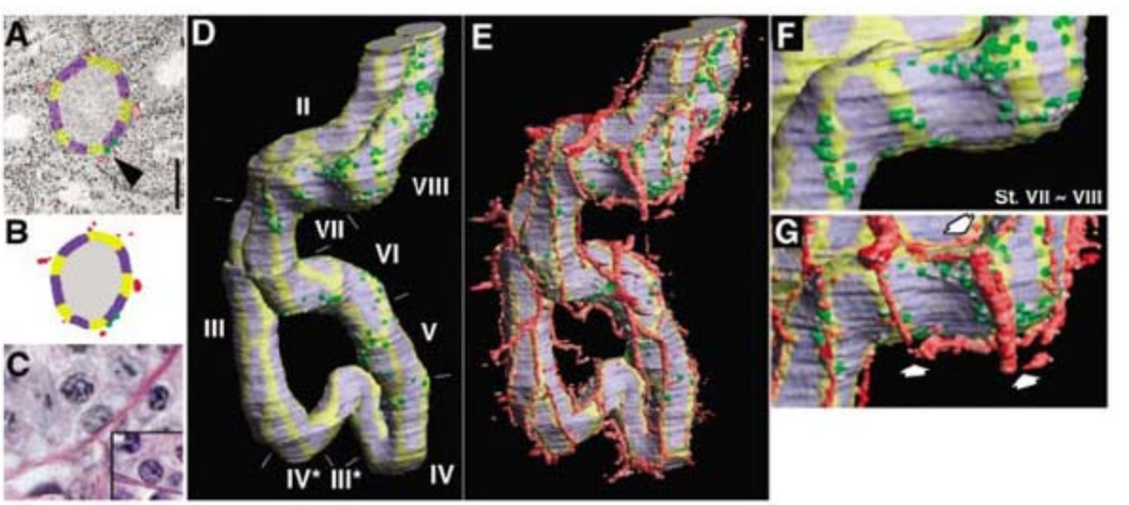

Fig. 4. Three-dimensional reconstitution of the seminiferous tubule, surrounding vasculature, and A_{undiff} localization. (**A** to **C**) Tracing of the components in each section. (A) A microscopic image of a serial section stained with periodic acid–Schiff and hematoxylin. The seminiferous tubule of interest was traced; its peripheral regions facing the interstitium (yellow), those facing the neighboring seminiferous tubules (blue), and the blood vessels (except capillaries; red) are shown. Traces of seminiferous tubules at stages from IV to VIII show A_{undiff} and nascent A_1 spermatogonia as green dots. Scale bar, 100 μm. (B), traced image and (C), a magnified view of an A_{undiff} spermatogonium indicated by the arrowhead in (A), with a pale homogeneous staining of the nuclear materials, and its comparison with a differentiating B spermatogonium found in the same section (inset). (**D** to **G**) Three-dimensional reconstituted images. (D) and (E) Entire views and [(F) and (G)] closer images with [(E) and (G)] and without [(D) and (F)] blood vessels. Seminiferous epithelial stages are indicated, with a small modulation in their order, as described (asterisks) (*9*). Arrows in (G) indicate the examples of blood vessel branch points associated with A_{undiff} clustering.

points (arrows in Fig. 4G). In stages IV to VI, a small number of A_{undiff} spermatogonia were tightly clustered near the interstitium. In stages VII to VIII, they increased in number and were more dispersed than in stages IV to VI, similar to what we had observed during the A_{undiff} to A_1 transition with live GFP-labeling (Figs. 1 to 3).

Rearrangement of A_{undiff} accompanies the vasculature pattern alteration. To assess the functional link between the vasculature pattern and A_{undiff} localization, seminiferous tubule fragments from donor mice (marked with ubiquitous GFP) were freed of the attaching vessels and interstitium, then transplanted beneath the tunica albuginea of a recipient testis (Fig. 5). After 3 months, the grafts survived in an unusual coiled configuration, and a significant part of them harbored donor-derived spermatogenesis with multilayered organization and an apparently normal seminiferous epithelial cycle (Fig. 5, A to E). Therefore, normal functioning of the stem cells was restored in the grafts.

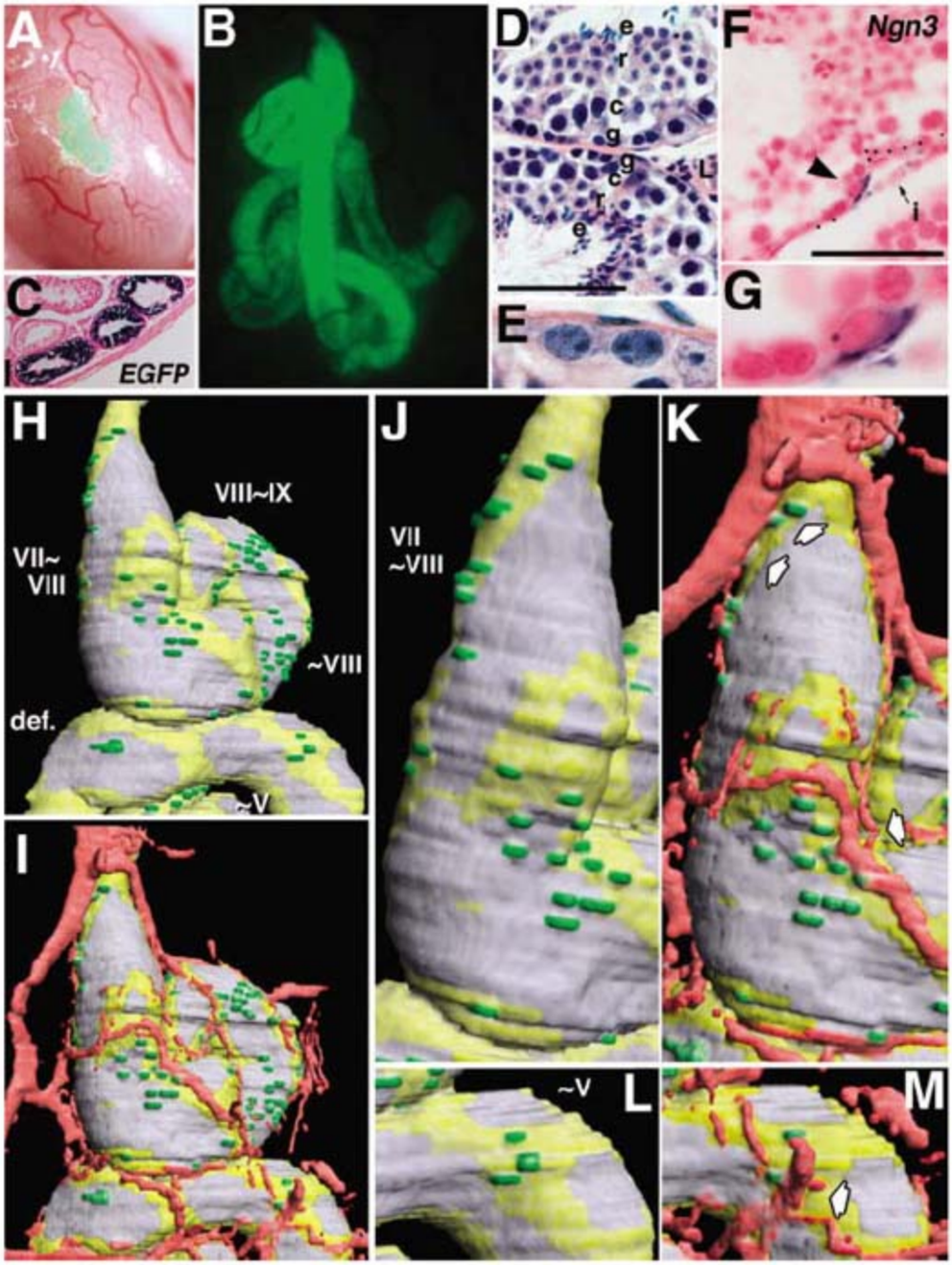

Fig. 5. Localization of spermatogonia in the transplanted seminiferous tubule fragment. (**A** and **B**) A GFP-positive seminiferous tubule fragment that survived in the host testis 3 months posttransplantation beneath the tunica albuginea. (A) An overlay of the bright-field and fluorescence images; (B) a closer fluorescence graft image; and (**C**) a section of the graft, hybridized in situ with the enhanced GFP probe. (**D**) A hematoxylin-and-eosin–stained section showing the donor seminiferous tubules harboring multiple germ cell layers. e, elongated spermatids; r, round spermatids; c, spermatocytes; g, spermatogonia; and i, interstitium. (**E**) Spermatogonia with the type-A morphology observed in the graft. (**F**) A section of the donor seminiferous tubules hybridized with the Ngn3 probe. Arrowhead indicates an Ngn3-positive spermatogonium. (**G**) A magnified image. Dots, the basement membrane; and i, interstitium. Scale bars, 100 μm. (**H** to **M**) Three-dimensional reconstitution of the same graft; [(J) to (M)], at higher magnifications. Most of the green dots represent the positions of spermatogonia with the type-A morphology, whereas some of them were identified on the basis of their Ngn3 expression determined by in situ hybridization [(F) and (G)]. Roman numerals indicate the approximate seminiferous epithelial stages, and arrows indicate the blood vessel branch points associated with A_{undiff} clusters. The region marked "def" contains defective spermatogenesis.

A three-dimensional reconstruction of a graft (Fig. 5, H to M) is represented in the same manner as in Fig. 4. The vasculature was established in good coordination with the abnormal shape of the graft (Fig. 5, B, H, and I), which suggested that the vasculature pattern was different from that present in the donor testis. Interstitial cells including the Leydig cells were also established surrounding the vasculature (Fig. 5D). The green dots represent the spermatogonia with a primitive morphology common to A_{undiff} and A_1 to A_4 spermatogonia (Fig. 5E), some of which were Ngn3-positive (Fig. 5, F and G). If we assume that the seminiferous epithelial cycle is normal in the graft, the green dots represent A_{undiff} localization before the transition into A_1 (stages V to VII). They preferentially localized to interstitial zones, and even to the branch points of the vessels (Fig. 5, J to M). In stages ~VIII to IX, they were no longer restricted to the interstitium and were also found in regions facing neighboring tubules (Fig. 5, H and I).

Therefore, a normal pattern of A_{undiff} localization reappeared when the surrounding vasculature and interstitium were reorganized. The intriguing correlation between the vessels, the shape of the graft, and the A_{undiff} localization suggest that the vasculature and interstitium play a causal role in the A_{undiff} relocation, although it is not excluded that the A_{undiff} may have also affected the vasculature to some extent.

A microenvironmental niche for A_{undiff} linked to the vasculature. In summary, in the mature mouse testis, A_{undiff} are preferentially located in restricted portions of the basal compartment within the seminiferous tubule, which are adjacent to the blood vessels and interstitium and are particularly close to the blood vessel branch points. On making the transition into differentiating spermatogonia, they migrate out of these areas and disperse over the entire basal compartment of the seminiferous epithelium. These limited regions can be considered the microenvironmental niche for A_{undiff}. The actual stem cells, which constitute an as-yet-unknown A_{undiff} subpopulation (*11*), might also reside in these regions, although it is still possible that the actual stem cells are localized differently and that only their immediate A_{undiff} progeny prefer this microenvironment. A_{undiff} spermatogonia do not behave uniformly in these niche regions. In some instances, they migrate out and transit into A_1; in other instances, they remain within the niche. This might reflect heterogeneity within the niche environments or within the A_{undiff} population.

Our study raises the question of why A_{undiff} localization recapitulates the vasculature pattern. One straightforward possibility is that blood vessels recruit A_{undiff}. Recently, a "vascular niche" has been described for several other stem and/or progenitor

cells (*23*–*26*). A similar interaction might be possible in the testis. However, unlike cells in the brain, bone marrow, and tumors, spermatogonia are not in direct contact with the vasculature.

Leydig cells are strongly associated, anatomically, with the blood vessels. Moreover, Leydig cells have been also proposed to originate from cells in blood vessels such as smooth muscle cells or pericytes (*27*). Therefore, the Leydig cells (or other types of interstitial cells) might contribute to the niche microenvironment by producing androgens or other factors. This is compatible with the observation that A_{undiff} are preferentially associated with blood vessels surrounded by Leydig cells. The preference for the branch points of blood vessels might reflect the importance of Leydig or other interstitial cells, because such regions are usually rich in these cells.

Vasculature-oriented niche specification in the mouse testis. Regardless of the identity of the primary somatic niche cell type, this study has shown that the niche for A_{undiff}, and possibly that for the stem cells, is associated with the vasculature pattern. The grand design of seminiferous tubules (testis cords in the fetal testis) and testicular vessels are established by developmental processes linked to sex differentiation (*28*). In contrast, the complex packaging of the highly convoluted seminiferous tubules (*29*) and the networking of the vasculature running between the tubules are not likely to be predetermined. Rather, the intrinsic pattern-forming activity of the vessels (*30*) appears to play an important role in the establishment of the local vasculature that surrounds the seminiferous tubules. Therefore, niche formation is unlikely to be a developmentally programmed process and is more likely to be an indirect consequence of vasculature formation. This conclusion is further supported by our grafting data, which showed that A_{undiff} rearrangement accompanied vasculature alteration (Fig. 5).

A vasculature-oriented niche formation has several attractive features. It allows niches to form at regular intervals all through the seminiferous tubule loops, whatever their length. Additionally, new niches could be added as the tissue increases in size or following tissue damage and revascularization. When the niche is regenerated, spermatogenesis could be reestablished after intratubular migration of the stem cells from neighboring unaffected regions. These features make a good contrast to that of the *Drosophila* or *Caenorhabditis elegans* germline niche, which is totally dependent on the developmentally determined somatic cells and, once damaged, niche cells never regenerate. Such niche plasticity could be particularly beneficial for continuous spermatogenesis during the long reproductive periods of mammals.

References and Notes

1. A. Spradling, D. Drummond-Barbosa, T. Kai, *Nature* **414**, 98 (2001).
2. D. T. Scadden, *Nature* **441**, 1075 (2006).
3. Y. M. Yamashita, M. T. Fuller, *Int. J. Hematol.* **82**, 377 (2005).
4. T. Ogawa, M. Ohmura, K. Ohbo, *Int. J. Hematol.* **82**, 381 (2005).
5. T. Shinohara, K. E. Orwig, M. R. Avarbock, R. L. Brinster, *Proc. Natl. Acad. Sci. U.S.A.* **98**, 6186 (2001).
6. R. A. Hess, P. S. Cooke, M. C. Hofmann, K. M. Murphy, *Cell Cycle* **5**, 1164 (2006).
7. C. Chen *et al.*, *Nature* **436**, 1030 (2005).
8. B. T. Hilton, T. T. Turner, in *Cell and Molecular Biology of the Testis*, C. Desjardins, L. L. Ewing, Eds. (Oxford Univ. Press, New York, 1993), pp. 238–265.
9. L. Russell, R. Ettlin, A. Sinha Hikim, E. Clegg, *Histological and Histopathological Evaluation of the Testis* (Cache River Press, Clearwater, FL, 1990).
10. Y. Nishimune, S. Aizawa, T. Komatsu, *Fertil. Steril.* **29**, 95 (1978).
11. T. Nakagawa, Y. Nabeshima, S. Yoshida, *Dev. Cell* **12**, 195 (2007).
12. C. P. Leblond, Y. Clermont, *Ann. N. Y. Acad. Sci.* **55**, 548 (1952).
13. D. G. de Rooij, L. D. Russell, *J. Androl.* **21**, 776 (2000).
14. R. A. Tegelenbosch, D. G. de Rooij, *Mutat. Res.* **290**, 193 (1993).
15. D. G. de Rooij, *Reproduction* **121**, 347 (2001).
16. T. Shinohara, K. E. Orwig, M. R. Avarbock, R. L. Brinster, *Proc. Natl. Acad. Sci. U.S.A.* **97**, 8346 (2000).
17. K. Ohbo *et al.*, *Dev. Biol.* **258**, 209 (2003).
18. H. Chiarini-Garcia, L. D. Russell, *Biol. Reprod.* **65**, 1170 (2001).
19. H. Chiarini-Garcia, J. R. Hornick, M. D. Griswold, L. D. Russell, *Biol. Reprod.* **65**, 1179 (2001).
20. S. Yoshida *et al.*, *Dev. Biol.* **269**, 447 (2004).
21. Materials and methods are available as supporting material on *Science* Online.
22. S. Yoshida *et al.*, *Development* **133**, 1495 (2006).
23. G. Nikolova, B. Strilic, E. Lammert, *Trends Cell Biol.* **17**, 19 (2007).
24. T. Sugiyama, H. Kohara, M. Noda, T. Nagasawa, *Immunity* **25**, 977 (2006).
25. T. D. Palmer, A. R. Willhoite, F. H. Gage, *J. Comp. Neurol.* **425**, 479 (2000).
26. C. Calabrese *et al.*, *Cancer Cell* **11**, 69 (2007).
27. M. S. Davidoff *et al.*, *J. Cell Biol.* **167**, 935 (2004).
28. J. Brennan, J. Karl, B. Capel, *Dev. Biol.* **244**, 418 (2002).
29. Y. Clermont, C. Huckins, *Am. J. Anat.* **108**, 79 (1961).
30. J. Folkman, C. Haudenschild, *Nature* **288**, 551 (1980).

31. We thank D. de Rooij for providing instructions regarding seminiferous epithelial stage determination; T. Obata for preparing sections; T. Fujimori and K. Kato for their suggestions about imaging; N. Yoshida, T. Nakagawa, and R. Sugimoto for critical reading of the manuscript. We also thank members of the Institute of Laboratory Animals, Graduate School of Medicine, Kyoto University, for animal care. This work was partly supported by Grants-in-Aid for Scientific Research from the Ministry of Education, Culture, Sports, Science and Technology, Japan. The initial part of this study was supported by the PRESTO program (Recognition and Formation), Japan Science and Technology Agency.

Supporting Online Material

www.sciencemag.org/cgi/content/full/1144885/DC1
Materials and Methods
Fig. S1
References
Movie S1

9 May 2007; accepted 16 August 2007
Published online 6 September 2007;
10.1126/science.1144885
Include this information when citing this paper.

REPORTS

Universality Classes for Domain Wall Motion in the Ferromagnetic Semiconductor (Ga,Mn)As

M. Yamanouchi,[1,2] J. Ieda,[3,4] F. Matsukura,[1,2] S. E. Barnes,[3,5] S. Maekawa,[3,4] H. Ohno[1,2]*

Magnetic domain wall motion induced by magnetic fields and spin-polarized electrical currents is experimentally well established. A full understanding of the underlying mechanisms, however, remains elusive. For the ferromagnetic semiconductor (Ga,Mn)As, we have measured and compared such motions in the thermally activated subthreshold, or "creep," regime, where the velocity obeys an Arrhenius scaling law. Within this law, the clearly different exponents of the current and field reflect different universality classes, showing that the drive mechanisms are fundamentally different.

A spin-polarized current can interact with a magnetic domain wall (DW) (*1*), thereby allowing the magnetization direction to be electronically controlled (*2*–*7*) with subsequent possible applications for nonvolatile memory (*8*). However, a full understanding of the underlying mechanism of magnetization reversal by DW motion is lacking (*9*–*15*). Recent progress in the nanofabrication of ferromagnetic structures has made possible the investigation of the dynamics of a single DW subject to a spin-polarized electrical current. Systematic experimental data, spanning five decades of DW velocity, v, for a current-driven microstructure made from the ferromagnetic semiconductor (Ga,Mn)As (*16*) has revealed that the DW velocity increases roughly linearly with the current density, j, beyond its threshold value, j_C. This can be understood in terms of the spin-transfer mechanism in which the angular momentum is transferred from the flow of spin-polarized carriers to the localized spins in the DW, thus producing a torque and resulting motion. In the subthreshold creep regime below j_C, it was found that the motion follows an unexplained empirical scaling law. Similarly, v is approximately linear

in the magnetic field, H, for modest values larger that a field threshold H_C (*17*). These facts suggest that there might be a linear relation between H and j that results in a given drive and v. We have made a comparison between the subthreshold DW motion resulting from these two driving influences. For both cases, an Arrhenius scaling law is obeyed but involves incompatibly distinct powers of H and j, showing that a linear relation between the field- and current-induced drives does not apply here. Whereas the field-driven data are compatible with the existing theory for the random-field universality class, the current-induced motion is not and does not appear to fit any known class. A theoretical framework to explain this behavior has been developed.

In this work, we used the (Ga,Mn)As device (Mn composition $x = 0.045$) thoroughly studied in our previous experiments on current-induced DW motion (*16*). Due to the tensile strain induced by (In,Al)As underlayer, there is a magnetic easy axis perpendicular to the plane. The device (topmost inset in Fig. 1) consists of two regions, I and II: The Curie temperature, T_C, of region I, within which is swept the DW, is 112 K. Through use of the thickness-dependent coercivity (*2*), the DW is initially placed at the etched step boundary by H. Once the DW is created in this channel, it can also be reset at the step boundary by a current. Micromagnetic calculations based on the p-d Zener model show that the DW of interest is a Bloch wall of width 17 nm (*18*). With $H = 0$, the DW, at the step boundary, is injected into region I by j or H pulse. The area swept by the DW observed by a magneto-optical Kerr effect (MOKE) microscope is used to determine the effective DW displacement, d_{eff}; the insets of Fig. 1, A and B, show typical images with various pulse durations, w_p. The moving head of DW has a wedge shape in the current-induced case, reflecting a nonuniform current distribution around the DW due to the polarity change of the anomalous Hall effect. For the field-induced (current-induced) case shown in Fig. 1A (Fig. 1B), initially d_{eff} increases gradually (rapidly) with w_p, and then the slope becomes almost constant for $d_{eff} > 15$ μm. We determined the effective DW velocity, v_{eff}, from the linear slope for $d_{eff} > 15$ μm. Figure 2, A and C, summarize the dependence of v_{eff} on $\mu_0 H$ ($\mu_0 H = 1.9$ to 11 mT for $T = 100$ to 104 K; μ_0: vacuum permeability) and j ($j = 4.5 \times 10^4$ to 1.1×10^6 A/cm^2 for $T = 98$ to 104 K), respectively. To compensate for the effects of Joule heating, we determined sample temperature, T, for the current-induced case using the device resistance as a thermometer (*16*). The temperature range for the measurements is restricted by the Joule heating for the current-induced case and by the temperature-dependent coercivity, i.e., the coercivity for region I becomes greater than that of region II below 96 K, for the field-induced case. The logarithmic plots of the velocity show a nonlinear dependence on both $\mu_0 H$ and j, strongly suggesting that the DW motion observed here is in the creep regime (*19*). We test the scaling of the DW creep velocities, v (v^*), with functional forms; $\ln(v/v_c) = a - bj^{-\mu}$ and $\ln(v^*/v_c^*) = a^* - b^*(\mu_0 H)^{-\mu^*}$ with a (a^*) and b (b^*) expressed as the power of the relative temperature ($T_C - T$) for current-induced and field-induced cases, respectively. Here, v_c (v_c^*) is the velocity at the threshold drive. From the linearity over a few decades of v_{eff} of the scaling plots (Fig. 2, B and D), we conclude that the above scaling functions describe well the data. Curves in Fig. 2D do not collapse because of the relatively strong temperature dependence of a. The parameters are determined as $\mu = 0.33 \pm 0.06$, $b \propto (T_C - T)^{2.0 \pm 0.2}$, and $\mu^* =$

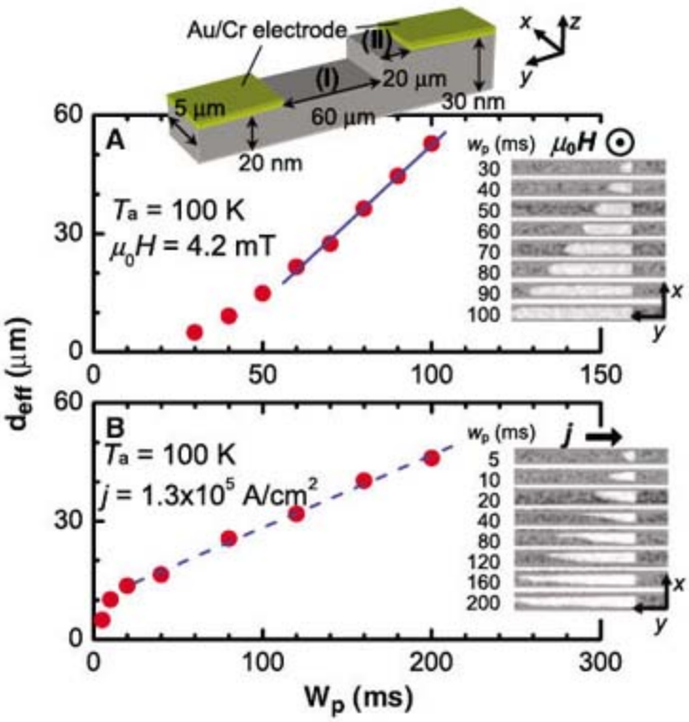

Fig. 1. The topmost inset shows a schematic of the device. A 5-μm-wide (Ga,Mn)As channel with a perpendicular easy axis was patterned into two regions, I (20 nm) and II (30 nm), to pattern the coercivity. Initially, a DW was prepared at the boundary between region I and II. Differential MOKE images (insets) before and after application of magnetic field or current pulses were used to determine the effective DW displacement, d_{eff}, defined as the area divided by channel width. The white regions in the insets are those swept out by the DW. Two main panels show the dependence of d_{eff} on the pulse width, w_p, at ambient temperature T_a = 100 K. **(A)** Magnetic field $\mu_0 H$ = 4.2 mT and **(B)** current density $j = 1.3 \times 10^5$ A/cm^2.

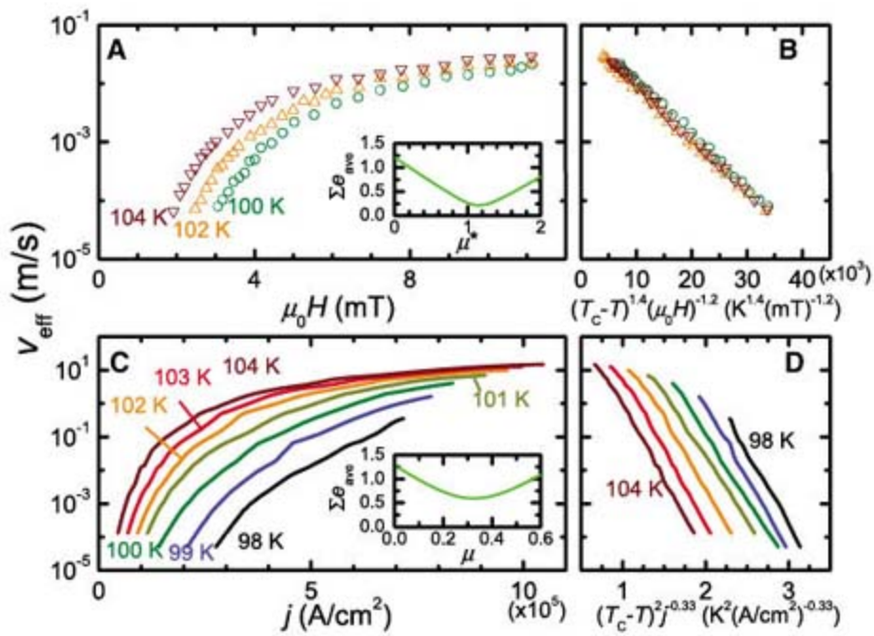

Fig. 2. **(A)** Logarithm of v_{eff} versus $\mu_0 H$ for 100 to 104 K. **(B)** Scaling of v_{eff} in magnetic field–induced case; logarithm of v_{eff} is plotted as a function of $(T_C - T)^{1.4}(\mu_0 H)^{-1.2}$. **(C)** Logarithm of v_{eff} versus j at 98 to 104 K. **(D)** Scaling of v_{eff} in the current-induced case; logarithm of v_{eff} is plotted as a function of $(T_C - T)^2 j^{-0.33}$. The insets in (A) and (C) show the sum of the averaged errors as a function of μ (μ^*) in scaling fits.

[1]Semiconductor Spintronics Project, Exploratory Research for Advanced Technology, Japan Science and Technology Agency, 1-18 Kitamemachi, Aoba-ku, Sendai 980-0023, Japan. [2]Laboratory for Nanoelectronics and Spintronics, Research Institute of Electrical Communication, Tohoku University, 2-1-1 Katahira, Aoba-ku, Sendai 980-8577, Japan. [3]Institute for Materials Research, Tohoku University, 2-1-1 Katahira, Aoba-ku, Sendai 980-8577, Japan. [4]Core Research for Evolutional Science and Technology, Japan Science and Technology Agency, 4-1-8 Honcho, Kawaguchi 332-0012, Japan. [5]Physics Department, University of Miami, Coral Gables, FL 33124, USA.

*To whom correspondence should be addressed: E-mail: ohno@riec.tohoku.ac.jp

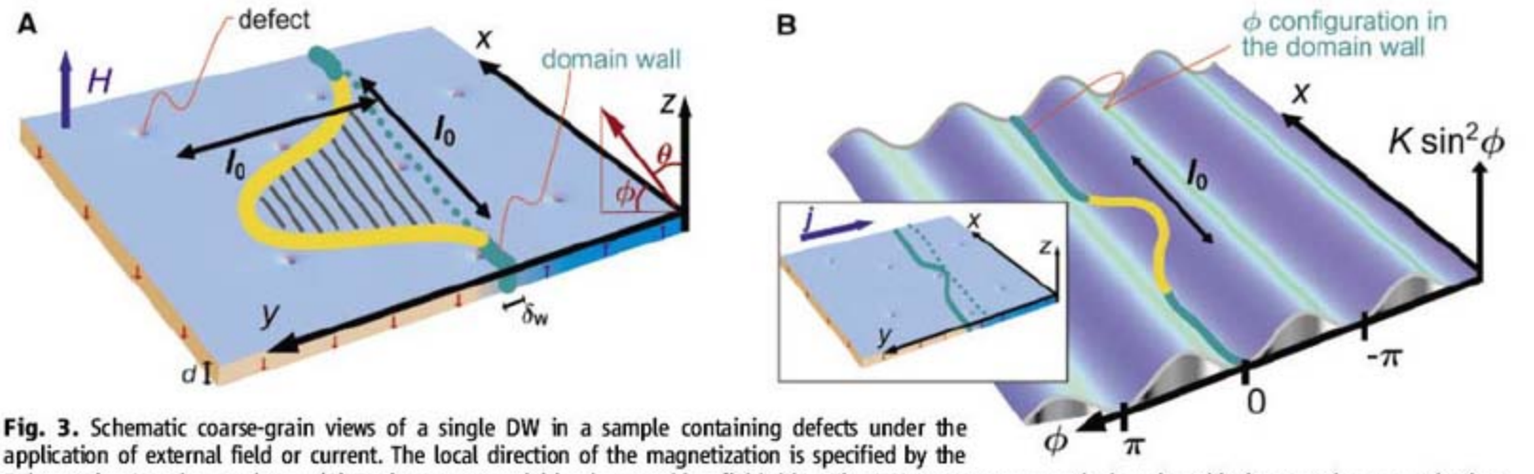

Fig. 3. Schematic coarse-grain views of a single DW in a sample containing defects under the application of external field or current. The local direction of the magnetization is specified by the Euler angles θ and φ, as shown. **(A)** Real-space potential landscape with a field drive. The DW separates magnetic domains with the opposite magnetization, as indicated by solid arrows. Dimples represent localized pinning defects. The dimension l_0, which advances in a thermal activation process, is determined by balancing the elastic energy and Zeeman energy as described in the text. **(B)** The potential landscape with current drive depends upon the internal angle φ. In the presence of a current, only segments that advance the wall φ profile have appreciable thermal weight and, as illustrated in (B), the effective dimension of such a segment, in the coarse-grained φ profile (modulo π), is the l_0 introduced in the text. In real space (inset), the DW advances because a finite $d\phi/dt$ is equivalent to a local magnetic field.

Table 1. Critical exponents from experiment and theory. The experimental values are determined by the least-square method and their error from the standard deviation.

	Field drive		Current drive	
	μ*	σ*	μ	σ
Experiment	1.2 ± 0.1	1.4 ± 0.1	0.33 ± 0.06	2.0 ± 0.2
Theory	1.0	1.5	0.5	1.25

1.2 ± 0.1, $b^* \propto (T_C - T)^{1.4 \pm 0.1}$, indicating that the creep velocities are scaled with different exponents for current-induced and field-induced cases.

To understand the origin of the different exponents, we have studied the creep motion based on a scaling theory. We first treat the field case and next develop the scaling law for the current-driven case in the same framework. As shown in Fig. 3A, we consider a single DW lying in a ferromagnetic wire (thickness d) containing random pinning sites, in a coordinate system with y along the wire (the hard axis) and z normal to the film (the easy axis). Because pinning prevents a uniform DW displacement, when a field H ($< H_C$) is applied along the z axis, only a segment of the DW with dimension l is displaced. Here, random-field disorder (*19*), with a length-scale shorter than the DW width, is assumed. The total free energy related to this displacement is estimated by $F(l) = e_0 l - e_1 l^2$. The first term with $e_0 = 4(A_S K_u)^{1/2} d$ denotes the elastic energy due to the partial wall extension with the spin exchange stiffness, A_S, and the uniaxial anisotropy energy density, K_u. The second term with $e_1 = MHd$ represents the Zeeman energy gain of the shaded region with magnetization, M, in Fig. 3A, relative to the original configuration. As is commonly done in creep problems, we assume that the characteristic energy scale in the random-energy landscape is unique and hence that the barrier height, U_b, scales in the same manner as the total free energy (*19*). Thus, the turning point of $F(l)$ with respect to H determines a characteristic length $l_0 = e_0/2e_1 \propto H^{-1}$. This gives the longest elapsed time in the energy valley separated by U_b and, imposing the Arrhenius law, a DW creep velocity, $v \sim \exp(-U_b/k_B T)$ with $U_b \sim F(l_0)$, where k_B is the Boltzmann constant. This procedure leads to the scaling formula, $\ln(v^*/v_c^*) = a^* - b^*(\mu_0 H)^{-\mu^*}$ with $\mu^* = 1$. Assuming $M \propto (T_C - T)^{\beta}$ and $A_S, K_u \propto M^2$ (*18*), we obtain $a^* \propto (T_C - T)^{2\beta}$ and $b^* \propto (T_C - T)^{3\beta}$.

The current-induced creep formula can be derived with the same steps as in the above treatment. Whereas the DW is uniformly driven by the current, the pinning centers locally modulate φ, the angle of the DW plane relative to the x-z plane, from a straight configuration at the bottom of the hard-axis anisotropy potential $K \sin^2\phi$ (Fig. 3B), where K is due to the stray field. The situation contrasts with that in which the global rotation of φ occurs due to, e.g., an external field. The modulation of φ along the DW lying in the x direction gives rise to a finite exchange torque, $f_A \propto A_S \partial^2\phi/\partial x^2$ (*20*), which is absent in the rigid wall approximation (*21*, *22*). Competition of the f_A with the spin transfer torque, $f_j \propto Pj$, where P is the spin polarization of the current, introduces a characteristic length in the φ landscape. The scaling of the characteristic length is determined by the requirement $f_j \sim f_A$. Replacing $\partial^2/\partial x^2$ by l_0^{-2} within this relation, we obtain $l_0 \propto j^{-1/2}$. U_b is given by the DW volume that passes over the barrier times the anisotropy barrier K (Fig. 3B), i.e., $U_b \sim K l_0 \delta_W d$, where $\delta_W = \pi(A_S/K_u)^{1/2}$ is the width of the DW (*16*). The Arrhenius law dictates that $\ln(v/v_c) = a - bj^{-\mu}$ with $\mu = 1/2$ with $P \propto M$ (*23*) and A_S, $K \propto M^2$; it then follows that $a \propto (T_C - T)^{2\beta}$ and $b \propto (T_C - T)^{5\beta/2}$.

In Table 1, we compare experimental results with the above scaling laws. In the magnetic field–induced case, $\mu^* = 1.0$, adopting the mean field value of $\beta = 0.5$ (experiment shows $\beta = 0.49 \pm 0.03$), we obtain $a^* \propto (T_C - T)^{\rho^*}$ with $\rho^* = 1$ and $b^* \propto (T_C - T)^{\sigma^*}$ with $\sigma^* = 1.5$. The values of μ^* and σ^* are consistent with the experimental results [$\mu^*(\text{exp}) = 1.2$ and $\sigma^*(\text{exp}) = 1.4$]. Thus, the results for magnetic field–induced DW creep are indeed compatible with random-field disorder, rather than random-bond disorder as observed for creep in metallic systems (*19*, *24*–*28*). The random fields most probably arise from the randomly distributed Mn moments, whereas random-bond disorder for metals is expected to originate from the surface roughness (*25*). In the current-induced case [$\mu(\text{exp}) = 0.33$ and $b \propto (T_C - T)^{\sigma}$ with $\sigma(\text{exp}) = 2$], μ and σ agree within a factor of 1.6 with our theoretical expectation ($\mu = 0.5$ and $\sigma = 1.25$). The theory also predicts that $a \propto (T_C - T)^{\rho}$ with $\rho = 1$. The different scaling exponents μ and μ* clearly indicate that the two cases belong to different universality classes. The values for ρ and ρ* cannot be accurately determined from experiment alone because of the uncertainty in v_c^* and v_c. However, the experimental results together with the theoretical values (ρ and $\rho^* = 1$) yield reasonable v_c^* and v_c, in the range of 0.02 to 0.03 m/s, less than the highest experimental creep velocity.

The DW velocities for subthreshold drive values of both the current density j and magnetic field H obey an Arrhenius scaling law but with different exponents. These measurements on (Ga, Mn)As lead us to conclude there is no simple physical relation, and an absence of a linear mathematical proportionality between these two forms of drive. In the context of the theory of creep in random media, we conclude that the two cases

correspond to different universality classes and have developed a theory that explains this difference.

References and Notes

1. L. Berger, *J. Appl. Phys.* **55**, 1954 (1984).
2. M. Yamanouchi, D. Chiba, F. Matsukura, H. Ohno, *Nature* **428**, 539 (2004).
3. A. Yamaguchi *et al.*, *Phys. Rev. Lett.* **92**, 077205 (2004).
4. N. Vernier, D. A. Allwood, D. Atkinson, M. D. Cooke, R. P. Cowburn, *Europhys. Lett.* **65**, 526 (2004).
5. E. Saitoh, H. Miyajima, T. Yamaoka, G. Tatara, *Nature* **432**, 203 (2004).
6. M. Klāui *et al.*, *Phys. Rev. Lett.* **94**, 106601 (2005).
7. M. Hayashi *et al.*, *Phys. Rev. Lett.* **97**, 207205 (2006).
8. S. S. P. Parkin, U.S. Patent 6834005 (2004).
9. G. Tatara, H. Kohno, *Phys. Rev. Lett.* **92**, 086601 (2004).
10. S. Zhang, Z. Li, *Phys. Rev. Lett.* **93**, 127204 (2004).
11. A. Thiaville, Y. Nakatani, J. Miltat, Y. Suzuki, *Europhys. Lett.* **69**, 990 (2005).
12. S. E. Barnes, S. Maekawa, *Phys. Rev. Lett.* **95**, 107204 (2005).
13. J. Xiao, A. Zangwill, M. D. Stiles, *Phys. Rev. B* **73**, 054428 (2006).
14. Y. Tserkovnyak, H. J. Skadsem, A. Brataas, G. E. W. Bauer, *Phys. Rev. B* **74**, 144405 (2006).
15. A. K. Nguyen, H. J. Skadsem, A. Brataas, *Phys. Rev. Lett.* **98**, 146602 (2007).
16. M. Yamanouchi, D. Chiba, F. Matsukura, T. Dietl, H. Ohno, *Phys. Rev. Lett.* **96**, 096601 (2006).
17. H. X. Tang, R. K. Kawakami, D. D. Awschalom, M. L. Roukes, *Phys. Rev. B* **74**, 041310(R) (2006).
18. T. Dietl, J. König, A. H. MacDonald, *Phys. Rev. B* **64**, 241201(R) (2001).
19. P. Chauve, T. Giamarchi, P. Le Doussal, *Phys. Rev. B* **62**, 6241 (2000).
20. A. P. Malozemoff, J. C. Slonczewski, *Magnetic Domain Walls in Bubble Materials* (Academic Press, New York, 1979).
21. G. Tatara, N. Vernier, J. Ferré, *Appl. Phys. Lett.* **86**, 252509 (2005).
22. R. A. Duine, A. S. Núñez, A. H. MacDonald, *Phys. Rev. Lett.* **98**, 056605 (2007).
23. T. Dietl, H. Ohno, F. Matsukura, *Phys. Rev. B* **63**, 195205 (2001).
24. T. Giamarchi, A. B. Kolton, A. Rosso, *Lect. Notes Phys.* **688**, 91 (2006).
25. S. Lemerle *et al.*, *Phys. Rev. Lett.* **80**, 849 (1998).
26. L. Krusin-Elbaum, T. Shibauchi, B. Argyle, L. Gignac, D. Weller, *Nature* **410**, 444 (2001).
27. F. Cayssol, D. Ravelosona, C. Chappert, J. Ferré, J. P. Jamet, *Phys. Rev. Lett.* **92**, 107202 (2004).
28. V. Repain *et al.*, *Europhys. Lett.* **68**, 460 (2004).

29. We thank T. Dietl, D. Chiba, T. Giamarchi, and G. Tatara for useful discussions. This work was partly supported by Grant-in-Aids from the Japan Society for the Promotion of Science and by the 21st Century Centers of Excellence program at Tohoku University.

22 May 2007; accepted 23 August 2007
10.1126/science.1145516

Signatures of Electron Fractionalization in Ultraquantum Bismuth

Kamran Behnia,[1]* Luis Balicas,[2] Yakov Kopelevich[3]

Because of the long Fermi wavelength of itinerant electrons, the quantum limit of elemental bismuth (unlike most metals) can be attained with a moderate magnetic field. The quantized orbits of electrons shrink with increasing magnetic field. Beyond the quantum limit, the circumference of these orbits becomes shorter than the Fermi wavelength. We studied transport coefficients of a single crystal of bismuth up to 33 tesla, which is deep in this ultraquantum limit. The Nernst coefficient presents three unexpected maxima that are concomitant with quasi-plateaus in the Hall coefficient. The results suggest that this bulk element may host an exotic quantum fluid reminiscent of the one associated with the fractional quantum Hall effect and raise the issue of electron fractionalization in a three-dimensional metal.

Electronic properties of bismuth have been extensively studied during the 20th century. As early as 1928, Kapitza discovered that bismuth's resistivity increases by several orders of magnitude in the presence of a large magnetic field and that it shows no sign of saturation (*1*). Two years later, studies of bismuth led to the discovery of quantum oscillations in both magnetization (*2*) and resistivity (*3*). Bismuth was the first metal whose Fermi surface was experimentally identified (*4*). Commenting on the exceptional role played by bismuth in the history of metal physics (*5*, *6*), Falkovskii wrote in 1968, "It is easiest to observe in bismuth the phenomena that are inherent in all metals" (*7*).

An extremely small Fermi surface and a very long mean-free path distinguish bismuth from other metals. The Fermi surface occupies 10^{-5} of the Brillouin zone (*5*), an order of magnitude lower than graphite, the closest rival and another celebrated semi-metal. The mean-free path at room temperature exceeds 2 μm (*8*), which is almost two orders of magnitude longer than in copper. Because of the low carrier density, the quantum limit in bismuth can be reached by the application of a magnetic field as small as 9 T along the trigonal axis. In this limit, electrons are all pushed to the lowest Landau level, and the magnetic length (the radius of the lowest-energy quantized isolated electron orbit in a magnetic field) becomes shorter than the Fermi wavelength. As recently noted (*9*), the quasi-linear magnetoresistance of bismuth (*1*) in this limit does not fit into the quasi-classical theory of electronic transport. The last experimental investigation of high-field magnetoresistance in bismuth, in the 1980s, found no evidence of saturation up to 45 T (*10*). Notably, this was contemporaneous with the discovery of fractional quantum Hall effect (FQHE) (*11*). Soon, the many-particle quantum theory succeeded in providing an elegant solution to this unexpected experimental finding (*12*). Today, the FQHE ground state is an established case of a quantum fluid whose elementary excitations are fractionally charged. Such a fluid emerges in high-mobility two-dimensional (2D) electron systems formed in semiconductor heterostructures in the presence of a magnetic field exceeding the quantum limit. In contrast with the integer quantum Hall effect (IQHE), which can be explained in a one-particle picture, the occurrence of FQHE implies strong interaction among electrons and their condensation to a many-body quantum state (*13*).

Recently, we reported on the giant quantum oscillations of the Nernst coefficient in bismuth in the vicinity of the quantum limit (*14*). The Nernst signal (the transverse voltage produced by a longitudinal thermal gradient) was found to peak markedly whenever a Landau level meets the Fermi level. Otherwise, it is severely damped. This observation was in qualitative agreement with a theoretical prediction (*15*) invoking a "quantum Nernst effect" associated with the IQHE. Here, we present measurements resolving distinct peaks in the Nernst signal deep in the ultra-quantum limit. Measurements of the Hall coefficient in the same field range reveal a series of quasi-plateaus extending over a window marked by fields at which the Nernst peaks occur. These findings raise the issue of the relevance of the FQHE physics in a clean 3D compensated semi-metal. They suggest that electron correlations in bismuth are stronger than what has been commonly assumed and that this elemental metal may host an exotic quantum fluid.

The lower panel of Fig. 1 contains our primary experimental observation: the detection of three peaks occurring at 13.3, 22.3, and 30.8 T in the Nernst response (*16*). These three peaks follow the rich structure found in the field dependence of the Nernst signal in the previous study limited to 12 T (*14*) and emerge well beyond the quantum limit.

The quantum limit in bismuth is set by the well-known topology of the Fermi surface in this compensated semi-metal (*5*, *17*): An ellipsoid associated with hole-like carriers around the T-point of the Brillouin zone and elongated along the trigonal axis and three cigar-like slightly tilted electron ellipsoids along the L points. The cross-section of the hole ellipsoid perpendicular to the trigonal axis is $A^h = 0.0608\ \mathrm{nm}^{-2}$. For each of the three electron ellipsoids, the corresponding area is $A^e = 0.0836\ \mathrm{nm}^{-2}$ (*17*) (Fig. 1A). These numbers set the quantum limit, which is attained by a magnetic field equal to $B_{QL} = (A/2\pi)(\hbar/e)$, where $\hbar$ is the reduced Planck constant and e is the charge of electron, which is 6.4 T for holes and 8.6 T for

[1]Laboratoire Photons Et Matière (CNRS-UPRS), ESPCI, 10 rue Vauquelin, 75231 Paris, France. [2]National High Magnetic Field Laboratory, Florida State University, Tallahassee, FL 32306, USA. [3]Instituto de Fisica "Gleb Wataghin," Universidade Estradual de Campinas, 13083-970 Campinas, São Paulo, Brazil.

*To whom correspondence should be addressed. E-mail: kamran.behnia@espci.fr

electrons. When $B = B_{QL}$, the condition $\lambda_F^{\perp} = 2\pi l_B$ is realized: The circumference of the quantized electronic orbit becomes equal to the Fermi wavelength. Here, $\lambda_F^{\perp}$ is the Fermi wavelength of the electrons traveling perpendicular to the field, and $l_B = \sqrt{\frac{\hbar}{eB}}$ is the magnetic length. In a 2D system, this corresponds to a Landau-level filling factor of unity. In a 3D system, there is an infinite degeneracy along the z axis. Nevertheless, analogous to the 2D case and in the absence of an established terminology, we use the expression "filling factor" for the ratio $\nu = (2\pi l_B/\lambda_F^{\perp})^2$.

The Fermi surface cross-sections correspond to the low-field response of the system, however. Strong magnetic field is known to modify the two Fermi surfaces in order to maintain charge neutrality (*18*, *19*). This feature together with Zeeman splitting leads to a slight enhancement of the quantum limit. It occurs at 8.9 T, and is marked by the most notable peak in the Nernst signal (S_{xy}). All previous studies (*10*, *18*–*20*) converge in detecting a dip in resistivity at 8.85 ± 0.25 T (±SD) and identifying it as the one corresponding to the first Landau level [supporting online material (SOM) text].

Bismuth is host to surface states quite distinct from the bulk semi-metal and with a much higher carrier density (*21*). It is very unlikely that their existence is relevant to our observations. The metallic state resolved by photoemission on the 111 surface (normal to the trigonal) has a Fermi surface whose radius is on the order of 0.5 to 3 nm^{-1} (*22*) and the expected quantum oscillations would have a frequency range of 100 to 1000 T.

Therefore, we conclude that the three peaks we observed emerge in the ultraquantum limit. Given the distance between the four distinct orbits in the reciprocal space, magnetic breakdown is an unlikely explanation. Moreover, the peaks resolved here do not display a B^{-1} periodicity. Figure 2 presents the high-field data as a function of B^{-1}. The peaks are situated at rational fractions (2/3, 2/5, and 2/7) of the first integer peak. The low-field data are presented in Fig. 2B. As seen in Fig. 2C, their B^{-1} positions are close to those of the dips resolved in resistivity (at temperature $T = 25$ mK and for $B < 18$ T) (*19*). In addition to these peaks [already identified in the previous report (*14*)], there are two unidentified peaks between $\nu = 1$ and $\nu = 2$ anomalies and one between the $\nu = 2$ and $\nu = 3$. Assuming that λ_F is constant between two successive integer peaks, these peaks occur close to $\nu = 4/3$, $\nu = 5/3$, and $\nu = 5/2$. Figure 2C summarizes the position of all Nernst peaks (both integer and fractional) and resistivity dips. The upward curvature was previously reported and attributed to the field-induced modification of the carrier density (*19*). This feature would imply a field-induced change in λ_F. Therefore, the values of ν for fractional peaks, which are extracted by linearly extrapolating the position of adjacent in-

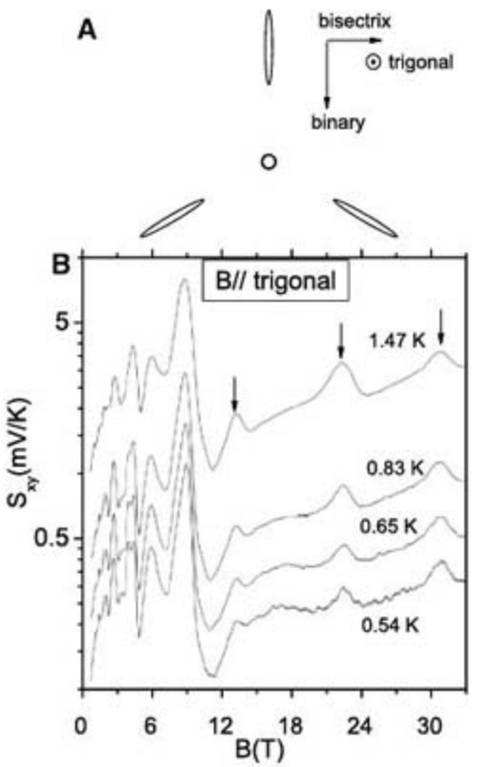

Fig. 1. (**A**) Cross section of the hole-like (center) and electron-like ellipsoid Fermi surfaces for a field applied along the trigonal axes. (**B**) The field dependence of the Nernst signal at different temperatures. The three peaks resolved in the ultraquantum limit are indicated by arrows.

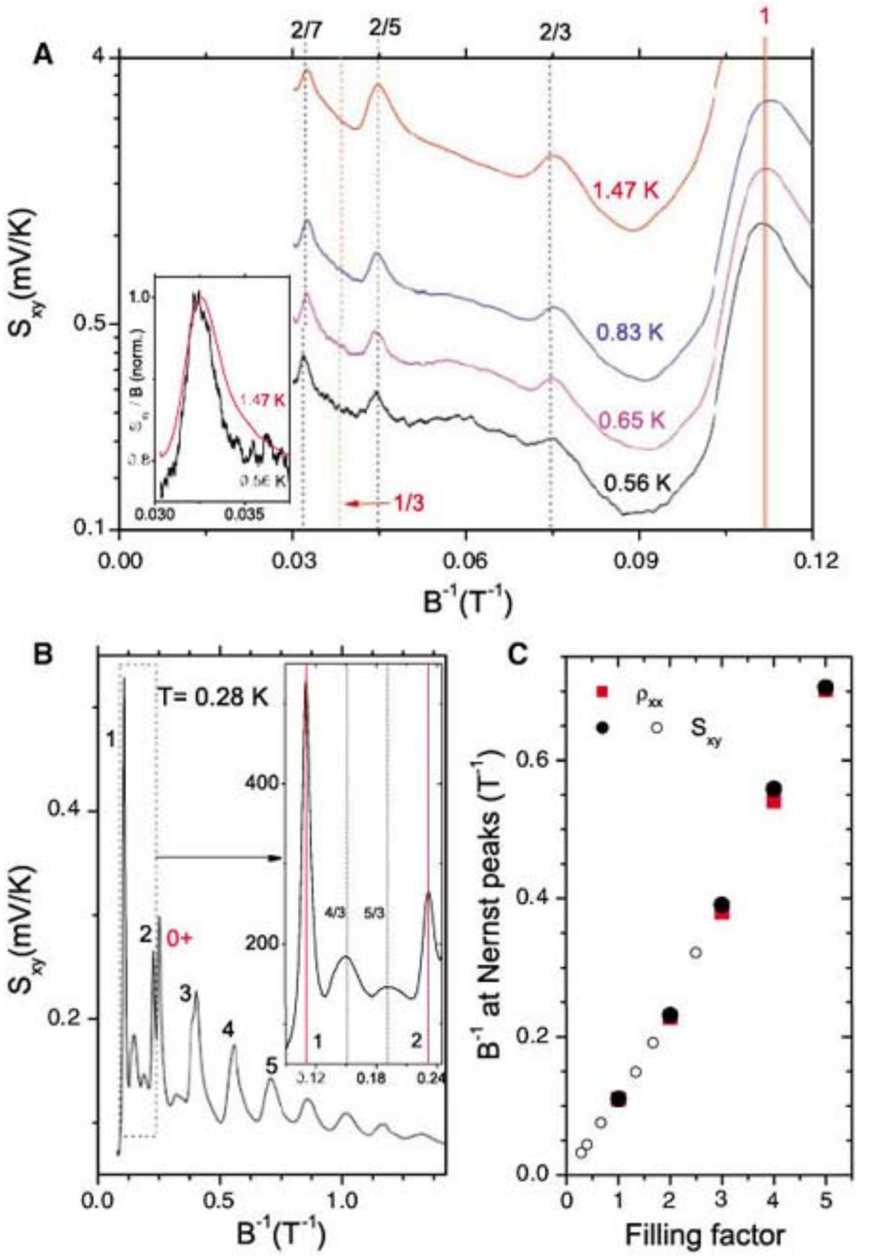

Fig. 2. (**A**) The high-field Nernst plotted as a function of B^{-1}. Dotted lines represent $B^{-1}_{p/q} = (p/q) \times 0.1118\ T^{-1}$. Note the position of the three peaks respective to these lines. The inset shows the thermal broadening of the peak at highest field. (**B**) Quantum oscillations observed in the low-field data (*14*). Identified peaks correspond to integer filling factors of the hole pocket. As seen in the inset, the B^{-1} positions of two previously unidentified peaks are very close to 4/3 and 5/3 filling factor. (**C**) The B^{-1} position of the Nernst (*14*) and resistivity (*19*) anomalies versus the filling factor associated with them. Open and closed circles represent integer and functional filling factors, respectively.

teger peaks are subject to caution. However, as there is no visible phase transition and the change in λ_F is continuous, the extracted values of ν are not expected to differ much from the effective ones.

We also performed low-resolution measurements of resistivity and the Hall coefficient on our sample at 0.44 K. In agreement with the previous high-field study (*10*), resistivity does not show any strong feature beyond the quantum limit (fig. S1). The Hall response, ρ_{xy} (Fig. 3) is strongly nonlinear for fields exceeding 3 T. Above this field, a rich structure including a sharp peak at 9.8 T is resolved. At still higher fields—i.e., in the ultraquantum limit—a succession of fast and slow regimes in the field-dependence of ρ_{xy} is visible. Comparing the relative position of these quasi-plateaus and the Nernst peaks clearly shows that each Nernst peak occurs between two successive Hall plateaus in agreement with the theoretical prediction invoking IQHE (*15*).

Below 3 T, the slope of ρ_{xy} yields the Hall number $R_H = 1.5 \times 10^{-5}$ m^3/C corresponding to a carrier density of 3.9×10^{17} cm^{-3}, only 30% larger than the hole carrier density. In the high-field regime, ρ_{xy} is 0.129 ohm-cm at $\nu = 1/2$ and 0.158 ohm-cm at $\nu = 1/3$. Therefore, when the filling factor passes from 1/2 to 1/3, ρ_{xy} jumps by 0.029 ohm-cm. Let us recall that, in a 2D electron gas in the FQHE, the magnitude of ρ^{2D}_{xy} at filling factor ν would be $h/(\nu e^2)$ and the passage from the $\nu = 1/2$ to $\nu = 1/3$ plateau would lead to a jump of $h/e^2 = 25.8$ kilo-ohms in ρ^{2D}_{xy}. Because in our 3D system, the jump in ρ_{xy} is 11.2 nm times h/e^2, it is tempting to consider the bulk crystal as an assembly of coherent 2D sheets each 11.2 nm thick. This length scale is very close to $\lambda_F^{\parallel} = 14$ nm, the Fermi wavelength of holes along the trigonal axis and the magnetic field and much longer than the atomic distance between layers (~0.2 nm).

These observations raise the issue of relevance of FQHE physics to bulk bismuth. The former is found in the context of high mobility, 2D and interacting electronic systems. To what extent do electrons in bismuth qualify for these attributes? The electronic mobility is undoubtedly large enough. In our crystal, it exceeds—by two orders of magnitude—the mobility of the GaAs/AlGaAs sample in which the FQHE was discovered in 1982 (*11*) (SOM text). It is true that bismuth is not commonly considered as a strongly interacting electron system. However, the very low level of carrier density undermines screening and favors Coulomb repulsion. Given that electrons in bismuth and in GaAs are comparable in their concentration and in their effective mass, it is reasonable to assume that Coulomb interaction is sufficiently strong to allow electron fractionalization.

The most serious obstacle for the realization of FQHE physics in bulk bismuth is dimensionality. IQHE (also a purely 2D effect) has already been observed in an anisotropic 3D electron gas (*23*) as well as a number of bulk systems (SOM text), and 3D FQHE has been a topic of theoretical investigation (*24*). Bismuth, with its weak anisotropy, was recently proposed as a candidate to exhibit the quantum spin Hall effect (*25*). However, according to our preliminary studies, in the vicinity of the quantum limit, the in-plane conductivity in bismuth is orders of magnitude lower than the perpendicular conductivity along the field axis. Instead of being an assembly of weakly coupled 2D sheets perpendicular to the field, the system is closer to a set of 1D wires oriented along the field (*26*). To the best of our knowledge, there is no appropriate theoretical frame for in-plane transport in such a context. Thus, bismuth in the ultraquantum limit emerges as an experimental playground for two distinct routes toward the electron fractionalization, the FQHE and the field-induced Luttinger liquid (*26*).

Several other questions remain. What happens to the electron-like carriers? For this field orientation, the three electron ellipsoids have been invisible in all studies of quantum oscillations. The complex structure of $\rho_{xy}(B)$ for $B <$ 14 T suggests competing responses of electrons and holes. However, in the ultraquantum limit, there is no definite signature of their presence in spite of the larger total area occupied by the three electron ellipsoids. This may be a consequence of their lower mobility. The absence of strong features in the raw $\rho_{xx}(B)$ data are also noteworthy. In 2D systems, the quantum Hall plateaus are associated with absence of dissipation and vanishing longitudinal conductivity. In bulk systems showing IQHE, plateaus in ρ_{xy} are concomitant with minima in ρ_{xx}. Extensive high-resolution studies of resistivity at lower temperatures on cleaner samples may help to identify the source of resistive dissipation at high fields. The 80-year-old mystery of magnetoresistance in bismuth (*1*, *9*) needs fresh experimental and theoretical attention.

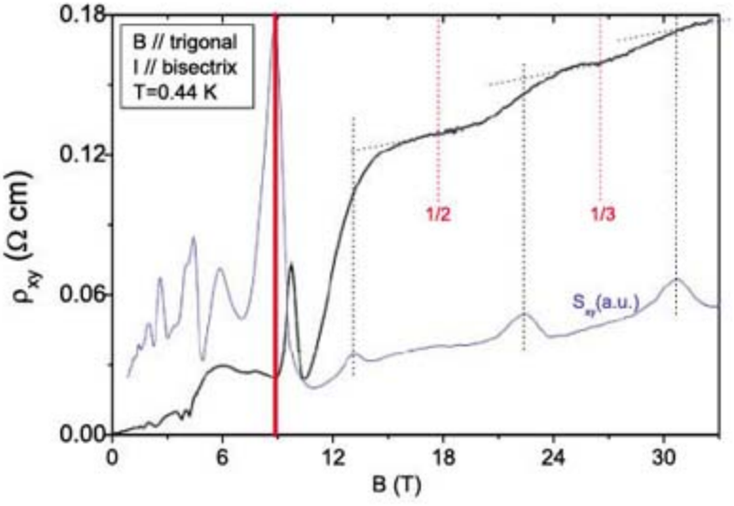

Fig. 3. The field dependence of the Hall resistivity. A complicated behavior in the intermediate field range precedes quasi-plateaus in the ultraquantum limit. The Nernst response at 0.83 K is also shown. The quantum limit is marked by a thick red line. Two red dotted lines mark the value of the filling factor. All other lines are guides to the eye. a.u., arbitrary units.

References and Notes

1. P. L. Kapitza, *Proc. R. Soc. London Ser. A* **119**, 358 (1928).
2. W. Y. de Haas, P. M. van Alphen, *Proc. Acad. Sci. Amsterdam* **33**, 1106 (1930).
3. L. Shubnikov, W. Y. de Haas, *Comm. Phys. Lab. Univ. Leiden* 207a, 207c, 207d, 210a (1930).
4. D. Shoenberg, *Proc. R. Soc. London Ser. A* **170**, 341 (1939).
5. V. S. Édelman, *Adv. Phys.* **25**, 555 (1976).
6. J.-P. Issi, *Aust. J. Phys.* **32**, 585 (1979).
7. L. A. Falkovskiĭ, *Sov. Phys. Usp.* **11**, 1 (1968).
8. A. B. Pippard, R. G. Chambers, *Proc. Phys. Soc. A* **65**, 955 (1952).
9. A. A. Abrikosov, *J. Phys. A* **36**, 9119 (2003).
10. K. Hiruma, N. Miura, *J. Phys. Soc. Jpn.* **52**, 2118 (1983).
11. D. C. Tsui, H. L. Stormer, A. C. Gossard, *Phys. Rev. Lett.* **48**, 1559 (1982).
12. R. B. Laughlin, *Phys. Rev. Lett.* **50**, 1395 (1983).
13. D. Yoshioka, *The Quantum Hall Effect* (Springer, Berlin, 2002).
14. K. Behnia, M.-A. Méasson, Y. Kopelevich, *Phys. Rev. Lett.* **98**, 166602 (2007).
15. H. Nakamura, N. Hatano, R. Shirasaki, *Solid State Comm.* **135**, 510 (2005).
16. Materials and methods, including details on measurement technique and sample characterization, are available as supporting material on *Science* Online.
17. D. Shoenberg, *Magnetic Oscillations in Metals* (Cambridge Univ. Press, Cambridge, 1984), pp. 228–234.
18. G. E. Smith, G. A. Baraff, J. M. Rowell, *Phys. Rev.* **135**, A1118 (1964).
19. S. G. Bompadre, C. Biagini, D. Maslov, A. F. Hebard, *Phys. Rev. B* **64**, 073103 (2001).
20. F. Y. Yang *et al.*, *Phys. Rev. B* **61**, 6631 (2000).
21. Ph. Hofmann, J. E. Gayone, G. Bihlmayer, Yu. M. Koroteev, E. V. Chulkov, *Phys. Rev. B* **71**, 195413 (2005).
22. M. Hengsberger, P. Segovia, M. Garnier, D. Purdie, Y. Baer, *Eur. Phys. J. B* **17**, 603 (2000).
23. H. L. Stormer, J. P. Eisenstein, A. C. Gossard, W. Wiegmann, K. Baldwin, *Phys. Rev. Lett.* **56**, 85 (1986).
24. L. Balents, M. P. A. Fisher, *Phys. Rev. Lett.* **76**, 2782 (1996).
25. S. Murakami, *Phys. Rev. Lett.* **97**, 236805 (2006).
26. C. D. L. Biagini, M. Maslov, Yu Reizer, L. I. Glazman, *Europhys. Lett.* **55**, 383 (2001).

27. We thank G. Boebinger, P. M. Chaikin, T. Giamarchi, and A. MacDonald for useful discussions and E. Palm and T. Murphy for their assistance. K.B. is supported by Agence Nationale de la Recherche (contract no. ANR-05-BLAN-0055-02) and by Délégation Générale pour l'Armement (subvention no. 06.60.031.00.470.75.01) and acknowledges a visiting scientist fellowship by National High Magnetic Field Laboratory (NHFML). L.B. is supported by the NHMFL in-house research program. Y.K. is supported by Conselho Nacional de Desenvolvimento Científico e Tecnológico (CNPq) and by Fundação de Amparo à Pesquisa do Estado de São Paulo (FAPESP). Research at the NHMFL is supported by NSF Cooperative Agreement no. DMR-0084173, by the State of Florida, and by the Department of Energy.

Supporting Online Material

www.sciencemag.org/cgi/content/full/1146509/DC1
Materials and Methods
SOM Text
Fig. S1
Table S1
References

14 June 2007; accepted 6 August 2007
Published online 16 August 2007;
10.1126/science.1146509
Include this information when citing this paper.

Free-Solution, Label-Free Molecular Interactions Studied by Back-Scattering Interferometry

Darryl J. Bornhop,[1]* Joey C. Latham,[2] Amanda Kussrow,[1] Dmitry A. Markov,[3] Richard D. Jones,[1] Henrik S. Sørensen[4]

Free-solution, label-free molecular interactions were investigated with back-scattering interferometry in a simple optical train composed of a helium-neon laser, a microfluidic channel, and a position sensor. Molecular binding interactions between proteins, ions and protein, and small molecules and protein, were determined with high dynamic range dissociation constants (K_d spanning six decades) and unmatched sensitivity (picomolar K_d's and detection limits of 10,000s of molecules). With this technique, equilibrium dissociation constants were quantified for protein A and immunoglobulin G, interleukin-2 with its monoclonal antibody, and calmodulin with calcium ion Ca^{2+}, a small molecule inhibitor, the protein calcineurin, and the M13 peptide. The high sensitivity of back-scattering interferometry and small volumes of microfluidics allowed the entire calmodulin assay to be performed with 200 picomoles of solute.

Measurement of the rate and affinity of biomolecular interactions, such as protein-protein binding or binding of small molecules, not only provides insight into basic cellular function but also can facilitate the development of therapeutics and serve as the basis for many diagnostic techniques. For measurements at very low concentrations, detection of molecules often requires labeling (such as fluorescent tags), but label-free studies can be performed in two main ways. Calorimetric methods, such as isothermal titration calorimetry (ITC) (*1*–*3*), are performed with all components in solution and have found relatively widespread acceptance. However, these methods have very low throughput, require large sample volumes (milliliters), and have low sensitivity (Table 1) (in the worst case, there is no sensitivity if the reaction enthalpy is near zero). The enthalpic array (*4*) has been used as a high-throughput embodiment of the microcalorimeter and can be used to perform homogeneous, label-free molecular interaction measurements with just 500 nl of sample. Yet the method suffers from poor concentration detection limits (~5×10^{-5} M) (Table 1) restricting the range of measurable binding affinities.

A larger group of related methods relies on immobilizing one of the binding partners to a surface. Several methods, including diffraction, interferometry, wave guiding and plasmon sensing, nanowire sensing (*5*), and microcantilever sensing (*6*), can then be used to detect changes in the surface layer. Although these surface methods are much more sensitive than calorimetry (for typical proteins of interest, detection limits for dissociation constant measurements are 1 to 100 pM versus 1 to 10 nM), surface immobilization of binding partners can raise several issues. The molecule's binding site may be near the surface (*7*) and may induce steric hindrances that could influence the binding energetics and/or kinetics. Surface preparation can be laborious, time-consuming, expensive to implement, and incompatible with some materials, and the surface layers often exhibit decreased activity over time (*8*). Finally, it is not possible to study unknown binding partners or binding partners that are not isolated in quantities sufficient for modification so that they can be bound to surfaces.

We now show that back-scattering interferometry (BSI), which we have previously used with surface immobilization methods (*9*, *10*), can now be used to measure a wide dynamic range (K_d spanning six decades) of molecular interactions in free solution. It provides high sensitivity (picomolar K_d and detection limits of tens of thousands of molecules), either through kinetic or end-point analysis of concentration-dependent binding data. Compatibility with microfluidics gives BSI the added advantage that either assay format can be done on small sample quantities, allowing the study of molecules that require labor-intensive synthesis or are prepared by tedious mutation or isolation methods.

Interferometry is one of the most sensitive optical interrogation methods known and has been used to screen molecular interactions in surface-binding modes. Examples include on-chip embodiments of a Mach-Zehnder (*11*–*14*) and Young Interferometer (*15*), dual polarization interferometer (*16*), porous Si (*17*) and nanoporous Al (*18*) sensors, diffraction optics technology (*19*), and the biological compact disk (BioCD) (*20*, *21*), as well as BSI (*9*, *10*, *22*). The Mach-Zehnder and Young dual polarization interferometers use wave guiding to monitor binding with surface interaction sensing, which requires relatively long sections of the channel to be coated with the target and large sample volumes to be introduced to facilitate micromolar to nanomolar detection limits. The BioCD is based on a disk that has a mirrored surface upon which periodic patterns of proteins can be bound, providing a periodic reflectance pattern that is phase modulated, changing in proportion to the surface bound mass. Porous Si and Al sensors depend on spectral fringe shifts and are limited to monitoring interactions near the surface where the target is attached. We recently demonstrated that BSI, implemented with a fast Fourier transform (FFT) fringe pattern interrogation approach, could be performed in poly(dimethylsiloxane) (PDMS) chips with rectangular channels. This system enabled substrate-immobilized, reversible, label-free molecular interactions on-chip (*9*, *10*). A three base pair mismatch was quantified, and the interaction between protein A and immunoglobulin G (IgG) was monitored at the attomole level (*10*). BSI (Fig. 1) has been effectively performed with cylindrical objects such as fused silica capillaries (*22*), semicircular shaped channels formed from isotropic etching of fused silica (*23*, *24*), and recently with rectangular channels (*9*, *10*). The latter shape was inspired by the simplicity of microfluidic chip production using PDMS (*25*).

Although it is well established that changes in refractive index (RI) at surfaces can be used to study molecular interactions (*9*, *10*, *26*, *27*), some studies (e.g., *28*) suggest that molecular interactions can be quantified in free solution by using an intrinsic signal other than temperature, as in ITC. Sota *et.al.* (*28*) used molar ellipticity of the sample molecule in combination with surface plasmon resonance (SPR), also an RI detector, to show a relation between surface and bulk signals. The underlying implication of their observations may be that an RI detector could be used to measure binding events in free solution. They show that SPR is sensitive to protein conformational changes and waters of hydration, but they also described their results as "counterintuitive." Other studies

Table 1. A comparison of free-solution, label-free molecular interaction techniques.

Technique	Compatibility with μ-fluidics	Minimum sample volume	Detection limits
Microcal ITC (*3*)	No	1.3 mL	1.0×10^{-6} M (1.3 nmol)
Enthalpy arrays (*4*)	No	500 nL	5.0×10^{-5} M (25 pmol)
BSI	Yes	350 pL	8.57×10^{-11} M (30 zmol)

[1]Department of Chemistry, Vanderbilt Institute of Chemical Biology, Vanderbilt University, VU Station B 351822, Nashville, TN 37235–1822, USA. [2]Department of Biochemistry, Vanderbilt University School of Medicine, 465 21st Avenue South, Suite 9160 MRBIII, Nashville, TN 37232, USA. [3]Department of Biomedical Engineering and Vanderbilt Institute for Integrative Biosystems Research and Education (VIIBRE), Vanderbilt University, 5824 Stevenson Center, Nashville, TN 37235, USA. [4]Optics and Plasma Research Department, Risø National Laboratory, Technical University of Denmark, Building 128, Frederiksborgvej 399–DK-4000-Roskilde, Denmark.

*To whom correspondence should be addressed. E-mail: darryl.bornhop@vanderbilt.edu

have shown that it is possible to measure the intrinsic properties of a solute, such as the molecular dipole or polarizability. Elkashef (*29*) used a dual-wavelength interferometer to measure structural properties of laser dye solvents (*29*) and Maroulis *et al.* (*30*) used RI measurements to study dipole, dipole-quadrupole, and dipole-octopole polarizability of adamantane (*30*). Given these findings, we suspected that structural modifications, as in ion-induced protein folding, protein-protein interactions, and small molecule-protein binding events, must be measurable using RI techniques. We now show that BSI can be implemented in free-solution and can detect a 25 pM binding event using a simple optical train based on a PDMS microfluidic chip.

Modeling of the physical mechanism behind the BSI optical phenomenon (*23*, *31*–*33*) indicates that a multipass configuration leads to a long effective path-length and high sensitivity. Impinging coherent parallel rays from a fiber-coupled He-Ne laser beam onto a micrometer-dimensioned rectangular channel in the PDMS chip produces a fan of scattered light. It contains a set of very high contrast interference fringes (Fig. 1A) and results from this beam-channel-fluid interaction. As the composition or RI of the medium contained within the channel changes, these fringes shift spatially (Fig. 1C). The transducer design (*10*) uses a high-resolution linear charge-coupled device and an FFT, which gives a readout in near-real time of the phase for a particular fringe frequency. Spatial phase detection methods allow us to measure RI change to greater than one part per million in picoliter volumes of solution.

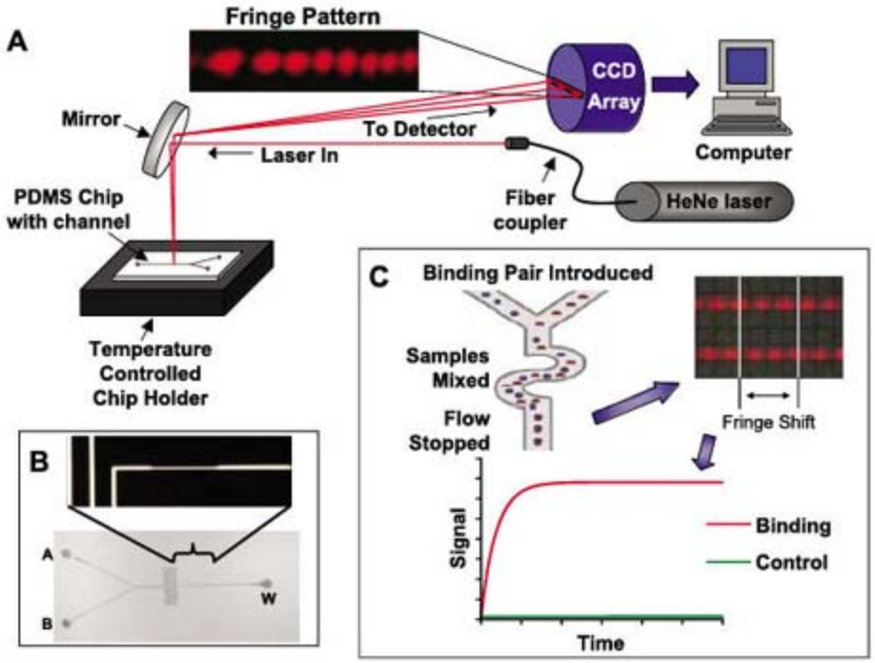

Fig. 1. (**A**) Experimental setup for BSI. (**B**) Microfluidic chip with serpentine mixer and restriction. (**C**) Photograph of representative fringe patterns showing a RI-induced position shift of the fringes, a representation of a binding event, and observed signal for a control and reactive pair binding event.

The chip contains a serpentine and a squeeze for rapid mixing (Fig. 1B). We adopted a modified "stop-flow" methodology (*34*), configured with two sample reservoirs, both connected to equal-length channels that converge into a single channel with a serpentine mixer made from a series of connected C shapes followed by a restriction (Fig. 1B). This simple microfluidic network, which allows for sample introduction and rapid mixing of the two interacting species, was fabricated using standard photolithography and replica molding techniques (*25*, *35*, *36*). It has a 50 μm by 70 μm rectangular channel that, when interrogated by the 100 μm diameter He-Ne laser beam, yields an optical probe volume of ~350 pL. Stop-flow determinations (*37*) and a simple kinetic model allow us to estimate dissociation constants K_d for an array of binding pairs, which are comparable to end-point determinations. A conservative estimate of the quantifiable signal over background for the antibody-antigen interaction studied here [interleukin-2 (IL-2) with its antibody, and applying a 0.3 s electronic filter for data smoothing] demonstrates that there are just 21 zeptomoles of IL-2 or 12,600 molecules and 0.6 attomoles of the antibody within the probe volume. Our calmodulin (CaM) results show that a species with nanomolar affinity can be assayed with just nanograms (picomoles) to micrograms (nanomoles) of protein or small molecule, which represents the use of one-thousandth the number of species required by ITC.

Because BSI is a highly sensitive RI detector, it is possible that the source of our observed signal was a temperature-induced RI change. However, the signals we measured changed during the course of reaction and then leveled off and remained constant after equilibrium had been reached. Thus, the signals must arise through a permanent change in the RI, because the heat sink would have quickly removed the reaction-generated heat from the chip and fluid and then returned the signal to the original value. A calculation presented in the supporting information (*38*) illustrates that even under the best-case scenario (i.e., the highest concentration of binding pairs), the temperature change resulting from the reaction in aqueous media would not produce a detectable signal in BSI. Even if the reaction produced a temperature change 10 times as high (resulting in a $\Delta RI = 10^{-8}$), our current detection limit of about $\Delta RI = 10^{-6}$ would not facilitate registration of the event.

Having ruled out thermal RI changes as a signal source, we still must account for the source of the binding signal in BSI. We note that binding

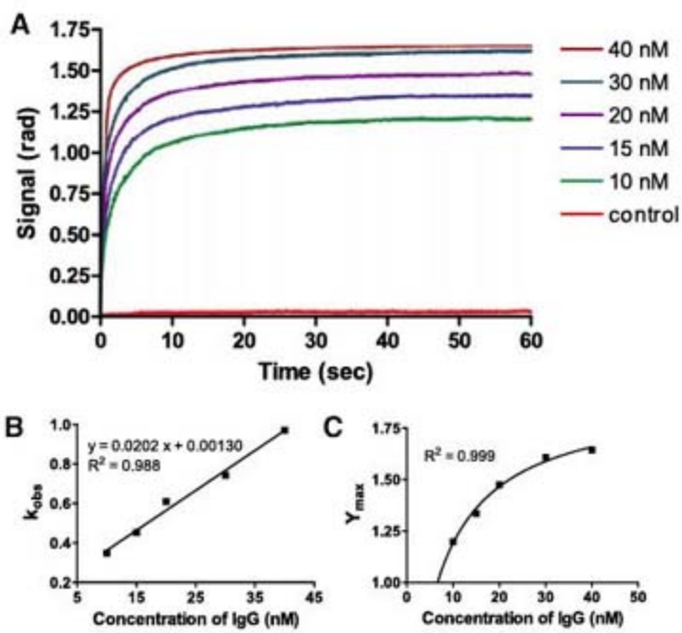

Fig. 2. (**A**) Real-time association plots are shown for P_A binding IgG at various nanomolar concentrations. In the stop-flow interaction experiments, a fixed concentration of 2.5 nM P_A was used, and sequential experiments with increasingly larger concentrations of the F_C region from IgG (i.e., from 10 to 40 nM) were performed. P_A was buffered at a pH = 7.2 with 15 mM Na_2HPO_4, 50 mM NaCl, 0.1 mM EGTA, and 0.02% sodium azide. All IgG solutions were made using the same buffer as P_A. The temperature of the solutions and microfluidic chip were held constant at 25°C ± 0.01°C throughout the experiment. (**B**) Extracted rates are plotted versus IgG concentration. (**C**) End-point values are plotted as a function of IgG concentration and analyzed by Prism software.

creates a new entity in solution that may have a very different refractive index (RI) or molecular dipole from that of either of the reacting analytes. We are not measuring the combined RI or sample mixing (fig. S7) (*38*) because there is virtually no measurable "binding event" signal produced by the controls. The effect of waters of hydration on the intrinsic dipole of a forming complex or folding protein are underestimated and could be a major contributing factor in BSI. For example, during Ca^{2+}-induced folding of CaM, many water molecules (>35/CaM molecule) are ejected from the compound (*39*). Such an event most certainly produces substantial electrostatic effects leading to a highly modified molecular dipole relative to that of the unfolded compound.

We now describe our results for several typical binding experiments. Protein A (P_A) binds the F_C region of several IgG species, including human and rabbit, with high affinity (K_d values from 5 to 34.5 nM) (*40*, *41*). The association reaction was monitored in real time during an interval of ~60 s. As expected, the "shape" of the binding curves changed and more rapidly reached the equilibrium point at higher concentrations of the antibody (IgG) at fixed concentration of the substrate (receptor).

The apparent binding affinity can be extracted from the data using a simple model that assumes first-order kinetics or single-mode binding (*38*) and plotting the observed rate (k_{obs}) versus the concentration of IgG (Fig. 2B). Least-squares analysis of the line generated by this method from the kinetics obtained from BSI yields a K_d for P_A-IgG of 7.92 nM (±1.71). Alternatively, a plot of the end-point values of phase for the reaction between P_A and IgG as a function of the concentration of IgG can be used as a second method to evaluate binding affinity of the complex. This plot (Fig. 2C) exhibits the expected hyperbolic shape often seen in enzyme kinetic studies and described by the law of mass action. Analysis of the end point yields a K_d value of 6.05 nM (±0.52), which correlates well with the results obtained from the kinetic analysis and with reported values (*41*). The quasi leveling-off observed at higher concentrations of the ligand in the end-point assay is attributed to a bulk RI signal, which becomes increasingly significant at higher concentrations of the ligand, IgG. Although this background signal is always present in the BSI experiment, we have studied its magnitude and have determined that the contribution is small compared with that of the binding event (3 to 5%, depending on the concentration and RI of the reacting species).

The control shown in Fig. 2A illustrates the result for mixing the 2.5-nM solution of P_A with a 40-nM solution of the F_{AB} fragment of IgG (rather than the F_C region) and shows that combining a high concentration of the noncomplementary receptor with the target results in a nominal response by BSI. The control shows <1.6% of the signal observed at equivalent P_A and IgG F_C concentrations and exhibits decidedly different kinetics. Although a bulk property change is expected and observed, the magnitude of this contribution is small.

The interaction assays by BSI benefit from the inherent advantages afforded by microfluidics, as

Table 2. The binding affinities determined by BSI compared with reported values.

Binding partners	K_d BSI		Reported	Detection method of published data
	Kinetic	Endpoint		
CaM-Ca^{2+}	3.40 μM	18.23 μM	1–10 μM	Equilibrium and flow dialysis (*43*)
CaM-TFP	4.73 μM	7.82 μM	4.5–5.8 μM	Affinity chromatography (*44*)
CaM-CaN	15.64 nM	11.39 nM	4–16 nM	Radioisotope (*46*, *47*) and affinity chromatography (*45*)
CaM-M13	2.89 nM	9.87 nM	1.9–5.5 nM	SPR (*48*)
P_A-IgG	7.92 nM	6.05 nM	5–34.5 nM	Acoustic waveguide (*41*) and others (*40*)
IL-2-Ab	25.91 pM		10–60 pM	Radioisotope (*52*)

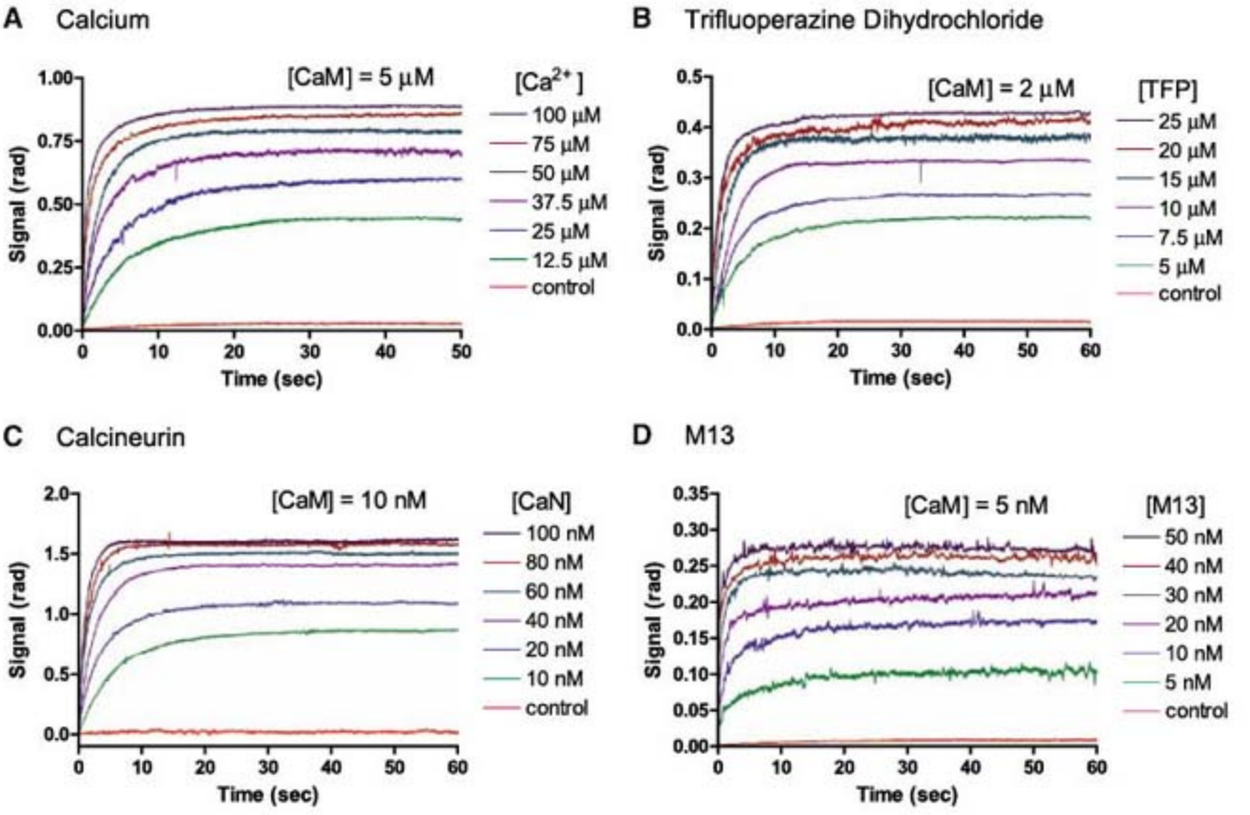

Fig. 3. Association curves of CaM with **(A)** Ca^{2+} using a constant buffered concentration of 5 μM CaM and Ca^{2+} concentrations from 12.5 to 100 μM. All CaM solutions used contained a small amount of EGTA to chelate any free Ca^{2+}. A 5 μM CaM solution and a 100 μM Ca^{2+} solution, both containing excess EGTA (i.e., 400 μM), served as the control. **(B)** TFP using a constant concentration of 2 μM activated CaM. TFP solutions were made in the same buffer and held at the same pH as CaM. A 2 μM solution of CaM and a 25 μM solution of TFP, both in the absence of Ca^{2+}, were mixed to serve as a control. **(C)** Calcineurin using a constant concentration of 10 nM activated CaM and a control of 10 nM solution of CaM and a 100 nM solution of Calcineurin, both in the absence of Ca^{2+}. **(D)** M13 using a concentration of activated CaM kept constant at 5 nM. A 5 nM solution of CaM and a 50 nM solution of M13, both devoid of CaM activating Ca^{2+} served as the control.

was also the case for entire syntheses performed on-chip (*42*). The macro-micro interface is less than optimal for our system, yet it was possible to perform the entire P_A-IgG binding assays with only 105×10^{-9} g (2.5 pmol) of P_A and just 287×10^{-9} g (5.75 pmol) of the F_C fragment of IgG. Under the best-case scenario, a comparable determination by ITC would require 300 to 1000 times as much mass (~300 μg) of each of the reactants.

We chose CaM, the ubiquitous calcium-binding protein that can bind to and regulate a multitude of different protein targets, to further demonstrate the utility of BSI. Upon binding to Ca^{2+}, CaM undergoes a conformational change thought to induce activity. Once activated by Ca^{2+}, CaM binds, among other targets, the protein calcineurin, a skeletal muscle myosin peptide, and small inhibitor molecules. Ligands ranging in size from ions such as Ca^{2+} to 77 kD proteins and spanning three decades in K_d (from a few micomolar to tens of nanomolar) provide an array of ligand-substrate interactions to evaluate BSI methodology. We quantified (i) CaM-Ca^{2+} interactions, (ii) interactions between CaM and the small-molecule inhibitor trifluoperazine dihydrochloride (TFP), (iii) CaM-calcineurin binding, and (iv) reactions of CaM with M13, a peptide from the sequence of skeletal muscle myosin light chain kinase (sk-MLCK), a known target of the Ca^{2+}-activated CaM complex. In all of these experiments performed at 25°C, the CaM solutions were buffered. For the latter three studies, CaM was activated with Ca^{2+}, and unactivated CaM, in the absence of Ca^{2+}, served as a control. The values reported previously and those we have measured are summarized in Table 2.

The reported K_d values for CaM-Ca^{2+} range from 1 to 10 μM (*43*). The control showed < 3% change in signal above that observed in the absence of excess EGTA at equivalent CaM and Ca^{2+} concentrations (Fig. 3A). Kinetic analysis with a single exponential gives rise to a plot of observed rates versus Ca^{2+} concentration that is linear (*38*). A linear least-squares analysis of the data gives the slope, the intercept, and their respective uncertainties. From this analysis, K_d was determined to be 3.40 μM (±2.86). Analysis of the plot of the end-point values monitored by BSI versus the concentration of Ca^{2+} yields a K_d value of 18.23 μM (±1.43), which is above the range previously reported. The disparity in these two values may arise from the use of an overly simplistic model of the reaction kinetics (for example, Ca^{2+} is known to bind more than one CaM site) and/or from the RI background present from unreacted ligand, particularly at high concentrations. Even four-site binding models provide questionable fits of kinetic data for this system (*43*).

The interaction between CaM and TFP was previously examined with affinity chromatography (*44*). This method required 30 μg per sample, with each sample analysis requiring 300 μl. In these chromatography studies, dissociation constants or affinities ranged from 4.5 to 5.8 μM. At equivalent CaM and TFP concentrations, the control showed <4% of the signal observed when Ca^{2+} was present (Fig. 3B). Kinetic analysis produces a linear relation between the observed rates over the concentration range of TFP used (*38*), and from the least-squares analysis, K_d was determined to be 4.73 μM (±0.48) for the CaM-TFP complex, which is within the range obtained by affinity chromatography (*44*). A plot of the BSI signal values at end-point versus TFP concentration was constructed and gave a K_d of 7.82 μM (±0.91).

Calcineurin is a protein phosphatase and the major CaM binding protein in the brain (*45*). The pair has been studied previously using both affinity chromatography and radioligand binding (*45*–*47*), with reported K_d's between 4 and 16 nM. The unactivated control showed <1.5% of the signal observed at the equivalent CaM and calcineurin concentrations in the presence of Ca^{2+} (Fig. 3C). Kinetic analysis yields a linear relation between the observed rates and calcineurin concentration (*38*). The slope and intercept from a least-squares analysis yields a K_d of 15.64 nM (±3.24), again within the range of reported values from affinity chromatography and radioligand binding (*45*–*47*). End-point analysis yielded a hyperbolic relation (*38*) and a K_d of 11.39 nM (±0.82).

M13, a peptide from sk-MLCK, is also a known target of the Ca^{2+}-activated CaM complex and has been shown by SPR to bind with high affinity (K_d = 1.9 to 5.5 nM) (*48*). A range of concentrations of M13 were reacted with CaM sequentially, and time-dependent association events were detected by interferometry (Fig. 3D). A control showed <2.6% of the signal observed when Ca^{2+} was present. A linear relation between the observed rates and the ligand concentration (M13) enabled the calculation of K_d. For the CaM-M13 pair, this value was 2.89 nM (±0.74), which compares well with the SPR values (*48*). Analysis with the end-point CaM-M13 signal values versus concentration yields a K_d value of 9.87 nM (±1.12) (*38*). The likely causes for the disparity between the end-point and kinetic affinity values are that this interaction produces less signal, requiring the assay to be done near the noise floor, and a relatively larger noninteraction RI change at higher concentrations of ligand.

Kinetic parameters can also be derived from BSI. For example, the interaction of CaM with M13 showed high consistency with stopped-flow kinetics performed previously (*49*). The association rate determined by BSI was $3.1 \times 10^7\ M^{-1}s^{-1}$, compared with $3.9 \times 10^7\ M^{-1}s^{-1}$ as determined by Török (*49*). Homogeneous assays based on calorimetry are problematic for very low and very high binding affinities. To effectively evaluate the interaction between pairs with picomolar binding affinities, it is desirable to perform the determination at subnanomolar concentrations, which is often not possible with ITC but is well within the range possible with BSI. To demonstrate this capability, we measured the interaction between IL-2 and a monoclonal antibody in buffer (*38*) and in cell-free media (Fig. 4). Activated T cells secrete IL-2 (*50*, *51*), which, among its other roles, is responsible for the proliferation of antigen-specific cells, as well as promoting the proliferation and differentiation of other immune cells. IL-2 and its antibody (IL-Ab) have been shown to bind with high affinity, with reported K_d values ranging from 10 to 60 pM (*52*). BSI was used to monitor real-time interactions IL-Ab with IL-2 in free solution and in cell media. The slight, nearly identical RI change observed for the blank and two controls was attributed to the mixing of the media. The kinetic analysis, as described above for the CaM and P_A- IgG pairs, yields a linear plot (*38*). From the analysis, a K_d of 25.91 pM (±5.24 pM) was determined, which falls within the published range of 10 to 60 pM (*52*).

Although additional work is required to completely understand the intricacies of free-solution interaction determinations by BSI, the observations presented here demonstrate that such measurements can be performed label-free with high sensitivity over a six-decade dynamic range for K_d determinations with values as low as 4 μM and as high as tens of pM. For example, using an unoptimized microfluidic network, the entire CaM study required the consumption of only about 200 picomoles or 3 μg CaM. To perform a similar analysis with ITC would have required about 250 times as much solute, or about 0.8 mg. The lower concentrations used in BSI may avoid errors resulting from solute aggregation. We note that all of the data presented were obtained using a single-channel system and, excluding the IL-2 results, with no active or passive signal filtering. It should also be possible to use this method to look for the presence of unknown binding partners, such

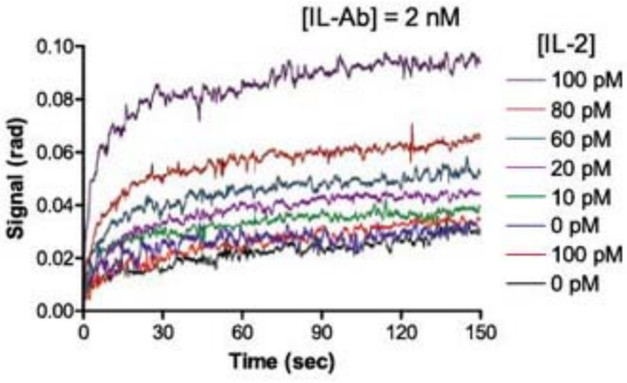

Fig. 4. IL-2-Ab binding curves with interaction assay performed in cell-free media. The IL-Ab concentration was held constant at 2 nM. Both the IL-2 and IL-Ab solutions were made using RPMI 1640 cell media with 1% fetal bovine serum and 10 μg/mL Cipro. A blank [0 M of both IL-2 and IL-Ab, (black)], as well as two controls [0 pM IL-2 reacted with 2 nM IL-Ab (blue); 100 pM IL-2 mixed on chip with 0 nM IL-Ab (red)] were evaluated.

as from cellular extracts, to a target of known concentration.

References and Notes

1. A. Velazquez-Campoy, E. Freire, *Biophys. Chem.* **115**, 115 (2005).
2. A. Ababou, J. E. Ladbury, *J. Mol. Recognit.* **20**, 4 (2007).
3. S. Leavitt, E. Freire, *Curr. Opin. Struct. Biol.* **11**, 560 (2001).
4. F. E. Torres *et al.*, *Proc. Natl. Acad. Sci. U.S.A.* **101**, 9517 (2004).
5. J. Hahm, C. M. Lieber, *Nano Lett.* **4**, 51 (2004).
6. G. Shekhawat, S. H. Tark, V. P. Dravid, *Science* **311**, 1592 (2006).
7. M. B. Kerby, R. S. Legge, A. Tripathi, *Anal. Chem.* **78**, 8273 (2006).
8. R. L. Rich, Y. S. N. Day, T. A. Morton, D. G. Myszka, *Anal. Biochem.* **296**, 197 (2001).
9. D. A. Markov, K. Swinney, D. J. Bornhop, *J. Am. Chem. Soc.* **126**, 16659 (2004).
10. J. C. Latham, D. A. Markov, H. S. Sorensen, D. J. Bornhop, *Angew. Chem. Int. Ed.* **45**, 955 (2006).
11. F. Brosinger *et al.*, *Sens. Actuators B Chem.* **44**, 350 (1997).
12. F. Prieto *et al.*, *Nanotechnology* **14**, 907 (2003).
13. F. Prieto *et al.*, *Sens. Actuators B Chem.* **92**, 151 (2003).
14. E. F. Schipper *et al.*, *Sens. Actuators B Chem.* **40**, 147 (1997).
15. A. Ymeti *et al.*, *Appl. Opt.* **42**, 5649 (2003).
16. M. J. Swann, L. L. Peel, S. Carrington, N. J. Freeman, *Anal. Biochem.* **329**, 190 (2004).
17. Y. Y. Li *et al.*, *Science* **299**, 2045 (2003).
18. S. L. Pan, L. J. Rothberg, *Nano Lett.* **3**, 811 (2003).
19. J. B. Goh, R. W. Loo, M. C. Goh, *Sens. Actuators B Chem.* **106**, 243 (2005).
20. M. Zhao *et al.*, *Clin. Chem.* **52**, 2135 (2006).
21. J. J. La Clair, M. D. Burkart, *Org. Biomol. Chem.* **1**, 3244 (2003).
22. H. S. Sorensen, N. B. Larsen, J. C. Latham, D. J. Bornhop, P. E. Andersen, *Appl. Phys. Lett.* **89**, 151108 (2006).
23. K. Swinney, D. Markov, D. J. Bornhop, *Anal. Chem.* **72**, 2690 (2000).
24. D. A. Markov, S. Dotson, S. Wood, D. J. Bornhop, *Electrophoresis* **25**, 3805 (2004).
25. D. C. Duffy, J. C. McDonald, O. J. A. Schueller, G. M. Whitesides, *Anal. Chem.* **70**, 4974 (1998).
26. G. J. Wegner, N. J. Lee, G. Marriott, R. M. Corn, *Anal. Chem.* **75**, 4740 (2003).
27. T. Sakai *et al.*, *Anal. Sci.* **20**, 279 (2004).
28. H. Sota, Y. Hasegawa, M. Iwakura, *Anal. Chem.* **70**, 2019 (1998).
29. H. Elkashef, *Opt. Mater.* **8**, 175 (1997).
30. G. Maroulis, D. Xenides, U. Hohm, A. Loose, *J. Chem. Phys.* **115**, 7957 (2001).
31. K. Swinney, D. Markov, D. J. Bornhop, *Rev. Sci. Instrum.* **71**, 2684 (2000).
32. H. J. Tarigan, P. Neill, C. K. Kenmore, D. J. Bornhop, *Anal. Chem.* **68**, 1762 (1996).
33. H. S. Sorensen, Thesis, Technical University of Denmark (2006).
34. B. J. Burke, F. E. Regnier, *Anal. Chem.* **75**, 1786 (2003).
35. G. M. Whitesides, E. Ostuni, S. Takayama, X. Y. Jiang, D. E. Ingber, *Annu. Rev. Biomed. Eng.* **3**, 335 (2001).
36. After the PDMS was cured and peeled from the mold, it was oxidized in O_2 plasma for 30 s and then placed on a 1-mm-thick microscope glass slide, creating an irreversible bond between the glass and PDMS. The glass slide was used to seal the microfluidic channels and allowed for the entire chip assembly to be handled and securely mounted onto a thermoelectrically temperature-controlled x-y translation stage. A shorter top piece of glass was also used as a faceplate, offering structural stability to minimize channel deformations during the sample introduction step. Nanoliter volumes of samples of each of the two binding pairs were placed in the reservoirs at the top of the "Y," then a slight negative pressure was applied to the chip exit well, drawing the two interacting species through the mixer and into the detection zone.
37. In our stop-flow experiments, the sample introduction pressure was chosen to optimize the flow rate and mixing of the solutes. The constraints of the mixer system made it necessary to balance the need for rapid, complete mixing to produce a homogeneous solution of the binding pair with the requirement that the reaction has not proceeded appreciably before flow is stopped and analysis begins. These parameters change slightly for each binding pair, with flow rates found to be in the range of 75 to 120 μL/min.
38. Materials and methods are available as supporting material on *Science* online.
39. E. Project, R. Friedman, E. Nachliel, M. Gutman, *Biophys. J.* **90**, 3842 (2006).
40. J. J. Langone, *Adv. Immunol.* **32**, 157 (1982).
41. K. Saha, F. Bender, E. Gizeli, *Anal. Chem.* **75**, 835 (2003).
42. C. C. Lee *et al.*, *Science* **310**, 1793 (2005).
43. H. Tsuruta, T. Sano, *Biophys. Chem.* **35**, 75 (1990).
44. L. Massom, H. Lee, H. W. Jarrett, *Biochemistry* **29**, 671 (1990).
45. C. B. Klee, M. H. Krinks, *Biochemistry* **17**, 120 (1978).
46. M. G. Speaker, S. J. Orlow, T. W. Sturgill, O. M. Rosen, *Proc. Natl. Acad.Sci. U.S.A.* **80**, 329 (1983).
47. M. J. Hubbard, C. B. Klee, *J. Biol. Chem.* **262**, 15062 (1987).
48. S. Montigiani, G. Neri, P. Neri, D. Neri, *J. Mol. Biol.* **258**, 6 (1996).
49. K. Török, *Biochem. Soc. Trans.* **30**, 55 (2002).
50. J. Theze, P. M. Alzari, J. Bertoglio, *Immunol. Today* **17**, 481 (1996).
51. A. K. Abbas, A. H. Lichtman, *Cellular and Molecular Immunology* (Saunders, Philadelphia, ed. 5, 2003).
52. G. H. Reem, N. H. Yeh, D. L. Urdal, P. L. Kilian, J. J. Farrar, *Proc. Natl. Acad. Sci. U.S.A.* **82**, 8663 (1985).

53. This research was supported by National Institute of Biomedical Imaging and Bioengineering at NIH, R-01 EB0003537-01A2, Vanderbilt Institute for Chemical Biology, Air Force Office of Scientific Research grants FA9550-04-1-0364 and FA9550-05-1-0349, and the Vanderbilt Institute for Integrative Biosystems and Education, as well as by vision sciences training grant T32-EY07135 and BIOP Graduate School grant 643-01-0092. We thank J. B. Haas for editorial assistance and P. E. Andersen, S. Dotson, S. Faley, R. Flowers, H. Mchaourab, and J. Wikswo for helpful discussions.

Supporting Online Material

www.sciencemag.org/cgi/content/full/317/5845/1732/DC1
Materials and Methods
SOM Text
Figs. S1 to S7
References
Movie S1

15 June 2007; accepted 8 August 2007
10.1126/science.1146559

Asymmetric Catalysis of the Transannular Diels-Alder Reaction

Emily P. Balskus and Eric N. Jacobsen*

Transannular chemical reactions are unparalleled in their ability to generate high degrees of stereochemical and architectural complexity in a single transformation. However, the successful application of this approach in synthesis depends on the ability to predict and control the outcome of the transannular reaction. Use of a chiral catalyst in this context represents an attractive, yet unused, strategy. This report describes a catalytic, asymmetric transannnular Diels-Alder (TADA) reaction that affords polycyclic products in high enantiomeric excess. This catalyst system can also alter the inherent diastereoselectivity of cyclizations with substrates containing chiral centers. Additionally, the catalytic enantioselective TADA has been used as the key step in a total synthesis of the sesquiterpene 11,12-diacetoxydrimane; this route may provide a general approach to the polycyclic carbon framework shared by many terpene natural products.

The challenge of constructing complex molecules has captured the attention of synthetic chemists for over a century. Polycyclic, stereochemically complex carbon frameworks are a common feature of many biologically active synthetic and naturally occurring targets. Among the possible strategies for assembling such compounds, transannular reactions constitute a particularly efficient approach (Fig. 1A). In this type of transformation, reacting centers are tethered together as part of a macrocycle; covalent bond formation occurs across the ring, resulting in the formation of a polycyclic product, often with concomitant formation of multiple stereogenic centers. The relative proximity of the reacting sites can confer an entropic advantage to transannular reactions, allowing reactions within sterically congested frameworks that are effectively inert in analogous inter- or acyclic intramolecular systems. However, successful application of transannular strategies in target-oriented synthesis depends on the ability to predict and influence the stereochemical course of the reaction.

In the vast majority of transannular transformations studied to date, stereoselectivity has relied on the intrinsic conformational properties of the reacting macrocycle. An appealing alternative strategy for controlling enantio- and diastereoselectivity in transannular reactions might involve use of a chiral catalyst or reagent. Despite numerous efforts in this direction, efficient asymmetric catalysis of transannular reactions has not been achieved (*1*–*5*).

The Diels-Alder reaction has long stood as one of the most useful complexity-generating

Department of Chemistry and Chemical Biology, Harvard University, Cambridge, MA 02138, USA.

*To whom correspondence should be addressed. E-mail: jacobsen@chemistry.harvard.edu

reactions in organic chemistry, and transannular variants have been studied extensively (*6*, *7*). In particular, the transannular Diels-Alder (TADA) has been used as a key step in many elegant total syntheses of complex polycylic natural products (*8*). The choice to explore asymmetric catalysis of the TADA was also influenced by the existence of numerous successful catalytic enantioselective inter- and acyclic intramolecular Diels-Alder reactions discovered over the past 2 decades (*9*).

The investigation began by screening a variety of chiral metal-based Lewis acids, Brønsted acids, and hydrogen bond donors for their ability to promote the TADA of macrolactone **1** (Fig. 1B). This macrocyclic substrate was accessed in only seven steps from commercially available materials, making sufficient quantities available for these initial experiments (*10*). Although most catalysts tested were unable to promote the desired cyclization under the conditions of our screens, use of 20 mole % (mol%) triflimide-activated oxazaborolidine Lewis acid **3a** provided excellent conversion of **1** to the *endo* TADA product **2**, albeit with low enantioselectivity (Table 1, entry 1). First reported by Corey, acid-activated chiral oxazaborolidine derivatives are among the most effective catalyst systems for enantioselective inter- and intramolecular Diels-Alder reactions (*11*–*13*).

In an effort to obtain higher enantioselectivity in the TADA, we synthesized and tested various chiral oxazaborolidine derivatives (Table 1, entries 2 to 8). As anticipated from earlier work on the intermolecular Diels-Alder reaction (*13*), replacing the methyl substituent on boron with a phenyl ring increased enantioselectivity (entry 2). However, the optimal catalyst for inter- and acyclic intramolecular Diels-Alder reactions, which contains an ortho tolyl group on boron (**3c**), was found to have a detrimental effect on both the enantioselectivity and the conversion of the TADA (entry 3). This difference may be attributed to the added steric demand associated with a macrocyclic substrate; the presence of alkyl groups at the ortho or meta positions of the boron aryl substituent diminished both reactivity and selectivity (entries 3 and 4). Substitution at the para position was better tolerated but did not lead to useful degrees of enantioselectivity (entry 5).

A breakthrough in catalyst optimization came with the introduction of a less sterically demanding fluorine substituent onto the boron aryl ring (entries 6 to 8). Monofluorinated catalysts provided excellent conversion to the desired product as well as an increase in enantioselectivity, with the ortho-fluorinated catalyst **3f** affording the best result of 86% enantiomeric excess (ee). Systematic variation of the other reaction parameters, including solvent, concentration, and temperature, identified optimal reaction conditions, which afford product in 90% ee and 69% isolated yield (entry 9).

The complex conformational properties of macrocycles might have necessitated a fairly specific match between catalyst and substrate, restricting the scope of any given catalyst. However, it was found instead that a variety of macrocycles containing *E,E* dienes provided products in good to excellent enantioselectivity and diastereoselectivity with catalyst **3f** under the optimal reaction conditions described above (Fig. 2). Notably,

entry	macrocycle	product	isolated yield	% ee/dr
1	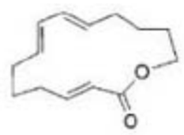	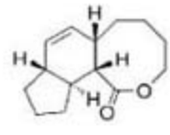	69%	90%/>19:1
2	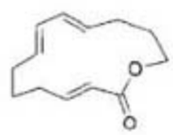	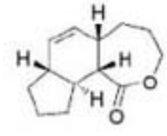	80%	92%/>19:1
3	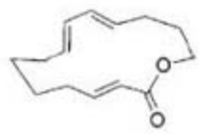	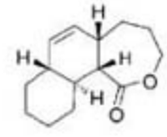	78%	90%/5.9:1
4*	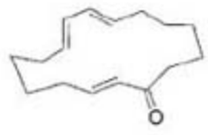	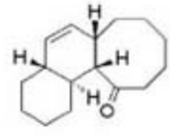	62% (83%)†	88%/8.8:1.1:1‡
5§	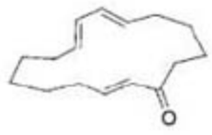	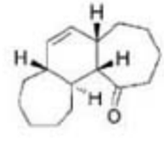	15% (25% conversion by ^{1}H NMR)	85%/5.0:1

Fig. 2. Substrate scope of the asymmetric catalytic TADA. All reactions were performed in toluene (0.3 M) for 20 hours at room temperature using 20 mol% of catalyst **3f**. Isolated yields were obtained after purification using silica gel chromatography. Dr values were measured with ^{1}H nuclear magnetic resonance analysis. Ee values of the major diastereomers were determined by gas chromatography (GC) analysis using commercial chiral columns. *Macrocycle was a 3.7:1 ratio of inseparable *E,E*:*E,Z* diene isomers; only the *E,E* diene reacted under these conditions. †Isolated yield based on *E,E* macrocycle. ‡Additional minor diastereomer may be the result of product epimerization or reaction of a geometric isomer. §Macrocycle was a 5.0:1 ratio of inseparable *E,E*:*E,Z* diene isomers; only the *E,E* diene reacted under these conditions.

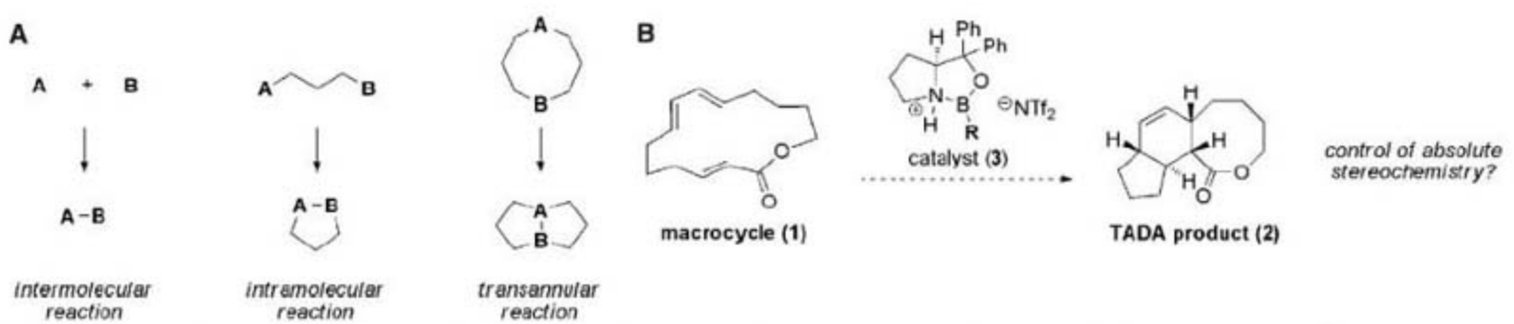

Fig. 1. (**A**) Comparison of intermolecular, intramolecular, and transannular chemical reactions. (**B**) Proposed asymmetric catalytic TADA reaction.

a number of different ring systems can be formed in this transformation, including medium-sized seven- and eight-membered rings. Changing the dienophile from an α,β-unsaturated lactone to a ketone is also possible (entries 4 and 5). The lowered energy barrier for this transannular process also permits the formation of a highly unusual 7-6-7 fused ring system with good enantioselectivity, albeit in low conversion (entry 5).

Table 1. Optimization of catalyst structure in the asymmetric TADA. Conversion of **1** to **2** was measured with ^{1}H nuclear magnetic resonance analysis, which also revealed >95:5 dr for all cases. Enantiomeric excesses (% ee) were determined by GC analysis using commercial chiral columns. All reactions were performed on a 0.01 mmol scale in toluene (0.05 M) for 20 hours at room temperature using 20 mol% of catalyst, except for entry 9 [reaction performed on a 0.02 mmol scale in toluene (0.3 M) for 20 hours at room temperature]. R refers to the boron substituent as in Fig. 1B.

Entry	Catalyst	% Conversion	% ee
1	R = CH_3 (**3a**)	85	10
2	R = C_6H_5 (**3b**)	66	80
3	R = 2-$CH_3C_6H_4$ (**3c**)	11	49
4	R = 3-$CH_3C_6H_4$ (**3d**)	10	48
5	R = 4-$CH_3C_6H_4$ (**3e**)	32	71
6	R = 2-FC_6H_4 (**3f**)	86	86
7	R = 3-FC_6H_4 (**3g**)	63	82
8	R = 4-FC_6H_4 (**3h**)	95	82
9	R = 2-FC_6H_4 (**3f**)	>95 (69% isolated)	90

In all TADA reactions examined, the *endo* diastereomer predominates, and the absolute stereochemical outcome of the reaction matches that found for other oxazaborolidine-catalyzed inter-and intramolecular processes [for details of absolute stereochemical assignment, see (*10*)]. A current limitation of this methodology is the requirement for an *E,E* diene in the macrocycle; substrates containing trisubstituted or *E,Z* dienes provide no product under the optimal reaction conditions. This lack of reactivity may be attributed to the inability of such macrocyclic dienes to achieve the required s-*cis* conformation at ambient temperatures (*6*, *7*). However, every macrocycle found to be reactive under the optimal, standardized conditions underwent cycloaddition in good to excellent enantioselectivity (>80% ee).

After establishing the broad substrate scope of the asymmetric catalytic TADA, our efforts turned toward applying the methodology to more

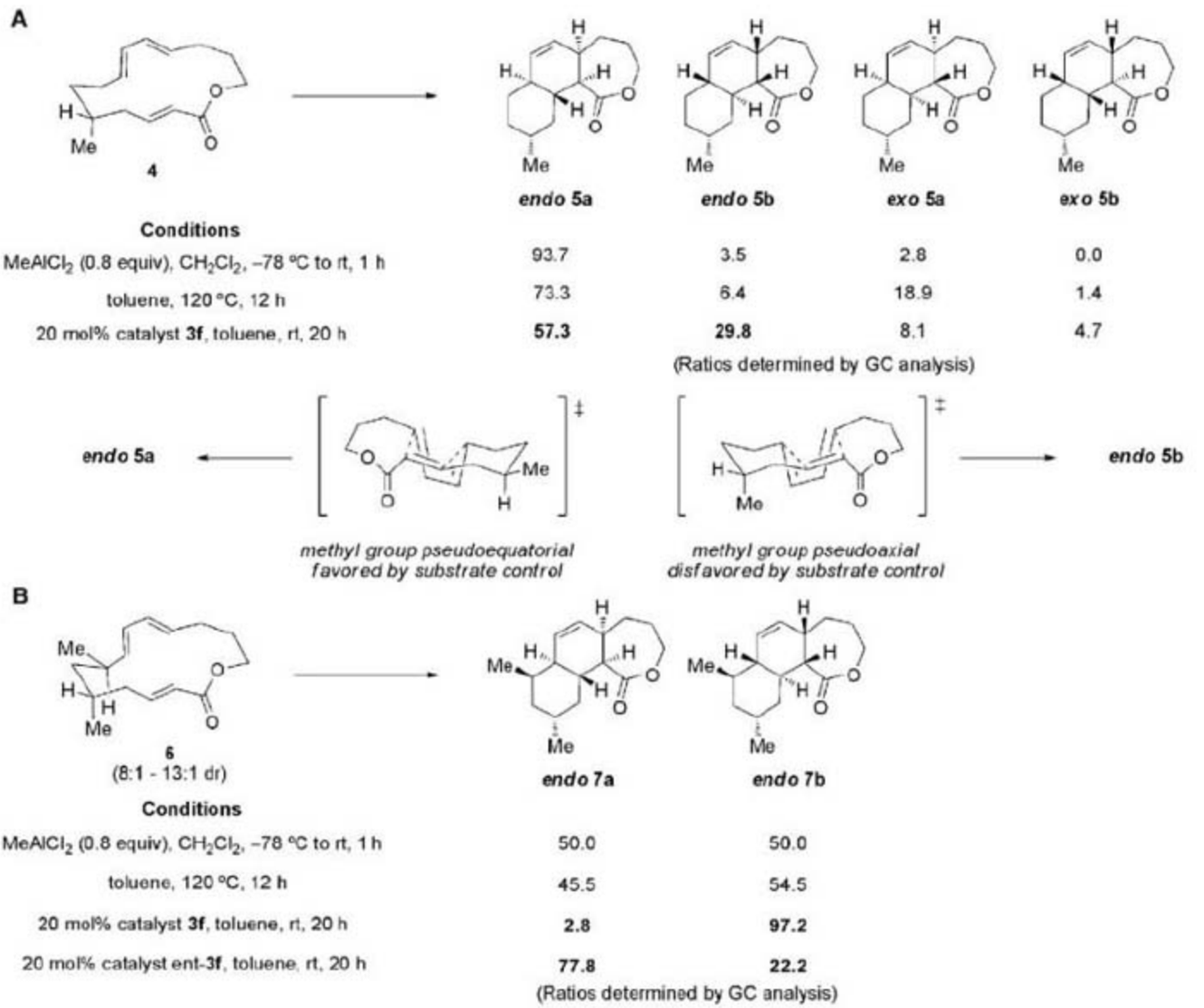

Fig. 3. **(A)** Catalyst-controlled diastereoselective TADA of a biased macrocycle. equiv., equivalents; rt, room temperature. **(B)** Catalyst-controlled diastereoselective TADA of an unbiased macrocycle.

elaborate macrocyclic substrates. Two areas emerged as worthwhile avenues for further investigation: catalyst-controlled diastereoselective cyclizations and synthesis of sterically congested natural product frameworks. Devising chiral catalysts to alter the inherent diastereoselectivity of reactions involving chiral substrates remains one of the greatest challenges in synthesis (*14*). In many cases, substrates exert a strong conformational bias toward formation of a particular diastereomer; pathways that lead to alternate diastereoselectivity have substantially higher activation barriers and therefore often proceed at impractically slow rates, even under the influence of highly stereoselective catalysts.

Initially, investigations began with the cyclization of a highly biased macrocycle (**4**), readily accessed from (+)-citronellol (Fig. 3A). In theory, there are four possible diastereomeric outcomes in this reaction. However, this macrocycle is expected to adopt conformations that place its methyl group in a pseudoequatorial position in the TADA transition state (*15*). Indeed, reaction of **4**, either in the presence of an achiral Lewis acid or under thermal conditions, proceeds with high diastereoselectivity to generate ***endo*-5a**, which results from reaction of such a conformation. Diastereomers resulting from cyclization of alternate conformers bearing the methyl group in pseudoaxial positions (***endo*-5b** and ***exo*-5b**) are obtained in only minor amounts. However, upon exposure of **4** to 20 mol% of catalyst **3f**, the alternate, otherwise inaccessible, ***endo*-5b** diastereomer is formed in useful quantities (30% yield). This type of catalyst-controlled, diastereoselective reaction may find use in structure-activity relationship studies and diversity-oriented synthesis, applications where access to every possible diastereomer of a particular carbon framework is desired (*16*).

Another useful application of catalyst-controlled diastereoselectivity would involve influencing the outcome of a poorly selective reaction. In order to assess the performance of the catalyst under these circumstances, macrocycle **6** was synthesized, which contains 1,3-*anti* methyl substitution (Fig. 3B) (*17*). The stereochemical relationship between these two groups should create a situation where both possible *endo* Diels-Alder transition states are destabilized to similar extents by the presence of a pseudoaxial methyl group. As expected, the TADA reaction of **6** proceeded with low selectivity between the two *endo* diastereomers (***endo*-7a** and ***endo*-7b**) in the presence of an achiral Lewis acid or under thermal conditions. However, exposure of macrocycle **6** to 20 mol% of catalyst **3f** dramatically favors formation of the ***endo*-7b** diastereomer, providing TADA product in a 34:1 diastereomeric ratio (dr) and excellent isolated yield. The opposite enantiomer of catalyst led to selective formation of ***endo*-7a**.

Given the many previous applications of the TADA in total synthesis, one would anticipate considerable utility of the catalytic enantioselec-

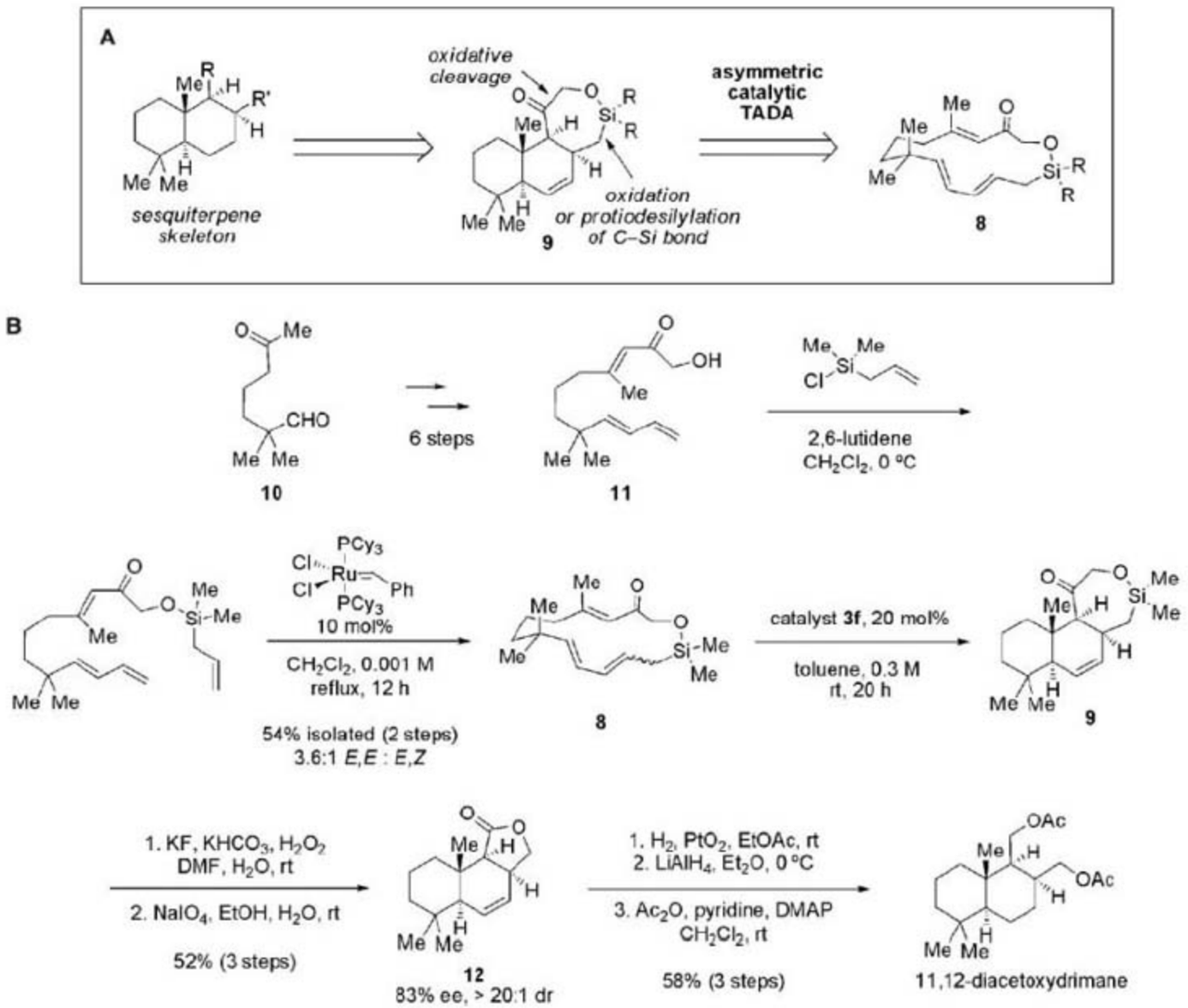

Fig. 4. **(A)** Retrosynthesis of sesquiterpene natural products using the catalytic asymmetric TADA. **(B)** Enantioselective total synthesis of 11,12-diacetoxydrimane.

tive version in the construction of natural products. To illustrate, the carbon skeleton of the sesquiterpene natural products, a large family with many biologically active members in both enantiomeric series, was targeted (*18*). The retrosynthesis involved constructing the polycyclic core of these molecules by using the TADA of silicon-containing macrocyclic ketone **8** (Fig. 4A) (*19*). Post-cyclization, straightforward synthetic manipulations of the tricyclic product **9** would provide access to various members of this interesting natural product class. Construction of such a decalin framework using traditional Diels-Alder partners that lack a macrocyclic tether is problematic because of the development of severe *syn* pentane-like interactions between the *gem*-dimethyl group and the methyl group of the dienenophile in the transition state (*20*).

Synthesis of the desired TADA substrate was achieved in eight steps from known ketoaldehyde **10** (Fig. 4B) (*21*). Silylation of alcohol **11** was followed by macrocyclization via diene-ene ring-closing metathesis using the Grubbs first-generation ruthenium catalyst, which proceeded in excellent conversion and with good selectivity for the *E,E* diene product **8** (*22*). Gratifyingly, exposure of this macrocycle to catalyst **3f** resulted in complete conversion of the *E,E* isomer to provide the desired TADA product **9** in >20:1 dr. Tamao oxidation of the crude reaction mixture (*23*), followed by oxidative cleavage of the resulting diastereomeric mixture of hemiketals, provided lactone **12** in 83% ee. This intermediate, which could potentially serve as a precursor to a number of sesquiterpene targets, was elaborated in three steps to a representative natural product, 11,12-diacetoxydrimane (*24*). In addition to providing a concise, enantioselective route to these terpene targets, the strategic use of a temporary transannular tether may constitute an important approach for dealing with difficult bond constructions in a variety of systems.

The successful application of a chiral catalyst to transannnular reactions is thus not only possible but is seen to be remarkably general across a broad range of macrocyclic substrates. This strategy should allow stereocontrolled assembly of polycyclic molecular architectures with unparalleled efficiency and elegance.

References and Notes

1. D. M. Hodgson *et al.*, *J. Chem. Soc. Perkin Trans. 1* 2151 (1998).
2. D. M. Hodgson, L. A. Robinson, *Chem. Commun.* 309 (1999).
3. D. M. Hodgson, I. D. Cameron, *Org. Lett.* **3**, 441 (2001).
4. O. Knopff, J. Kuhne, C. Fehr, *Angew. Chem. Int. Ed.* **46**, 1307 (2007).
5. M. Inoue *et al.*, *J. Org. Chem.* **72**, 3065 (2007).
6. P. Deslongchamps, *Pure Appl. Chem.* **64**, 1831 (1992).
7. P. Deslongchamps, *Aldrichchimica Acta* **24**, 43 (1991).
8. E. Marsault, A. Toró, P. Nowak, P. Deslongchamps, *Tetrahedron* **57**, 4243 (2001).
9. D. A. Evans, J. S. Johnson, in *Comprehensive Asymetric Catalysis*, E. N. Jacobsen, A. Pfaltz, H. Yamamoto, Eds. (Springer-Verlag, Berlin, 1999), vol. 3, ch. 33.1.
10. Materials and methods are available on *Science* Online.
11. E. J. Corey, T. Shibata, T. W. Lee, *J. Am. Chem. Soc.* **124**, 3808 (2002).
12. D. H. Ryu, E. J. Corey, *J. Am. Chem. Soc.* **125**, 6388 (2003).
13. G. Zhou, Q.-Y. Hu, E. J. Corey, *Org. Lett.* **5**, 3979 (2003).
14. S. Masamune, W. Choi, J. S. Petersen, L. R. Sita, *Angew. Chem. Int. Ed.* **24**, 1 (1985).
15. D. J. Witter, J. C. Vederas, *J. Org. Chem.* **61**, 2613 (1996).
16. M. D. Burke, S. L. Schreiber, *Angew. Chem. Int. Ed.* **43**, 46 (2004).
17. A. G. Myers *et al.*, *J. Am. Chem. Soc.* **119**, 6496 (1997).
18. B. M. Fraga, *Nat. Prod. Rep.* **23**, 943 (2006); and references therein.
19. G. Stork, T. Y. Chan, G. A. Breault, *J. Am. Chem. Soc.* **114**, 7578 (1992).
20. For related examples of utilizing a TADA, see (*8*).
21. M. Negi, G. V. Subbaraju, M. S. Manhas, A. K. Bose, *Enzyme Microb. Technol.* **15**, 483 (1993).
22. K. Lu *et al.*, *Org. Lett.* **8**, 1193 (2006); and references therein.
23. K. Tamao, N. Ishida, M. Kumada, *J. Org. Chem.* **48**, 2120 (1983).
24. A. Montagnac, M.-T. Martin, C. Debitus, M. Pais, *J. Nat. Prod.* **59**, 866 (1996).

25. Financial support was provided by the NIH (GM-59316). E.P.B. is the recipient of a predoctoral fellowship from NSF and an American Chemical Society Division of Organic Chemistry fellowship sponsored by Schering-Plough.

Supporting Online Material

www.sciencemag.org/cgi/content/full/317/5845/1736/DC1
Materials and Methods
Figs. S1 to S13
References

25 June 2007; accepted 6 August 2007
10.1126/science.1146939

Spin Transition Zone in Earth's Lower Mantle

Jung-Fu Lin,[1] György Vankó,[2,3] Steven D. Jacobsen,[4] Valentin Iota,[1] Viktor V. Struzhkin,[5] Vitali B. Prakapenka,[6] Alexei Kuznetsov,[6] Choong-Shik Yoo[1*]

Mineral properties in Earth's lower mantle are affected by iron electronic states, but representative pressures and temperatures have not yet been probed. Spin states of iron in lower-mantle ferropericlase have been measured up to 95 gigapascals and 2000 kelvin with x-ray emission in a laser-heated diamond cell. A gradual spin transition of iron occurs over a pressure-temperature range extending from about 1000 kilometers in depth and 1900 kelvin to 2200 kilometers and 2300 kelvin in the lower mantle. Because low-spin ferropericlase exhibits higher density and faster sound velocities relative to the high-spin ferropericlase, the observed increase in low-spin (Mg,Fe)O at mid-lower mantle conditions would manifest seismically as a lower-mantle spin transition zone characterized by a steeper-than-normal density gradient.

Electronic spin-pairing transitions of iron and associated effects on the physical properties of host phases have been reported in lower-mantle minerals, including ferropericlase, silicate perovskite, and possibly in post-silicate perovskite at high pressures, but so far only at room temperature experimentally (*1*–*12*). These mineral physics studies have prompted geophysicists and geodynamicists to reevaluate the state of the lower mantle and, in particular, the possible sources of seismic (*13*–*15*) and chemical (*16*, *17*) heterogeneities, as well as the thermal stability of massive upwellings (*18*, *19*) in terms of spin-pairing phenomena. Changes in the electronic structure of iron are thought to promote partitioning of iron into ferropericlase relative to perovskite (*1*), although experimental evidence is lacking under lower mantle conditions (*6*, *11*, *16*, *17*). Recent theoretical calculations predict that the spin transition of Fe^{2+} in ferropericlase, $(Mg_{1-x}Fe_x)O$ ($x < 0.2$), would occur continuously over an extended pressure range—and thus would be more accurately referred to as a spin crossover—under the pressure-temperature conditions of the lower mantle (*6*, *11*). In this case, the associated effects would be gradual and therefore less likely to permit seismological detection. Because the Earth's lower mantle varies in pressure from 22 to 140 GPa and in temperature from 1800 K to 4000 K (*20*), experimental determination of the simultaneous pressure-temperature effect on the spin transitions of lower-mantle phases is essential.

We have studied the electronic spin states of iron in ferropericlase [$(Mg_{0.75},Fe_{0.25})O$] and its crystal structure under relevant lower-mantle conditions using x-ray emission spectroscopy (XES) and x-ray diffraction with a laser-heated diamond anvil cell (LHDAC) (*5*, *21*–*23*). The spin states of iron in $(Mg_{0.75},Fe_{0.25})O$ at high pressures and temperatures were probed by in situ XES in a

[1]Lawrence Livermore National Laboratory (LLNL), 7000 East Avenue, Livermore, CA 94550, USA. [2]KFKI Research Institute for Particle and Nuclear Physics, Post Office Box 49, H-1525 Budapest, Hungary. [3]European Synchrotron Radiation Facility, Boîte Postal 220 F-38043, Grenoble Cedex 9, France. [4]Department of Earth and Planetary Sciences, Northwestern University, Evanston, IL 60208, USA. [5]Geophysical Laboratory, Carnegie Institution of Washington, 5251 Broad Branch Road, NW, Washington, DC 20015, USA. [6]Consortium for Advanced Radiation Sources, University of Chicago, Chicago, IL 60637, USA.

*Present address: Department of Chemistry and Institute for Shock Physics, Washington State University, Pullman, WA 99164, USA.

LHDAC. The samples were preoriented <110> crystal plates (*5*) or polycrystalline (*9*) samples of $(Mg_{0.75},Fe_{0.25})O$ composition measuring ~12 μm thick and 70 μm in diameter. Samples were loaded into diamond cells with Be gaskets and boron or cubic BN gasket inserts. Dried NaCl layers acted as thermal insulators between the sample and diamond anvils, as well as the pressure medium and the pressure calibrant (*24*).

A Rowland circle spectrometer with 1-m diameter in the vertical scattering geometry was configured around the double-sided laser-heating system at the GeoSoilEnviro Consortium for Advanced Radiation Sources (GSECARS) sector of the Advanced Photon Source (APS), Argonne National Laboratory (ANL) for XES of iron in the sample under high pressures and temperatures (*5*, *21*). A monochromatic x-ray beam of 14 keV was focused down to ~5 μm vertically and horizontally at the sample position, and a near-infrared laser beam 25 μm in diameter at the sample position was used to heat the sample from both sides of the DAC. The Fe Kβ emission spectra were collected by a silicon detector through the Be gasket and a Si (333) analyzer in the Rowland circle geometry. During the laser-heating experiments, the energy of the monochromatic x-ray was adjusted to higher energy to allow x-ray diffraction measurements with an image plate (MAR345). The details of the experimental set-up and sample synthesis are reported in supporting online material (*22*).

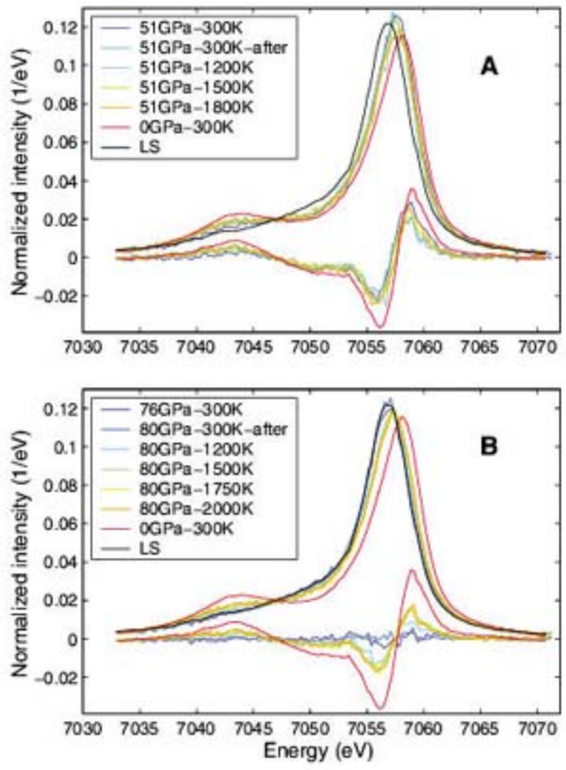

Fig. 1. Representative x-ray emission spectra of Fe Kβ collected from ferropericlase-$(Mg_{0.75},Fe_{0.25})O$ at high pressures and temperatures. **(A)** 51 GPa and high temperatures; **(B)** 80 GPa and high temperatures. High-quality XES spectra collected at ambient pressure and 80 GPa are used as references for the IAD analysis (*23*) of the high-spin and low-spin states, respectively. Differences from the low-spin line shape, shown below the spectra, are used to derive the ratio of the high-spin to low-spin states in the sample. An energy shift of ~1.6 eV in the main emission peak (Kβ) can also be seen across the spin transition.

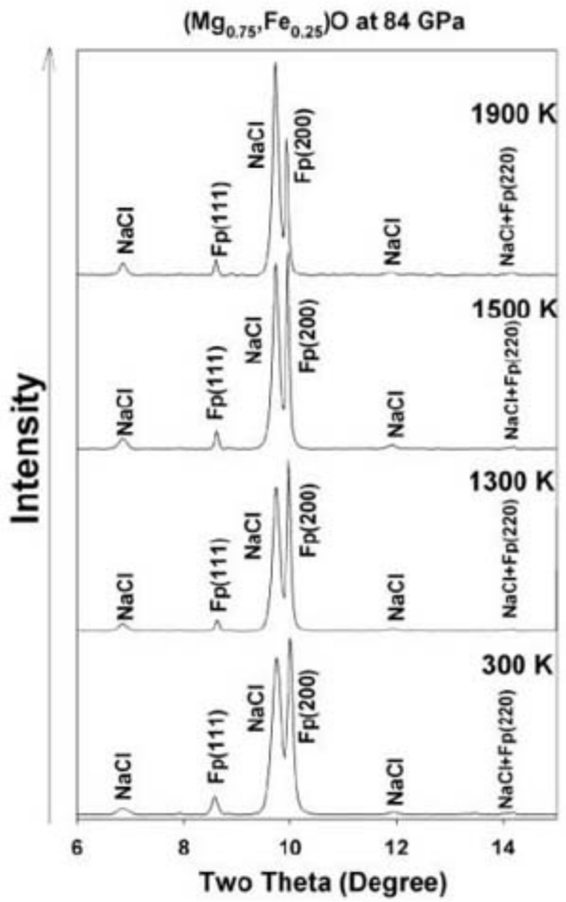

Fig. 2. Representative angle-dispersive x-ray diffraction patterns of $(Mg_{0.75},Fe_{0.25})O$ at ~84 GPa and high temperatures collected from a laser-heated diamond cell. A monochromatic beam of 0.3344 Å in wavelength was used as the x-ray source, and the diffracted x-rays were collected by an image plate (MAR345). The diffraction patterns were integrated with the FIT2D program, and the backgrounds were subtracted for clarity. $(Mg_{0.75},Fe_{0.25})O$ is stable in the B1 structure up to 1900 K and remains in the B1 structure after hours of laser heating (*26*). Fp, $(Mg_{0.75},Fe_{0.25})O$; NaCl, thermal insulator in the B2 structure. Temperature uncertainties in the experiments were approximately 100 to 150 K. Optical observation of the laser-heated sample shows no evidence of a phase separation.

The XES spectra of the Fe Kβ fluorescence lines in $(Mg_{0.75},Fe_{0.25})O$ were collected up to 95 GPa and 2000 K, and x-ray diffraction patterns were collected from some of the samples before, during, and after laser heating at high pressures (Figs. 1 and 2). To quantitatively derive the 3*d* spin momentum and the ratio of the high-spin and low-spin states, the XES spectra were analyzed using the line-shape analysis by integrating the absolute values of the difference spectra and comparing these integrals with that obtained on references [integrated absolute difference (IAD) analysis] (Fig. 1 and figs. S1 and S2) (*23*). The IAD analysis uses the information of the full Fe Kβ spectrum and is model independent. It has been shown that the derived IAD values linearly correlate with the spin momentum at the transition between two spin states and provide a reliable method for determining the ratio of the high-spin and low-spin states in the sample (*23*).

The derived fractions of the high-spin state were used to construct the spin-crossover phase diagram of iron in $(Mg_{0.75},Fe_{0.25})O$ up to 95 GPa and 2000 K (Fig. 3). Whereas the XES results reveal an electronic spin crossover with a mixed population of high-spin and low-spin states of iron in ferropericlase at high pressures and temperatures, x-ray diffraction patterns show that the $(Mg_{0.75},Fe_{0.25})O$ sample is stable in the B1 structure before, during, and after the experiments up to 95 GPa and 2000 K (Fig. 2 and fig. S3) (*25*, *26*). High temperatures do not significantly affect the fraction of the high-spin state below 50 GPa and above 95 GPa, but much stronger temperature effects on the spin crossover are observed from ~50 to 90 GPa. The observed spin crossover is found to be readily reversible in temperatures and cannot be simply explained as the result of sluggish transition and kinetics. The spin-crossover zone clearly widens with increasing temperatures at high pressures (Fig. 3). Although previous high-pressure and room-temperature experiments showed that low-spin and high-spin states have characteristic physical properties, such as volume, incompressibility, and sound velocities, and can be categorized as two distinct phases, high-spin ferropericlase and low-spin ferropericlase (*5*, *7*, *9*),

the spin crossover in the ferropericlase observed in our current XES and diffraction experiments likely involves a mixed population of high-spin and low-spin states in the same crystal structure, an isosymmetric transition involving the substitution of low-spin ions for high-spin ions without change in the structure of the host (*6*, *11*).

Comparison with the model geotherm of the Earth's lower mantle (*20*) indicates that the high-spin to low-spin crossover of iron likely occurs from the middle part to the lower part of the lower mantle from ~1000 km in depth and 1900 K to ~2200 km and 2300 K, and that the low-spin ferropericlase with the B1 structure exists in the lower mantle, that is, at depths below ~2200 km. The observed width of the spin crossover in ferropericlase is much narrower than that predicted by the existing theoretical models (*6*, *11*). Although the temperature effect on the spin transitions in the silicate perovskite and post-perovskite is yet to be studied (*2*–*4*, *8*, *12*), we propose that this spin-crossover phenomenon should also occur in silicate perovskite because it is subject to similar thermal energy in the lower mantle as that required to overcome the spin-pairing energy.

The spin crossover of iron in the lower-mantle phases substantially affects its implications for the geophysics and geodynamics of Earth's lower mantle. The continuous nature of the spin crossover observed here explains why no significant change in iron partitioning between ferropericlase and perovskite has been observed in recent high pressure-temperature experiments with a pyrolitic and olivine composition (*16*, *17*), as opposed to a proposed dramatic change in partitioning and chemical layering in the lower mantle (*1*, *2*). Because the low-spin ferropericlase exhibits relatively high density (*5*, *11*), fast sound velocities (*5*, *9*), and lower radiative thermal conductivity (*7*) than the high-spin ferropericlase, the spin crossover in ferropericlase would result in continuously enhanced density and reduced radiative thermal conductivity of ferropericlase from the middle part to the lower part of the lower mantle. However, slowing in sound velocities and lowering in pressure derivatives of the sound velocities are expected within the transition region (*9*). The observed increase of the low-spin (Mg,Fe)O at the mid-lower mantle conditions would manifest seismically as a lower-mantle spin transition zone (STZ), characterized by a steeper-than-normal density gradient between ~1000 km and 2200 km in depth (*13*–*15*) (Fig. 4). Spin transition may therefore account for some of the seismic wave heterogeneity in that region, and the existence of the low-spin (Mg,Fe)O at the lowermost mantle conditions may affect the thermal stability of the mantle upwellings (*18*, *19*).

Because the spin crossover of iron occurs in the lower-mantle minerals such as ferropericlase at high pressures and temperatures, the thermal compression curves and sound velocities of the lower-mantle minerals will be continuously influenced by the ratio of the high-spin and low-spin states along the lower-mantle geotherm (Figs. 3 and 4). This renders the use of the classical equations of state with lattice finite strain theory unreliable for modeling the density and sound velocity behavior across the spin crossover (*24*, *27*–*29*). For example, a density increase of ~3 to 4% is observed across the high-spin to low-spin transition in ferropericlase at ~50 GPa (*5*, *11*, *22*). Using a pyrolite lower-mantle composition model (*29*, *30*) with ~33% of ferropericlase and assuming a similar thermal compression behavior in high-spin/low-spin (Mg,Fe)O with various iron content (*22*, *31*, *32*), we predict the spin crossover of iron in (Mg,Fe)O would result in a density difference of ~1% between the extrapolated high-spin and low-spin density profiles, affecting our understanding of the lower-mantle chemistry. Such density increase is equivalent to the addition of ~5.0% FeO into MgO in ferropericlase (*32*) and may be further enhanced if the stiffer low-spin ferropericlase (*5*) exhibits less thermal expansion than that extrapolated using the thermal equation of state of the high-spin ferropericlase (*31*). Therefore, knowledge of the ratio of the high-spin to low-spin states in ferropericlase as well as in the silicate perovskite and post-perovskite is essential to evaluate reliably the composition, geophysics, and dynamics of Earth's lower mantle.

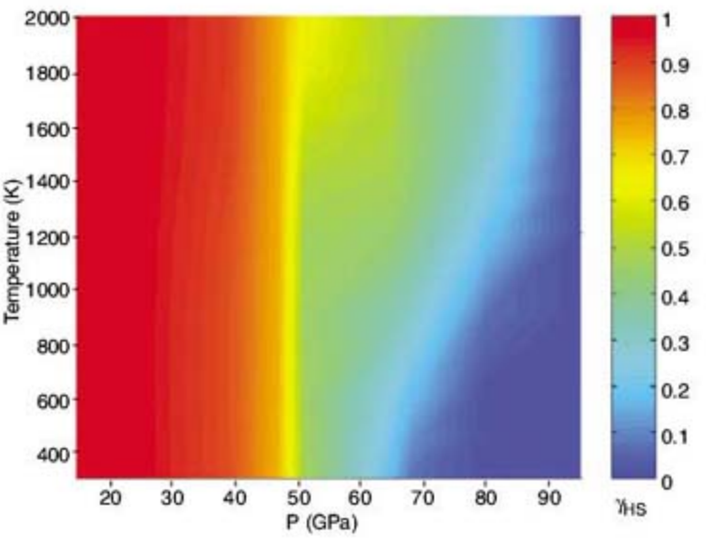

Fig. 3. Isosymmetric spin crossover of Fe^{2+} in $(Mg_{0.75}, Fe_{0.25})O$. The phase diagram is constructed from the interpolation and extrapolation of the derived fractions of the high-spin state in the sample (fig. S2). Colors in the vertical column on the right represent fractions of the high-spin iron, γ_{HS}, in $(Mg_{0.75},Fe_{0.25})O$.

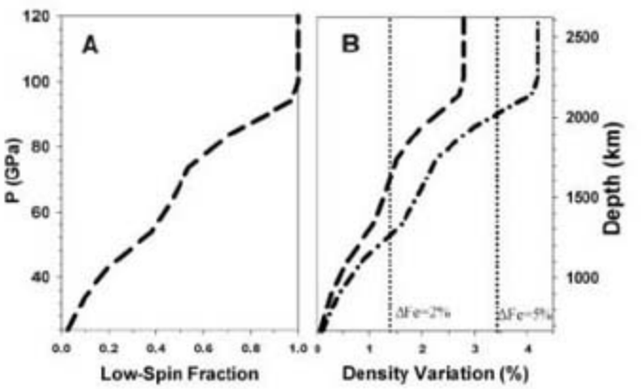

Fig. 4. Derived fractions of the low-spin ferropericlase (**A**) and density variation (**B**) along a model lower-mantle geotherm (*20*). Fraction of the low-spin ferropericlase is derived from an extrapolation of the experimental data in Fig. 3. Density variations in ferropericlase across the spin-crossover region assume that the density varies linearly with the fraction of the low-spin iron (*22*). Dashed line and dash-dotted line represent derived density variations using maximum variations of 2.8% and 4.2% across the spin-crossover region from evaluation of recent experimental (*5*) and theoretical (*11*) data, respectively. Vertical bars represent the density variations caused by 2% and 5% perturbation of total iron content in ferropericlase, respectively, at ambient conditions (*32*).

References and Notes

1. J. Badro *et al.*, *Science* **300**, 789 (2003).
2. J. Badro *et al.*, *Science* **305**, 383 (2004).
3. J. Li *et al.*, *Proc. Natl. Acad. Sci. U.S.A.* **101**, 14027 (2004).
4. J. M. Jackson *et al.*, *Am. Miner.* **90**, 199 (2005).
5. J. F. Lin *et al.*, *Nature* **436**, 377 (2005).
6. W. Sturhahn, J. M. Jackson, J. F. Lin, *Geophys. Res. Lett.* **32**, L12307 (2005).
7. A. F. Goncharov, V. V. Struzhkin, S. D. Jacobsen, *Science* **312**, 1205 (2006).
8. A. M. Hofmeister, *Earth Planet. Sci. Lett.* **243**, 44 (2006).
9. J. F. Lin *et al.*, *Geophys. Res. Lett.* **33**, L22304 (2006).
10. K. Persson, A. Bengtson, G. Ceder, D. Morgan, *Geophys. Res. Lett.* **33**, L16306 (2006).
11. T. Tsuchiya, R. M. Wentzcovitch, C. R. S. da Silva, S. de Gironcoli, *Phys. Rev. Lett.* **96**, 198501 (2006).
12. F. Zhang, A. R. Oganov, *Earth Planet. Sci. Lett.* **249**, 436 (2006).
13. L. H. Kellogg, B. H. Hager, R. D. van der Hilst, *Science* **283**, 1881 (1999).
14. R. D. van der Hilst, H. Kárason, *Science* **283**, 1885 (1999).
15. J. Trampert, F. Deschamps, J. Resovsky, D. Yuen, *Science* **306**, 853 (2004).
16. Y. Kobayashi *et al.*, *Geophys. Res. Lett.* **32**, L19302 (2005).
17. M. Murakami, K. Hirose, N. Sata, Y. Ohishi, *Geophys. Res. Lett.* **32**, L03304 (2005).

18. C. Matyska, D. A. Yuen, *Earth Planet. Sci. Lett.* **154**, 196 (2006).
19. J. B. Naliboff, L. H. Kellogg, *Geophys. Res. Lett.* **33**, L12S09 (2006).
20. J. M. Brown, T. J. Shankland, *Geophys. J. R. Astr. Soc.* **66**, 579 (1981).
21. J. F. Lin *et al.*, *J. Synchrotron Rad* **12**, 637 (2005).
22. Materials and methods are available as supporting material on *Science* Online.
23. G. Vankó *et al.*, *J. Phys. Chem. B* **110**, 11647 (2006).
24. F. Birch, *J. Geophys. Res.* **91**, 4949 (1986).
25. L. S. Dubrovinsky *et al.*, *Science* **289**, 430 (2000).
26. J. F. Lin *et al.*, *Proc. Natl. Acad. Sci. U.S.A.* **100**, 4405 (2003).
27. G. F. Davies, A. M. Dziewonski, *Phys. Earth Planet. Int.* **10**, 336 (1975).
28. T. S. Duffy, D. L. Anderson, *J. Geophys. Res.* **94**, 1895 (1989).
29. E. Mattern, J. Matas, Y. Ricard, J. Bass, *Geophys. J. Int.* **160**, 973 (2005).
30. A. E. Ringwood, *J. Geol.* **90**, 611 (1982).
31. W. van Westrenen *et al.*, *Phys. Earth Planet. Int.* **151**, 163 (2005).
32. S. D. Jacobsen *et al.*, *J. Geophys. Res.* **107**, 2037 (2002).
33. We acknowledge GSECARS, APS, and ANL for the use of the synchrotron and laser facilities and the High Pressure Collaborative Access Team for the use of the ruby system. We thank F. de Groot, J.-P. Rueff, W. Sturhahn, T. Tsuchiya, and W. J. Evans for helpful discussions and G. Shen, M. Hu, and K. Visbeck for their assistance in the experiments. Use of the APS was supported by U.S. Department of Energy (DOE), Office of Science, Basic Energy Sciences, under contract DE-AC02-06CH11357. GSECARS is supported by NSF Earth Sciences (EAR-0622171) and DOE Geosciences (DE-FG02-94ER14466). This work at LLNL was performed under the auspices of the U.S. DOE by University of California and LLNL under contract W-7405-Eng-48. J.-F.L. is also supported by the Lawrence Livermore Fellowship. S.D.J. acknowledges financial support from NSF/EAR 0721449, and V.V.S. acknowledges financial support from DOE.

Supporting Online Material

www.sciencemag.org/cgi/content/full/317/5845/1740/DC1
Materials and Methods
Figs. S1 to S3
References

11 May 2007; accepted 24 July 2007
10.1126/science.1144997

The Primitive Wrist of *Homo floresiensis* and Its Implications for Hominin Evolution

Matthew W. Tocheri,[1]* Caley M. Orr,[2,3] Susan G. Larson,[4] Thomas Sutikna,[5] Jatmiko,[5] E. Wahyu Saptomo,[5] Rokus Awe Due,[5] Tony Djubiantono,[5] Michael J. Morwood,[6] William L. Jungers[4]

Whether the Late Pleistocene hominin fossils from Flores, Indonesia, represent a new species, *Homo floresiensis*, or pathological modern humans has been debated. Analysis of three wrist bones from the holotype specimen (LB1) shows that it retains wrist morphology that is primitive for the African ape-human clade. In contrast, Neandertals and modern humans share derived wrist morphology that forms during embryogenesis, which diminishes the probability that pathology could result in the normal primitive state. This evidence indicates that LB1 is not a modern human with an undiagnosed pathology or growth defect; rather, it represents a species descended from a hominin ancestor that branched off before the origin of the clade that includes modern humans, Neandertals, and their last common ancestor.

The debate over the affinity of the Late Pleistocene hominin fossils from the island of Flores has focused primarily on the craniodental remains of the first specimen (LB1) recovered from Liang Bua cave (*1*–*6*). LB1 is the holotype specimen of a new species, *Homo floresiensis* (*1*, *7*), but some argue that it is a pathological modern human (*4*, *6*). Here we examine the morphology of three wrist bones attributed to LB1 to test these competing hypotheses.

Wrist morphology can be a powerful indicator of phylogenetic relationships in Mammalia because of variation in the number and shape of carpal elements and in the configuration of the articular surfaces (*8*–*12*). In primates, the trapezoid is the wrist bone situated directly proximal to the index finger. The modern human trapezoid is shaped like a boot (*9*, *13*, *14*), wherein the palmar half of the bone is radio-ulnarly and proximo-distally wide (Fig. 1). In contrast, other primates have a trapezoid that is more wedge-shaped with a narrow palmar tip and a wide dorsal base (*9*, *13*–*15*). This difference between human and nonhuman primate trapezoid shape is concomitantly reflected by the shapes and articular configurations of the carpals that articulate with the trapezoid, and all of these carpals are derived in modern humans in comparison to those in other primates (Figs. 2 and 3) (*9*, *13*). Upper Paleolithic *Homo sapiens* and Neandertals share these derived morphological features with modern humans, suggesting that they are most likely inherited from a recent common ancestor (*13*). A capitate attributed to *Homo antecessor* (*16*) and dated to ~0.8 million years ago (Ma) (*17*) also shares the derived condition (*13*, *16*). Thus, the current paleontological evidence suggests that this complex of wrist features evolved by at least 800,000 years ago.

Three complete carpals—a trapezoid, scaphoid, and capitate—all of which are from a left wrist, were recovered along with the cranium, mandible, and additional postcranial material of LB1 in Spit No. 59 of Sector VII during the September 2003 excavation (fig. S1 and table S3) (*1*, *2*, *18*). Each is well preserved and shows no signs of pathology or abnormal development. As shown in Figs. 1 to 3, these three articulating bones display none of the shared, derived features of modern human and Neandertal carpals (*13*). Instead, they show the general symplesiomorphic pattern exhibited by all extant African apes, as well as fossil hominins that preserve comparable wrist morphology and date before 1.7 Ma (*13*, *19*–*22*). Like other nonhuman primates, LB1's trapezoid is (i) wedge-shaped; (ii) the ulnar side of its second metacarpal articulation is oriented more sagittally (Fig. 1, top and bottom rows); (iii) its scaphoid articular surface is more triangular in shape (Fig. 1, middle row); and (iv) it lacks the expanded palmar nonarticular area (Fig. 1, top row) and the more palmarly placed capitate articulation observed in modern humans and Neandertals (Fig. 1, bottom row). We quantified these shape differences using three-dimensional (3D) methods measuring the relative areas and angles of carpal articular surfaces (*13*, *14*, *18*, *23*). Multivariate statistical analysis of these data distinguishes modern humans and Neandertals from the great apes, *Papio*, and LB1 (Fig. 1). Primarily, the trapezoids of modern humans and Neandertals are distinct in their shape and articular configuration as a consequence of the large expansion of palmar nonarticular area, which tends to square off the entire palmar half of the bone (Fig. 1, top row) (*13*).

The scaphoid and capitate of LB1 both exhibit the shapes and articular configurations that occur concomitantly with the primitive hominid trapezoid condition (*13*, *18*), and multivariate analyses of these carpals provide similar results (Figs. 2 and 3). For example, LB1's capitate lacks the enlarged palmarly placed articular surface for the trapezoid observed in modern humans and Neandertals (*9*, *13*) and, instead, shows the waisted neck characteristic of extant

[1]Human Origins Program, Department of Anthropology, National Museum of Natural History, Smithsonian Institution, Washington, DC 20013, USA. [2]School of Human Evolution and Social Change, Arizona State University, AZ 85287, USA. [3]Institute of Human Origins, Arizona State University, AZ 85287, USA. [4]Department of Anatomical Sciences, School of Medicine, Stony Brook University, NY 11794, USA. [5]The National Research and Development Centre for Archaeology, Jakarta, Indonesia. [6]School of Earth and Environmental Sciences, University of Wollongong, NSW 2522, Australia.

*To whom correspondence should be addressed. E-mail: tocherim@si.edu

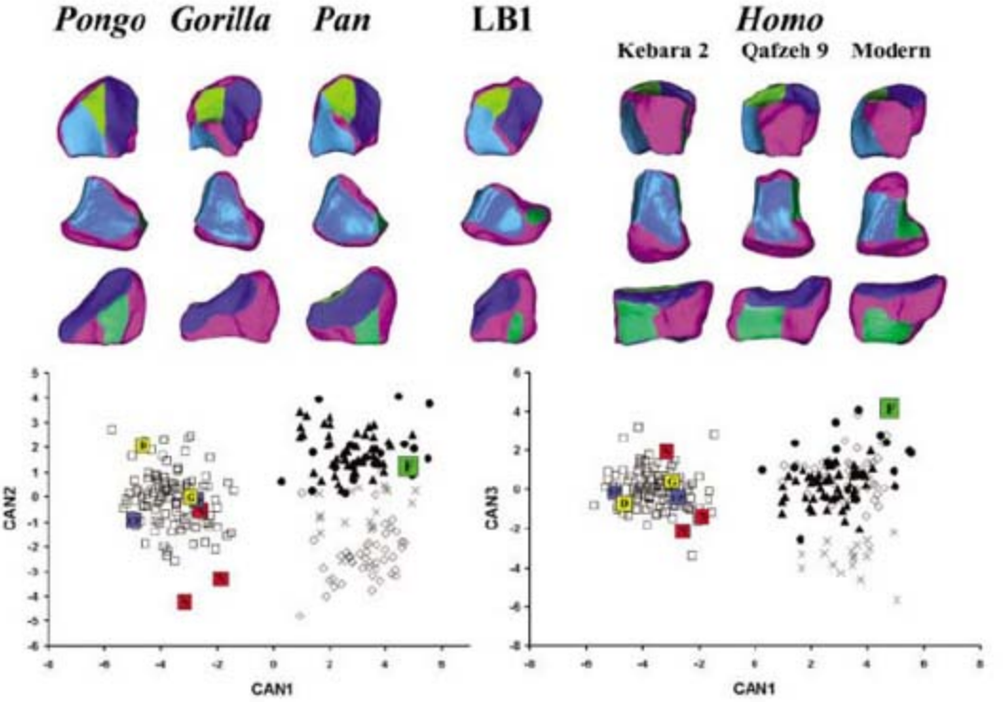

Fig. 1. **(Top)** Palmar (top row), proximal (middle row), and ulnar views (bottom row) of trapezoid morphology (the distal, palmar, and distal borders, respectively, shown toward the page top). All bones are scaled to approximately the same size and shown as from the left wrist. Articular surfaces are as follows: 2nd metacarpal (radial side), yellow; 2nd metacarpal (ulnar side), dark blue; capitate, green; trapezium, light blue; scaphoid, medium blue; nonarticular, pink. **(Bottom)** Plots of the canonical variables (CAN1 to CAN3) generated from 3D trapezoid shape analysis (*13*, *14*, *18*). CAN1 accounts for 76% of the variation, CAN2 accounts for 14%, and CAN3 8% (modern humans, open squares; *Pan*, closed triangles; *Gorilla*, open diamonds; *Pongo*, closed circles; *Papio*, X's; Upper Paleolithic *H. sapiens* (e.g., Qafzeh 9), blue squares (UP); Neandertals (e.g., Kebara 2), red squares (N); modern human pituitary dwarf, yellow square (D); modern human pituitary giant, yellow square (G); *H. floresiensis* (LB1), green square (F).

great apes and *Australopithecus* (Fig. 3, middle row) (*20*). Similarly, the articular surface for the trapezium on LB1's scaphoid does not extend out onto the scaphoid tubercle as it does in modern humans and Neandertals (Fig. 2, middle row) (*13*). However, LB1's scaphoid includes a fused centrale, as does the OH7 scaphoid from Olduvai Gorge (Fig. 2) (*21*, *24*). Congenital fusion of these two carpal elements is a synapomorphy of *Gorilla*, *Pan*, and *Homo* (*25*), and the fossil evidence from LB1 and OH7 further indicates that fusion is the most likely primitive condition for all hominins.

The consistent carpal shape differences between human and nonhuman primates are the result of differences in the cavitation of the carpal mesenchyme during embryonic development (*18*, *26*). In modern humans, the trapezoid, capitate, and trapezium arise in the mesenchyme in essentially their adult form by the 11th week of development, long before the processes of chondrification and ossification are complete, and the remaining carpal elements achieve their distinctive shapes shortly thereafter (*26*). Because of the timing of carpal formation, dysostoses (i.e., errors in cell patterning) or disruptions (i.e., through exposure to toxic substances or infection) may result in malformation of the initial carpal shape (*27*, *28*). However, the transient characteristics of such disturbances most often produce localized skeletal shape abnormalities (e.g., individual bones are affected) that are not typically associated with skeletal dwarfism (*27*, *28*). In contrast, dysplasias usually involve systemic errors in ossification and growth, frequently resulting in dwarfism (*27*, *28*). The genes that result in dysplasias, however, do not normally become expressed until after normal shape formation of the carpal mesenchyme (*27*). Although skeletal dysplasias may include carpal and digit abnormalities related to ossification errors, as well as various forms of microcephaly (*27*), none are known to result in abnormal carpal morphology that closely mimics a plesiomorphic state. Our diverse modern human sample includes a pituitary dwarf (USNM 314306) and a

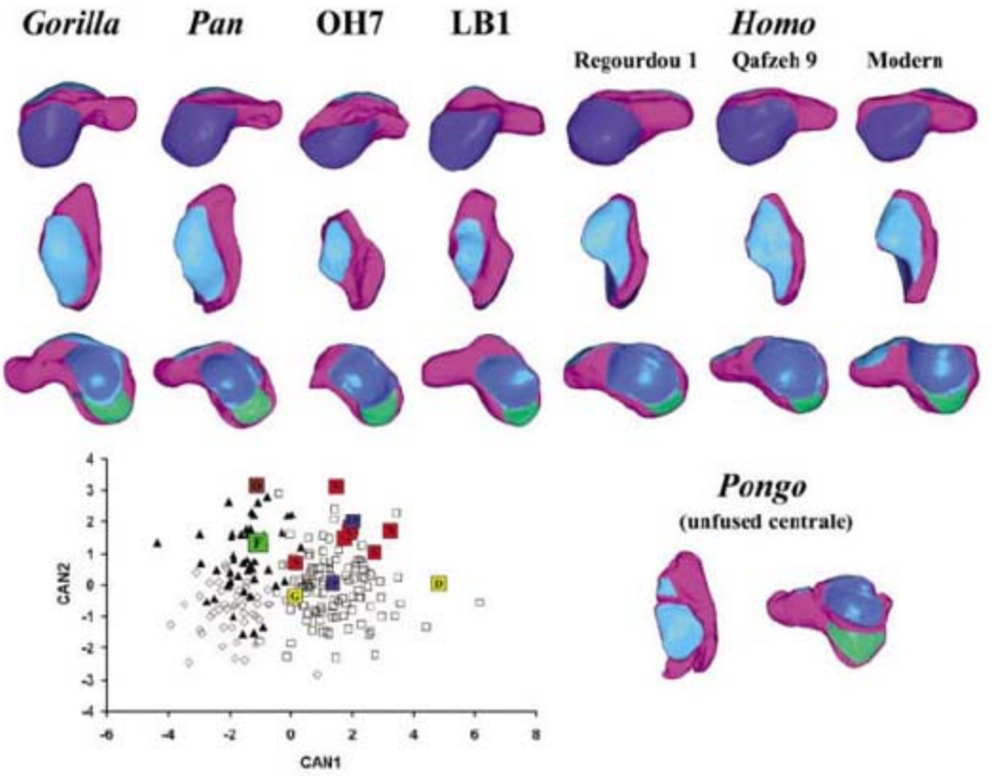

Fig. 2. **(Top)** Radial (top row), distal (middle row), and ulnar views (bottom row) of scaphoid morphology (the distal, palmar, and distal borders, respectively, shown toward the page top). All bones are scaled to approximately the same size and shown as from the left wrist. Regourdou 1 is a Neandertal. Articular surfaces are as follows: radius, dark blue; trapezium-trapezoid, light blue; capitate, medium blue; lunate, green; nonarticular, pink. **(Bottom left)** Plot of the canonical variables (CAN1, CAN2) generated from 3D scaphoid shape analysis (*13*, *18*). CAN1 accounts for 89% of the variation, CAN2 accounts for 11% [symbols as in Fig. 1 plus *H. habilis* (OH7), brown square (O)]. **(Bottom right)** The separate centrale (the primitive condition in primates) is shown articulated with the scaphoid in *Pongo*.

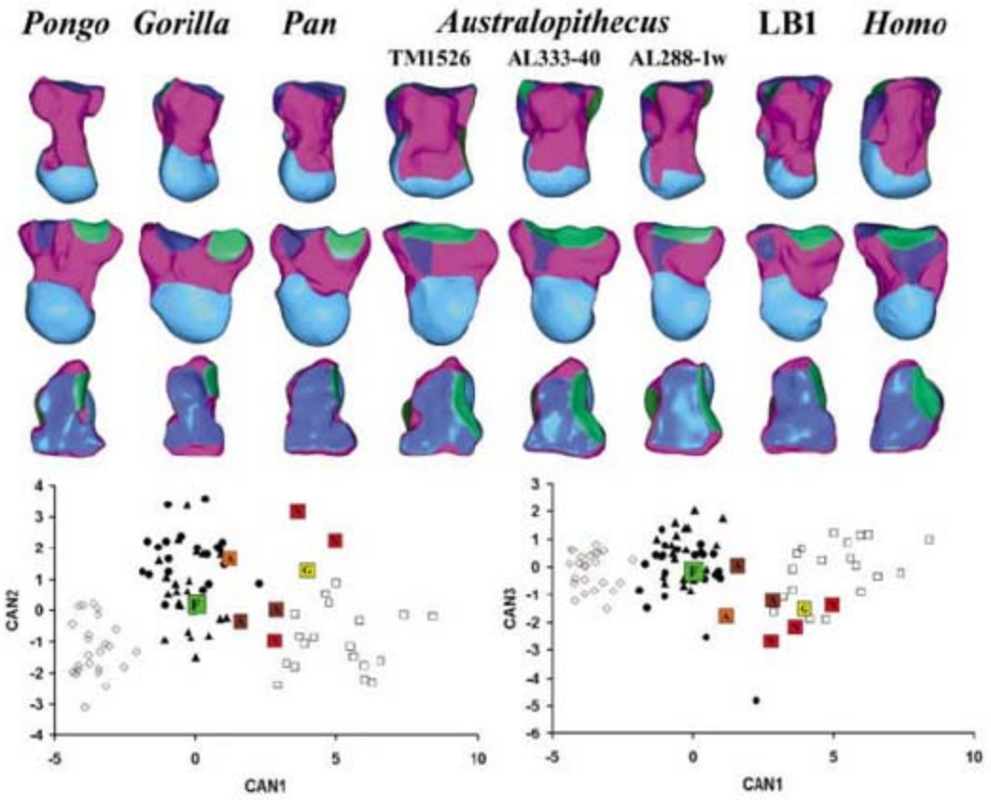

Fig. 3. (Top): Palmar (top row), radial (middle row), and distal views (bottom row) of capitate morphology (the distal, distal, and palmar borders, respectively, shown toward the page top). All bones are scaled to approximately the same size and shown as from the left wrist. Articular surfaces as follows: trapezoid, dark blue; scaphoid-lunate, light blue; 3rd metacarpal, medium blue; 2nd metacarpal, green; nonarticular, pink. **(Bottom)** Plots of the canonical variables (CAN1 to CAN3) generated from 3D capitate shape analysis (*18*). CAN1 accounts for 86% of the variation, CAN2 accounts for 13%, and CAN3 1% [symbols as in Fig. 1 plus *A. africanus* (TM1526), orange square (A); *A. afarensis* (AL333-40 and AL288-1w), brown squares (A)].

pituitary giant (USNM 227508) (tables S1 and S2). Both show normal modern human carpal shapes and articular configurations despite their abnormal sizes, demonstrating that LB1's wrist morphology is not the result of allometric scaling, errors in metabolism, or a skeletal growth disorder.

Our analyses support hypotheses that LB1 is descended from a hominin ancestor that migrated out of Africa before the evolution of the shared, derived wrist morphology that is characteristic of modern humans, Neandertals, and their last common ancestor. The association of LB1 with direct evidence of stone flaking technology comparable to that found at Oldowan or other Lower Paleolithic sites throughout the Old World (*29*) provides additional support for the hypothesis that the earliest hominins to use and make stone tools retained primitive hominin wrist morphology (*13*, *21*, *30*, *31*). The structurally modified wrist of modern humans and Neandertals probably evolved sometime between 1.8 and 0.8 Ma (*13*). These structural modifications form a morphological complex that may represent an adaptation for better distribution of forces radio-ulnarly across the wrist to facilitate the full commitment to tool-related manipulative behaviors that arose in the hominin lineage leading to modern humans and Neandertals (*13*).

The wrist morphology of LB1 may ultimately help falsify or support specific hypotheses regarding the phylogenetic position of *H. floresiensis* (*1*, *5*, *7*). Unfortunately, no carpals are attributed to *Homo erectus* sensu lato, which is otherwise well represented in the fossil record between 1.8 and 0.8 Ma, with the exception of a partial lunate from Zhoukoudian (*32*). However, if hominin carpals that date within this period of time are discovered, their primitive or derived morphology will allow a firmer assessment of their phylogenetic relationship to other Pleistocene hominin species, such as modern *H. sapiens* and *H. floresiensis*.

References and Notes

1. P. Brown *et al.*, *Nature* **431**, 1055 (2004).
2. M. J. Morwood *et al.*, *Nature* **431**, 1087 (2004).
3. D. Falk *et al.*, *Science* **308**, 242 (2005).
4. R. D. Martin, A. M. MacLarnon, J. L. Phillips, W. B. Dobyns, *Anat. Rec.* **288A**, 1123 (2006).
5. D. Argue, D. Donlon, C. Groves, R. Wright, *J. Hum. Evol.* **51**, 360 (2006).
6. T. Jacob *et al.*, *Proc. Natl. Acad. Sci. U.S.A.* **103**, 13421 (2006).
7. M. J. Morwood *et al.*, *Nature* **437**, 1012 (2005).
8. Q. Ji *et al.*, *Nature* **416**, 816 (2002).
9. O. J. Lewis, *Functional Morphology of the Evolving Hand and Foot* (Clarendon, Oxford, UK, 1989).
10. E. E. Sarmiento, E. Stiner, K. Mowbray, *New Anat.* **269**, 50 (2002).
11. B. J. Stafford, R. W. Thorington Jr., *J. Morphol.* **235**, 135 (1998).
12. R. W. Thorington Jr., K. Darrow, *J. Morphol.* **246**, 85 (2000).
13. M. W. Tocheri, thesis, Arizona State University, Tempe (2007).
14. M. W. Tocheri, A. Razdan, R. C. Williams, M. W. Marzke, *J. Hum. Evol.* **49**, 570 (2005).
15. E. E. Sarmiento, *Am. Mus. Novit.* **3091**, 1 (1994).
16. C. Lorenzo, J. L. Arsuaga, J. M. Carretero, *J. Hum. Evol.* **37**, 501 (1999).
17. C. Falgueres *et al.*, *J. Hum. Evol.* **37**, 343 (1999).
18. Additional information is available as supporting material on *Science* Online.
19. M. W. Marzke, *J. Hum. Evol.* **12**, 197 (1983).
20. H. M. McHenry, *Am. J. Phys. Anthropol.* **62**, 187 (1983).
21. J. R. Napier, *Nature* **196**, 409 (1962).
22. C. V. Ward, M. G. Leakey, A. Walker, *Evol. Anthropol.* **7**, 197 (1999).
23. M. W. Tocheri *et al.*, *Am. J. Phys. Anthropol.* **122**, 101 (2003).
24. R. L. Susman, N. Creel, *Am. J. Phys. Anthropol.* **51**, 311 (1979).
25. T. L. Kivell, D. R. Begun, *J. Hum. Evol.* **52**, 321 (2007).
26. R. Čihák, *Ergeb. Anat. Entwicklungsgesch.* **46**, 1 (1972).
27. J. W. Spranger, P. W. Brill, A. K. Poznanski, *Bone Dysplasias: An Atlas of Genetic Disorders of Skeletal Development* (Oxford Univ. Press, Oxford, UK, ed. 2, 2002).
28. E. Zelzer, B. R. Olsen, *Nature* **423**, 343 (2003).
29. M. W. Moore, A. Brumm, *J. Hum. Evol.* **52**, 85 (2007).
30. M. A. Panger, A. S. Brooks, B. G. Richmond, B. Wood, *Evol. Anthropol.* **11**, 235 (2002).
31. S. Semaw *et al.*, *Nature* **385**, 333 (1997).
32. F. Weidenreich, *Paleontol. Sin. Ser. D* **5**, 1 (1941).

33. We thank the people and staff of the National Research and Development Centre for Archaeology (formerly the Indonesian Centre for Archaeology) for their kind and continuing assistance in the field and lab; L. Cornish for conservation efforts on the Flores hominins funded by the Wenner-Gren Foundation; R. Potts, D. Ortner, C. Tryon, B. Pobiner, K. Kovarvic, C. Campisano, J. Clark, B. Frohlich, J. Yellen, A. Brooks, C. Ward, J. Hodgkins, L. Delezene, J. Scott, and M. Nargowalla for thoughtful discussions; and D. Hunt, L. Gordon, R. Thorington, B. Latimer, L. Jellema, E. Gilissen, W. Wendelen, B. Kimbel, D. Johanson, and E. Trinkaus for access to comparative material. Additional thanks to M. Marzke, R. Williams, A. Razdan, J. Femiani, G. Farin, D. Collins, and the Partnership for Research In Spatial Modeling (PRISM) at Arizona State University (ASU). Aspects of this research were supported in part by NSF [grant IIS-998016 to A. Razdan (ASU), grant BCS-0218511 to R. Potts (Smithsonian)], a Social Sciences and Humanities Research Council of Canada Doctoral Fellowship (award 752-2002-0432 to M.W.T.), a Smithsonian Institution Predoctoral Fellowship (M.W.T.), a Discovery Project Grant from the Australian Research Council (M.J.M.), and grants from the University of New England (M.J.M.). Additional support from the School of Human Evolution and Social Change at ASU, the Leakey Foundation, the National Geographic Society, and the Human Origins Program and Department of Anthropology at the Smithsonian Institution National Museum of Natural History is also greatly appreciated.

Supporting Online Material

www.sciencemag.org/cgi/content/full/317/5845/1743/DC1
SOM Text
Fig. S1
Tables S1 to S11
References

28 June 2007; accepted 15 August 2007
10.1126/science.1147143

Structure of the Zinc Transporter YiiP

Min Lu and Dax Fu*

YiiP is a membrane transporter that catalyzes Zn^{2+}/H^{+} exchange across the inner membrane of *Escherichia coli*. Mammalian homologs of YiiP play critical roles in zinc homeostasis and cell signaling. Here, we report the x-ray structure of YiiP in complex with zinc at 3.8 angstrom resolution. YiiP is a homodimer held together in a parallel orientation through four Zn^{2+} ions at the interface of the cytoplasmic domains, whereas the two transmembrane domains swing out to yield a Y-shaped structure. In each protomer, the cytoplasmic domain adopts a metallochaperone-like protein fold; the transmembrane domain features a bundle of six transmembrane helices and a tetrahedral Zn^{2+} binding site located in a cavity that is open to both the membrane outer leaflet and the periplasm.

Zinc is essential for cellular growth and differentiation. The total zinc content in a living cell is sustained at submillimolar levels, mostly in a protein-bound form (*1*). The ligated zinc can serve as catalytic or structural cofactors in a host of biological processes ranging from gene expression to immune functions (*2*). A pool of loosely bound zinc in the brain plays an additional role in modulating neurotransmission (*3*). Presynaptic vesicles of glutamatergic neurons and insulin-containing secretory vesicles of pancreatic β cells are particularly rich in zinc, with concentrations exceeding 1 mM (*4*, *5*). Although zinc is abundant in certain specialized subcellular organelles, abnormally elevated zinc concentrations in the cytoplasm may exert cytotoxic effects. For instance, excessive zinc may contribute to neuronal cell death during brain ischemia (*6*) and to β-amyloid deposition in Alzheimer's disease (*7*, *8*). Therefore, the free cytoplasmic zinc concentration of a living cell is maintained well below the nanomolar level (*9*).

A family of ubiquitous zinc transporters, termed cation diffusion facilitator (CDF), is critically involved in controls of cytoplasmic zinc build-ups, either by facilitating zinc efflux to the cell exterior or by accumulating the excess zinc in intracellular storage organelles (*10*, *11*). These zinc transporters move Zn^{2+} across the otherwise impermeable membrane barriers. In glutamatergic synapses, a mammalian CDF, known as ZnT-3 (zinc transporter-3), is responsible for sequestering cytoplasmic Zn^{2+} into presynaptic vesicles (*12*). In pancreatic β cells, yet another mammalian CDF, ZnT-8 (*SLC30A8*), stimulates zinc accumulation in the insulin secretory vesicles (*13*). Emerging evidence has linked ZnT-8 to the pathogenesis of type 2 diabetes (*14*). At present, little is known about the structure and molecular mechanism of ZnTs. Three bacterial CDF homologs, YiiP and ZitB from *Escherichia coli* and CzcD from *Ralstonia metallidurans*, have been characterized functionally and are related to their mammalian counterparts with 25 to 30% sequence identity (Fig. 1). YiiP is a homodimer of two 33-kD integral membrane proteins (*15*), each composed of six transmembrane segments (TMs) and a hydrophilic C-terminal domain (CTD) located in the cytoplasm (*16*). Metal binding and transport by YiiP have been mapped to strictly conserved D49 and D157 in the transmembrane domain (TMD) with binding affinities for Zn^{2+} and Cd^{2+} in the submicromolar range (*17*). The transcription of *yiiP* gene in *E. coli* is inducible by both Zn^{2+} and Fe^{2+} (*18*, *19*), although YiiP expression seems to promote iron detoxification only. However, direct transport measurement using native membrane vesicles indicated that YiiP catalyzes Zn^{2+}/H^{+} antiport (*19*).

We obtained YiiP crystals following an extensive screening for crystallization conditions. Although several metal ions improved the stability of YiiP in detergent micelles, only Zn^{2+} yielded crystals of diffraction quality. X-ray diffraction data were obtained from native crystals and 12 heavy-atom derivative crystals for multiple isomorphous replacement and anomalous scattering phasing (table S1) (*20*). The resulting experimental maps to 3.8 Å revealed two YiiP protomers per asymmetric unit, one of which could be readily traced as a continuous polypeptide chain (figs. S1 and S2), whereas the other is more disordered as a result of less favorable crystal contacts. Protein sequence registration was established by using electron densities for bulky side chains and 11 major heavy metal binding sites (table S2). Subsequent structure refinement and model rebuilding resulted in a structural model with R_{cryst} and R_{free} of 32.2% and 32.9%, respectively. The final model contained all but the first 4 and the last 10 residues of the 300 amino acids in each protomer.

The physiological YiiP homodimer is arranged around a two-fold crystallographic axis oriented perpendicular to the membrane plane (Fig. 2A). Two bands of aromatic residues on the protein surface suggest the boundaries of the membrane-embedded region. The CTDs protrude into the cytoplasm and juxtapose each other in parallel to form the major dimerization contact. At the CTD and TMD juncture, intracellular loops form another dimerization contact, from which two TMDs swing outward and plunge into the membrane with a 60° crossing angle. Viewed from the membrane plane, this dimeric structure exhibits a Y-shaped architecture, with each arm formed by a TMD; the bulk of the Y stem is provided by the associated CTDs. Given this orientation within

Fig. 1. Sequence alignment of YiiP and representative members of the CDF protein family. Conserved and homologous residues are colored in magenta and light-brown respectively. Regions of secondary structural elements in YiiP are outlined. Magenta and cyan dots indicate residues involved in Zn^{2+} binding and dimerization contacts, respectively. Dots within the two human sequences indicate omitted residues in a loop (IL2) between TM4 and TM5. The signature sequence suggested for the CDF family corresponds to the aligned YiiP sequence from residues 36 to 49 (*27*).

Department of Biology, Brookhaven National Laboratory, Upton, NY 11973, USA.

*To whom correspondence should be addressed. E-mail: dax@bnl.gov

the membrane, the void space observed between two TMDs is likely to be filled with phospholipids in vivo. Viewed from extracellular side down the two-fold axis (Fig. 2B), the lower protein density between TMDs is consistent with a distinctive constriction of electron density at the dimer interface of a YiiP projection map obtained in the native *E. coli* lipid bilayer (*15*).

Residues from 1 to 211 of YiiP are folded into the TMD as a compact six-helix bundle (Fig. 2). Interdigitations of helices in YiiP all fall into the "knobs-into-holes" type of contact, and the crossing angles between helices are within the optimal range. A lack of helix-breaking proline residues in the middle of transmembrane helices suggests a rather limited conformational flexibility in the TMD. Threading across the membrane six times, transmembrane helices are linked together by three extracellular loops, denoted as EL1 to EL3, and two intracellular loops, IL1 and IL2 (Fig. 1). An additional intracellular loop, IL3, connects TM6 to the CTD. IL1 extends toward the dimer interface and forms a dimerization contact with IL3 from the neighboring subunit (Fig. 2B). Related by the two-fold symmetry, IL3 and IL1 of the neighboring subunit form another dimerization contact. IL2 makes a short connection between TM4 and TM5, with only four residues from position 141 to 144 (Fig. 2A).

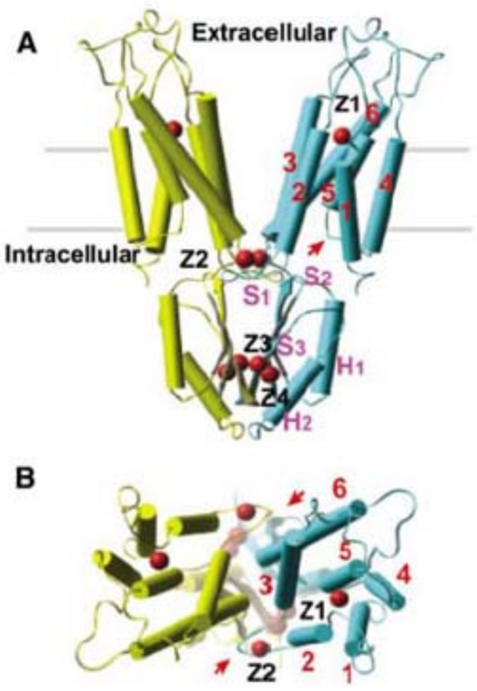

Fig. 2. YiiP with bound Zn^{2+}. **(A)** YiiP homodimer (yellow and cyan for each protomer) viewed from the membrane plane. Zn^{2+} ions are represented by red spheres and labeled as Z1 to Z4. Transmembrane helixes are numbered 1 to 6, α helices and β strands in CTD are labeled as H1 and H2, and S1 to S3, respectively. IL2 is indicated by an arrow. **(B)** View from the extracellular side along the membrane normal. Dimerization contacts between IL1 and IL3 are indicated by arrows.

The length of TM5 is conspicuously short, accounting for three and a half helical turns from residue V147 to M159. This short helix is largely sequestered in the center of the six-helix bundle, thereby giving rise to one extracellular and one intracellular cavity on either side of the membrane (Fig. 3A). The extracellular cavity is accessible from the bulk solvent and exposed to the membrane outer leaflet (Fig. 3C). This cavity spans nearly half of the membrane thickness and anchors a Zn^{2+} ion near the bottom. The intracellular cavity is confined between the TMD and CTD (Fig. 3A). The extended IL1 and IL3 partially obstruct lateral solvent accessibility to the cavity along the cytoplasmic face of the membrane, while the short IL2 makes room for full solvent access from the distal side of the dimer interface. The dome of the intracellular cavity is capped by three highly conserved residues at the amino end of TM5, V147, R148, and A149. Directly under the dome lie the conserved R11 from TM1, E79 from TM3, E200 from TM6, and a variable Q145 from IL2 (Fig. 3D). The two cavities are open to different sides of the membrane and point toward each other within the membrane, but no connecting channel exists between them (Fig. 3B).

Residues from 212 to 300 of CTD are folded into an open α-β domain with two α helices (H1 and H2) aligned on one side and a three-stranded mixed β sheet (S1 to S3) on the other side (fig. S3). The CTD exhibits an overall structural similarity with the copper metallochaperone Hah1 (*21*), although there is no sequence homology between CTD and Hah1. To a first approximation, the topologies of the CTD αβ-βαβ and the Hah1 βαβ-βαβ fold are identical except that the first β strand in Hah1 loops out as IL3 in YiiP. The αβ-βα structural core of CTD from H1 to H2 can be superimposed onto the equivalent portion of Hah1 with a root mean square deviation of 1.8 Å for 42 common Cα positions. To date, all known structures of metallochaperones and their target domains have shared a common metallochaperone-like fold (*22*, *23*). The fold of CTD places it into the same structural category as a possible Zn^{2+} receiving domain.

Anomalous difference Fourier maps of native crystals were computed using experimental phases and diffraction data collected at the zinc edge. Four strong anomalous peaks indicate the presence of four Zn^{2+}-populated sites (designated as Z1 to Z4) in each protomer (Fig. 4). Calorimetric titrations of EDTA pretreated YiiP yielded 2.6 Zn^{2+} stoichiometric units per YiiP protomer, corresponding to two Zn^{2+}-binding sites with an overall dissociation constant (K_d) of 0.24 μM and a low-affinity component (K_d = 145 μM) (*16*). The free Zn^{2+} concentration in the crystallization solution is buffered by citrate within the micromolar range (*24*); thus, only the two high-affinity sites (K_d = 0.24 μM) may have been mostly saturated to become visible in electron density maps. Anomalous peak heights from site Z1 to Z4 increase progressively from 4.6 and 5.8 to 9.6 and 9.6 σ, revealing a rank order of Zn^{2+} occupancy consistent with Z1 and Z2 as being EDTA chelatable, and Z3 and Z4 as EDTA resistant. The EDTA-resistant sites did not respond to calorimetric titrations, but they likely exist because prolonged EDTA chelation denatured YiiP (*25*).

The Zn^{2+} in site Z1 is tetracoordinated by highly conserved D45, D49 from TM2, and H153, D157 from TM5 (Fig. 4). All these res-

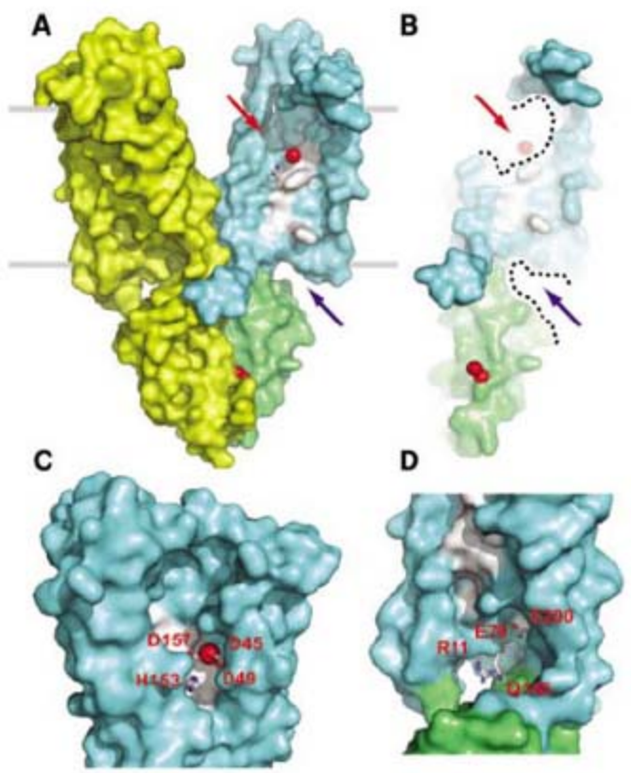

Fig. 3. Extracellular and intracellular cavities. **(A)** YiiP dimer is viewed from the membrane plane. The front portions of TM1, TM2, and CTD of one protomer (cyan) are removed to reveal the embedded TM5 (gray patch), the extracellular cavity (red arrow), and the intracellular cavity (blue arrow). TMD and CTD are colored cyan and green, respectively. **(B)** A cross section of a YiiP monomer with both the front and back portions removed to highlight the barrier that separates two cavities. The cavity boundaries are outlined by dashed lines. **(C)** Close-up view of the extracellular cavity along the red arrow. A bound Zn^{2+} near the bottom is colored red, and its coordination residues are drawn as sticks. **(D)** Close-up view of the intracellular cavity along the blue arrow, with R11, E79, Q145, and E200 drawn as sticks.

idues are essential for Zn^{2+} transport activity (*17*). The tetrahedral coordination is a preferred geometry for Zn^{2+} binding. Consistently, metal binding to cysteine substitutes of D49 and D157 is selective for Zn^{2+} and its isomorphous Cd^{2+} but discriminative against Ca^{2+}, Mg^{2+}, Ni^{2+}, Co^{2+}, and Mn^{2+}, all of which favor different coordination geometries (*16*, *17*). Site Z1 is located near the bottom of the extracellular cavity and exposed to aliphatic lipid chains, where hydrophobic mismatch between packing lipids and the irregular cavity surface may create water-filled packing defects in the lipid matrix.

The Zn^{2+} in site Z2 binds to the intracellular loop that connects TM2 and TM3 (IL1) (Fig. 4). This loop is semiconserved and harbors many potential Zn^{2+} ligating residues. Side chains in this region are not well resolved, but the primary Zn^{2+} coordination shell appears to involve D68 and H75. Additional coordination residues may complete the tetrahedral coordinate geometry. Although the functional role of site Z2 has yet to be defined, its involvement in subunit dimerization is evident. Site Z2 is adjacent to a cluster of highly conserved residues at the dimer interface, including S72 and F73 from IL1, K77 and L81 from the amino end of TM3, and L205, L206, and D207 from IL3 of the neighboring subunit. These residues make direct hydrogen bonds and Van der Waals interactions across the dimer interface.

Located within a cleft between two CTDs, sites Z3 and Z4 appear to be bridged by the highly conserved D285 through a bidentate coordination (Fig. 4). The two Zn^{2+} ions align nearly perpendicular to the long axis of the β sheet, thereby straddling all three β strands of one subunit and coordinating residues from H2 of the neighboring subunit. Unambiguous placement of side chains was not feasible in the β-sheet region, but it is evident that the binuclear Zn^{2+} binding establishes a coordination network at least involving H232 from S1, H283 and D285 from S3, and H261 from H2 of the neighboring subunit. Furthermore, a two-fold related binuclear Zn^{2+} cluster is located on the opposite side of the CTD dimer interface (Fig. 4). The positioning of two Zn^{2+} clusters and their resistance to EDTA chelation suggest a structural role that they may play in strengthening the dimerization contact.

The structure of YiiP provides a model for rationalizing mutagenic results from CzcD and ZitB (*26*) (Fig. 1). In TM1, a $CzcD^{E31k}$ mutation abolished the transport activity. The YiiP equivalent of $CzcD^{E31}$ is a membrane-embedded K27, which seems to be stabilized by D45 of site Z1. In CzcD, an H49 is in place of $YiiP^{D45}$, which is incapable of stabilizing the positive charge on $CzcD^{E31K}$. In TM2, mutations of $CzcD^{H49}$, $CzcD^{D53}$, $ZitB^{H53}$, and $ZitB^{D57}$ resulted in functionless proteins, because their YiiP equivalents (D45 and D49) contribute to site Z1. In TM4, $ZitB^{N135}$ is required for function, and its YiiP equivalent (T128) wedges between TM1 and TM5 into a hydrophobic pocket near site Z1. In TM5, mutations of $CzcD^{E154}$, $CzcD^{D158}$, $ZitB^{H159}$, and $ZitB^{D163}$ abolished transport activity, and these residues in YiiP (H153 and D157) contribute to site Z1. Near the amino end of TM6, a strictly conserved $YiiP^{D179}$ is involved in crystal contacts, obscuring its functional implications. In addition, $ZitB^{E214A}$, $CzcD^{H237R}$, and $CzcD^{H280}$ impaired transport activity. Their YiiP equivalents are all involved in dimerization contacts. The emerging pattern of structure-function correlation is the clustering of loss-of-function mutations around site Z1 and the dimer interface. Although two TMDs in the YiiP structure swing out as separated transmembrane units, dimerization seems essential for YiiP function.

The low-resolution YiiP structure is characterized by two water-filled cavities, which collectively penetrate more than half of the membrane thickness from opposite membrane surfaces. The tetrahedral Zn^{2+} binding site (site Z1) near the bottom of the extracellular cavity is separated from a cluster of conserved residues located near the dome of the intracellular cavity. Although no Zn^{2+} binding was observed within the intracellular cavity of the current structure, a similar cation (Cd^{2+}) can be placed at the cavity entrance by superimposing one subunit of an Hah1-Cd^{2+}-Hah1 dimer onto the YiiP CTD. We propose that the binding of a putative Zn^{2+} metallochaperone to YiiP CTD may deliver a cytoplasmic Zn^{2+} to the intracellular cavity where the Zn^{2+} is then translocated across the membrane to site Z1 in the extracellular cavity.

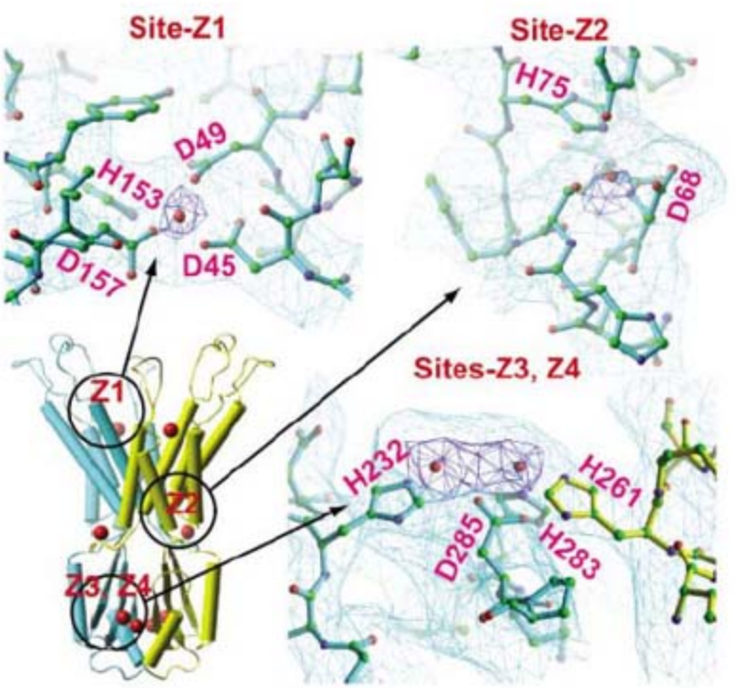

Fig. 4. Zn^{2+} binding sites. Zn^{2+} ions are represented by red spheres. The overall locations of sites Z1 to Z4 in the Yiip dimer are circled. Protein residues (cyan and yellow) and their experimental electron densities (light cyan) at 1.2 σ contour levels overlay zinc difference anomalous Fourier maps (blue) contoured at 3.5 σ, 4.0 σ, and 6.0 σ for sites Z1, Z2, and Z3-Z4, respectively.

References and Notes

1. B. L. Vallee, K. H. Falchuk, *Physiol. Rev.* **73**, 79 (1993).
2. J. M. Berg, Y. Shi, *Science* **271**, 1081 (1996).
3. K. Hirzel *et al.*, *Neuron* **52**, 679 (2006).
4. C. J. Frederickson, A. Bush, *Biometals* **14**, 353 (2001).
5. G. Dodson, D. Steiner, *Curr. Opin. Struct. Biol.* **8**, 189 (1998).
6. J. Y. Koh *et al.*, *Science* **272**, 1013 (1996).
7. A. I. Bush *et al.*, *Science* **265**, 1464 (1994).
8. J. Y. Lee *et al.*, *Proc. Natl. Acad. Sci. U.S.A.* **99**, 7705 (2002).
9. C. E. Outten, T. O'Halloran, *Science* **292**, 2488 (2001).
10. R. D. Palmiter, S. Findley, *EMBO J.* **14**, 639 (1995).
11. D. H. Nies, S. Silver, *J. Ind. Microbiol.* **14**, 186 (1995).
12. T. B. Cole *et al.*, *Proc. Natl. Acad. Sci. U.S.A.* **96**, 1716 (1999).
13. F. Chimienti *et al.*, *J. Cell Sci.* **119**, 4199 (2006).
14. R. Sladek *et al.*, *Nature* **445**, 881 (2007).
15. Y. Wei, H. Li, D. Fu, *J. Biol. Chem.* **279**, 39251 (2004).
16. Y. Wei, D. Fu, *J. Biol. Chem.* **280**, 33716 (2005).
17. Y. Wei, D. Fu, *J. Biol. Chem.* **281**, 23492 (2006).
18. G. Grass *et al.*, *J. Bacteriol.* **183**, 4664 (2001).
19. G. Grass *et al.*, *Arch. Microbiol.* **183**, 9 (2005).
20. Materials, methods, and structure statistics are available as supporting material on *Science* Online.
21. A. K. Wernimont *et al.*, *Nat. Struct. Biol.* **7**, 766 (2000).
22. A. C. Rosenzweig, T. V. O'Halloran, *Curr. Opin. Chem. Biol.* **4**, 140 (2000).
23. L. A. Finney, T. V. O'Halloran, *Science* **300**, 931 (2003).
24. T. E. Furia, *Handbook of Food Additives* (CRC Press, Cleveland, ed. 2, 1980).
25. Y. Chao, D. Fu, *J. Biol. Chem.* **279**, 17173 (2004).
26. A. Anton *et al.*, *J. Bacteriol.* **186**, 7499 (2004).
27. I. T. Paulsen, M. J. Saier, *J. Membr. Biol.* **156**, 99 (1997).

28. We thank A. Heroux, A. Soares, and A. Saxena for assistance in data collection and J. Shanklin, P. Freimuth, P. Maloney, and C. Anderson for comments. This work was supported by the National Institutes of Health (D.F.) and the Biology Department of Brookhaven National Laboratory, U.S. Department of Energy. The coordinates for the structure have been deposited in the Protein Data Bank under the accession code 2QFI.

Supporting Online Material

www.sciencemag.org/cgi/content/full/1143748/DC1
Materials and Methods
Figs. S1 to S3
Tables S1 and S2
References

12 April 2007; accepted 7 August 2007
Published online 23 August 2007;
10.1126/science.1143748
Include this information when citing this paper.

Multicolor Super-Resolution Imaging with Photo-Switchable Fluorescent Probes

Mark Bates,[1] Bo Huang,[2,3] Graham T. Dempsey,[4] Xiaowei Zhuang[2,3,5]*

Recent advances in far-field optical nanoscopy have enabled fluorescence imaging with a spatial resolution of 20 to 50 nanometers. Multicolor super-resolution imaging, however, remains a challenging task. Here, we introduce a family of photo-switchable fluorescent probes and demonstrate multicolor stochastic optical reconstruction microscopy (STORM). Each probe consists of a photo-switchable "reporter" fluorophore that can be cycled between fluorescent and dark states, and an "activator" that facilitates photo-activation of the reporter. Combinatorial pairing of reporters and activators allows the creation of probes with many distinct colors. Iterative, color-specific activation of sparse subsets of these probes allows their localization with nanometer accuracy, enabling the construction of a super-resolution STORM image. Using this approach, we demonstrate multicolor imaging of DNA model samples and mammalian cells with 20- to 30-nanometer resolution. This technique will facilitate direct visualization of molecular interactions at the nanometer scale.

As one of the most versatile imaging modalities in biology, fluorescence microscopy allows noninvasive imaging of cells and tissues with molecular specificity. The availability of fluorescent probes in many colors and the ability to label specific gene products enable visualization of molecular interactions in biological samples. However, the spatial resolution of optical microscopy, classically limited by the diffraction of light to ~300 nm, is inconveniently situated one to two orders of magnitude above the typical molecular length scales in cells. Various "super-resolution" optical imaging techniques have been developed to overcome this limit (*1*, *2*). Among these methods, stimulated emission depletion microscopy (STED) and reversible saturable optically linear fluorescent transition (RESOLFT) techniques (*2*, *3*), saturated structured illumination microscopy (SSIM) (*4*), stochastic optical reconstruction microscopy (STORM) (*5*), and photoactivated localization microscopy (PALM) (*6*, *7*) have achieved 20- to 50-nm resolution in the far field and promise to preserve the inherent noninvasive imaging capability of optical microscopy. In certain cases, binding kinetics or translational motions of individual molecules have also been used to map out high-resolution structures in cells (*8*–*10*).

Nonetheless, multicolor super-resolution imaging remains a difficult task, leaving many biological questions beyond the reach of optical methods. Among the various multicolor imaging techniques, fluorescence resonance energy transfer (FRET) is particularly powerful for probing molecular interactions on the nanometer scale (*11*–*14*), although it is difficult to determine the precise locations and organizations of molecules from a FRET image. Fluorescence colocalization offers another approach to detect molecular interactions, but has traditionally been used within the boundaries of diffraction-limited imaging and would benefit from a combination with super-resolution techniques (*15*). Here, we report a family of photo-switchable probes with distinct colors and demonstrate multicolor STORM imaging with 20- to 30-nm resolution.

STORM relies on the detection of single fluorescent molecules (*16*) and the localization of these molecules with nanometer accuracy (*17*–*21*). Limited only by the number of photons detected (*17*), localization accuracies as high as 0.1 to 1 nm can be achieved for bright fluorescent or scattering objects (*22*–*25*). By using photo-switchable probes, one can modulate the fluorescence emission profile of individual fluorophores in time such that only an optically resolvable subset of fluorophores are activated at any moment, allowing their localization with high accuracy. Over the course of multiple activation cycles, the positions of numerous fluorophores are determined and used to construct a high-resolution STORM image (*5*–*7*). The development of multicolor STORM thus depends on the construction of bright, photo-switchable probes with distinct colors.

To search for chromatically distinguishable photo-switchable probes, we turned to cyanine dyes with various lengths of polymethine chains (fig. S1) (*26*–*28*). We constructed a series of dye pairs, each consisting of a cyanine dye and a shorter-wavelength chromophore, as inspired by our earlier work on photo-switchable Cy5 (*27*). These dye pairs were conjugated to double-stranded DNA or antibody and immobilized on microscope slides for single-molecule detection (*26*). A series of cyanine dyes with distinct absorption and emission spectra displayed robust photo-switching behavior when paired with a Cy3 molecule in close proximity (fig. S1) (*26*). Figure 1A shows fluorescence time traces obtained from single molecules of Cy5, Cy5.5, and Cy7 as they undergo multiple switching cycles. Upon illumination with a red laser (657 nm), each of the three dyes was initially fluorescent and then quickly switched into a nonfluorescent, dark state. A brief exposure to a green laser pulse (532 nm) led to reactivation of the dyes back to the fluorescent state. Without a proximal Cy3, the reactivation of Cy5, Cy5.5, or Cy7 was barely detectable under our excitation conditions. We therefore refer to the Cy3 dye as the "activator" and Cy5, Cy5.5, or Cy7 as the photo-switchable "reporter." These reporters typically can be switched on and off for hundreds of cycles before permanently photobleaching.

The rate constant of switching from the fluorescent to the dark state, designated k_{off}, scaled linearly with the red laser power (Fig. 1B). Consistent with this observation, the average number of photons detected per switching cycle was a constant, independent of the laser power. The number of photons detected was ~3000 for Cy5 and Cy5.5 and ~500 for Cy7 under prism-type total internal reflection fluorescence (TIRF) imaging geometry, and these numbers doubled under objective-type TIRF imaging geometry (*26*). The activation rate, k_{on}, from the dark to the fluorescent state, was linear with respect to the green laser power (Fig. 1B). The linear dependence of both rate constants extended over the entire range of laser powers tested, suggesting that faster switching rates are possible at higher laser intensities. As shown previously, their distinct emission spectra (fig. S1) allow Cy5, Cy5.5, and Cy7 to be distinguished at the single-molecule level (*29*), suggesting one approach to accomplish multicolor STORM imaging.

The above results indicate that chromatically distinguishable photo-switchable reporters can be activated by the same activator dye. As a further exploration, we tested whether other dyes with distinct spectral properties can be used as activators. To this end, Cy3, Cy2, and Alexa Fluor 405 (fig. S1) (*26*) were paired with Cy5. Switching traces for individual pairs are shown in Fig. 1C. Again, Cy5 was quickly switched into the dark state upon illumination with a red laser. The activation of Cy5, however, required different-colored lasers corresponding to the absorption wavelengths of the activators. The Alexa 405-Cy5 pair was efficiently activated by a violet laser (405 nm), but was much less sensitive to blue (457 nm) and green (532 nm) activation light. Similarly, the Cy2-Cy5 pair and Cy3-Cy5 pair were most sensitive to the blue and green lasers, respectively. To determine the activation specificity quantitatively, we measured the activation rate constants for these dye pairs at the

[1]School of Engineering and Applied Sciences, Harvard University, Cambridge, MA 02138, USA. [2]Howard Hughes Medical Institute, Harvard University, Cambridge, MA 02138, USA. [3]Department of Chemistry and Chemical Biology, Harvard University, Cambridge, MA 02138, USA. [4]Graduate Program in Biophysics, Harvard University, Cambridge, MA 02138, USA. [5]Department of Physics, Harvard University, Cambridge, MA 02138, USA.

*To whom correspondence should be addressed. E-mail: zhuang@chemistry.harvard.edu

three wavelengths: 405, 457, and 532 nm. For each wavelength, the pair with the appropriate activator was activated rapidly, with a rate at least 10 times as high as those measured for the other two pairs (Fig. 1D), indicating high activation specificity.

This selective activation provides a second parameter for multicolor detection. Not only can different activator-reporter pairs be distinguished by their emission color, as determined by the reporter dye, but they can also be differentiated by the color of light which activates them, as

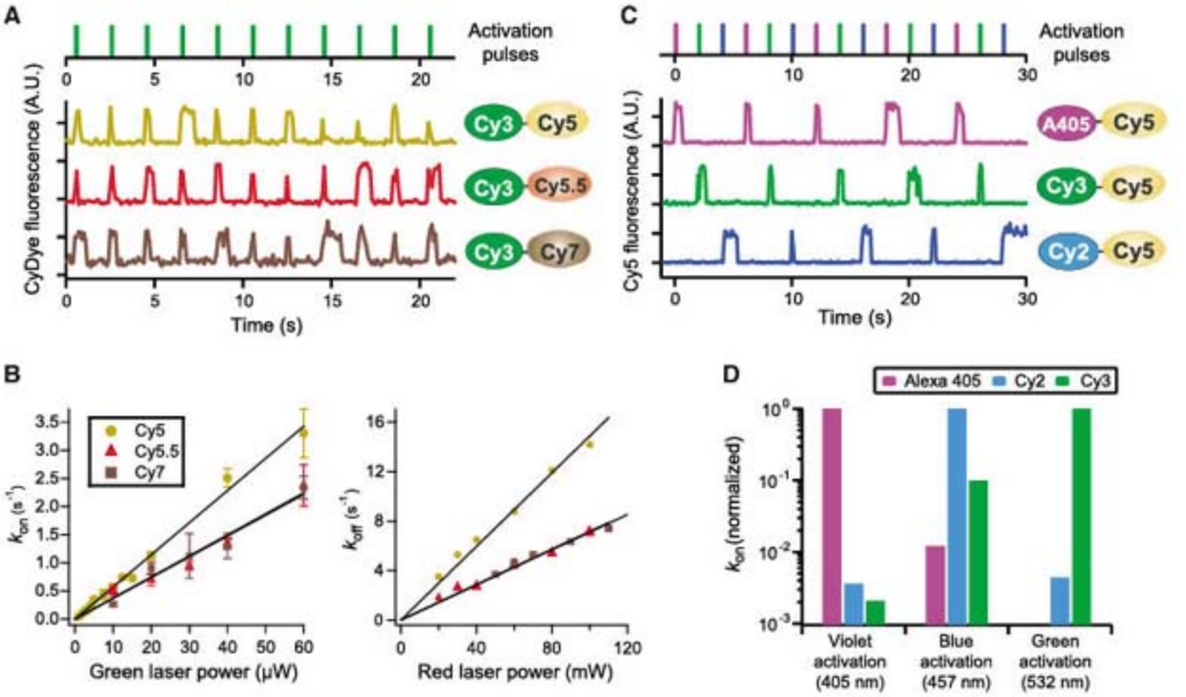

Fig. 1. Photo-switchable probes constructed from activator-reporter pairs. **(A)** Spectrally distinct reporters exhibit photo-switching behavior. The lower panel shows the fluorescence time traces of three photo-switchable reporters Cy5 (dark yellow line), Cy5.5 (red line), and Cy7 (brown line), each paired with a Cy3 dye as the activator on a DNA construct. The upper panel shows the green laser pulses (532 nm) used to activate the reporters. The red laser (657 nm) was continuously on, serving to excite fluorescence from the reporters and to switch them to the dark state. Traces were shifted relative to each other for clarity. **(B)** Switching rate constants k_{on} and k_{off} of the Cy3-Cy5, Cy3-Cy5.5, and Cy3-Cy7 pairs as a function of green and red laser power. Error bars indicate SEM from about three data sets. The laser power to intensity calibration may vary between different samples because of moderate differences in the laser spot size at the sample. **(C)** The same reporter can be activated by spectrally distinct activators. The lower panel shows the fluorescence time traces of Cy5 paired with three different activators, Alexa 405 (magenta line), Cy2 (blue line), and Cy3 (green line). The upper panel shows the violet (405 nm, magenta line), blue (457 nm, blue line), and green (532 nm, green line) activation pulses. **(D)** Normalized activation rate constants of the three dye pairs at three activation wavelengths: 405, 457, and 532 nm. The k_{on} values of Alexa 405-Cy5, Cy2-Cy5, and Cy3-Cy5 were used for normalization at 405, 457, and 532 nm, respectively. The absolute activation rates were rapid for each pair at its corresponding optimal wavelength, with values of 10 s^{-1} or greater at only a few hundred μW of laser power. The activation rate of the Alexa 405-Cy5 pair by the 532-nm laser was too small to be measured reliably.

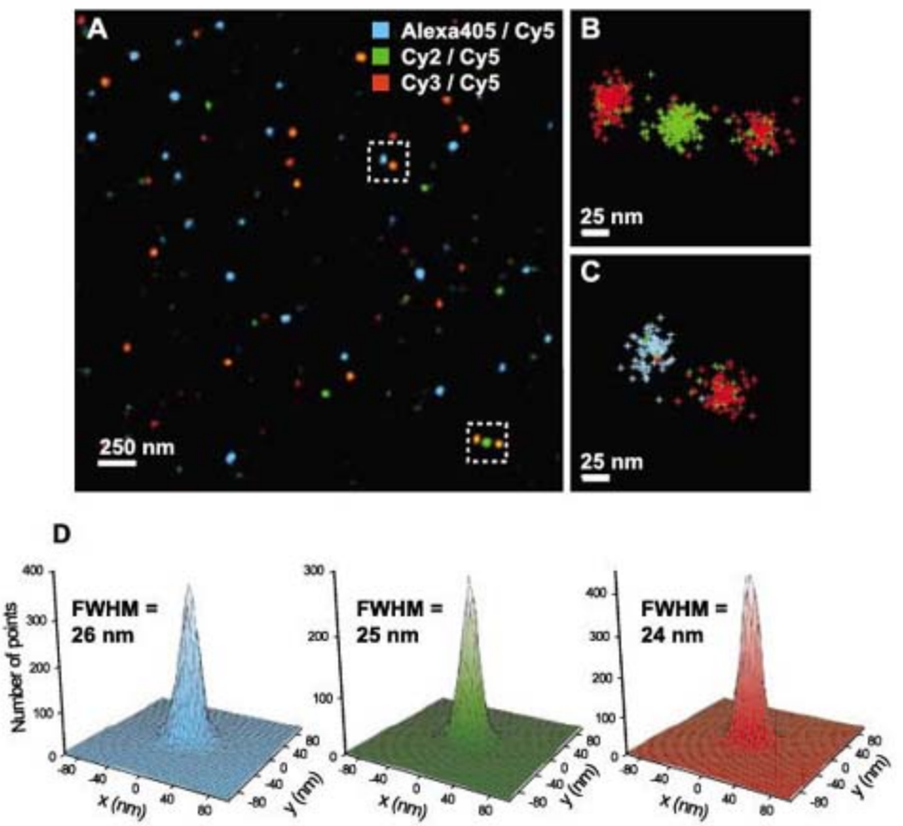

Fig. 2. Three-color STORM imaging of a model DNA sample. **(A)** Three-color STORM image of three different DNA constructs labeled with Alexa 405-Cy5, Cy2-Cy5, or Cy3-Cy5 mixed at a high surface density on a microscope slide. The image was plotted by rendering each localization as a Gaussian peak, the width of which was scaled with the theoretical localization accuracy given by the number of photons detected (*26*). Each colored spot in this image represents a cluster of localizations from a single DNA molecule. A conventional fluorescence image of the same area is shown in fig. S3 for comparison. **(B** and **C)** Higher-magnification views of the boxed regions in (A) show several examples of closely spaced DNA molecules. Each localization was plotted as a cross, colored according to the following code: If the molecule was activated by a 405-, 457-, or 532-nm laser pulse, the color of the cross was assigned as blue, green, or red, respectively. **(D)** The localization distributions of the blue, green, or red clusters. The two-dimensional histograms of localizations were generated by aligning multiple (50 to 60) clusters by their center of mass. The histograms were fit to a Gaussian profile to determine their FWHM.

determined by the activator dye. A combinatorial pairing of the three reporters and three activators reported here could generate up to nine distinguishable fluorescent probes, but requires only four light sources for excitation and three spectrally distinct channels for detection. Photoswitching appeared not to be limited by the spectral separation between the dyes, as illustrated by efficient activation of Cy7 by Alexa 405 (fig. S2), even though the two dyes lie at opposite extremes of the visible spectrum with absorption maxima ~350 nm apart (fig. S1) (*26*). We expect this combinatorial scheme to substantially expand multicolor imaging capabilities at both conventional and subdiffraction limit resolutions.

Here, we use the selective activation scheme as an initial demonstration of multicolor STORM imaging. Three different DNA constructs labeled with Alexa 405-Cy5, Cy2-Cy5, or Cy3-Cy5 were mixed and immobilized on a microscope slide at a high surface density such that individual DNA molecules could not be resolved in a conventional fluorescence image (fig. S3) (*26*). To generate a STORM image, the sample was first exposed to a red laser (633 nm) to switch off nearly all Cy5 dyes in the field of view. The sample was then periodically excited with a sequence of violet (405 nm), blue (457 nm), and green (532 nm) laser pulses, each of which activated a sparse, optically resolvable subset of fluorophores. In between activation pulses, the sample was imaged with the red laser. The image of each activated fluorescent spot was analyzed to determine its centroid position (referred to as a localization), and a color was assigned according to the preceding activation pulse. Because the same imaging laser and detection channel were used for all three dye pairs, there was no need for correction of chromatic aberration. After thousands of activation cycles, a STORM image was constructed by plotting all of the colored localizations (Fig. 2, A to C). In contrast to the conventional image (fig. S3), the STORM image showed clearly separated clusters of localizations, each cluster corresponding to an individual DNA molecule and resulting from repetitive localizations of a single Cy5 molecule over multiple switching cycles. Most of the localizations within each cluster displayed the same color, identifying the type of activator dye present on the DNA and illustrating multicolor imaging capability through selective activation. We identified two origins of crosstalk between colors: false activation by laser pulses of incorrect colors (for example, activation of the Cy3-Cy5 pair by blue pulses) and nonspecific activation by the red imaging laser (*26*). Both effects were quantitatively small (fig. S4) (*26*). The localizations within each cluster approximately follow a Gaussian distribution with a full width at half maximum (FWHM) of 26 ± 1 nm, 25 ± 1 nm, and 24 ± 1 nm for the Alexa 405, Cy2, and Cy3 clusters, respectively (Fig. 2D), suggesting an imaging resolution of ~25 nm for three-color STORM imaging. This resolution is lower than the theoretical limit predicted from the number of photons detected (*26*), likely due to the residual stage drift that was not completely accounted for by the drift correction.

Applying STORM to cell imaging, we first performed single-color immunofluorescence imaging of microtubules, filamentous cytoskeleton structures important for many cellular functions. BS-C-1 cells were immunostained with primary antibodies and then with activator-reporter–labeled secondary antibodies (*26*). Cy3 was used as the activator and Alexa Fluor 647, a cyanine dye with structural, spectral, and photo-switching properties very similar to those of Cy5, was used as the reporter (fig. S1). The STORM image shows a drastic improvement in the resolution of the microtubule network as compared to the conventional fluorescence image (Fig. 3, A to F). In the regions where microtubules were densely packed and undefined in the conventional image, individual microtubule filaments were clearly resolved by STORM (Fig. 3, C to F). For example, two filaments 80 nm apart appeared well separated in the STORM image (Fig. 3G). Whole-cell STORM images, including ~10^6 single-molecule localizations, were acquired in 2 to 30 min, an improvement of one to two orders of magnitude over the previously reported imaging speed of PALM (*6*). Super-resolution microtubule structures began to emerge after only 10 to 20 s of STORM imaging.

To determine the imaging resolution more quantitatively, we identified pointlike objects in the cell, appearing as small clusters of localizations away from any discernable microtubule filaments. These clusters likely represent individual antibodies nonspecifically attached to the cell. The width (FWHM) of the localization clusters was 24 ± 1 nm (fig. S5) (*26*), giving a measure of the image resolution inside the cell. Next, we measured the apparent width of an individual microtubule filament in the STORM

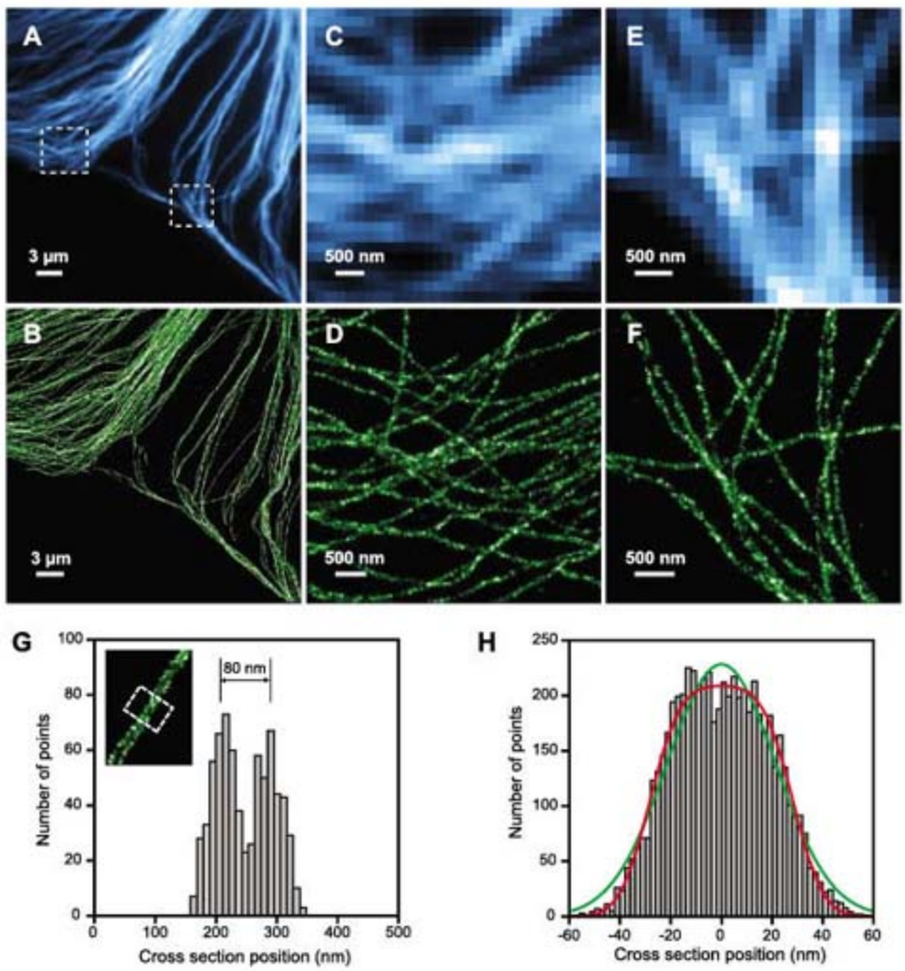

Fig. 3. STORM imaging of microtubules in a mammalian cell. **(A)** Conventional immunofluorescence image of microtubules in a large area of a BS-C-1 cell. **(B)** STORM image of the same area. **(C** and **E)** Conventional and **(D** and **F)** STORM images corresponding to the boxed regions in (A). **(G)** Cross-sectional profiles of two nearby microtubule filaments in the cell. The inset shows the STORM image, and the histogram shows the cross-sectional distribution of localizations within the small regions specified by the white box. **(H)** Cross-sectional profile of a microtubule segment determined from the STORM image. A relatively long segment (~7 μm) was chosen to obtain good statistics. The histogram shows the cross-sectional distribution of localizations. The green line is a single Gaussian fit with FWHM = 51 nm. The red line shows the fit obtained by convolving a rectangular function of width = *d* with a Gaussian function of FWHM = *r*. The fit yields *d* = 56 nm and *r* = 22 nm, corresponding to the antibody-coated microtubule width and the imaging resolution, respectively.

image by examining its cross-sectional profile. Figure 3H shows a cross-sectional distribution of localizations for a microtubule segment. A simple Gaussian fit to the profile yielded a FWHM of 51 nm but deviates significantly from the actual distribution, which appeared flat-topped presumably due to the finite width of the microtubule. A better fit was obtained by simulating the actual microtubule cross-section as a rectangular function of width d, but convolving it with a Gaussian function with FWHM r to model our image resolution. From the fit, we obtained an intrinsic imaging resolution of $r = 22$ nm, consistent with the localization accuracy determined from the point-like objects. The microtubule width derived from the fit, $d = 56$ nm, is in agreement with the 60-nm width of antibody-stained microtubules previously determined by electron microscopy (*30*). However, this apparent width is significantly larger than the diameter of a bare microtubule without antibody coating, pointing out a commonly appreciated aspect of super-resolution imaging—the effective resolution is determined by a combination of the intrinsic imaging resolution and the size of the labels. Improvement in the effective resolution may be achieved by using direct immunofluorescence staining with dye-labeled primary antibodies or Fab fragments.

To demonstrate multicolor STORM imaging in cells, we simultaneously imaged microtubules and clathrin-coated pits (CCPs), cellular structures used for receptor-mediated endocytosis. Microtubules and clathrin were immunostained with primary antibodies and then activator-reporter–labeled secondary antibodies. The activator-reporter pairs used were Cy2-Alexa 647 for microtubules and Cy3-Alexa 647 for clathrin. The 457- and 532-nm lasers were used to selectively activate the two pairs. Cross talk between the two color channels due to false and nonspecific activations was subtracted from the image after statistical analysis (*26*). Figure 4 shows the two-color STORM image presented at different scales. The intrinsic imaging resolution, as determined from the FWHM of pointlike clusters of localizations, was 30 ± 1 nm for each of the two color channels, slightly larger than the resolution determined for the single-color STORM images (fig. S6) (*26*). The green channel (457-nm activation) revealed filamentous structures as expected for microtubules, with a width quantitatively similar to that obtained from the single-color STORM image. The red channel revealed predominantly spherical structures, representing clathrin-coated pits and vesicles (Fig. 4 and fig. S7A) (*26*). In contrast to the STORM images, the conventional TIRF images of CCPs appeared as diffraction-limited spots without any discernable shape (fig. S7A). Side-by-side CCPs that were clearly resolved by STORM appeared as a single spot in the conventional image (fig. S7A). Many of the spherical CCPs appeared to have a doughnut shape with a higher density of localizations toward the periphery, which is consistent with the two-dimensional projection of a three-dimensional cage structure. Finally, the STORM image allowed us to measure the size distribution of CCPs (fig. S7B), which agrees quantitatively with the size distribution determined by electron microscopy (*31*). In summary, our two-color STORM images of cells clearly revealed ultrastructural information not discernable in conventional fluorescence images. This technique may be readily expanded to include more colors by using the photo-switchable activator-reporter pairs reported here, substantially enhancing our ability to visualize molecular interactions in cells and tissues. Further development of cell-delivery methods with molecular specificity will facilitate live cell imaging with these probes (*14*, *32*).

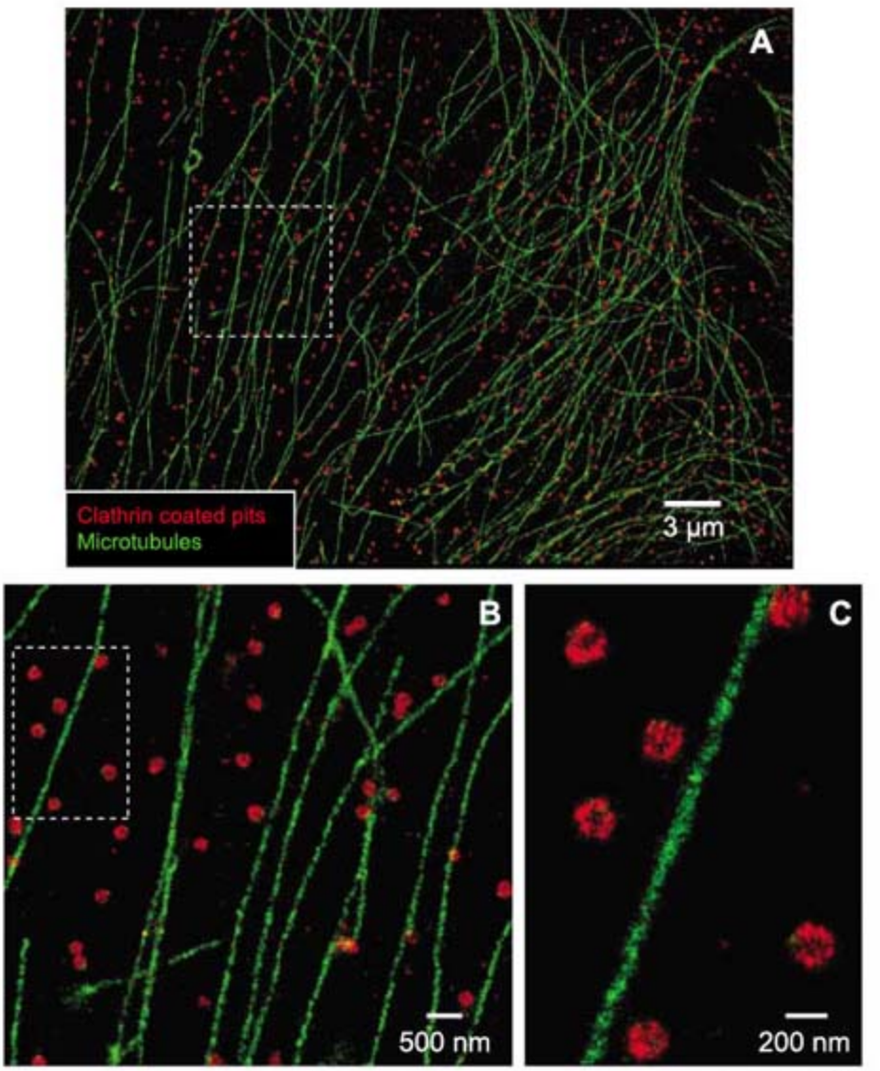

Fig. 4. Two-color STORM imaging of microtubules and CCPs in a mammalian cell. **(A)** STORM image of a large area of a BS-C-1 cell. The secondary antibodies used for microtubule staining were labeled with Cy2 and Alexa 647, and those for clathrin were labeled with Cy3 and Alexa 647. The 457- and 532-nm laser pulses were used to selectively activate the two pairs. Each localization was false colored according to the following code: green for 457-nm activation and red for 532-nm activation. **(B)** STORM image corresponding to the boxed region in (A) shown at a higher magnification. **(C)** Further magnified view of the boxed region in (B).

References and Notes

1. L. Novotny, B. Hecht, *Principles of Nano-optics* (Cambridge Univ. Press, Cambridge, 2006).
2. S. W. Hell, *Science* **316**, 1153 (2007).
3. S. W. Hell, *Nat. Biotechnol.* **21**, 1347 (2003).
4. M. G. L. Gustafsson, *Proc. Natl. Acad. Sci. U.S.A.* **102**, 13081 (2005).
5. M. J. Rust, M. Bates, X. Zhuang, *Nat. Methods* **3**, 793 (2006).
6. E. Betzig *et al.*, *Science* **313**, 1642 (2006).
7. S. T. Hess, T. P. K. Girirajan, M. D. Mason, *Biophys. J.* **91**, 4258 (2006).
8. A. Ponti, M. Machacek, S. L. Gupton, C. M. Waterman-Storer, G. Danuser, *Science* **305**, 1782 (2004).
9. S. Y. Kim, Z. Gitai, A. Kinkhabwala, L. Shapiro, W. E. Moerner, *Proc. Natl. Acad. Sci. U.S.A.* **103**, 10929 (2006).
10. A. Sharonov, R. M. Hochstrasser, *Proc. Natl. Acad. Sci. U.S.A.* **103**, 18911 (2006).
11. L. Stryer, R. P. Haugland, *Proc. Natl. Acad. Sci. U.S.A.* **58**, 719 (1967).
12. T. Ha *et al.*, *Proc. Natl. Acad. Sci. U.S.A.* **93**, 6264 (1996).
13. T. Ha *et al.*, *Proc. Natl. Acad. Sci. U.S.A.* **96**, 9077 (1999).
14. B. N. G. Giepmans, S. R. Adams, M. H. Ellisman, R. Y. Tsien, *Science* **312**, 217 (2006).
15. G. Donnert *et al.*, *Biophys. J.* **92**, L67 (2007).
16. W. E. Moerner, M. Orrit, *Science* **283**, 1670 (1999).
17. R. E. Thompson, D. R. Larson, W. W. Webb, *Biophys. J.* **82**, 2775 (2002).

18. A. Yildiz *et al.*, *Science* **300**, 2061 (2003).
19. M. P. Gordon, T. Ha, P. R. Selvin, *Proc. Natl. Acad. Sci. U.S.A.* **101**, 6462 (2004).
20. X. Qu, D. Wu, L. Mets, N. F. Scherer, *Proc. Natl. Acad. Sci. U.S.A.* **101**, 11298 (2004).
21. K. A. Lidke, B. Rieger, T. M. Jovin, R. Heintzmann, *Opt. Exp.* **13**, 7052 (2005).
22. C. Kural *et al.*, *Science* **308**, 1469 (2005).
23. X. L. Nan, P. A. Sims, P. Chen, X. S. Xie, *J. Phys. Chem. B* **109**, 24220 (2005).
24. E. A. Abbondanzieri, W. J. Greenleaf, J. W. Shaevitz, R. Landick, S. M. Block, *Nature* **438**, 460 (2005).
25. S. Dumont *et al.*, *Nature* **439**, 105 (2006).
26. See supporting material on *Science* Online.
27. M. Bates, T. R. Blosser, X. Zhuang, *Phys. Rev. Lett.* **94**, 108101 (2005).
28. M. Heilemann, E. Margeat, R. Kasper, M. Sauer, P. Tinnefeld, *J. Am. Chem. Soc.* **127**, 3801 (2005).
29. S. Hohng, C. Joo, T. Ha, *Biophys. J.* **87**, 1328 (2004).
30. K. Weber, P. C. Rathke, M. Osborn, *Proc. Natl. Acad. Sci. U.S.A.* **75**, 1820 (1978).
31. J. E. Heuser, R. G. W. Anderson, *J. Cell Biol.* **108**, 389 (1989).
32. I. Chen, A. Y. Ting, *Curr. Opin. Biotechnol.* **16**, 35 (2005).
33. We thank M. Rust for initial discussions of this work, W. Wang for help with analysis on dye-labeled antibodies, and S. Liu for providing some DNA constructs. This work was supported in part by the National Institutes of Health (grant GM 068518) and a Packard Science and Engineering Fellowship (to X.Z.). X.Z. is a Howard Hughes Medical Institute Investigator.

Supporting Online Material

www.sciencemag.org/cgi/content/full/1146598/DC1
Materials and Methods
Figs. S1 to S7
References

18 June 2007; accepted 3 August 2007
Published online 16 August 2007;
10.1126/science.1146598
Include this information when citing this paper.

Widespread Lateral Gene Transfer from Intracellular Bacteria to Multicellular Eukaryotes

Julie C. Dunning Hotopp,[1]*†‡ Michael E. Clark,[2]* Deodoro C. S. G. Oliveira,[2] Jeremy M. Foster,[3] Peter Fischer,[4] Mónica C. Muñoz Torres,[5] Jonathan D. Giebel,[2] Nikhil Kumar,[1]‡ Nadeeza Ishmael,[1]‡ Shiliang Wang,[1] Jessica Ingram,[3] Rahul V. Nene,[1]§ Jessica Shepard,[1]‖ Jeffrey Tomkins,[5] Stephen Richards,[6] David J. Spiro,[1] Elodie Ghedin,[1,7] Barton E. Slatko,[3] Hervé Tettelin,[1]‡¶ John H. Werren[2]¶

Although common among bacteria, lateral gene transfer—the movement of genes between distantly related organisms—is thought to occur only rarely between bacteria and multicellular eukaryotes. However, the presence of endosymbionts, such as *Wolbachia pipientis*, within some eukaryotic germlines may facilitate bacterial gene transfers to eukaryotic host genomes. We therefore examined host genomes for evidence of gene transfer events from *Wolbachia* bacteria to their hosts. We found and confirmed transfers into the genomes of four insect and four nematode species that range from nearly the entire *Wolbachia* genome (>1 megabase) to short (<500 base pairs) insertions. Potential *Wolbachia*-to-host transfers were also detected computationally in three additional sequenced insect genomes. We also show that some of these inserted *Wolbachia* genes are transcribed within eukaryotic cells lacking endosymbionts. Therefore, heritable lateral gene transfer occurs into eukaryotic hosts from their prokaryote symbionts, potentially providing a mechanism for acquisition of new genes and functions.

The transfer of DNA between diverse organisms, lateral gene transfer (LGT), facilitates the acquisition of novel gene functions. Among Eubacteria, LGT is involved in the evolution of antibiotic resistance, pathogenicity, and metabolic pathways (*1*). Rare LGT events have also been identified between higher eukaryotes with segregated germ cells (*2*), demonstrating that even these organisms can acquire novel DNA. Although most described LGT events occur within a single domain of life, LGT has been described both between Eubacteria and Archaea (*3*) and between prokaryotes and phagotrophic unicellular eukaryotes (*4*, *5*). However, few interdomain transfers involving higher multicellular eukaryotes have been found.

Wolbachia pipientis is a maternally inherited endosymbiont that infects a wide range of arthropods, including at least 20% of insect species, as well as filarial nematodes (*6*). It is present in developing gametes (*6*) and so provides circumstances conducive for heritable transfer of bacterial genes to the eukaryotic hosts. *Wolbachia*-host transfer has been described in the bean beetle *Callosobruchus chinensis* (*7*) and in the filarial nematode *Onchocerca* spp. (*8*).

We have found *Wolbachia* inserts in the genomes of additional diverse invertebrate taxa, including fruit flies, wasps, and nematodes. A comparison of the published genome of the *Wolbachia* endosymbiont of *Drosophila melanogaster* (*9*) and assemblies of *Wolbachia* clone mates (*10*) from fruit fly whole-genome shotgun sequencing data revealed a large *Wolbachia* insert in the genome of the widespread tropical fruit fly *D. ananassae*. Numerous contiguous, overlapping, clone sequences (contigs) were found that harbored junctions between *Drosophila* retrotransposons and *Wolbachia* genes. The large number of these junctions and the deep sequencing coverage across the junctions indicated that these inserts were probably not due to chimeric libraries or assemblies. To validate these observations, we amplified five *Drosophila-Wolbachia* junctions with polymerase chain reaction (PCR) and verified the end sequences for three of them. Fluorescence in situ hybridization (FISH) of banded polytene chromosomes with fluorescein-labeled probes of two *Wolbachia* genes (*11*) revealed the presence of *Wolbachia* genes on the 2L chromosome of *D. ananassae* (Fig. 1).

We found that nearly the entire *Wolbachia* genome was transferred to the fly nuclear genome, as evidenced by the presence of PCR-amplified products from 44 of 45 physically distant *Wolbachia* genes in cured strains of *D. ananassae* Hawaii verified by microscopy to be lacking the endosymbiont after treatment with

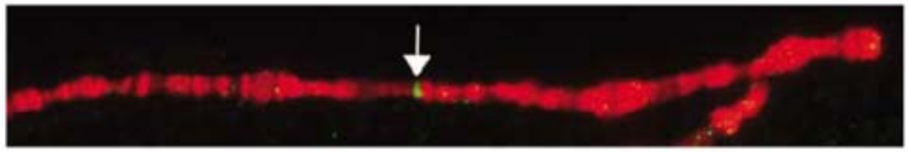

Fig. 1. Fluorescence microscopy evidence supporting *Wolbachia*/host LGT. DNA in the polytene chromosomes of *D. ananassae* were stained with propidium iodide (red), whereas a probe for the *Wolbachia* gene WD_0484 bound to a unique location (green, arrow) on chromosome 2L.

[1]The Institute for Genomic Research, J. Craig Venter Institute, 9712 Medical Center Drive, Rockville, MD 20850, USA. [2]Department of Biology, University of Rochester, Rochester, NY 14627, USA. [3]Molecular Parasitology Division, New England Biolabs Incorporated, 240 County Road, Ipswich, MA 01938, USA. [4]Department of Internal Medicine, Infectious Diseases Division, Washington University School of Medicine, St. Louis, MO 63110, USA. [5]Clemson University Genomics Institute, 304 BRC, 51 New Cherry Street, Clemson, SC 29634, USA. [6]Human Genome Sequencing Center, Baylor College of Medicine, Houston, TX 77030, USA. [7]Division of Infectious Diseases, University of Pittsburgh School of Medicine, Pittsburgh, PA 15261, USA.

*These authors contributed equally to this work.
†To whom correspondence should be addressed. E-mail: jhotopp@som.umaryland.edu
‡Present address: Institute for Genome Sciences, University of Maryland School of Medicine, Health Sciences Facility II, Room S-445, 20 Penn Street, Baltimore, MD 21201, USA.
§Present address: Brown University, Providence, RI 02912, USA.
‖Present address: Pace University, New York, NY 10038, USA.
¶These authors contributed equally to this work.

antibiotics (fig. S1) (*11*). In contrast, only spurious, incorrectly sized, and weak amplification was detected from a cured control line lacking these inserts (Townsville). The 45 genes assayed (table S1) are spaced throughout the *Wolbachia* genome. Thus, the high proportion of amplified genes suggests gene transfer of nearly the entire *Wolbachia* genome to the insect genome.

A 14-kb region containing four *Wolbachia* genes with two retrotransposon insertions was sequenced (*11*) from a single bacteria artificial chromosome (BAC), constituting an independent source of DNA as compared with the largely plasmid-derived whole-genome sequence of *D. ananassae*. The two retroelements each contained 5–base pair (bp) target site duplications (9/10 bp identical), long terminal repeats, and *gag-pol* genes (Fig. 2A) indicating that the *Wolbachia* insert is accumulating retroelements. Insertion of this region appears to be recent, as shown by the nearly identical target site duplications and the >90% nucleotide identity between corresponding endosymbiont genes and sequenced homologs in the *D. ananassae* chromosome.

Crosses between *Wolbachia*-free Hawaii males (with the insert) and *Wolbachia*-free Mexico females (without the insert) revealed that the insert is paternally inherited by offspring of both sexes, confirming that *Wolbachia* genes are inserted into an autosome. Because *Wolbachia* infections are maternally inherited, this also confirms that PCR amplification in the antibiotic-treated line is not due to an undetectable infection. Furthermore, the Hawaii and Mexico crosses revealed Mendelian, autosomal inheritance of *Wolbachia* inserts [paternal $N = 57$, proportion of offspring with *Wolbachia* genes (k) = 0.49; maternal $N = 40$, $k = 0.58$]. Six physically distant, inserted *Wolbachia* genes perfectly cosegregated in F_2 maternal inheritance crosses (*11*), suggesting they also are closely linked.

PCR amplification and sequencing (*11*) of 45 *Wolbachia* loci in 14 *D. ananassae* lines from widely dispersed geographic locations revealed large *Wolbachia* inserts in lines from Hawaii, Malaysia, Indonesia, and India (table S2). Sequence comparisons of the amplicons from these four lines revealed that all open reading frames (ORFs) remained intact with >99.9% identity between inserts. This is compared to an average of 97.7% identity for the inserts compared with *w*Mel, the *Wolbachia* endosymbiont of *D. melanogaster*. These results indicate the widespread prevalence of *D. ananassae* strains with similar inserts of the *Wolbachia* genome, probably because of a single insertion from a common ancestor.

In addition, reverse transcription PCR (RT-PCR) followed by sequencing (*11*) demonstrated that ~2% of *Wolbachia* genes (28 of 1206 genes assayed; table S3) are transcribed in cured adult males and females of *D. ananassae* Hawaii. The complete 5′ sequence of one of the transcripts, WD_0336, was obtained with 5′–rapid amplification of cDNA ends (RACE) on uninfected flies (*11*), suggesting that this transcript has a 5′ mRNA cap, a form of eukaryotic posttranscriptional modification. Analysis of the transcript quantities of inserted *Wolbachia* genes with quantitative RT-PCR (qRT-PCR) (*11*) revealed that they are 10^4 times to 10^7 times less abundant than the fly's highly transcribed actin gene (*act5C*; table S3). There is no cutoff that defines a biologically relevant amount of transcription, and assessment of transcription in whole insects can obscure important tissue-specific transcription. Therefore, it is unclear whether these transcripts are biologically meaningful, and further work is needed to determine their importance.

Screening of public shotgun sequencing data sets has identified several additional cases of LGT in different invertebrate species. In *Wolbachia*-cured strains of the wasp *Nasonia*, six small *Wolbachia* inserts (<500 bp) were verified by PCR and sequencing (*11*) that have >96% nucleotide identity to native *Wolbachia* sequences, in some cases with short insertion site duplications. These include four in *Nasonia vitripennis*, one in *N. giraulti*, and one in *N. longicornis* (table S4 and Fig. 2B). Amplification and sequencing of 14 to 18 geographically diverse strains of each species indicated that the inserts are species-specific. For example, three *Wolbachia* inserts in *N. vitripennis* are not found in the closely related

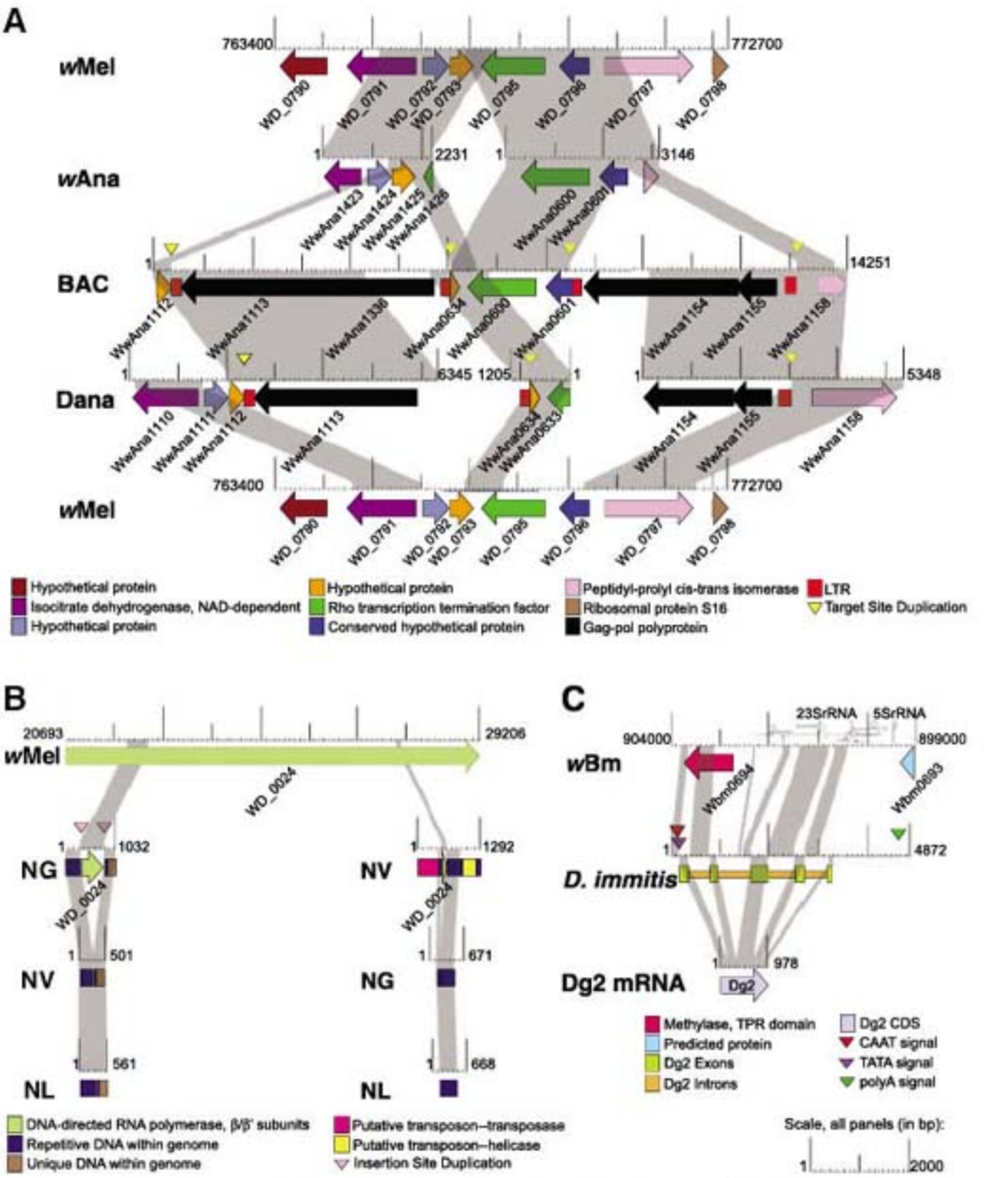

Fig. 2. Schematics of *Wolbachia* inserts in host chromosomes. **(A)** Contigs containing *Wolbachia* sequences generated from the *D. ananassae* Hawaii shotgun sequencing project are segregated into sequences coming from the endosymbiont (*w*Ana) or from the *D. ananassae* chromosome (Dana) on the basis of presence or absence of eukaryotic genes in the contigs. These are compared to those from the reference *D. melanogaster Wolbachia* genome (*w*Mel) and a *D. ananassae* BAC. NAD, nicotinamide adenine dinucleotide. **(B)** Fragments of the *Wolbachia* gene WD_0024 gene have inserted into different positions in the *N. giraulti* (NG) and *N. vitripennis* (NV) genomes with unique insertions in each lineage, including *N. longicornis* (NL). **(C)** A region in the *D. immitis* genome (Dg2) that is transcribed has introns similar to sequences from the *Wolbachia* infecting *B. malayi* (*w*Bm). All matches in (A) and (B) have >90% nucleotide identity; those in (C) have >75% nucleotide identity. TPR, tetratrico peptide repeat; CDS, coding sequence.

Table 1. Summary of *Wolbachia* sequences and evidence for LGT in public databases. Junctions were validated by PCR amplification and sequencing (*11*), with the number of successful reactions compared to the number attempted. Species marked with a plus sign are described in the literature as being infected with *Wolbachia*. All whole-genome shotgun sequencing reads were downloaded for 26 arthropod and nematode genomes (*11*). Organisms identified as lacking *Wolbachia* sequences either had no match or matches only to the prokaryotic ribosomal RNA. Because the *Nasonia* genomes are from antibiotic-cured insects, they were identified as having a putative LGT event merely on identification of *Wolbachia* sequences in a read. All other organisms were considered to have putative LGT events if the trace repository contained ≥1 read with (i) >80% nucleotide identity over 10% of the read to a characterized eukaryotic gene, (ii) >80% identity over 10% of the read to a *Wolbachia* gene, and (iii) manual review of the BLAST results for 1 to 20 reads to ensure significance (*11*). NA, not applicable.

Organism	Total traces screened	*Wolbachia* traces	LGT	Junctions validated	*Wolbachia* infection
	Trace repository sequences				
Acyrthosiphon pisum (aphid)	4,285,120	0			+
Aedes aegypti (mosquito)	16,238,263	0			–
Anopheles gambiae (mosquito)	5,456,630	0			–
Apis mellifera (honeybee)	3,941,137	0			–
Brugia malayi (filarial nematode)	1,260,214	22,524	+	10/12	+
Culex pipiens quinquefasciatus (mosquito)	7,380,430	21,304	+	0/0	+
Daphnia pulex (crustacean)	2,724,768	0			–
D. ananassae (fruit fly)	3,878,537	38,605	+	6/7	+
D. erecta (fruit fly)	2,916,936	0			–
D. grimshawi (fruit fly)	2,874,111	0			–
D. melanogaster (fruit fly)	1,001,855	0			+
D. mojavensis (fruit fly)	3,130,180	107*	–		–
D. persimilis (fruit fly)	1,375,313	0			–
D. pseudoobscura (fruit fly)	5,161,792	0			–
D. sechellia (fruit fly)	1,203,722	1	+	0/0	+
D. simulans (fruit fly)	2,321,958	7473	+	0/0	+
D. virilis (fruit fly)	3,632,492	0			–
D. willistoni (fruit fly)	2,332,565	2519	–		+
D. yakuba (fruit fly)	2,269,952	0			+
Ixodes scapularis (tick)	13,088,763	44	–		+
N. giraulti (wasp)	540,102	2	+	1/1	+
N. longicornis (wasp)	447,736	1	+	1/1	+
N. vitripennis (wasp)	3,360,694	30	+	4/4	+
Pediculus humanus (head louse)	1,480,551	0			+
Pristonchus pacificus (nematode)	2,292,543	0			–
Tribolium castaneum (beetle)	1,918,906	0			–
	GenBank sequence				
Dirofilaria immitis (filarial nematode)	NA	NA	+		+

*This isolate was previously shown to have *Wolbachia* reads in its trace repositories that are contaminating reads from the *D. ananassae* genome sequencing project (*10*).

species *N. giraulti* or *N. longicornis*, which diversified ~1 million years ago (*12*). These data suggest that the *Wolbachia* gene inserts are of relatively recent origin, similar to the inserts in *D. ananassae*.

Nematode genomes also contain inserted *Wolbachia* sequences. Because *Wolbachia* infection is required for fertility and development of the worm *Brugia malayi*, the genomes of both organisms were sequenced simultaneously, complicating assemblies and leading to the removal of *Wolbachia* reads during genome assembly [>98% identity over 90% of the read length on the basis of the independent BAC-based genome sequence of *w*Bm, the *Wolbachia* endosymbiont of *B. malayi* (*13*)]. Despite this, the genome of *B. malayi* contains 249 contigs with *Wolbachia* sequences (e value $< 10^{-40}$), nine of which were confirmed by long-range PCR and end-sequencing (*11*). These include eight large scaffolds containing >1-kb *Wolbachia* fragments within 8 kb of a *B. malayi* gene (table S5). Comparisons of *w*Bm homologs to these regions suggested that all of these *Wolbachia* genes within the *B. malayi* genome are degenerate. In addition, a single region <1 kb was examined that contains a degenerate fragment of the *Wolbachia* aspartate aminotransferase gene (Wbm0002). Its location was confirmed by PCR and sequencing in *B. malayi* as well as in *B. timori* and *B. pahangi* (*11*).

Of the remaining 21 arthropod and nematode genomes in the trace repositories (*11*), we found six containing *Wolbachia* sequences. Potential *Wolbachia*-host LGT was detected in three: *D. sechellia*, *D. simulans*, and *Culex pipiens* (Table 1), as revealed by the presence of reads containing homology to both endosymbiont and host genomes (*11*).

The sequencing of *w*Bm also facilitated the discovery of a *Wolbachia* insertion in *Dirofilaria immitis* (dog heartworm). The *D. immitis Dg2* chromosomal region encoding the D34 immunodominant antigen (*14*, *15*) contains *Wolbachia* DNA within its introns and in the 5′ untranslated region (5′-UTR) (Fig. 2C). These *Wolbachia* genomic fragments have maintained synteny with the *w*Bm genome (*13*), suggesting they may have inserted as a single unit and regions were replaced by exons of *Dg2*. A second gene (*DgK*) has been identified in other *D. immitis* lines that has 91% nucleotide identity in the exon sequences but contains differing number, position, size, and sequence of introns (*16*) and has no homology to known *Wolbachia* sequences.

Whole eukaryote genome sequencing projects routinely exclude bacterial sequences on the assumption that these represent contamination. For example, the publicly available assembly of *D. ananassae* does not include any of the *Wolbachia* sequences described here. Therefore, the argument that the lack of bacterial genes in these assembled genomes indicates that bacterial LGT does not occur is circular and invalid. Recent bacterial LGT to eukaryotic genomes will continue to be difficult to detect if bacterial sequences are routinely excluded from assemblies without experimental verification. And these LGT events will remain understudied despite their potential to provide novel gene functions and affect arthropod and nematode genome evolution. Because *W. pipientis* is among the most abundant intracellular bacteria (*17*, *18*) and its hosts are among the most abundant animal phyla, the view that prokaryote-to-eukaryote transfers are uncommon and unimportant needs to be reevaluated.

References and Notes

1. Y. Boucher *et al.*, *Annu. Rev. Genet.* **37**, 283 (2003).
2. S. B. Daniels, K. R. Peterson, L. D. Strausbaugh, M. G. Kidwell, A. Chovnick, *Genetics* **124**, 339 (1990).
3. K. E. Nelson *et al.*, *Nature* **399**, 323 (1999).
4. J. O. Andersson, *Cell. Mol. Life Sci.* **62**, 1182 (2005).
5. W. F. Doolittle, *Trends Genet.* **14**, 307 (1998).
6. R. Stouthamer, J. A. Breeuwer, G. D. Hurst, *Annu. Rev. Microbiol.* **53**, 71 (1999).
7. N. Kondo, N. Nikoh, N. Ijichi, M. Shimada, T. Fukatsu, *Proc. Natl. Acad. Sci. U.S.A.* **99**, 14280 (2002).
8. K. Fenn *et al.*, *PLoS Pathog.* **2**, e94 (2006).
9. M. Wu *et al.*, *PLoS Biol.* **2**, e69 (2004).
10. S. L. Salzberg *et al.*, *Genome Biol.* **6**, R23 (2005).
11. Materials and methods are available as supporting material on *Science* Online.
12. B. C. Campbell, J. D. Steffen-Campbell, J. H. Werren, *Insect Mol. Biol.* **2**, 225 (1993).
13. J. Foster *et al.*, *PLoS Biol.* **3**, e121 (2005).
14. S. Sun, K. Sugane, *J. Helminthol.* **68**, 259 (1994).
15. S. H. Sun, T. Matsuura, K. Sugane, *J. Helminthol.* **65**, 149 (1991).
16. K. Sugane, K. Nakayama, H. Kato, *J. Helminthol.* **73**, 265 (1999).
17. J. H. Werren, *Annu. Rev. Entomol.* **42**, 587 (1997).
18. J. H. Werren, D. M. Windsor, *Proc. Biol. Sci. R. Soc. London Ser. B* **267**, 1277 (2000).
19. The *D. ananassae* BAC 01L18 sequence is deposited in GenBank (EF426679); the *D. ananassae* sequence comparisons from the four lines are deposited in GenBank (EF611872 to EF611985); the *D. ananassae* RACE sequence is deposited in dbEST (46867557) and GenBank (ES659088); the *Nasonia* sequences are deposited in

GenBank (EF588824 to EF588901); the *Brugia malayi* contigs are available in GenBank (DS237653, DS238272, DS238705, DS239028, DS239057, DS239291, DS239377, and DS239315); the *Brugia malayi* scaffolds are available in GenBank (AAQA01000958, AAQA01000097, AAQA01001500, AAQA01000425, AAQA01001819, AAQA01001498, AAQA01000384, AAQA01001952, AAQA01000736, AAQA01000571, and AAQA01000369); and the microarray primers sequences that were used for RT-PCR are deposited in ArrayExpress (A-TIGR-28). This work was supported by an NSF grant to J.H.W. and H.T., a National Institute of Allergy and Infectious Diseases grant to E.G., and New England Biolabs Incorporated support to B.E.S.

Supporting Online Material
www.sciencemag.org/cgi/content/full/1142490/DC1
Materials and Methods
Fig. S1
Tables S1 to S5
References

13 March 2007; accepted 2 July 2007
Published online 30 August 2007;
10.1126/science.1142490
Include this information when citing this paper.

Draft Genome of the Filarial Nematode Parasite *Brugia malayi*

Elodie Ghedin,[1,2]# Shiliang Wang,[2] David Spiro,[2] Elisabet Caler,[2] Qi Zhao,[2] Jonathan Crabtree,[2] Jonathan E. Allen,[2]* Arthur L. Delcher,[2]† David B. Guiliano,[3] Diego Miranda-Saavedra,[4]‡ Samuel V. Angiuoli,[2] Todd Creasy,[2] Paolo Amedeo,[2] Brian Haas,[2] Najib M. El-Sayed,[2]§ Jennifer R. Wortman,[2] Tamara Feldblyum,[2] Luke Tallon,[2] Michael Schatz,[2]† Martin Shumway,[2] Hean Koo,[2] Steven L. Salzberg,[2]† Seth Schobel,[2] Mihaela Pertea,[2]† Mihai Pop,[2]† Owen White,[2] Geoffrey J. Barton,[4] Clotilde K. S. Carlow,[5] Michael J. Crawford,[6] Jennifer Daub,[7]‖ Matthew W. Dimmic,[6] Chris F. Estes,[8] Jeremy M. Foster,[5] Mehul Ganatra,[5] William F. Gregory,[7] Nicholas M. Johnson,[9] Jinming Jin,[10] Richard Komuniecki,[11] Ian Korf,[12] Sanjay Kumar,[5] Sandra Laney,[13] Ben-Wen Li,[14] Wen Li,[13] Tim H. Lindblom,[8] Sara Lustigman,[15] Dong Ma,[5] Claude V. Maina,[5] David M. A. Martin,[4] James P. McCarter,[6,16] Larry McReynolds,[10] Makedonka Mitreva,[16] Thomas B. Nutman,[17] John Parkinson,[18] José M. Peregrín-Alvarez,[1] Catherine Poole,[5] Qinghu Ren,[2] Lori Saunders,[13] Ann E. Sluder,[19] Katherine Smith,[11] Mario Stanke,[20] Thomas R. Unnasch,[21] Jenna Ware,[5] Aguan D. Wei,[22] Gary Weil,[14] Deryck J. Williams,[7] Yinhua Zhang,[5] Steven A. Williams,[13] Claire Fraser-Liggett,[2]¶ Barton Slatko,[5] Mark L. Blaxter,[7] Alan L. Scott[23]

Parasitic nematodes that cause elephantiasis and river blindness threaten hundreds of millions of people in the developing world. We have sequenced the ~90 megabase (Mb) genome of the human filarial parasite *Brugia malayi* and predict ~11,500 protein coding genes in 71 Mb of robustly assembled sequence. Comparative analysis with the free-living, model nematode *Caenorhabditis elegans* revealed that, despite these genes having maintained little conservation of local synteny during ~350 million years of evolution, they largely remain in linkage on chromosomal units. More than 100 conserved operons were identified. Analysis of the predicted proteome provides evidence for adaptations of *B. malayi* to niches in its human and vector hosts and insights into the molecular basis of a mutualistic relationship with its *Wolbachia* endosymbiont. These findings offer a foundation for rational drug design.

The phylum Nematoda is speciose and abundant and, although most species are free-living, many are parasitic. Over one-third of all humans, mainly in the developing world, carry a nematode infection. Parasitic worms typically cause chronic, debilitating infections that are often difficult to treat and that, despite the high cost to human health, have been neglected in biomedical research. Current knowledge of nematode molecular genetics and developmental biology is largely based on extensive studies of the free-living, bacteriovorous species *Caenorhabditis elegans*. Here, we present the initial analysis of the genome of the human filarial parasite *Brugia malayi*.

Brugia malayi is endemic in Southeast Asia and Indonesia. Like other filarial nematodes, *B. malayi* develops through four larval stages into an adult male or female (fig. S1), entirely within one of two host species—a mosquito vector (*Culex*, *Aedes*, and *Anopheles*) and humans, where adult worms can live for more than a decade. *B. malayi* was chosen for whole-genome sequencing (*1*) because it is the only major human filarial pathogen that can be maintained in small laboratory animals. Most filarial nematodes, including *B. malayi*, carry three genomes: nuclear, mitochondrial (available at GenBank, accession no. AF538716), and that of an alphaproteobacterial endosymbiont, *Wolbachia*. We present here the draft assembly and annotated genome of the TRS strain of *B. malayi*. We provide comparative analyses with *Caenorhabditis* and another well-annotated member of the superphylum Ecdysozoa, *Drosophila melanogaster*, to further illuminate the origins of novelty and loss of ancestral characters in the model species and the parasite. Comparative genome analysis reveals key features of Nematoda that define the scope of molecular diversity that has contributed to the success of the phylum. The analysis also uncovers adaptations that appear to have evolved in the *B. malayi* genome in response to the pressures of parasitism and to the presence of the parasite's *Wolbachia* endosymbiont, *w*Bm.

The *B. malayi* nuclear genome is organized as five chromosomes (*2*), including an XY sex-determination pair, and has been estimated to be 80 to 100 megabases (Mb) (*3*, *4*). The sequence of the *B. malayi* nuclear genome was obtained to ~9× coverage with the use of whole-genome shotgun (WGS) sequencing (*1*, *5*). The sequences were assembled into scaffolds totaling ~71 Mb of data with a further ~17.5 Mb of contigs not integrated into any scaffold (orphan contigs). The repeat content of the *B. malayi* genome, estimated at ~15% (*1*), may have contributed significantly to assembly difficulties (*5*, *6*). From these sequence data, we estimate that the *B. malayi* genome is 90 to 95 Mb (Table 1) (*5*). In comparison, the *C. elegans* genome is 100 Mb and the *Caenorhabditis briggsae* genome 104 Mb. The overall G + C content (30.5%) is lower than that of *C. elegans* (35.4%) or *C. briggsae* (37.4%) (*6*).

The complement of protein-coding genes was derived by automated gene prediction from the ~71-Mb assembly and by manual annotation of selected gene families (table S1). The 11,515 robustly predicted gene-coding regions occupy ~32% of the sequence at an average density of 162 genes/Mb (Table 1).

After inclusion of genes estimated to be found in the unannotated portion of the genomic sequence (*5*), we infer that *B. malayi* has between 14,500 and 17,800 protein-coding genes, agreeing with previous estimates (*7*). Even the higher estimate is lower than the 19,762 (WormBase data release WS133) and 19,507 (*6*) genes reported for *C. elegans* and *C. briggsae*, respectively, which suggests that parasitic nematode genomes have fewer genes than their free-living counterparts, echoing a pattern observed in bacterial pathogens.

For the six scaffolds longer than 1 Mb, totaling ~25 Mb of the genome, the arrangement of *B. malayi* genes was compared with that of their *C. elegans* orthologs (Fig. 1). Linkage is in general conserved: For large regions of the *B. malayi* genome, orthologs map predominantly to one (or, in the case of scaffold 14972, two) *C. elegans* chromosome(s) (Fig. 1, A to C), which indicates maintenance of linkage of these genes despite ~350 million years of separation (*8*). However, local gene order is not conserved (Fig. 1D). The largest, 6.5-Mb scaffold contains interdigitating blocks of genes that map to chromosomes 4 and X of *C. elegans*, which suggests there were ancient breakage and fusion events between linkage groups. These data support a model where within-linkage group rearrangements have been many times more common than between-linkage group transloca-

tions (*7*, *9*), a pattern that may be typical of nematode genomes (*6*, *10*).

Operons are a common form of gene organization in bacteria and some protozoa, but in Metazoa, operons have been identified only in nematodes, platyhelminths, and urochordates (*11*, *12*). Using 1000 base pairs (bp) as the upper limit of intergenic spacing, 838 potential operons (*5*), containing ~1800 genes (16% of the total; 2 to 5 genes per operon), were found in the assembled genome (Fig. 2 and fig. S2). Of these putative operons, only 10% of the gene pairs were also in operons in *C. elegans* (table S2).

To obtain an estimate of the core complement of proteins that defines the phylum Nematoda, we compared the proteomes of *B. malayi*, *C. elegans*, and *C. briggsae*. Comparisons with the arthropod *D. melanogaster* were also made to help define a list of lineage-restricted genes. We identified 3979 sets of orthologs with representatives in all four species and 1726 sets of orthologs limited to the three nematode species (fig. S3A; tables S3 to S8). The average pairwise identity of *B. malayi* proteins with orthologs from either caenorhabditid species is ~48%. The genes conserved in nematodes but absent from the fly include cathepsin Z–like cysteine proteases, major sperm proteins, and cuticle collagens, as well as several families of unknown function. In addition, these orthologs were significantly enriched (2.4- to 4.4-fold; $P > 0.0017$) for genes with RNA interference (RNAi) phenotypes in *C. elegans* (fig. S4), which is consistent with a gene set essential to the core of nematode biochemisty and cell biology. These lineage-restricted families may define a molecular "bauplan" of Nematoda.

As noted above, the *B. malayi* genome appears to have fewer genes than *C. elegans*. On examination, much of the disparity in gene numbers can be accounted for by the extent to which gene families in *Brugia* and *Caenorhabditis* have undergone lineage-specific expansion. More than 8% of the 5780 *B. malayi*–*C. elegans* ortholog clusters were expanded in *C. elegans* (fig. S3C).

Comparing the occurrence of protein domains in *B. malayi*, *C. elegans*, *C. briggsae*, and *D. melanogaster* (figs. S3B and S5 and table S9) revealed, to our surprise, that *B. malayi* is in some ways more similar to the fly than to

Table 1. General features and genome content of *B. malayi*, with *C. elegans* values for comparison. Scaffolds are also called super-contigs, they are assembled into large regions of ordered sequence fragments separated by gaps. Orphan-contigs are sequence fragments (contigs) that do not have information allowing them to be linked to other fragments and into scaffolds. Singletons are sequences that cannot be assembled into sequence fragments (contigs). N50 is a length-weighted average of contig or scaffold size, such that the average nucleotide in an assembly will appear in a contig (or scaffold) of N50 size or greater.

Features	*B. malayi*	*C. elegans*
Overall		
Estimated size of genome (Mb)	90–95	
Total number of bp of assembled sequence (bp)	88,363,057	
Number of scaffolds	8,180	
N50 of scaffolds (bp)	93,771	
Maximum length of scaffold (bp)	6,534,162	
Number of bp assembled into scaffolds (bp)	70,837,048	
Number of orphan contigs	18,868	
Number of bp assembled into orphan contigs (bp)	17,526,009	
Number of singletons	176,099	
Number of bp in singletons (bp)	108,289,205	
Protein-coding regions		
Percent of genome containing protein-coding sequence (%)	17.84	
Number of gene models	11,515*	
Number of proteins	11,508 (9,839)†	
Max/average protein length (amino acids)	9,445/371	18,563/440
Gene density (genes per Mb)	162	228
Number of exons	83,672	
Mean/median exon size (bp)	159/140	307/147
Mean/median number of exons per gene	7.27/5	6.38/6
Number of bp included in exons	13,282,846	
Number of introns	72,157	
Mean/median intron size (bp)	311/219	320/68
Number of bp included in introns	22,512,502	
Mean length of intergenic region (bp)	3,783	2218
Overall G + C content (%)	30.5	35.4
Exons, G + C content (%)	39.6	42.9
Introns, G + C content (%)	27.6	29.1
Intergenic regions, G + C content (%)	30.9	32.5
Non–protein coding genes		
Transfer RNA (tRNA) genes (+ tRNA pseudogenes)	~233 (+26)	
5S ribosomal RNA (found in scaffolds and orphan contigs)	~400	

*This number includes seven pseudogenes. †The number of proteins 100 amino acids long or larger.

[1]Division of Infectious Diseases, University of Pittsburgh School of Medicine, Pittsburgh, PA 15261, USA. [2]The Institute for Genomic Research (TIGR) and the J. Craig Venter Institute, 9712 Medical Center Drive, Rockville, MD 20850, USA. [3]Division of Cell and Molecular Biology, Biochemistry Building, Imperial College London, Exhibition Road, South Kensington, London, SW7 2AZ, UK. [4]School of Life Sciences Research, University of Dundee, Dow Street, Dundee, DD1 5EH, UK. [5]Division of Parasitology, New England BioLabs, Inc., 240 County Road, Ipswich, MA 01938, USA. [6]Divergence, Inc., 893 North Warson Road, St. Louis, MO 63141, USA. [7]Institute of Evolutionary Biology and Institute of Immunology and Infection Research, University of Edinburgh, Edinburgh EH9 3JT, UK. [8]Division of Science, Lyon College, 2300 Highland Road, Batesville, AR 72501, USA. [9]School of Biochemistry and Molecular Biology, The Australian National University, Canberra, ACT 0200, Australia. [10]Division of RNA Biology, New England Biolabs, Inc., 240 County Road, Ipswich, MA 01938, USA. [11]Department of Biological Sciences, University of Toledo, 2801 West Bancroft Street, Toledo, OH 43606–3390, USA. [12]Genome Center, Section of Molecular Biology, Division of Biological Sciences, University of California at Davis, Davis, CA 95616, USA. [13]Clark Science Center, Smith College, Northampton, MA 01063, USA. [14]Infectious Diseases Division, Washington University School of Medicine, 660 South Euclid Avenue, St. Louis, MO 63110, USA. [15]Laboratory of Molecular Parasitology, Lindsley F. Kimball Research Institute, New York Blood Center, 310 East 67th Street, New York, NY 10021, USA. [16]Genome Sequencing Center, Washington University School of Medicine, 4444 Forest Park Avenue, St. Louis, MO 63108, USA. [17]Laboratory of Parasitic Diseases, National Institute of Allergy and Infectious Diseases, National Institutes of Health, 6610 Rockledge Drive, Bethesda, MD 20892–6612, USA. [18]Program in Molecular Structure and Function, Hospital for Sick Children, TMDT Building, 101 College Street, 15th Floor, East Tower, Toronto, ON, Canada, M5G 1L7. [19]Cambria Biosciences, 8A Henshaw Street, Woburn, MA 01801, USA. [20]Department of Bioinformatics, University of Göttingen, Goldschmidtstrasse 1, 37077 Göttingen, Germany. [21]Division of Geographic Medicine, University of Alabama at Birmingham, BBRB 203, 1530 Third Avenue South, Birmingham, AL 35294–2170, USA. [22]Department of Anatomy and Neurobiology, Washington University School of Medicine, 660 South Euclid Avenue, St. Louis, MO 63110, USA. [23]Department of Molecular Microbiology and Immunology, Bloomberg School of Public Health, Johns Hopkins University, 615 North Wolfe, Baltimore, MD 21205, USA.

*Present address: Lawrence Livermore National Laboratory, 7000 East Avenue, Livermore, CA 94550, USA.
†Present address: Center for Bioinformatics and Computational Biology, University of Maryland, College Park, MD 20742, USA.
‡Present address: Cambridge Institute for Medical Research, Wellcome Trust/MRC Building, Addenbrooke's Hospital, Hills Road, Cambridge CB2 0XY, UK.
§Present address: Department of Cell Biology and Molecular Genetics, 2105 H. J. Patterson Hall, and Center for Bioinformatics and Computational Biology, 3115 Biomolecular Sciences Building, University of Maryland, College Park, MD 20742, USA.
‖Present address: The Wellcome Trust Sanger Institute, Hinxton Genome Campus, Cambridge CB10 1SA, UK.
¶Present address: Institute for Genome Sciences, University of Maryland School of Medicine, 800 West Baltimore Street, Baltimore, MD 21201, USA.
#To whom correspondence should be addressed. E-mail: GhedinE@dom.pitt.edu

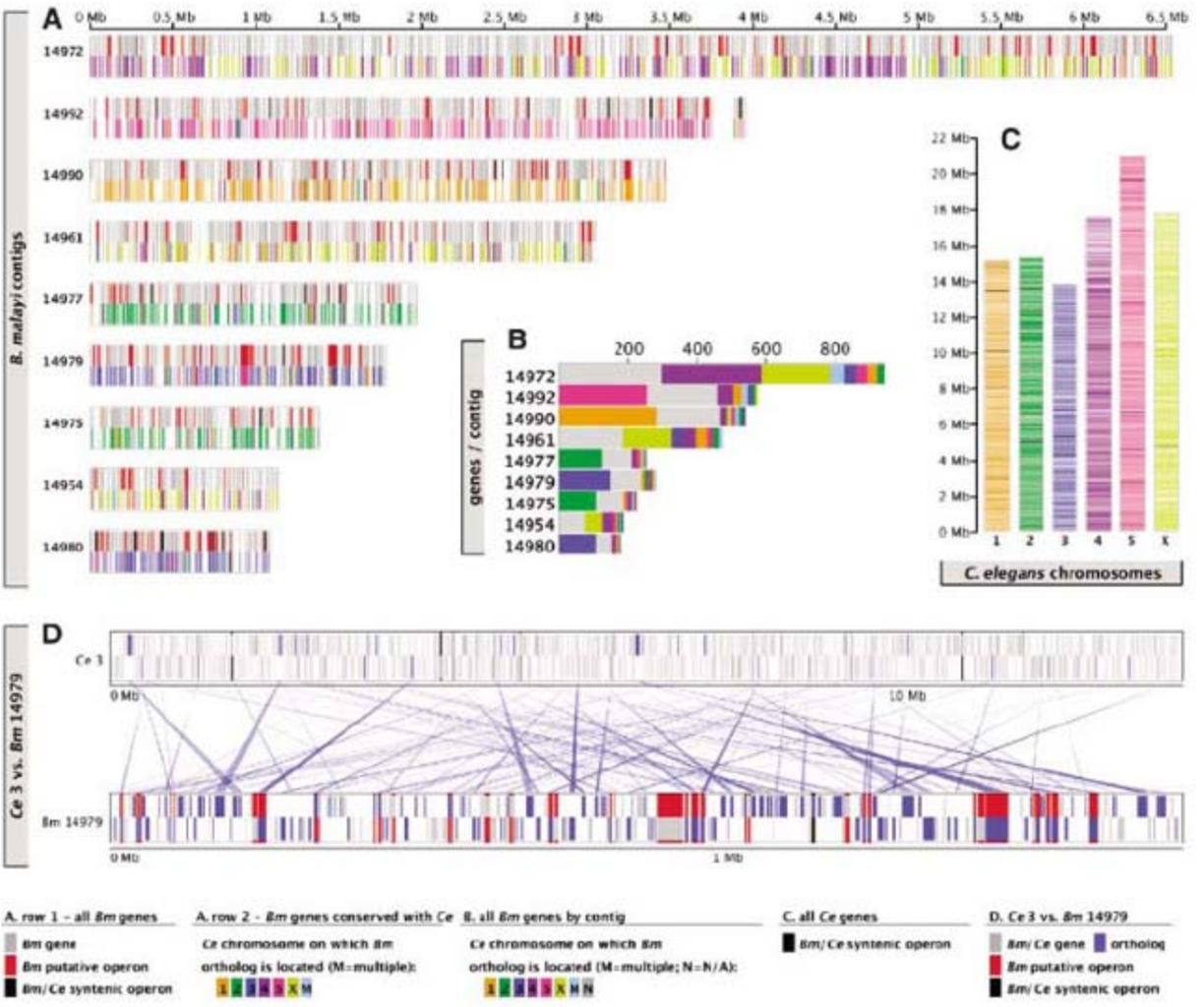

Fig. 1. Genome organization of *B. malayi* in comparison with *C. elegans*. **(A)** Genes on the eight largest *B. malayi* scaffolds. The upper part of each scaffold cartoon represents genes in conserved operons (black) or *B. malayi*–specific operons (red) or genes not in operons (gray). The lower part indicates genes with orthologs in *C. elegans*, colored to indicate the *C. elegans* chromosome on which the ortholog is located. **(B)** Numbers of genes on the longest *B. malayi* scaffolds that have orthologs on each of the six *C. elegans* chromosomes. **(C)** Distribution on the six chromosomes of *C. elegans* of orthologs of *B. malayi* genes. Orthologs map to both the conserved, central cores of the autosomes and to the less well conserved genes on the autosome arms. **(D)** Relative arrangements of the genes on *B. malayi* scaffold 14979 and their orthologs on *C. elegans* chromosome 3. Forward- and reverse-strand genes are distinguished (forward on top, reverse below). Red rectangles correspond to putative *B. malayi* operons, and black rectangles correspond to conserved operon structures.

the model worms. For example, *B. malayi* and *D. melanogaster* have similar numbers of genes of the most abundant domains, whereas several of the most abundant domains in the caenorhabditid nematodes rank much lower in or are absent from the filarial or fly genomes (fig. S5). For domains with high abundance in all four species, *C. elegans* tends to have 1.5- to 2-fold as many instances as do *B. malayi* or *D. melanogaster* (fig. S5).

The distinctive biology of *B. malayi* is likely to be underpinned by novel proteins with unique functions. After extensive comparative analyses, 20% of the predicted proteins were found to be *B. malayi*-specific (fig. S6 and table S10). More than one-third of the 1977 hypothetical proteins found only in *B. malayi* were confirmed by *B. malayi* expressed sequence tags. These genes constitute an interesting list of initial candidates for functional studies of putatively filaria-specific gene products.

The drugs used for treatment of filarial parasites, although effective in the short-term control of worm burden and transmission, require extended courses of treatment that have traditionally compromised their long-term effectiveness. Recently, issues of the emergence of drug resistance have become a concern (*13*, *14*). From the genome sequence we can identify several systems likely to be fruitful targets for the discovery of additional drug targets. (i) Molting: The *B. malayi* genome contains many homologs of genes that encode molecules required for molting in *C. elegans* (*15*) including proteases, protease inhibitors, nuclear hormone receptors (NRs), cuticular collagens, and chitinases (table S11). (ii) Nuclear receptors: Twenty-seven members of the NR family were identified in the *B. malayi* genome including orthologs of *Ecr* (not present in the caenorhabditids) and other NRs acting in the *D. melanogaster* ecdysone-response cascade (table S12). (iii) Collagens and collagen processing: *B. malayi* has ~82 genes that encode for a collagen repeat (including cuticular collagens and basement membrane collagens) (table S13), which is less than half the number of collagens found in the *C. elegans* genome (~180). It also encodes enzymes important for cuticular collagen processing such as blisterase-like proteases, protease inhibitors, tyrosinases, mixed-function oxidases, and peptidyl-prolyl isomerase (table S1). (iv) Neuronal signaling: Seven putative biogenic amine heterotrimeric guanosine 5′-triphosphate–binding protein (G protein)–coupled receptors, 44 Cys-loop receptors, and 36 genes encoding potassium channels (table S14) were identified in *B. malayi*, a number of which are orthologs of *C. elegans* genes that can be mutated to give paralytic or uncoordinated phenotypes. (v) The *B. malayi* kinome: The *B. malayi* genome encodes ~205 conventional and ~10 atypical protein kinases (Table 2), of which 142 appear to be of fundamental importance based on the severity of their RNAi phenotypes in *C. elegans* (table S15). (vi) Reliance on host and endosymbiont metabolism: As 9 of 10 enzymes required for de novo purine synthesis, 6 of 7 genes required for heme biosynthesis, and all 5 enzymes required for de novo riboflavin biosynthesis are absent from the *B. malayi* genome, the worm may be forced to meet requirements for these key metabolic factors by active uptake of host-supplied molecules (*16*) or through reliance on *w*Bm, which has complete purine, heme, and riboflavin synthesis pathways (*17*).

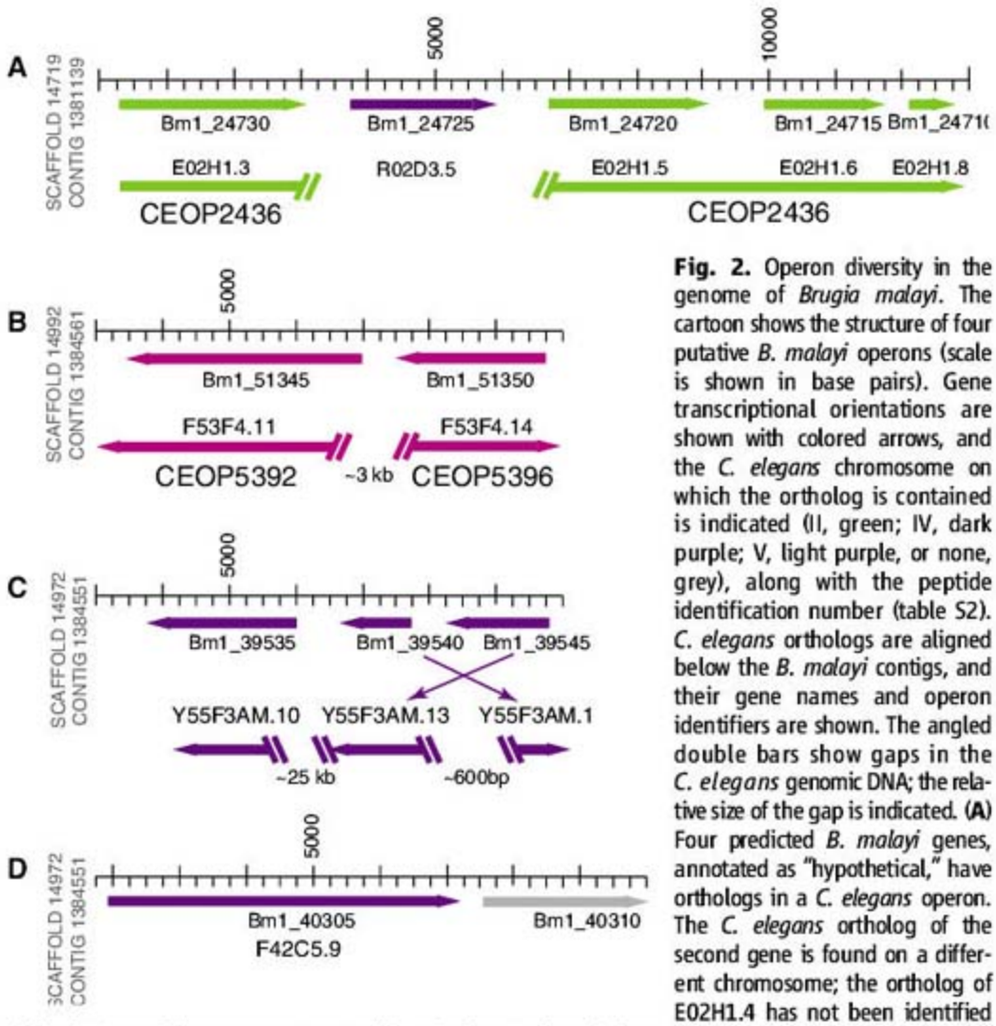

Fig. 2. Operon diversity in the genome of *Brugia malayi*. The cartoon shows the structure of four putative *B. malayi* operons (scale is shown in base pairs). Gene transcriptional orientations are shown with colored arrows, and the *C. elegans* chromosome on which the ortholog is contained is indicated (II, green; IV, dark purple; V, light purple, or none, grey), along with the peptide identification number (table S2). *C. elegans* orthologs are aligned below the *B. malayi* contigs, and their gene names and operon identifiers are shown. The angled double bars show gaps in the *C. elegans* genomic DNA; the relative size of the gap is indicated. **(A)** Four predicted *B. malayi* genes, annotated as "hypothetical," have orthologs in a *C. elegans* operon. The *C. elegans* ortholog of the second gene is found on a different chromosome; the ortholog of E02H1.4 has not been identified within the *B. malayi* genome sequence. **(B)** In *C. elegans*, the orthologs of these genes are found in operons adjacent to each other but in opposing transcriptional orientations. **(C)** The *C. elegans* orthologs of genes found in this operon are relatively close to each other but are not in an operon. **(D)** The *C. elegans* ortholog of the first gene is not in the operon while the downstream gene (independently verified GenBank accession CAD22104) has no identifiable *C. elegans* ortholog.

Effective RNAi by soaking worms in double-stranded RNA (dsRNA) has been demonstrated in *B. malayi* adults (*18*). We therefore expected to find components of the RNAi pathway in the genome (table S16). However, some genes necessary for systemic RNAi in *C. elegans* appear to be absent from *B. malayi*, including *sid-1*, a membrane channel that transfers dsRNA molecules from a source cell to neighboring cells (*19*); *sid-2*; *sid-3*; and *rsd-6*. The presence of a putative *drsh-1* ortholog suggests that *B. malayi* is also capable of microRNA processing. The effectiveness of RNAi in *B. malayi* implies either that these genes are rapidly evolving or are not required in *B. malayi* or that alternate pathways for siRNA transfer exist. Improvement of RNAi protocols for filarial nematodes would offer an attractive testing platform for verifying candidate drug targets.

Mapping *B. malayi* genes onto the *C. elegans* protein-protein interaction network (*20*) reveals an interesting pattern of evolutionarily conserved relations within the context of interconnected functional modules (figs. S7 and S8). Of 957 *B. malayi* genes that could be mapped, only 30 were found to be nematode-specific (supporting online text), revealing the overall conserved nature of the protein interaction network (*21*). Given the low level of sequence similarity between the two nematodes, the identification of conserved functional modules indicates that results from investigations of these complexes within *C. elegans* may be effectively translated to *B. malayi*.

B. malayi interacts with two hosts during its life cycle and is thought to have evolved mechanisms to suppress, subvert, or exploit host defense systems (*22*). Comparison of sequences of predicted proteins of *B. malayi* to that of interleukins, chemokines, and other signaling molecules from humans identified intriguing candidates including two genes encoding members of the macrophage migration inhibition (MIF) family of signaling molecules (*23*), transforming growth factor beta (TGFβ) homologs (including *Bm-tgh-1*) (*24*), and a member of the PDZ domain/interleukin 16 family (table S17). These proteins may be immune modulators that promote parasite survival or growth and differentiation factors important in parasite development. In addition, members of the ALT (abundant larval transcript) family of proteins have been implicated as virulence factors through their ability to modulate macrophage function (*25*). The *B. malayi* genome sequence revealed an unexpected diversity of 13 ALT genes (table S17), most of which are expressed by adult parasites. Note that the ALTs represent one of the few gene families that are expanded in *B. malayi* but not in *C. elegans* (which has only one member).

The innate immune systems encoded in the *B. malayi* genome have a complexity comparable to those of *C. elegans* (*26*) and include thioester proteins, scavenger receptors, C-type lectins, and galectins. However, both nematodes lack the peptidoglycan-recognition and lipopolysaccharide-binding proteins found in arthropods. Although there are orthologs of some components of the DAF-2, TGFβ, and p38 mitogen-activated protein (MAP) kinase signaling cascades in *B. malayi* and *C. elegans*, there is no evidence for the nuclear factor κB and Dif pathways. None of the small antibacterial peptides described from *C. elegans* and *Ascaris suum* (*27*) were identified in *B. malayi*, which suggests that the parasite might have a unique set of small peptide effectors or may lack this effector arm altogether. *B. malayi* gene products implicated in defense against and interaction with mammalian and insect immune systems were found, including seven genes encoding antioxidants deployed at the cuticle surface, where they may protect against oxyradical attack (*28*) (table S17).

Four representative organisms involved in the maintenance of Brugian filariasis have now been sequenced: the nematode parasite; its *Wolbachia* endosymbiont, *w*Bm; mosquito vectors (*Aedes* and *Anopheles*); and the human host. Together these present opportunities for a systems-based approach to understanding the molecular basis of parasitism and for identification of targets for intervention. In addition, defining the molecular mechanisms that allow filarial worms to persist for decades in an immunologically competent host may yield new strategies for the control of autoimmunity and the management of transplanted tissues.

The differences in genome content and organization between *Caenorhabditis* and *B. malayi* underscore the importance of obtaining additional genome data from representative species from across the diversity of the Nematoda (*29*). The ability to carry out large-scale comparative genomics within Nematoda will be key in defining molecules and pathways unique to nematode development and parasitism that can serve as the targets for the next generation of anti-nematode drugs and vaccines.

References and Notes

1. E. Ghedin, S. Wang, J. M. Foster, B. E. Slatko, *Trends Parasitol.* **20**, 151 (2004).
2. Y. Sakaguchi, I. Tada, L. R. Ash, Y. Aoki, *J. Parasitol.* **69**, 1090 (1983).
3. B. K. Sim, J. Shah, D. F. Wirth, W. F. Piessens, *Ciba Found. Symp.* **127**, 107 (1987).

Table 2. The kinomes of the nematodes *B. malayi*, *C. elegans*, and *C. briggsae* in comparison with that of *Homo sapiens*. Eukaryotic protein kinases are mainly defined on the basis of sequence similarity of their catalytic domains, plus knowledge of accessory domains and any known modes of regulation. Conventional protein kinases (EPKs) include AGC [adenosine 3′,5′-monophosphate–dependent protein kinase/protein kinase G/protein kinase C] kinases regulated by cyclic-nucleotide and calcium-phospholipid binding; casein kinase 1 and close relatives (CK1); calmodulin-dependent kinases (CaMK), cyclin-dependent kinases (CDK)/mitogen-activated protein kinases/glycogen synthase kinases/CDK-like kinases (CMGC); receptor guanylate cyclase (RGC); a group including many kinases functioning in MAP kinase cascades (STE); tyrosine kinases (TK); tyrosine kinase-like kinases (TKL). Atypical protein kinases (APKs) include Alpha (exemplified by myosin heavy chain kinase of *Dictyostelium discoideum*); phosphatidylinositol 3-kinase–related kinases (PIKK); pyruvate dehydrogenase kinases (PHDK); "right open reading frame" (RIO) [named as such as it was one of two adjacent genes that were found to be transcribed divergently from the same intergenic region].

Protein kinases	Organism				Kinases shared by all 3 nematodes
	H. sapiens	*C. elegans*	*C. briggsae*	*B. malayi*	
EPKs					
AGC	84	35	46	22	19
CAMK	98	63	69	41	23
CK1	12	91	77	31	13
CMGC	70	56	60	33	28
RGC	5	27	24	4	4
STE	61	35	27	27	16
TK	93	96	73	35	21
TKL	55	22	21	12	9
Total	478	425	397	205	133
APKs					
PIKK	6	5	4	5	4
Alpha	6	1	1	1	1
PDHK	5	1	1	1	1
RIO	3	3	3	3	3
Total	20	10	9	10	9

4. L. A. McReynolds, S. M. DeSimone, S. A. Williams, *Proc. Natl. Acad. Sci. U.S.A.* **83**, 797 (1986).
5. Materials and methods are available as supporting material on *Science* Online.
6. L. D. Stein *et al.*, *PLoS Biol.* **1**, E45 (2003).
7. C. Whitton, J. Daub, M. Thompson, M. Blaxter, *Methods Mol. Biol.* **270**, 75 (2004).
8. J. R. Vanfleteren *et al.*, *Mol. Phylogenet. Evol.* **3**, 92 (1994).
9. D. B. Guiliano *et al.*, *Genome Biol.* **3**, RESEARCH0057.1 (2002).
10. K. Z. Lee, A. Eizinger, R. Nandakumar, S. C. Schuster, R. J. Sommer, *Nucleic Acids Res.* **31**, 2553 (2003).
11. T. Blumenthal, *Brief. Funct. Genomic. Proteomic.* **3**, 199 (2004).
12. D. B. Guiliano, M. L. Blaxter, *PLOS Genetics* **2**, e198 (2006).
13. K. Awadzi *et al.*, *Ann. Trop. Med. Parasitol.* **98**, 231 (2004).
14. A. E. Schwab, D. A. Boakye, D. Kyelem, R. K. Prichard, *Am. J. Trop. Med. Hyg.* **73**, 234 (2005).
15. A. R. Frand, S. Russel, G. Ruvkun, *PLoS Biol.* **3**, e312 (2005).
16. S. N. Chen, R. E. Howells, *Exp. Parasitol.* **51**, 296 (1981).
17. J. Foster *et al.*, *PLoS Biol.* **3**, e121 (2005).
18. A. A. Aboobaker, M. L. Blaxter, *Mol. Biochem. Parasitol.* **129**, 41 (2003).
19. W. M. Winston, C. Molodowitch, C. P. Hunter, *Science* **295**, 2456 (2002).
20. S. Li *et al.*, *Science* **303**, 540 (2004).
21. R. Sharan *et al.*, *Proc. Natl. Acad. Sci. U.S.A.* **102**, 1974 (2005).
22. J. Murray, W. F. Gregory, N. Gomez-Escobar, A. K. Atmadja, R. M. Maizels, *Mol. Biochem. Parasitol.* **118**, 89 (2001).
23. D. V. Pastrana *et al.*, *Infect. Immun.* **66**, 5955 (1998).
24. N. Gomez-Escobar, E. Lewis, R. M. Maizels, *Exp. Parasitol.* **88**, 200 (1998).
25. N. Gomez-Escobar *et al.*, *BMC Biol.* **3**, 8 (2005).
26. S. Alper, S. J. McBride, B. Lackford, J. H. Freedman, D. A. Schwartz, *Mol. Cell. Biol.* **27**, 5544 (2007).
27. Y. Kato, S. Komatsu, *J. Biol. Chem.* **271**, 30493 (1996).
28. X. Ou, L. Tang, M. McCrossan, K. Henkle-Duhrsen, M. E. Selkirk, *Exp. Parasitol.* **80**, 515 (1995).
29. M. L. Blaxter, *Adv. Parasitol.* **54**, 101 (2003).

30. Funding for this project was provided by a grant from the National Institute for Allergy and Infectious Diseases, NIH (NIAID/NIH U01-AI50903) awarded to E.G. and A.L.S. We would like to acknowledge our colleagues in the Filarial Genome Consortium and the filarial research community for their continued support and encouragement. The Filarial Genome Consortium was initiated by grants from the United Nations Special Programme for Research and Training in Tropical Diseases (TDR), which is cosponsored by the U.N. Children's Fund (UNICEF), U.N. Development Programme (UNDP), World Bank, and World Health Organization (WHO) (T23/79/152 to A.L.S.; T23/79/153 to B.S.; and T23/79/157 to S.A.W.). This whole-genome shotgun project has been deposited at the DNA Databank of Japan (DDBJ), European Molecular Biology Laboratory (EMBL), and GenBank under the project accession AAQA00000000. The version described in this paper is the first version AAQA01000000. The data are also available in WormBase release WS175.

Supporting Online Material

www.sciencemag.org/cgi/content/full/317/5845/1756/DC1
Materials and Methods
SOM Text
Figs. S1 to S8
Tables S1 to S17
References

8 May 2007; accepted 14 August 2007
10.1126/science.1145406

UHRF1 Plays a Role in Maintaining DNA Methylation in Mammalian Cells

Magnolia Bostick,[1]* Jong Kyong Kim,[2]* Pierre-Olivier Estève,[2] Amander Clark,[1] Sriharsa Pradhan,[2]† Steven E. Jacobsen[1,3]†

Epigenetic inheritance in mammals relies in part on robust propagation of DNA methylation patterns throughout development. We show that the protein UHRF1 (ubiquitin-like, containing PHD and RING finger domains 1), also known as NP95 in mouse and ICBP90 in human, is required for maintaining DNA methylation. UHRF1 colocalizes with the maintenance DNA methyltransferase protein DNMT1 throughout S phase. UHRF1 appears to tether DNMT1 to chromatin through its direct interaction with DNMT1. Furthermore UHRF1 contains a methyl DNA binding domain, the SRA (SET and RING associated) domain, that shows strong preferential binding to hemimethylated CG sites, the physiological substrate for DNMT1. These data suggest that UHRF1 may help recruit DNMT1 to hemimethylated DNA to facilitate faithful maintenance of DNA methylation.

Cytosine methylation is an epigenetic mark used for the silencing of transposable elements and for the regulation of development (*1*, *2*). Once established, DNA methylation is often stable through mitosis, in part because CG methylation is faithfully main-

tained after DNA replication by DNMT1 (*3*). The SRA domain present in the *Arabidopsis* KRYPTONITE histone methyltransferase, and also in UHRF1 family proteins found in plants and animals, was found to bind methylated DNA in either a CG, CHG (where H indicates A, T, or C), or asymmetrical sequence context (*4*–*7*). KRYPTONITE is required for maintenance of CHG DNA methylation, and the *Arabidopsis* UHRF1 homolog VIM1/ORTH2 is required for maintenance of CG methylation at centromeric repeat sequences (*6*, *7*). Mammalian UHRF1, formerly known as NP95 (nuclear protein 95) in mouse and ICBP90 (inverted CCAAT box binding protein 90) in human, contains several domains, including UBL (ubiquitin-like), RING (really interesting new gene), and PHD (plant homeo domain) domains and an SRA domain that can bind methylated DNA (*4*, *5*, *8*–*10*). Prior analysis has implicated UHRF1 in DNA damage control, regulation of S phase, and transformation to malignancy (*5*, *11*–*14*), although the mechanism behind these effects is unknown. In this study, we explored the interaction between UHRF1 and DNMT1 in maintaining mammalian CG DNA methylation.

[1]Department of Molecular Cell and Developmental Biology, University of California, Los Angeles, Los Angeles, CA 90095, USA. [2]New England BioLabs, Ipswich, MA 01938, USA. [3]Howard Hughes Medical Institute, University of California, Los Angeles, Los Angeles, CA 90095, USA.

*These authors contributed equally to this work.
†To whom correspondence should be addressed. E-mail: pradhan@neb.com (S.P.); jacobsen@ucla.edu (S.E.J.)

Methylation of genomic DNA from wild-type and *mUhrf1*$^{-/-}$ (mouse *Uhrf1*) embryonic stem (ES) cells (*15*) was analyzed by Southern blots and genomic bisulfite sequencing (*16*). We observed massive global losses of DNA methylation in *mUhrf1*$^{-/-}$ cells, as evidenced by a decrease in the size of genomic DNA after digestion with the CG methylation–sensitive restriction enzyme HpaII (Fig. 1A). We also observed decreased methylation of two well-characterized, heavily methylated, high copy number loci, the minor satellite and *IAP* (intracisternal A particle) elements (Fig. 1, B and C). We quantified the change in DNA methylation by using bisulfite sequencing of wild-type and *mUhrf1*$^{-/-}$ genomic DNA. We observed a decrease of *IAP* element CG DNA methylation from 91% in the

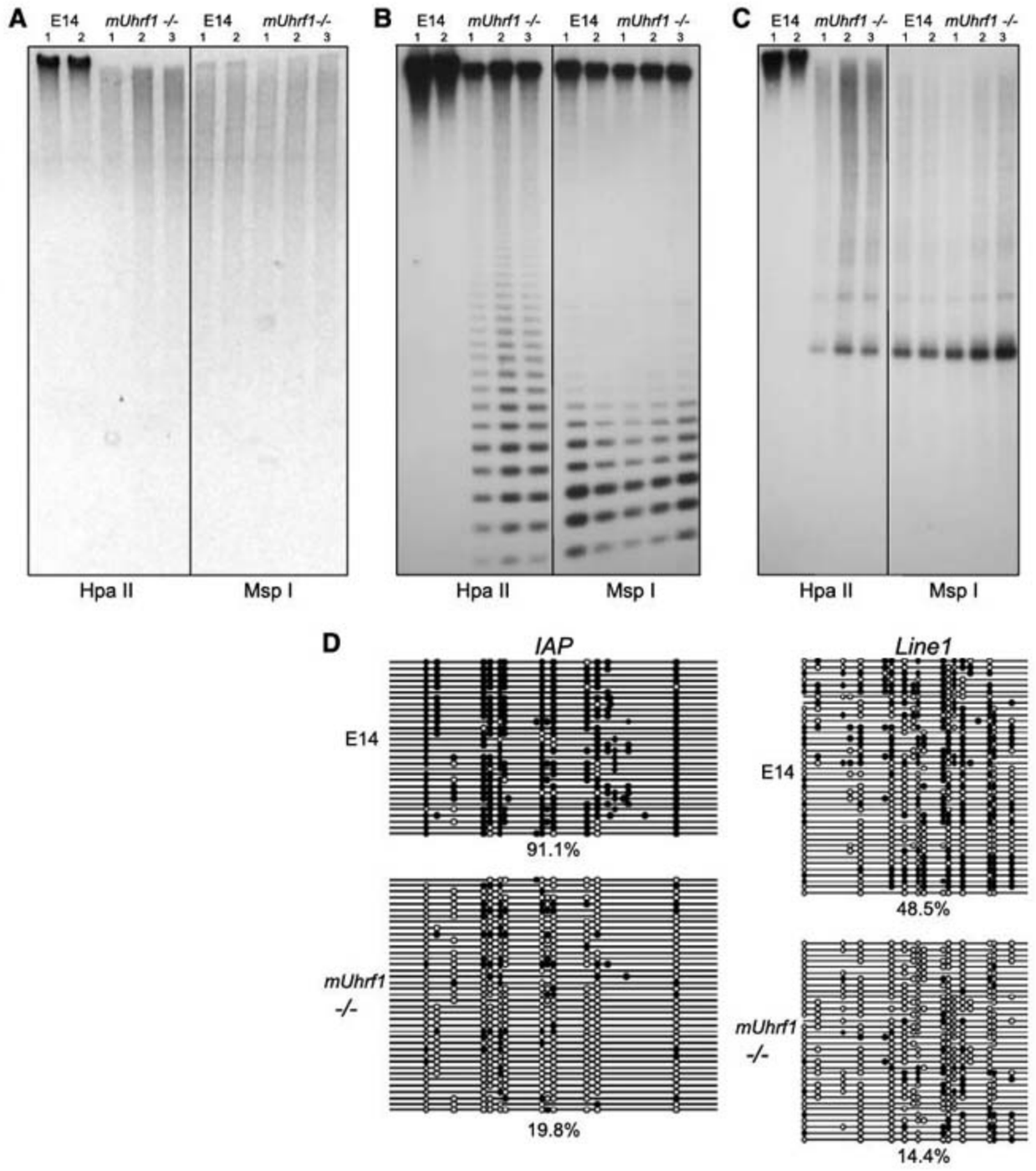

Fig. 1. Decreased DNA methylation in *mUhrf1*$^{-/-}$ ESC. (**A**) Ethidium bromide–stained genomic DNA from two wild-type (E14) and three *mUhrf1*$^{-/-}$ independent sets of ES cells digested with a CG methylation–sensitive enzyme (HpaII) or –insensitive enzyme (MspI). (**B** and **C**) Southern blots probed with a minor satellite (B) or *IAP* (C) probe. (**D**) Bisulfite sequencing methylation patterns at *IAP* (left) or *Line-1* (right) sequences. CG dinucleotides are represented by circles, solid if methylated and open if unmethylated. Percentages of methylated CG dinucleotides are below each pattern.

wild type to 19% in *mUhrf1*$^{-/-}$ and a decrease in *Line-1* (another abundant element) methylation from 49% to 14% (Fig. 1D). This loss of methylation phenotype was not a secondary consequence of decreases in DNA methyltransferases, because we observed that DNMT1, DNMT3a, and DNMT3b amounts were not reduced in the *mUhrf1*$^{-/-}$ cells (fig. S1).

Loss of DNMT1 activity also led to decreased genomic DNA methylation at *Line-1* (*17*), *IAP* (*18*), and minor satellite (*19*) sequences. Furthermore, both UHRF1- and DNMT1-depleted ES cells failed to properly differentiate and showed embryonic lethality, but both remained proliferative as ES cells (*15*, *20*). Lastly, the subnuclear localization of DNMT1 (*21*, *22*) and UHRF1 (*14*, *23*) have been studied as cultured cells progress through the cell cycle, and both were found at multiple foci during S phase. During mid-S phase, both UHRF1 and DNMT1 were shown to be at replication foci, as judged by colocalization with proliferating cell nuclear antigen (PCNA) and 5-bromo-2′-deoxyuridine (BrdU), and in late S phase both proteins were also found associated with 4′,6′-diamidino-2-phenylindole (DAPI)–staining heterochromatin (*14*, *23*–*25*). Consistent with these earlier findings, we found that, in COS-7 cells, mUHRF1 and DNMT1 colocalized as synchronized cells were allowed to progress from G1 though S phase (Fig. 2). As the cells entered S phase, both proteins moved from a diffuse pattern throughout the nucleus (excluded from the nucleolus) to primarily being localized to multiple foci (Fig. 2). Merged images of DNMT1 and mUHRF1 confirmed that these foci contained both proteins. The colocalization was especially evident in late S phase, when highly methylated heterochromatin is replicated (Fig. 2). This colocalization was repeated with hUHRF1 (human UHRF1) and DNMT1, giving very similar results (fig. S2). Consistent with the immunolocalization data, we found that hUHRF1 and DNMT1 were chromatin-associated proteins whose abundance in HeLa cell chromatin increased as cells progressed from G1 though S phase (fig. S3).

By using a coprecipitation assay, we found that UHRF1 and DNMT1 were physically asso-

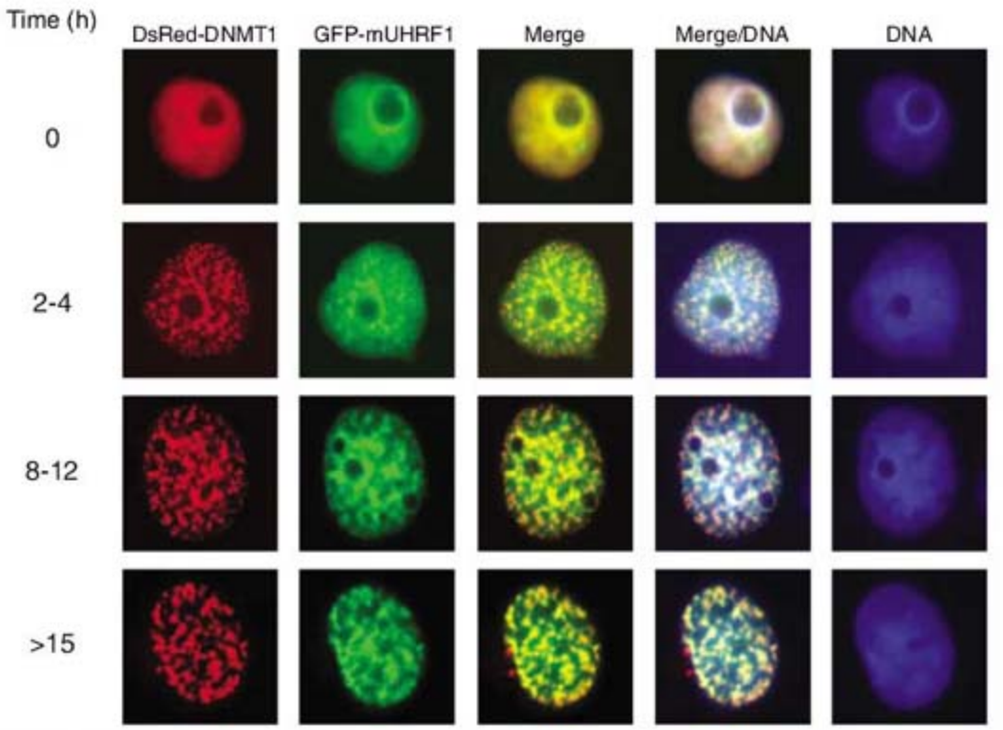

Fig. 2. Colocalization of mUHRF1 and DNMT1. Detection of DsRed-DNMT1 and green fluorescent protein (GFP)–mUHRF1 transiently expressed in synchronized COS-7 cells. Cells were released from G1 arrest and followed for the given number of hours (h) through S phase. DNA was visualized with Hoechst stain.

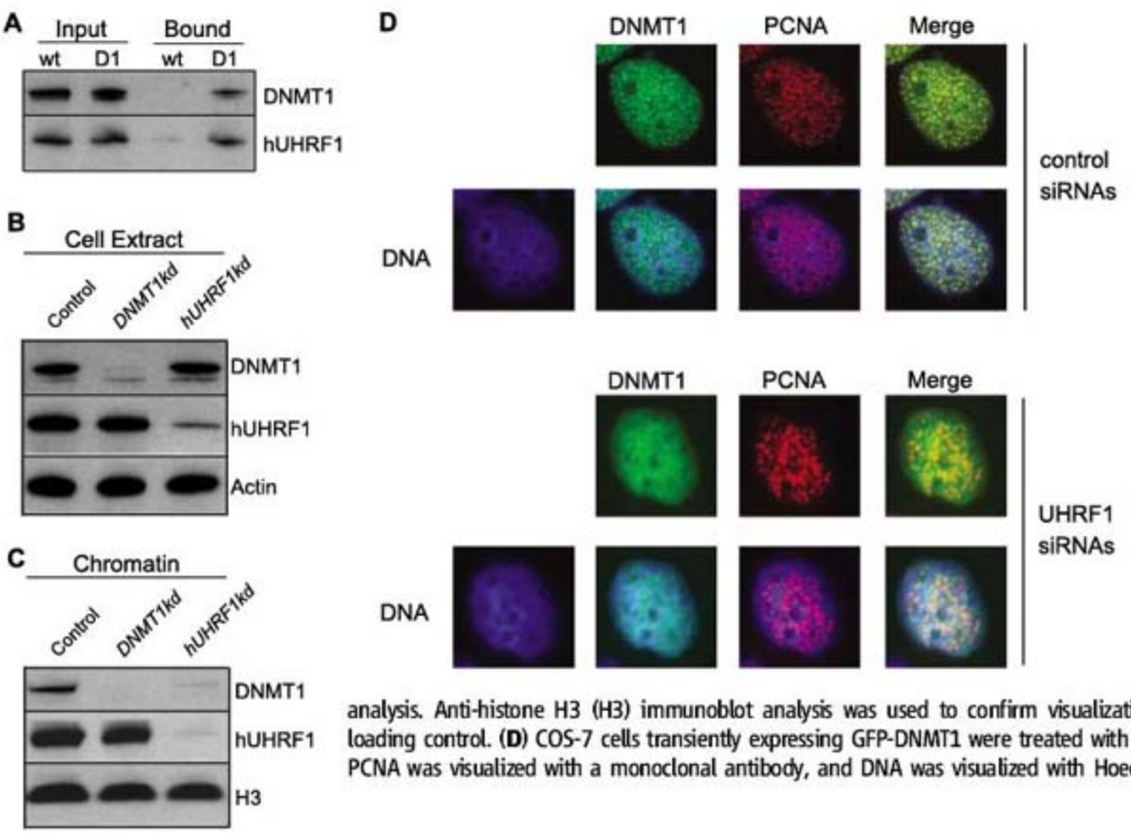

Fig. 3. hUHRF1 interacts with DNMT1 and is required for its association with chromatin. (**A**) Wild-type HEK293T cells (wt) or those stably expressing DNMT1 fused to CBD (D1) were used for coprecipitation experiments. Chitin sepharose was used to precipitate DNMT1. hUHRF1 and DNMT1 were detected by immunoblot analysis from total protein fractions (Input) or precipitation fractions (Bound) using antibodies against DNMT1 or hUHRF1. (**B**) Total proteins were extracted from mock-treated control HeLa cells (Control) or cells treated with siRNAs for *DNMT1* (*DNMT1* kd) or *hUHRF1* (*hUHRF1* kd). Decreased protein quantities were verified by immunoblot analysis, with antibodies against actin used as a loading control. (**C**) Chromatin was purified from wild-type HeLa cells (Control), *DNMT1* kd cells, or *hUHRF1* kd cells, and DNMT1 and hUHRF1 were detected by immunoblot analysis. Anti-histone H3 (H3) immunoblot analysis was used to confirm visualization of the chromatin fraction and as a loading control. (**D**) COS-7 cells transiently expressing GFP-DNMT1 were treated with mock (top) or *hUHRF1* (bottom) siRNAs. PCNA was visualized with a monoclonal antibody, and DNA was visualized with Hoechst stain.

ciated. We used a human cell line [human embryonic kidney–293 (HEK293T) cells] stably expressing a chitin binding domain (CBD) affinity-tagged DNMT1. We captured DNMT1-CBD fusion proteins with chitin sepharose beads and assayed for the presence of hUHRF1 in the precipitates by immunoblot analysis using an hUHRF1 antibody. hUHRF1 was highly enriched in the bound fraction (Fig. 3A). An additional analysis with recombinant DNMT1 and mUHRF1 demonstrated a direct interaction of the two proteins (fig. S4).

We next tested whether hUHRF1 depletion would affect the association of DNMT1 with chromatin. Small interfering RNAs (siRNAs) were used to reduce the amounts of endogenous hUHRF1 or DNMT1 in HeLa cells, and immunoblots of the knockdown cell extracts using hUHRF1- or DNMT1-specific antibodies confirmed that only the protein of interest was suppressed (Fig. 3B). Methylation-specific polymerase chain reaction (PCR) confirmed that methylation levels were decreased in these cells at both repeated sequences and at the *RAR*-β2 locus that is hypermethylated in HeLa cells (fig. S5). We then isolated chromatin from these cells and assayed for the presence of hUHRF1 and DNMT1 by immunoblotting of chromatin-associated proteins. In mock treated HeLa cells, DNMT1, hUHRF1, and histone H3 (a positive control) were all associated with chromatin (Fig. 3C). As expected, siRNA-mediated knockdown of hUHRF1 or DNMT1 depleted the respective protein from isolated chromatin. In addition, knockdown of hUHRF1 severely reduced the association of DNMT1 with chromatin, but knockdown of DNMT1 did not reduce the association of hUHRF1 with chromatin (Fig. 3C). We also analyzed the dependence of DNMT1 subnuclear localization on UHRF1. Whereas DNMT1 colocalized with the replication factor PCNA in wild-type cells, we found that, in both COS-7 cells treated with UHRF1 siRNAs (Fig. 3D) or in the *mUhrf1*$^{-/-}$ ES cells (fig. S6), DNMT1 showed a more dispersed pattern throughout the nucleoplasm. Together, these results suggest a model in which UHRF1 helps to tether DNMT1 to chromatin.

We studied the methyl DNA binding properties of the UHRF1 SRA domain by using electrophoretic mobility shift assays and a bacterially expressed and purified glutathione *S*-transferase (GST) fusion with the mUHRF1 SRA domain. We used double-stranded oligonucleotides that contained either unmethylated, fully methylated, or hemimethylated cytosines found in three different sequence contexts (CG, CHG, and asymmetric CHH; fig. S7). The mUHRF1 SRA only bound to DNA methylated in a CG context (Fig. 4A), consistent with the prevalence of this type of methylation in mammalian genomes. In addition, the mUHRF1 SRA domain bound better to hemimethylated CG DNA, whether it was methylated on the sense strand (hs) or the antisense strand (ha), than it did to fully methylated DNA (Fig. 4, A and B). We quantified this difference and found a sevenfold higher affinity for hemimethylated DNA (K_d = 1.8 ± 0.4 nM for hs and K_d = 1.7 ± 0.1 nM for ha) than for fully methylated DNA (K_d = 12.1 ± 1.7 nM) (mean ± SD, Fig. 4B and fig. S8). The mUHRF1 SRA domain did not bind to hemimethylated CNG-containing DNA or to asymmetrically methylated DNA (which is also methylated on only one strand), confirming its preference for CG methylation (Fig. 4A). In addition, negative control binding assays with purified GST alone showed no detectable binding even at greatly increased GST concentrations. We confirmed the specificity of the mUHRF1 SRA domain for hemimethylated DNA by performing competition studies where GST-mUHRF1SRA bound to the hemimethylated CG DNA (hs) was competed with unmethylated, fully methylated, or hemimethylated DNA (Fig. 4, C and D). Lastly, we found that hUHRF1 also shows a preference for hemimethylated CG DNA (fig. S9).

We found that the affinity for binding to hemimethylated DNA is not a general property of SRA domains, because this specificity was not observed for the *Arabidopsis* SRA-SET protein, SUVH6 (fig. S10) (*6*). This confirms our earlier finding that SRA domains from different proteins show a wide variation in binding properties for differentially methylated DNA (*6*).

In summary, we found that UHRF1 is required for maintenance of CG DNA methylation, physically interacts and colocalizes with DNMT1, and is required for the stable association of DNMT1 with chromatin. The affinity of the UHRF1 SRA domain for hemimethylated DNA suggests a model in which UHRF1 can bind to hemimethylated DNA and recruit DNMT1 to facilitate efficient maintenance CG methylation. Two other important factors are known to contribute to maintenance methylation. The first is the inherent preference of DNMT1's catalytic activity for hemimethylated DNA (*26*, *27*). The second is the recruitment of DNMT1 to replication foci through its interaction with PCNA

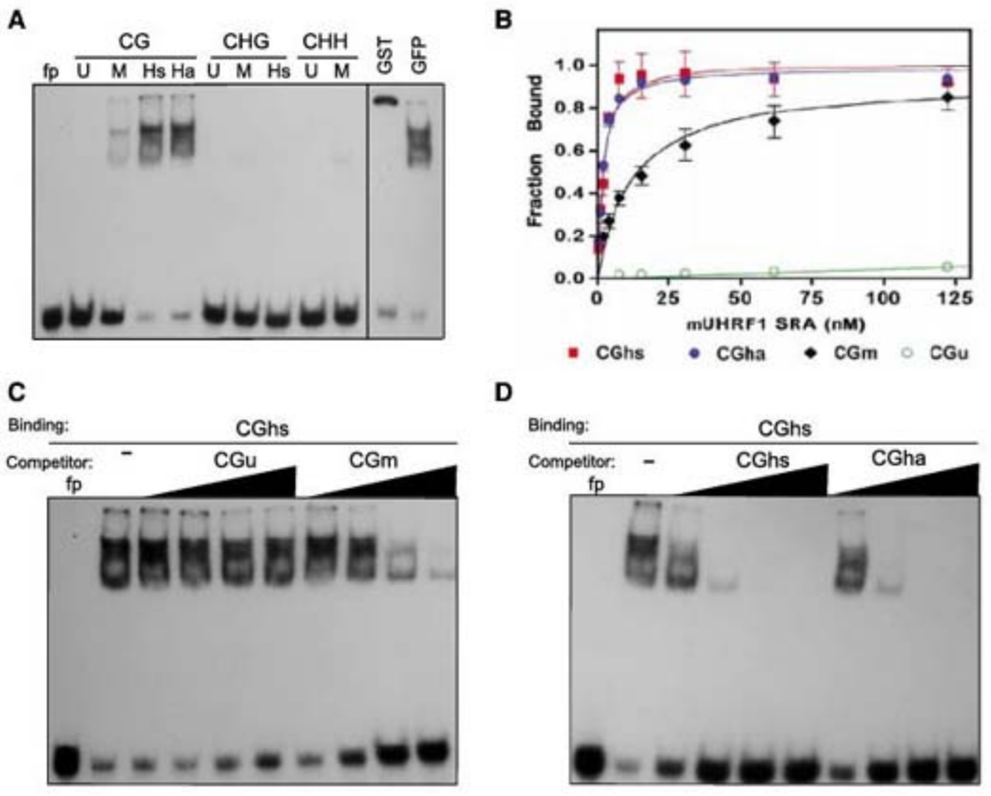

Fig. 4. SRA domain of mUHRF1 preferentially binds hemimethylated CG dinucleotides. **(A)** Electrophoretic mobility shift assays with GST-mUHRF1SRA binding to double-stranded oligonucleotides containing unmethylated (U), fully methylated (M), or hemimethylated DNA with the methyl cytosine on sense (Hs) or antisense (Ha) strands, in either a CG, CHG, or CHH sequence context. Antibody against GST (GST) added to the assay before electrophoresis supershifted the GST-mUHRF1SRA/DNA complex, whereas the nonspecific control antibody GFP (GFP) did not. **(B)** Quantification of binding of GST-mUHRF1SRA to unmethylated (CGu, circles), fully methylated (CGm, diamonds), or hemimethylated (CGhs, squares; CGha, solid circles) oligonucleotides. Points represent mean ± SD. **(C** and **D)** Competition assays with GST-mUHRF1 bound to CGhs and competed with 10×, 100×, 500×, and 1000× of unmethylated, fully methylated, or hemimethylated cold DNA. fp is free probe.

(*28*), although recent studies suggest that disruption of the PCNA-DNMT1 interaction results in only a small decrease in the efficiency of maintenance methylation (*25*, *29*, *30*). Together with the activity of UHRF1, these factors likely contribute to the high fidelity of CG maintenance methylation that contributes to epigenetic inheritance.

References and Notes

1. I. R. Henderson, S. E. Jacobsen, *Nature* **447**, 418 (2007).
2. C. B. Schaefer, S. K. T. Ooi, T. H. Bestor, D. Bourc'his, *Science* **316**, 398 (2007).
3. T. Bestor, A. Laudano, R. Mattaliano, V. Ingram, *J. Mol. Biol.* **203**, 971 (1988).
4. M. Unoki, T. Nishidate, Y. Nakamura, *Oncogene* **23**, 7601 (2004).
5. M. Jeanblanc *et al.*, *Oncogene* **24**, 7337 (2005).
6. L. M. Johnson *et al.*, *Curr. Biol.* **17**, 379 (2007).
7. H. R. Woo, O. Pontes, C. S. Pikaard, E. J. Richards, *Genes Dev.* **21**, 267 (2007).
8. E. Citterio *et al.*, *Mol. Cell. Biol.* **24**, 2526 (2004).
9. A. Fujimori *et al.*, *Mamm. Genome* **9**, 1032 (1998).
10. M. Mousli *et al.*, *Br. J. Cancer* **89**, 120 (2003).
11. I. M. Bonapace *et al.*, *J. Cell Biol.* **157**, 909 (2002).
12. M. Muto *et al.*, *Cell Prolif.* **28**, 645 (1995).
13. A. Sakai *et al.*, *Biol. Pharm. Bull.* **26**, 347 (2003).
14. R. Papait *et al.*, *Mol. Biol. Cell* **18**, 1098 (2007).
15. M. Muto *et al.*, *J. Biol. Chem.* **277**, 34549 (2002).
16. Materials and methods are available on *Science* Online.
17. D. M. Woodcock, M. E. Linsenmeyer, W. D. Warren, *Gene* **206**, 63 (1998).
18. C. P. Walsh, J. R. Chaillet, T. H. Bestor, *Nat. Genet.* **20**, 116 (1998).
19. M. Kim, B. N. Trinh, T. I. Long, S. Oghamian, P. W. Laird, *Nucleic Acids Res.* **32**, 5742 (2004).
20. E. Li, T. H. Bestor, R. Jaenisch, *Cell* **69**, 915 (1992).
21. H. Leonhardt, A. W. Page, H. U. Weier, T. H. Bestor, *Cell* **71**, 865 (1992).
22. Y. Liu, E. J. Oakeley, L. Sun, J. P. Jost, *Nucleic Acids Res.* **26**, 1038 (1998).
23. M. Miura, H. Watanabe, T. Sasaki, K. Tatsumi, M. Muto, *Exp. Cell Res.* **263**, 202 (2001).
24. H. P. Easwaran, L. Schermelleh, H. Leonhardt, M. C. Cardoso, *EMBO Rep.* **5**, 1181 (2004).
25 L. Schermelleh *et al.*, *Nucleic Acids Res.* **35**, 4301 (2007).
26. T. H. Bestor, *EMBO J.* **11**, 2611 (1992).
27. S. Pradhan, A. Bacolla, R. D. Wells, R. J. Roberts, *J. Biol. Chem.* **274**, 33002 (1999).
28. L. S. Chuang *et al.*, *Science* **277**, 1996 (1997).
29. G. Egger *et al.*, *Proc. Natl. Acad. Sci. U.S.A.* **103**, 14080 (2006).
30. F. Spada *et al.*, *J. Cell Biol.* **176**, 565 (2007).

31. We thank L. Johnson, A. Khattar, A. Conway, and N. Mohan for technical assistance and H. Koseki, M. Muto, G. Fan, and T. Bestor for reagents and advice. M.B. was partially funded by the American Heart Association Postdoctoral Fellowship 0625014Y. S.P. would like to thank R. Roberts, D. Comb, and New England Biolabs for support. Work in the Jacobsen lab is funded by NIH grant GM060398. S.E.J. is an Investigator of the Howard Hughes Medical Institute.

Supporting Online Material

www.sciencemag.org/cgi/content/full/1147939/DC1
Materials and Methods
Figs. S1 to S10
References

17 July 2007; accepted 26 July 2007
Published online 2 August 2007;
10.1126/science.1147939
Include this information when citing this paper.

MicroRNA Inhibition of Translation Initiation in Vitro by Targeting the Cap-Binding Complex eIF4F

Géraldine Mathonnet,[1*] Marc R. Fabian,[1*] Yuri V. Svitkin,[1] Armen Parsyan,[1] Laurent Huck,[1] Takayuki Murata,[1] Stefano Biffo,[2,3] William C. Merrick,[4] Edward Darzynkiewicz,[5] Ramesh S. Pillai,[6] Witold Filipowicz,[6] Thomas F. Duchaine,[1]† Nahum Sonenberg[1]†

MicroRNAs (miRNAs) play an important role in gene regulatory networks in animals. Yet, the mechanistic details of their function in translation inhibition or messenger RNA (mRNA) destabilization remain controversial. To directly examine the earliest events in this process, we have developed an in vitro translation system using mouse Krebs-2 ascites cell–free extract that exhibits an authentic miRNA response. We show here that translation initiation, specifically the 5′ cap recognition process, is repressed by endogenous let-7 miRNAs within the first 15 minutes of mRNA exposure to the extract when no destabilization of the transcript is observed. Our results indicate that inhibition of translation initiation is the earliest molecular event effected by miRNAs. Other mechanisms, such as mRNA degradation, may subsequently consolidate mRNA silencing.

MicroRNAs (miRNAs) are short [~21 nucleotides (nt) in length] regulatory RNAs encoded within the genomes of organisms ranging from plants to animals. They are implicated in the regulation of a wide variety of biological processes (*1*–*7*). miRNAs act in association with Argonaute (Ago) proteins as components of the RNA-induced silencing complex (RISC) to repress mRNA expression (*8*, *9*). Studies using in vivo systems reported that miRNAs either inhibit translation or lead to the degradation of the target mRNA or proteolysis of the nascent polypeptide (*10*–*17*). An important limitation to the in vivo studies is the fact that the outcome of mRNA silencing has been examined hours or days after the initial mRNA target recognition. Thus, the development of an in vitro system is necessary to understand the biochemistry of miRNA function, especially the early steps after the recruitment of RISC to the mRNA.

We chose the mouse Krebs-2 ascites cell extract as an in vitro translation system because it supports efficient translation and exhibits many endogenous and viral translational control mechanisms (*18*, *19*). We generated two constructs encoding the *Renilla* luciferase (Rluc) open reading frame fused to a 3′UTR (untranslated region) containing or lacking six target sites for let-7 miRNA (termed RL and RL-6xB, respectively), followed by a poly(A) tail of 98 nucleotides (*20*) (Fig. 1A). On the basis of quantitative real-time polymerase chain reaction (PCR) analyses, we estimated the total concentration of let-7a and let-7f miRNAs [which are the most abundant let-7 miRNAs in human tissues (*21*)] in the extract at ~150 pM. In vitro transcribed mRNAs were translated at concentrations varying from 3 pM to 3 nM. At the lowest concentration (3 pM), RL-6xB mRNA translation was only 25% of that of RL mRNA (Fig. 1B). In contrast, a decrease in translation was not observed at an mRNA concentration of 3 nM, consistent with a limiting concentration of let-7 miRNAs in the extract (Fig. 1B and fig. S1, A and B). In addition, the same degree of translation inhibition was observed when Rluc activity was normalized against firefly luciferase (Fluc) activity, expressed from Fluc mRNA used as an internal control (fig. S1, A and B). Moreover, the RL and RL-6xB mRNAs were translated with similar efficiency in a wheat germ extract where let-7 is absent (fig. S1C). These results show that target mRNA repression is sensitive to the relative concentrations of the mRNA and miRNA. The degree of inhibition by let-7 miRNA for a 1-hour reaction varied between 35 and 75% among the different extract preparations.

To address the specificity of the inhibition of RL-6xB mRNA translation by let-7, we supplemented the Krebs-2 ascites extract with an antisense 2′-*O*-methyl (2′-*O*-Me) oligoribonucleotide complementary to let-7 miRNA. This resulted in an ~2.5-fold increase in translation of RL-6xB mRNA (an increase from 28 to 71% relative to RL mRNA at 10 nM), but had no effect on translation of the control RL mRNA (Fig. 1C). Control 2′-*O*-Me oligonucleotides tar-

[1]Department of Biochemistry and McGill Cancer Center, McGill University, Montreal, Quebec, Canada, H3G 1Y6. [2]Department of Environmental and Life Sciences, University of Eastern Piedmont, 15100 Alessandria, Italy. [3]Laboratory of Molecular Histology, San Raffaele Scientific Institute, 20132 Milan, Italy. [4]Department of Biochemistry, Case Western Reserve University, Cleveland, OH 44106–4935, USA. [5]Department of Biophysics, Institute of Experimental Physics, Warsaw University, 02-089 Warsaw, Poland. [6]Friedrich Miescher Institute for Biomedical Research, Post Office Box 2543, 4002 Basel, Switzerland.

*These authors contributed equally to this work.
†To whom correspondence should be addressed. E-mail: nahum.sonenberg@mcgill.ca (N.S.); thomas.duchaine@mcgill.ca (T.F.D).

geting either miR-122a or miR-1 miRNAs failed to relieve translational inhibition even at a concentration of 10 nM (Fig. 1C).

With few exceptions, perfect complementarity of base pairing between the mRNA and the seed region of mRNA is required for repression. Translation of a reporter mRNA containing mutations in nucleotides complementary to the let-7 seed sequences (RL-6xBMut) (*10*) (Fig. 1A) was almost as efficient (~90%) as control RL mRNA (Fig. 1D), which indicated the importance of the let-7 seed region for inhibition of mRNA expression. These data show that the Krebs-2 ascites cell–free translation system faithfully recapitulates the properties of miRNAs established in vivo.

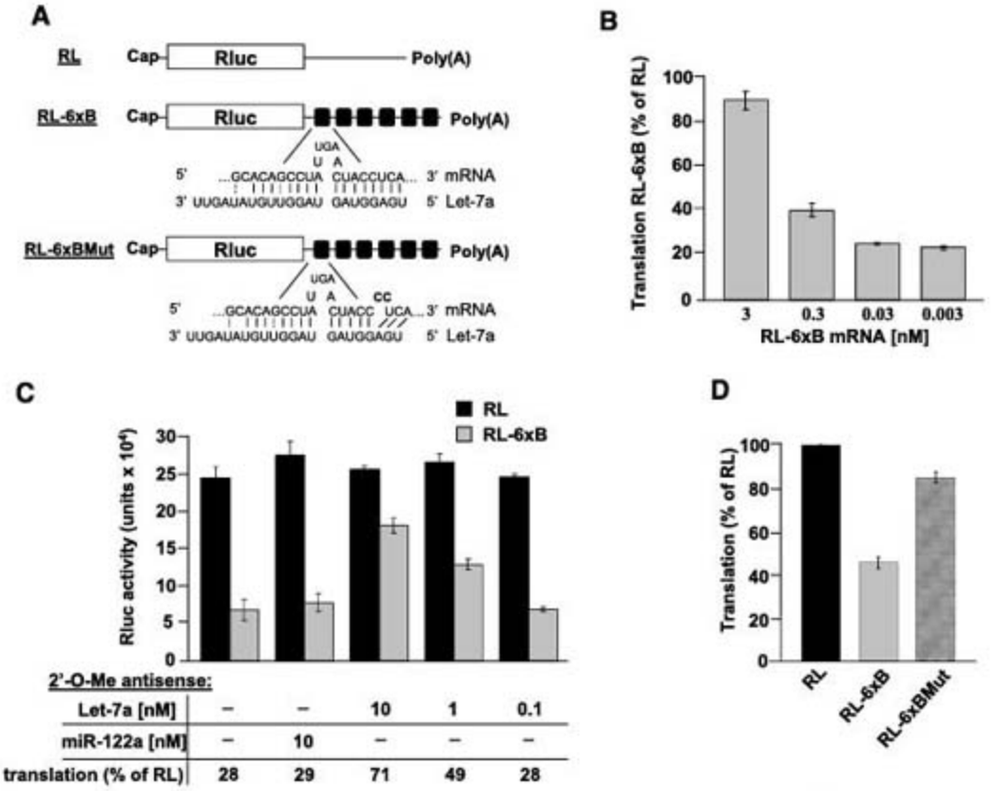

Fig. 1. Repression of protein synthesis by let-7 miRNA in an ascites extract. **(A)** Schematic representation of the *Renilla* luciferase (Rluc) reporter mRNAs. Sequences of the let-7a–binding sites (RL-6xB) and mutated seed sites (RL-6xBMut) are shown below the drawings. **(B)** Effect of mRNA concentration on RL-6xB inhibition. **(C)** Relief of RL-6xB mRNA repression by anti–let-7 2′-*O*-Me oligonucleotide. Where indicated, antisense 2′-*O*-Me oligonucleotides to let-7a or miR-122a were incubated for 20 min at 30°C with the extract before a 1-hour translation reaction. **(D)** Requirement for intact let-7 seed sequence for efficient RL-6xB inhibition. Experiments in (C) and (D) were performed at an mRNA concentration of 0.03 nM. Values represent means ± SD for $n \geq 3$.

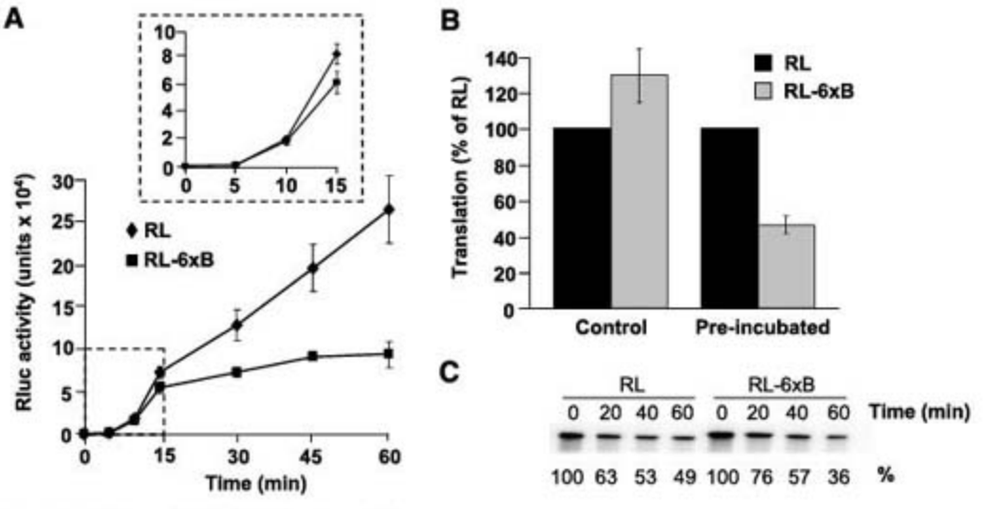

Fig. 2. let-7 miRNA inhibits translation without affecting mRNA stability in an ascites extract. **(A)** Time course of RL and RL-6xB mRNAs translation. [Inset] The first 15 min of translation enlarged. **(B)** Effect of mRNA preincubation on RL-6xB repression. Preincubation was carried out at 16°C for 20 min, followed by incubation for 10 min. **(C)** Time course of mRNA stability, as determined by autoradiography in the absence (top) or presence (bottom) of 10 nM anti–let-7 2′-*O*-Me oligonucleotide. Percent sign indicates percentage of intact mRNA relative to starting time. The data shown are representative of three independent experiments. Values in panels (A) and (B) represent means ± SD for $n = 3$.

Analysis of the kinetics of let-7–mediated inhibition revealed a decrease (~25%) in translation of RL-6xB mRNA relative to RL mRNA, first detected after 15 min of incubation (Fig. 2A); a stronger inhibition occurred at later times. The 15-min delay may reflect the time required to assemble the RISC complex on the mRNA. Consistent with this idea, preincubation of the reaction mixture at 16°C for 20 min (conditions that are unfavorable for translation) resulted in 30 to 50% inhibition as early as 10 min after transfer to 30°C (Fig. 2B and fig. S2), which demonstrated that the let-7 miRNA–associated machinery, once assembled on the mRNA, rapidly represses translation.

To determine whether the differential inhibition of RL-6xB mRNA expression might be the result of its faster degradation relative to control mRNA, we examined mRNA decay by measuring the integrity of uniformly labeled mRNAs. Both RL-6xB and RL decayed with similar kinetics during translation for up to 40 min of incubation, which indicated that degradation could not account for the differences in translation at the early time points (Fig. 2C). A 13% (±2) difference in stability between RL and RL-6xB mRNAs was observed at 1 hour (Fig. 2C, top). This difference in mRNA stability was abolished when anti–let-7 2′-*O*-Me was included in the reaction (Fig. 2C, bottom). These results indicate that mRNA degradation is not responsible for the inhibition of translation mediated by let-7 seen at early times.

A salient advantage of the in vitro translation extract over the published in vivo systems is that the step of translation that miRNAs inhibit can be precisely determined. Thus, we examined 80*S* ribosomal complex formation by performing glycerol gradient centrifugation. At 10 min of incubation, after preincubation at 16°C for 20 min [resulting in 50% inhibition of translation (Fig. 2B)], formation of the 80*S* complex on the RL-6xB mRNA was reduced by about half when compared with RL, and this inhibition was almost fully relieved in the presence of anti–let-7 2′-*O*-Me (Fig. 3). These results demonstrate that let-7 miRNA rapidly inhibits ribosome recruitment to the mRNA.

To determine whether let-7 targets the cap-recognition step in translation initiation, we examined the translation of a reporter mRNA containing the internal ribosome entry site (IRES) of encephalomyocarditis virus (EMCV) (Fig. 4A). Internal translation initiation by the EMCV IRES requires neither a functional cap

nor the cap-binding initiation factor eIF4E, a component of the eIF4F complex (*22*). The EMCV–RL-6xB mRNA was translated efficiently (90%) when compared with the control EMCV-RL mRNA, and the anti–let-7 2′-*O*-Me oligonucleotide did not stimulate its translation (Fig. 4B). Thus, we conclude that EMCV IRES-dependent translation is refractory to inhibition by let-7. Next, we substituted the 7-methylguanosine cap (m^7GpppG) with ApppG on the reporter mRNAs. Although the translation of the ApppG-capped mRNA was, as expected, dramatically reduced (1% of m^7GpppG-capped mRNA), there was no apparent difference in translation between the ApppG-capped RL and RL-6xB mRNAs (Fig. 4C). These results demonstrate the necessity of a functional cap structure for miRNA-mediated mRNA repression.

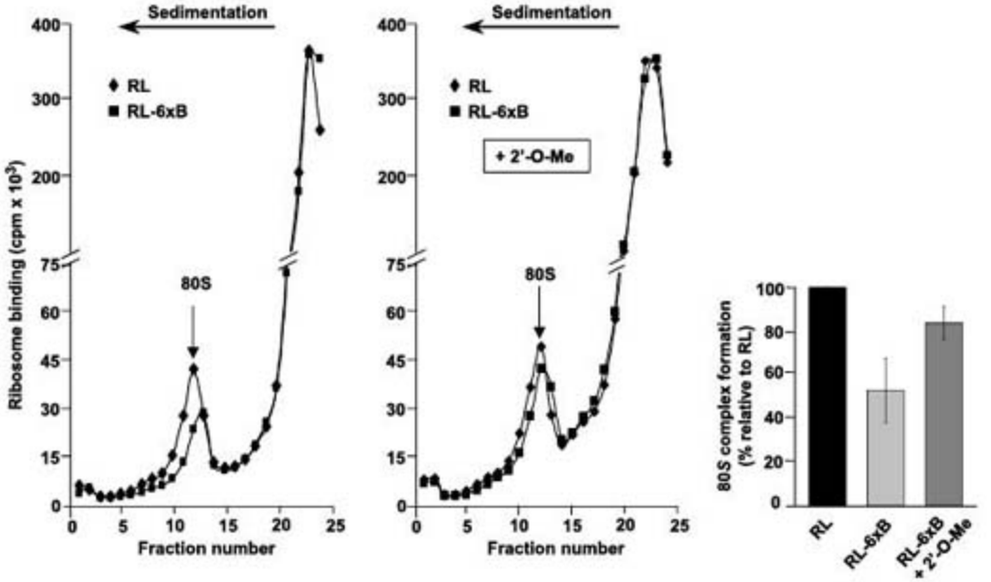

Fig. 3. let-7 miRNA inhibits ribosome binding. Ribosome binding assay of RL and RL-6xB mRNAs in the absence (**left**) or presence of anti–let-7 2′-*O*-Me (**middle**). Ascites extract was preincubated at 16°C for 20 min, followed by a 10-min incubation at 30°C. The position of the 80*S* ribosomes was determined by recording absorbance at 254 nm. mRNA concentration was 0.03 nM. The right panel represents the percentage of the area under the 80*S* peak, calculated from three independent experiments, relative to RL. The number of counts per minute in each fraction was normalized to correct for differences in total cpm recovery between RL and RL-6xB gradients. (**Right**) Values represent means ± SD for $n = 3$.

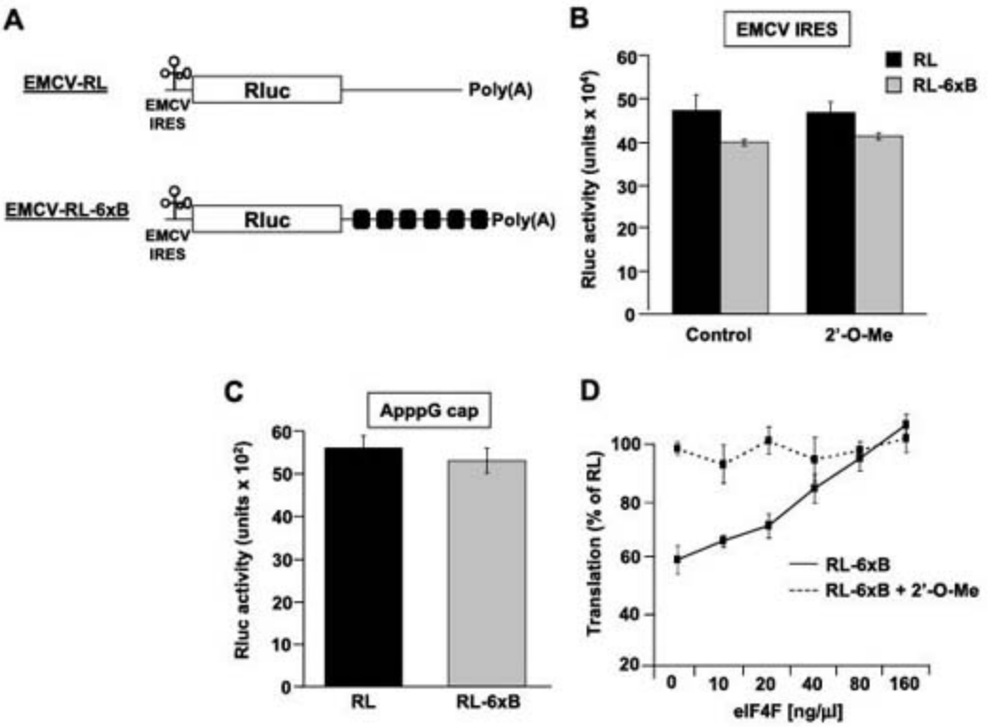

Fig. 4. let-7 miRNA inhibits cap-dependent, but not cap-independent, translation in an ascites extract. (**A**) Schematic structure of mRNAs containing the EMCV IRES. (**B**) The EMCV IRES confers resistance to repression of RL-6xB translation. EMCV IRESs containing mRNAs were translated for 1 hour in the presence or absence of anti–let-7 2′-*O*-Me oligonucleotides. (**C**) ApppG-capped RL-6xB mRNA is refractory to let-7–mediated inhibition. (**D**) Effect of eIF4F addition on miRNA-mediated repression. Extracts were supplemented with the indicated amounts of purified eIF4F, and Rluc activity was assayed after a 1-hour translation reaction. Data are depicted as a percentage of translation relative to RL in the presence or absence of anti–let-7 2′-*O*-Me oligonucleotide. Assays contained 0.03 nM mRNA. Values in (B), (C), and (D) represent means ± SD for $n = 3$.

The levels of many miRNAs change in cancer (*28*), whereas eIF4E and eIF4G function as oncogenes (*29*). Our results raise the intriguing possibility that eIF4E and eIF4G function to

counteract the activity of miRNAs in cancer development and progression.

References and Notes

1. V. Ambros, *Nature* **431**, 350 (2004).
2. N. Bushati, S. M. Cohen, *Annu. Rev. Cell Dev. Biol.* published online 21 May 2007, 10.1146/annurev.cellbio.23.090506.123406, in press.
3. W. P. Kloosterman, R. H. Plasterk, *Dev. Cell* **11**, 441 (2006).
4. C. Z. Chen, L. Li, H. F. Lodish, D. P. Bartel, *Science* **303**, 83 (2004).
5. T. Du, P. D. Zamore, *Development* **132**, 4645 (2005).
6. L. He, G. J. Hannon, *Nat. Rev. Genet.* **5**, 522 (2004).
7. G. Meister, T. Tuschl, *Nature* **431**, 343 (2004).
8. R. S. Pillai, S. N. Bhattacharyya, W. Filipowicz, *Trends Cell Biol.* **17**, 118 (2007).
9. R. J. Jackson, N. Standart, *Sci. STKE* **2007**, re1 (2007).
10. R. S. Pillai *et al.*, *Science* **309**, 1573 (2005).
11. D. T. Humphreys, B. J. Westman, D. I. Martin, T. Preiss, *Proc. Natl. Acad. Sci. U.S.A.* **102**, 16961 (2005).
12. C. P. Petersen, M. E. Bordeleau, J. Pelletier, P. A. Sharp, *Mol. Cell* **21**, 533 (2006).
13. S. Bagga *et al.*, *Cell* **122**, 553 (2005).
14. L. Wu, J. Fan, J. G. Belasco, *Proc. Natl. Acad. Sci. U.S.A.* **103**, 4034 (2006).
15. S. Nottrott, M. J. Simard, J. D. Richter, *Nat. Struct. Mol. Biol.* **13**, 1108 (2006).
16. I. Behm-Ansmant *et al.*, *Genes Dev.* **20**, 1885 (2006).
17. P. H. Olsen, V. Ambros, *Dev. Biol.* **216**, 671 (1999).
18. Y. V. Svitkin, N. Sonenberg, *Methods Mol. Biol.* **257**, 155 (2004).
19. A. Kahvejian, Y. V. Svitkin, R. Sukarieh, M. N. M'Boutchou, N. Sonenberg, *Genes Dev.* **19**, 104 (2005).
20. Materials and methods are available as supporting material on *Science* Online.
21. C. K. Raymond, B. S. Roberts, P. Garrett-Engele, L. P. Lim, J. M. Johnson, *RNA* **11**, 1737 (2005).
22. T. V. Pestova, C. U. Hellen, I. N. Shatsky, *Mol. Cell. Biol.* **16**, 6859 (1996).
23. M. Kiriakidou *et al.*, *Cell* **129**, 1141 (2007).
24. R. Thermann, M. W. Hentze, *Nature* **447**, 875 (2007).
25. T. P. Chendrimada *et al.*, *Nature* **447**, 823 (2007).
26. P. A. Maroney, Y. Yu, J. Fisher, T. W. Nilsen, *Nat. Struct. Mol. Biol.* **13**, 1102 (2006).
27. B. Wang, T. M. Love, M. E. Call, J. G. Doench, C. D. Novina, *Mol. Cell* **22**, 553 (2006).
28. A. Esquela-Kerscher, F. J. Slack, *Nat. Rev. Cancer* **6**, 259 (2006).
29. Y. Mamane *et al.*, *Oncogene* **23**, 3172 (2004).

30. We thank M. Costa-Mattioli, A. Rosenfeld, and D. Arvanitis for comments. Supported by Human Frontiers Science Foundation (N.S.), Howard Hughes Medical Institute (E.D.), NIH (W.C.M.). Postdoctoral support by Fonds de Recherche en Santé du Québec (FRSQ) to G.M., Natural Sciences and Engineering Research Council and Richard H. Tomlinson (M.R.F.), Fonds National Suisse (L.H.), Japanese Society for the Promotion of Science (T.M.), Canadian Institute of Health Research and FRSQ awards (T.F.D.). Friedrich Miescher Institute is supported by the Novartis Research Foundation.

Supporting Online Material

www.sciencemag.org/cgi/content/full/1146067/DC1
Materials and Methods
Figs. S1 to S3
References

5 June 2007; accepted 17 July 2007
Published online 26 July 2007;
10.1126/science.1146067
Include this information when citing this paper.

Dynamic Visualization of Thrombopoiesis Within Bone Marrow

Tobias Junt,[1] Harald Schulze,[2]* Zhao Chen,[2] Steffen Massberg,[1] Tobias Goerge,[1] Andreas Krueger,[2]† Denisa D. Wagner,[1] Thomas Graf,[4] Joseph E. Italiano Jr.,[3] Ramesh A. Shivdasani,[2]‡ Ulrich H. von Andrian[1]‡

Platelets are generated from megakaryocytes (MKs) in mammalian bone marrow (BM) by mechanisms that remain poorly understood. Here we describe the use of multiphoton intravital microscopy in intact BM to visualize platelet generation in mice. MKs were observed as sessile cells that extended dynamic proplatelet-like protrusions into microvessels. These intravascular extensions appeared to be sheared from their transendothelial stems by flowing blood, resulting in the appearance of proplatelets in peripheral blood. In vitro, proplatelet production from differentiating MKs was enhanced by fluid shear. These results confirm the concept of proplatelet formation in vivo and are consistent with the possibility that blood flow–induced hydrodynamic shear stress is a biophysical determinant of thrombopoiesis.

Blood platelets are required to maintain hemostasis in mammals. The relative paucity of MKs in normal BM contrasts with the relative abundance of platelets in peripheral blood and implies that platelet assembly and release are highly efficient, dynamic processes. The prevalent model for thrombopoiesis, the proplatelet or flow model (*1*, *2*), receives support mostly from MK differentiation cultures (*3*–*5*), which deprive MKs of cellular contacts and signals found in intact BM (*6*, *7*). The flow model proposes that MKs extend plump pseudopodia that give rise to long (>100-μm) branched proplatelet processes that appear "beaded" by virtue of intermediate swellings (*3*, *4*, *8*). It is unclear whether proplatelets detach from MKs in bulk and fragment further into platelets (*4*) or whether barbell-shaped platelet pairs detach exclusively from proplatelet ends (*8*), but eventually the MK cytoplasm is exhausted as a result of fragment release. Previous in situ imaging approaches, such as electron microscopy, helped define the morphology and environment of MKs in the BM (*1*, *2*, *9*), but they provided only static snapshots that leave room for alternative mechanistic concepts of thrombopoiesis. For example, the platelet territory model proposes that vesicles from internal MK demarcation membranes are released as mature platelets (*10*–*12*). Another conundrum pertains to how newly formed platelets traverse BM vessel walls and escape activation by subendothelial prothrombotic factors.

To observe thrombopoiesis in vivo, we studied mouse skull BM by multiphoton intravital microscopy (MP-IVM) (*13*, *14*). To identify MKs and their progeny, we used *CD41-EYFP*$^{ki/+}$ mice in which enhanced yellow fluorescent protein (EYFP) was expressed as a targeted transgene from the endogenous gene locus for *CD41*, an MK- and platelet-specific integrin (*15*). We used heterozygous *CD41-EYFP*$^{ki/+}$ mice and confirmed that EYFP$^+$ MKs in BM of these animals generate fully functional platelets at normal frequency (fig. S1).

MKs showed considerable morphological diversity; they occurred mostly as isolated cells but occasionally in clusters, and they were always found in close contact with BM sinusoids (Fig. 1, A and B, and movie S1). MKs were largely sessile, exhibiting minimal migratory tracks or three-dimensional (3D) instantaneous velocities as compared with other BM-resident cell types (Fig. 1C). To facilitate imaging of normally rare MKs, we pretreated some mice with thrombopoietin (TPO), which increased MK numbers but did not alter their perivascular localization (fig. S2 and movie S2). Another physiologic activity of TPO is the differentiation of immature MKs, which are small and compact, toward larger mature cells that assemble and release platelets (*16*). Indeed, 3D reconstructions of intravital recordings (Fig. 1, D and E) revealed that TPO treatment increased maximal MK diameters (Fig. 1F) and volumes (Fig. 1G) and caused more irregular MK shapes (Fig. 1H).

Many MKs exhibited fragmented protrusions (Fig. 1, I and J, and movie S3), whereas others were surrounded by scattered EYFP$^+$ particles (Fig. 1A and movie S4), which may represent proplatelets that remained connected to the MK cell body. However, particle connections were mostly inferred based on near-linear alignment and close proximity of particles to large MK bodies (Fig. 1J), because insuffi-

[1]Immune Disease Institute and Department of Pathology, Harvard Medical School, Boston, MA 02115, USA. [2]Dana-Farber Cancer Institute, Boston, MA 02115, USA. [3]Hematology Division, Brigham and Women's Hospital, Boston, MA 02115, USA. [4]Centre de Regulacio Genomica, Parc de Recesca Biomedica de Barcelona, 08003 Barcelona, Spain.

*Present address: Klinik für Allgemeine Pädiatrie, Charite, Labor für Pädiatrische Molekularbiologie, 10117 Berlin, Germany.
†Present address: Institute of Immunology, Hannover Medical School, 30625 Hannover, Germany.
‡To whom correspondence should be addressed. E-mail: uva@hms.harvard.edu (U.H.v.A.); ramesh_shivdasani@dfci.harvard.edu (R.A.S.)

cient signal intensity limited direct visualization. The farnesylated EYFP reporter protein in *CD41-EYFP*$^{ki/+}$ MK localizes to external and internal membranes (*15*, *17*); intermediate and distal proplatelet swellings contain numerous internal membranes and thus generate a robust fluorescent signal, whereas proplatelet shafts contain little membrane (*18*) and tend to fall below the detection limit. Nevertheless, we captured the formation of MK fragments on 1- to 2-μm-thick, branching filaments budding from one MK pole (fig. S3A and movie S5), reminiscent of proplatelet formation in vitro (*8*). Consistent with TPO-induced MK maturation, interstitial MK fragments tended to be smaller in TPO-treated mice (Fig. 1K). However, almost all MK fragments were 10 to 100 times as large as circulating platelets (Fig. 1K), implying that few mature platelets get released within the BM interstitium. Most EYFP$^+$ fragments in the BM were immotile, but some moved with a median 3D instantaneous velocity of 3.9 μm/min (fig. S3, B and C, and movie S6). Because proplatelet elongation from cultured MKs occurs at ~0.85 μm/min (*19*), these observations suggest that the BM microenvironment enhances the motility of MK extensions.

Consistent with ultrastructural observations (*1*, *2*, *20*), MKs extended cellular processes into BM microvessels in TPO-treated and untreated mice (Fig. 2A, movie S7, and fig. S2). These intravascular EYFP$^+$ extensions had a mean volume of 3295 μm^3 (Fig. 2B), corresponding to ~6% of the average MK volume or 824 times the mean volume of mature murine platelets (4 μm^3). These fragments may represent multiple intertwined or single immature proplatelets. MP-IVM recordings also captured MKs extending plump perivascular pseudopodia, reportedly the first step of platelet release in vitro (*8*, *18*), over the span of <15 min (Fig. 2C and movie S8). On one occasion, an unusually large EYFP$^+$ MK fragment entered a BM vessel, and intravascular fluorescein isothiocyanate (FITC)–dextran tracer accumulated upstream, indicating transient vascular occlusion (Fig. 2D and movie S9). Such observations imply that BM sinusoidal diameter imposes size constraints on released MK fragments and that transsinusoidal migration of whole MKs (*21*) is probably rare. Smaller, spherical MK fragments typically protruded through the sinusoidal wall (Fig. 2E), moved in the direction of blood flow, and were eventually released into the lumen, either slowly along the endothelium (Fig. 2E and movie S10) or briskly (movie S11).

These observations collectively reveal that MKs routinely release heterogeneous particles, with properties resembling immature proplatelets, into BM microvessels. Shedding events in TPO-treated mice were recorded about once every 7 hours per field of view. Even these seemingly infrequent events likely contribute substantially toward physiological platelet outputs. Assuming that the platelet lifespan is 5 to 6 days and that TPO treatment doubled the normal platelet number in mice [~2.2 × 10^9 to ~4.4 × 10^9 platelets (*22*)], we calculate the steady-state platelet production in TPO-treated animals as 0.8 × 10^9 platelets per day. Mouse BM and spleen contain a total of ~180,000 MKs (*14*), whose number is also doubled after TPO treatment (*22*). If each MK releases one fragment every 7 hours, the total intravascular discharge amounts to 1.2 × 10^6 fragments per 24 hours, with a combined mean volume (Fig. 2B) corresponding to ~1 × 10^9 platelets. Thus, even if we consider that proplatelet cytoplasmic mass may not completely convert into mature platelets as it diminishes during further fragmentation (*8*, *18*), these calculations suggest that intravascular proplatelet shedding by juxtasinusoidal MKs may account for the bulk of thrombopoiesis. However, it should be cautioned that we cannot exclude additional thrombopoieitic events that may occur below the limit of MP-IVM resolution or in regions that are inaccessible to intravital imaging.

To assess how intravascular shedding of MK fragments relates to the presumptive MK maturation sequence, we first classified nonshedding MKs in TPO-treated mice into two groups ("small" and "large") according to how their maximal diameter related to the mean diameter calculated in Fig. 1F. Based on 3D reconstruc-

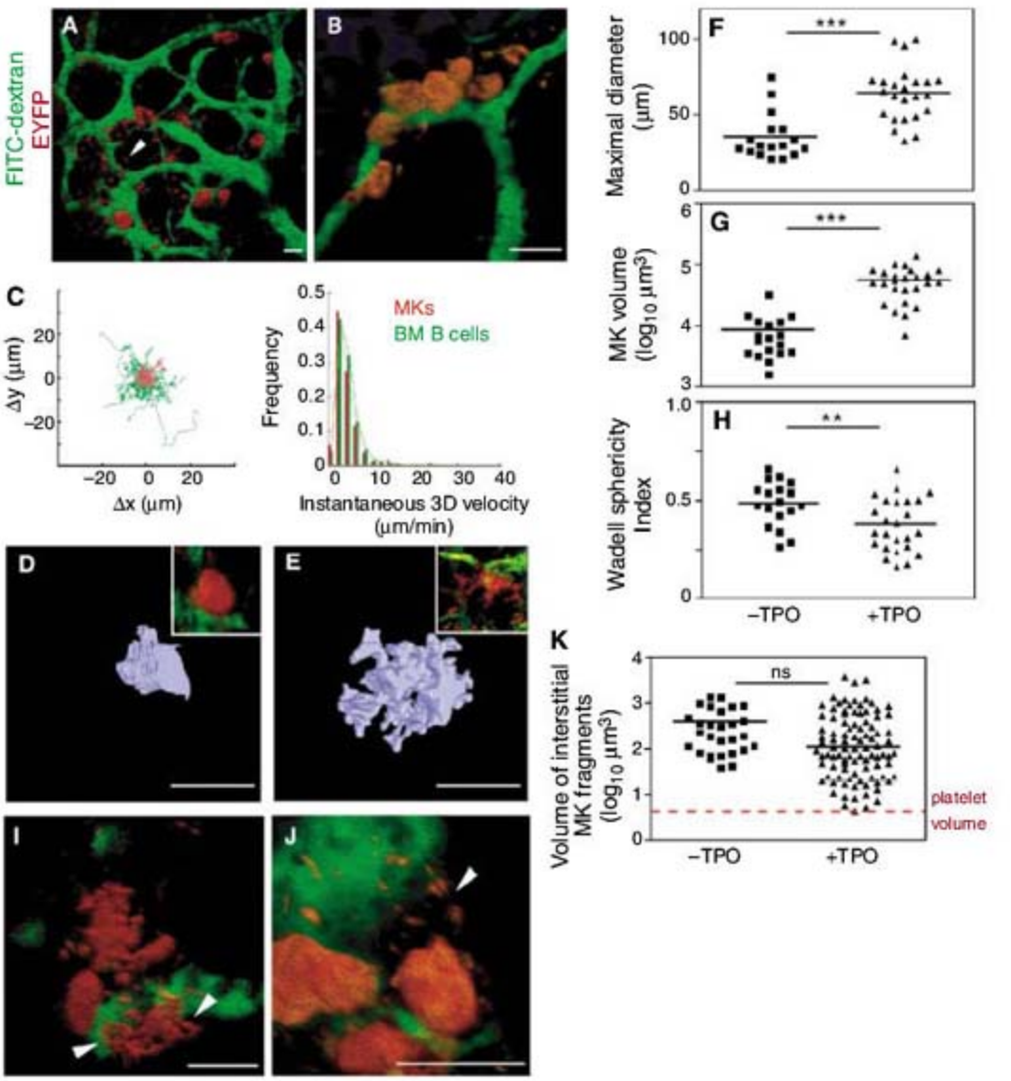

Fig. 1. Localization of EYFP$^+$ MKs in BM of living mice. (**A**) EYFP$^+$ MKs (red) and surrounding areas of fragmentation (arrowhead) in close proximity to BM sinusoids, which were outlined by intravenous injection of FITC-dextran (green). (**B**) Clusters of MKs along a BM sinusoidal vessel. (**C**) Cumulated tracks and instantaneous 3D velocities of BM MKs (red) and B lymphocytes (green). One representative of four movies for B cells, combined with cumulative data from four MK movies, is shown. (**D** and **E**) Representative 3D reconstructions of MKs from time-lapse MP-IVM; insets show renderings of intravital recordings. (**F** to **H**) Maximal diameters (F), volumes (G), and Wadell sphericity indices (H) of MKs in BM cavities of mice without (squares) or after (triangles) TPO treatment. $^{**}P < 0.01$, $^{***}P < 0.001$; unpaired Student's *t* test. (**I**) Representative MKs with proplatelet-like protrusions (arrowheads). (**J**) Zones of aligned EYFP$^+$ interstitial fragments close to an MK (arrowhead), possibly tethered to the cell body. Scale bars in (A), (B), (D), (E), (I), and (J), 50 μm. (**K**) Volumes of interstitial MK fragments with or without apparent connection to MK cell bodies and with or without TPO treatment. The dashed line denotes mean platelet volume. Data were compared with an unpaired Student's *t* test. ns, not significant. Horizontal bars in [(F) to (H)] and (K) indicate means.

tions, we determined MK volumes, surface areas, and Wadell sphericity indices (Fig. 2, F to H). Small MKs displayed a higher average sphericity index than large cells, indicating that the latter were less compact and shaped more irregularly. These findings agree with morphological changes recorded in cultured MKs before proplatelet formation (*3*, *5*) and hold true whether TPO was administered or not (fig. S4), confirming that TPO does not alter MK differentiation qualitatively (*23*). Size and shape parameters of MKs that were actively shedding intravascular fragments were statistically similar to those of large nonshedding MKs (Fig. 2, F to H). Thus, vascular release of MK fragments occurred

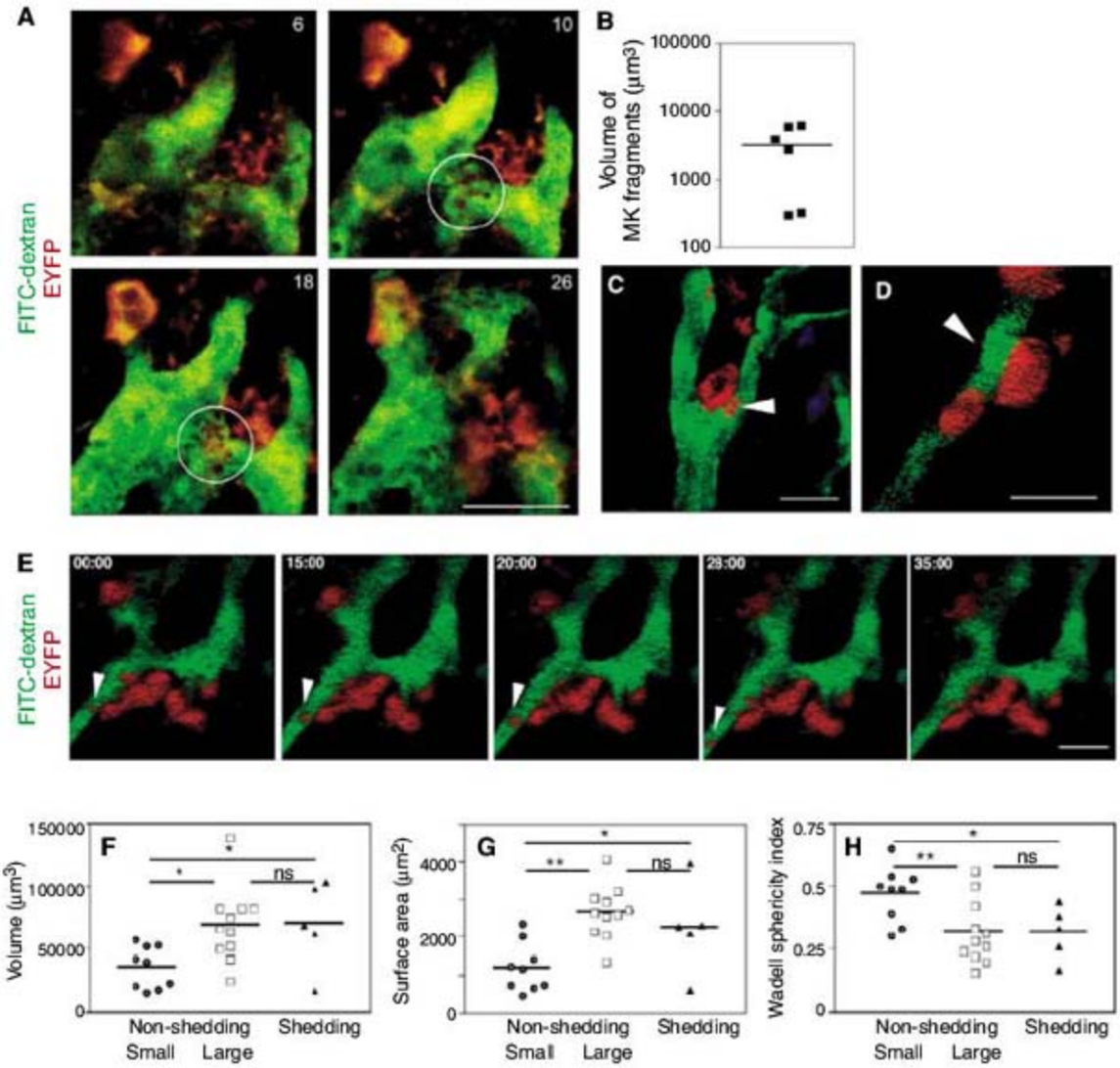

Fig. 2. Intravascular MK fragmentation. (**A**) EYFP$^+$ MK (red) with proplatelet extensions inside BM sinusoids (see circles), which were demarcated by FITC-dextran injection (green). Numbers at top right in each panel denote image depth in μm. (**B**) Volume of EYFP$^+$ fragments released from MKs into BM sinusoids (bar represents mean: 3295 μm^3). (**C**) Apparent pseudopodium elaboration (arrowhead) by a perivascular MK. (**D**) Presence of a very large MK fragment in a sinusoidal vessel, with upstream accumulation (arrowhead) of FITC-dextran tracer. (**E**) Intravascular shedding of a MK fragment (arrowhead). Numbers at top left in each panel correspond to minutes and seconds. Scale bars in (A) and (C) to (E), 50 μm. (**F** to **H**) Volumes (F), surface areas (G), and Wadell sphericity indices (H) of small and large nonshedding MKs and of MKs captured in the process of shedding intravascular fragments. Data were analyzed with one-way analysis of variance tests with Bonferroni's post-test. *$P < 0.05$, **$P < 0.01$. Horizontal bars in (B) and (F) to (H) indicate means.

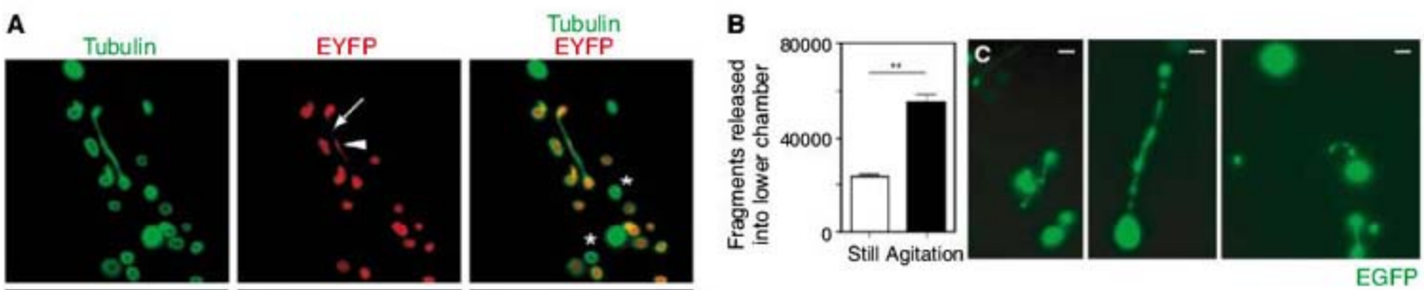

Fig. 3. Proplatelets in the circulation and proplatelets released from cultured MKs under shear stress. (**A**) Platelets and proplatelets in the peripheral blood of *CD41-EYFP$^{ki/+}$* mice. Immunostaining for β1 tubulin (green) highlights characteristic microtubule coils and identifies structures as bona fide platelets or platelet precursors. EYFP signal (red) is mostly found in intermediate swellings (arrowheads); proplatelet shafts carry low EYFP content (arrows). As expected (*15*), some *CD41-EYFP$^{ki/+}$* platelets lack EYFP expression (white asterisks). Scale bar, 10 μm. (**B**) Number of fragments released through 5-μm pores into lower transwell chambers, with (black bar) or without (white bar) agitation after mouse MKs were transduced with EGFP-expressing retrovirus and cultured to maturity. Means of triplicates are shown from one of two similar experiments; error bars indicate SEM. **$P < 0.01$; Student's *t* test. (**C**) Morphology of EGFP$^+$ MK fragments released through transwell filters after agitation. Scale bars, 10 μm.

concomitant to the expansion of MK size and loss of sphericity, most likely late in MK maturation, as predicted by proplatelet-based models of thrombopoiesis.

Because most shed MK fragments exceeded platelet dimensions, we inferred the presence of proplatelets in the systemic circulation, as proposed by Behnke (*24*). Indeed, beaded proplatelets and barbell-shaped platelet pairs (Fig. 3A) carrying characteristic β1-tubulin$^+$ marginal bands (*25*) were readily identified in peripheral blood of *CD41-EYFP*$^{Cre+}$ mice. Proplatelet morphogenesis is thought to continue in peripheral blood to engender individual platelets (*24*), possibly assisted by intravascular shear forces in pulmonary arterioles. This idea is consistent with observations that proplatelet counts are higher in prepulmonary vessels than in post-pulmonary vessels (*26*), whereas platelet counts are higher in the latter (*27*).

Our observations raise the possibility that blood flow–induced shear stress [1.3 to 4.1 dynes/cm^2 in BM sinusoids (*15*)] may help separate intravascular cell fragments from the MK proper. Thus, we reasoned that mature MKs may be particularly susceptible to such forces in vitro. Indeed, MKs cultured on top of 5-μm transwells shed significantly more proplatelet-like fragments into the lower chamber when they were gently agitated as compared with MKs in static cultures (Fig. 3, B and C). Together with our MP-IVM observations, these results support the idea that intravascular release of fragments protruding from mature MKs is aided by hydrodynamic fluid shear in BM sinusoids.

Our in vivo observations permit refinement of thrombopoiesis models. Although cell growth and maturation, early events in MK ontogeny, are modulated by factors like TPO, later steps may be directed by chemokines or by localized expression of ligands for MK surface receptors. For example, CXCL12 (stromal-derived factor 1) is a potent MK chemoattractant (*7*), and fibrinogen present along BM sinusoids promotes proplatelet formation through $\alpha_{IIb}\beta_3$ integrin on MKs (*28*). However, newly synthesized platelets entering BM microvessels must avoid procoagulant activation and local clotting when they traverse the subendothelial space. We propose that MKs may circumvent this problem by extending voluminous processes into the lumen of local sinusoidal vessels. These processes are sheared off and may serve as an intravascular source of new platelets. Our observations also provide evidence for partial MK fragmentation within the BM interstitium, but further studies will be needed to determine if these structures give rise to viable platelets or serve other local functions.

References and Notes

1. R. P. Becker, P. P. De Bruyn, *Am. J. Anat.* **145**, 183 (1976).
2. J. M. Radley, G. Scurfield, *Blood* **56**, 996 (1980).
3. E. S. Ogawa, J. L. Mitchell, M. M. Hebert, A. C. Hunsfeld, P. Hunt, *Blood* **85**, 402 (1995).
4. E. M. Cramer *et al.*, *Blood* **89**, 2336 (1997).
5. P. Jackson *et al.*, *Blood* **92**, 3030 (1998).
6. A. Eder *et al.*, *Blood Cells* **17**, 447 (1991).
7. S. I. Avecilla *et al.*, *Nat. Med.* **10**, 64 (2004).
8. J. E. Italiano Jr., P. Lecine, R. A. Shivdasani, J. H. Hartwig, *J. Cell Biol.* **147**, 1299 (1999).
9. M. A. Eckstein, J. K. Chamberlain, W. Strom, P. A. Santillo, *Am. J. Hematol.* **4**, 303 (1978).
10. E. Yavuzlu, *Acta Anat.* **29**, 267 (1957).
11. D. Zucker-Franklin, S. Petursson, *J. Cell Biol.* **99**, 390 (1984).
12. G. Bucki, *Int. J. Hematol.* **81**, 204 (2005).
13. I. B. Maas *et al.*, *J. Exp. Med.* **188**, 445 (1998).
14. *Materials and Methods are available as supporting material on Science Online.*
15. J. Zhang *et al.*, *Exp. Hematol.* **35**, 414 (2007).
16. K. Kaushansky, *Blood* **86**, 419 (1995).
17. H. Sibelius *et al.*, *Blood* **107**, 3618 (2006).
18. S. R. Patel, J. H. Hartwig, J. E. Italiano Jr., *J. Clin. Invest.* **115**, 3348 (2005).
19. S. R. Patel *et al.*, *Blood* **106**, 4076 (2005).
20. C. Paulet *et al.*, *Blood* **82**, 2482 (1993).
21. M. Kaushansky, *Blood* **55**, 517 (1980).
22. K. Kobaya *et al.*, *Stem Cells* **14**, 513 (1996).
23. S. Berking *et al.*, *Blood* **90**, 1423 (1997).
24. O. Behnke, A. Forer, *Int. J. Hematol. Suppl.* **63**, 3 (1998).
25. P. Lecine, J. E. Italiano Jr., S. W. Kim, J. L. Villeval, R. A. Shivdasani, *Blood* **96**, 1366 (2000).
26. P. J. Hindenburg, B. F. Feldman, N. C. Jain, T. B. Farver, C. S. Kaneps, *Am. J. Vet. Res.* **48**, 362 (1987).
27. W. H. Howell, D. D. Donahue, *J. Exp. Med.* **65**, 177 (1937).
28. M. K. Larson, S. P. Watson, *Blood* **108**, 1509 (2006).

29. We thank A. Abuarqub, H. Leung, J. Richardson, and S. Blanchard for advice. This work was funded by NIH grants HL56949 to U.H.v.A., HL61543 to R.A.S., and HL68130 to J.E.I. J.E.I. is a fellow of the Swiss National Science Foundation, E.Gu. is a fellow, and S.M. is a Heisenberg fellow of the Deutsche Forschungsgemeinschaft. The authors do not have competing financial interests.

Supporting Online Material

www.sciencemag.org/cgi/content/full/317/5845/1764/DC1
Materials and Methods
Figs. S1 to S4
References
Movies S1 to S11

11 June 2007; accepted 7 August 2007
10.1126/science.1146304

X-Ray Fluorescence Spectrometer

The Nanohunter benchtop total reflection x-ray fluorescence spectrometer is designed to offer comprehensive trace element and materials characterization analysis to a broader range of research disciplines, and in more diverse analytical settings, than was possible with previous technology. Whether for geologists, chemists, biochemists, biologists, materials scientists, or engineers, non-destructive trace element analysis is attainable, with minimal sample preparation, for applications that span from metallo-protein research to environmental assessment and semiconductor wafer metrology. Nanohunter features a patented, switchable wavelength and automated variable x-ray incidence angle excitation design. The instrument can analyze the full range of elements in solids, liquids, and powders. It also provides chemical information as a function of analysis depth for profiling surface characteristics of materials. For example, for researchers involved in nano-technology, this ability allows surface layers to be characterized as particles on a substrate, a homogenous thin film, or as something in between.

Rikagu For information 281-362-2300 www.rigaku.com

Stirring Hotplate

The Carousel Stirring Hotplate is a third-generation system with a host of new features to enable faster heating, more powerful stirring, greater accuracy, and superior safety. Offering adjustable speed control from 0 to 1200 rpm and a stirring capacity of up to 20 liters of water, the hotplate can perform a wide range of laboratory tasks. A digital display offers accuracy in setting stirring speeds and temperature. A removable PT1000 temperature sensor is standard.

Radleys For information +44-1799-513320 www.radleys.com

NIR Reference Materials

New certified reference materials for the near infrared (NIR) region of the spectrum are now available. The NIR region has recently found new and important applications, and verification of the wavelength scale in the region is particularly important because small wavelength errors can cause significant problems. Convenient reference materials have been hard to come by because they have too few peaks across the region or require the use of volatile solvents. This new reference material provides 13 certified and traceable peak values.

Starna Scientific For information +44 (0) 20 8501 5550 www.starna.com

Centrifugal Evaporator

The EZ-2 Series centrifugal evaporators combine performance and safety in a compact benchtop unit. Similar in size to a rotary evaporator, these instruments' innovative design presents advantages in parallel synthesis and medicinal chemistry, as well as for general-purpose solvent removal in life science laboratories. Technological innovations guard against overheating or losing samples through solvent bumping. The evaporator offers true unattended operation and requires no user training. Solvents collect in an insulated, plastic-coated glass vessel, enabling the user to see the progress of evaporation and determine when the trap should be emptied. With no defrosting required, the glass vessel is removed by a quarter turn, allowing the solvent to be poured directly into the waste container. The evaporator can concentrate or completely dry samples. It accommodates a wide selection of sample holders, enabling evaporation from most common sample container formats, including round-bottom flasks up to 500 ml, tubes up to 160 mm long, custom reaction blocks, and shallow-well or deep-well microplates.

Genevac For information +44 1473 240000 www.genevac.com

Purification Resin

Ni-NTA Superflow resin for the purification of histidine-tagged proteins is now available in pre-filled 1 ml and 5 ml cartridges for purification on liquid chromatography platforms such as the FPLC, AKTA, and BioLogic systems. Ni-NTA matrices are the most cited solutions for purifying 6× histidine-tagged proteins. Their high stability means that they are compatible with a wide range of buffer components, including strong denaturants, detergents, and even reducing agents.

Qiagen For information 800-426-8157 www.qiagen.com

Microarray Services

LC Sciences offers custom products and specialty microarray services of nucleic acid and protein analysis, biomarker discovery, novel drug screening, and custom development of miniaturized assay devices for diagnostics and biosensing applications. These products and services are based on a proprietary technology that integrates multiple high-throughput bioanalyses on a single platform. The mParaflo microfluidics technology integrates high throughput parallel synthesis, microfluidics, and digital photolithography to create custom microarrays of DNA, RNA, and peptides. Specific services include a microRNA Profiling Microarray Service, a Small Non-coding RNA Discovery Microarray Service, and a Peptide Microarray Service. Custom services include protein-binding oligonucleotide arrays for detection and profiling of transcription factors, nuclear receptors, DNA/RNA binding proteins, peptides, enzyme co-factors, carbohydrates, and metabolite molecules, and peptidomimetic arrays for lead drug or novel ligand discovery.

LC Sciences For information 888-528-8818 www.lcsciences.com

Ribonuclease R

Ribonuclease R is a magnesium-dependent 3′ → 5′ exoribonuclease that digests essentially all linear RNAs but will not digest lariat or circular RNA structures. Intron RNA can be isolated from total RNA samples by digestion with ribonuclease R. After digestion, only lariat structures that are produced during the pre-messenger RNA splicing of intron regions remain. Applications include alternative splicing studies, gene expression studies, intron complementary DNA production, and intronic screening of complementary DNA libraries.

Epicentre Biotechnologies For information 800-284-8474 www.EpiBio.com

Newly offered instrumentation, apparatus, and laboratory materials of interest to researchers in all disciplines in academic, industrial, and government organizations are featured in this space. Emphasis is given to purpose, chief characteristics, and availability of products and materials. Endorsement by *Science* or AAAS of any products or materials mentioned is not implied. Additional information may be obtained from the manufacturer or supplier.

Science Careers

From the journal *Science* AAAS

Classified Advertising

From life on Mars to life sciences

For full advertising details, go to www.sciencecareers.org and click on **For Advertisers,** or call one of our representatives.

United States & Canada

E-mail: advertise@sciencecareers.org
Fax: 202-289-6742

IAN KING Recruitment Sales Manager
Phone: 202-326-6528

ALLISON MILLAR
Industry–US & Canada
Phone: 202-326-6572

ALEXIS FLEMING
Northeast Academic
Phone: 202-326-6578

TINA BURKS
Southeast Academic
Phone: 202-326-6577

DARYL ANDERSON
Midwest/Canada Academic
Phone: 202-326-6543

NICHOLAS HINTIBIDZE
West Academic
Phone: 202-326-6533

Europe & International

E-mail: ads@science-int.co.uk
Fax: +44 (0) 1223 326532

TRACY HOLMES Sales Manager
Phone: +44 (0) 1223 326525

ALEX PALMER
Phone: +44 (0) 1223 326527

ALESSANDRA SORGENTE
Phone: +44 (0) 1223 326529

MARIUM HUDDA
Phone: +44 (0) 1223 326517

LOUISE MOORE
Phone: +44 (0) 1223 326528

Japan

JASON HANNAFORD
Phone: +81 (0) 52-757-5360
E-mail: jhannaford@sciencemag.jp
Fax: +81 (0) 52-757-5361

To subscribe to *Science*:
In U.S./Canada call 202-326-6417 or 1-800-731-4939
In the rest of the world call +44 (0) 1223-326-515

Science makes every effort to screen its ads for offensive and/or discriminatory language in accordance with U.S. and non-U.S. law. Since we are an international journal, you may see ads from non-U.S. countries that request applications from specific demographic groups. Since U.S. law does not apply to other countries we try to accommodate recruiting practices of other countries. However, we encourage our readers to alert us to any ads that they feel are discriminatory or offensive.

POSITIONS OPEN

BIOLOGICAL CHEMISTRY FACULTY POSITION
Wayne State University

The Department of Chemistry at Wayne State University seeks applications for a tenure-track position in the Division of Biological Chemistry. Preference will be given toward candidates at the **ASSISTANT PROFESSOR** level. Candidates must have a Ph.D. and the potential to develop a nationally recognized, externally funded research program of outstanding quality in any area of biological chemistry. The Department offers exciting opportunities for candidates with research interests complementing a large group of faculty working in the areas of DNA, RNA and protein biochemistry, enzymology, carcinogenesis, biophysical, bioorganic, and bioinorganic chemistry, as well as molecular and cellular biology (see departmental **website: http://chem.wayne.edu** for further information).

The Department of Chemistry has a supportive academic environment and a strong graduate program. Excellent opportunities exist for collaborative research with individuals in the Department of Biological Sciences, the basic science departments in the highly ranked School of Medicine, the College of Pharmacy and Health Sciences, as well as in the Center for Molecular Medicine and Genetics, the Institute for Environmental Health Sciences, and the Barbara Ann Karmanos Cancer Institute. The Department of Chemistry offers an excellent research environment that includes ample, newly renovated research laboratories and a fully staffed Central Instrument Facility that manages state-of-the-art equipment for: electrospray ionization and MALDI-TOF mass spectrometry, circular dichroism, electron parametic resonance, surface plasmon resonance, transmission electron microscopy, and nuclear magnetic resonance (NMR) (including a 700 megahertz [MHz] NMR with cryoprobe). The Wayne State faculty also have access to the resources of the Michigan Core Technology Alliance **(website: http://www.ctaalliance.org/),** which includes facilities for bioinformatics, proteomics, genomics, animal models and structural biology, including 900 MHz NMR and a dedicated synchrotron beamline for X-ray crystallography.

Applicants should submit a complete resume and description of future research plans, as well as three letters of recommendation addressing both research and teaching potential. All materials should be sent to: **Professor Charles H. Winter, Associate Chair, 141 Chemistry, Wayne State University, 5101 Cass Avenue, Detroit, MI 48202-3489.** In addition to the materials noted above, applicants must complete an online application at **website: https://jobs.wayne.edu.** Please apply for all chemistry faculty positions listed. Review of applications will begin in October 2007. *Women and minority candidates are encouraged to apply. Wayne State University is an Equal Opportunity and Affirmative Action Employer.*

CHAIR, BIOLOGY DEPARTMENT
East Carolina University

The Department of Biology at East Carolina University seeks an energetic, well-established Investigator to lead the Department's expanding research and teaching programs beginning on or before August 11, 2008. The successful candidate must have a Ph.D. or equivalent research degree in one of the biological sciences, administrative and teaching experience, and a record of distinguished scholarly achievements and funded research appropriate for appointment at the rank of **PROFESSOR.** Applicants must complete a candidate profile and submit statements of research interests and future plans, administrative philosophy, educational philosophy, curriculum vitae, and contact information for four current references online at **website: http://www.jobs.ecu.edu.** Address specific inquiries to **Dr. John Sutherland, e-mail: sutherlandj@ecu.edu;** for information about the Biology Department see **website: http://www.ecu.edu/biology.** Screening of applications will begin on November 1, 2007, and continue until the position is filled. *Equal Employer Opportunity/Affirmative Action Employer. Official transcript required upon employment.*

POSITIONS OPEN

POSTDOCTORAL POSITION in HEPATOBILIARY CANCER RESEARCH

Postdoctoral position available to participate in long-term NIH-funded research on the molecular pathogenesis and experimental therapeutics of hepatobiliary cancer. Candidates should possess a Ph.D. in cell and molecular biology or in a related field of study and be eligible for U.S. postdoctoral fellowship awards. Experience in gene expression profiling, siRNA technology, and laser capture microdissection are highly desirable. Applicants should send curriculum vitae and contact information for three references to: **Dr. Alphonse E. Sirica, Professor and Division Chair, Division of Cellular and Molecular Pathogenesis, Department of Pathology, Virginia Commonwealth University School of Medicine, Richmond, VA 23298-0297.** E-mail: asirica@mcvh-vcu.edu. *Virginia Commonwealth University is an Equal Opportunity/Affirmative Action Employer. Women and minority candidates and persons with disabilities are encouraged to apply.*

ASSISTANT/ASSOCIATE PROFESSOR
RNAi in Gene Regulation and Small RNAs as Biopharmaceutical Agents

The Center for Pharmaceutical Biotechnology and the Department of Biopharmaceutical Sciences, University of Illinois at Chicago, invite applications for a tenure-track faculty position at the level of **ASSISTANT or ASSOCIATE PROFESSOR** in a general area of RNAi-based gene regulation and/or small RNAs as biopharmaceutical agents. Responsibilities include developing a strong, externally funded research program and teaching in graduate and professional programs. The successful candidate will have joint appointments in the Center for Pharmaceutical Biotechnology and the Department of Biopharmaceutical Sciences. Ph.D. and at least one year of postdoctoral experience in areas related to biology of RNAi and/or small RNAs are required. Candidates at the Assistant Professor level must have strong potential for attracting extramural funding; candidates at the Associate Professor level must have a strong record of successful extramural funding. Position available spring 2008. For fullest consideration, send curriculum vitae, description of research interests and three letters of reference by October 15, 2007, to **e-mail: cpbhr@uic.edu** or: **Dr. Alexander Mankin, RNA Search Committee, Center for Pharmaceutical Biotechnology, M/C 870, University of Illinois at Chicago, 900 S. Ashland Avenue, 3052 MBRB, Chicago, IL 60607-7173** (electronic applications encouraged). *UIC is an Affirmative Action/Equal Opportunity Employer.*

ASSISTANT PROFESSOR, PLANT BIOLOGY

The Department of Biological Sciences, California State University, Los Angeles, seeks to fill a Tenure-Track Position in plant biology beginning fall 2008. A Ph.D. in biology, botany, or related field is required, with a minimum of one year of postdoctoral experience preferred. The candidate is expected to teach undergraduate and graduate courses, participate in program development, and establish an externally funded research program involving undergraduate and Master's students. The candidate is also expected to participate in University service, and to provide academic advisement to students. Submit curriculum vitae, research plans, statement of teaching philosophy, and three letters of reference to: **Search Committee Chair - Plant Biologist, Department of Biological Sciences, California State University, Los Angeles, 5151 State University Drive, Los Angeles, CA 90032 (e-mail: plapolt@exchange.calstatela.edu).** Review of completed applications will begin November 1, 2007, and may continue until position is filled. *EO/Title IX/ADA Employer. Qualified women and minorities are encouraged to apply.*

A STRATEGY FOR THE FUTURE

As nations compete for scientific recognition, Germany is boosting its fight. Over the past few years, the Bundesministerium für Bildung und Forschung (BMBF)—Germany's ministry of education and research—has upped the science budget and encouraged initiatives that require universities and scientists to be more innovative. The intention is to promote competition to improve the nation's science reputation. **By Gunjan Sinha**

Last year the federal and state governments announced the first winners of the Excellence Initiative—a measure introduced by the Deutsche Forschungsgemeinschaft (DFG) and the Wissenschaftsrat, a scientific commission that advises political decision makers. For the first time in decades, universities and collaborative research groups have a chance at winning substantial extra funding if they prove worthy.

"My view on the development of the science system in Germany is not to have a flat field but a picture of the Alps," says **Matthias Kleiner,** president of the DFG, Germany's primary science funding agency.

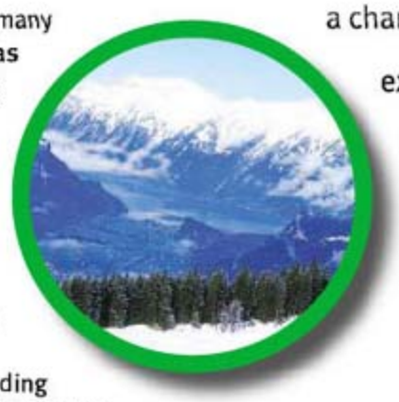

Germany's "flat field" is its university system. For decades the notion of equality in education has driven the nation's science funding strategy. Until last year, all universities received the same lump sum from state and federal governments, regardless of quality. But while all universities are similarly prestigious, they haven't been able to compete internationally and lure in top talent.

The Excellence Initiative offers €1.9 billion in additional funding through 2011. Last year the DFG and the Wissenschaftsrat doled out €873 million of that sum in the program's three categories: 12.7 percent went to support graduate schools, 63.4 percent went to research clusters (projects involving scientists from several institutions), and 23.9 percent was awarded to universities for devising strategies for future development.

Federal and state governments plan to announce a second round of winners this October. Overall 40 graduate schools and 30 research clusters will win the coveted extra funds after a lengthy application process. In addition, universities will also receive a supplementary allowance of 20 percent of the funding to cover indirect expenses.

Universities aren't the only science research centers to get a financial boost. BMBF also promised a 3 percent per year increase in funding through 2011 to Germany's nonuniversity research institutes: the Hermann von Helmholtz Association of National Research Centers, Max Planck Society, Fraunhofer Society, and Gottfried Wilhelm Leibniz Science Association. The total science budget increase amounts to an additional €6 billion over five years.

German research is striking back in other ways too. Construction of a new European X-ray laser facility in Hamburg is slated to begin this year—it will be the only one of its kind in Europe. And the Deutsches continued »

> "For the first time in decades, universities and collaborative research groups have a chance at winning substantial extra funding if they prove worthy."

CREDIT: (ALL) ©2007 JUPITERIMAGES CORPORATION

UPCOMING FEATURES

Careers for B.S./M.S. — September 28

Focus on Diversity— October 5

Top Employers Survey— October 12

MAX-PLANCK-GESELLSCHAFT

World-Class Science ...

The Max Planck Society is renowned for outstanding basic research in the life sciences, the natural sciences and the humanities. Max Planck scientists perform their research at the frontiers of knowledge. They seek answers to fundamental questions, and the work they do with their discoveries and insights contributes significantly to our future.

The scientists build important foundations for innovations that significantly impact economy and society. They train thousands of junior scientists, submit patent applications, generate revenues through licenses, establish companies and create jobs. Thus, in the long run, investing in basic research of the highest quality pays off many times over.

The Max Planck Society enjoys an excellent reputation both at home and abroad. It can hold its own in the global competition for the best minds as no other scientific organization in the country can. This competitiveness is one of the advantages of being located in Germany in today's world - and will be that much more so in tomorrow's. Scientific publications, patents and highly qualified junior scientists substantiate the quality of the research done at Max Planck Institutes.

... made in Germany

www.mpg.de

Gabler

Technical Research Assistant - NanoSIMS operator

The Max Planck Institute for Marine Microbiology (MPI), Bremen, Germany, is seeking highly motivated applicants with a strong interest in multi-disciplinary research to support our nanoSIMS analytical facility for environmental microbiology. The successful candidate will be responsible for the day-to-day operation of the Cameca nanoSIMS 50L and carry out routine maintenance and repairs.

Additionally, the successful candidate will support scientists from the MPI and external academic collaborators in carrying out high quality SIMS analysis on a wide range of environmental samples, and advise and assist in sample preparation and data interpretation. The active development of independent research projects will be encouraged. Candidates should have at least a Bachelor of Science degree or equivalent qualification in physical sciences. Prior experience with SIMS, particularly with Cameca SIMS instrumentation, is desired. Knowledge of UNIX operating system is also beneficial.

We offer a 3-year full-time appointment, with the possibility of permanent employment. The salary is according to the German system for public employees (TVöD E 12). The position is available immediately.

Further information can be obtained at www.mpi-bremen.de or from Dr. Marcel M.M. Kuypers or Dr. Tim Ferdelman.

Applications should include a curriculum vitae and a list of three references. Written or electronic applications are invited until October 15, 2007 and should be sent to:

Max Planck Institute for Marine Microbiology
Administration -NanoSims-
Celsiusstr. 1, D-28359 Bremen, Germany, E-mail: nanosims@mpi-bremen.de

---

At the Max Planck Institute for Terrestrial Microbiology

Postdoctoral fellow positions in

- **intercellular signalling in bacteria**
- **regulation of motility in bacteria**

are available immediately for outstanding, highly motivated scientists to study the molecular and cellular biology of fruiting body formation in Myxococcus xanthus. Specific areas of research include mechanisms of intercellular signalling, signal transduction with special emphasis on two-component regulatory systems, regulation of type IV pili function, and regulation of motility.

Qualifications:
Applicants should be enthusiastic and self-motivated and have a strong interest in molecular and cellular microbiology. Experience in one or more of the areas of molecular genetics, protein purification and characterization, and cell imaging is advantageous.

Further information can be obtained from Prof. Dr. Lotte Sogaard-Andersen (sogaard@mpi-marburg.mpg.de).

The MPI for Terrestrial Microbiology (http://www.mpi-marburg.mpg.de/) consists of four departments and offers a stimulating and interdisciplinary research environment. The daily language in the Institute is English.

Applications should be send as a single pdf file by e-mail to Anabela Krah (akrah@mpi-marburg.mpg.de). Please include your CV, names and email addresses of three academic referees, statements of previous research and career goals (no more than two A4 pages for each).

For more detailed information on our research see: http://www.mpi-marburg.mpg.de/sogaard/

MPI
Max Planck Institute for Terrestrial Microbiology
Karl-von-Frisch-Straße
35043 Marburg, Germany
Applications should be received by October 15.

The Max Planck Institute of Biochemistry is one of the leading research institutes within the fields of biochemistry, cell- and structural biology, and biomedicine. With its ten scientific departments, twelve junior research groups, and a staff of around 800 people, the institute is one of the largest institutes within the Max Planck Society.

Within the Department of Cell Biology applications are invited for a

Project Leader Position (ref. no. 35.07)

The research in the department is focused on the molecular mechanisms that govern cell division, the contribution of mitotic errors to chromosomal instability in tumor cells, and centrosome/centriole function.

Specific areas of research include:
- **the regulation of mitotic progression**
- **the spindle assembly checkpoint**
- **the centrosome cycle**
- **the function of the primary cilium**

A special strength of the MPIB is its broad expertise in the areas of protein chemistry (including mass spectrometry, crystallography), molecular biology and cell biology. Important support is also provided by an outstanding central core facility (e.g. for DNA- and protein sequence analysis, peptide-synthesis, biophysical measurements, live cell imaging, etc.).

The successful applicant must have a doctoral degree, a strong research record in biochemistry/cell biology/molecular biology and, preferably, prior experience in one of the above research areas. The project leader is expected to supervise both undergraduate and graduate students and should enjoy working in a collegial and highly interactive environment.

The starting date is flexible and remuneration will be according to prior experience and qualification up to 14 TVöD (public service payment tariff scale). The duration of the appointment will be initially for 2 years.

Applications, including CV, list of publications, and addresses of three referees, should be sent (preferably before 30. November 2007) to:

Max Planck Institute of Biochemistry
Prof. Dr. Erich A. Nigg, Department of Cell Biology
Am Klopferspitz 18, D-82152 Martinsried, Germany
e-mail: nigg@biochem.mpg.de, www.biochem.mpg.de

The Max Planck Institute for Demographic Research (MPIDR) seeks to recruit a

Research Scientist

to conduct research for the Laboratory of Demographic Data. Qualified demographers, sociologists, statisticians, and other scientists with a research background in the social sciences are invited to apply. We intend to fill the position as soon as possible. The duration of the contract will initially be limited to three years. The salary is paid according to qualification and in accordance with the rules of federal employees in Germany, up to level 14 TVöD.

The successful applicant must have completed a Ph.D. degree in demography or a related field. He or she must have a proven record of scientific work and theoretical experience in the field of fertility and its determinants in Europe and other industrialized societies as well as knowledge of the relevant literature.

The candidate will in the main process and analyze population and survey data on fertility. The position requires expertise in statistical and demographic analyses and practical skills in handling demographic data. Fluency in English is essential

Applications should include a CV with a statement of academic interests and relevant experience, a list of publications, two recommendations, and contact details of two referees.

Please send all materials **by 21st October 2007** to the:

Max Planck Institute for Demographic Research
Attn. Edelgard Katke, Konrad-Zuse-Str. 1, 18057 Rostock, Germany
Email: katke@demogr.mpg.de

A 5 year research group leader position

in the area **Mycorrhiza or fungal plant pathogens** will open in April 2008. Interested candidates with a strong record in fungal genetics are expected to focus their work on the fungal side of the respective system, apply or seriously plan to develop reverse genetics and incorporate comparative genomics approaches. The group will be housed in the department of Organismic Interactions where we focus on the molecular analysis of disease mechanisms in smut fungi. Fruitful and stimulating interactions with the existing groups are expected to develop.

The successful candidate will be provided with lab space for a group of 6, substantial core support and fellowships for two PhD students/postdocs. Applicants should be in the early stages of their career, ideally in the 1st or 2nd postdoctoral period.

Inquiries can be made by email kahmann@mpi-marburg.mpg.de

Please send your applications including a CV, publication list, research proposal and names of two referees to:

MPI Max Planck Institute for Terrestrial Microbiology
Prof. Dr. Regine Kahmann, Karl-von-Frisch-Straße, D-35043 Marburg, Germany
Applications are accepted until the position is filled.

The **Max Planck Institute for Demographic Research** seeks up to
10 Ph.D., Post-Doc and Research Scientists to pursue

Theoretical Evolutionary Demography across the Tree of Life

- The length of life is long for some species and short for others. What underlying processes govern lifespan?
- Some species suffer senescence after reproductive maturity whereas others enjoy extended periods of constant or decreasing mortality and constant or increasing fertility. What fundamental dynamics explain mortality and fertility trajectories?
- Species differ in body size, growth rates, age at first reproduction, number and size of offspring, parental care and sociality. What general principles produce this diversity?

Exploiting phylogenetic knowledge about coalescence times and the characteristics of species across the tree of life, the EvoDemo group will use mathematical methods, biological theory, and demographic and economic concepts to develop unifying frameworks and discover deep connections by focusing on these basic questions. The group will pursue interdisciplinary research at the intersection of

mathematical modeling and optimization, demography, phylogenetics, comparative biology, life history theory, and evolutionary ecology.

Max Planck Institute for Demographic Research
To learn more or to apply, see **www.demogr.mpg.de/go/evodemojobs**

The Max-Planck-Institute of Molecular Plant Physiology in Potsdam invites applications for a

Scientist (code 26/07)

Our research is focused on microarray data analysis, using visualization and GUI tools enabling the end-user to use statistical methods and ontological information.

To extend and improve our tools MapMan, Pageman and ROBIN, we seek a life scientist with strong programming skills (preferred), or a (bio)informatician/computer scientist with a strong background in biology. The candidate should have experience in the field of literature curation or be willing to learn it, and possess programming skills in Java. A knowledge in statistics and especially microarray analysis and/or PERL is a plus.

The candidate is expected to work in an interdisciplinary field involving both pathway curation as well as software development/data analysis. She/he should be able to work in an international environment and display strong team-working capabilities.

The position is initially funded for 3 years. For further information please contact Dr Björn Usadel, e-mail: usadel@mpimp-golm.mpg.de. Applications including a cover letter, curriculum vitae and the names of two referees should be sent to:

Max-Planck-Institut für Molekulare Pflanzenphysiologie
Personalverwaltung
Wissenschaftspark Golm, Am Mühlenberg 1, 14476 Potsdam

MAX-PLANCK-GESELLSCHAFT

Research of the highest international calibre ...

Basic research is continuously facing new challenges. In the Max Planck Society, more than 4,300 scientists dedicate themselves to exploring and expanding the boundaries of human knowledge. They are annually joined by 10,500 student assistants, doctoral students, post docs and visiting scientists and supported by a staff of 8,000 in the financial, technical and administrative areas.

In its 78 institutes, the Max Planck Society promotes basic research of the highest international standards. Its annual budget is 1.38 billion euros. Max Planck scientists make groundbreaking discoveries and lay the foundations for new medical applications and materials of the future.

The Max Planck Institutes are ranked among the most popular employers and among the 30 "best employers of postdocs" (internet survey conducted by the US magazine The Scientist, February 2003). They are among the 10 best research institutions outside of the USA (Young Career 2004). This is your opportunity to work for a major, internationally renowned research organisation that offers long-term career prospects.

... a challenge for you

www.mpg.de

As an equal opportunity employer, the Max Planck Society is committed to employing more individuals with disabilities. We therefore actively encourage individuals with disabilities to apply. We also seek to increase the percentage of female employees in areas where they are under-represented. Qualified women are therefore strongly encouraged to apply.

Science Careers | online @sciencecareers.org
FOCUS ON GERMANY

Krebsforschungszentrum (DKFZ)—German Cancer Research Center—recently launched The National Center for Tumor Diseases in Heidelberg with the goal of translating basic research into better treatments for cancer patients.

Germany isn't the only nation within the European Union to strengthen its scientific prowess. The nation's efforts are the manifestation of the European Council's decision in 2000 to transform the European Union into "a competitive and dynamic knowledge-based economy" by 2010. The so-called Lisbon Strategy calls on all member states to increase spending on research and development to 3 percent of GDP by 2010.

But instead of keeping the status quo, Germany wants to shake up the system by requiring institutions and scientists to compete for those extra funds. Germany isn't alone in this regard. The French government has a bill pending that would also give French universities, which are government controlled, more freedom to manage budgets, investments, and real estate. Italy and Spain are also moving in similar directions. But while they continue to debate the pros and cons of a competitive system, in Germany the idea is no longer controversial.

"No one talks anymore about equal funding and possibilities for everyone," says **Thomas Vogt,** spokesperson for the Leibniz Association. "This [initiative] is to strengthen the strong."

Current (bottom) and future (top) National Center for Tumor Diseases (NCI) building in Heidelberg.

The Winners

While Germany's research institutes such as Max Planck, Leibniz, and Helmholtz have strong reputations, its university research has been lackluster. In the 2006 list drawn up by the *Times* Higher Education Supplement, for example, the University of Heidelberg came in at number 58—that was the best rank of any German university.

"Germany was one of the leading nations in science," says Kleiner. "But the loss of science during the Second World War has been long lasting. There must be a movement toward excellence in science again."

Toward that goal, DFG and the Wissenschaftsrat implemented the Excellence Initiative in 2005 that introduces competition into the system to improve the quality of research. Last year, reviewers selected 22 universities to receive additional funding; a few came out ahead of the class. Technical University Karlsruhe (TUK), the University of Munich (LMU), and Technical University Munich (TUM) won in all three categories—future development, graduate programs, and cluster participation—making the city of Munich the program's biggest winner.

TUK's future strategy centers on its longstanding cooperation with the Forschungszentrum Karlsruhe, an institute governed by the Helmholtz Association. The two propose to create the Karlsruhe Institute of Technology, modeled on the Massachusetts Institute of Technology in the United States.

TUK also won funds for its proposal to establish a department of optics and photonics and for collaborating with the DFG Center for Functional Nanostructures, which will form the epicenter of a nanotechnology research cluster.

The Karlsruhe School of Optics and Photonics graduate school, which the university intends to establish in collaboration with three other research institutions, is intended to plug a hole in graduate study. The optics and photonics industry grows annually by about 20 percent according to the Association of German Engineers. However, optics and photonics are not distinct disciplines at German universities.

LMU's future strategy is a concept it refers to as "working brains – networking minds – living knowledge." It plans to introduce student recruitment, conduct more fund raising—a rarity in continued »

Helmholtz Association
www.helmholtz.de

Leibniz Association
www.wgl.de

Max Planck Institut für Eisenforschung
www.mpie.de

Nationales Centrum für Tumorerkrankungen
www.dkfz.de/en/nct

Technische Universität
portal.mytum.de/welcome

Universität München LMU
www.uni-muenchen.de

University of Karlsruhe
www.uni-karlsruhe.de

CREDIT: (TOP) BEHNISCH ARCHITEKTEN; (BOTTOM) COPYRIGHT, PRESS CENTER OF THE HEIDELBERG UNIVERSITY MEDICAL SCHOOL

"We have pretty modern equipment. That gives us the possibility to pursue science that is really new."
—Anke Pyzalla

Germany—and use peer evaluation to improve and update teaching quality.

LMU also intends to launch a graduate school of systematic neurosciences and participate in three research clusters: the Munich Center for Integrated Protein Science, the Munich Center for Advanced Photonics, and the Nanosystems Initiative Munich.

The third university to take top honors was TUM. It proposed to transform itself into an "entrepreneurial university" by adopting a series of measures that ensure greater information exchange between the university and industry, selectively recruiting students and professors, and conducting more fund raising. It also plans to further develop its new Institute for Advanced Studies, modeled on the one in Princeton, New Jersey, which will free some of its top professors from part of their teaching loads.

"Both universities in Munich are really outstanding," comments Kleiner." But there are no losers in this competition, he adds. Working on proposals to apply for the additional funds has helped universities focus on the future—a task they were never encouraged to do. Even the universities that don't win Excellence Initiative funding, Kleiner says, profit from the exercise of applying.

"Our goal is not only to do excellent science but also to do things that will last beyond the research itself."
—Korinna Bauer

Nonuniversity Research

Established within the past 60 years, German nonuniversity research centers such as Max Planck, Leibniz, and Helmholtz already have reputations for conducting strong science. Contributing to their success, says Leibniz's Vogt, is the fact that they are relatively new and that they function independently. Moreover, scientists can pursue research without the constraints imposed by teaching.

"We have pretty modern equipment," says **Anke Pyzalla,** director of the Max Planck Institut für Eisenforschung in Düsseldorf. "That gives us the possibility to pursue science that is really new." The institute for iron research is one of the very few that are financed partly by the Stahlinstitut VDEh, she adds, an industrial partner. The collaboration helps the institute conduct projects that would be of interest to the steel industry that are potentially profitable. It's a model that many institutes and universities would like to emulate.

To bring university research up to par, one explicit aim of the Excellence Initiative is to foster more collaboration between universities, nonuniversity research centers, and industry when possible—an effort that has so far been fruitful. Seventy percent of the 17 research clusters thus far awarded funding as part of the Excellence Initiative are being driven by Max Planck Institutes, says **Bernd Wirsing,** spokesperson at Max Planck. Among them are the Frankfurt cluster on macromolecular complexes and the clusters of astrophysical science and cellular networks both centered at the University of Heidelberg.

The Leibniz Association participates in four clusters and the Helmholtz Association participates in six—collaborations that have greatly benefited university scientists and graduate students who have access to the better infrastructure that exists at research centers. But the research centers benefit too, says Wirsing, because cluster participation and the accompanying financial resources enable them to branch out into new areas. Leibniz, for example, has broadened its research to include ocean science, nanotechnology, and cellular biology.

Collaboration among researchers across institutions and industry participation is the norm in the US. But inertia within the system has prevented such collaboration from becoming widespread in Germany. Funding that promotes research clusters will establish a framework for collaboration, says Kleiner.

Just as beneficial, say experts, is the 3 percent annual funding increase promised by BMBF. It's the first time that the research centers can count on at least a 3 percent annual increase, perhaps indefinitely, says Vogt. Leibniz has mostly put the extra funds toward salary increases and internal costs.

Helmholtz Association, however, has taken a slightly different tack. It has used much of the funding to launch a number of initiatives that mirror the Excellence Initiative. In 2002, for example, Helmholtz introduced the President's Initiative and Networking Fund that has so far doled out €150 million toward three types of projects: collaborative research that includes different Helmholtz centers, universities, international partners, and industry; financial packages to support young scientists and graduate schools; and establishing a framework to improve working conditions for researchers.

After a scientific review process, the president can distribute the additional funds at his discretion, says **Korinna Bauer,** project officer for the Helmholtz continued »

CREDIT: (BOTTOM) DAVID AUSSERHOFER/HELMHOLTZ ASSOCIATION

"It has been very difficult to offer internationally competitive salaries because of the mandatory tariff."
—Christof von Kalle

Alliances scheme, which funds the collaborative research projects. For very large clusters, the senate must also give its consent. Still, it's a much less complicated process than doling out institutional funds, which requires a lengthy review process, she adds.

Two collaborative projects approved earlier this year, for example, are Physics at the Teraskala and Mem-Brain. Physics at the Teraskala aims to investigate the nature of matter and the forces operating directly after the Big Bang. Particle physicists from two Helmholtz Centers, Deutsches Elektronen-Synchrotron (DESY) and Forschungszentrum Karlsruhe, have joined forces with colleagues from 17 universities and the Max Planck Institut für Physik in Munich. This alliance will receive a total of €25 million over the next five years.

The Mem-Brain project pools scientific talent from four Helmholtz centers, universities, industry, and research institutions both in Germany and abroad. The goal is to develop ceramic membranes to lower pollutant and carbon dioxide emissions in coal-fired power plants. This alliance will receive €11 million over the next three years.

The fund has been so successful that Helmholtz plans to more than double it next year to €57 million. But the extra funds won't necessarily go into the same programs.

"The idea is to do some structural innovation," Bauer explains. "Our goal is not only to do excellent science, but also to do things that will last beyond the research itself." Reaching out to young, talented scientists, for example, ensures a steady supply of fresh talent that will be interested in working with Helmholtz long into the future, Bauer adds.

Other Projects

Earlier this year, BMBF officially launched the construction of the European X-ray laser facility (XFEL)—a particle accelerator that will send electrons hurtling down a 3.4 km underground tunnel to generate pulses of brilliant X-ray light.

Expected to provide bursts of light that are orders of magnitude brighter than any existing light source, XFEL will enable researchers to film at atomic detail the precise sequence of events in chemical reactions, material deformation, and biological processes.

The XFEL will be built in Hamburg and Schenefeld and is scheduled to be complete by 2013. The project is a pan-European effort but Germany is funding the bulk: Twelve countries will contribute at least 25 percent of the estimated €1.082 billion cost; German federal and local governments will finance the rest.

The facility's closest rival is across the Atlantic, where engineers are working on the US Department of Energy–funded Linac Coherent Light Source—a machine that will produce X-rays in a manner similar to XFEL, emitting pulses a thousand times shorter than existing instruments. It is scheduled to be complete by 2009.

Less grand but equally important is Germany's new National Tumor Center in Heidelberg. For the past 40 years DKFZ has carried out basic cancer research and cancer patients have been treated at the nearby University of Heidelberg hospital. But the collaboration between basic and clinical researchers has been limited, explains **Christof von Kalle,** director of the new center. The new center aims to translate basic research into new therapies. In 2004, the Helmholtz Association gave DKFZ a startup grant to support the project with €13 million over five years.

"That's not a huge amount," von Kalle acknowledges. But the DKFZ, Heidelberg University, and two neighboring hospitals have agreed to split the remaining costs 50/50, he adds.

Right now the center is operating out of Heidelberg University hospital. But in two years, it will occupy its own space and become the first comprehensive cancer clinic in Germany. Deutsche Krebshilfe, a nonprofit cancer aid society, has agreed to foot the bill for a new facility scheduled to be complete in 2009. The new facility will occupy 5,500 square meters of space, five times the space the center presently occupies. The society has also agreed to finance the building for 10 years, after which Heidelberg University Hospital and DKFZ will take over. The center's primary goal will be to take promising basic research from DKFZ and put it into clinical trials conducted at the center.

Measuring Success

Overall the changes and additions in the German science landscape bode well for scientists—more money means more jobs. But whether they go far enough to achieve their intended goals is anybody's guess. And Germany has other issues that some say hold back the nation's science. One problem echoed by many is the salary system.

The German government still considers scientists civil servants and fixes their salaries via a tariff system. "It has been very difficult to offer internationally competitive salaries because of the mandatory tariff," von Kalle complains. Recent changes do offer a scheme whereby institutions can top up salaries based on performance, but at the same time the government has reduced base salaries and even cut university funding in several areas, says von Kalle.

Gender is also an issue. Only 14 percent of professors are female in Germany—about half the percentage in other nations. But change is afoot. There's lots of discussion over initiatives that keep women in science. Several universities that won additional DFG funding, for example, plan to actively recruit more female professors.

In fact, the Excellence Initiative has been so successful, says Kleiner, that he has been discussing extending it beyond its scheduled five-year life span, perhaps indefinitely. "This isn't a process that will be finished in five years. We want to make it permanent and the response from politicians so far has been very positive."

Gunjan Sinha is a freelance writer living and working in Berlin, Germany.

10.1126/science.opms.r0700039

CREDIT: COPYRIGHT, PRESS CENTER OF THE HEIDELBERG UNIVERSITY MEDICAL SCHOOL

Bayer AG sets up new foundation

INCREASED COMMITMENT TO EDUCATION AND SCIENCE

Bayer has a long tradition of setting up foundations. The company established its first foundation way back in 1923 in order to enable students of medicine and natural sciences to spend time abroad. The Leverkusen-based Group has now increased its commitment to education & science by grouping together its previous foundation-related activities and establishing a new foundation for science and education: the Bayer Science & Education Foundation. Together with the recently established Bayer Cares Foundation and the Hermann Strenger and Herbert Grünewald Foundations, both of them with a long standing history of funding, a total of 20.7 million euros is being invested in foundations.

Overview of the Bayer Science & Education Foundation.

Convinced of the fact that today society needs to invest more than ever in its brightest talent, the objective of the Bayer Science & Education Foundation is to promote natural sciences and research and improve educational opportunities in the long term.

The foundation sponsors people who demonstrate particular commitment and outstanding achievement, even, and particularly, when they are just starting out in a science-related career. The scope of sponsorship offered therefore extends from school and scholarship programs right through to the honoring of renowned scientists.

The work of the foundation is inspired by the Bayer Group's mission statement: "Bayer: Science For A Better Life". One particular focus of the sponsored programs is therefore on segments which combine the topics of health care, nutrition and high-tech materials in an innovative manner.

Individual projects

Germany's future lies in fundamental and industrial research. In order to promote these areas, the Bayer Science & Education Foundation will award the Otto Bayer and Familie Hansen prizes on an alternate annual basis to young scientists from German-speaking countries for outstanding research achievements in new fields of chemistry, biochemistry and natural science/medicine-related topics.

Supporting school projects located in and around Bayer's registered sites also plays a special role in the Foundation's activities. Through this sponsorship, the Foundation hopes to implement innovative science-related school projects that will have a lasting effect. Some examples of the forms these can take are the provision of special teaching material for students with disabilities, the introduction of innovative teaching methods or the promotion of initiatives to improve the continuing professional training of teachers.

Arasch Waifasade studies human medicine at the University of Cologne in Germany. His scholarship of the Bayer foundations allowed him to gather valuable experiences as a member of the Department of Surgery at the Downtown Hospital in New York, USA.

The *Bayer Fellowship Program* assists people in achieving particular study-related aims. Undergraduate and post-graduate studies as well as internships, theses and PHD proposals are sponsored by the program. Internationality is a key aspect of the sponsorship program and for this reason scholarships are preferably awarded to allow individuals to spend time abroad and to enable foreign scholars to study in Germany. In addition to the Bayer and Carl Duisberg scholarships for those studying biology, biochemistry, biotechnology, biochemical engineering, chemistry, chemical engineering, pharmacy, physics and medicine, there are also Kurt Hansen scholarships for trainee science teachers. The Kurt Hansen Program, which is a unique Germany-wide program, was set up by the Foundation particularly in response to the increasing importance in the teaching profession of having experience of living in a foreign country. It funds trainee science teachers during time spent abroad and enables prospective teachers from abroad to spend time in Germany. Applications can still be made as part of the current selection cycle up until October 31.

Thimo V. Schmitt-Lord
Bayer Science & Education Foundation.
c/o Bayer AG
51368 Leverkusen
foundationoffice@bayer-stiftungen.de
www.bayer-foundations.com

Bayer Science & Education Foundation

POSITIONS OPEN

Research Fellowships

to be held at the Babraham Institute, Cambridge

The Babraham Institute is a charity which is world renowned for its research in life sciences that leads to new medicines and treatments for human diseases.

The Babraham Institute seeks to encourage and support the careers of highly promising postdoctoral scientists who have the clear potential to become Group Leaders. We are interested to hear from such scientists, in any area of biomedicine that interfaces well with our research strengths in cell signalling and epigenetics, who wish to apply for prestigious Fellowship schemes, such as those offered by BBSRC, MRC and Wellcome Trust, in order to build their career at the Institute. We would particularly welcome applications from those studying RNA biology, epigenomics, nutrient sensing, stem cell biology or immunology, and from mathematical and structural biologists who would wish to be involved in expansion in these areas. Those successful in obtaining Fellowship support will be granted "tenure-track" Group Leader status at the Institute. Successful candidates will receive mentoring with their Fellowship applications by the appropriate senior colleagues at the Institute.

Application forms are available on the Babraham website (**www.babraham.ac.uk**) or by contacting our Recruitment Line (01223 496365). Completed application forms and/or CVs (including names of three academic referees), and a two to three page research outline should be addressed to the Director, Professor Michael Wakelam and sent or emailed to the Institute's Personnel Department (**babraham.personnel@bbsrc.ac.uk**). Applicants should ask their referees to send letters of reference by the deadline below. Informal enquiries may be made to michael.wakelam@bbsrc.ac.uk, wolf.reik@bbsrc.ac.uk, or len.stephens@bbsrc.ac.uk. Further information about the Institute can be found on our website. **The deadline for applications is 31 October 2007.**

An Equal Opportunities employer. An Institute supported by the Biotechnology and Biological Sciences Research Council.

www.babraham.ac.uk

FOCUS ON GERMANY

Research in Germany

Alexander von Humboldt
Stiftung/Foundation

The Alexander von Humboldt Foundation enables highly qualified scientists and scholars of all nationalities and fields to conduct extended periods of research in Germany. Fellowships are awarded solely on the basis of the applicant's academic record, the quality and feasibility of the proposed research and the candidate's international publications. The Humboldt Foundation particularly welcomes applications from qualified, female junior researchers.

Research Fellowship for Postdoctoral Researchers who have completed a doctoral degree within the past four years.

- Allows for a stay of 6-24 months in Germany; monthly stipend of 2,250 EUR plus additional allowances

Research Fellowship for Experienced Researchers who have completed a doctoral degree within the past twelve years.

- Allows for a stay of 6-18 months in Germany; fellowships may be divided into a maximum of three visits lasting three months or longer; monthly stipend of 2,450 EUR plus additional allowances

www.humboldt-foundation.de

POSITIONS OPEN

MUSCLE PHYSIOLOGIST

ASSISTANT PROFESSOR

Section of Neurobiology, Physiology and Behavior
University of California, Davis

The Section of Neurobiology, Physiology and Behavior, in the College of Biological Sciences, University of California, Davis, invites applications for a faculty position in Physiology at the assistant professor level. The section is continuing its initiative to build a program emphasis in Muscle Biology and encourages applicants specializing in skeletal, cardiac or smooth muscle physiology to apply. Areas of significant interest include, but are not limited to, exercise physiology and adaptation, muscle growth and atrophy, motor control, metabolic signaling and control, calcium signaling, and muscle mechanics. Successful applicants will be expected to establish a vigorous research program supported by extramural funding, and contribute to the teaching mission of the Section, including the Exercise Biology major. The successful applicant will be part of a growing group of muscle biologists that include two recent hires with interests in thick filament regulation of muscle contraction (**Samantha Harris, Ph.D.**; University of Washington) and the role of the proteosome in muscle disease (**Aldrin Gomes, Ph.D.**; UCLA).

The Section has grown steadily since its inception in 1993 to include 32 ladder rank faculty who conduct research encompassing a general theme of integrative biology, ranging from muscle physiology and biomechanics, molecular endocrinology, environmental physiology, cell physiology, aging, molecular, cellular, and developmental neurobiology, systems neuroscience, and animal behavior. In addition, UC Davis has one of the largest concentrations of life scientists in the world, with vibrant units across campus that would provide the successful candidate with a wide range of collaborative interactions. These units include the Department of Physiology and Membrane Biology in the School of Medicine, the UC Davis Genome Center, the Mouse Biology Program, the Clinical Nutrition Research Unit, the Molecular, Cellular, and Integrative Physiology and Exercise Science Graduate Groups, the Center for Neuroscience, the Department of Biomedical Engineering, and other physiology-related departments of the Schools of Medicine and Veterinary Medicine and College of Agriculture and Environmental Sciences.

Candidates must possess a Ph.D. or M.D. degree with significant post-doctoral experience. Applicants should send a letter describing their research plan and teaching interests, a curriculum vitae, copies of representative publications, and the names of at least five persons from whom references can be obtained to: **Sue Bodine, Chair, Muscle Physiology Search Committee, Section of Neurobiology, Physiology, and Behavior, One Shields Avenue, University of California, Davis, CA, 95616-8519**. All materials must be received by **January 4, 2008** to be assured full consideration. For more information on the position and UC Davis in general, please visit the following web site: **www.npb.ucdavis.edu/facultypositions/**.

The University of California is an Affirmative Action/Equal Opportunity Employer.

POSITIONS OPEN

Johns Hopkins Medical Institutions Tenure-Track Positions

Influenza and Respiratory Virus Translational Research

Human Immunology, Vaccinology, Pharmacology

The Division of Infectious Diseases of the Johns Hopkins School of Medicine is recruiting 1-2 faculty at the Assistant or Associate Professor level to contribute to an emerging institutional Respiratory Viruses Program. Our focus is on persons with proven capabilities to conduct independent research on respiratory infections, especially investigations that contribute to the prevention or treatment of influenza in humans. This recruitment contributes to expanding programs in influenza virology, structural biology, and vaccine testing. Emphasis will be given to researchers with complementary research such as in molecular biology of viral replication, host virus interactions, and quantitative analysis of viral dynamics.

Candidates must have earned an MD and/or PhD degree and have a record of acquiring research funding and producing outstanding scholarship. Salary and resources will match experience.

Candidates should provide a curriculum vitae, a one-page statement of career interest, and 3 professional references to: **Dr. David Thomas, Chief Infectious Diseases, Johns Hopkins School of Medicine, Suite 437 1830 Monument Street, Baltimore, Maryland 21205** or by email care of Nadia Hay **nhay@jhmi.edu**. Application review will begin in Fall 2007.

Johns Hopkins is an Equal Opportunity Employer.

Tenure-Track Investigator Position in the Laboratory of Immunology

The Laboratory of Immunology (LI), Division of Intramural Research, National Institute of Allergy and Infectious Diseases, National Institutes of Health invites applications for a tenure-track investigator position in immunology. Applicants should have a Ph.D., M.D., or equivalent degree; an outstanding record of postdoctoral accomplishment; and an interest in any area of biomedical research related to immunology.

Specifically, we seek a highly creative individual who will establish an independent, forward-looking, world class research program that takes full advantage of the special opportunity afforded by the stable, long-term funding of the Intramural Research Program at NIH. She/he should be interested in developing and applying novel approaches to the study of problems of major biological and /or medical importance, which could include a major clinical research effort. There are ample opportunities to participate in trans-NIH initiatives involving technology development, translational investigation, and multidisciplinary science.

Generous ongoing support for salary, technical personnel, postdoctoral fellows, equipment, and research supplies will be provided. Available cores or collaborative facilities include flow cytometry, advanced optical imaging, microarray generation and analysis, computational biology, production of transgenic and gene- manipulated mice, chemical genomics and support for projects involving RNAi screening. In addition to an outstanding international postdoctoral community, a superior pool of graduate and undergraduate students is available to the successful applicant.

NIAID's Laboratory of Immunology has a distinguished history of accomplishment in immunology. We strongly encourage outstanding early career investigators who can continue and enhance this record of achievement to apply. Current LI principal investigators are Ronald Germain, Michael Lenardo, Rose Mage, David Margulies, William Paul, Ethan Shevach and Tsan Xiao.

Application Process: To apply, e-mail your CV, bibliography, and an outline of a proposed research program (no more than two pages) to **Ms. Wanda Jackson at jacksonwa@niaid.nih.gov or mail to Ms. Wanda Jackson, 10 Center Drive MSC 1356, Building 10, Rm. 4A-26, Bethesda, Maryland 20892-1356. E-mail is preferred.**

Reference Letters: Three letters of recommendation must be sent directly from the referees to **Ms. Wanda Jackson via e-mail or U.S. mail**. Please refer to **Ad #016** on all communications. Further information about this position may be obtained by contacting **Dr. William Paul (301 496-5046; wpaul@niaid.nih.gov)**. Applications must be received by **October 19, 2007**.

A full package of benefits (including retirement, health, life and long term care insurance, 401-k plan) is available. Women and minorities are especially encouraged to apply. U.S. citizenship is not required.

NATIONAL CANCER INSTITUTE

HIV and AIDS Malignancy Branch
Center for Cancer Research
Tenure Track or Tenure Eligible Position in Viral Oncogenesis

The HIV and AIDS Malignancy Branch (HAMB), NCI, is searching for a tenure track or tenure eligible investigator in the field of viral oncogenesis. It is anticipated that the investigator will establish an independent research program targeted to the study of viral-induced tumors, especially those associated with AIDS. The research program should be able to interface with the branch's existing clinical and basic programs in AIDS-associated malignancies. A particular interest will be for a research program in gammaherpesviruses, but other areas of viral oncogenesis will be considered as well. Current areas of laboratory research in HAMB focus on the molecular biology of Kaposi's sarcoma-associated herpesvirus (KSHV/HHV-8) and human papillomavirus (HPV), pathogenesis of tumors caused by these viruses, and the development of novel therapeutic interventions for HIV infection. The clinical research program in HAMB is primarily directed at AIDS-related malignancies. HAMB is located on the Bethesda campus of the NIH (**http://ccr.cancer.gov/labs/lab.asp?labid=63**). Candidates for the position should have an M.D./Ph.D., Ph.D., or M.D. and strong research credentials. Applicants for this position should submit a curriculum vitae including bibliography, a statement of research interests, a two-page outline of the proposed research program, and the names of three references to **Chairman, Search Committee, HAMB, NCI, Attention Jan Huque, 301-435-4627, fax 301-480-5955, Building 10, Rm. 6N106, 10 Center Drive, MSC 1868, Bethesda, MD 20892-1868 no later than November 18, 2007**. You may also e-mail your application to: **huquej@mail.nih.gov.**

Tenure-Track Position
Vascular Medicine Branch

The Vascular Medicine Branch within the Division of Intramural Research of the National Heart, Lung and Blood Institute is seeking an individual to direct an independent research program in lipoprotein metabolism and vascular therapeutics. Demonstrated research accomplishment and excellence in the area of lipoprotein metabolism will be considered, however, preference will be given to those working in the area of HDL metabolism and potential therapeutic approaches. The candidate may have an M.D., Ph.D. or both and have an outstanding record of research accomplishments as evidenced by publications in major peer-reviewed journals. The position is tenure-track and comes with generous start up support. Also available is open access to various core facilities, including transgenic and knockout mouse facility, confocal and electron microscopy cores, multi-modality non-invasive mouse imaging facility, siRNA resources, fluorescent activated cell sorting facility and state of the art genomics, microarray and proteomics facilities.

The successful candidate will be offered a competitive salary commensurate with experience and qualifications. Appointees must be US citizens, resident aliens or non-resident alien with a valid employment visa. Applications must be received by October 31, 2007. Please submit a curriculum vitae and brief statement of research interests along with three letters of reference to Ross Heffer at heffer@mail.nih.gov or mail to:

Robert S. Balaban, Ph.D., Scientific Director, NHLBI, c/o Mr. Ross Heffer, Administrative Officer, NHLBI, 10, Center Drive, MSC 1670, Building 10, Room 7N220, Bethesda, MD 20892-1670.

NORTHWESTERN
UNIVERSITY

The Department of Biochemistry, Molecular Biology and Cell Biology seeks outstanding individuals whose research programs complement the existing interdisciplinary strengths of the department.

The department is a vibrant and exciting research and training environment located on the undergraduate campus in Evanston, IL. The openings of the Pancoe/ENH Life Sciences Pavilion and soon to be completed Silverman Hall are part of an ongoing expansion of the life sciences at Northwestern. Please visit our website at **www.biochem.northwestern.edu**.

SENIOR FACULTY – TWO POSITIONS
Associate or Full Professor

Applicants should submit electronically a single Adobe PDF or Microsoft Word file containing a cover letter, curriculum vitae, research summary and statement of teaching experience to **bmbcb@northwestern.edu** using "BMBCB Senior Search" as the subject.

JUNIOR FACULTY – TWO POSITIONS
Assistant Professor

We are particularly interested in individuals using state-of-the-art imaging or biophysical approaches to answer fundamental questions in biology. Applicants should submit electronically a single Adobe PDF or Microsoft Word file containing a cover letter, curriculum vitae, research summary, statement of future research goals and statement of teaching interests to **bmbcb@northwestern.edu** using "BMBCB Junior Search" as the subject. Applicants should also arrange for four letters of recommendation to be sent on their behalf. Review of completed applications for all positions will begin on **November 1, 2007**. To ensure full consideration, all material should be submitted by that date.

Northwestern University is an AA/EOE. Women and minorities are especially encouraged to apply.

DEPARTMENT OF THE NAVY
ONR
Science & Technology

HEAD, WARFIGHTER PERFORMANCE
S&T DEPARTMENT

The Office of Naval Research (ONR) is seeking an outstanding individual to serve in this Civil Service position in the Senior Executive Service (SES). Salary range is $111,676 to $168,000 per year, depending on qualifications. In addition to salary, career SES appointees are eligible to compete for performance awards and bonuses.

As a Department Head, the incumbent participates with other top management officials in advising on matters concerning the policies and personnel of the science and technology program and in recommending to the Chief of Naval Research the scientific and technical contents of an integrated science and technology program. In support of the approved program and overall Office of Naval Research mission requirements, the incumbent manages an extensive Departmental research and development program focused on the integration of basic research, applied research, and advanced technology development in the fields of science and technology such as computational neuroscience, cognitive science, manpower, personnel, training, human factors, occupational and environmental health, medicine of naval operations (undersea, Marine Corps, surface, aerospace) and combat/contingency medicine. The incumbent is responsible and accountable for planning and executing the Department's program. The incumbent: provides leadership to and establishes the broad direction of the program; establishes the objectives, policies, and priorities pertinent to the program; oversees and ensures the effective accomplishment of the extensive activities of the Department's Divisions; and coordinates and cooperates with other Departments in working to achieve a fully integrated science and technology program in the Office of Naval Research.

For detailed information on qualifications and how to apply, applicants may download a copy of Announcement # NW7-XXXX-00-4H673666-SES from the ONR web site http://www.onr.navy.mil/hr. Applications must be received in the Human Resources Service Center, Northwest by the close of business October 12, 2007. Emailed, faxed or postmarked applications will not be accepted.

ONR IS AN EQUAL EMPLOYMENT OPPORTUNITY EMPLOYER
AND PROMOTES DIVERSITY IN THE WORKPLACE.
WOMEN AND MINORITIES ARE ENCOURAGED TO APPLY.

COLUMBIA UNIVERSITY
Department of Biological Sciences

The Department of Biological Sciences of Columbia University invites applications for a tenure-track position. We anticipate that the appointment will be at the Assistant Professor level, but we will consider applications from more senior individuals. We are looking for individuals with outstanding and innovative research records and future plans, and who will complement the current strengths of the Department. Our Department has a long history of leadership in modern biology and a broad multidisciplinary focus (see http://www.columbia.edu/cu/biology). We are located on the main campus of Columbia University, surrounded by other basic science and engineering departments, and have strong ties to our Medical School. We expect that the successful candidate will develop a vigorous research program and also participate in undergraduate and graduate teaching. Ph.D. in biological sciences or related field required.

Send CV, statement of research goals, and three letters of reference by November 1, 2007, by e-mail (preferred) to:

biologysearch@biology.columbia.edu

or mail to:

Search Committee
Department of Biological Sciences
Columbia University
600 Fairchild, MC2402
New York, NY 10027

Columbia University is an equal opportunity/affirmative action employer. Minorities and women are encouraged to apply.

Tenure-Track Faculty Position in Chemistry or Chemical Biology Sloan-Kettering Institute

Sloan-Kettering Institute is seeking an innovative individual at the Assistant Member level, with strong research accomplishments in synthetic or mechanistic organic chemistry, or chemical biology to be part of a research program which addresses problems relating to bioorganic chemistry and cancer research. A doubling of chemical research resources and core facilities are now available on campus. Faculty will be eligible to hold graduate school appointments in the Gerstner Sloan-Kettering Graduate School of Biomedical Sciences, the Weill Graduate School of Medical Sciences of Cornell University, as well as the Tri-Institutional MD/PhD Training Program and Tri-Institutional Training Program In Chemical Biology.

MSKCC offers a unique and exciting research environment with programs in Chemistry, Pharmacology, Immunology, Molecular Biology, Computational Biology, Genetics, Cell Biology, Developmental Biology, Cancer Pathogenesis and Structural Biology. The presence on campus of world-renowned clinical programs in cancer research, treatment and prevention offers many opportunities for creative collaboration.

Applicants must have a Ph.D. in chemistry and a dedication to engage in collaborative research efforts at the interface of chemistry and biology. Both a strong record of achievement and the potential to secure external funding are required.

Candidates should e-mail their application, preferably in PDF format, to **chembio@mskcc.org** by November 15, 2007. The application should include a CV, a description of past research, a description of proposed research, and copies of three representative publications. Candidates should arrange to have three signed letters of reference sent by e-mail to **chembio@mskcc.org** or regular mail to: **David Gin, PhD and Sam Danishefsky, PhD, c/o Marie Aiello/Box 428, Molecular Pharmacology and Chemistry Program, Memorial Sloan-Kettering Cancer Center, 1275 York Avenue, New York, NY 10021.** Memorial Sloan-Kettering Cancer Center is an affirmative action, equal opportunity employer.

Memorial Sloan-Kettering Cancer Center
The Best Cancer Care, Anywhere.
www.mskcc.org

Pfizer

Working for a healthier world™

Biotherapeutics Research

When does a discovery become a miracle?

Imagine what you can achieve at a biotech start-up with unrivaled global resources. Imagine translating leading research into life-saving biotherapeutics. Imagine a biotech company atmosphere within one of the world's largest pharmaceutical organizations.

At Pfizer Biotherapeutics Research, we're not content waiting to witness the evolution of our industry. Instead, we are building on our current successes and capabilities, with a goal of developing the most compelling story of biotherapeutic scientific discoveries - and through this a compelling portfolio of biological therapies.

Our emphasis on innovation in Biotherapeutics has brought to market a wide range of ground-breaking medicines, such as Fragmin, Genotropin, Macugen, Somavert and our first-in-class inhaled insulin product Exubera. Our accomplishments, to date, make us the eighth-largest biotech in the world with an anticipated $1.5 billion in sales. But there is much more work to be done, and we are staged to deliver on our challenging goals with a blossoming pipeline.

Playing an integral part of the Biotherapeutics line in Pfizer Research is Vaccines Research. The vaccines research departments in Sandwich, UK and La Jolla, CA seek to discover novel vaccines (prophylactic and therapeutic) for the prevention and treatment of significant human diseases (infectious diseases, oncology, CNS and Allergy and Respiratory) using a variety of vaccines technology platforms combined with immunomodulatory agents.

Another essential part of Biotherapeutics Research is Rinat PGRD, which is comprised of skilled protein engineers, pharmacologists and biochemists that have expertise in developing novel protein-based therapeutics. Rinat is currently collaborating with other PGRD sites to conduct research that addresses significant unmet medical needs in Neurology, Oncology, Infectious Disease and Cardiovascular, Metabolic and Endocrine Diseases.

The Research team in St. Louis, MO also plays a key role in Biotherapeutics by focusing on the generation of novel therapeutic proteins, aptamers, and antibodies to treat diseases in numerous therapeutic areas. The St. Louis scientists, using key strategic alliances with Medarex, MorphoSys, Archemix and Noxxon, work in a collaborative fashion with Pfizer Research sites around the globe to deliver both monoclonal antibodies and macromolecular therapeutics. Additionally, one of the key research interests in St. Louis is applying protein engineering to support improving pharmaceutic properties of Biotherapeutics.

Your talents can change the world. Join Pfizer Biotherapeutics Research and turn discoveries into miracles.

To apply or to learn more about our people, our pipeline, and our plans for the future visit **www.pfizerbiotherapeutics.com**

We're proud to be an equal opportunity employer and welcome applications from people with different experiences, backgrounds and ethnic origins.

UCMERCED

Two Life Sciences Faculty Positions
University of California, Merced

UC Merced is the 10th UC campus and the first new US research university of the 21st century. The School of Natural Sciences at UC Merced seeks applicants for two faculty positions at the assistant, associate, or full professor ranks to continue building a life sciences program with a strong biomedical emphasis. Candidates must have a Ph.D. or equivalent, a record of research, publication, and teaching commensurate with a faculty appointment at the UC, and a strong interest in creating a curriculum characterized by strong cross-disciplinary links. Applicants are sought in the following two areas:

Complex Diseases: defined as diseases that are influenced by the actions of multiple genes, and include but are not limited to Alzheimer's disease, cardiovascular disease, Crohn's disease, asthma, cancer, diabetes, persistent infection, and metabolic disorders.

Developmental Biology: including observation of embryonic development from the single cell to mature organism, gene regulation, intercellular communication, intracellular signaling, cell fate decisions, organization of body plans, and evolution of developmental mechanisms.

For more information or to apply, please visit:
http://jobs.ucmerced.edu/n/academic/listings.jsf?seriesId=1

Applications must be received by **November 30, 2007**. For further information please contact **Prof. David Ojcius** (Complex Diseases): **dojcius@ucmerced.edu**, or **Prof. Michael Colvin** (Developmental Biology): **mcolvin@ucmerced.edu**.

AA/EOE

Department of
Biochemistry &
Molecular Biology
Indiana University School of Medicine
Indianapolis, Indiana

TENURE-TRACK FACULTY POSITIONS
Department of Biochemistry and Molecular Biology
Indiana University School of Medicine

The Department of Biochemistry and Molecular Biology is seeking applicants for several TENURE-TRACK FACULTY POSITIONS at any rank. This search continues a vigorous expansion of the Department in which 5-8 new faculty members will be added over the next few years. Indiana University School of Medicine offers a highly interactive scientific environment with many multidisciplinary centers and state-of-the-art core facilities including transgenic, imaging, genomic, proteomic, and chemical genomics (**http://www.medicine.iu.edu/research**). Candidates with research interests that complement or strengthen the existing research activities (**http://www.biochemistry.iu.edu**), or who bring novel approaches and/or expertise in chemical biology, structural biology, signaling mechanisms, systems biology, proteomics/genomics, RNA-mediated processes, epigenetics, stem cells, and genetic/disease model systems are encouraged to apply. Successful applicants are expected to develop a strong, independent extramurally funded research program and participate in graduate and medical student teaching. Highly competitive salary, start-up funds and laboratory space will be provided. Applicants must have a Ph.D., M.D. or equivalent degree, post-doctoral experience, and clear evidence of research productivity. The search committee will begin consideration of applications immediately and continue until positions are filled. Applicants should submit curriculum vitae, a brief summary of past accomplishments and future research plans, and the names and email addresses of at least three references electronically to: **biomjobs@iupui.edu** or by mail to:

Dr. Zhong-Yin Zhang, Professor and Chair
c/o Patty Dilworth
Department of Biochemistry and Molecular Biology
Indiana University School of Medicine
635 Barnhill Drive, MS 4053
Indianapolis, IN 46202-5122

Indiana University is an Equal Opportunity/Affirmative Action Employer, Educator and Contractor, M/F/D.

Faculty Position in Chemical Biology

The Life Sciences Institute (LSI) at the University of Michigan invites applications for a position at the rank of Assistant or Associate Professor in the field of chemical biology. Chemical biology is broadly defined and the successful applicant will use chemical methods to address an important biological question.

The LSI is a scientific enterprise at the University of Michigan dedicated to opening new scientific paths by blending diverse research talents in a state-of-the-art collaborative physical space (www.lsi.umich.edu). The LSI is currently home to 26 interactive faculty in the areas of cell biology, genetics, bioinformatics, structural biology, signaling, and chemistry.

Candidates are expected to develop an internationally recognized program of scholarly research and to excel in teaching at undergraduate and graduate levels. The positions will remain open until filled but preference will be given to applicants who have submitted all requested materials prior to **October 15, 2007**. Applicants should send the following (in PDF format): a curriculum vitae, copies of up to three reprints, a one- to two-page summary of research plans, and arrange to have three letters of reference sent directly to: **lsichembio@umich.edu**.

The University of Michigan is supportive of the needs of dual career couples and is a non-discriminatory, Affirmative Action Employer. Women and minorities are encouraged to apply.

lifesciencesinstitute

CHAIR ● DEPARTMENT OF BIOLOGY

The Department of Biology at the College of Charleston invites applications and nominations for **DEPARTMENT CHAIR.** Located in historic Charleston, South Carolina, the College of Charleston is a public liberal arts and sciences institution with approximately 11,000 undergraduate and graduate students. The Department of Biology is located on the main campus and at nearby Grice Marine Laboratory, and is comprised of 32 full-time faculty who actively pursue research in a broad range of biological disciplines both individually and collaboratively with local, state and national partners. Faculty research is supported by NIH, NSF, and USDA, among others. With over 800 undergraduate majors, the department awards B.A. and B.S. degrees in biology with emphases in marine biology, molecular biology, and biology teaching and supports interdisciplinary minors in neuroscience, environmental studies, and discovery informatics. It offers M.S. degrees in marine biology with an optional emphasis in genomics, and in environmental studies. The department values and promotes independent research by undergraduate and graduate students. Further information is available at **http://www.cofc.edu/~biology.** We are seeking a dynamic and innovative leader with an established research program, commitment to excellence in teaching, and significant administrative experience. Applicants should send a cover letter, *Curriculum vitae*, and contact information for four references, at least one of whom can address the applicant's administrative skills, to: **George Pothering, Biology Chair Search Committee, Department of Biology, College of Charleston, Charleston, SC 29424. Telephone: (843) 953-5504. Email: biologychair@cofc.edu.** For fullest consideration, nominations and applicant materials should be received by 10/31/07, however, applications will be accepted until the position is filled. For more information contact the committee chair via email or phone

The College of Charleston is an Affirmative Action/Equal Opportunity Employer and encourages applications from women and minorities.

COLLEGE of CHARLESTON
SCHOOL OF SCIENCES AND MATHEMATICS

Wellman Center for Photomedicine

MGH 1811

HST

Assistant or Associate Professor

The Wellman Center for Photomedicine (WCP) at Harvard Medical School and the Harvard University-Massachusetts Institute of Technology Division of Health Sciences and Technology (HST) are jointly recruiting new faculty members at the Assistant or Associate level. A broad range of areas will be considered including, but not limited to pathology, image guided therapy, applications of nanotechnology to photomedicine, advanced microscopy and molecular imaging, high throughput gene, protein, and molecular analysis, and photodynamic therapy. A competitive start-up package will be provided.

Candidates will be expected to promote and foster multidisciplinary research within Wellman, HST, and the larger MGH and Harvard research communities. The Wellman Center, located on the Massachusetts General Hospital Campus, will be the primary location. The Wellman Center for Photomedicine is the largest academic research facility dedicated to investigating the effects of light on human biology and to the development of light-mediated, minimally invasive diagnostic and therapeutic technologies. A pioneer in light-based biomedical research, the Center has been the source of many of the most successful transfers of this research to clinical applications (**http://www.mgh.harvard.edu/wellman**)

The ideal candidate would combine a record of achievement in scientific research and a demonstrated interest in translational research, with M.D., Ph.D. or M.D.-Ph.D. degrees. An outstanding publication record and demonstrated ability to obtain independent peer-reviewed funding is expected. Applicants should submit: (i) curriculum vitae, (ii) statement of research interests and goals, (iii) statement of teaching interests, (iv) brief ideas of potential collaborative possibilities with WCP and HST faculty (**http://hst.mit.edu**), (v) plans for future funding, and (vi) reprints of selected recent publications. Applicants should have three letters of recommendation sent directly to the Search Committee Chair.

Although applications will be accepted until the position is filled, complete applications (including reference letters) will be reviewed beginning **November 1, 2007**, and should be mailed to: **Gary Tearney, M.D., Ph.D., Chair of Faculty Search Committee, c/o Susan Weeks, Wellman Center for Photomedicine/MGH, 40 Blossom Street BAR 604, Boston, MA 02114**. Electronic versions of the application materials should also be sent to (**WCPFacultySearch@partners.org**)

Massachusetts General Hospital, Harvard University and Massachusetts Institute of Technology are Equal Opportunity Employers. Women and minorities are encouraged to apply.

UCMERCED

Faculty Positions in Ecology

Three tenure/ tenure-track faculty positions open in Ecology at UC Merced, the newest 10th campus in the University of California system. We seek outstanding individuals with research interests in any area of ecology using experimental, field, computational, and/or theoretical approaches and working at population to ecosystem scales.

For more information/ to apply, visit: **http://jobs.ucmerced.edu/n/academic/listings.jsf?seriesId=1** under job codes: **ASNS1219A** and **ASNS1221A**.

Deadline is **November 12, 2007**.

AA/EOE

HEAD of DEPARTMENT and PROFESSOR
Department of Bioengineering
University of Illinois at Urbana-Champaign

Bioengineering education and research in the 21st century will exploit the revolution in biomolecular sciences, building on the spectacular advances in imaging and devices that have fundamentally changed biomedical diagnosis, therapy and research. Exploration of the human body at vastly different scales, coupling of macroscopic physiology to microscopic biology, creative development of micro and nano sensors, and massive computational approaches in bioinformatics all constitute grand challenges in education and research. The new generation of highly engaged bioengineering students will transform the workforce and society's ability to improve our quality of life.

Against this backdrop, the College of Engineering of the UIUC (**www.engr.uiuc.edu**) established the Department of Bioengineering (**www.bioen.uiuc.edu**) in 2003. Today, the Department offers undergraduate (BS), and graduate (MS, PhD) educational and research programs focused on bioimaging, cellular and tissue engineering, computational bioengineering/systems biology, and nano- and microsystems technology. The Department has six full-time faculty members, will triple in size over the next five years, and has a network of affiliated faculty. Expanding collaborations with related activities across the Colleges of Engineering, Medicine, Veterinary Medicine, and Liberal Arts & Sciences enrich the Department's education and research programs. Bioengineering faculty participate actively in campus-wide initiatives located at the Beckman Institute for Advanced Science and Technology, Institute for Genomic Biology, Coordinated Sciences Laboratory, Fredrick Seitz Materials Research Laboratory, the Micro and Nanotechnology Laboratory, and will have key role in the campus priority on translational biomedical education and research.

Applications and nominations are sought for the position of Head of the Department. We seek a visionary leader with organizational skills to advance this young Department into a preeminent position of research and education. Applicants must have an earned PhD/MD in a relevant field, recognition as a distinguished researcher and scholar, and a strong interest in developing the research and teaching programs of the Department. The Department Head is the chief administrative officer with responsibilities for leading the faculty in the development of research, teaching and public service, external fund raising, and for administrative, budgetary and promotion decisions. The Department Head holds the rank of Professor in Bioengineering with tenure and reports to the Dean of the College of Engineering.

The proposed date of appointment is June 2008 or as soon as possible thereafter. Salary is negotiable. To ensure full consideration, applications must be received by **December 1, 2007**. Submit applications electronically as a single PDF document to: **cee-searches@uiuc.edu**. Electronic applications should include a letter of application and a complete resume. The cover letter should be addressed to: **Professor Robert H. Dodds, Jr., Chair of the Bioengineering Search Committee, 1114 Newmark Civil Engineering Laboratory, 205 North Mathews Avenue, Urbana, IL 61801. Telephone: 217-333-6378**.

The College is committed to building a diverse environment; minorities, women and other designated class members are encouraged to apply. The University of Illinois is an AA/EO Employer.

Stanford University
Ecology Faculty Position

The Department of Biological Sciences at Stanford University invites applications for a tenure-track faculty position as Assistant Professor with a research and teaching specialization in ecology. Research interests may include behavioral, population and/or community ecology with reference to animals, plants and/or microorganisms, and may employ theoretical, experimental, and/or comparative methods.

Applicants are expected to develop a vigorous research program and to participate in undergraduate, graduate, and postdoctoral education and training. For information about the Department consult our web page: **http://biology.stanford.edu/**.

Applicants are requested to provide a cover letter, a curriculum vitae including list of publications, a statement of research accomplishments and future research plans, a description of teaching experience and aspirations, and the names of three persons whom we can contact for letters of recommendation.

Applicant materials must be received by **November 15, 2007**. The appointment is anticipated to begin September 1, 2008.

Interested candidates should apply online at **AcademicJobsOnline.Org**

Stanford University is an Equal Opportunity Employer and is committed to increasing the diversity of its faculty. It welcomes nominations of and applications from women and minority groups, as well as others who would bring additional dimensions to the university's research, teaching and clinical mission.

PHARMACOLOGY CHAIR
UNIVERSITY OF ALABAMA SCHOOL OF MEDICINE AT UAB

The University of Alabama School of Medicine at UAB is seeking applications and nominations for the position of Professor & Chair of the Department of Pharmacology. This is a tenured position. The successful candidate will be an internationally recognized MD or PhD scientist who has demonstrated success in teaching, research, and administration. The UAB Department of Pharmacology currently has 18 full-time faculty with 30 active grants and 23,000 square feet of research space. The new Chair will have the opportunity and resources to implement an aggressive and visionary approach to Pharmacology, and will have substantial leeway in implementing their vision for the Department. UAB seeks an innovative new Chair who will position the Department as a leading academic and research enterprise nationally. The University is the largest state employer with more than 20,000 employees and a $1.9 billion budget.

Nominations and applications should include a curriculum vitae, bibliography and the names and addresses of at least three references and should be sent electronically (preferably) to **Mroser@uab.edu** or mailed to:

Dr. David Sweatt, Chairman
Pharmacology Search Committee
C/O Margarete Roser
University of Alabama School of Medicine at UAB
1530 3rd Ave S; FOT 1230
Birmingham, Alabama 35294-3412

The University of Alabama at Birmingham is an Equal Opportunity/ Affirmative Action Employer.

Immunology
Tenure-track Faculty Position

The Department of Immunology at the University of Connecticut Health Center seeks outstanding investigators for a tenure-track position at the Assistant/Associate Professor level. Although all areas of immunology will be considered, we are particularly interested in individuals using molecular and cellular approaches to study immune system function in vivo. Areas of priority include dendritic cell biology or innate immunity, immune cell signaling and immunity to infection. Salary and start-up funds are highly competitive and outstanding core facilities are available. Applicants must have a Ph.D., D.Sc. and/or M.D. with postdoctoral experience and a quality publication record. For the Associate Professor level, applicants should have a record of substantial productivity and sustained extramural funding.

Please submit curriculum vitae, two-page summary of research interests and the names of three references to:

Leo Lefrançois, Ph.D., Chair
Immunology Search Committee
Department of Immunology MC1319
UCONN Health Center
263 Farmington Ave.
Farmington, CT 06030-1319

Email: **fiorente@nso1.uchc.edu**
For further information on UCHC please visit **immune.uchc.edu**.

UCHC is an Equal Opportunity Employer M/F/V/PwD.

Beth Israel Deaconess Medical Center
A teaching hospital of Harvard Medical School

FACULTY POSITION in
THE TUMOR MICROENVIRONMENT

The Department of Pathology at Beth Israel Deaconess Medical Center is seeking a full-time scientist at the Assistant Professor level. The Center is a major teaching hospital of Harvard Medical School and is undergoing an ambitious program of growth and is expanding the strength and depth of its faculty. In 2008, we will move into a new state-of-the-art research building which will become the epicenter for basic science research.

We are seeking candidates of exceptional promise who have strong records of research creativity and productivity in basic or translational research. The department has expertise in all areas of cancer cell biology and seeks to expand into related areas, especially in tumor microenvironment. Examples include but are not limited to angiogenesis, inflammation, tumor immunology, stem cell and stromal cell biology.

The successful candidate will receive a highly competitive start-up package and appointment to the faculty of HMS. We strongly encourage interactions among research and clinical faculty and provide opportunities to access a human tumor resource through its Divisions of Anatomic Pathology and Laboratory Medicine. The Medical Center provides an exceptional opportunity for scientists who aspire to work in a setting that combines the power of HMS and its affiliated institutions with an unusually collegial, supportive and interactive environment.

Applicants must hold a PhD and/or MD degree. BIDMC is committed to increasing the representation of women and members of minority groups on its faculty. Interested applicants should submit a CV, a statement outlining existing and planned research activities and the names of three references to:

Alex Toker, Ph.D.
Beth Israel Deaconess Medical Center
Department of Pathology
330 Brookline Avenue, RN-237
Boston MA 02215
E-Mail: atoker@bidmc.harvard.edu

Center for Epigenetics
Johns Hopkins University

The **Center for Epigenetics** is a major new initiative of the **Institute for Basic Biomedical Sciences** at the **Johns Hopkins School of Medicine** to establish the first interdisciplinary research center devoted to epigenetics research. Members of the Center work in a collaborative and interactive environment on the mechanisms of epigenetic regulation and the role of epigenetics in development and human disease. The Center seeks new faculty working in fields related to epigenetics, including biochemical and structural studies of chromatin and DNA modifications, the epigenetics of humans and model organisms, and novel computational and systems biology approaches. A strong infrastructure is provided by an NIH funded Center of Excellence in Genome Sciences in Epigenetics. Faculty will reside in new laboratories on the Medical School campus and receive primary appointments in an existing departments within the School of Medicine.

Applications will be considered on a rolling basis, but should be submitted no later than January 15, 2008. Please email a CV, research plan, names and emails of three references and up to three publications, all in pdf format to IBBScenters@jhmi.edu. Indicate CE in the email subject line.

The Johns Hopkins University is committed to diversity and equality in education and employment and encourages applicants from under-represented groups.

THE UNIVERSITY OF KANSAS

Faculty Position in Bioinformatics/Computational Biology

The Center for Bioinformatics and the Department of Molecular Biosciences at the University of Kansas invite applications for a tenure-track assistant professor position expected to begin August 18, 2008. Applicants should have a clear interest in the modeling of protein interactions in networks or systems. The interdisciplinary Center for Bioinformatics (**www.bioinformatics.ku.edu**) complements existing strengths in the Department of Molecular Biosciences (**www.molecularbiosciences.ku.edu**), including structural biology, computational chemistry, proteomics, and developmental/molecular genetics. The Center fosters international activities in Bioinformatics and combines outstanding research and an affiliated Ph.D. program. **Duties:** To establish and maintain an externally-funded research program, to participate in teaching, and to provide service. **Required Qualifications:** Ph.D. and postdoctoral experience in a discipline related to Bioinformatics; potential for excellence in research in Bioinformatics as evidenced by publications in highly ranked journals and innovative research objectives; and commitment to teaching life sciences courses evidenced by teaching philosophy statement. The successful candidate for the position should be eligible to work in the U.S. prior to the starting date of the position. For the full position announcement, refer to: **www.clas.ku.edu** Email application as a single file including CV, letter of application, statement of past and future research and teaching interests and philosophy to: **rweaver@ku.edu** Have at least three letters of reference sent separately to **Dr. Robert F. Weaver, Professor and Associate Dean, College of Liberal Arts and Sciences, 1450 Jayhawk Blvd., Lawrence, KS 66045-7535**. Initial review of applications begins November 1st and will continue until the position is filled.

EO/AA Employer. Women, minorities, and candidates who will contribute to the climate of diversity in the College, including a diversity of scholarly approaches, are encouraged to apply.

UNIVERSITY OF CALIFORNIA, BERKELEY ASSISTANT PROFESSOR

The Department of Nutritional Sciences and Toxicology, the University of California-Berkeley, is recruiting for an assistant professor (nine-month tenure-track) starting as early as July 1, 2008.

We expect the appointee to develop a vigorous and independent research program investigating metabolic regulation, control of metabolic systems, and/or the relationship among nutrients, phytochemicals, toxicants, genetics, and disease. Applicants should have a bioscience Ph.D., M.D., or equivalent degree, with training and experience in experimental biology. The appointee will have opportunity to work with Ph.D. students in four interdepartmental programs: Molecular and Biochemical Nutrition; Molecular Toxicology; Comparative Biochemistry; Endocrinology. The appointee will also contribute to educating undergraduates seeking degrees in nutritional biology and molecular toxicology. Numerous opportunities exist for interactions with colleagues at UCB and in the Bay Area.

Applications should include a curriculum vitae, a statement of current and proposed research, copies of publications, and the names and addresses of at least three references. Applicants should have their referees send references to us directly, and should refer their referees to the UC Berkeley Statement of Confidentiality at: http://apo.chance.berkeley.edu/evalltr.html. Applications should be submitted to **DNSTsearch@berkeley.edu** (electronic submissions strongly preferred) or to: Search Committee Chair, Department of Nutritional Sciences and Toxicology, 119 Morgan Hall, University of California, Berkeley, CA 94720-3104. The deadline for receipt of applications is **December 1, 2007**. Late applications will not be accepted.

The University of California is an Equal Opportunity, Affirmative Action Employer. We are especially interested in a diverse applicant pool.

Faculty Positions

Yale Stem Cell Center

Yale University School of Medicine

The newly established Yale Stem Cell Center invites applications for faculty positions at the rank of Assistant, Associate, or Full Professor. Rank and tenure will be commensurate with experience. Applicants should have a Ph.D. and/or M.D. degree. Each successful candidate will be expected to develop a vigorous, externally funded research program on fundamental questions related to the biology of embryonic or adult stem cells. Investigators will join a vibrant stem cell research community at Yale with over 40 labs working on various aspects of stem cell biology and medicine, and will have opportunities to compete for Connecticut State funding for stem cell research, including research on non-federally approved human embryonic stem cell lines. Investigators will also contribute to teaching graduate and/or medical students as well as shaping stem cell research at Yale.

Applicants should mail a three-page research statement and CV, and arrange to have three reference letters sent to:

Haifan Lin, Ph.D., c/o Kristin Dugan
Director's Office, Yale Stem Cell Center
P.O. Box 208073, Yale University School of Medicine
10 Amistad Street, New Haven CT 06509

Application deadline is **December 15, 2007**. Follow-up inquiries should be sent to: **kristin.dugan@yale.edu**.

Yale is an Affirmative Action/Equal Opportunity Employer.

HARVARD UNIVERSITY CENTER FOR BRAIN SCIENCE FACULTY POSITION

The Center for Brain Science is seeking an Assistant Professor in the area of animal behavioral genetics and neurobiology, broadly construed. We are particularly interested in candidates whose research programs are driven by behavioral and psychological questions, and who explore neural and genetic mechanisms using innovative techniques. Potential research areas include, but are not limited to, spatial knowledge and navigation, decision-making, social relationships, and psychopathology. Successful candidates will hold an academic appointment in a participating department, such as Psychology or Molecular and Cellular Biology.

The Center for Brain Science brings together scientists involved in research on systems neuroscience (see **http://cbs.fas.harvard.edu**). Our aims include mapping neural circuits that underlie experimentally accessible behaviors in diverse species, and elucidating the biological bases of individual differences in behavior. CBS fosters interactions across disciplinary boundaries: faculty from several academic departments will be housed in common research space, and its connections reach out across the University.

Candidates should have demonstrated a promise of excellence in both research and teaching. Teaching duties will include offerings at both undergraduate and graduate levels. Applications are due by **December 10, 2007**. Please send a cover letter, curriculum vitae, and 2 to 4 page research plan, and arrange for submission of 3 letters of recommendation. Application materials can be submitted electronically by emailing **cbs@fas.harvard.edu**, or by sending mail to:

Joshua R. Sanes
Center for Brain Science Search Committee
Harvard University
7 Divinity Ave.
Cambridge, MA 02138

Applications from, or nominations of, women and minority candidates are encouraged. Harvard is an Affirmative Action/Equal Opportunity Employer.

Imperial College London

100 years of living science 100

Division of Cell and Molecular Biology,
Faculty of Natural Sciences

Research Associate x 2

Salary in the range of £24,570 - £35,800 per annum

Imperial College is ranked in the top ten universities of the world, according to the 2006 Times Higher Education Supplement league tables.

Imperial College London invites applications for the following vacancies in the joint group of Prof. Fotis C. Kafatos and Dr. George K. Christophides at Imperial College London.

You will be members of a large research team working on innate immunity and functional genomics of the malaria vector Anopheles gambiae. You will work on a programme aiming to understand the mosquito innate immune system and its interactions with Plasmodium parasites capitalizing on a variety of postgenomic tools. Required skills include standard molecular biology techniques with emphasis on protein biochemistry, including 2D-PAGE, mass spectrometry, purification of secreted proteins and protein expression. Experience in cell culture techniques is preferred.

You will also be skilled molecular biologists with a PhD in a relevant field and a track record of publications.

These positions are available immediately and funding is available for up to 3 years.

A job description and an application form can be obtained from: www.imperial.ac.uk/employment

For further details please contact Rabeya Sultana, email: r.sultana@imperial.ac.uk

Completed application forms accompanied by a CV and the name and contact details of two referees should be sent to Rabeya Sultana, BioMalPar Administrator, Cell & Molecular Biology, Imperial College London, Sir Alexander Fleming Building, South Kensington Campus, London SW7 2AZ, r.sultana@imperial.ac.uk

Closing date: 30 September 2007.

(Conference call interviews are possible for international candidates)

Valuing diversity and committed to equality of opportunity

UNIVERSITY OF DELAWARE

Assistant Professor in Animal Infectious Disease

The Department of Animal and Food Sciences is seeking a tenure-track Assistant or Associate Professor to develop an animal infectious disease research and teaching program. The individual will join an internationally-recognized team focusing on avian health, genomics and food safety. The major portion of the person's appointment will be allocated to research. The successful candidate will be expected to develop a vigorous and competitive research program in an area that complements animal infectious disease expertise at the University of Delaware. Possible areas of focus include immunology, virology, bacteriology, mathematical modeling and computational biology. Collaboration is expected with scientists within the Department, the Avian Biosciences Center, the Delaware Biotechnology Institute or other appropriate academic departments. A portion of the person's appointment will be allocated to teaching activities consistent with the individual's background and the needs of the Department. The individual will be responsible for the academic advisement and supervision of undergraduate and graduate students and is expected to participate in the University's nationally-recognized undergraduate student research program. Qualifications: Ph.D. or DVM/Ph.D. with postdoctoral training. The individual must be able to communicate effectively with academic, government, and industry colleagues and with students.

Applicants should submit a letter of interest addressing the required qualifications, curriculum vitae, a statement of research interests and teaching philosophy and the names and addresses of three references by email (preferred) to **Parcells@Udel.edu**; or to Dr. Mark S. Parcells, Search Committee Chair, Department of Animal and Food Sciences, 044 Townsend Hall, University of Delaware, Newark, DE 19716-2150; or by fax to (302) 831-2822. Application deadline is October 15, 2007.

The UNIVERSITY OF DELAWARE is an Equal Opportunity Employer which encourages applications from Minority Group Members and Women.

ÉCOLE POLYTECHNIQUE FÉDÉRALE DE LAUSANNE

Tenure Track Assistant Professor in Cognitive Development

Nestlé Chair on "Nutrition and Brain Development" at Ecole Polytechnique Fédérale de Lausanne (EPFL)

The Brain Mind Institute of EPFL invites applications for a Tenure Track Assistant Professor position in Cognitive Development. We are especially interested in candidates focusing on events taking place from the early postnatal period to puberty/adolescence, and on the role of nutrition. A range of research topics within these areas will be considered (e.g., development of mental representations, executive function or cognitive control, development of reasoning/problem solving, social and emotional development, emergence of different cognitive functions, molecular mechanisms of memory). Candidates whose work bridges the cognitive level with underlying molecular and cellular mechanisms relies on multidisciplinary approaches (such as a combination of molecular, behavioral and neuroimaging-based experimentation) and involves human subjects and/or animal models are particularly sought. Successful candidates will develop an independent and vigorous research program, will be committed to excellence in undergraduate/graduate teaching, and supervise PhD students.

Start-up resources and state-of-the-art research infrastructure will be available, within the framework of a campus that fosters very strong interactions between life sciences, basic science, informatics and engineering. Salaries and benefits are internationally competitive.

Applications should be submitted through the Internet http://bmisearch-cogdev.epfl.ch and should include the following documents in PDF format: curriculum vitae, publication list, brief statement of research and teaching interests, names and addresses (including e-mail) of 3 references. Deadline for applications: **October 31st 2007.**

Further questions can be addressed to:

Professor Pierre J. Magistretti, Co-Director
Brain Mind Institute
School of life sciences, EPFL
pierre.magistretti@epfl.ch

For additional information on EPFL, please consult http://www.epfl.ch and http://sv.epfl.ch/

The EPFL School of life sciences aims for a very strong presence of women amongst its faculty, and qualified female candidates are strongly encouraged to apply.

Tufts UNIVERSITY

DEPARTMENT OF CHEMISTRY

The Department of Chemistry is beginning a phase of significant expansion. Applications are invited for three tenure-track positions at the rank of assistant professor with research interests at the interface of chemistry and biology. All areas of chemistry will be considered. The department has a particular interest in hiring at least one candidate who has research plans at this interface with a strong synthetic organic chemistry component. Successful candidates will demonstrate the potential to develop an internationally recognized research program and excel in teaching. The Chemistry Department at Tufts is a well-funded, thriving community of researchers with collaborations spanning across the university. Excellent resources are available for new investigators interested in building a program in the Life Sciences—one of the university's strengths. Teaching responsibilities will include graduate and undergraduate courses in chemistry and/or the biochemistry curriculum. Additional information about the department can be found at **http://chem.tufts.edu**.

Send CV, a research plan and three letters of recommendation to:

Faculty Search Committee
Department of Chemistry
Tufts University
Medford, MA 02155

Evaluation of candidates will begin **October 15, 2007** and continue until the positions are filled.

Tufts University is an Affirmative Action/Equal Opportunity Employer. We are committed to increasing the diversity of our faculty. Applications from women and members of underrepresented groups are strongly encouraged.

www.aucmed.edu

IMMUNOLOGIST/MICROBIOLOGIST

The **American University of the Caribbean School of Medicine (AUC)**, an accredited institution with over 3,500 graduated physicians, seeks to appoint an Immunologist / Microbiologist.

The university seeks an individual with a strong teaching background in immunology and microbiology. Candidates should possess a Ph.D. and/or Ph.D./M.D., with a positive commitment to teaching, good communications skills, and a strong comfort level with electronic based learning.

The position is contained within the Department of Immunology and Microbiology. These disciplines are team taught over the course of a semester. Modern research facilities, a comprehensive library, and state of the art e-learning paradigms are available to support the department.

The position is to be fulfilled at the Basic Sciences campus on the island of St. Maarten in the Netherlands Antilles, approximately 3 hours by air from Miami. AUC possesses an exceptional faculty composed of both basic scientists and clinicians. Students complete their basic sciences training on the island, and then go on to complete clinical clerkships in the U.S., U.K. or Ireland.

Interested parties should send a brief statement of teaching philosophy, their CV, and contact information for three professional references to Kathi Shupe, Ph.D., at **kshupe@aucmed.edu**.

American University of the Caribbean
School of Medicine

Hutchison China

The China operations group of Hutchison Whampoa Limited

CAREER OPPORTUNITIES in SHANGHAI, CHINA

Hutchison Whampoa Limited (HWL) is a Hong Kong based multinational conglomerate with over 150,000 employees worldwide. Hutchison MediPharma Limited is its subsidiary division focused on innovative drug development for the global markets. Currently, the Company has the following opening for research management position in its R&D Center located in Shanghai, China;

Biomarker R&D, Director/Associate Director

This position is responsible for the quantitative analysis of biomarkers for our leading new drug candidates including development, characterization, & assay for biomarkers for informed decision making in our new drug pipeline development for cancers and autoimmune diseases. The qualified candidate should have a Doctorate degree with minimal 5 years of industrial drug discovery experience in a relevant field. A good understanding of cancer and autoimmune diseases biology is essential. Experience in development, characterization, and implementation of quantitative bio-analytical assays and excellent communication and leadership skills are required.

If you share our goal to become one of the global leaders in new drug discovery and development, and a leader in the ever-growing healthcare industry in China, we encourage you to apply. Please submit a cover letter, your CV, and your expected compensation package by **e-mail to hr@hmplglobal.com or fax us at 011-86-21-50793595.**

Our website: www.hmplglobal.com

The University of North Dakota
School of Medicine & Health Sciences
501 N. Columbia Road Stop 9037
Grand Forks, ND 58202

UND

Associate Dean for Research

Applications are invited for an accomplished senior investigator to fill the position of Associate Dean for Research with an appointment as Professor in a suitable research-focused academic department. The School of Medicine and Health Sciences at the University of North Dakota has excellent space, state-of-the-art equipment, and a young and ambitious faculty who receive over $20M per year in extramural support for their research activities. The successful candidate will be expected to maintain an active extramurally-funded research program, participate in graduate and medical education, and provide creative leadership and guidance to develop, promote, and sustain an increased culture of research excellence and productivity within the School of Medicine and Health Sciences. Applications will be reviewed as received and the position will remain open until filled.

Please send current curriculum vitae, contact information for at least three individuals willing to serve as references, and descriptions of administrative, research, teaching and service activities to **Dr. Jonathan D. Geiger, Chair of Search Committee and Professor and Chair, Department of Pharmacology, Physiology and Therapeutics, Box 9037, University of North Dakota, School of Medicine and Health Sciences, Grand Forks, ND 58203 (Ph. 701-777-2183, Fax 701-777-4490, jgeiger@medicine.nodak.edu)**. The University of North Dakota, with about 13,000 students, is located in Grand Forks, ND, a family-oriented community of over 50,000 people with excellent schools, parks, and abundant year-round outdoor recreational activities.

The University of North Dakota is an Equal Opportunity/Affirmative Action Employer and invites applications from all qualified individuals.

www.med.und.nodak.edu

Department of Health and Human Services
National Institutes of Health
Office of the Director
Office of Biotechnology Activities
Office of Science Policy

INTERESTED IN APPLYING YOUR SCIENTIFIC OR CLINICAL EXPERIENCE TO ENHANCING FEDERAL POLICIES GOVERNING CLINICAL RESEARCH?

JOIN A FEDERAL INITIATIVE TO COORDINATE AND STREAMLINE CLINICAL RESEARCH POLICIES

The National Institutes of Health (NIH) Clinical Research Policy Analysis and Coordination (CRpac) program is recruiting exceptional candidates for several analytical and management positions. The CRpac program is located within the Office of Biotechnology Activities of the Office of Science Policy within the Office of the Director, NIH. The CRpac program staff is responsible for identifying and pursuing opportunities for harmonization, streamlining, and coordination of Federal clinical research policies and will ensure focused attention on NIH efforts in this regard. Among other initiatives, the CRpac program is exploring and developing strategic approaches to 1) harmonizing adverse event reporting requirements, 2) clarifying agency views on the acceptability of IRB models for various types of clinical research activities, 3) coordinating the development of DSMB policies and clarifying their roles and responsibilities, and 4) developing guidance on informed consent processes for those considering participation in clinical research. See our website at **http://crpac.od.nih.gov/** for more information about the CRpac program.

Incumbent must have an expert knowledge of the HIPPA Privacy Rule, particularly as it applies to research, as well as any related HHS regulations, policies, and procedures. Incumbent must also have expert knowledge of the range of administrative laws, policies, regulations, and precedents applicable to the protection of human subjects and privacy and confidentiality in research.

Incumbent must have an expert knowledge and understanding of the mission, goals, and objectives of CRpac/OBA as well as its relationship with other research programs throughout NIH, the federal government, and the nation. A broad knowledge of the Department s programs, regulations, and practices, the missions of agencies within the Department, and Congressional and Executive Branch initiatives with regard to the conduct of research is imperative.

Finally, incumbent must have a knowledge and understanding of current state-of-the-art in clinical research, including past and current legislation. Knowledge of the complexity of biomedical research, a broad understanding of scientific principles of science and technology areas, and familiarity with the structure and interrelationship of scientific research programs.

Salary is commensurate with experience and includes a full benefits package. A detailed vacancy announcement with the mandatory qualifications and application procedures can be obtained in **USAJOBS** at **www.usajobs.gov (announcement number OD-07-200861-DE)** and the NIH web site at **http://jobs.nih.gov**. Applications must be received by midnight eastern standard time **on closing date indicated in order to be considered**. Questions on the application procedures maybe addressed to **Felicia Royster on 301-496-3531**.

DHHS and NIH are Equal Opportunity Employers

Endowed Professorship for Dementia Research

The Department of Neurology and the Neuroscience Center at the University of North Carolina School of Medicine are seeking candidates with an interest in degenerative neurological diseases that produce cognitive impairment for appointment to full professor on the tenure track. The qualified candidate will have an M.D. or M.D./Ph.D. and an established record of excellence in research as reflected by peer-reviewed publications and independent external funding. He/she will be expected to conduct a laboratory-based research program investigating mechanisms of cellular death and dysfunction in neurodegenerative diseases using state-of-the-art cellular and molecular techniques. The position includes an endowed professorship of $1 million, ample modern laboratory space in the UNC Neuroscience Center and a generous start-up package. The UNC Neuroscience Center maintains outstanding Core Facilities that support confocal and multiphoton imaging, vector construction and ES cell electroporation for generation of mouse genetic models, and Affymetrix GeneChip technology for expression profiling and SNP analysis.

Interested candidates should contact: **William J. Powers, MD, H. Houston Merritt Professor and Chair, Department of Neurology, 3114 Bioinformatics Building CB 7025, University of North Carolina School of Medicine, Chapel Hill, NC 27599-7025; (919) 966-8178; holzmachere@neurology.unc.edu.**

EOE

ÉCOLE POLYTECHNIQUE FÉDÉRALE DE LAUSANNE

Tenure Track Assistant Professor in Interoception and Visceral Physiology

Nestlé Chair on "Gut-brain interactions" at Ecole Polytechnique Fédérale de Lausanne (EPFL)

The Brain Mind Institute of EPFL is searching for a tenure track Assistant Professor in Interoception and Visceral Physiology. Approaches of particular interest include, but are not limited to, perceptual, cognitive, and affective neuroscience in humans (or animals) for studying the gut-brain axis and the impact of nutrition. Experience in how interoception and visceral physiology relates to mood and emotions will be beneficial. Applications from candidates with strong quantitative skills in gastroenterology, physiology and/or neuroimaging are particularly welcome as is an active interest in the behavioural and neurophysiological effects of nutrients. Successful candidates will develop an independent and vigorous research program, will be committed to excellence in undergraduate/graduate teaching, and supervise PhD students.

Start-up resources and state-of-the-art research infrastructure will be available, within the framework of a campus that fosters very strong interactions between life sciences, basic sciences, informatics and engineering. Salaries and benefits are internationally competitive.

Applications should be submitted through the Internet http://bmisearch-interocept.epfl.ch and should include the following documents in PDF format: curriculum vitae, publication list, brief statement of research and teaching interests, names and addresses (including e-mail) of 3 references. Deadline for applications: **October 31st 2007.**

Further questions can be addressed to:

Professor Pierre J. Magistretti, Co-Director
Brain Mind Institute
School of life sciences, EPFL
pierre.magistretti@epfl.ch

For additional information on EPFL, please consult http://www.epfl.ch and http://sv.epfl.ch/

The EPFL School of life sciences aims for a very strong presence of women amongst its faculty, and qualified female candidates are strongly encouraged to apply.

Science Careers | online @sciencecareers.org

PHYSIOLOGY UCLA
Assistant Professor

The **Department of Physiology** at the **David Geffen School of Medicine at UCLA** invites applications for a tenure track faculty position, preferably at the level of Assistant Professor.

We are especially interested in candidates using molecular physiological approaches such as functional genomics, proteomics, molecular imaging, or systems biology. Areas of departmental strength include molecular biophysics, neuroscience, and cardiovascular research, and candidates in these disciplines are encouraged to apply. However, we will consider applicants in all areas of modern physiology. Areas in which we might hope to expand include renal and respiratory physiology. Candidates are expected to have a strong background in cellular and molecular biology and a demonstrated interest in addressing fundamental physiological problems.

The successful candidate will be expected to develop an independent research program and participate in the teaching mission of the Department.

Interested applicants should email their curriculum vitae, a letter with a statement of research interests and career goals, and the names of three references to **Ms. Debra Moorehead** at **PhysiologySearch@mednet.ucla.edu**. Applicants should also arrange for three letters of reference to be sent to Ms. Moorehead at the same email address.

UCLA is an Affirmative Action/Equal Opportunity Employer. Women and minorities are encouraged to apply.

ASSISTANT/ASSOCIATE PROFESSOR OF BIOCHEMISTRY

The Department of Biochemistry, University of Missouri-Columbia, invites applications for a tenure-track Assistant or Associate Professor position from scientists applying biochemical and molecular approaches to the study of fundamental biological processes related to health and disease. We are particularly interested in individuals that would complement existing research strengths in neurodegenerative diseases, inflammation, radiopharmaceuticals, molecular nutrition, diabetes/cardiovascular disease, and cancer. The University is noted for interdisciplinary research programs including a multidisciplinary Life Sciences Center, a NIH-supported Imaging Center that complements a productive institutional nuclear reactor and a new International Institute for Nano and Molecular Medicine. Position qualifications include a Ph.D. and/or M.D. in biochemistry or a related field and postdoctoral experience. Successful applicant will develop or continue an outstanding research program and contribute to Departmental teaching activities.

Submit a curriculum vitae and descriptions of current and planned research activities, and have three letters of reference sent to:

Chair Biochemistry Search Committee
Department of Biochemistry
117 Schweitzer Hall
University of Missouri-Columbia
Columbia, MO 65211

Electronic submission to **biochemsearch@missouri.edu** is encouraged. Review of applications will begin **October 31, 2007**.

MU is an EEO/AA/ADA Employer, and encourages applications from women and minorities. For ADA accommodations, please contact our ADA Coordinator at (573) 884-7278 (V/TTY).

UNIVERSITY OF KANSAS MEDICAL CENTER

ASSISTANT/ASSOCIATE PROFESSOR – MOLECULAR BIOTECHNOLOGY

The Department of Clinical Laboratory Sciences at the KU Medical Center invites applications for a full-time tenure-track 12 month appointment (rank commensurate with experience). Candidates must have a Ph.D. (or equivalent degree) in a molecular life science, postdoctoral experience, demonstrated excellence in research, and be committed to quality graduate education.

The successful applicant will have the opportunity to collaborate with faculty in the many interdisciplinary programs at KU Medical Center (www.kumc.edu), and will be expected to maintain an externally-funded research program that utilizes molecular biological/biotechnology approaches. The area of research specialty is open, but individuals with interests relevant to human health and/or disease states are encouraged to apply. Teaching responsibilities will include graduate courses in molecular biology/biotechnology, and academic teaching experience is preferred.

Information about the CLS Department and its programs is available at www.cls.kumc.edu and www.biotech.kumc.edu.

TO APPLY

Visit position J0030505 at http://jobs.kumc.edu to apply and to view the complete position description. Besides completing the on-line application, please send a statement of research interests, statement of teaching interests and philosophy, up to three reprints and three letters of reference to Dr. Eric Elsinghorst, Mail Stop 4048, 3901 Rainbow Blvd., Kansas City, KS 66160. Review of applications begins November 26, 2007, and will continue until the position is filled. KU is an EO/AA Employer.

KU THE UNIVERSITY OF KANSAS Medical Center

Department of Physiology
Tenure Track Faculty Positions

The Department of Physiology at The University of Texas Health Science Center at San Antonio (UTHSCSA) is continuing its major expansion. This year we seek to hire two tenure track faculty to begin by August 2008. The intention is to hire Assistant Professors, but exceptional candidates at more senior levels will be considered. At present, the Department of Physiology has clusters of research strength in neuroscience, cardiovascular function, ion channel biophysics, and the molecular biology of aging. Although candidates that can extend or bridge these areas are encouraged to apply, we are most interested in talented investigators using cutting edge techniques and/or model systems to elucidate fundamental physiological mechanisms at the molecular, cellular, or integrative levels. Candidates will be expected to contribute to the teaching mission that includes training medical, dental, and graduate students.

UTHSCSA is a Tier 1 Research Institution. Plans and resources are in place to continue to grow both the University as a whole and the Department of Physiology in particular. Competitive start-up packages and ample resources will be offered to those selected to be a part of this exciting endeavor. UTHSCSA is located in the Northwest section of San Antonio and sits as a gateway to the picturesque Texas Hill Country. San Antonio is a vibrant, dynamic, and multicultural city with much to offer including an attractive cost-of-living.

Candidates should submit a Curriculum Vitae as well as a description of research accomplishments/goals (not to exceed two pages) as a single PDF to:

David S. Weiss, Ph.D., Professor and Chair
Department of Physiology
E-Mail: PhysioSearch@uthscsa.edu
Website: www.physiology.uthscsa.edu

Also, arrange for three letters of recommendation to be forwarded to the above e-mail address. Candidates who wish to be considered for this position should ensure that their applications are complete by **November 30, 2007**.

All faculty appointments are designated as security sensitive positions. The University of Texas Health Science Center at San Antonio is an Equal Employment Opportunity/Affirmative Action Employer.

Department of Health and Human Services
National Institutes of Health
Office of the Director
Office of Biotechnology Activities
Office of Science Policy

INTERESTED IN THE NATIONAL SECURITY IMPLICATIONS OF LIFE SCIENCE RESEARCH?

JOIN A FEDERAL INITIATIVE TO ADDRESS RESEARCH WITH "DUAL USE" POTENTIAL

The National Institutes of Health (NIH) Office of Biotechnology Activities (OBA) is seeking exceptional candidates for several analytical and management positions within a program looking at the biosecurity implications of life sciences research. OBA is located within the Office of Science Policy, a component of the Office of the Director, National Institutes of Health (NIH). OBA is the focal point within the U.S. Department of Health and Human Services (DHHS) for addressing the scientific, clinical, safety, ethical, legal, and societal impacts of pioneering biologic research programs. This includes policy issues in recombinant DNA and gene transfer research, clinical research, genetics, biosafety, and dual use life sciences research. In this context, dual use research is life sciences research with legitimate scientific purpose that may also be misused to pose a biologic threat to public health and/or national security.

OBA s activities regarding dual use research include: (1) providing executive, analytic, and administrative support to the National Science Advisory Board for Biosecurity (NSABB), a federal advisory committee providing policy recommendations in this arena; (2) coordinating the development of dual use research policies within DHHS and across the US government; (3) soliciting broad-based input from government, industry, academic institutions, and the public at-large regarding developing policies for the oversight of dual use research; (4) identifying unresolved and emerging issues raised by the conduct and oversight of dual use research and recommending appropriate strategies to address these issues; (5) advising the Director, NIH; the Secretary, DHHS; and the heads of other federal departments and agencies that support or conduct life sciences research on dual use research policies; (6) representing the NIH and/or DHHS and/or US government in dual use research-related activities; and (7) fostering awareness of the dual use issue and the development of sound policies at the international level. Additional information on the NSABB and the dual use research program can be found at **http://www.biosecurityboard.gov.**

The incumbent of this position serves under the direction of the Executive Director to the NSABB. As such, the incumbent provides scientific administrative support to the NSABB in fulfilling its role of advising the HHS Secretary and the NIH Director on specific strategies for the efficient and effective oversight of dual-use biological research, taking into consideration both national security concerns and the needs of the research community. The incumbent provides expertise in one or more of the following areas of specialization: molecular biology, virology, health science, biosafety, and/or clinical medicine.

Researches, reviews, and analyzes data and collaborates with the Executive Director in developing criteria for identifying dual-use research and research results. Provides policy expertise to the Executive Director, NSABB, in advising the Secretary and NIH Director on the development and/or revision of national policies regarding the conduct of dual-use biological research. This includes, but is not limited to, strategies for addressing national security concerns as well as for fostering continued rapid progress in public health research (e.g., new diagnostics, treatments, vaccines, and other prophylactic measures, and detection methods).

Salary is commensurate with experience and includes a full benefits package. A detailed vacancy announcement with the mandatory qualifications and application procedures can be obtained in **USAJOBS** at **www.usajobs.gov (announcement number OD-07-202635-DE)** and the NIH web site at **http://jobs.nih.gov**. Applications must be received by midnight eastern standard time **on closing date indicated in order to be considered**. Questions on the application procedures maybe addressed to **Felicia Royster on 301-496-3531.**

DHHS and NIH are Equal Opportunity Employers

INTEGRATIVE ANIMAL BEHAVIOR
Vassar College

The Department of Biology at Vassar College invites applications for a tenure-track faculty position at the level of assistant professor beginning Fall 2008. Vassar College is an equal opportunity/affirmative action employer and is strongly and actively committed to diversity within its community. We seek a broadly trained integrative biologist whose research and teaching interests may include but need not be limited to animal behavior, behavioral genetics, behavioral ecology, evolution, neurophysiology, sensory biology, or computational biology. The ideal candidate will demonstrate the ability to span several levels of biological organization in their teaching and research. The successful candidate will be expected to develop an upper-level course in his/her specialty as well as teach at the intermediate and introductory levels. There is an opportunity to teach in the interdepartmental program of Neuroscience and Behavior. Development of a productive research program with student participation will be expected and start-up funding and personal laboratory space will be provided. A Ph.D. is required and postdoctoral experience is preferred. Applicants should submit a curriculum vitae, representative reprints, a statement of research interests and goals, a statement of teaching interests and philosophy, and three letters of reference. To apply please visit **https://employment.vassar.edu/**. Referees should send reference letters directly to **behaviorbiology@vassar.edu**. Website: **http://biology.vassar.edu/**. Consideration of applications will begin on **15 October 2007**.

Department of Health and Human Services
National Institutes of Health
Office of the Director
Office of Biotechnology Activities
Office of Science Policy

INTERESTED IN THE SCIENTIFIC, SAFETY, AND ETHICAL IMPLICATIONS OF CUTTING EDGE CLINICAL RESEARCH?

JOIN A TEAM ADVANCING SCIENTIFIC UNDERSTANDING ABOUT HUMAN GENE TRANSFER RESEARCH

The National Institutes of Health (NIH) Office of Biotechnology Activities (OBA) is seeking applications from exceptional candidates for the position of **Medical Officer**. OBA is located within the Office of Science Policy, which is a component of the Office of the Director, NIH in Bethesda, Maryland. OBA is the focal point within the U.S. Department of Health and Human Services (DHHS) for addressing the scientific, clinical, safety, ethical, legal, and societal impacts of pioneering biologic research programs. This includes policy issues in recombinant DNA and gene transfer research, clinical research, genetics, biosafety, and biosecurity and dual use life sciences research.

As part of addressing these policy issues, NIH OBA currently provides analytical, administrative, and executive secretariat functions for the NIH Recombinant DNA Advisory Committee (RAC), which recommends policies and biosafety guidelines concerning basic and clinical research involving recombinant DNA and focuses particular attention on human gene transfer research.

As a member of the team supporting the activities of the RAC, the incumbent in this position provides expert clinical advice and analysis, especially with regard to clinical trials that involve the transfer of recombinant DNA to humans. Responsibilities include analyzing practices and policies applicable to the conduct of recombinant DNA and gene transfer clinical research activities, conducting in-depth analyses of a wide range of recommendations developed by a national advisory committee and identifying human gene transfer experiments deserving of public discussion by the RAC.

Candidates are required to have Doctor of Medicine or Doctor of Osteopathy from a school in the United States or Canada approved by a recognized accrediting body. Salary is commensurate with experience and includes a full benefits package. A detailed vacancy announcement with the mandatory qualifications and application procedures can be obtained in **USAJOBS** at **www.usajobs.gov (announcement number OD-07-184675-DE)** and the NIH web site at **http://jobs.nih.gov**. Applications must be received by midnight eastern standard time **on closing date indicated in order to be considered**. Questions on the application procedures maybe addressed to **Felicia Royster on 301-496-3531.**

DHHS and NIH are Equal Opportunity Employers

Science Careers online @sciencecareers.org

POSITIONS OPEN

DEPARTMENT HEAD and PROFESSOR
Department of Plant Sciences
The University of Arizona
Tucson, Arizona

The College of Agriculture and Life Sciences invites applications and nominations for the position of Head of the Department of Plant Sciences and Professor. The Department of Plant Sciences, in addition to serving the agricultural industry of the state of Arizona, has extensive collaborative interactions with faculty in the biological sciences across the University. The Department consists of 40 faculty members who reside on the main campus in Tucson and at several off-campus experimental stations located elsewhere in the state. The Department is also home to the University of Arizona (UA) Campus Herbarium, the largest herbarium in the southwest. Strong innovative, interdisciplinary leadership in an academic environment is being sought to lead the Department in the areas of extension, research, and teaching. The candidate should have established scholarly credentials in an area that could be considered a part of a contemporary interdisciplinary department of plant sciences, including agronomy, biochemistry, botany, controlled environment agriculture, genetics, genomics, horticulture, molecular and cellular biology, plant microbe-interactions, plant-insect interactions, plant physiology or development. The successful candidate will be encouraged to maintain an extension, research, or teaching program.

A Ph.D. is required, preferably in one of the above fields or areas of study. Strong evidence of managerial and leadership abilities, the capacity to articulate a vision for the Department, and a strong appreciation for diversity and for the land-grant mission are essential.

Applicants should submit an online application by November 1, 2007, and attach a current curriculum vitae, the names, addresses (including e-mail), telephone numbers of six references, and a statement of qualifications and goals for job number 39057 to the UA Human Resources at **website: http://www.hr.arizona.edu.**

This appointment will be available 1 July 2008.

The University of Arizona is an Equal Employment Opportunity/Affirmation Action Employer. Women and minorities are especially encouraged to apply.

ASSISTANT/ASSOCIATE/FULL PROFESSOR
(Quantitative Ecologist/Tenure-Track)
Department of Biological Sciences

The Department of Biological Sciences at Louisiana State University invites applications for an Assistant/Associate/Full Professor (quantitative ecology/tenure-track) position. Required qualifications: Ph.D. or equivalent in a biological science or related field; teaching abilities that can augment new directives to increase the quantitative skills (e.g., quantitative theory, modeling, experimental design, statistics) of our graduate and undergra duate students. Additional qualifications desired: postdoctoral experience. Responsibilities: develops a strong, competitively funded research program in ecology, at any level of biological organization (e.g., population, community, ecosystem). For additional information visit our departmental **website: http://www.biology.lsu.edu.** We encourage applications from women and minorities. An offer of employment is contingent on a satisfactory pre-employment background check. Application deadline is November 1, 2007, or until a candidate is selected. Send curriculum vitae (including e-mail address), statements of research and teaching interests, three letters of recommendation, and no more than three representative publications to:

Dr. Kyle Harms
Chair of Quantitative Ecologist Search
Department of Biological Sciences
202 Life Sciences Building
Louisiana State University
Reference #025301
Baton Rouge, LA 70803

LSU is an Equal Opportunity/Equal Access Employer.

POSITIONS OPEN

INSTITUT PASTEUR

POSTDOCTORAL FELLOWSHIPS
Institut Pasteur, Paris, France

Founded in 1887 by Louis Pasteur and located in the heart of Paris, the Institut Pasteur is a world-renowned private research organization. The Pasteur Foundation of New York is seeking outstanding fellowship applicants. Candidates may apply to any laboratory within 10 Departments: Cell Biology and Infection, Developmental Biology, Genomes and Genetics, Immunology, Infection and Epidemiology, Microbiology, Neuroscience, Parasitology and Mycology, Structural Biology and Chemistry, and Virology. See website for details. Annual package is $70,000 for three years. This is a biannual call for applicants; see website for deadlines. *U.S. citizenship required.*

E-mail: pasteurus@aol.com. Website: http://www.pasteurfoundation.org.

CHEMICAL ENGINEER
Focusing on Environmental Issues

The Center for Environmental Sciences and Engineering and the Chemical Engineering Program of the Department of Chemical, Materials, and Biomolecular Engineering at the University of Connecticut invite applications for tenure-track positions in chemical engineering, with a focus on environmental research, especially in the areas of air and water pollution, bioenergy, or green engineering. Qualified candidates will be considered at the rank of **ASSISTANT or ASSOCIATE PROFESSOR.** The successful candidate will have a Ph.D. in chemical engineering or a closely related field, and is expected to establish and maintain vigorous independent research programs in environmental sciences and engineering, collaborate in multidisciplinary environmental research initiatives, and teach at the undergraduate and graduate levels in the Chemical Engineering Program. Salary and rank will be commensurate with qualifications.

Candidates should submit curriculum vitae, a description of research plans of less than five pages, a one-page teaching statement, and arrange for three letters of recommendation to be sent to: **Center for Environmental Sciences and Engineering/Chemical Engineering Faculty Search, Chemical, Materials and Biomolecular Engineering, University of Connecticut, 191 Auditorium Road, Storrs, CT 06269-3222.** Review of applications will start on October 1, 2007, and continue until the positions are filled.

At the University of Connecticut, our drive to excel includes a commitment to building a culturally diverse community. *We encourage members of underrepresented groups, including minorities, women, and people with disabilities, to apply.*

POSTDOCTORAL POSITION. A Postdoctoral position funded by the National Institutes of Health is available, to study the roles of insulin, nitric oxide, and protein tyrosine phosphatases in regulation of vascular smooth muscle cell signaling and neointima formation in vascular injury. Our projects address important basic science questions and also have relevance to clinical problems. Experience in molecular biology and a good command of the English language are essential. Competitive salary is offered. Please send curriculum vitae and the names of three references to: **Dr. Aviv Hassid, Department of Physiology, University of Tennessee, 894 Union Avenue, Memphis, TN 38163. E-mail: ahassid@tennessee.edu; fax: 901-448-7126.** *The University of Tennessee is an Equal Employment Opportunity/Affirmative Action Title VI/Title IX/Section 504/ADA/ADEA Institution in the provision of its education and employment programs and services.*

POSITIONS OPEN

BUCKNELL
Biology

The Biology Department at Bucknell University invites applications for two entry-level tenure-track **ASSISTANT PROFESSOR** positions to begin August 2008.

The successful candidates will teach introductory courses for majors or nonmajors and upper-level courses in their area of specialty. The successful candidate is expected to establish a research program that involves talented undergraduates and attracts extramural funding. Ph.D. or all-but-dissertation, evidence of teaching effectiveness, and a strong research record are required. Postdoctoral experience is preferred.

We are seeking a broadly trained **ORGANISMAL, ECOLOGICAL, or EVOLUTIONARY BIOLOGIST.** We especially welcome applicants who can contribute to the interdisciplinary programs of neuroscience, animal behavior, or environmental studies, but all research areas will be considered.

We are also seeking a broadly trained **CELL or MOLECULAR BIOLOGIST.** Applications from candidates with expertise in any cell or molecular biology discipline will be considered; areas of particular interest that would complement existing strengths in the Department are neurobiology, immunology, or signal transduction.

Bucknell University is a premier liberal arts university with a long-standing tradition of excellence in the sciences. Startup funds and internal funding for research are available. Institutional support for faculty research includes shared facilities for tissue culture, confocal and scanning electron microscopy. Faculty members typically teach one course and two laboratories, or the equivalent, each semester.

To apply, please refer to **website: http://www.bucknell.edu/jobs.** Review of applications will begin on October 15, 2007. The search will remain open until the position is filled.

Bucknell University values a diverse college community and is committed to excellence through diversity in its faculty, staff, and students. An Equal Opportunity/Affirmative Action Employer, Bucknell University especially welcomes applications from women and minority candidates.

ASSISTANT or ASSOCIATE PROFESSOR
(Toxicology)
Department of Pharmaceutical Sciences
University of Maryland School of Pharmacy

The Department of Pharmaceutical Sciences is seeking outstanding **BIOMEDICAL SCIENTISTS** for a tenure-track or tenured position at the level of Assistant or Associate Professorship with an anticipated start date of summer 2008. The candidate will have current research expertise in the broad area of toxicology and pharmacology with a strong record of recent accomplishments as a postdoctoral fellow or sustained productivity as an established faculty member. Preference will be given to those with the potential for interactions with current research programs in the Department of Pharmaceutical Sciences. Expertise in translational research is particularly welcome. Successful applicants are expected to establish an extramurally funded research program or to have an established program in place.

Applicants should have a Ph.D. or equivalent terminal degree in toxicology, pharmacology, or related field, as participation in the teaching of both Pharm.D. and Ph.D. students is required. Interested individuals should submit a letter of intent, curriculum vitae, statement of research and teaching philosophy, and addresses of three references to **Dr. H. Wang, Chair of Toxicology Search Committee,** at **e-mail: hwang@rx.umaryland.edu** or mail to: **Department of Pharmaceutical Sciences, University of Maryland School of Pharmacy, 20 Penn Street, Baltimore, MD 21201-1180.** For additional information, please visit our **website: http://www.pharmacy.umaryland.edu.** Review of applications will begin on December 2, 2007, and will continue until the position is filled. *The University of Maryland is an Affirmative Action/Equal Opportunity/ADA Employer. Minorities and women are encouraged to apply.*

Nanobiotechnology
Tenure-Track Faculty Position

The University of Maryland Biotechnology Institute (UMBI) and University of Maryland College Park (UMCP) invite applications for a tenure track position at the level of Assistant Professor. UMBI and UMCP have initiated a new multi-disciplinary program that combines Biosciences and Engineering Faculty from the Center for Biosystems Research (CBR: **http://www.umbi.umd.edu/CBR**) and the Fischell Department of Bioengineering (UMCP-BioE: **http://www.bioe.umd.edu/**) to address emerging topics in nanobiotechnology. This position will be a joint appointment between UMBI-CBR and UMCP-BioE and will be located at College Park. The successful applicant will benefit from existing strengths in nanobiotechnology and pathobiology at UMBI-CBR, and cellular and tissue engineering, biomaterials/BioMEMS, synthetic biology, biomechanics and drug delivery at UMCP-BioE.

The successful applicant will have demonstrated exceptional accomplishments and promise in a research and teaching area that integrates biology with nanoscale engineering. Examples include but are not limited to: the use of biological components or systems for harvesting solar or chemical energy; the application of molecular motors for signaling and transduction; the synthesis and characterization of self-assembling biological structures for novel functions; the interfacing of biological molecules or assemblies to devices; and the development of hybrid nano-bio structures for imaging and drug delivery. The investigator is expected to build a competitively funded research group within the setting of an interdisciplinary research institute located in the Washington D.C./Baltimore metropolitan area. For full consideration submit a brief description of your research, curriculum vitae and summary of future research plans (all in pdf format) and arrange for three letters of recommendation to be sent to:

Faculty Search Committee – Position # 300893
cbrsrch@umbi.umd.edu

Review of applications will begin **November 16, 2007** and continue until the position is filled. For additional information please see (**http://www.umbi.umd.edu/index.php/cbr-job-opportunities**).

UMBI is committed to Affirmative Action and Equal Opportunity Employment. As required by the 1986 Immigration Act, applicants should be prepared to present acceptable documentation showing their identities, their U.S. citizenship or alien status, and their authorization to work in the United States.

Neuroscientist
University of Wyoming

The Department of Zoology and Physiology and the Graduate Neuroscience Program at the University of Wyoming invites applications for a full-time, nine-month, tenure-track **Assistant Professor FACULTY POSITION**, starting August 2008. Area of research is open but applicants who complement existing strengths in the Neuroscience Program, which include sensory neurophysiology, neuronal plasticity, neuroendocrinology, and neuropharmacology are especially encouraged to apply. The successful candidate must have a PhD or equivalent, post-doctoral experience and evidence of research productivity. Teaching responsibilities will include a graduate level functional neuroanatomy course. S/he will be expected to develop an externally funded research program and participate in the Graduate Neuroscience Program and the NIH funded Neuroscience Center of Biomedical Research Excellence. The successful applicant will have access to outstanding Microscopy and Macromolecular Analytic Facilities. A competitive start-up package is available.

Interested applicants should send a curriculum vitae, a statement of research and teaching experience, three publications, and three letters of recommendation to:

Neuroscience Search Committee
Dept 3166
1000 E University Avenue
Laramie, WY 82071

Fax: **307-766-5625**
Website: **http://www.uwyo.edu/NeuroScience** and **http://uwyo.edu/Zoology**;
Email: **zprequest@uwyo.edu**

Review of applications will begin in **December 2007**.

The University is a Carnegie Foundation Research/Doctoral Extensive Institution, and is an AA/EEO Employer.

Appalachian STATE UNIVERSITY

FOUNDING DIRECTOR
Research Institute for Environment, Energy, and Economics
(Search Continues)

Appalachian State University invites applications and nominations for the position of **Founding Director of the Research Institute for Environment, Energy, and Economics,** with a starting date as early as 1 July 2008. The Founding Director will report to the Provost, and work with various constituencies in all colleges and schools at Appalachian. Qualifications for this position include:

- Significant academic and research credentials in one or more of the Institute's core areas or in a closely related discipline.
- Senior-level administrative experience, preferably in an academic setting or research center or institute.
- Success in managing research by multidisciplinary teams in the relevant areas.
- Significant track record of external funding from state, federal and private sources for research in environment, energy, and/or economics. Success in assisting others to secure funding for multidisciplinary research.
- Effective interaction with public, political and academic audiences.

Appalachian faculty have built a reputation for solid basic and applied research, education, and public programming in environment, energy, and economics. In addition, Appalachian offers related graduate programs in biology, physics, public administration, and technology, and undergraduate programs in chemistry, economics, geology, sustainable development, appropriate technology, and building science. The University is committed to strengthening these areas of excellence by developing the Research Institute for Environment, Energy, and Economics to encourage and coordinate basic and applied research, emphasize the University's commitment to energy and environmental studies, and facilitate educational and community outreach programs. With a formal focus on environment, energy, and economics, the Institute will facilitate research that brings together faculty and students whose interests lie at the intersections between and among these areas.

Appalachian State University (**www.appstate.edu**) is a member institution of the University of North Carolina System. Located in Boone, North Carolina, Appalachian has approximately 15,000 students in undergraduate and graduate programs at the Boone campus and several distance education sites. Information about the proposed Institute and about University activities in energy and the environment is available at **www.web.appstate.edu/research/**.

Applicants are invited to send a letter of application, a current c.v., and contact information of five references. Completed applications in pdf or paper should be sent to **resdirector@appstate.edu** with **"Institute Director Search"** in the subject line, or to **Institute Director Search, Cratis D. Williams Graduate School, Appalachian State University, Box 32068, Boone, NC 28608.** Application review begins **November 1, 2007**, continuing until the position is filled.

Appalachian State University is an Equal Opportunity Employer. Women and minorities are strongly encouraged to apply.

Science Careers | online @sciencecareers.org

POSITIONS OPEN

The Department of Environmental Sciences at the University of Toledo invites applications for a tenure-track position at the **ASSISTANT PROFESSOR** level in earth surface processes to complement existing University and departmental strengths in ecology, hydrology, geology, geography, and environmental engineering. Competitive candidates must have a Ph.D. in the geosciences or a closely related field; postdoctoral experience is desirable. The successful candidate will be expected to provide instruction at the introductory level for nonmajors as well as for the undergraduate and graduate programs in geology and environmental science.

Our Department is a rapidly growing, multidisciplinary, research-oriented academic unit with 23 tenured/tenure-track full-time faculty. The primary research focus envisioned for the candidate is on physical interactions at the land-lake-air interfaces, with application to the Lake Erie Basin. Applicants should have expertise in the application and utilization of remote sensing and computerized geospatial analysis in their research. Research opportunities are particularly promising in the western Lake Erie basin, where the confluence of an intensively used agro-urban watershed and an economically and ecologically critical water body produce an ideal natural laboratory for environmental research. This person will be expected to develop an externally funded research program as well as collaborate with colleagues in ongoing large scale, multidisciplinary research projects including watershed investigations, remediation, and wetlands restoration.

It is anticipated that this position will begin in mid August 2008. Review of applications will begin October 19, 2007, and continue until the position is filled. Salary, fringe benefits, and startup funds are competitive. Applicants should submit curriculum vitae, descriptions of teaching and research interests, and the names and addresses of three references to: **Alison Spongberg, Chair, Search Committee, Earth Surface Processes, Department of Environmental Sciences, Mail Stop #604, University of Toledo, Toledo, OH 43606-3390.** *The University of Toledo is an Equal Opportunity, Equal Access, Affirmative Action Employer and Educator. Minorities/Females/Veterans/Persons with Disabilities are encouraged to apply.* For more information visit the departmental **website: http://www.eeescience.utoledo.edu.**

FACULTY POSITION at MIT
Department of Biology

The Massachusetts Institute of Technology Department of Biology is seeking an outstanding Scientist for a tenure-track position as an **ASSISTANT PROFESSOR.** We are interested in candidates with important research contributions, the ability to develop a significant and independent research program, and a commitment to excellence in undergraduate and graduate education.

The applicant's research program should involve the study of cells, organisms or the interactions among them. Areas of interest include, but are not limited to, cell biology, developmental biology, immunology, evolutionary biology and mammalian biology, including stem cells, aging, and disease.

We require that applicants submit curriculum vitae, summary of current and proposed research programs, and three letters of recommendation online at **website: http://www.academicjobsonline.org.**

Consideration of completed applications will begin on November 1, 2007.

We request that your letters of reference be submitted by the reviewers online via **website: academicjobsonline.org.** Alternatively, they may be submitted as PDF attachments emailed to **e-mail: lucasm@mit.edu** or as paper copies mailed to:

Biology Search Committee
Attn: Dr. Lenny Guarente
MIT Room 68-132
77 Massachusetts Avenue
Cambridge, MA 02139

MIT is an Affirmative Action/Equal Opportunity Employer. Qualified women and minority candidates are especially encouraged to apply.

POSITIONS OPEN

Washington University in St. Louis
SCHOOL OF MEDICINE

FACULTY POSITION in DEPARTMENT of CELL BIOLOGY and PHYSIOLOGY
Molecular Oncology Program

The Department of Cell Biology and Physiology at Washington University School of Medicine invites applications for a tenure-track appointment at the rank of **ASSISTANT PROFESSOR.** The successful candidate will join the Molecular Oncology Program, a joint program between the Departments of Cell Biology and Internal Medicine at Washington University School of Medicine. The Molecular Oncology Program is comprised of a vibrant group of interactive investigators studying cell cycle control, checkpoint control, cell death, G-protein signaling, telomere biology, HIV pathogenesis, metastasis, oncogenes, and tumor suppressors. Outstanding individuals investigating fundamental problems in molecular oncology are encouraged to apply. Candidates must demonstrate the ability to develop an independent research program and a commitment to excellence in graduate education. Applicants must have a Ph.D. and/or M.D. and postdoctoral experience. Please send curriculum vitae, a summary of current and proposed research programs, and arrange for three letters of recommendation to be sent to:

Drs. Helen Piwnica-Worms and Kendall J. Blumer, Co-Chairs
Cell Biology and Physiology Search Committee
Washington University School of Medicine
660 South Euclid Avenue - Campus Box 8228
St. Louis, MO 63110
E-mail: facultysearch@cellbiology.wustl.edu

Applications should be received by February 1, 2008. *Washington University is committed to increasing representation of women and members of minority groups on its faculty and particularly encourages applications from such candidates.*

BIO-ORGANIC CHEMIST. The Williams College Chemistry Department invites application for a tenure-track position at the **ASSISTANT PROFESSOR** level for fall 2008. Senior appointment possible in exceptional circumstances. Initial teaching assignment, depending upon the successful candidate's subspecialty, will include two courses from: sophomore-level organic chemistry, enzyme kinetics and reaction mechanisms, biochemistry, and a course for nonscience majors. A semester teaching load normally includes complete responsibility for one course and two laboratory sections, and supervision of student research projects. Candidates should have the Ph.D. or completed dissertation by September 2008 (postdoctoral experience is preferred). The successful candidate must have a strong commitment both to teaching at the undergraduate level and to developing a productive research program. Williams College is a highly selective, coeducational liberal arts institution of approximately 230 faculty and 2,000 undergraduates, located in northwestern Massachusetts. The Chemistry Department is composed of 12 faculty members and graduates about 25 to 30 majors each year; the Department has excellent facilities for teaching and research. The College is actively working to increase the diversity of its science majors and seeks an individual who can help us meet these goals. Mail resume, undergraduate and graduate transcripts, descriptions of teaching philosophy and research projects for undergraduates, and three letters of recommendation to: **Prof. Enrique Peacock-López, Chair, Department of Chemistry, Williams College, Williamstown, MA 01267,** by November 12, 2007. Electronic applications will not be accepted. For additional information about the Chemistry Department, please visit our **website: http://www.williams.edu/Chemistry.**

Williams College is an Equal Opportunity/Affirmative Action Employer.

POSITIONS OPEN

ASSISTANT PROFESSOR - ECOSYSTEM ECOLOGIST

The Department of Ecology and Evolutionary Biology at the University of Tennessee seeks to fill a tenure-track Assistant Professor position in terrestrial ecosystem ecology to start August 1, 2008. We seek candidates who work on interactions and feedbacks between plants, soil, and soil biota in a global change context. Applicants are sought who (1) will develop strong collaborations with scientists at Oak Ridge National Laboratory and at the University of Tennessee, (2) show evidence of the ability to secure external research funding, and (3) have a demonstrated interest in mentoring undergraduate and graduate students. An earned Ph.D. and refereed publications in a relevant field are required. Teaching will include courses in ecology and advanced courses in the applicant's specialty. Internal applicants are welcome. For more information visit the Department **website: http://eeb.bio.utk.edu.** Candidates should apply to: **Dr. Susan E. Riechert, Department of Ecology and Evolutionary Biology, 569 Dabney Hall, University of Tennessee, Knoxville, TN 37996.** Applicants should send curriculum vitae, statements of research and teaching experience and goals, and arrange for three reference letters to be submitted. Applications will be reviewed beginning October 8, 2007, and will continue until the position is filled. *The University of Tennessee is an Equal Employment Opportunity/Affirmative Action/Title VI/Title IX/Section 504/ADA/ADEA Institution in the provision of its education and employment programs and services. All qualified applicants will receive equal consideration for employment without regard to race, color, national origin, religion, sex, pregnancy, marital status, sexual orientation, age, physical or mental disability, or covered veteran status.*

TWO CHEMISTRY FACULTY POSITIONS
Energy for the Future
Initiative at the University of California, Davis

The University of California (UC), Davis, Department of Chemistry **(website: http://www.chem.ucdavis.edu/)** invites applications for two chemistry faculty positions associated with the UC Davis Energy for the Future Initiative targeting major energy issues facing California and the nation. One position is at the **ASSISTANT PROFESSOR** level, and the other position could be at a tenured rank **(ASSOCIATE or FULL PROFESSOR).** Online applications for these positions are available at **website: http://energy.ucdavis.edu.** This website also provides further information about the Energy for the Future Initiative, which brings a total of fourteen new faculty positions to the campus, including a total of four positions in the Chemistry Department to be filled over a two to three year period.

The search is open to all areas of fundamental chemistry targeting energy science and technology. However, two areas are of special interest: (i) new materials for energy applications, and (ii) bio-inspired, biochemical, and biological approaches to energy generation and utilization. Competitive candidates will bring a strong research program in chemistry relevant to energy, as well as a strong commitment to undergraduate and graduate teaching. A Ph.D. or equivalent degree in chemistry or related disciplines is required. The positions are open until filled; but to assure full consideration, online applications should be submitted no later than October 15, 2007, for a targeted start date of July 1, 2008.

The University of California is an Affirmative Action/Equal Opportunity Employer.

The Department of Pediatrics at the University of Louisville is seeking an **ASSISTANT PROFESSOR** engaged in diabetes or obesity research. Applications are welcome from individuals with excellent publication records in translational or basic science research. The successful applicant will be expected to obtain independent research funding within three years. Candidates with an M.D. and/or Ph.D. will be considered. E-mail **(e-mail: paul.epstein@louisville.edu)** curriculum vitae and names of three references to: **Paul N. Epstein, Professor, Department of Pediatrics, University of Louisville School of Medicine.**

Rat der Eidgenössischen Technischen Hochschulen ETH-Rat | Conseil des écoles polytechniques fédérales CEPF | Consiglio dei politecnici federali CPF | Cussegl da las scolas politecnicas federalas CSPF | Board of the Swiss Federal Institutes of Technology ETH Board

The ETH Board wishes to appoint the

Director of the Paul Scherrer Institute / PSI *(www.psi.ch)*

The Paul Scherrer Institute is a multidisciplinary research centre and one of the world's leading user laboratories. With over 1200 members of staff, this autonomous institution is part of the ETH Domain and focuses on the fields of solid state research and materials sciences, elementary particle physics, energy and environmental research as well as biology and medicine. As a user laboratory, it operates large, complex research facilities such as the Swiss Light Source (SLS), the Swiss Spallation Neutron Source (SINQ) and the 590 MeV proton accelerator. It also develops novel research instruments for the Swiss and international research community.

The Director will be an innovative, charismatic, decisive personality with international experience and excellent academic qualifications in one of the above fields. He or she will take over the operational management of PSI and assume responsibility for its long-term development. The new Director will already have successfully demonstrated leadership qualities as a scientist and head of a large research unit. The successful candidate must be able to take decisions unassisted, create an efficient management culture with no unnecessary hierarchical levels and at the same time proactively integrate the diverse aspects of the institution. The person appointed must have excellent communication skills in dealing with both the general public and the scientific community. Experience in managing a large user facility would be an asset. The successful candidate will qualify for a professorship at the Federal Institute of Technology in Zurich or Lausanne.

Please send your written application with comprehensive curriculum vitae marked "Private and Confidential" by 10 October 2007 to: Dr. Klara Sekanina, ETH Board, Haeldeliweg 15, 8092 Zurich, Switzerland. Your application will be treated in strictest confidence. For further details call +41 44 632 20 64 or e-mail sekanina@ethrat.ch.

University of Louisville Post-doctoral Fellowship in Stem Cell Biology

The Department of Ophthalmology & Visual Sciences at the University of Louisville is one of the leading academic departments of ophthalmology in the nation. It is a major recipient of NIH funding with 22 full-time clinical and basic science faculty. The successful candidate will perform research in a closely mentored program focused on retinal regeneration using bone-marrow derived, as well as ocular-derived stem cells. The primary mentors for this program are Douglas Dean, Ph.D. and Henry J. Kaplan, M.D.

The UofL Post-doctoral Fellowship in Stem Cell Biology is for a two-year commitment. Training and basic research will be complemented by participation in basic science and clinical conferences in the Department of Ophthalmology & Visual Sciences, as well as other disciplines within the University of Louisville Health Sciences Center.

Applicants should be U.S. citizens or permanent residents, and have received their PhD within the past two years. The Fellowship position is available starting in the 2007 - 2008 academic year. For additional information please contact:

Henry J. Kaplan @ 502-852-3716 or via email at hank.kaplan@louisville.edu
or
Douglas Dean @ 502-852-4882 or via email at dcdean01@louisville.edu

UofL Health Care

University of Louisville
Louisville, Kentucky

The University of Louisville is an equal opportunity and affirmative action employer. Women and minorities are strongly encouraged to apply.

PURDUE UNIVERSITY

Department of Biological Sciences Faculty Positions

The Department of Biological Sciences invites applications for faculty positions in the following four areas: (1) Cancer Biology with an emphasis on stem cells or epigenetics, (2) Microbiology with an emphasis on biofuels, (3) Molecular Evolution, and (4) Evolutionary Ecology. We expect to fill academic year appointments at the Assistant Professor level; however appointments at a higher rank will be considered for qualified applicants.

The Department has over 50 faculty members directing research in a wide range of fields from bioinformatics, through molecular and systems levels, to evolutionary biology and ecology. The Department directs a transgenic mouse core facility in conjunction with the Purdue Cancer Center and maintains an animal facility. Further information about the Department is available at **http://www.bio.purdue.edu/**. The University is expanding Life Sciences on campus and as part of this initiative several new buildings have been completed or under construction. These include the Jischke Hall of Biomedical Engineering, the Hockmeyer Hall of Structural Biology, and the Bindley Bioscience Center, which houses shared facilities for image analysis, genomics, quantitative and functional proteomics, and biological instrumentation for systems level analyses. In addition, as part of its strategic plan, the College of Science at Purdue is hiring faculty in several interdisciplinary areas that span multiple departments including Biological Sciences: **http://www.science.purdue.edu/hiring/**.

Successful applicants must have a Ph.D. or equivalent in an appropriate discipline and at least 2 years of postdoctoral experience. We seek applicants with a strong potential for excellence in research, the promise of extramural funding and a commitment to excellence in teaching. Applications must be submitted electronically as a PDF file that includes a detailed curriculum vitae, the names and addresses of three referees, a summary of research interests, and a one-page teaching statement to **Search@bio.purdue.edu**. Inquiries should be directed to: **Faculty Search Committee, Department of Biological Sciences, Purdue University, 915 W. State St., West Lafayette, IN 47907-2054**. Review of applications will begin **October 1, 2007** and continue until the positions are filled.

Purdue University is an Equal Opportunity/Equal Access/Affirmative Action Employer and is committed to building a diverse faculty of excellence.

POSITIONS OPEN

FACULTY POSITION, TOXICOLOGY
The University of Texas at Austin

The Division of Pharmacology and Toxicology in the College of Pharmacy is seeking a tenure-track position at the level of **ASSISTANT or ASSOCIATE PROFESSOR** with an anticipated start date of fall 2008. The successful candidate will be expected to establish a nationally recognized research program focused around current departmental strengths. These areas include apoptosis, breast cancer, mitochondrial and oxidant signaling, reproductive biology, and neuroscience. Qualifications include a Ph.D. (or equivalent doctoral degree), a strong publication record, and excellent communication skills. Preference will be given to individuals with independent research funding and also to individuals with training in pharmacology/toxicology, as participation in the teaching of both Pharm.D. and Ph.D. students is required. A competitive startup package and laboratory space are available. The Division of Pharmacology and Toxicology is a joint participant with the M.D. Anderson Cancer Center in a National Institute of Environmental Health Sciences Environmental Center Grant **(website: http://sciencepark.mdanderson.org/cred/)** and also directs two NIH predoctoral training programs in toxicology and alcoholism. Details of the pharmacology and toxicology educational program, affiliated academic programs and associated research centers, can be found at **website: http://www.utexas.edu/pharmacy/divisions/pharmtox/.** Interested individuals should submit curriculum vitae, a statement of their research plans, and only a list of three references to: **Dr. John H. Richburg, Search Committee Chair, The University of Texas at Austin, PHAR-Pharmacology PHR 5.218, 1 University Station A1915, Austin, TX 78712-0125;** applications may also be sent via e-mail to **e-mail: pharmtox@uts.cc.utexas.edu.** The application deadline is November 15, 2007, but applications will be reviewed until a suitable candidate is selected. *UT-Austin is an Equal Opportunity/Affirmative Action Employer. Qualified women and minorities are encouraged to apply. This is a security sensitive position requiring a criminal background check of the successful applicant.*

ASSISTANT PROFESSOR
The University of Chicago
Department of Chemistry

The Department of Chemistry of the University of Chicago invites applications from outstanding individuals for the position of Assistant Professor of Chemistry. This search is in the areas broadly defined as inorganic, organic, and physical chemistry. Applications must include curriculum vitae, a list of publications, and a succinct outline of research plans, and be supported by three letters of recommendation. Submit materials by mail addressed, as appropriate, to: **Inorganic Search Committee, Organic Search Committee, or Physical Search Committee, Department of Chemistry, Office of the Chairman (Ghj 222), The University of Chicago, 5735 S. Ellis Avenue, Chicago, IL 60637.** Review of completed applications will begin October 1, 2007; to ensure full consideration, all material should be submitted by that date. *University of Chicago is an Affirmative Action/Equal Opportunity Employer.*

FACULTY POSITION
Cancer Biology
Vanderbilt University Medical Center

The Department of Cancer Biology in the School of Medicine at Vanderbilt University is accepting applications for tenure-track faculty positions at the **ASSISTANT or ASSOCIATE PROFESSOR** level for investigators with research interests focused on the tumor microenvironment. Investigators with an interest in transdisciplinary and/or translational cancer research are particularly encouraged to apply. Send curriculum vitae, statement of research interests and future research plans, and contact information for three individuals willing to write letters of recommendation to: **Lynn M. Matrisian, 2220 Pierce Avenue/771 PRB, Nashville TN 37232-6840. Website: http://canbio.vanderbilt.edu/.** *Vanderbilt is an Affirmative Action/Equal Opportunity Institution.*

POSITIONS OPEN

FRED HUTCHINSON CANCER RESEARCH CENTER
A LIFE OF SCIENCE

M.D. or M.D./Ph.D. PHYSICIAN/SCIENTIST or Ph.D. TRANSLATIONAL SCIENTIST
Position Available
Fred Hutchinson Cancer Research Center
Seattle, Washington

The Fred Hutchinson Cancer Research Center (FHCRC) is recruiting a faculty member at the **ASSISTANT, ASSOCIATE, or FULL MEMBER** level with active laboratory research related to breast cancer. Physician/Scientists with strong laboratory research and clinical expertise in a breast cancer-related discipline or Ph.D. candidates with active translational research interests in breast cancer are strongly encouraged to apply. The successful candidate will join the large Breast Cancer Research group within the FHCRC/University of Washington Cancer Consortium; a dynamic cross-disciplinary research team dedicated to improving prevention, detection, diagnosis, prognosis, and treatment of breast cancer. The primary appointment will be in the Clinical Research Division of the FHCRC. If desired, a joint appointment may be made to other divisions at the Center and to the full-time faculty in an appropriate department at the University of Washington.

Interested individuals should forward their curriculum vitae, including a research plan and the names of five references, to: **Suzanne Lentz, Fred Hutchinson Cancer Research Center, 1100 Fairview Avenue N., Mail-Stop: C1-015, P.O. Box 19024, Seattle, WA 98109.** The closing date for applications is November 1, 2007.

The Fred Hutchinson Cancer Research Center is an Affirmative Action, Equal Opportunity Employer. We are dedicated to building a culturally diverse faculty and strongly encourage applications from women, minorities, individuals with disabilities, and covered veterans.

ASSISTANT and/or ASSOCIATE PROFESSOR of HUMAN GENETICS

The Department of Human Genetics at the University of Utah School of Medicine is continuing a new major expansion, recruiting three new investigators over the next three years to build upon existing strengths in human genetics and developmental biology.

We are seeking outstanding applicants at the level of **ASSISTANT and/or ASSOCIATE PROFESSOR** in the broad fields of genetics and functional genomics, including but not limited to human genetics, genetic approaches to complex disease, population genetics, behavioral genetics, regenerative medicine, developmental genetics, and animal models of human disease and development. Our Department has a strong history in human genetics and resources, such as the Utah Population Data Base, that are unique in the world. These resources have created a highly productive and collaborative environment between researchers, clinicians, and the community.

Creative scientists with a record of achievement and commitment to excellence in both research and teaching are encouraged to apply. Successful candidates will receive a substantial startup package and enjoy a stimulating and supportive research environment.

Applicants should submit curriculum vitae, a summary of research plans, relevant reprints and/or preprints, and three letters of reference to:

Dr. Mario R. Capecchi
Co-Chair, Department of Human Genetics
Howard Hughes Medical Institute
University of Utah School of Medicine
15 North 2030 East, Room 2130
Salt Lake City, UT 84112-5330

Application materials, including letters of reference, should be submitted by November 9, 2007.

The University of Utah is an Equal Opportunity/Affirmative Action Employer, encourages nominations and applications from women and minorities, and provides reasonable accommodation to the known disabilities of applicants and employees.

POSITIONS OPEN

INORGANIC CHEMIST. The Williams College Chemistry Department invites applications for a tenure-track position at the **ASSISTANT PROFESSOR** level for fall 2008 in the general area of inorganic chemistry. (Senior appointment possible in exceptional circumstances.) Initial teaching assignment, depending upon the successful candidate's subspecialty, will include two courses from: introductory chemistry, sophomore inorganic and physical chemistry, advanced inorganic/organometallic chemistry, and instrumental methods of analysis. A semester's teaching load normally includes complete responsibility for one course and two laboratory sections, and supervision of student research projects. Candidates should have the Ph.D. or completed dissertation by September 2008 (postdoctoral experience is preferred). The successful candidate must have a strong commitment both to teaching at the undergraduate level and to developing a productive research program. Williams College is a highly selective, coeducational liberal arts institution of approximately 230 faculty and 2,000 undergraduates, located in northwestern Massachusetts. The Chemistry Department is composed of 12 faculty members and graduates about 25 to 30 majors each year; the Department has excellent facilities for teaching and research. The College is actively working to increase the diversity of its science majors and seeks an individual who can help us meet these goals. Mail resume, undergraduate and graduate transcripts, descriptions of teaching philosophy and research projects for undergraduates, and three letters of recommendation to: **Prof. Enrique Peacock-López, Chair, Department of Chemistry, Williams College, Williamstown, MA 01267,** by November 12, 2007. Electronic applications will not be accepted. For additional information about the Chemistry Department, please visit our **website: http://www.williams.edu/Chemistry.**

Williams College is an Equal Opportunity/Affirmative Action Employer.

ACADEMIC POSITIONS OPEN
TENURE-TRACK FACULTY POSITION
at Florida State University Physical Chemistry

The Department of Chemistry and Biochemistry invites applications for a tenure-track ASSISTANT PROFESSOR position in experimental physical chemistry (broadly defined) to begin in fall 2008. Candidates are expected to mount a highly creative interdisciplinary research program that is externally funded, and to contribute to graduate and undergraduate teaching in the Physical Chemistry Program in the Department. Applicants should send curriculum vitae, research plan, a statement of teaching philosophy and interests, and arrange to have three letters of recommendation sent to: **Chair, Physical Chemistry Search Committee, Department of Chemistry and Biochemistry, Florida State University, 95 Chieftain Way, Tallahassee, FL 32306-4390.** Review of applications will begin November 1, 2007, and will continue until the position is filled. *FFSU is an Affirmative Action Equal Opportunity Employer: women, veterans, disabled persons, and members of underrepresented minorities are encouraged to apply.*

NATIONAL UNIVERSITY of SINGAPORE
Department of Chemical and Biomolecular Engineering

The Department of Chemical and Biomolecular Engineering at National University of Singapore invites applications for **TENURE-TRACK FACULTY POSITIONS** at all levels. The Department is one of the largest internationally with excellent in-house infrastructure for experimental and computational research. A Ph.D. in chemical engineering or related areas and a strong research record with excellent publications are required. Please refer to **website: http://www.chbe.nus.edu.sg/** for more information on the areas of interest and for application details. Applicants should send full curriculum vitae (including key publications), a detailed research plan, a statement of teaching interest, and a list of names of at least three references to: **Professor Raj Rajagopalan, Head of Department (attention: Ms. Nancy Chia, e-mail: nancychia@nus.edu.sg).**

Science Careers online @sciencecareers.org

KU THE UNIVERSITY OF KANSAS

ASSISTANT PROFESSOR
Department of Molecular Biosciences

The Department of Molecular Biosciences at the University of Kansas seeks applications from outstanding individuals for a tenure-track ASSISTANT PROFESSOR position in Chemical Biology. Appointment is expected to begin August 18, 2008. Applicants must have a clear interest in studying the function of enzymes at the molecular level using approaches at the interface of chemistry and biology and a doctoral degree (Ph.D., M.D., M.D./Ph.D.) in biological or chemical sciences expected by start date of appointment. For full job announcement visit: **http://www.molecularbiosciences.ku.edu/positions/assistantprof.shtml** Successful candidates will be expected to develop and maintain an active research program and contribute to the teaching and training programs in the department. Interested applicants should send a cover letter, curriculum vitae, statement of planned research and statement of teaching interests and philosophy to the address below. Applicants should also arrange for three letters of reference to be sent directly to the address below. To ensure full consideration, complete applications should be received by November 1st, 2007. The application can be submitted as a single PDF file to **chembiosearch@ku.edu**, or by mail to **Linda Wiley, Administrative Associate, Chemical Biology Search, Dept. Molecular Biosciences, Univ. of Kansas, 1200 Sunnyside Dr., Room 2034, Lawrence, KS 66045-7534**.

For more information about the Department of Molecular Biosciences, consult our website **http://www.molecularbiosciences.ku.edu/**

EO/AA Employer.

Université Claude Bernard Lyon 1

UNIVERSITE CLAUDE BERNARD LYON 1, LYON, FRANCE
Fifty faculty positions in 2008 and in 2009

Université Claude Bernard University Lyon 1 will offer, each year in 2008 and in 2009, about 50 tenure-track positions (associate and full professors) in the following fields: mathematics, physics, chemistry, computer science, mechanical engineering, electronics, biochemistry, biology, pharmaceutical and medical sciences. Applicants are invited to consult our web site **www.univ-lyon1.fr** and to click on "employement". They will find as examples, a short description of the different positions offered in 2007 (click on "the jobs"). Appointees will be selected through national and local scientific committees. Indications on the selection procedure, and the salary ranges can be found on our web site (download the pdf "devenir v2" following the "**faculty members and researchers**" *link)*. The appointed faculty members are expected to establish a successful research program and secure extramural funding. They will be involved in undergraduate and graduate student education and research. The university is one of the largest in France with more than 30 000 students involved in all the domains of science including life science and engineering. It can boast of a very strong and efficient research activity taking place in more than 80 laboratories carrying out cutting-edge research focusing on three main domains : health, material and environmental sciences. Lyon, in the heart of France's second most important region area is the third largest city with 1.2 million people famous for its industrial network, higher education and gastronomy. More information about Lyon can be found in the Higher Education and Research Researcher's Guide **http://www.lyoncampus.org/pagesguide/etab3.htm.** Applications will be accepted early in 2008 for positions opened in september 2008. Inquiries are handled by Email only by Prof. J.F. Mornex, Vice–President in charge of research **mornex@univ-lyon1.fr**

STANFORD UNIVERSITY DEPARTMENT OF CHEMICAL AND SYSTEMS BIOLOGY

The Department of Chemical and Systems Biology at Stanford University School of Medicine invites applications for a tenure-track or tenured position at the **ASSISTANT or ASSOCIATE PROFESSOR** level. We are particularly interested in candidates who have research interests at the interface of biomedical and physical sciences (e.g., chemical biology, quantitative biology, systems biology). Candidates could focus on either specific methodologies (e.g. mass spectroscopic approaches to proteomics) or specific biological problems where chemical and systems-level approaches are particularly well-suited. However, outstanding applicants in any area of signal transduction or cellular regulation are welcome. Stanford offers an outstanding environment for creative interdisciplinary biomedical research. Rank and salary are dependent on the candidate's qualifications. The predominant criterion for appointment in the University Tenure Line is a major commitment to research and teaching.

Candidates should have a Ph.D. and/or M.D. degree and postdoctoral research experience. Stanford University is an equal opportunity employer and is committed to increasing the diversity of its faculty. It welcomes nominations of and applicants from women and minority groups, as well as others who would bring additional dimensions to the university's research, teaching, and clinical missions. Candidates should send curriculum vitae, a description of future research plans and the names of three potential referees by November 16 to:

James Ferrell, Professor and Chair
c/o Jean Kavanagh, FAA
Department of Chemical and Systems Biology
269 Campus Drive, CCSR Bldg Room 3145A
Stanford University School of Medicine
Stanford CA 94305-5174

Department of Health and Human Services
National Institutes of Health
Office of the Director
Office of Biotechnology Activities
Office of Science Policy

INTERESTED IN APPLYING YOUR SCIENTIFIC OR CLINICAL EXPERIENCE TO ENHANCING FEDERAL POLICIES GOVERNING CLINICAL RESEARCH?

JOIN A FEDERAL INITIATIVE TO COORDINATE AND STREAMLINE CLINICAL RESEARCH POLICIES

The National Institutes of Health (NIH) Clinical Research Policy Analysis and Coordination (CRpac) program is recruiting exceptional candidates for several analytical and management positions. The CRpac program is located within the Office of Biotechnology Activities of the Office of Science Policy within the Office of the Director, NIH. The CRpac program staff is responsible for identifying and pursuing opportunities for harmonization, streamlining, and coordination of Federal clinical research policies and will ensure focused attention on NIH efforts in this regard. Among other initiatives, the CRpac program is exploring and developing strategic approaches to 1) harmonizing adverse event reporting requirements, 2) clarifying agency views on the acceptability of IRB models for various types of clinical research activities, 3) coordinating the development of DSMB policies and clarifying their roles and responsibilities, and 4) developing guidance on informed consent processes for those considering participation in clinical research. See our website at **http://crpac.od.nih.gov/** for more information about the CRpac program.

We are recruiting for Health Science Policy Analyst. The incumbent of this position performs senior level scientific program planning, evaluation, and analysis responsibilities in support of this new initiative. In addition, the incumbent is the lead policy analyst and advisor on one of the following new initiatives: centrally-administered versus locally-administered Institutional Review Board (IRBs); harmonization of diverse adverse event reporting requirements to include improving their understanding, compliance, and use; and development of standards for electronic submission of safety data.

Salary is commensurate with experience and includes a full benefits package. A detailed vacancy announcement with the mandatory qualifications and application procedures can be obtained in **USAJOBS** at **www.usajobs.gov (announcement number OD-07-201997-DE)** and the NIH web site at **http://jobs.nih.gov**. Applications must be received by midnight eastern standard time **on closing date indicated in order to be considered**. Questions on the application procedures maybe addressed to **Felicia Royster on 301-496-3531.**

DHHS and NIH are Equal Opportunity Employers

POSITIONS OPEN

BIOLOGY DEPARTMENT
Eukaryotic Developmental/Cell Biology

The Department of Biology seeks applicants for a tenure-track position to begin late August 2008. The successful candidate must have a Ph.D. and must have demonstrated excellence in undergraduate teaching; postdoctoral research experience preferred. Preference will be given to candidates working in animal or fungal systems who can take advantage of existing facilities. This person will teach introductory biology, molecular cell biology, genetics, and electives in area of expertise, and is expected to maintain an active research program that involves undergraduates. Colorado College is committed to increasing the diversity of its community and curriculum. Candidates are encouraged to identify the ways in which they can contribute to that goal. Application deadline is October 14, 2007. To apply send letter of application, curriculum vitae, graduate and undergraduate transcripts, statements of teaching philosophy and research interests, and three letters of reference to: **Dr. Marc Snyder, Department of Biology, Colorado College, 14 E. Cache la Poudre Street, Colorado Springs, CO 80903.** Colorado College is a highly selective national liberal arts college with a unique one-course-at-a-time curriculum. *The College is an Equal Opportunity Employer that does not discriminate on the basis of race, color, age, religion, sex, sexual orientation, national origin, or disability in its educational programs, activities, or employment practices.*

The biology division of the Illinois Institute of Technology invites applications for a **TENURE-TRACK POSITION** in any area at the forefront of modern biology. The exact area is secondary to the quality of the candidate, but Experimentalists who apply molecular, cellular, or biochemical techniques to problems in genomics, proteomics, systems, or synthetic biology are particularly invited to apply. The biology division exists within the Department of Biological, Chemical, and Physical Sciences at IIT, providing a vibrant, highly interdisciplinary environment.

The successful candidate will contribute to teaching of both undergraduates and graduate students, and set up an active research laboratory. An attractive startup package will be provided, but external funding or evidence of near term fundability is crucial.

Send curriculum vitae, separate research and teaching statements, and the names and contact information of three professional references who will be contacted for shortlisted applicants to **e-mail: biology_search@bcps.iit.edu.** For full consideration, packages should arrive by 1 November 2007, although the position will remain open until filled. *Illinois Institute of Technology is an Equal Opportunity, Affirmative Action Employer. Women and minorities are strongly encouraged to apply.*

The Department of Biological Sciences at Wellesley College invites applications for a tenure-track position at the rank of **ASSISTANT PROFESSOR** to begin August 2008. We are seeking a broadly trained **BIOLOGIST** who is strongly committed to excellence in both teaching and research in a liberal arts college environment. The position is open to any field of biology, however, we are interested in candidates in developmental biology, endocrinology, or behavior. The sucessful candidate will teach courses at all levels of the curriculum and develop an active research program that involves undergraduates.

A Ph.D. and postdoctoral experience are required. Applications should incude a cover letter, curriculum vitae, statements of teaching and research interests, and three letters of recommendation.

Materials should be submitted in Word or PDF format to **e-mail: bio07search@wellesley.edu** or mailed to: **Kaye Peterman, Department of Biological Sciences, Wellesley College, Wellesley, MA 02481.** The deadline for receipt of all application materials is October 15, 2007.

POSITIONS OPEN

Oregon State UNIVERSITY | **College of Health and Human Sciences**

FACULTY POSITION in MUSCULOSKELETAL HEALTH

The Department of Nutrition and Exercise Sciences in the College of Health and Human Sciences at Oregon State University invites applications for a tenure-track, nine-month, full-time faculty position in the newly created Center for Healthy Aging Research with the rank of **ASSISTANT or ASSOCIATE PROFESSOR.** The successful applicant will be expected to establish or maintain a competitive research program in one of the following two areas: (1) effects of aging on the cellular and physiological function of bone and/or muscle, or (2) translational research pertaining to human musculoskeletal health and/or physical function in aging. This research should have a mechanistic focus related to diet and/or exercise. The successful applicant will also be expected to teach core undergraduate courses in nutrition or exercise science, and graduate courses in area of expertise. To view a full announcement or to apply, visit **website: http://www.oregonstate.edu/jobs.** Refer to posting #0001434. Application deadline is December 3, 2007. For additional information: **Russell Turner, telephone: 541-737-9545** or **e-mail: russell.turner@oregonstate.edu.** *OSU is an Affirmative Action/Equal Opportunity Employer.*

ASSISTANT PROFESSOR in DEVELOPMENTAL BIOLOGY
University of Missouri at St. Louis

The Department of Biology at University of Missouri at St. Louis invites applications for a tenure-track Assistant Professor position in developmental biology. Applicants with expertise in any aspect of developmental biology will be considered; however, we are particularly interested in applicants who focus on nonmammalian systems and use interdisciplinary approaches, including molecular biology, cell biology, biochemistry, bioinformatics, and functional genomics. The successful candidate will be expected to establish a vigorous, externally funded research program and participate in teaching and advising of both undergraduate and graduate students. Applicants must have a Ph.D. (or equivalent) and postdoctoral experience in an appropriate discipline with evidence of high quality research. Complete applications will include a cover letter, curriculum vitae, a concise outline of research plans, copies of up to five publications, a statement of teaching interests and philosophy, and three letters of reference. Send application documents to **Maryann Hempen (e-mail: hempen@umsl.edu), Department of Biology, University of Missouri at St. Louis, One University Boulevard, St. Louis, MO 63121. Telephone: 314-516-6202; fax: 314-516-6233.** Review of applications will begin October 31, 2007, and will continue until the position is filled. *University of Missouri is an Affirmative Action/Equal Opportunity Employer committed to excellence through diversity.*

A SENIOR RESEARCH TECHNOLOGIST position is immediately available in Cleveland Clinic Foundation. The candidate must have a Bachelor's or higher degree in biological sciences or related field, and very strong background in molecular biology, and extensive experience on genomic DNA cloning and gene mapping. The successful candidate will be required to define the gene structure, design experimental approaches to make transgenic constructs from bacterial artificial chromosome clones. The knowledge and experience on embryonic stem cell culture will be a plus, but not necessary. Interested applicants please submit curriculum vitae and names and contact information of three references to: **Dr. Xiaoxia Li, Department of Immunology, Lerner Research Institute, 9500 Euclid Avenue N.E. 40, Cleveland, OH 44195,** or via **e-mail: lix@ccf.org.**

POSITIONS OPEN

SENIOR FACULTY in CANCER BIOLOGY
Department of Chemistry and Molecular Biology
North Dakota State University

The Department of Chemistry and Molecular Biology **(website: http://www.chem.ndsu.nodak.edu)** is seeking outstanding applicants for a tenure-track senior faculty **(ASSOCIATE PROFESSOR or HIGHER)** position in, but not limited to, cellular processes controlling tumorigenesis.

The Department has excellent modern facilities with an annual research expenditure exceeding $3 million. Since 2001, faculty from the Department have spearheaded a nationally competitive Center of Biomedical Research Excellence **(website: http://www.ndsu.nodak.edu/cobre).** The Center has recently secured five additional years of NIH support and its scientific goals are focused on human health disorders, including cancer and asthma. The Center has state-of-the-art biology and synthetic chemistry core facilities. The candidate is expected to maintain a vigorous NIH-supported research program and participate in the educational mission of the Department by teaching graduate and undergraduate students. The Department offers M.S. and Ph.D. degrees in both chemistry and biochemistry/molecular biology.

The candidate should have a Ph.D. or M.D./Ph.D. degree in chemistry, biochemistry, molecular biology, or a related field. A demonstrated record of a nationally competitive research program in cancer biology or a related field is required. Applicants must be able to communicate effectively in spoken and written English. This position will have a competitive startup package and salary will be commensurate with experience. Review of applications will begin November, 1, 2007, and will continue until filled. Qualified applicants should send a letter of interest, statement of research interests, curriculum vitae and three letters of reference to:

Mukund Sibi, Ph.D.
Department of Chemistry and Molecular Biology
North Dakota State University
1231 Albrecht Boulevard
P.O. Box 5516
Fargo, ND 58105-5516

E-mail inquiries may be sent to **e-mail: rose.nichols@ndsu.edu.**

North Dakota State University is an Equal Opportunity Institution.

POSTDOCTORAL POSITION
Neurophysiology of Visuo-Motor Control

To study synaptic interactions between identified neurons in various visuo-motor coordination pathways during movements to visual targets in cats. The specific question being addressed is how cortex, thalamus, and cerebellum interact to ensure the precise positioning of feet during walking. The activity of single identified neurons in cerebellum, thalamus, and cortex will be analyzed in relation to mechanics of movements and local pharmacological manipulations (microinjections or iontophoresis of synaptically active compounds). Learn more at **website: http://www.beloozerova.com.**

The most important qualifications needed are the demonstrated strong reasoning skills and a passion for experimentation. Experience with electrophysiology is a great plus. Good writing skills, advanced skills in computer applications, and some experience with animal training are also pluses. The ideal candidate will be able to conduct experiments with only limited help from technical personnel, and to produce data and a good draft for at least one publication per year. The position is for one year; it will be renewed based on demonstrated productivity. The successful candidate will be supported to also pursue research in the area of his/her own interest in the field of motor control, and to apply for independent funding.

Send curriculum vitae, names of three references, summary of previous work and research interests to: **Irina Beloozerova, Barrow Neurological Institute, Phoenix, AZ 85013; e-mail: ibelooz@chw.edu.** Applications are reviewed continuously until the position is filled. *Equal Opportunity Employer.*

Post-Doctoral Position
Cellular and Molecular Regulation of Angiogenesis and Vascular Regression

Principal Investigator:
Roberto Nicosia, MD, PhD

Candidate will have up to three years of post-doctoral experience, and a strong background in cell and molecular biology. Desired background includes vascular biology, extracellular matrix biology, and immunology. Position is in the Department of Pathology, University of Washington/VA Medical Center, Seattle, WA

Send your CV and cover letter electronically to:
nicosialab@gmail.com
or by post to:
Eric Fogel
1660 S. Columbian Way
Mailstop S-151
Seattle, WA 98108

ROSALIND FRANKLIN UNIVERSITY
OF MEDICINE AND SCIENCE

Assistant/Associate Professor
Membrane Protein Structural Biology

As part of a University-wide initiative, the Department of Biochemistry and Molecular Biology (BMB) continues to undergo significant expansion and invites applications for a tenure-track Assistant or Associate Professor in the area of membrane protein structural biology. We seek candidates employing cutting-edge biophysical techniques that will provide fundamental insight into the structure-based mechanisms of membrane proteins. **Although preference will be given to candidates using X-ray crystallography, outstanding candidates employing other biophysical approaches are also encouraged to apply.** BMB is a well-funded active department that enjoys strong University commitment to development of membrane protein structural biology. In addition to faculty recruitment in this area, the University commitment includes recent development of the Rosalind Franklin Structural Biology Laboratories (consisting of state-of-the-art facilities for X-ray diffraction, mass spectrometry/proteomics, and electron paramagnetic resonance) and a Biophysical Instrumentation Facility, as well as access to the nearby APS via participation in the SERCAT beamline consortium. Candidates at the Assistant Professor level must have outstanding research potential and a commitment to excellence in teaching, whereas applicants at the Associate Professor level must demonstrate outstanding research accomplishment including national recognition and extramural funding, as well as a track record in graduate training. The successful candidate will receive a highly competitive salary, an attractive start-up package and space, and is expected to develop or maintain an externally funded research program, as well as teach at the medical and graduate school levels. Further information about the department can be viewed at **www.rosalindfranklin.edu/cms/biochem**.

Interested applicants should submit their C.V., a 2 page summary of research interests, copies of representative publications, and the names of at least 3 references to: **Dr. Ronald S. Kaplan, Chair, Dept. of Biochemistry and Molecular Biology, Rosalind Franklin University of Medicine and Science, 3333 Green Bay Rd., North Chicago, IL 60064** or as an attached document to: **ronald.kaplan@rosalindfranklin.edu**. Review of applications will begin immediately and will continue until the position is filled.

Rosalind Franklin University of Medicine and Science is an Equal Opportunity/Affirmative Action Employer.

THE UNIVERSITY *of* TEXAS
HEALTH SCIENCE CENTER AT HOUSTON
A part of The University of Texas Health Science Center at Houston

Microbiology and Molecular Genetics
Tenure-Track Assistant Professor

The Department of Microbiology and Molecular Genetics in the Medical School of the University of Texas Health Science Center - Houston seeks an exceptional scientist for a tenure track position at the Assistant Professor level. Candidates must have a Ph.D. and/or M.D. and several years of postdoctoral experience. Demonstrated excellence in research is more significant than the area of research. The successful candidate will join faculty using diverse microbial systems to study cell biology, regulatory biology, signal transduction, development, and pathogenesis by bacteria, fungi, and viruses. In addition to directing an extramurally funded research program, the successful candidate will be expected to participate in teaching graduate and medical students. The position affords a competitive salary, start-up package, and unparalleled opportunities to interact with basic scientists as well as clinical and translational researchers. New research facilities, including BSL-3 laboratories, will provide significant opportunities for the successful applicant. As part of the Texas Medical Center, departmental faculty collaborate and interact with the other academic and health components including Baylor College of Medicine, M.D. Anderson Cancer Center, Rice University, the Texas A&M Institute of Bioscience and Technology, and the UTHSC-H Institute for Molecular Medicine. The breadth and quality of biomedical science in the Texas Medical Center rivals that of any academic medical center in the world.

Applicants should submit a curriculum vitae, a statement of research interests and plans, and contact information for at least three referees. For full consideration, completed applications should be submitted by **December 15, 2007**. Applications should be directed to: **Samuel Kaplan, Ph.D., Microbiology and Molecular Genetics, The University of Texas Medical School, 6431 Fannin St., MSB 1.206, Houston, TX 77030-1501; E-mail: Lyska.Morrison@uth.tmc.edu.**

The University of Texas Health Science Center at Houston is an EO/AA Employer. M/F/D/V.This position is subject to Texas Education Code § 51.215. A background check will be required for the final candidate. Women and minorities are encouraged to apply.

DEPARTMENT OF THE NAVY
ONR
Science & Technology

PROGRAM OFFICER,
OCEAN COASTAL GEOSCIENCE
(Oceanographer GS-1360)

The Office of Naval Research is seeking a qualified individual to manage sponsored basic/applied research, and advanced development programs and projects in the broad area of ocean coastal geoscience. The sponsored efforts are conducted principally at U.S. universities and industry or Federal laboratories. This is a Federal Civil Service position at the GS-13/14/15 level ($79,397 - $143,471) depending on individual qualifications.

The position requires knowledge and experience in the fundamental theories, concepts, and current state-of-the art research and/or technology development in the area of ocean coastal geoscience, including but not limited to, wave mechanics and prediction, nearshore circulation, boundary layer physics, sediment mechanics, coastal geology, and river dynamics.

For information on qualifications and how to apply, see ONR's Job Announcements at our website http://www.onr.navy.mil/hr. Applications must be submitted by the date noted in the job announcement. For technical information contact us at hrdeptjobs@onr.navy.mil.

U.S. CITIZENSHIP REQUIRED • AN EQUAL OPPORTUNITY EMPLOYER

Science Careers | online @sciencecareers.org

POSITIONS OPEN

PHYSIOLOGICAL ECOLOGIST
University of Arkansas at Little Rock

The Biology Department at the University of Arkansas at Little Rock (UALR) invites applications for a full-time, tenure-track **ASSISTANT PROFESSOR** position (job #389) to begin fall 2008. We seek a Physiological Ecologist who will teach mammalian or comparative physiology, as well as develop advanced courses in his/her area of expertise. The successful candidate must have a strong commitment to teaching and is expected to develop an extramurally funded research program. Applicants must have a Ph.D. in biological science; postdoctoral experience is expected.

The Department of Biology offers both the B.S. and M.S. degrees and participates fully in the applied biosciences and bioinformatics Ph.D. programs. The University of Arkansas at Little Rock is a metropolitan university with a current enrollment of over 11,500 students. Visit **website: http://www.ualr.edu/biology** for more information about the University and the Department.

To apply, submit a letter of application referencing job #389, curriculum vitae, transcripts, statements of research interests and teaching philosophy, and three letters of recommendation to: **Dr. Steve Yanoviak (e-mail: spyanoviak@ualr.edu), Department of Biology, University of Arkansas at Little Rock, 2801 S. University, Little Rock, AR 72204-1099.** Review of applications will begin November 1, 2007, and continue until the position is filled.

The University of Arkansas at Little Rock is an Affirmative Action, Equal Opportunity Employer, and actively seeks the candidacy of qualified minorities, women, and persons with disabilities. Under Arkansas law, all applications are subject to disclosure. Persons hired must have, or be able to obtain, proof of legal authority to work in the United States.

The Department of Biochemistry at Brandeis University invites applications for a tenure-track faculty position at the rank of **ASSISTANT PROFESSOR** beginning fall 2008. We are searching for a creative scientist who will establish a vigorous independent research program and also excel at teaching. The research program should address fundamental biological questions at the molecular level and complement existing Department strengths in analysis of protein structure and function. Research fields of particular interest include nucleic acid biochemistry, chemical biology, and biochemistry of complex systems.

Brandeis University offers the rare combination of an internationally recognized research university in a small college setting. The suburban campus is just 20 minutes from the bustling academic and biotechnology centers of Boston and Cambridge.

Candidates should submit their curriculum vitae, a brief research proposal, and three letters of reference to:

Christopher Miller, Professor of Biochemistry
Brandeis University
MS 013
P.O. Box 549110
Waltham, MA 02454-9110

First consideration will be given to applications received by November 15, 2007.

Brandeis University is an Equal Opportunity Employer, committed to building a culturally diverse intellectual community, and strongly encourages applications from women and minority candidates.

The Division of Public Health Sciences of the Fred Hutchinson Cancer Research Center invites applications from laboratory-based scientists with an interest in molecular diagnostics, including but not limited to aspects of predictive medicine, early detection, diagnosis, treatment response, and risk assessment.

Further information is available at **website: http://www.fhcrc.org/about/jobs/** and selecting job posting identification # KW-21205.

POSITIONS OPEN

DIRECTOR
Institute of Arctic and Alpine Research
University of Colorado, Boulder

The University of Colorado, Boulder, seeks applications for Director of the Institute of Arctic and Alpine Research (INSTAAR). The successful candidate will also be a tenured **PROFESSOR** in an appropriate academic department. INSTAAR research spans geochronology, human and ecosystem ecology, hydrology, glaciology, oceanography, landscape evolution, biogeochemistry, and climate in a range of Quaternary and modern environments. The Institute is connected to seven departments, administers the Mountain Research Station, and maintains ties with federal laboratoriess including the U.S. Geological Survey, National Oceanic and Atmospheric Administration, and National Center for Atmospheric Research. The Director has primary responsibility for INSTAAR's management, and reports to the Vice-Chancellor for Research and Dean of the Graduate School. Applicants should have an outstanding record of scientific achievement and leadership, and be able to balance INSTAAR's management with a vigorous research program and a commitment to graduate education. All correspondence including applications should be sent to **e-mail: aardir@colorado.edu.** Applications should include a letter of interest, current curriculum vitae, and the names of four references. Review of applications will begin on October 22, 2007, and continue until the position is filled. See **website: http://instaar.colorado.edu/director** for more information on this position and INSTAAR.

RANDOLPH-MACON COLLEGE
Biology Department

The Department of Biology invites applications for two tenure-track positions at the rank of **ASSISTANT PROFESSOR** beginning August 2008. The department seeks an **EVOLUTIONARY BIOLOGIST** and an **ECOLOGIST.** The standard teaching load is two lecture/laboratory courses per semester, which is equivalent to a combination of lecture and lecture/laboratory courses that total 24 teaching credit hours. The successful candidates will teach annually in an innovative inquiry-based introductory biology course and will contribute to its ongoing development. They will also be expected to develop upper-level courses in their specialty. Ongoing scholarly activity involving undergraduates is expected. Applicants must have a Ph.D. and be able to demonstrate teaching effectiveness. Review of applications will begin on October 31, 2007, and continue until the positions are filled. Applicants should indicate which position they are applying for and submit: (1) curriculum vitae, (2) a statement of their teaching philosophy and research plans, and (3) three letters of reference. Applications and inquiries to: **Ms. Barb Wirth, Randolph-Macon College, P.O. Box 5005, Ashland, VA 23005.** *Applications are especially encouraged from minorities and women. Randolph-Macon College is an Equal Opportunity Employer.*

The Department of Chemistry at Duke University invites applications for a faculty position at the **ASSISTANT PROFESSOR** level in theoretical chemistry commencing in the fall of 2008. Applicants developing programs with links to the rich interdisciplinary opportunities in the sciences, engineering, and biomedicine at Duke University are particularly encouraged to apply. All candidates should be committed to excellence in education at the undergraduate and graduate levels. Applications received by November 15, 2007, will be given full consideration. To guarantee timely evaluation of applications, all applicants should e-mail full curriculum vitae and a description of proposed research activities (in PDF format) to **e-mail: positions@chem.duke.edu** and should request that three letters of recommendation be submitted electronically to this address. *Duke University is an Affirmative Action/Equal Opportunity Employer and is eager to identify minority candidates and women with appropriate qualifications.*

POSITIONS OPEN

INTERDISCIPLINARY LAND USE/LAND COVER SCIENTIST

Stanford University's School of Earth Sciences and the Woods Institute for Environment jointly seek applications for a tenure-track faculty appointment at either the **ASSISTANT, ASSOCIATE, or FULL PROFESSOR** level in the area of land use and land cover (LU/LC) change. We welcome applications from individuals with research interests in the causes, nature, and consequences of LU/LC change. Research topics could include: evaluating land-use dynamics (e.g. urban growth, agricultural expansion, or intensification); understanding the primary drivers of LU/LC change; understanding and modeling impacts of LU/LC change on biogeochemical or hydrological processes, and their consequences for biological and social systems; and/or forecasting future patterns of LU/LC change. The successful candidate will have strong quantitative and spatial modeling skills; experience integrating field data with geographic information system, and/or remote sensing; the ability to collaborate with a broad range of natural and social scientists; and a strong desire to teach at the graduate and undergraduate levels, in the Department of Environmental Earth System Science and on interdisciplinary topics.

Applications, including curriculum vitae, a statement outlining research and teaching experience and interests, and the names and addresses of four references should be sent in either electronic (PDF only) format or paper.

Submit electronic applications to: **lu-lcsearch@sesmail.stanford.edu,** or if preferred, paper applications to:

Land Use/Land Cover Search Committee
School of Earth Sciences
Mitchell Building #101
Stanford, CA 94305-2215 U.S.A.

Applications received by October 22, 2007, will receive full consideration.

Stanford University is an Equal Opportunity Employer and is committed to increasing the diversity of its faculty. It welcomes nominations of and applications from women and minority groups, as well as others who would bring additional dimensions to the University's research, teaching, and clinical missions.

University of Illinois at Chicago, Department of Chemistry invites applications for a tenure-track position in chemistry. Although preference will be given to a prospective **ASSISTANT PROFESSOR,** applications at higher levels may be considered. While the search is open in terms of research area, candidates who have a demonstrated interdisciplinary approach to chemistry will be preferred. Areas of interest include chemical biology, biological and bioanalytical chemistry, organometallic, materials, and bio-inorganic chemistry. The successful candidate will be expected to carry out a full and vigorous program of innovative research and to contribute to the teaching of graduate and undergraduate students. Please submit applications, including curriculum vitae, list of publications, summary of past research, plans for future research, and letters of reference from three individuals who are familiar with the candidate's work by October 22, 2007, to the: **Chair of the Chemistry Search Committee, Department of Chemistry (M/C 111), The University of Illinois at Chicago, 845 W. Taylor Street, Chicago, Illinois 60607-7061.** Final authorization of this position depends upon availability of state funding. *UIC is an Affirmative Action/Equal Opportunity Employer. Women and minority candidates are strongly encouraged to apply.*

SENIOR SCIENTIST. Quantitative analysis of pharmaceuticals in physiologic buffers and biological matrices. Design/conduct experiments. Analyze, review, interpret data, write reports, and present findings. Write manuscripts and review manuscripts of others. Identify technology problems and find solutions. Initiate new research directions, contracts, and collaborations. Master's degree in pharmaceutical science or related field plus two years of relevant experience. Resume to: **Tamara Spalding, Absorption Systems, 436 Creamery Way 600, Exton, PA 19341.**

Tenure Track Faculty Position Cancer Pharmacology, Drug Discovery, and Biochemistry Sloan-Kettering Institute

Sloan-Kettering Institute is seeking an innovative individual, for a tenure-track position at the Assistant or Associate Member level, with strong research accomplishments in biochemistry, pharmacology, prevention or chemical biology who wishes to address problems of relevance to cancer research or cancer drug discovery and development. Faculty will be eligible to hold graduate school appointments in the Gerstner Sloan-Kettering Graduate School of Biomedical Sciences, the Weill Graduate School of Medical Sciences of Cornell University, as well as the Tri-Institutional MD/PhD Training Program and Tri-Institutional Training Program in Chemical Biology.

MSKCC offers a unique and exciting research environment with programs in Immunology, Pharmacology, Chemistry, Molecular Biology, Informatics, Genetics, Cell Biology, Developmental Biology, Cellular Biochemistry and Structural Biology. The presence of world-renowned clinical programs in cancer research, treatment and prevention offers unique opportunities for creative collaboration.

Applicants should have a Ph.D. or MD degree, postdoctoral experience, and dedication to important problems at the interface of biology, biochemistry and chemistry as they relate to cancer pharmacology.

Candidates should send by November 15, 2007 their curriculum vitae, research objectives and copies of three representative publications to: **molphar@mskcc.org.** Candidates should arrange to have three signed letters of reference sent by E-mail to: molphar@mskcc.org or regular mail to: **David Scheinberg, MD, PhD, c/o Marie Aiello/Box 428, Molecular Pharmacology and Chemistry Program, Memorial Sloan-Kettering Cancer Center, 1275 York Avenue, New York, NY 10021.**

Memorial Sloan-Kettering Cancer Center is an affirmative action, equal opportunity employer.

Memorial Sloan-Kettering Cancer Center
The Best Cancer Care. Anywhere.
www.mskcc.org

TEMPLE UNIVERSITY®

Faculty Positions in Ecology/ Environmental Biology

The Department of Biology at Temple University is expanding its faculty and anticipates adding several new faculty members in the next year. Applications for tenure-track faculty positions at all levels in the general field of Ecology and Environmental Biology are invited. Successful candidates should have a strong publication record and an innovative research program with level-appropriate external funding. Contribution to teaching at both the undergraduate and graduate levels is expected.

Applicants for junior positions with a Ph.D. and postdoctoral experience should send curriculum vitae, a description of research interests, a statement of teaching philosophy, and three letters of reference to: **Dr. Robert Sanders, Search Committee Chair, Department of Biology, Temple University, 1900 N. 12th St., Philadelphia, PA 19122.** Senior applicants should provide curriculum vitae and the names and contact information for references. Review of applications will begin October 15, 2007. Temple University is an equal opportunity, equal access, affirmative action employer committed to achieving a diverse community. AA, EOE, m/f/d/v.

THE OHIO STATE UNIVERSITY

FACULTY POSITION IN BIOCHEMISTRY

The Ohio State University

The Department of Biochemistry at The Ohio State University invites applications for a **Tenure-Track Faculty Position**, preferably at the Assistant Professor level, as part of a multi-year effort to develop excellence in macromolecular structure and function-related research. Consideration will be given to qualified candidates with research interests spanning all areas of biochemical research including chemical and structural biology, mechanistic and metabolic biochemistry, bioinformatics, proteomics, biopolymer folding and assemblyC especially those that complement the research strengths of the department (see http://www.biosci.ohio-state.edu/~biochem).

The candidate should have a Ph.D. degree or its equivalent with a strong background in biochemistry, at least two years of postdoctoral experience, and an established record of accomplishment. A strong commitment to the development of a vigorous and innovative independent research program supported with extramural funds, the integration of teaching and research, and the rigorous training and instruction of graduate and undergraduate students is essential.

Please send a curriculum vitae, a summary of research accomplishments, and a three-page description of future research plans to the **Faculty Search Committee, Department of Biochemistry, The Ohio State University, 484 West 12th Avenue, Columbus, OH 43210.** Candidates should also have three letters of recommendation sent to this address. For full consideration, applications should be received by **November 1, 2007,** but will be accepted until the position is filled.

In its commitment to build a diverse workforce, The Ohio State University encourages applications from minorities, veterans, women and individuals with disabilities. Flexible work options are available. OSU is an Equal Opportunity/Access and Affirmative Action Employer

ANNOUNCEMENTS

CYSTINOSIS RESEARCH FOUNDATION
NATALIE'S WISH

$1.2 Million Available

2007 Autumn Call for Funding Proposals

The Cystinosis Research Foundation's (CRF) ultimate goal is a cure for this disease. Research awards will be given for up to three years. The CRF has over $1.2 million dollars in research funds available. The number of awards and their value will depend on the number of outstanding proposals and the funds available at the time.

- Research Proposal — The CRF is pleased to announce its second 2007 call for research proposals. The CRF is prepared to fund proposals to improve the immediate care of children and young adults with Cystinosis and to develop new understanding and treatment of Cystinosis to help these children.
- Pre- or Post-Doctoral Fellowships — The CRF has established the first pre- or post-doctoral research fellowship program in the United States to encourage young investigators to establish careers in Cystinosis research. Fellows will be funded for one to three years for a maximum of $75,000/year.

For the current funding cycle, proposals and fellowship applications must be received by November 2, 2007. Decisions for funding will be made in January 2008. **For instructions on how to prepare proposals, visit www.natalieswish.org and click on research/grant guidelines.**

Review Process — Proposals are reviewed by a Scientific Review Board comprised of experts on Cystinosis who then advise the CRF on the scientific merit of each proposal. The CRF will balance the eventual funding to support clinical and bench research, and fellowships.

POSITIONS OPEN

The American Chemistry Council (ACC), a national trade association representing the world's leading chemical and plastics manufacturers, currently has an opportunity for a **DIRECTOR** within our Long-Range Research Initiative (LRI) Department in the Washington, DC metro area. This position directs the research management process for the LRI, additionally providing the focal point for the chemical risk assessment/health effects component of the research program. The LRI is a major program of the ACC that sponsors an independent research program ($17 million in 2007) that advances the science of risk assessment of the health effects of chemicals to enhance decision making by government, industry, and the public. The primary duties are to (1) serve as the lead for several Request-for-Proposal (RfP) Teams, which develop and implement RfPs via a competitive process; (2) perform senior-level administrative functions related to resources and research contracts; and (3) provide outreach and communication about the program. To learn minimum qualifications, more details about the position, and application instructions, visit our **website: http://www.americanchemistry.com/jobs.** To learn more about the LRI, please visit **website: http://www.americanchemsitry.com/lri.** ACC offers a salary commensurate with experience and excellent benefits.

POSTDOCTORAL POSITION in the Cell Differentiation and Development Center at Marshall University to study the molecular mechanisms which govern skeletal muscle growth and atrophy. The successful candidate will have Ph.D. and/or M.D., a strong background in physiology and molecular biology, and exceptional oral and written communication skills. Experience with animal models is highly desirable. The candidate will be expected to present research findings at scientific conferences, prepare manuscripts, assist in experimental design, and apply for extramural postdoctoral funding. Salary is nationally competitive and will be commensurate with experience. Please e-mail curriculum vitae and a brief description of career goals, along with names and contact information of three references to: **Eric Blough, Ph.D., Laboratory of Molecular Physiology, 241N Byrd Biotechnology Science Center, 1700 3rd Avenue, Huntington WV 25755 U.S.A.; e-mail: blough@marshall.edu.** *Marshall University is an Equal Opportunity/Affirmative Action Employer.*

COMPUTATIONAL STRUCTURAL BIOLOGY/BIOPHYSICS
Oregon Health & Science University

A **POSTDOCTORAL POSITION** is available for the development of computer methods to fit atomic models to electron microscope reconstructions. It involves the testing of optimization algorithms and development of restraints applicable at low resolution **(website: http://xtal.ohsu.edu).** Test applications to the ribosome will be in collaboration with **Joachim Frank.** Candidates should have experience of software development in computational or experimental structural biology (electron microscopy or x-ray crystallography). E-mail curriculum vitae and contact information for three references to **Michael Chapman** at **e-mail: chapmami@ohsu.edu.**

POSTDOCTORAL POSITIONS
Available at
Sloan-Kettering Institute

Seeking Research Scientists with postdoctoral experience to join a laboratory studying the molecular events underlying normal or leukemic hematopoiesis. Applicants must have interest and expertise in the study of hematopoietic stem cell biology using mouse models and/or in vitro culture techniques. Send a description of your research interests, curriculum vitae, and the names and telephone: numbers of three references to: **Dr. Stephen D. Nimer, Memorial Sloan-Kettering Cancer Center, 1275 York Avenue, P.O. Box 575, New York, NY 10021.**

POSITIONS OPEN

FACULTY POSITION in CELL and DEVELOPMENTAL BIOLOGY
Vanderbilt University Medical Center

The Department of Cell and Developmental Biology invites applications for a tenure-track faculty position. Established investigators with a strong record of productivity and extramural funding are especially encouraged to apply for appointment at the level of **ASSOCIATE or FULL PROFESSOR.** We seek candidates using cutting-edge cellular, molecular, biochemical, structural and/or genetic approaches in any area of cell and developmental biology and eukaryotic model systems. Special consideration will be given to those using *C. elegans* or *Drosophila* to investigate fundamental problems in neurobiology such as mechanisms of axon guidance and synapse assembly or function, nuclear organization and dynamics, vesicular trafficking, and tissue differentiation. Successful candidates will receive substantial startup packages and will be housed in newly constructed/renovated facilities. The appointee will also benefit from a broad array of core facilities, active graduate programs, and an interdisciplinary environment. Complete applications should include curriculum vitae, reprints of recent publications, a brief statement of present and future research plans, and three letters of recommendation, solicited by the applicant. Deadline for receipt of full application materials is December 1, 2007.

Submission instructions: cover letter, curriculum vitae, research plan, and at least three reprints should be submitted as one PDF file to **e-mail: cdb.recruiting@vanderbilt.edu.** Reference letters should be emailed directly from the referee.

Vanderbilt University Medical Center is strongly committed to diversity in attracting faculty to fill this position and is an Affirmative Action, Equal Opportunity Employer.

VERTEBRATE PHYSIOLOGY

The Department of Biology seeks candidates for the position of **ASSISTANT PROFESSOR** effective August 2008. Responsibilities include instruction of the following: animal physiology course, undergraduate/graduate course in the area of candidate's specialty, and introductory courses for majors and nonmajors. The successful candidate will be expected to have earned a Ph.D. from an accredited institution by May 31, 2008. A demonstration of teaching effectiveness and evidence of a commitment to understanding diverse populations will be required as part of the on-campus interview. Qualified candidates should submit a letter of interest, a brief statement of teaching philosophy and research interests, curriculum vitae, undergraduate and graduate transcripts (unofficial for application, official prior to interview), and the names and contact information for three references to: **Dr. Michael McNichols, Chair Physiology Search Committee, Biology Department, Shippensburg University, 1871 Old Main Drive, Shippensburg, PA 17257; e-mail: mjmcni@ship.edu; fax: 717-477-4064.** Review of applications begins January 10, 2008, and will continue until the position is filled. *Upon appointment, candidates must furnish proof of eligibility to work in the U.S. Offers of employment are contingent upon successful completion of a criminal background check. Shippensburg University is an Equal Opportunity Employer.*

CAREER OPPORTUNITY

This unique program offers the candidate with an earned Doctorate in the life sciences the opportunity to obtain the Doctor of Optometry (O.D.) degree in 27 months (beginning in March of each year). Employment opportunities exist in research, education, industry, and private practice. Contact the **Admissions Office, telephone: 800-824-5526** at the **New England College of Optometry, 424 Beacon Street, Boston, MA 02115.** Additional information at **website: http://www.neco.edu, e-mail: admissions@neco.edu.**

POSITIONS OPEN

EVOLUTIONARY DEVELOPMENTAL BIOLOGIST

The Department of Zoology, University of Hawaii invites Evolutionary Developmental Biologists to apply for a tenure-track **ASSISTANT or ASSOCIATE PROFESSOR** position. Teaching responsibilities will include an advanced undergraduate course in developmental biology and a graduate course in the individual's specialty. Applicants must have a Ph.D. and relevant postdoctoral experience, evidence of significant research accomplishments, and a commitment to excellence in teaching. Desirable qualifications include college teaching experience, research that interfaces developmental and evolutionary biology, evidence of successful grantsmanship, management of a research project, and ability to interface with a diverse range of faculty interests and to work with an ethnically diverse student population. To apply: Send letter of application, curriculum vitae, statement of research accomplishments and goals, reprints of three publications, and names of three references to: **Search Committee Department of Zoology, 2538 McCarthy Mall, University of Hawaii, Honolulu, HI 96822.** Closing date: November 2, 2007.

ANNOUNCEMENTS

INDO-U.S. SCIENCE and TECHNOLOGY FORUM (IUSSTF)
Announces
Indo-U.S. Research Fellowships

Indo-U.S. Science and Technology Forum (IUSSTF) in association with the Science and Engineering Research Council (SERC) of Department of Science and Technology (DST), Government of India has launched Indo-U.S. Research Fellowships to enable Indian researchers under the age of 40 years to carry out R&D in frontier areas of S&T at any premier institution in the United States up to a period of one year. Fellowship will cover (i) monthly stipend, (ii) return airfare, and (iii) preparatory and conference allowances.

Areas covered under the Fellowship are: atmospheric and earth sciences, chemical sciences, engineering sciences, life sciences, medical sciences, mathematical and computational sciences, and physical sciences.

Young Indian researchers interested in availing the above fellowship and American counterparts willing to host an outstanding Indian Fellow may refer to **website: http://www.indousstf.org** for application details.

Application deadline: 31 December 2007.

Additional job postings not featured in this issue can be viewed online at **website: http://www.sciencecareers.org.** New jobs are added daily!

MARKETPLACE

Widely Recognized Original & Guaranteed
KlenTaq 1
8¢/u
Truncated Taq DNA Polymerase Withstand 99°C
US Pat #5,436,149
Call: Ab Peptides
Fax: 314•968•8988
e-mail: abpeps@msn.com
1•800•383•3362
www.abpeps.com

Oligo Synthesis Reagents
Specialty CPG Supports
Linkers, Spacers, & Modifiers
Bulk Reagent Pricing Available
BIOSEARCH TECHNOLOGIES
Advancing Nucleic Acid Technology™
+1.800.GENOME.1
www.btisynthesis.com

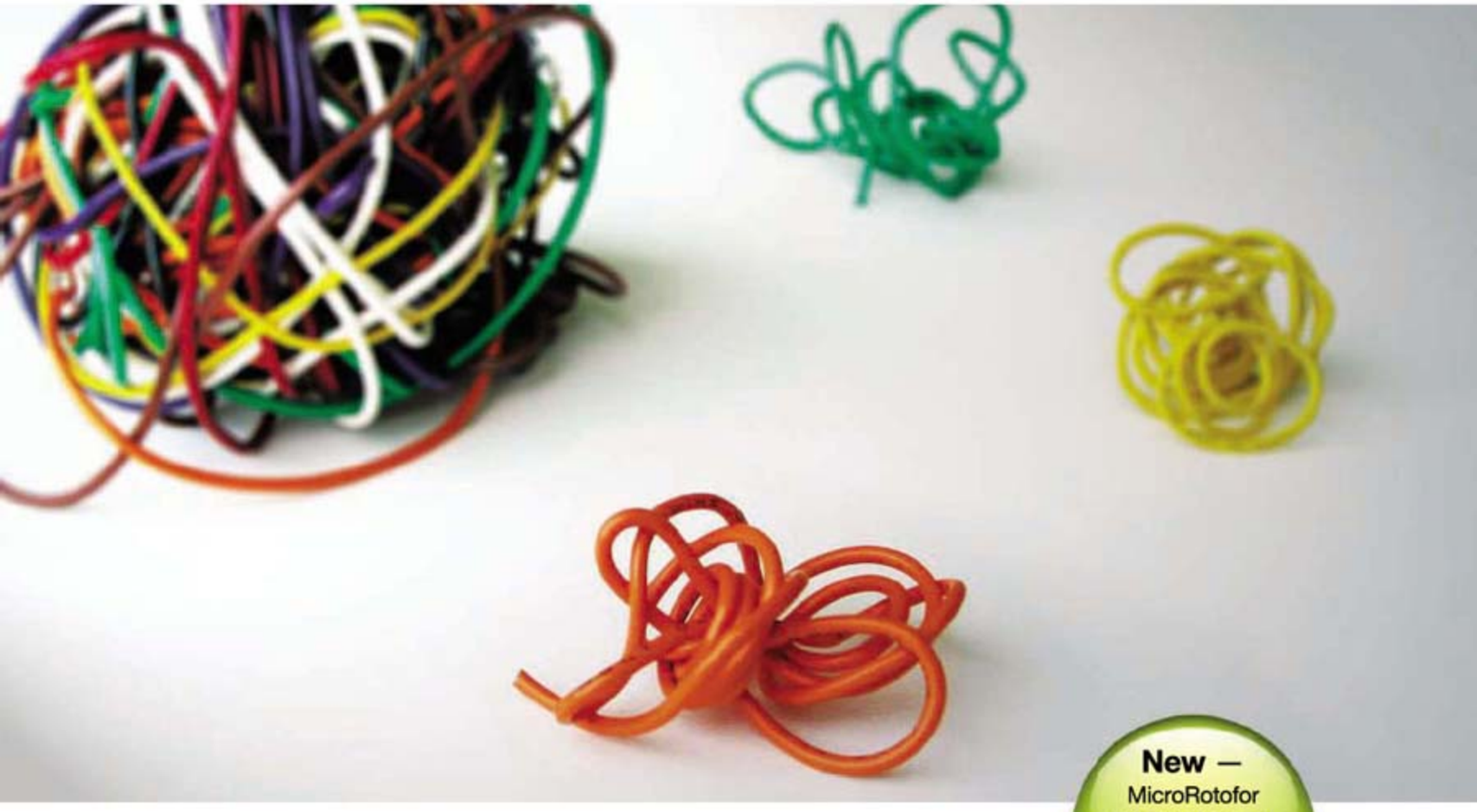

New — MicroRotofor lysis kits for easy, effective cell lysis and protein extraction

Fractionation just got simpler.

Reduce the complexity of your protein sample with the MicroRotofor™ system.

Fractionation is an essential step for increasing protein resolution in proteomic workflows. By fractionating, you reduce your sample complexity and enrich low-abundance proteins, both of which are central to biomarker discovery. Bio-Rad offers the MicroRotofor system for fractionation of proteins prior to most downstream proteomic applications, including 2-D gel electrophoresis and LC-MS/MS analysis.

- Handles small volumes (~2.5 ml) of precious samples
- Is compact and easy to use
- Separates proteins by liquid-phase isoelectric focusing
- Fractionates complex protein mixtures under native and denaturing conditions
- Offers customizable pH gradients to further enhance resolution of proteins of interest

MicroRotofor system

For more information, visit us on the Web at **www.bio-rad.com/microrotofor/**

Visit us on the Web at **discover.bio-rad.com**
Call toll free at 1-800-4BIORAD (1-800-424-6723);
outside the US, contact your local sales office.

BIO-RAD